KINETIC DETERMINANTS OF $GABA_A$ RECEPTOR FUNCTION

By

Emmanuel J. Botzolakis

Dissertation

Submitted to the Faculty of the

Graduate School of Vanderbilt University

in Partial Fulfillment of the requirements

for the degree of

DOCTOR OF PHILOSOPHY

in

Neuroscience

May, 2010

Nashville, Tennessee

Approved:

Robert L. Macdonald, M.D., Ph.D.

Louis J. De Felice, Ph.D.

Randy D. Blakely, Ph.D.

Sebastian Joyce, Ph.D.

To Liya, for supporting me on this journey.

ACKNOWLEDGEMENTS

In a letter to Robert Hooke, Isaac Newton once wrote, "If I have seen further, it is by standing on the shoulders of giants." No statement could be more relevant to this dissertation. Indeed, if I contributed at all to our understanding of channel kinetics and their role in shaping neurotransmission, it is only because I had the honor and privilege to work with an extremely long list of exceptional people. First and foremost, I am deeply indebted to my thesis advisor, Dr. Robert Macdonald, who gave me unprecedented freedom to explore new ideas and new techniques, to forge collaborations, and, despite the possible risk to his scientific reputation, to challenge dogma. I thank him for being an amazing mentor, for teaching me the rules of this game we call science, and for sharing his lunch on so many occasions. I also owe a great debt to Dr. Matt Bianchi, who took me under his scientific wing many years ago and taught me the fundamentals of channel kinetics. Nearly every idea presented in these pages represents a direct extension of his thesis work, and at one point or another, was discussed with him in great detail. I thank him for being a constant source of motivation, encouragement, and support, and for being a wonderful friend and collaborator. I am also grateful to many current and former members of the Macdonald Lab for their help and guidance. Dr. David Hinkle and Dr. Dorothy Jones-Davis helped integrate me into the lab and provided invaluable advice for surviving graduate school. Dr. Andre Lagrange taught me the basics of patch clamping and solution switching, and since I first joined the lab, has been a valued sounding board and collaborator. Katharine Gurba deserves a great deal of thanks, not only for helping me assemble the references for the Introduction in the final hours, but also for proofreading so many lengthy kinetics manuscripts. I also thank her for helping me re-

learn English grammar, for running countless control experiments, and for single-handedly keeping the flow cytometry project alive. The PDMS project could never have been completed without Ankit Maheshwari. I thank him for dedicating more than a year of his life to perfecting the fabrication process, something that required enormous creativity and persistence. I thank Dr. Hua-jun Feng for inviting me to work with him on the penicillin project and for his valuable contributions to the PDMS and repetitive stimulation projects. Dr. Ningning Hu and Dr. Wangzhen Shen provided excellent technical assistance on every project, and I thank them for their hard work and incredible patience (I must have asked them to sequence constructs hundreds of times). I credit Dr. Aleksandar Stanic-Kostic for teaching me the art of experimental design during our collaboration on the flow cytometry project (which I promise, Aleks, will get published eventually). Devon Smith deserves a great deal of thanks for proofreading several of the kinetics manuscripts, for running thousands of simulations, and for countless stimulating discussions. Sandra Camp is the reason things run smoothly in the Macdonald lab, and I thank her for rushing supply orders and dealing with the insufferable paperwork needed for travel reimbursements. I thank Dr. Martin Gallagher and Dr. Gregory Matthews for many stimulating discussions and for valuable career advice. Dr. Lou DeFelice, Dr. Randy Blakely, and Dr. Sebastian Joyce deserve great thanks for serving on my thesis committee. I sincerely appreciate their patience, encouragement, constructive criticism, and tolerance of my wandering scientific interests over the last few years. Thanks also to my MSTP advisor, Dr. Roger Chalkley, and former MSTP director, Dr. David Robertson, for bringing me into the Vanderbilt family. On the verge of giving up on graduate school in 2002, they gave me the chance to start over, and I will be forever grateful for that

opportunity. I am also grateful to the current director of the MSTP, Dr. Terry Dermody, for a great deal of valuable advice over the years. My presentation skills are undoubtedly better because of his constructive feedback, as is my general approach to and outlook on science. The Vanderbilt University School of Graduate Studies deserves special thanks for their generosity. In addition to funding my travel to national meetings on four separate occasions, they were kind enough to support the work presented in Chapter VI with a Dissertation Enhancement Grant. Outside of the University, numerous family and friends also deserve special recognition. I could not possibly have survived graduate school without the unwavering support of my wife, Dr. Liya Beyderman, who spent countless hours hearing about experiments gone wrong, obnoxious reviewers, and various other things that made graduate school frustrating, and who always picked up the slack at home when I needed to work late. Indeed, despite being a mommy of two little monsters, a Child Neurology resident, and moonlighter extraordinaire, she always manages to keep the house running like a finely tuned machine. She is truly a superhero, and I strive every day to be more like her. I thank my parents (all 3 of them) for nurturing my scientific interests from a young age, for letting me find my own path and voice, and for their incredible patience over the years. I know that raising me was probably one of the most demanding things they have ever done, and I am incredibly grateful that they never considered putting me up for adoption. Dr. Adam Wegner has been a close friend since my first day of classes at Vanderbilt. I thank him for countless fun nights of beer and darts, and for showing me how to properly culture cells. Farid Hekmat also deserves tremendous thanks, not only for his valued friendship over the last 15 years, but also for his help with the proofs shown in the Appendices. Again, thank you all. -- EJB

The great tragedy of science - the slaying of a beautiful hypothesis by an ugly fact.
Thomas Huxley

How wonderful that we have met with a paradox. Now we have some hope of making progress.
Niels Bohr

If we knew what it was we were doing, it wouldn't be called research, would it?
Albert Einstein

Research is the act of going up alleys to see if they are blind.
Marston Bates

All truths are easy to understand once they are discovered; the point is to discover them.
Galileo Galilei

Chance favors the prepared mind.
Louis Pasteur

Facts are stubborn, but statistics are more pliable.
Mark Twain

Science is facts; just as houses are made of stone, so is science made of facts; but a pile of stones is not a house, and a collection of facts is not necessarily science.
Jules Poincaré

The greater the ignorance the greater the dogmatism.
William Osler

I don't mind your thinking slowly; I mind your publishing faster than you think.
Wolfgang Pauli

Many people would sooner die than think. In fact, many do.
Bertrand Russell

Inventions have long since reached their limit, and I see no hope for further development.
Julius Frontinus (highly respected engineer in Rome, 1st century A.D.)

The hardest thing to explain is the glaringly evident which everybody had decided not to see.
Ayn Rand

Desensitization is more of an experimental nuisance than a physiologically interesting phenomenon.
David Colquhoun (prominent electrophysiologist)

TABLE OF CONTENTS

LIST OF TABLES

LIST OF FIGURES

Chapter II Page

Chapter III

Chapter V

Chapter VI

LIST OF ABBREVIATIONS

AChBP	acetylcholine binding protein
ANOVA	analysis of variance
AP2	clathrin-adaptor protein 2
ATP	adenosine triphosphate
B	open-channel blocked state
BI	bicuculline
BIG2	brefeldin-A-inhibited GDP/GTP exchange factor 2
BiP	immunoglobulin heavy-chain-binding protein
BDZ	benzodiazepine
C	closed state
CA1	cornu ammonis area 1
CAE	childhood absence epilepsy
C_b	bound closed state
cDNA	complementary deoxyribonucleic acid
CI	confidence interval
CNS	central nervous system
C_u	unbound closed state
D	desensitized state
D_f	fast desensitized state
D_i	intermediate desensitized state
D_s	slow desensitized state

D_5	dopamine receptor type 5
DMCM	methyl-6,7-dimethoxy-4-ethyl-beta-carboline-3-carboxylate
DMEM	Dulbecco's Modified Eagle's Medium
DZP	diazepam
EC_{50}	effective concentration that yields half-maximal response
E_{Cl}	chloride equilibrium potential
EGTA	ethylene glycol tetraacetic acid
eIPSC	evoked inhibitory post-synaptic current
ER	endoplasmic reticulum
FBS	fetal bovine serum
GABA	γ-aminobutyric acid
$GABA_A$	GABA receptor type A
$GABA_B$	GABA receptor type B
$GABA_C$	GABA receptor type C
GABARAP	$GABA_A$ receptor-associated protein
GABA-T	GABA transaminase
GAD	glutamic acid decarboxylase
GAT	GABA transporter
GEFS+	generalized epilepsy with febrile seizures plus
GHB	γ-hydroxybutyrate
GlyR	glycine receptor
GPCR	G-protein coupled receptor
GRIF1	$GABA_A$ receptor interacting factor 1 (aka, TRAK2)

GST	glutathione S-transferase
HEK	human embryonic kidney cell
HEPES	4-(2-hydroxyethyl)-1-piperazineethanesulfonic acid
IGE	idiopathic generalized epilepsy
I_{peak}	peak current
IPSC	inhibitory post-synaptic current
JME	juvenile myoclonic epilepsy
KCC2	potassium-chloride co-transporter
kDa	kilodalton
LGIC	ligand-gated ion channel
mIPSC	miniature inhibitory post-synaptic current
mRNA	messenger ribonucleic acid
M1	first transmembrane domain
M2	second transmembrane domain
M3	third transmembrane domain
M4	fourth transmembrane domain
nAChR	nicotinic acetylcholine receptor
O	open state
PB	pentobarbital
PBS	phosphate buffered saline
PDMS	polydimethylsiloxane
PDS	paroxysmal depolarizing shift
PG	penicillin G

PLIC1	protein linking integrin-associated protein to cytoskeleton-1
PKA	protein kinase A (aka, cAMP-dependent protein kinase)
PKC	protein kinase C
PKG	protein kinase G (aka, cGMP-dependent protein kinase)
PPI	paired-pulse inhibition
PRIP	phospholipase-C-related catalytically inactive proteins
PTC	premature termination codon
PX	picrotoxin
P_2X	purinergic receptor (aka, ATP-gated ion channel)
Ro 15-4513	ethyl 8-azido-6-dihydro-5-methyl-6-oxo-4H-imidazo[1,5-a][1,4] benzodiazepine-3-carboxylate
RPE	repeated pulse enhancement
RPI	repeated pulse inhibition
RT-PCR	reverse transcription polymerase chain reaction
SEM	standard error of the mean
sIPSC	spontaneous inhibitory post-synaptic current
SNAT	sodium-coupled neutral amino acid transporter
SSA	succinic semialdehyde
SSADH	succinic semialdehyde dehydrogenase
SU-8	negative, near-UV photoresist consisting of gamma butyrolactone (22-60%), triarylsulfonium/hexafluoroantimonate salt (<1%/1-3%), propylene carbonate (1-5%), and epoxy resin (35-75%)
TBPS	t-butylbicyclophosphorothionate
THDOC	tetrahydrodeoxycorticosterone
THIP	4,5,6,7-tetrahydroisoxazolo[5,4-c-]pyridin-3-ol

TM	transmembrane
UV	ultraviolent
VGAT	vesicular GABA transporter
WT	wild-type
ZAC	zinc-activated channel
5-HT_3R	5-hydroxytryptamine type 3 serotonin receptor

CHAPTER I

INTRODUCTION

Emmanuel J. Botzolakis and Robert L. Macdonald

GABA is important for proper functioning of the CNS

Present in ~30% of nerve terminals (Bloom and Iversen, 1971), γ-aminobutyric acid (GABA) is the most abundant inhibitory neurotransmitter in the central nervous system (CNS) (Curtis and Crawford, 1969; Hebb, 1970). Although GABA has also been detected in the pancreas, lung, kidney, and uterus (Hedblom and Kirkness, 1997; Wendt et al., 2004; Sarang et al., 2008; Jin et al., 2008) and in several stem cell lineages (Andang et al., 2008), its levels are highest in the brain and spinal cord (Awapara et al., 1950; Roberts and Frankel, 1950), where it plays an important role in sensory-motor integration (Middleton et al., 2008), learning and memory (Liu et al., 2007; McNally et al., 2008), maintenance of circadian rhythms and sleep (Liu and Reppert, 2000; Gillespie et al., 1997; Mintz et al., 2002; Steriade, 2005; Agosto et al., 2008), regulation of reward pathways (Johnson and North, 1992; Steffensen et al., 1998), mediation and perception of pain (Jasmin et al., 2003; Enna and McCarson, 2006), and even neuronal proliferation, migration, and differentiation (Owens and Kriegstein, 2002; McClellan et al., 2008). It is therefore not surprising that impaired GABA signaling has been implicated in a wide variety of neurological and psychiatric disorders including epilepsy, anxiety, insomnia, neuropathic pain, spasticity, schizophrenia, autism, depression, and drug addiction

(Malan et al., 2002; Wong et al., 2003; Rudolph and Möhler, 2004; Cryan and Kaupmann, 2005; Akbarian and Huang, 2006; Krystal et al., 2006; Enoch, 2008; Maguire and Mody, 2008). Although many of these disorders are undoubtedly polygenic, the recent discovery of inherited epilepsy syndromes caused by point mutations or polymorphisms in genes encoding GABA receptors (Macdonald et al., 2006) highlights the vulnerability of neuronal circuitry to loss of GABAergic inhibition and underscores the need to better understand this important neurotransmitter system.

Synthesis and degradation of GABA

GABA is synthesized from glutamate in presynaptic nerve terminals by the pyridoxal phosphate-requiring enzyme L-glutamic acid decarboxylase (GAD). (Notably, this reaction converts the predominant excitatory neurotransmitter into the predominant inhibitory one.) There are two isoforms of GAD (GAD_{65} and GAD_{67}; Erlander et al., 1991), each having different kinetic properties and subcellular localizations (Esclapez et al., 1994; Kanaani et al., 1999; Battaglioli et al., 2003). Once synthesized, GABA is packaged into presynaptic vesicles by the vesicular GABA transporter (VGAT) (Chaudhry et al., 1998). Following exocytic release into the synaptic cleft, GABA is cleared rapidly (in less than 1 ms; Clements, 1996; Glavinovic, 1999) by a combination of diffusion and reuptake, the latter being mediated by GABA transporters (GATs) expressed on the surface of presynaptic neurons and neighboring glia (Minelli et al., 1995). Interestingly, despite the classical view that individual synapses release a single type of neurotransmitter (Dale, 1935), several studies have shown that GABA can be co-released with other neurotransmitters such as glycine (Jonas et al., 1998), ATP (Jo and

Schlichter, 1999), glutamate (Gutierrez, 2005), and dopamine (Maher and Westbrook, 2008).

Once cleared from synapses, GABA is either repackaged into presynaptic vesicles by VGAT or converted back to glutamate by the "GABA shunt", a series of enzymatic reactions occurring in glia (Martin, 1993). The first step requires the mitochondrial enzyme GABA transaminase (GABA-T), which converts GABA to succinic semialdehyde (SSA). SSA is then converted by SSA dehydrogenase (SSADH) to succinate, which enters the Krebs cycle and is converted eventually to α-ketoglutarate. Glutamate is then regenerated from α-ketoglutarate during the process of GABA deamination by GABA-T, thereby ensuring that GABA catabolism is directly coupled with regeneration of its precursor. Glutamate, however, cannot be converted to GABA in glia due to their lack of GAD expression (Wuenschell et al., 1986). It is therefore converted by glutamine synthetase to glutamine, which is pumped out of glia and into the extracellular space by sodium-coupled neutral amino acid transporters (SNAT3/5) (Mackenzie and Erickson, 2003). From there, glutamine is pumped back into neurons by members of the same transporter family (SNAT1/2), where it is reconverted to glutamate by the enzyme glutaminase and thus available again for GABA synthesis (Mackenzie and Erickson, 2003).

Types of GABA receptors

GABAergic synaptic transmission is mediated by three receptor classes. The most widely expressed are the $GABA_A$ receptors (Laurie et al., 1992; Wisden et al., 1992), a large family of ligand-gated chloride channels responsible for the effects of

benzodiazepines (BDZs), barbiturates, anesthetics, neurosteroids, and ethanol (Olsen and Macdonald, 1992; Macdonald and Olsen, 1994; Rabow et al., 1995). In most adult neurons, $GABA_A$ receptor activation decreases the likelihood of neuronal firing by promoting membrane hyperpolarization. This occurs because the chloride reversal potential is typically lower than the resting membrane potential, reflecting the relatively low concentration of intracellular chloride due to expression of the potassium-chloride exporter, KCC2 (Rivera et al., 1999). Notably, lack of KCC2 expression is responsible for $GABA_A$ receptor activation causing membrane depolarization (i.e., excitation) during development, as this permits chloride to accumulate intracellularly and, consequently, efflux upon $GABA_A$ receptor channel opening (Ben-Ari, 2002; Stein and Nicoll, 2003). Although most $GABA_A$ receptors are expressed postsynaptically, where they give rise to fast inhibitory postsynaptic currents (IPSCs), they can also be found presynaptically, where they serve to inhibit neurotransmitter release (Kullmann et al., 2005).

In contrast, $GABA_B$ receptors are metabotropic G-protein-coupled receptors (GPCRs) that exert slow inhibitory effects either by activating outwardly rectifying voltage-gated potassium channels (Wagner and Dekin, 1993) or by inhibiting voltage-gated calcium channels (Mintz and Bean 1993). These effects are blocked by pertussis toxin, indicating that receptor coupling to its effector channels is mediated by $G_{i\alpha}$- or $G_{o\alpha}$-type G proteins (Bowery et al., 2002). Like $GABA_A$ receptors, $GABA_B$ receptors are expressed both pre- and postsynaptically, where they decrease the likelihood of neurotransmitter release and neuronal firing, respectively. However, unlike $GABA_A$ receptors, which are expressed at high levels throughout the brain, $GABA_B$ receptors have a more limited distribution. They are most highly expressed in cerebral cortex,

thalamus, cerebellum, interpeduncular nucleus, and spinal cord (Wilkin et al., 1981; Bowery et al., 1987; Chu et al., 1990). $GABA_B$ receptors are targeted by several clinically relevant compounds, including baclofen, an anti-spasticity agent (Bowery et al., 1980), and γ-hydroxybutyrate (GHB), an endogenous metabolite of GABA and common drug of abuse (Schweitzer et al., 2004).

A third type of GABA receptor, termed the $GABA_C$ receptor, has been identified in the retina and brainstem (Enz and Cutting, 1998; Bormann, 2000; Milligan et al., 2004). However, its classification as a separate entity from the $GABA_A$ receptor remains a matter of debate (Barnard et al., 1998; Zhang et al., 2001). Although $GABA_A$ and $GABA_C$ receptors have slightly different functional and pharmacological properties, they are both nevertheless ligand-gated chloride channels assembled from the same family of homologous subunits (Collingridge et al., 2008). Indeed, it should be emphasized that if differences in receptor function and pharmacology were sufficient for independent classification, then the $GABA_A$ receptor family would need to be further subdivided into perhaps as many as 30 different receptor classes (see below). Moreover, although $GABA_C$ receptors were originally thought to assemble from a different subunit subtype than $GABA_A$ receptors, recent studies have found that hybrid $GABA_{A/C}$ receptors can form and that they have unique biophysical and pharmacological properties (Qian and Ripps, 1999; Pan et al., 2001; Ekema et al., 2002; Milligan et al., 2004; Qian and Pan, 2002; Pan and Qian, 2004).

Classification issues aside, it is generally agreed that $GABA_A$ receptors mediate the majority of GABAergic signaling and are thus most important for maintaining inhibitory tone in the mammalian brain. Pharmacological blockade of $GABA_A$ receptors

rapidly induces seizures in animals (Kapur et al., 1997; Poulter et al., 1999) and epileptiform activity in neuronal slice preparations (De Deyn, et al., 1990; Schneiderman, 1997). Conversely, enhancement of $GABA_A$ receptor function leads to sedation and, ultimately, coma. Targeting $GABA_A$ receptors has thus been an effective approach for treating neuropsychiatric disorders characterized by neuronal hyperexcitability (e.g., epilepsy, anxiety, and insomnia). The properties of $GABA_A$ receptors will therefore be the focus of this dissertation.

Molecular biology of $GABA_A$ receptors

Like other members of the Cys-loop superfamily of LGICs, which includes the nicotinic acetylcholine receptor (nAChR; Noda et al., 1983), the 5-hydroxytryptamine type 3 serotonin receptor (5-HT_3R; Maricq et al., 1991), the zinc-activated channel (ZAC; Davies et al., 2003), and the glycine receptor (GlyR; Langosch et al., 1988), $GABA_A$ receptors are assembled as heteropentamers from a large family of homologous subunits (Schofield et al., 1987; Mamalaki et al., 1989; Nayeem et al., 1994; Knight et al., 1998; Barrera et al., 2008). Molecular cloning studies have identified eight subunit families (α, β, γ, δ, ε, θ, π, and ρ), thus providing enormous potential for receptor heterogeneity. Some of these subunit families are comprised of multiple subtypes (α1-6, β1-3, γ1-3, ρ1-3), splice variants (e.g., β2S and β2L; β3-v1 and β3-v2; γ2S and γ2L), and alternatively edited transcripts (e.g., α3I and α3M), further increasing the potential for heterogeneity (Schofield et al., 1987; Levitan et al., 1988; Pritchett et al., 1989; Shivers et al., 1989; Ymer et al., 1989a; Ymer et al., 1989b; Whiting et al., 1990; Herb et al., 1992; Kirkness and Fraser, 1993; Davies et al., 1997; Hedblom and Kirkness, 1997; Bonnert et al., 1999;

Simon et al., 2004; Ohlson et al., 2007). Sequence homology is ~60–80 % among members of the same $GABA_A$ receptor family, ~20-40 % among members of different families, and ~10-20 % among members of the $GABA_A$ receptor and other Cys-loop receptor families (Olsen and Tobin, 1990).

Most genes encoding human $GABA_A$ receptor subunits are found in tight clusters comprising 1 or 2 α subunits, 1 β subunit, and 1 γ subunit gene (in the order β-α-[α]-γ). Chromosome 4 contains α2, α4, β1, and γ1 subunit genes; chromosome 5 contains α1, α6, β2, and γ2 subunit genes; and chromosome 15 contains α5, β3, and γ3 subunit genes (Buckle et al., 1989; Wilcox et al., 1992; Russek and Farb, 1994; Hicks et al., 1994; McLean et al., 1995; Glatt et al., 1997; Simon et al., 2004). The gene encoding the α3 subunit is found on the X chromosome near the genes encoding θ and ε subunits (Bell et al., 1989; Wilke et al., 1997), which are most homologous to β and γ subunits, respectively (Wilke et al., 1997; Bonnert et al., 1999). Thus, it is believed that the incredible diversity of $GABA_A$ receptor subunits arose following duplication of a progenitor α-β-γ cluster (Hicks et al., 1994; Russek and Farb, 1994; Greger et al., 1995; McLean et al., 1995; Wilke et al., 1997; Darlison et al., 2005). The exceptions are the relatively isolated genes encoding the δ (chromosome 1; Sommer et al., 1990), π (chromosome 5; Bailey et al., 1999a), and ρ (chromosomes 3 and 6; Cutting et al., 1992; Bailey et al., 1999b; Simon et al., 2004) subunits, which given their lower degree of homology to other subunit subtypes, likely resulted from earlier gene duplication and transposition (Simon et al., 2004).

Although the functional significance of gene clustering remains uncertain, it may be important for coordinating transcription, and consequently, for limiting receptor

heterogeneity (Russek and Farb, 1994; McLean et al., 1995; Wilke et al., 1997; Darlison et al., 2005). Indeed, it is remarkable that the most abundant $GABA_A$ receptor isoforms in the cortex ($\alpha1\beta2\gamma2$; McKernan and Whiting, 1996; Pirker et al., 2000) and cerebellum ($\alpha6\beta2\gamma2$; McKernan and Whiting, 1996; Pirker et al., 2000) are composed of subunits encoded by genes clustered on chromosome 5, and similarly, that brain regions known to express the $\alpha3$ subunit also express the ε and θ subunits, which form the X chromosome cluster (Fritschy et al., 1992; Moragues et al., 2000; Moragues et al., 2002). Additional support for this hypothesis comes from the observation that genomic disruption of $\alpha6$ subunit expression leads to decreased transcript levels for co-clustered subunits (Uusi-Oukari et al., 2000). There are, however, many examples of receptor isoforms (see below) comprised of subunits encoded by non-clustered genes (McKernan and Whiting, 1996), reflecting the fact that individual neurons can simultaneously express as many as 10 different subunit subtypes (Brooks-Kayal et al., 2001).

Assembly of $GABA_A$ receptors

$GABA_A$ receptors, like other Cys-loop receptors, are assembled in a complex, multi-step process that occurs in the endoplasmic reticulum (ER). Assembly is thought to be slow and relatively inefficient (Green and Millar, 1995), relying heavily on luminal and cytoplasmic molecular chaperones (Bollan et al., 2003; Wanamaker and Green, 2007; Sarto-Jackson and Sieghart, 2008). Luminal chaperones include calnexin, which recognizes immature glycans (Helenius and Aebi, 2004); immunoglobulin heavy-chain-binding protein (BiP), which recognizes exposed hydrophobic residues (Gething, 1999); and protein disulfide isomerase, which catalyzes the formation of appropriate disulfide

bonds (Maattanen et al., 2006). Working together, these proteins facilitate the folding and oligomerization of $GABA_A$ receptor subunits and provide a stringent quality control system (Ellgaard and Frickel, 2003; Bollan et al., 2003). Although less is known about the role of cytoplasmic chaperones in $GABA_A$ receptor assembly, their involvement has been inferred based on the known interaction between α4β2 nAChRs and 14-3-3η (Jeanclos et al., 2001; Exley et al., 2006), a member of a large family of cytoplasmic regulatory, scaffolding, and adaptor proteins (Wang and Shakes, 1996).

In addition to these cellular requirements, there are also specific subunit requirements for $GABA_A$ receptor assembly that serve to limit receptor heterogeneity (Angelotti et al., 1993). Although most subunit combinations appear capable of oligomerization (Connolly et al., 1996), sucrose density centrifugation studies indicate that only a small subset can form pentamers, a prerequisite for receptor function and surface expression (lower molecular weight oligomers are retained in the ER and degraded) (Gorrie et al., 1997; Connolly et al., 1996; Connolly et al., 1999; Taylor et al., 2000; Klausberger et al., 2001; Bollan et al., 2003; Lo et al., 2008; Sarto-Jackson and Sieghart, 2008). For example, when recombinant α1, β2, or γ2 subunits were expressed individually in heterologous cells, primarily monomers and dimers were formed (Gorrie et al., 1997; Connolly et al., 1999; Taylor et al., 1999; Lo et al., 2008; Sarto-Jackson and Sieghart, 2008). Similarly, co-expression of either α1 or β3 subunits with γ2 subunits yielded primarily dimers and trimers (Tretter et al., 1997; Sarto-Jackson and Sieghart, 2008). In contrast, co-expression of α1 and β2/3 subunits formed pentamers, as did co-expression of α1, β2/3, and γ2 subunits (Gorrie et al., 1997; Tretter et al., 1997; Connolly et al., 1999; Taylor et al., 2000; Klausberger et al., 2001; Lo et al., 2008; Sarto-Jackson

and Sieghart, 2008). Thus, the presence of both α and β subunits is required for pentameric assembly (Angelotti et al., 1993). Known exceptions are the β3 and ρ1 subunits, which efficiently form homopentameric receptors when expressed individually (Taylor et al., 1999; Pan et al., 2006).

Interestingly, ternary receptors appear to assemble with higher efficiency than binary receptors, suggesting the existence of an assembly hierarchy within the subunit family that further limits receptor heterogeneity. For example, co-expression of α and β subunits with either γ, δ, ε, or π subunits yields a relatively homogeneous receptor population with kinetic properties distinct from receptors formed following co-expression of only α and β subunits (Angelotti and Macdonald, 1993; Saxena and Macdonald, 1994; Fisher and Macdonald, 1997; Haas and Macdonald, 1999; Neelands et al., 1999; Neelands and Macdonald, 1999; Lagrange et al., 2007). Similarly, despite the functional and pharmacological signature of αβ receptors having been identified in a subset of hippocampal neurons (Mortensen and Smart, 2006), the overwhelming majority of native receptors are thought to be composed of ternary subunit combinations (McKernan and Whiting, 1996; Olsen and Sieghart, 2008). The most widely expressed are αβγ and αβδ receptors, though αβε, αβθ, and αβπ receptors may be important in certain brain regions (see below). The α1β2γ2 isoform is the most abundant, accounting for ~40% of all $GABA_A$ receptors (McKernan and Whiting, 1996; Olsen and Sieghart, 2008).

For αβγ receptors, a subunit stoichiometry of 2α:2β:1γ (Chang et al., 1996; Tretter et al., 1997; Farrar et al., 1999) and a subunit arrangement of γ-β-α-β-α (counterclockwise when viewed top-down from the synaptic cleft; Baumann et al., 2001; Baumann et al., 2002; Baur et al., 2006) was proposed. Atomic force microscopy studies

suggested a similar stoichiometry and arrangement for αβδ receptors, with the δ subunit taking the place of the γ subunit in the pentamer (i.e., δ-β-α-β-α; Barrera et al., 2008). It should be noted, however, that there is evidence for alternate patterns of assembly. For example, multiple γ subunit subtypes have been identified in a subset of native (Quirk et al., 1994; Khan et al., 1994; Benke et al., 1996) and recombinant (Backus et al., 1993) receptors. Although it is unclear if multiple δ subunits can also be incorporated in the same pentamer, recent evidence using concatenated subunits suggests that at least two additional arrangements are possible: δ-α-β-β-α (GABA-gated) and δ-α-β-α-β (THDOC-gated) (Kaur *et al*., 2009). The ε subunit, which is highly homologous to the γ subunit (Wilke et al., 1997), appears particularly promiscuous (at least when expressed in heterologous systems), as it can form not only αβε receptors with multiple stoichiometries (2α:2β:1ε and 2α:1β:2ε), but can also co-assemble with α, β, and γ subunits to form αβγε receptors (Neelands et al., 1999; Davies et al., 2001; Wagner et al., 2005; Jones and Henderson, 2007; Bollan et al., 2008). The θ and π subunits, which are most homologous to β and δ subunits, respectively (Simon et al., 2004), exhibit similar promiscuity (again, when expressed in heterologous systems), having been shown to assemble as both ternary (αβθ and αβπ) and quaternary (αβγθ and αβγπ) receptors (Bonnert et al., 1999; Neelands and Macdonald, 1999).

Spatial and temporal regulation of $GABA_A$ receptor expression

Expression of $GABA_A$ receptors is tightly regulated both spatially and temporally, with individual subunits having distinct, but often overlapping, distributions. Based on *in situ* hybridization (Zhang et al., 1991; Laurie et al., 1992a, 1992b; Wisden et al., 1992)

and immunohistochemical (Fritschy et al., 1994; Fritschy and Mohler, 1995; Pirker et al., 2000) studies, α1 subunits appear to be widely expressed in the adult, but not the developing, brain. In contrast, α2 subunits are widely expressed during development (though not in cerebellum) but are limited to cortex, hippocampus, basal ganglia, amygdala, certain thalamic nuclei, and hypothalamus in the adult. α3 subunits have a similar spatiotemporal pattern, with high expression in most brain areas during development but limited expression in the adult, when it is found mainly in cortex and certain thalamic nuclei (most notably in the nucleus reticularis). Of note, α2 and α3 subunits are the predominant α subtypes in brainstem and spinal cord. α4 subunits have little expression during development; in the adult, their highest levels are found in cortex, hippocampus, and thalamus. α5 and α6 subunits have the most restricted distributions of all α subtypes, being localized mainly to hippocampus and cerebellum, respectively. α5 subunits, however, are expressed highly during development (except in cerebellum, where α3 subunits predominate). Among β subunits, β2 subunits are most widely expressed in the adult, except in hippocampus, where β1 and β3 subunits predominate (particularly in the dentate gyrus). Conversely, β3 subunits are most widely expressed during development, though β2 subunits are also expressed in cortex. γ2 subunits are the most widely expressed of the γ subunits, both in developing and adult brain. γ1 subunits are expressed in basal ganglia, forebrain, amygdala, and cerebellum, whereas γ3 subunits are expressed in cortex, basal ganglia, and certain thalamic nuclei (Herb et al., 1992). δ subunits are virtually absent during early development, but in the adult, are found in cortex, hippocampus, basal ganglia, thalamus, and cerebellum. Expression of ε subunits was initially undetectable in whole brain mRNA (Wilke et al., 1997), but upon closer

evaluation, was identified in amygdala, thalamus, and the subthalamic nucleus (Davies et al., 1997). θ subunits are found at low levels in cortex, intermediate levels in hypothalamus, and high levels in amygdala, hippocampus, and brainstem (Bonnert et al., 1999). Although π subunits are found mainly in peripheral tissues, low levels have been identified in hippocampus and temporal cortex (Hedblom and Kirkness, 1997). ρ subunits are expressed in retina on bipolar cells (Enz et al., 1996), cerebellum during development, and adult brainstem and spinal cord (Boue-Grabot et al., 1998; López-Chavez et al., 2005; Mejía et al., 2008).

Using information provided by mRNA co-localization studies, testable hypotheses were generated regarding possible subunit combinations that might exist *in vivo* (as opposed to what subunits could theoretically assemble *in vitro*). For example, transcripts encoding α1, β2, and γ2 subunits were co-expressed throughout the brain, while transcripts encoding α4, β2, and δ subunits were co-expressed in thalamus and hippocampus, suggesting they had a high probability of co-assembly in those areas. However, many brain regions were found to simultaneously express a variety of subunit subtypes (dentate gyrus, for example, expresses α1-5, β1-3, γ1-3, and δ subunits; Wisden et al., 1992), making the potential for receptor heterogeneity tremendous. As a result, early estimates put the total number of different isoforms in the adult brain at nearly 800 (Barnard et al., 1998)! To address this issue more directly, immunoprecipitation and immunoaffinity chromatography studies were performed using subunit-specific antibodies (Quirk et al., 1995; Jechlinger et al., 1998; Sur et al., 1999; Sieghart and Sperk, 2002). These studies, combined with detailed electrophysiological and pharmacological profiling of native receptors demonstrated that receptor heterogeneity *in*

vivo is surprisingly limited (Sieghart and Sperk, 2002; Olsen and Sieghart, 2008). In total, only 11 receptor isoforms (α1β2γ2, α2β2γ2, α3β2γ2, α4β2γ2, α4β2δ, α4β3δ, α5βxγ2, α6βxγ2, α6β2δ, α6β3δ, and ρx) were identified "unequivocally" (Olsen and Sieghart, 2008). An additional 8 isoforms (α1β3γ2, α1βxδ, α5β3γ2, αxβ1γ, αxβ1δ, αxβx, α1α6βxγ, and α1α6βxδx) were thought to exist with "high probability", and the existence of an additional 9 isoforms (αxβxγ1, αxβxγ3, αxβxε, αxβxθ, αxβxπ, αxαyβxγ2, ρ1, ρ2, and ρ3) were considered "tentative" (Olsen and Sieghart, 2008). Note that some of the listed isoforms contain multiple α subunit subtypes, which confer unique functional and pharmacological properties upon receptors (Duggan et al., 1991; Lüddens and Wisden, 1991; Lüddens et al., 1991). The same is thought to be true for β subunit subtypes, but evidence for this is more equivocal (Li and De Blas, 1997; Olsen and Sieghart, 2008).

Of these isoforms, α1βxγ2, α1βxδ, α2βxγ2, α3βxγ2, and α4βxδ isoforms are the predominant cortical receptors; α1βxγ2, α4βxγ2, and α4βxδ isoforms are the predominant thalamic receptors (α3βxγ2 is also important in the nucleus reticularis); α1βxγ2, α2βxγ2, and α5βxγ2 isoforms are the predominant hypothalamic receptors; α1βxγ2, α1βxδ, α2βxγ2, α4βxδ, and α5β3γ2 isoforms are the predominant hippocampal receptors; and α1βxγ2, α1βxδ, α1α6βxγ2, α1α6βxδ, α6βxγ2, and α6βxδ isoforms are the predominant cerebellar receptors (Wisden et al., 1992; McKernan and Whiting, 1996; Pirker et al., 2000; Brickley et al., 2001; Caraiscos et al., 2004; Farrant and Nusser, 2005; Glykys and Mody, 2007). Interestingly, subunit composition is an important determinant of receptor subcellular localization. For example, receptors containing γ subunits are typically found in synapses, while those containing δ subunits are typically found in peri- and/or extrasynaptic compartments (Nusser et al., 1998; Brickley et al., 2001; Farrant and

Nusser, 2005). The known exceptions are α4 and α5 subunit-containing αβγ receptors, which are thought to be primarily peri- and extrasynaptic (Caraiscos et al., 2004; Glykys and Mody, 2007). Similarly, receptors assembled without γ and δ subunits (i.e., αβ receptors) are localized extrasynaptically (Mortensen and Smart, 2006). Interestingly, β subunit subtype was recently shown to be an important determinant of subcellular localization in dentate gyrus (Herd et al., 2008).

Structure of $GABA_A$ receptors

Although a crystal structure of the $GABA_A$ receptor is unavailable, several experimental approaches have provided important insight into its tertiary and quaternary structure. These include imaging by electron and atomic force microscopy (Nayeem et al., 1994; Barrera et al., 2008), scanning for accessibility of substituted cysteine residues (Akabas, 2004), and homology modeling based on high resolution structures of the *Torpedo marmorata* nAChR (Unwin, 1993; Miyazawa et al., 2003; Unwin, 2005) and its soluble molluscan cousin, the acetylcholine binding protein (AChBP; Brejc et al., 2001) (Cromer et al., 2002; Ernst et al., 2003; Trudell and Bertaccini, 2004; O'Mara et al., 2005; Campagna-Slater and Weaver, 2007). The recent crystallization of the nAChR extracellular domain (Dellisanti et al., 2007) and a prokaryotic Cys-loop receptor (Hilf and Dutzler, 2008) has also provided important validation for the predicted $GABA_A$ receptor structure.

Hydropathy analysis suggests that individual $GABA_A$ receptor subunits are composed of a large (~200 amino acids) extracellular N-terminal domain, followed by four α-helical transmembrane domains (M1, M2, M3, and M4) that are connected by

cytoplasmic (M1-M2 and M3-M4) and extracellular (M2-M3) linkers (Olsen and Tobin, 1990; Macdonald and Olsen, 1994; Smith and Olsen, 1995). When viewed from the synaptic cleft (i.e., perpendicular to the plasma membrane), assembled $GABA_A$ receptors have a circular structure (~80 Å in diameter), with individual subunits arranged pseudo-symmetrically around a central ion-conducting pore (~20 Å in diameter). When viewed from their side (i.e., parallel to the plasma membrane), $GABA_A$ receptors are inverted wedge-shaped structures (~160 Å in length). The ion pore runs the length of the receptor and is divided into four sections. Most extracellular is a large funnel shaped vestibule (~50 Å in length). Just exterior to the plasma membrane, the vestibule connects to a smaller oval chamber (~20 Å in length), which is connected in turn to a long transmembrane channel (~50 Å in length). The latter contains the narrowest point of the pore (~4 Å in the closed conformation and ~6 Å in the open conformation; Bormann et al., 1987; Fatima-Shad and Barry, 1993; O'Mara et al., 2005) and determines ion selectivity ($Cl^- > Br^- > SCN^- > F^-$; Bormann et al., 1987). There may also be an additional vestibule located in the intracellular domain that contains lateral windows for ion movement (Unwin, 2005; Hales et al., 2006).

The extracellular domain is composed of two sets of β-sheets joined by a highly conserved disulphide bridge (the Cys-loop), for which the receptor superfamily is named (Unwin, 2005). These β-sheets contain seven major "loops" that are important for agonist binding, three on each side of the extracellular domain. The "principal" side of the extracellular domain (also referred to as the "+" side) is composed of the A, B, and C loops, whereas the "complementary" side (the "-" side) is composed of the D, E, F, and G loops (Ernst et al., 2003). GABA binding occurs at the interface between the principal

side of the β subunit and the complementary side of the α subunit. In contrast, BDZs bind at the interface between the principal side of the α subunit and the complementary side of the γ subunit (assuming the γ-β-α-β-α arrangement is correct, this predicts that each αβγ receptor has two GABA binding sites and one BDZ binding site). Interestingly, the BDZ and GABA binding sites are highly homologous, suggesting that the BDZ binding site evolved from a former GABA binding site (Galzi and Changeux, 1994). An endogenous ligand for the BDZ binding site, however, has yet to be identified. Of note, in addition to containing binding sites for a variety of agonists, antagonists, and allosteric modulators (Macdonald and Olsen, 1994; Olsen et al., 2004), the extracellular subunit domain is the primary determinant of receptor assembly (Hackam et al., 1997; Hackam et al., 1998; Enz and Cutting, 1999; Taylor et al., 1999; Klausberger et al., 2000; Taylor et al., 2000).

The M1 domain contains residues important for determining receptor kinetic properties and sensitivity to allosteric modulators such as BDZs and neurosteroids (Bianchi et al., 2001; Bianchi and Macdonald, 2002; Engblom et al., 2002; Jones-Davis et al., 2005; Keramidas et al., 2006; Akk et al., 2008). The M2 domain lines the transmembrane portion of the pore, determines ion selectivity and channel conductance, and contains the channel gate (Giraudat et al., 1986; Imoto et al., 1986, 1988; Akabas et al., 1994; Xu and Akabas, 1996; Serafini et al., 2000; Wilkins et al., 2002; Keramidas et al., 2004; Gonzales, et al., 2008). A leucine residue at the 9' position is highly conserved among members of the Cys-loop family and has therefore been the focus of active investigation. This residue is thought to line the narrowest part of the pore, and consequently, mutation of this residue has profound effects on channel function (Chang

and Weiss, 1998; Bianchi and Macdonald, 2001; Scheller and Forman, 2002; Bianchi et al., 2007). The M3 and M4 domains are packed somewhat loosely with respect to the M1 and M2 domains, creating cavities where allosteric modulators such volatile and intravenous anesthetics bind (Schofield and Harrison, 2005; Richardson et al., 2007). The lipid-facing M4 domain is farthest from the channel pore and is thought mainly to provide subunit stability in the plasma membrane. In nAChRs, for example, the M4 domain can be replaced by an unrelated transmembrane domain without abolishing channel function, whereas replacement of any other transmembrane domain renders channels non-functional (Tobimatsu et al., 1987).

The amino acid linkers connecting the transmembrane domains are also important determinants of receptor function. The intracellular M1-M2 linker extends the channel pore and contributes to charge selectivity (Jensen et al., 2002; Filippova et al., 2004; Wotring and Weiss, 2008). The extracellular M2-M3 linker is responsible for transducing ligand binding in the N-terminal domain to channel gating in the transmembrane domain. Based on charge swapping mutations, this appears to involve a salt bridge between loop 2 (and possibly, loop 7) in the N-terminal domain and a highly conserved lysine residue in the M2-M3 linker (Kash et al., 2003). Of note, mutation of this conserved residue in the γ2 subunit of the $GABA_A$ receptor (K289M) has been associated with generalized epilepsy with febrile seizures plus (Baulac et al., 2001), and mutations of the same residue in the α1 subunit of the GlyR (K276E and K276Q) have been associated with hyperekplexia (Langosch et al., 1994; Harvey et al., 2008). In each case, mutation of the conserved lysine substantially inhibited channel function (Bianchi & Macdonald, 2002), consistent with a role for this domain in transducing binding to

gating. Interestingly, the mechanisms underlying the coupling of binding and gating appear to be highly conserved within the Cys-loop superfamily. Functional chimeras have been generated between nAChR subunit extracellular domains and 5-HT_3R subunit transmembrane domains and, similarly, between $GABA_A$ receptors and GlyRs (Eisele et al., 1993; Mihic et al., 1997). These chimeric receptors are gated by ligands specific for the extracellular domain, but have functional properties that depend on the identity of the transmembrane domain. The large intracellular M3-M4 linker (~100-200 amino acids) is also thought to play a role in channel function, having recently been shown in 5-HT_3Rs and nAChRs to contain a motif (the "MA" stretch) that is an important determinant of single-channel conductance (Kelley et al., 2003; Peters et al., 2005; Hales et al., 2006).

The M3-M4 linker, however, has a variety of other functions. Indeed, this domain serves as the primary interface between the $GABA_A$ receptor and the intracellular milieu. It contains phosphorylation sites for PKA, PKC, and PTK (Brandon et al., 2002; Kittler and Moss, 2003; Jacob et al., 2008), and protein binding domains that are important for receptor clustering, sorting, targeting, and trafficking (Kittler and Moss, 2003; Chen and Olsen, 2007; Jacob et al., 2008). Known interacting proteins include AP2, which promotes endocytosis by recruiting receptors into clathrin-coated pits (Kittler et al., 2005; Smith, et al., 2008); GRIF1, which regulates kinesin-mediated vesicular transport (Beck et al., 2002; Brickley et al., 2005); gephyrin, which clusters and stabilizes receptors in synapses (Essrich et al., 1998; Kneussel et al., 2000; Tretter et al., 2008); BIG2, which facilitates vesicular transport (Charych et al., 2004); GABARAP, which promotes receptor trafficking from the Golgi to the cell surface (Wang et al., 1999; Chen et al., 2000); PRIPs, which modulate phosphatase activity (Kanematsu et al., 2002, 2007);

and PLIC1, which stabilizes receptors on the cell surface by preventing ubiquitination-mediated degradation (Bedford et al., 2001). The M3-M4 linker is also thought to mediate the direct interaction between $GABA_A$ receptors and other neurotransmitter receptors such as the $GABA_B$, D_5, and P_2X receptors (Liu et al., 2000; Balasubramanian et al., 2004; Boué-Grabot et al., 2004). In addition, recent evidence suggests that motifs in the M3-M4 linker are required for complete pentameric assembly (Lo et al., 2008).

Biophysical and kinetic properties of $GABA_A$ receptor channels

$GABA_A$ receptor channels are relatively impermeant to cations (permeability ratio of K+ to Cl- < 0.05) but highly permeable to anions such as Cl^- and HCO_3^- (Bormann *et al.*, 1987). The channel is considerably more permeable to Cl^- than to HCO_3^- (Cl^-:HCO_3^- permeability is ~5:1), and consequently, the majority of charge transfer that follows channel activation *in vivo* is Cl^- mediated. However, HCO_3^- may play an important role when the Cl^- gradient is collapsed (Grover *et al.*, 1993; Perkins and Wong, 1997; Dallwig *et al.*, 1999; Kim *et al.*, 2009), as may be the case in immature neurons and in a subset of mature neurons. Interestingly, GABA-mediated HCO_3^- efflux has been shown to trigger Ca^{2+} influx (Kulik *et al.*, 2000; Chavas *et al.*, 2004), which may underlie the ability of GABA to serve as a trophic signal in maturing networks (Ben-Ari, 2002; Owens and Kriegstein, 2002).

The canonical $\alpha1\beta x\gamma2$ $GABA_A$ receptor opens to a main conductance level of 26-30 pS and to several less frequent sub-conductance levels (Macdonald et al., 1989; Twyman et al., 1990; Newland et al., 1991; Fisher and Macdonald, 1997; Haas and Macdonald, 1999; Burkat et al., 2001). The channel is almost exclusively chloride

selective with a permeability ratio of potassium to chloride ions less than 0.05 (Bormann et al., 1987). To fully activate the receptor, binding of two molecules of GABA (to independent sites) is required. Once bound with GABA, the channel exhibits complex patterns of activity. Detailed kinetic analysis of native (Macdonald et al., 1989; Twyman et al., 1990; Newland et al., 1991) and recombinant (Fisher & Macdonald, 1997; Haas & Macdonald, 1999; Burkat et al., 2001) receptors demonstrated the existence of three open states and at least five closed states (based on exponential fitting of open and closed time distributions). When activated by a saturating concentration of GABA (1 mM), open times of 0.3, 2.0, and 3.5 ms (referred to as O1, O2, and O3) were observed with relative amplitudes of 24, 48, and 28 %, respectively, the overall mean open time being 2.1 ms (Haas and Macdonald, 1999). The overall mean closed time was 21.0 ms (with individual components ranging from 0.2 to 990 ms in duration), thus yielding an open probability of ~0.1 when activated by 1 mM GABA (note that this may be an overestimation, as recordings are rarely obtained from patches containing a "single" channel).

Channel openings tended to occur in bursts (a series of openings separated by brief closures), of which there were at least three types, each containing a single type of opening (i.e., either O1 or O2 or O3). This indicated that receptors could not transition directly from one open state to another. Interestingly, activating receptors with progressively lower GABA concentrations increased the relative contribution of O1 openings at the expense of both O2 and O3 openings, without altering individual open times (though the overall mean open time was decreased since the lifetime of O1 is short). Considering that receptors have negligible spontaneous activity, these data have

been interpreted to mean that O1 and O2/O3 represent receptor sojourns in mono- and di-liganded open states, respectively (Twyman et al., 1990). What remains unclear, however, is why O1 openings were detectable at all in the context of a saturating GABA concentration, as this should have effectively driven receptor occupancy in mono-liganded states near zero. One possibility is that two O1 states exist with similar mean open times, one mono-liganded and the other di-liganded. In other words, there may actually be four open states, two of which are simply indistinguishable with classical exponential fitting of open time distributions (Lagrange et al., 2007).

Given the complex channel activity observed at the microscopic level, it is not surprising that $GABA_A$ receptor macroscopic current properties (i.e., the ensemble response of hundreds or thousands of channels) are also quite complex (Haas and Macdonald, 1999; Bianchi and Macdonald, 2001; Mozrzymas et al., 2003; Lagrange et al., 2007). Rapid application of a saturating GABA concentration to excised outside-out patches from hippocampal neurons or HEK293T cells transiently expressing $\alpha 1\beta x\gamma 2$ receptors gives rise to large amplitude currents that activate in the sub-millisecond time domain. In the context of prolonged agonist exposure, these currents undergo extensive multi-phasic desensitization, typically with three to four time constants ranging from <10 ms to >1000 ms (Celentano and Wong, 1994; Haas and Macdonald, 1999; Bianchi and Macdonald, 2002; Lagrange et al., 2007). This phenomenon (also referred to as current "sag") is not caused by receptor internalization or loss of the chloride gradient, but rather, is an intrinsic property of the channel, reflecting the progressive accumulation of receptors in long-lived non-conducting (desensitized) states (Celentano and Wong, 1994; Bianchi and Macdonald, 2002). Interestingly, desensitization has a steep concentration-

dependence (Haas and Macdonald, 1999; Bianchi et al., 2007). Although this has been suggested to reflect a concentration-dependent entry rate into the microscopic desensitized state, multiple modeling studies have demonstrated that this gating structure is not actually required (Haas and Macdonald, 1999; Bianchi et al., 2007). Instead, the loss of desensitization associated with application of low concentrations of GABA is most likely caused by failure to synchronously activate receptors, which masks the otherwise concentration-independent process (much like slow application of agonist; Jones and Westbrook, 1995; Bianchi and Macdonald, 2002). Evidence for this comes from detailed kinetic analysis of macroscopic desensitization, which shows that while the relative contribution of each desensitization time constant changes with GABA concentration, the actual time constants do not (Haas and Macdonald, 1999).

Following GABA washout, currents typically deactivate bi-phasically (Jones and Westbrook, 1995; Haas and Macdonald, 1999), though multi-phasic deactivation has been described (Lagrange et al., 2007). The time course of deactivation depends strongly on the duration of GABA exposure prior to washout, with longer applications being associated with slower deactivation (Jones and Westbrook, 1995; Haas and Macdonald, 1999; Bianchi et al., 2007; Botzolakis et al., 2008). This reflects the inability of GABA to unbind from receptors in desensitized states (note that GABA is also "trapped" on receptors in open and pre-open states; Bianchi et al., 2002), which represent an increasing fraction of receptors with longer GABA applications (Bianchi et al., 2007). Although desensitized states are functionally identical to other closed states, their long lifetimes provide channels with the opportunity to re-open long after GABA washout, the macroscopic correlate of which is prolonged deactivation (Jones and Westbrook, 1995,

1996). As a result, the phenomena of desensitization and deactivation are commonly referred to as being "coupled" (Jones and Westbrook, 1995; Bianchi et al., 2001).

Both the macroscopic and microscopic kinetic properties of $GABA_A$ receptors are highly influenced by subunit composition, thus providing a mechanism for neurons to fine tune their sensitivity to GABA (Angelotti and Macdonald, 1993; Saxena and Macdonald, 1994; Burgard et al., 1996; Fisher and Macdonald, 1997a, 1997b; Fisher et al., 1997; Neelands et al., 1999; Neelands and Macdonald, 1999; Haas and Macdonald, 1999; Bianchi et al., 2002; Feng and Macdonald, 1994; Feng et al., 2004; Barberis et al., 2007; Bianchi et al., 2007; Lagrange et al., 2007; Picton and Fisher, 2007; Rula et al., 2008). For example, in contrast to αβγ receptors, αβδ receptors have only two open states, both of which are relatively short-lived (0.3 and 1.0 ms). The shorter of these accounts for 80% of all openings, yielding an overall mean open time of only 0.4 ms (Fisher and Macdonald, 1997; Haas and Macdonald, 1999). In addition, αβδ receptors have a longer mean closed time (~36 ms), reflecting their increased likelihood of entering long-lived closed states. This, combined with their decreased mean open time, makes their overall open probability when activated by 1 mM GABA much lower than that of αβγ receptors (~0.02 vs. ~0.1, respectively). Consequently, macroscopic currents evoked from αβδ receptors have kinetic properties that are different from those evoked from αβγ receptors. Indeed, αβδ receptor currents are typically small, slowly activating, minimally desensitizing, and rapidly deactivating (Saxena and Macdonald, 1996; Fisher and Macdonald, 1997; Haas and Macdonald, 1999; Bianchi and Macdonald, 2002). Interestingly, while comparing αβδ and αβγ *macroscopic* currents provides support for the idea that desensitization and deactivation are coupled phenomena, at the *microscopic*

level, αβδ receptors actually appear to have similar, if not increased, access to long-lived closed states (Fisher and Macdonald, 1997; Haas and Macdonald, 1999). This suggests that macroscopic desensitization may not simply reflect receptor accumulation in any particular state or set of states, but rather, may depend on a more complex interplay between all rate constants in the gating scheme (Mozrzymas et al., 2003; Bianchi et al., 2007). Similarly, although deactivation may be influenced by receptor trapping in desensitized states, other rate constants (such as the unbinding rate) undoubtedly also contribute to its time course.

A variety of mathematical approaches have been used to describe the behavior of ion channels; however, it is generally agreed that Markov models comprising multiple, reversibly connected states, each corresponding to a distinct receptor conformation (i.e., open or closed), provide the best fits of channel data (Korn and Horn, 1988; McManus et al., 1988; Sansom et al., 1989). Although applying Markov models to ion channels involves several assumptions (primarily, that state transitions are probabilistic and independent of previous channel activity), thus far, they have proven extremely useful for describing the behavior not only of $GABA_A$ receptors (Twyman and Macdonald, 1989; Weiss and Magleby, 1989; Celentano and Wong, 1994; Jones and Westbrook, 1995; Haas and Macdonald, 1999; Lagrange et al., 2007), but also of numerous other ligand- and voltage-gated channels (Horn and Vandenberg, 1984; Zagotta et al., 1994; Schoppa and Sigworth, 1998; Rothberg and Magleby, 2000; Sigg and Bezanilla, 2003; Burzomato et al., 2004; Chakrapani et al., 2004; Lape et al., 2008). Indeed, Markov models have provided an important conceptual framework for interpreting the effects of disease-causing mutations and a variety of modulators (Twyman and Macdonald, 1992; Twyman

et al., 1989a, 1989b, 1992; Bianchi and Macdonald, 2001; Feng et al., 2004; Mercik et al., 2006; Mozrzymas et al., 2007; Plested et al., 2007). However, for models to have any practical utility, they must account for both microscopic and macroscopic channel behavior (that being said, simple models are often quite valuable for systematically exploring the relationship between microscopic rate constants and macroscopic phenomena, and for that purpose, will be relied upon as much as comprehensive models in this dissertation). Considering that receptor responses under both microscopic and macroscopic conditions are critical, as neither can independently provide enough information for a unique reaction scheme to be generated with certainty. Macroscopic currents, for example, constrain gating schemes by providing non-equilibrium kinetic data, which is typically unavailable from near-equilibrium single-channel studies. Single channel data, in contrast, provides direct information regarding channel open and closed states, including the number of each, their connectivity, and in the case of the open states, their approximate lifetimes. The first comprehensive model was developed by Haas and Macdonald (1999) and was based on an earlier model by Twyman et al. (1990) that described the behavior of single channels. This model contained two GABA binding steps and a total of 16 states - 3 open and 13 closed. Three of closed states were given the special designation of "desensitized" states, as they allowed for the macroscopic phenomenon of desensitization to occur. Although this model has been updated recently to take into account several additional macroscopic and microscopic observations, its core gating structure has not changed in almost a decade (Lagrange et al., 2007).

Pharmacological properties of $GABA_A$ receptors

$GABA_A$ receptors have a rich pharmacology (for a review, see Macdonald and Olsen, 1994, or Johnston, 1996). In addition to GABA, a number of GABA analogues can directly activate the receptor, including the plant alkaloid muscimol and its conformationally restricted analogue tetrahydroisoxazolopyridinol (THIP). Endogenous agonists include taurine and β-alanine, both of which are found at relatively high concentrations in the brain (Lerma et al., 1986). Interestingly, although each of these agonists has a different microscopic affinity for GABA (muscimol > GABA > β-alanine ≈ THIP), when used at EC-equivalent concentrations, all give rise to similar microscopic and macroscopic currents (Jones et al., 1998; Bianchi et al., 2007). $GABA_A$ receptor currents can be competitively antagonized by the convulsant drug, bicuculline, and by the pyridazinyl derivative of GABA, gabazine (SR95531). Of note, bicuculline can also block spontaneously active $GABA_A$ receptors (Bianchi and Macdonald, 2002), indicating it should also be classified as an inverse $GABA_A$ receptor agonist along with β-carbolines such as DMCM. Non-competitive antagonists include the convulsants picrotoxin, TBPS, pentylenetetrazole, and penicillin, the latter being a classic open channel blocker of $GABA_A$ receptors (Twyman et al., 1989; Feng et al., 2009). The anticonvulsant barbiturates and BDZs allosterically enhance $GABA_A$ receptor currents, but through different binding sites and by different mechanisms (Twyman et al., 1989). Barbiturates increase the fraction of long (O3) openings at the expense of short (O1 and O2) openings, thus increasing channel mean open time. In contrast, BDZs increase the microscopic affinity of GABA for the receptor without altering channel mean open time, thus increasing channel opening frequency (at sub-saturating concentrations of GABA)

(Bianchi et al., 2009). The BDZ binding site is targeted by several agents, including the inverse agonist β-carbolines, the imidazolpyridines (zolpidem, alpidem), the BDZ inverse agonist Ro 15-4513, and the BDZ antagonist, flumazenil. Other positive allosteric modulators include ethanol, neurosteroids (THDOC and allopregnanolone), and several volatile and intravenous anesthetics (halothane, diethylether, enflurane, isoflurane, alphaxalone, ketamine, and propofol). Negative allosteric modulators include pregnenolone sulfate, zinc, and furosemide. In addition, there are several classes of allosteric modulators with mixed effects (i.e., positive and negative modulation depending on GABA concentration and context of receptor activation). These include the insecticides dieldrin and lindane, the anti-helminthic ivermectin, lanthanum, and pH.

The pharmacological properties of $GABA_A$ receptors, much like their kinetic properties, are highly sensitive to subunit composition (for a review, see Hevers and Lüddens, 1998). For example, BDZ modulation requires the presence of a γ subunit; however, only α(1, 2, 3, or 5)βγ receptor isoforms are BDZ sensitive. Conversely, α(1, 2, 3, or 5)βγ receptor isoforms are less sensitive to furosemide, while those containing α4 and α6 subunits are highly sensitive. Zolpidem has highest affinity for α1 subtype-containing receptors, low affinity for α2 and α3 subtype-containing receptors, and almost no affinity for α5 subtype-containing receptors. Receptors containing β2 or β3 subtypes are highly sensitive to loreclezole, whereas those containing the β1 subtype are relatively insensitive. Inclusion of a γ subunit dramatically reduces receptor sensitivity to zinc and neurosteroids. Receptor incorporation of δ subunits increases receptor sensitivity to neurosteroids and ethanol. In some cases, subunit composition determines the polarity of modulation (i.e., enhancement vs. inhibition). For example, while Ro 15-4513 is an

inverse agonist at the BDZ binding site for α(1, 2, 3, or 5)βγ receptor isoforms, it is an agonist of α4 and α6 subtype-containing receptors. Similarly, while lanthanum enhances α1βγ receptor currents, it blocks α6βγ receptor currents.

Modes of GABAergic inhibition

$GABA_A$ receptors mediate two modes of inhibitory neurotransmission. The first, termed "phasic" inhibition, involves the transient activation of postsynaptic $GABA_A$ receptors by nearly saturating concentrations of GABA released from presynaptic vesicles. This process gives rise to inhibitory postsynaptic currents (IPSCs) that activate rapidly (rise times of ~1 ms or less) but decay slowly (time constants of 10s to 100s of ms) (Maconochie et al., 1994; Jones and Westbrook, 1995). In the experimental setting, several types of IPSCs can be recorded, each having slightly different kinetic properties (Otis and Mody, 1992a, 1992b; Otis et al., 1994; Kirmse et al., 2006; Liang et al., 2006). These include "miniature" IPSCs (mIPSCs), "spontaneous" IPSCs (sIPSCs), and "evoked" IPSCs (eIPSCs). mIPSCs are triggered by the spontaneous release of GABA from a single synaptic vesicle (i.e., action potential independent). In contrast, sIPSCs are triggered by spontaneously occurring action potentials in presynaptic terminals and typically involve release of GABA from multiple synaptic vesicles. eIPSCs are triggered following experimentally induced action potentials, and like sIPSCs, involve release of GABA from multiple synaptic vesicles. The properties of IPSCs are highly variable, depending on brain region, developmental stage, and neuron type (Vicini et al., 2001; Mozrzymas, 2004). While both pre- and postsynaptic factors influence IPSC shape, it is generally accepted that postsynaptic factors are the primary determinants. Indeed, the

GABA transient is thought to reach nearly saturating concentrations in <100 μs and decay in <1 ms due to a combination of diffusion and reuptake (Clements, 1996; Glavinovic, 1999; Ventriglia and Di, 2003). Thus, IPSC duration significantly outlasts the presence of GABA in the synaptic cleft, suggesting that IPSCs are shaped primarily by the intrinsic properties of postsynaptic receptors. In support of this hypothesis, application of ultra-brief pulses of nearly saturating GABA to membrane patches excised from mammalian cell lines expressing recombinant $GABA_A$ receptors gives rise to currents with kinetic properties that resemble IPSCs (Jones and Westbrook, 1995; Haas and Macdonald, 1999). Currents evoked from receptors containing the γ subunit are most similar to IPSCs, as they activate rapidly and deactivate slowly (Jones and Westbrook, 1995; Haas and Macdonald, 1999; Lagrange et al., 2007). This should not imply, however, that presynaptic factors cannot also influence IPSC shape. Several studies suggest that the GABA transient may actually decay with a time constant as brief as 100 μs (Mozrzymas, 2004). Kinetic modeling studies predict that such ultra-brief exposures prevent postsynaptic receptors from reaching maximal activation, thus leading to smaller amplitude and more rapidly deactivating IPSCs (Mozrzymas, 2004; Lagrange et al., 2007). In addition, while the concentration of GABA in synapses is generally thought to be nearly saturating (~1 mM) (Edwards et al., 1990; Otis and Mody, 1992; Jones and Westbrook, 1995; Strecker et al., 1999), the observation that diazepam can increase IPSC amplitudes in some brain regions suggests this may not always be the case (i.e., if GABA is truly saturating in the synapse, then increasing receptor affinity for GABA with a BDZ should not affect IPSC amplitude, as the postsynaptic receptors are already fully-liganded) (Frerking et al., 1995; Defazio and Hablitz, 1998; Hill et al., 1998). Activating

receptors with sub-saturating concentrations of GABA can significantly impact IPSC kinetics, as the time courses of $GABA_A$ receptor activation and deactivation are both highly sensitive to GABA concentration (slower and faster, respectively) (Bianchi et al., 2007; Lagrange et al., 2007).

In addition to mediating fast synaptic inhibition, there is now compelling evidence that $GABA_A$ receptors are also involved in slower forms of nonsynaptic inhibition, a phenomenon termed "tonic" inhibition (Farrant and Nusser, 2005). This is mediated by peri- and extrasynaptic $GABA_A$ receptors that are persistently activated by sub-saturating concentrations of ambient GABA. While the sources and precise concentration of ambient GABA are still uncertain (unlike other neurotransmitters such as dopamine and serotonin, the GABA concentration cannot be measured directly), it is generally believed to arise from a combination of synaptic overflow and non-vesicular release, and to reach concentrations of ~1 μM (Attwell et al., 1993; Nusser et al., 1998; Zoli et al., 1999; Bach-y-Rita, 2001; Farrant and Nusser, 2005). Interestingly, the contribution of the tonic current to overall inhibitory tone may actually be greater than the summed charge transfer of phasic currents (Brickley et al., 1996; Hamann et al., 2002). It should also be noted that tonic and phasic inhibition are differentially modulated by various pharmacological agents (Feng and Macdonald, 2004; Feng et al., 2004; Feng et al., 2008) and that they play distinct roles in the pathogenesis of neurological disorders such as epilepsy (Dibbens et al., 2004; Feng et al., 2006; Eugène et al., 2007). This reflects the fact that tonic currents are mediated by a different subset of receptor isoforms, which have kinetic properties distinct from those mediating phasic currents. α4βxδ and α6βxδ receptor isoforms are thought to be the primary mediators of tonic inhibition (Brickley et al.,

2001; Farrant and Nusser, 2005), though α1βxδ and α5βxγ2 receptors may also play an important role in the hippocampus (Glykys et al., 2008). Indeed, properties conferred by the δ subunit are consistent with a role in tonic inhibition; αβδ receptors desensitize much slower and less extensively than αβγ receptors and have a lower GABA EC_{50}, ideal for receptors that must respond to very low concentrations of GABA for extended periods of time (Saxena and Macdonald, 1996; Haas and Macdonald, 1999; Lagrange et al., 2007).

Involvement of $GABA_A$ receptors in epilepsy

Epilepsy is associated with abnormal hypersynchronous activation of large neuronal populations. Although the mechanistic bases for partial and generalized forms of epilepsy are uncertain, there is considerable evidence that impaired GABAergic inhibition underlies several types of epilepsy. Indeed, pharmacological blockade of GABAergic inhibition with $GABA_A$ receptor antagonists such as penicillin, picrotoxin, or bicuculline produces paroxysmal bursting in isolated neurons and partial seizures in experimental animals (Schwartzkroin & Prince, 1980). Similar experiments have shown that $GABA_A$ receptor blockade produces paroxysmal depolarization shifts (PDSs), which are the interictal manifestations of epileptiform events. This local paroxysmal bursting can spread to involve large areas of hippocampus or generalize to cortex when inhibition is further weakened and when other synchronizing factors occur, such as altered extracellular concentrations of potassium and calcium (Korn et al., 1987; Traynelis and Dingledine, 1988).

However, conclusive evidence that loss of GABAergic inhibition was involved in the pathogenesis of human epilepsy syndromes did not come until the recent discovery of mutations in genes encoding $GABA_A$ receptor subunits that were associated with idiopathic generalized epilepsies (Macdonald et al., 2006). The first α subunit mutation to be reported was the α1 subunit mutation, A322D, in a family with juvenile myoclonic epilepsy (JME). Mutant receptors had substantially reduced maximal currents and increased GABA EC_{50} (Cossette et al., 2002). This was caused by reduced levels of $GABA_A$ receptor surface expression, which resulted from ER retention and accelerated proteosomal and lysosomal degradation of subunits following failure of the M3 domain to insert properly in the plasma membrane (Gallagher et al., 2004, 2005, 2007; Bradley et al., 2008). Another α1 subunit mutation, a single base-pair deletion predicted to produce a frameshift and a premature translation-termination codon, 975delC, S326fs328X, was recently identified as a *de novo* mutation in an individual with childhood absence epilepsy (CAE) (Maljevic et al., 2006). Little is known regarding the mechanisms by which this mutation causes disease, except that current was not detectable when the mutant subunit was co-expressed with β2 and γ2 subunits. Whether this was caused by impaired channel function or trafficking, however, remains unknown. Three β3 subunit mutations, β3(S15F), β3(P11S), and β3(G32R), were also reported recently in families with CAE (Tanaka et al., 2008). These mutations were found to decrease the amplitude of GABA-evoked currents, a finding likely attributable to altered channel trafficking since mutant subunits has altered glycosylation in the absence of altered total protein expression. In the δ subunit, two epilepsy susceptibility variants, E177A and R220H, were discovered in small GEFS+ families (Dibbens et al., 2004). When co-expressed

with α1 and β2 subunits, these variants reduced single channel mean open time and the levels of $GABA_A$ receptor surface expression, thus substantially decreasing whole cell current amplitudes (Feng et al., 2006).

Interestingly, more mutations have been identified in the γ2 subunit than in all other subunit subtypes combined. A family with generalized epilepsy with febrile seizures plus (GEFS+) was found to have a γ2 subunit mutation, K289M, located in the extracellular M2-M3 linker (Baulac et al., 2001), a region implicated in transduction of ligand binding to channel gating (Kash et al., 2003). Consistent with the known importance of this protein domain to channel function, recordings from HEK293T cells expressing α1β2γ2(K289M) receptors were found to have defective channel gating (shortened mean open times) and accelerated deactivation (Bianchi et al., 2002). A family with CAE and febrile seizures had a γ2 subunit mutation, R43Q, located in the N-terminal extracellular domain in the BDZ binding domain (Wallace et al., 2001). This mutation reduced peak current amplitudes without altering channel kinetics (Bianchi et al., 2002). The basis for the reduced current was reduced surface expression due to retention of the receptor in the ER (Kang and Macdonald, 2004; Sancar and Czajkowski, 2004), possibly due to disruption of inter-subunit contacts at the γ-β subunit interface (Hales et al., 2005). However, it has been reported that γ2(R43Q) subunits may assemble with α3 subunits (Frugier et al., 2007), suggesting the effects of the mutation may depend on the specific α subunit subtype involved. The γ2 subunit mutation, R139G, altered BDZ sensitivity and accelerated desensitization (Audenaert et al., 2006). A γ2 subunit mutation, Q351X, which introduced a PTC in the M3-M4 linker was identified in a family with GEFS+ (Harkin et al., 2002). Mutant receptors had no GABA sensitivity

when expressed in oocytes, probably due to ER retention. A γ2 subunit splice donor site mutation, IVS6+2T-G, was identified in a family with CAE and febrile seizures (Kananura et al., 2002). The effect of this mutation is unknown but was predicted to lead to nonfunctional receptors. A γ2 subunit, mutation Q1X, that introduced a PTC (Q1X) between the signal peptide and the mature peptide was identified in a family with severe myoclonic epilepsy of infancy (Hirose et al., 2004). The functional consequence of the mutation is unknown but may be haploinsufficiency, since the mutation would likely trigger nonsense mediated mRNA decay, thus preventing production of even a signal peptide.

Rationale for experimental chapters

One of the greatest challenges in science is extracting microscopic mechanisms from data sets containing primarily macroscopic observations. Indeed, while there are myriad experimental techniques for monitoring the functional properties of biological machinery, few techniques provide direct information regarding the behavior of individual molecules. Scientists are therefore forced to deduce how molecules behave (or, in the case of disease, how the behavior of molecules is altered) at the microscopic level by carefully constructing experiments at the macroscopic level. This typically involves perturbing the system with multiple experimental protocols, each designed to eliminate one or more possible explanations, and then using the combined results to constrain mechanistic hypotheses. Perhaps the best-known illustration of the potential power of this experimental approach is the popular childhood road-trip game "20 questions", which challenges one player to guess what object another has in mind simply

by asking a series of twenty "yes" or "no" questions. While this may initially seem difficult (if not impossible) given the seemingly countless named objects in the known universe, the binary nature of the questions allows for as many as 2^{20} different objects to be unambiguously identified, a number nearly double the total number of characters (including spaces) in this entire dissertation. However, what has challenged scientists, quite simply, is knowing what questions to ask. While even a child can list the defining features of dogs (e.g., four legs, tails, barking, etc.), and thus, can rule out dogs immediately when the answer to the question "does it have a shell?" is "yes", scientists are often unaware of the microscopic determinants of many macroscopic phenomena, or if they do know, do not enough about the system to meaningfully combine the macroscopic observations to discriminate among possible microscopic mechanisms.

Nowhere is this challenge more relevant than in the field of ion channel research, where despite the availability of a Nobel Prize-winning technique that allows the behavior of individual channels to be monitored (i.e., single-channel recording), the mechanistic bases for a variety of macroscopic phenomena remain unclear. For example, what determines the extent and time course of receptor current desensitization? Why does desensitization often appear "uncoupled" from deactivation (i.e., more desensitization in the context of accelerated deactivation, or vice versa)? What is the kinetic basis for repeated pulse inhibition? Worse yet, the literature is replete with conclusions regarding the microscopic effects of disease-causing mutations or potential therapeutic compounds based on isolated macroscopic observations, ignoring the work of many investigators that has illustrated the complex relationship between microscopic rate constants and certain macroscopic current properties. Colquhoun (1998), for example,

demonstrated that changes in EC_{50} (and, by extension, binding affinity) should never, under any circumstances, be used to draw conclusions regarding the microscopic affinity of the channel for an agonist or allosteric modulator, as changes in efficacy can shift EC_{50} just as easily as changes in affinity (and importantly, without any appreciable change in the apparent maximal open probability). Nevertheless, despite this cautionary note, changes in a variety of macroscopic properties are often attributed incorrectly to changes in individual rate constants. Altered rise time is often attributed to changes in the channel opening rate; altered desensitization is often attributed to changes in the stability of desensitized states; and altered deactivation is often attributed to changes in the unbinding rate.

However, one could argue that the hands of investigators are effectively tied; that while Colquhoun and others may have illustrated the difficulties faced in bridging the gap between macroscopic and microscopic channel properties, they have failed to provide investigators with the ability to unambiguously discriminate among microscopic mechanisms. For example, a valid experimental algorithm has yet to be proposed for discriminating changes in the entry or exit rates from desensitized states from changes in the rates connecting other non-conducting states (or even the channel opening rate). While tempting to suggest that investigators resort to single-channel analysis, it should be noted that this is much easier said than done, as patches rarely, if ever, include only a single channel, and even when they do, distinguishing changes in the entry and exit rates from desensitized states from changes in other rate constants requires assumption of a kinetic model (for a discussion, see Shelley and Magleby, 2008). Indeed, these rates cannot simply be extracted from exponential fitting of closed time distributions, as

decreased desensitized state stability can be caused either by a decreased entry rate into the desensitized state or an increased rate into another state (open or closed). Moreover, the very nature of desensitized states substantially decreases the practical utility of single-channel analysis, as they are by definition long-lived (dwell times can be 1000 ms or greater), meaning that there will not only be far fewer events available for analysis per recording, but also that their lifetimes will be underestimated by the presence of multiple channels in the patch.

The first goal of this dissertation was therefore to determine the kinetic basis for several $GABA_A$ receptor macroscopic current properties including the non-equilibrium phenomena of desensitization and deactivation. This was accomplished with two approaches. The first involved a combination of kinetic modeling using Markov models of $GABA_A$ receptor function and mathematical analysis of the differential equations governing the behavior of these models. The second involved comparing the predictions of these theoretical studies with electrophysiological data acquired from receptors that a) had different kinetic properties, b) were activated by different agonists or allosteric modulators, or c) were activated under different experimental conditions (e.g., short vs. long pulses of GABA, high vs. low GABA). Once the kinetic bases for these macroscopic phenomena were determined, an experimental algorithm for interpreting changes in macroscopic currents in terms of microscopic mechanisms was generated, the first of its kind. This algorithm was then applied to answer several long-standing questions in the field of $GABA_A$ receptor research. These included determining how desensitized states were arranged with respect to other states in the gating scheme; determining why receptor isoforms with access to long-lived non-conducting states failed

to exhibit macroscopic desensitization; determining the kinetic basis for the phenomenon of desensitization-deactivation uncoupling; determining the specific rate constant targeted by the most widely prescribed class of $GABA_A$ receptor modulator, the benzodiazepines; and determining the kinetic basis for the seemingly paradoxical effects of open channel block on macroscopic currents. In addition, the kinetic lessons learned from these studies allowed the comprehensive $GABA_A$ receptor gating scheme generated by Haas and Macdonald (1999) to be expanded, such that it accounted for several additional microscopic and macroscopic experimental observations.

Having identified the kinetic determinants of macroscopic desensitization and deactivation, the physiological relevance of these phenomena (and by extension, their kinetic determinants) was then explored. While deactivation is known to determine the decay of IPSCs, the relevance of desensitization to GABAergic synaptic transmission remains unclear. Indeed, some investigators have gone so far as to state that desensitization is more of an experimental nuisance than a physiologically interesting phenomenon, as agonist is not present *in vivo* at saturating concentrations for extended durations. Others have disagreed, arguing that desensitization is important not only for shaping the decay of individual IPSCs (Jones and Westbrook, 1995, 1996; Haas and Macdonald, 1999), but also for shaping the pattern of IPSCs during high-frequency stimulation (Overstreet et al., 2000; Bianchi and Macdonald, 2002). To explore this important issue further, a combination of theoretical modeling and electrophysiological recording studies were again performed. Taken together, the results suggested that desensitization was indeed likely to have physiological significance, as it was both necessary and sufficient for currents to undergo repeated pulse inhibition (defined as the

loss of current amplitude during high-frequency stimulation). In fact, desensitization was found to represent an important boundary condition for the time course of repeated pulse inhibition, and also for the time course of IPSC decay. The results also suggested that desensitization may have physiological relevance to peri- and extrasynaptic inhibitory neurotransmission, as the underlying desensitized states effectively "buffered" open state fractional occupancy, protecting it from fluctuations in the concentration of ambient GABA or negative modulators of $GABA_A$ receptor function. In other words, desensitized states appeared to offer stability to tonic currents at the expense of efficacy.

It should be noted that many of the aforementioned experiments could not have been performed without an ultra-fast drug application system, as resolving the fastest phases of desensitization required resolution of the true peak current amplitude, which is achieved by many receptor isoforms in the sub-millisecond time domain. However, investigating the physiological significance of desensitization required that the drug application system not only be capable of applying GABA to receptor-containing membrane preparations rapidly, but also that it be able to terminate the GABA pulse after synaptically relevant durations. Moreover, these experiments required that the drug application system be capable of delivering synaptically relevant pulses at extremely high frequencies, as many GABAergic neurons are known to reach extremely high firing rates for short periods of time. Unfortunately, the latter two criteria were not met by our existing drug application system, necessitating the development of a novel approach to solution switching. This was accomplished using PDMS microfluidics. This system, the first of its kind, allowed GABA to be applied rapidly (solution exchange times < 100 μs), briefly (total exposure times < 400 μs), and at high frequencies (up to 80 Hz).

GLOSSARY

Activation: the process by which a *macroscopic* current reaches its peak following application of an agonist; typically quantified as the 10-90% rise time, but can also be fit to a sum of exponentials; determined by a complex relationship between all rate constants in the gating scheme, and therefore, does not simply equal the microscopic rate constant of channel opening (β)

Affinity: the ratio of the microscopic binding rate (K_{on}) to the microscopic unbinding rate (K_{off}) (i.e., increasing affinity increases the fraction of receptors that are bound with GABA); commonly reported as the K_a, which is actually the inverse of affinity, such that high K_a means an agonist is relatively low affinity (and vice versa)

Deactivation: the return of a *macroscopic* current to baseline following agonist washout; typically quantified by fitting to a sum of exponentials and calculating a weighted time constant; correlates with the average time channels are bound with GABA (see Appendix II), which is influenced by every rate constant in the gating scheme except that of agonist binding; sometimes referred to as the "washout" current

Desensitization: the loss of *macroscopic* current in the continued presence of agonist; also referred to as "sag" or "decay"; typically quantified either by fitting to a sum of exponentials or by calculating the amount of current lost relative to peak (referred to as the extent of desensitization); note that the time course of macroscopic desensitization does not equal the microscopic entry rate into the desensitized state, and similarly, the extent of macroscopic desensitization does not equal the fractional occupancy of receptors in the microscopic desensitized state

Dwell Time: the average lifetime of a receptor in an individual state; equal to the reciprocal sum of the exit rates from that state

Efficacy: classically defined as the ratio of the microscopic channel opening rate (β) to the microscopic channel closing rate (α); however, often used inappropriately in the macroscopic sense to describe the peak open probability; typical indices include mean open duration, burst duration, and open time per burst

Fractional Occupancy: the fraction of all receptors in a given state; mathematically the same as the probability that an individual receptor occupies a given state at any moment in time (see Appendix I)

Gating: generic term that describes the microscopic process of receptor transition among ligand-bound states

Macroscopic: involving many receptors; the "population" or "ensemble" response

Microscopic: involving a single receptor; note that while macroscopic currents can reach equilibrium, microscopic or "single channel" currents are never at equilibrium

Rate: a term used to describe the time course of a macroscopic current property

Rate Constant: a microscopic term used to describe the probability per unit time that a receptor transitions from one state to another

Stability: the ratio of the entry rate to the exit rate of a given state; the same as efficacy for open states

REFERENCES

Agosto, J., Choi, J. C., Parisky, K. M., Stilwell, G., Rosbash, M., & Griffith, L. C. (2008). Modulation of GABAA receptor desensitization uncouples sleep onset and maintenance in Drosophila. *Nat.Neurosci.* **11**, 354-359.

Akabas, M. H., Kaufmann, C., Archdeacon, P., & Karlin, A. (1994). Identification of acetylcholine receptor channel-lining residues in the entire M2 segment of the alpha subunit. *Neuron* **13**, 919-927.

Akabas, M. H. (2004). GABAA receptor structure-function studies: a reexamination in light of new acetylcholine receptor structures. *Int.Rev.Neurobiol.* **62**, 1-43.

Akbarian, S. & Huang, H. S. (2006). Molecular and cellular mechanisms of altered GAD1/GAD67 expression in schizophrenia and related disorders. *Brain Res.Rev.* **52**, 293-304.

Akk, G., Li, P., Bracamontes, J., Reichert, D. E., Covey, D. F., & Steinbach, J. H. (2008). Mutations of the GABA-A receptor alpha1 subunit M1 domain reveal unexpected complexity for modulation by neuroactive steroids. *Mol.Pharmacol.* **74**, 614-627.

Andang, M., Hjerling-Leffler, J., Moliner, A., Lundgren, T. K., Castelo-Branco, G., Nanou, E., Pozas, E., Bryja, V., Halliez, S., Nishimaru, H., Wilbertz, J., Arenas, E., Koltzenburg, M., Charnay, P., El Manira, A., Ibanez, C. F., & Ernfors, P. (2008). Histone H2AX-dependent GABA(A) receptor regulation of stem cell proliferation. *Nature* **451**, 460-464.

Angelotti, T. P. & Macdonald, R. L. (1993). Assembly of GABAA receptor subunits: alpha 1 beta 1 and alpha 1 beta 1 gamma 2S subunits produce unique ion channels with dissimilar single-channel properties. *J.Neurosci.* **13**, 1429-1440.

Attwell, D., Barbour, B., & Szatkowski, M. (1993). Nonvesicular release of neurotransmitter. *Neuron* **11**, 401-407.

Audenaert, D., Schwartz, E., Claeys, K. G., Claes, L., Deprez, L., Suls, A., Van Dyck, T., Lagae, L., Van Broeckhoven, C., Macdonald, R. L., & De Jonghe, P. (2006). A novel GABRG2 mutation associated with febrile seizures. *Neurology* **67**, 687-690.

Awapara, J., Landua, A. J., Fuerst, R., & Seale, B. (1950). Free gamma-aminobutyric acid in brain. *J.Biol.Chem.* **187**, 35-39.

Bach-y-Rita, P. (2001). Nonsynaptic diffusion neurotransmission in the brain: functional considerations. *Neurochem.Res.* **26**, 871-873.

Backus, K. H., Arigoni, M., Drescher, U., Scheurer, L., Malherbe, P., Mohler, H., & Benson, J. A. (1993). Stoichiometry of a recombinant GABAA receptor deduced from mutation-induced rectification. *Neuroreport* **5**, 285-288.

Bailey, M. E., Matthews, D. A., Riley, B. P., Albrecht, B. E., Kostrzewa, M., Hicks, A. A., Harris, R., Muller, U., Darlison, M. G., & Johnson, K. J. (1999a). Genomic mapping and evolution of human GABA(A) receptor subunit gene clusters. *Mamm.Genome* **10**, 839-843.

Bailey, M. E., Albrecht, B. E., Johnson, K. J., & Darlison, M. G. (1999b). Genetic linkage and radiation hybrid mapping of the three human GABA(C) receptor rho subunit genes: GABRR1, GABRR2 and GABRR3. *Biochim.Biophys.Acta* **1447**, 307-312.

Balasubramanian, S., Teissere, J. A., Raju, D. V., & Hall, R. A. (2004). Hetero-oligomerization between GABAA and GABAB receptors regulates GABAB receptor trafficking. *J.Biol.Chem.* **279**, 18840-18850.

Barberis, A., Mozrzymas, J. W., Ortinski, P. I., & Vicini, S. (2007). Desensitization and binding properties determine distinct alpha1beta2gamma2 and alpha3beta2gamma2 GABA(A) receptor-channel kinetic behavior. *Eur.J.Neurosci.* **25**, 2726-2740.

Barnard, E. A., Skolnick, P., Olsen, R. W., Mohler, H., Sieghart, W., Biggio, G., Braestrup, C., Bateson, A. N., & Langer, S. Z. (1998). International Union of Pharmacology. XV. Subtypes of gamma-aminobutyric acidA receptors: classification on the basis of subunit structure and receptor function. *Pharmacol.Rev.* **50**, 291-313.

Barrera, N. P., Ge, H., Henderson, R. M., Fitzgerald, W. J., & Edwardson, J. M. (2008). Automated analysis of the architecture of receptors, imaged by atomic force microscopy. *Micron.* **39**, 101-110.

Barrera, N. P., Henderson, R. M., & Edwardson, J. M. (2008). Determination of the architecture of ionotropic receptors using AFM imaging. *Pflugers Arch.* **456**, 199-209.

Barrera, N. P., Betts, J., You, H., Henderson, R. M., Martin, I. L., Dunn, S. M., & Edwardson, J. M. (2008). Atomic force microscopy reveals the stoichiometry and subunit arrangement of the alpha4beta3delta GABA(A) receptor. *Mol.Pharmacol.* **73**, 960-967.

Battaglioli, G., Liu, H., & Martin, D. L. (2003). Kinetic differences between the isoforms of glutamate decarboxylase: implications for the regulation of GABA synthesis. *J.Neurochem.* **86**, 879-887.

Baulac, S., Huberfeld, G., Gourfinkel-An, I., Mitropoulou, G., Beranger, A., Prud'homme, J. F., Baulac, M., Brice, A., Bruzzone, R., & LeGuern, E. (2001). First genetic evidence of GABA(A) receptor dysfunction in epilepsy: a mutation in the gamma2-subunit gene. *Nat.Genet.* **28**, 46-48.

Baumann, S. W., Baur, R., & Sigel, E. (2001). Subunit arrangement of gamma-aminobutyric acid type A receptors. *J.Biol.Chem.* **276**, 36275-36280.

Baumann, S. W., Baur, R., & Sigel, E. (2002). Forced subunit assembly in alpha1beta2gamma2 GABAA receptors. Insight into the absolute arrangement. *J.Biol.Chem.* **277**, 46020-46025.

Baur, R., Minier, F., & Sigel, E. (2006). A GABA(A) receptor of defined subunit composition and positioning: concatenation of five subunits. *FEBS Lett.* **580**, 1616-1620.

Beck, M., Brickley, K., Wilkinson, H. L., Sharma, S., Smith, M., Chazot, P. L., Pollard, S., & Stephenson, F. A. (2002). Identification, molecular cloning, and characterization of a novel GABAA receptor-associated protein, GRIF-1. *J.Biol.Chem.* **277**, 30079-30090.

Bedford, F. K., Kittler, J. T., Muller, E., Thomas, P., Uren, J. M., Merlo, D., Wisden, W., Triller, A., Smart, T. G., & Moss, S. J. (2001). GABA(A) receptor cell surface number and subunit stability are regulated by the ubiquitin-like protein Plic-1. *Nat.Neurosci.* **4**, 908-916.

Bell, M. V., Bloomfield, J., McKinley, M., Patterson, M. N., Darlison, M. G., Barnard, E. A., & Davies, K. E. (1989). Physical linkage of a GABAA receptor subunit gene to the DXS374 locus in human Xq28. *Am.J.Hum.Genet.* **45**, 883-888.

Ben-Ari, Y. (2002). Excitatory actions of gaba during development: the nature of the nurture. *Nat.Rev.Neurosci.* **3**, 728-739.

Benke, D., Honer, M., Michel, C., & Mohler, H. (1996). GABAA receptor subtypes differentiated by their gamma-subunit variants: prevalence, pharmacology and subunit architecture. *Neuropharmacology* **35**, 1413-1423.

Bianchi, M. T. & Macdonald, R. L. (2001). Mutation of the 9' leucine in the GABA(A) receptor gamma2L subunit produces an apparent decrease in desensitization by stabilizing open states without altering desensitized states. *Neuropharmacology* **41**, 737-744.

Bianchi, M. T. & Macdonald, R. L. (2001). Agonist Trapping by GABAA Receptor Channels. *J.Neurosci.* **21**, 9083-9091.

Bianchi, M. T., Haas, K. F., & Macdonald, R. L. (2001). Structural determinants of fast desensitization and desensitization-deactivation coupling in GABAa receptors. *J.Neurosci.* **21**, 1127-1136.

Bianchi, M. T. & Macdonald, R. L. (2002). Slow phases of GABA(A) receptor desensitization: structural determinants and possible relevance for synaptic function. *J.Physiol* **544**, 3-18.

Bianchi, M. T., Haas, K. F., & Macdonald, R. L. (2002). Alpha1 and alpha6 subunits specify distinct desensitization, deactivation and neurosteroid modulation of GABA(A) receptors containing the delta subunit. *Neuropharmacology* **43**, 492-502.

Bianchi, M. T., Song, L., Zhang, H., & Macdonald, R. L. (2002). Two different mechanisms of disinhibition produced by GABAA receptor mutations linked to epilepsy in humans. *J.Neurosci.* **22**, 5321-5327.

Bianchi, M. T., Botzolakis, E. J., Haas, K. F., Fisher, J. L., & Macdonald, R. L. (2007). Microscopic kinetic determinants of macroscopic currents: insights from coupling and uncoupling of GABAA receptor desensitization and deactivation. *J.Physiol* **584**, 769-787.

Bianchi, M.T., Botzolakis, E.J., Lagrange, A.H., and Macdonald, R.L. (2009) Benzodiazepine modulation of GABA(A) receptor opening frequency depends on activation context: a patch clamp and simulation study. Epilepsy Research **85**, 212-220.

Bloom, F. E. & Iversen, L. L. (1971). Localizing 3H-GABA in nerve terminals of rat cerebral cortex by electron microscopic autoradiography. *Nature* **229**, 628-630.

Bollan, K., Robertson, L. A., Tang, H., & Connolly, C. N. (2003). Multiple assembly signals in gamma-aminobutyric acid (type A) receptor subunits combine to drive receptor construction and composition. *Biochem.Soc.Trans.* **31**, 875-879.

Bollan, K. A., Baur, R., Hales, T. G., Sigel, E., & Connolly, C. N. (2008). The promiscuous role of the epsilon subunit in GABAA receptor biogenesis. *Mol.Cell Neurosci.* **37**, 610-621.

Bonnert, T. P., McKernan, R. M., Farrar, S., le Bourdelles, B., Heavens, R. P., Smith, D. W., Hewson, L., Rigby, M. R., Sirinathsinghji, D. J., Brown, N., Wafford, K. A., & Whiting, P. J. (1999). theta, a novel gamma-aminobutyric acid type A receptor subunit. *Proc.Natl.Acad.Sci.U.S.A* **96**, 9891-9896.

Bormann, J., Hamill, O. P., & Sakmann, B. (1987). Mechanism of anion permeation through channels gated by glycine and gamma-aminobutyric acid in mouse cultured spinal neurones. *J.Physiol* **385**, 243-286.

Bormann, J. (2000). The 'ABC' of GABA receptors. *Trends Pharmacol.Sci.* **21**, 16-19.

Botzolakis, E. J., Maheshwari, A., Feng, H. J., Lagrange, A. H., Shaver, J. F., Kassebaum, N. J., Venkataraman, R., Baudenbacher, F. J., & Macdonald, R. L. (2008). Achieving synaptically relevant pulses of neurotransmitter using PDMS microfluidics. *J.Neurosci.Methods* **177**, 294-302..

Boue-Grabot, E., Roudbaraki, M., Bascles, L., Tramu, G., Bloch, B., & Garret, M. (1998). Expression of GABA receptor rho subunits in rat brain. *J.Neurochem.* **70**, 899-907.

Boue-Grabot, E., Toulme, E., Emerit, M. B., & Garret, M. (2004). Subunit-specific coupling between gamma-aminobutyric acid type A and P2X2 receptor channels. *J.Biol.Chem.* **279**, 52517-52525.

Bowery, N. G., Hill, D. R., Hudson, A. L., Doble, A., Middlemiss, D. N., Shaw, J., & Turnbull, M. (1980). (-)Baclofen decreases neurotransmitter release in the mammalian CNS by an action at a novel GABA receptor. *Nature* **283**, 92-94.

Bowery, N. G., Hudson, A. L., & Price, G. W. (1987). GABAA and GABAB receptor site distribution in the rat central nervous system. *Neuroscience* **20**, 365-383.

Bowery, N. G., Bettler, B., Froestl, W., Gallagher, J. P., Marshall, F., Raiteri, M., Bonner, T. I., & Enna, S. J. (2002). International Union of Pharmacology. XXXIII. Mammalian gamma-aminobutyric acid(B) receptors: structure and function. *Pharmacol.Rev.* **54**, 247-264.

Bradley, C. A., Taghibiglou, C., Collingridge, G. L., & Wang, Y. T. (2008). Mechanisms involved in the reduction of GABAA receptor alpha1-subunit expression caused by the epilepsy mutation A322D in the trafficking-competent receptor. *J.Biol.Chem.* **283**, 22043-22050.

Brandon, N., Jovanovic, J., & Moss, S. (2002). Multiple roles of protein kinases in the modulation of gamma-aminobutyric acid(A) receptor function and cell surface expression. *Pharmacol.Ther.* **94**, 113-122.

Brejc, K., van Dijk, W. J., Klaassen, R. V., Schuurmans, M., van Der, O. J., Smit, A. B., & Sixma, T. K. (2001). Crystal structure of an ACh-binding protein reveals the ligand-binding domain of nicotinic receptors. *Nature* **411**, 269-276.

Brickley, K., Smith, M. J., Beck, M., & Stephenson, F. A. (2005). GRIF-1 and OIP106, members of a novel gene family of coiled-coil domain proteins: association in vivo and in vitro with kinesin. *J.Biol.Chem.* **280**, 14723-14732.

Brickley, S. G., Cull-Candy, S. G., & Farrant, M. (1996). Development of a tonic form of synaptic inhibition in rat cerebellar granule cells resulting from persistent activation of GABAA receptors. *J.Physiol* **497 (Pt 3)**, 753-759.

Brickley, S. G., Revilla, V., Cull-Candy, S. G., Wisden, W., & Farrant, M. (2001). Adaptive regulation of neuronal excitability by a voltage-independent potassium conductance. *Nature* **409**, 88-92.

Brooks-Kayal, A. R., Shumate, M. D., Jin, H., Rikhter, T. Y., Kelly, M. E., & Coulter, D. A. (2001). gamma-Aminobutyric acid(A) receptor subunit expression predicts

functional changes in hippocampal dentate granule cells during postnatal development. *J.Neurochem.* **77**, 1266-1278.

Buckle, V. J., Fujita, N., Ryder-Cook, A. S., Derry, J. M., Barnard, P. J., Lebo, R. V., Schofield, P. R., Seeburg, P. H., Bateson, A. N., Darlison, M. G., & . (1989). Chromosomal localization of GABAA receptor subunit genes: relationship to human genetic disease. *Neuron* **3**, 647-654.

Burgard, E. C., Tietz, E. I., Neelands, T. R., & Macdonald, R. L. (1996). Properties of recombinant gamma-aminobutyric acid A receptor isoforms containing the alpha 5 subunit subtype. *Mol.Pharmacol.* **50**, 119-127.

Burkat, P. M., Yang, J., & Gingrich, K. J. (2001). Dominant gating governing transient GABA(A) receptor activity: a first latency and Po/o analysis. *J.Neurosci.* **21**, 7026-7036.

Burzomato, V., Beato, M., Groot-Kormelink, P. J., Colquhoun, D., & Sivilotti, L. G. (2004). Single-channel behavior of heteromeric alpha1beta glycine receptors: an attempt to detect a conformational change before the channel opens. *J.Neurosci.* **24**, 10924-10940.

Campagna-Slater, V. & Weaver, D. F. (2007). Molecular modelling of the GABAA ion channel protein. *J.Mol.Graph.Model.* **25**, 721-730.

Caraiscos, V. B., Elliott, E. M., You, T., Cheng, V. Y., Belelli, D., Newell, J. G., Jackson, M. F., Lambert, J. J., Rosahl, T. W., Wafford, K. A., MacDonald, J. F., & Orser, B. A. (2004). Tonic inhibition in mouse hippocampal CA1 pyramidal neurons is mediated by alpha5 subunit-containing gamma-aminobutyric acid type A receptors. *Proc.Natl.Acad.Sci.U.S.A* **101**, 3662-3667.

Celentano, J. J. & Wong, R. K. (1994). Multiphasic desensitization of the GABAA receptor in outside-out patches. *Biophys.J.* **66**, 1039-1050.

Chakrapani, S., Bailey, T. D., & Auerbach, A. (2004). Gating dynamics of the acetylcholine receptor extracellular domain. *J.Gen.Physiol* **123**, 341-356.

Chang, Y., Wang, R., Barot, S., & Weiss, D. S. (1996). Stoichiometry of a recombinant GABAA receptor. *J.Neurosci.* **16**, 5415-5424.

Chang, Y. & Weiss, D. S. (1998). Substitutions of the highly conserved M2 leucine create spontaneously opening rho1 gamma-aminobutyric acid receptors. *Mol.Pharmacol.* **53**, 511-523.

Charych, E. I., Yu, W., Miralles, C. P., Serwanski, D. R., Li, X., Rubio, M., & De Blas, A. L. (2004). The brefeldin A-inhibited GDP/GTP exchange factor 2, a protein involved in vesicular trafficking, interacts with the beta subunits of the GABA receptors. *J.Neurochem.* **90**, 173-189.

Chaudhry, F. A., Reimer, R. J., Bellocchio, E. E., Danbolt, N. C., Osen, K. K., Edwards, R. H., & Storm-Mathisen, J. (1998). The vesicular GABA transporter, VGAT, localizes to synaptic vesicles in sets of glycinergic as well as GABAergic neurons. *J.Neurosci.* **18**, 9733-9750.

Chavas, J., Forero, M.E., Collin, T., Llano, I., Marty, A. (2004). Osmotic tension as a possible link between GABA(A) receptor activation and intracellular calcium elevation. Neuron **44**, 701-713.

Chen, L., Wang, H., Vicini, S., & Olsen, R. W. (2000). The gamma-aminobutyric acid type A (GABAA) receptor-associated protein (GABARAP) promotes GABAA receptor clustering and modulates the channel kinetics. *Proc.Natl.Acad.Sci.U.S.A* **97**, 11557-11562.

Chen, Z. W. & Olsen, R. W. (2007). GABAA receptor associated proteins: a key factor regulating GABAA receptor function. *J.Neurochem.* **100**, 279-294.

Chu, D. C., Albin, R. L., Young, A. B., & Penney, J. B. (1990). Distribution and kinetics of GABAB binding sites in rat central nervous system: a quantitative autoradiographic study. *Neuroscience* **34**, 341-357.

Clements, J. D. (1996). Transmitter timecourse in the synaptic cleft: its role in central synaptic function. *Trends Neurosci.* **19**, 163-171.

Collingridge, G. L., Olsen, R. W., Peters, J., & Spedding, M. (2008). A nomenclature for ligand-gated ion channels. *Neuropharmacology*.

Colquhoun, D. (1998). Binding, gating, affinity and efficacy: the interpretation of structure-activity relationships for agonists and of the effects of mutating receptors. *Br.J.Pharmacol.* **125**, 924-947.

Connolly, C. N., Krishek, B. J., McDonald, B. J., Smart, T. G., & Moss, S. J. (1996). Assembly and cell surface expression of heteromeric and homomeric gamma-aminobutyric acid type A receptors. *J.Biol.Chem.* **271**, 89-96.

Connolly, C. N., Kittler, J. T., Thomas, P., Uren, J. M., Brandon, N. J., Smart, T. G., & Moss, S. J. (1999). Cell surface stability of gamma-aminobutyric acid type A receptors. Dependence on protein kinase C activity and subunit composition. *J.Biol.Chem.* **274**, 36565-36572.

Cossette, P., Liu, L., Brisebois, K., Dong, H., Lortie, A., Vanasse, M., Saint-Hilaire, J. M., Carmant, L., Verner, A., Lu, W. Y., Wang, Y. T., & Rouleau, G. A. (2002). Mutation of GABRA1 in an autosomal dominant form of juvenile myoclonic epilepsy. *Nat.Genet.* **31**, 184-189.

Cromer, B. A., Morton, C. J., & Parker, M. W. (2002). Anxiety over GABA(A) receptor structure relieved by AChBP. *Trends Biochem.Sci.* **27**, 280-287.

Cryan, J. F. & Kaupmann, K. (2005). Don't worry 'B' happy!: a role for GABA(B) receptors in anxiety and depression. *Trends Pharmacol.Sci.* **26**, 36-43.

Curtis, D. R. & Crawford, J. M. (1969). Central synaptic transmission--microelectrophoretic studies. *Annu.Rev.Pharmacol.* **9**, 209-240.

Cutting, G. R., Curristin, S., Zoghbi, H., O'Hara, B., Seldin, M. F., & Uhl, G. R. (1992). Identification of a putative gamma-aminobutyric acid (GABA) receptor subunit rho2 cDNA and colocalization of the genes encoding rho2 (GABRR2) and rho1 (GABRR1) to human chromosome 6q14-q21 and mouse chromosome 4. *Genomics* **12**, 801-806.

Dale, A. S. (1935). The relation between metabolic processes and the ventricular electrogram. *J.Physiol* **84**, 433-453.

Dallwig, R., Deitmer, J.W., Backus, K.H. (1999). On the mechanism of GABA-induced currents in cultured rat cortical neurons. Pflugers Arch. **437**, 289-297.

Darlison, M. G., Pahal, I., & Thode, C. (2005). Consequences of the evolution of the GABA(A) receptor gene family. *Cell Mol.Neurobiol.* **25**, 607-624.

Davies, P. A., Kirkness, E. F., & Hales, T. G. (1997). Modulation by general anaesthetics of rat GABAA receptors comprised of alpha 1 beta 3 and beta 3 subunits expressed in human embryonic kidney 293 cells. *Br.J.Pharmacol.* **120**, 899-909.

Davies, P. A., Hanna, M. C., Hales, T. G., & Kirkness, E. F. (1997). Insensitivity to anaesthetic agents conferred by a class of GABA(A) receptor subunit. *Nature* **385**, 820-823.

Davies, P. A., Kirkness, E. F., & Hales, T. G. (2001). Evidence for the formation of functionally distinct alphabetagammaepsilon GABA(A) receptors. *J.Physiol* **537**, 101-113.

Davies, P. A., Wang, W., Hales, T. G., & Kirkness, E. F. (2003). A novel class of ligand-gated ion channel is activated by Zn2+. *J.Biol.Chem.* **278**, 712-717.

De Deyn, P. P. & Macdonald, R. L. (1990). Guanidino compounds that are increased in cerebrospinal fluid and brain of uremic patients inhibit GABA and glycine responses on mouse neurons in cell culture. *Ann.Neurol.* **28**, 627-633.

Defazio, T. & Hablitz, J. J. (1998). Zinc and zolpidem modulate mIPSCs in rat neocortical pyramidal neurons. *J.Neurophysiol.* **80**, 1670-1677.

Dellisanti, C. D., Yao, Y., Stroud, J. C., Wang, Z. Z., & Chen, L. (2007). Crystal structure of the extracellular domain of nAChR alpha1 bound to alpha-bungarotoxin at 1.94 A resolution. *Nat.Neurosci.* **10**, 953-962.

Dibbens, L. M., Feng, H. J., Richards, M. C., Harkin, L. A., Hodgson, B. L., Scott, D., Jenkins, M., Petrou, S., Sutherland, G. R., Scheffer, I. E., Berkovic, S. F., Macdonald, R. L., & Mulley, J. C. (2004). GABRD encoding a protein for extra- or peri-synaptic GABAA receptors is a susceptibility locus for generalized epilepsies. *Hum.Mol.Genet.* **13**, 1315-1319.

Duggan, M. J., Pollard, S., & Stephenson, F. A. (1991). Immunoaffinity purification of GABAA receptor alpha-subunit iso-oligomers. Demonstration of receptor populations containing alpha 1 alpha 2, alpha 1 alpha 3, and alpha 2 alpha 3 subunit pairs. *J.Biol.Chem.* **266**, 24778-24784.

Edwards, F. A., Konnerth, A., & Sakmann, B. (1990). Quantal analysis of inhibitory synaptic transmission in the dentate gyrus of rat hippocampal slices: a patch-clamp study. *J.Physiol* **430**, 213-249.

Eisele, J. L., Bertrand, S., Galzi, J. L., Devillers-Thiery, A., Changeux, J. P., & Bertrand, D. (1993). Chimaeric nicotinic-serotonergic receptor combines distinct ligand binding and channel specificities. *Nature* **366**, 479-483.

Ekema, G. M., Zheng, W., & Lu, L. (2002). Interaction of GABA receptor/channel rho(1) and gamma(2) subunit. *Invest Ophthalmol.Vis.Sci.* **43**, 2326-2333.

Ellgaard, L. & Frickel, E. M. (2003). Calnexin, calreticulin, and ERp57: teammates in glycoprotein folding. *Cell Biochem.Biophys.* **39**, 223-247.

Engblom, A. C., Carlson, B. X., Olsen, R. W., Schousboe, A., & Kristiansen, U. (2002). Point mutation in the first transmembrane region of the beta 2 subunit of the gamma--aminobutyric acid type A receptor alters desensitization kinetics of gamma--aminobutyric acid- and anesthetic-induced channel gating. *J.Biol.Chem.* **277**, 17438-17447.

Enna, S. J. & McCarson, K. E. (2006). The role of GABA in the mediation and perception of pain. *Adv.Pharmacol.* **54**, 1-27.

Enoch, M. A. (2008). The role of GABA(A) receptors in the development of alcoholism. *Pharmacol.Biochem.Behav.* **90**, 95-104.

Enz, R., Brandstatter, J. H., Wassle, H., & Bormann, J. (1996). Immunocytochemical localization of the GABAc receptor rho subunits in the mammalian retina. *J.Neurosci.* **16**, 4479-4490.

Enz, R. & Cutting, G. R. (1998). Molecular composition of GABAC receptors. *Vision Res.* **38**, 1431-1441.

Enz, R. & Cutting, G. R. (1999). Identification of 70 amino acids important for GABA(C) receptor rho1 subunit assembly. *Brain Res.* **846**, 177-185.

Erlander, M. G., Tillakaratne, N. J., Feldblum, S., Patel, N., & Tobin, A. J. (1991). Two genes encode distinct glutamate decarboxylases. *Neuron* **7**, 91-100.

Ernst, M., Brauchart, D., Boresch, S., & Sieghart, W. (2003). Comparative modeling of GABA(A) receptors: limits, insights, future developments. *Neuroscience* **119**, 933-943.

Esclapez, M., Tillakaratne, N. J., Kaufman, D. L., Tobin, A. J., & Houser, C. R. (1994). Comparative localization of two forms of glutamic acid decarboxylase and their mRNAs in rat brain supports the concept of functional differences between the forms. *J.Neurosci.* **14**, 1834-1855.

Essrich, C., Lorez, M., Benson, J. A., Fritschy, J. M., & Luscher, B. (1998). Postsynaptic clustering of major GABAA receptor subtypes requires the gamma 2 subunit and gephyrin. *Nat.Neurosci.* **1**, 563-571.

Eugene, E., Depienne, C., Baulac, S., Baulac, M., Fritschy, J. M., Le Guern, E., Miles, R., & Poncer, J. C. (2007). GABA(A) receptor gamma 2 subunit mutations linked to human epileptic syndromes differentially affect phasic and tonic inhibition. *J.Neurosci.* **27**, 14108-14116.

Exley, R., Moroni, M., Sasdelli, F., Houlihan, L. M., Lukas, R. J., Sher, E., Zwart, R., & Bermudez, I. (2006). Chaperone protein 14-3-3 and protein kinase A increase the relative abundance of low agonist sensitivity human alpha 4 beta 2 nicotinic acetylcholine receptors in Xenopus oocytes. *J.Neurochem.* **98**, 876-885.

Farrant, M. & Nusser, Z. (2005). Variations on an inhibitory theme: phasic and tonic activation of GABA(A) receptors. *Nat.Rev.Neurosci.* **6**, 215-229.

Farrar, S. J., Whiting, P. J., Bonnert, T. P., & McKernan, R. M. (1999). Stoichiometry of a ligand-gated ion channel determined by fluorescence energy transfer. *J.Biol.Chem.* **274**, 10100-10104.

Fatima-Shad, K. & Barry, P. H. (1993). Anion permeation in. *Proc.Biol.Sci.* **253**, 69-75.

Feng, H. J. & Macdonald, R. L. (2004). Multiple actions of propofol on alphabetagamma and alphabetadelta GABAA receptors. *Mol.Pharmacol.* **66**, 1517-1524.

Feng, H. J., Bianchi, M. T., & Macdonald, R. L. (2004). Pentobarbital differentially modulates alpha1beta3delta and alpha1beta3gamma2L GABAA receptor currents. *Mol.Pharmacol.* **66**, 988-1003.

Feng, H. J., Kang, J. Q., Song, L., Dibbens, L., Mulley, J., & Macdonald, R. L. (2006). Delta subunit susceptibility variants E177A and R220H associated with complex epilepsy alter channel gating and surface expression of alpha4beta2delta GABAA receptors. *J.Neurosci.* **26**, 1499-1506.

Feng, H. J., Mathews, G. C., Kao, C., & Macdonald, R. L. (2008). Alterations of GABA A-receptor function and allosteric modulation during development of status epilepticus. *J.Neurophysiol.* **99**, 1285-1293.

Feng, H.J., Botzolakis, E.J., and Macdonald, R.L. (2009). Context-dependent modulation of alphabetagamma and alphabetadelta GABA-A receptors by penicillin: implications for phasic and tonic inhibition. Neuropharmacology **56**, 161-173.

Filippova, N., Wotring, V. E., & Weiss, D. S. (2004). Evidence that the TM1-TM2 loop contributes to the rho1 GABA receptor pore. *J.Biol.Chem.* **279**, 20906-20914.

Fisher, J. L. & Macdonald, R. L. (1997). Single channel properties of recombinant GABAA receptors containing gamma 2 or delta subtypes expressed with alpha 1 and beta 3 subtypes in mouse L929 cells. *J.Physiol* **505 (Pt 2)**, 283-297.

Fisher, J. L., Zhang, J., & Macdonald, R. L. (1997). The role of alpha1 and alpha6 subtype amino-terminal domains in allosteric regulation of gamma-aminobutyric acida receptors. *Mol.Pharmacol.* **52**, 714-724.

Fisher, J. L. & Macdonald, R. L. (1997). Functional properties of recombinant GABA(A) receptors composed of single or multiple beta subunit subtypes. *Neuropharmacology* **36**, 1601-1610.

Frerking, M., Borges, S., & Wilson, M. (1995). Variation in GABA mini amplitude is the consequence of variation in transmitter concentration. *Neuron* **15**, 885-895.

Fritschy, J. M., Benke, D., Mertens, S., Oertel, W. H., Bachi, T., & Mohler, H. (1992). Five subtypes of type A gamma-aminobutyric acid receptors identified in neurons by double and triple immunofluorescence staining with subunit-specific antibodies. *Proc.Natl.Acad.Sci.U.S.A* **89**, 6726-6730.

Fritschy, J. M., Paysan, J., Enna, A., & Mohler, H. (1994). Switch in the expression of rat GABAA-receptor subtypes during postnatal development: an immunohistochemical study. *J.Neurosci.* **14**, 5302-5324.

Fritschy, J. M. & Mohler, H. (1995). GABAA-receptor heterogeneity in the adult rat brain: differential regional and cellular distribution of seven major subunits. *J.Comp Neurol.* **359**, 154-194.

Frugier, G., Coussen, F., Giraud, M. F., Odessa, M. F., Emerit, M. B., Boue-Grabot, E., & Garret, M. (2007). A gamma 2(R43Q) mutation, linked to epilepsy in humans, alters GABAA receptor assembly and modifies subunit composition on the cell surface. *J.Biol.Chem.* **282**, 3819-3828.

Gallagher, M. J., Song, L., Arain, F., & Macdonald, R. L. (2004). The juvenile myoclonic epilepsy GABA(A) receptor alpha1 subunit mutation A322D produces asymmetrical, subunit position-dependent reduction of heterozygous receptor currents and alpha1 subunit protein expression. *J.Neurosci.* **24**, 5570-5578.

Gallagher, M. J., Shen, W., Song, L., & Macdonald, R. L. (2005). Endoplasmic reticulum retention and associated degradation of a GABAA receptor epilepsy mutation that inserts an aspartate in the M3 transmembrane segment of the alpha1 subunit. *J.Biol.Chem.* **280**, 37995-38004.

Gallagher, M. J., Ding, L., Maheshwari, A., & Macdonald, R. L. (2007). The GABAA receptor alpha1 subunit epilepsy mutation A322D inhibits transmembrane helix formation and causes proteasomal degradation. *Proc.Natl.Acad.Sci.U.S.A* **104**, 12999-13004.

Galzi, J. L. and Changeux J. P. (1995). Neuronal nicotinic receptors: Molecular organization and regulations. *Neuropharmacology* **34**, 563-582.

Gething, M. J. (1999). Role and regulation of the ER chaperone BiP. *Semin.Cell Dev.Biol.* **10**, 465-472.

Gillespie, C. F., Mintz, E. M., Marvel, C. L., Huhman, K. L., & Albers, H. E. (1997). GABA(A) and GABA(B) agonists and antagonists alter the phase-shifting effects of light when microinjected into the suprachiasmatic region. *Brain Res.* **759**, 181-189.

Giraudat, J., Dennis, M., Heidmann, T., Chang, J. Y., & Changeux, J. P. (1986). Structure of the high-affinity binding site for noncompetitive blockers of the acetylcholine receptor: serine-262 of the delta subunit is labeled by [3H]chlorpromazine. *Proc.Natl.Acad.Sci.U.S.A* **83**, 2719-2723.

Glatt, K., Glatt, H., & Lalande, M. (1997). Structure and organization of GABRB3 and GABRA5. *Genomics* **41**, 63-69.

Glavinovic, M. I. (1999). Monte carlo simulation of vesicular release, spatiotemporal distribution of glutamate in synaptic cleft and generation of postsynaptic currents. *Pflugers Arch.* **437**, 462-470.

Glykys, J., Peng, Z., Chandra, D., Homanics, G. E., Houser, C. R., & Mody, I. (2007). A new naturally occurring GABA(A) receptor subunit partnership with high sensitivity to ethanol. *Nat.Neurosci.* **10**, 40-48.

Glykys, J., Mann, E. O., & Mody, I. (2008). Which GABA(A) receptor subunits are necessary for tonic inhibition in the hippocampus? *J.Neurosci.* **28**, 1421-1426.

Gonzales, E. B., Bell-Horner, C. L., Dibas, M. I., Huang, R. Q., & Dillon, G. H. (2008). Stoichiometric analysis of the TM2 6' phenylalanine mutation on desensitization in alpha1beta2 and alpha1beta2gamma2 GABA A receptors. *Neurosci.Lett.* **431**, 184-189.

Gorrie, G. H., Vallis, Y., Stephenson, A., Whitfield, J., Browning, B., Smart, T. G., & Moss, S. J. (1997). Assembly of GABAA receptors composed of alpha1 and beta2 subunits in both cultured neurons and fibroblasts. *J.Neurosci.* **17**, 6587-6596.

Green, W. N. & Millar, N. S. (1995). Ion-channel assembly. *Trends Neurosci.* **18**, 280-287.

Greger, V., Knoll, J. H., Woolf, E., Glatt, K., Tyndale, R. F., DeLorey, T. M., Olsen, R. W., Tobin, A. J., Sikela, J. M., Nakatsu, Y., & . (1995). The gamma-aminobutyric acid receptor gamma 3 subunit gene (GABRG3) is tightly linked to the alpha 5 subunit gene (GABRA5) on human chromosome 15q11-q13 and is transcribed in the same orientation. *Genomics* **26**, 258-264.

Grover, L.M., Lambert, N.A., Schwartzkroin, P.A., Teyler, T.J. (1993). Role of HCO3- ions in depolarizing GABAA receptor-mediated responses in pyramidal cells of rat hippocampus. J. Neurophysiol. **69**, 1541-1555.

Gutierrez, R. (2005). The dual glutamatergic-GABAergic phenotype of hippocampal granule cells. *Trends Neurosci.* **28**, 297-303.

Haas, K. F. & Macdonald, R. L. (1999). GABAA receptor subunit gamma2 and delta subtypes confer unique kinetic properties on recombinant GABAA receptor currents in mouse fibroblasts. *J.Physiol* **514 (Pt 1)**, 27-45.

Hackam, A. S., Wang, T. L., Guggino, W. B., & Cutting, G. R. (1997). The N-terminal domain of human GABA receptor rho1 subunits contains signals for homooligomeric and heterooligomeric interaction. *J.Biol.Chem.* **272**, 13750-13757.

Hackam, A. S., Wang, T. L., Guggino, W. B., & Cutting, G. R. (1998). Sequences in the amino termini of GABA rho and GABA(A) subunits specify their selective interaction in vitro. *J.Neurochem.* **70**, 40-46.

Hales, T. G., Tang, H., Bollan, K. A., Johnson, S. J., King, D. P., McDonald, N. A., Cheng, A., & Connolly, C. N. (2005). The epilepsy mutation, gamma2(R43Q) disrupts a highly conserved inter-subunit contact site, perturbing the biogenesis of GABAA receptors. *Mol.Cell Neurosci.* **29**, 120-127.

Hales, T. G., Dunlop, J. I., Deeb, T. Z., Carland, J. E., Kelley, S. P., Lambert, J. J., & Peters, J. A. (2006). Common determinants of single channel conductance within the large cytoplasmic loop of 5-hydroxytryptamine type 3 and alpha4beta2 nicotinic acetylcholine receptors. *J.Biol.Chem.* **281**, 8062-8071.

Hamann, M., Rossi, D. J., & Attwell, D. (2002). Tonic and spillover inhibition of granule cells control information flow through cerebellar cortex. *Neuron* **33**, 625-633.

Harkin, L. A., Bowser, D. N., Dibbens, L. M., Singh, R., Phillips, F., Wallace, R. H., Richards, M. C., Williams, D. A., Mulley, J. C., Berkovic, S. F., Scheffer, I. E., & Petrou, S. (2002). Truncation of the GABA(A)-receptor gamma2 subunit in a family with generalized epilepsy with febrile seizures plus. *Am.J.Hum.Genet.* **70**, 530-536.

Harvey, R. J., Topf, M., Harvey, K., & Rees, M. I. (2008). The genetics of hyperekplexia: more than startle! *Trends Genet.* **24**, 439-447.

Hebb, C. (1970). CNS at the cellular level: identity of transmitter agents. *Annu.Rev.Physiol* **32**, 165-192.

Hedblom, E. & Kirkness, E. F. (1997). A novel class of GABAA receptor subunit in tissues of the reproductive system. *J.Biol.Chem.* **272**, 15346-15350.

Helenius, A. & Aebi, M. (2004). Roles of N-linked glycans in the endoplasmic reticulum. *Annu.Rev.Biochem.* **73**, 1019-1049.

Herb, A., Wisden, W., Luddens, H., Puia, G., Vicini, S., & Seeburg, P. H. (1992). The third gamma subunit of the gamma-aminobutyric acid type A receptor family. *Proc.Natl.Acad.Sci.U.S.A* **89**, 1433-1437.

Herd, M. B., Haythornthwaite, A. R., Rosahl, T. W., Wafford, K. A., Homanics, G. E., Lambert, J. J., & Belelli, D. (2008). The expression of GABAA beta subunit isoforms in synaptic and extrasynaptic receptor populations of mouse dentate gyrus granule cells. *J.Physiol* **586**, 989-1004.

Hicks, A. A., Bailey, M. E., Riley, B. P., Kamphuis, W., Siciliano, M. J., Johnson, K. J., & Darlison, M. G. (1994). Further evidence for clustering of human GABAA receptor subunit genes: localization of the alpha 6-subunit gene (GABRA6) to distal chromosome 5q by linkage analysis. *Genomics* **20**, 285-288.

Hilf, R. J. & Dutzler, R. (2008). X-ray structure of a prokaryotic pentameric ligand-gated ion channel. *Nature* **452**, 375-379.

Hill, M. W., Reddy, P. A., Covey, D. F., & Rothman, S. M. (1998). Contribution of subsaturating GABA concentrations to IPSCs in cultured hippocampal neurons. *J.Neurosci.* **18**, 5103-5111.

Hirose, S. (2004). [Genetic approach to the pathogeneses of epilepsy]. *Rinsho Shinkeigaku* **44**, 975-978.

Horn, R. & Vandenberg, C. A. (1984). Statistical properties of single sodium channels. *J.Gen.Physiol* **84**, 505-534.

Imoto, K., Methfessel, C., Sakmann, B., Mishina, M., Mori, Y., Konno, T., Fukuda, K., Kurasaki, M., Bujo, H., Fujita, Y., & . (1986). Location of a delta-subunit region determining ion transport through the acetylcholine receptor channel. *Nature* **324**, 670-674.

Imoto, K., Busch, C., Sakmann, B., Mishina, M., Konno, T., Nakai, J., Bujo, H., Mori, Y., Fukuda, K., & Numa, S. (1988). Rings of negatively charged amino acids determine the acetylcholine receptor channel conductance. *Nature* **335**, 645-648.

Jacob, T. C., Moss, S. J., & Jurd, R. (2008). GABA(A) receptor trafficking and its role in the dynamic modulation of neuronal inhibition. *Nat.Rev.Neurosci.* **9**, 331-343.

Jasmin, L., Rabkin, S. D., Granato, A., Boudah, A., & Ohara, P. T. (2003). Analgesia and hyperalgesia from GABA-mediated modulation of the cerebral cortex. *Nature* **424**, 316-320.

Jeanclos, E. M., Lin, L., Treuil, M. W., Rao, J., DeCoster, M. A., & Anand, R. (2001). The chaperone protein 14-3-3eta interacts with the nicotinic acetylcholine receptor alpha 4 subunit. Evidence for a dynamic role in subunit stabilization. *J.Biol.Chem.* **276** , 28281-28290.

Jechlinger, M., Pelz, R., Tretter, V., Klausberger, T., & Sieghart, W. (1998). Subunit composition and quantitative importance of hetero-oligomeric receptors: GABAA receptors containing alpha6 subunits. *J.Neurosci.* **18**, 2449-2457.

Jensen, M. L., Timmermann, D. B., Johansen, T. H., Schousboe, A., Varming, T., & Ahring, P. K. (2002). The beta subunit determines the ion selectivity of the GABAA receptor. *J.Biol.Chem.* **277**, 41438-41447.

Jin, N., Guo, Y., Sun, P., Bell, A., Chintagari, N. R., Bhaskaran, M., Rains, K., Baviskar, P., Chen, Z., Weng, T., & Liu, L. (2008). Ionotropic GABA receptor expression in the lung during development. *Gene Expr.Patterns.* **8**, 397-403.

Jo, Y. H. & Schlichter, R. (1999). Synaptic corelease of ATP and GABA in cultured spinal neurons. *Nat.Neurosci.* **2**, 241-245.

Johnson, S. W. & North, R. A. (1992). Opioids excite dopamine neurons by hyperpolarization of local interneurons. *J.Neurosci.* **12**, 483-488.

Johnston, G. A. (1996). GABAA receptor pharmacology. *Pharmacol.Ther.* **69**, 173-198.

Jonas, P., Bischofberger, J., & Sandkuhler, J. (1998). Corelease of two fast neurotransmitters at a central synapse. *Science* **281**, 419-424.

Jones-Davis, D. M., Song, L., Gallagher, M. J., & Macdonald, R. L. (2005). Structural determinants of benzodiazepine allosteric regulation of GABA(A) receptor currents. *J.Neurosci.* **25**, 8056-8065.

Jones, B. L. & Henderson, L. P. (2007). Trafficking and potential assembly patterns of epsilon-containing GABAA receptors. *J.Neurochem.* **103**, 1258-1271.

Jones, M. V. & Westbrook, G. L. (1995). Desensitized states prolong GABAA channel responses to brief agonist pulses. *Neuron* **15**, 181-191.

Jones, M. V. & Westbrook, G. L. (1996). The impact of receptor desensitization on fast synaptic transmission. *Trends Neurosci.* **19**, 96-101.

Jones, M. V., Sahara, Y., Dzubay, J. A., & Westbrook, G. L. (1998). Defining affinity with the $GABA_A$ receptor. *J.Neurosci.* **18**, 8590-8604.

Kanaani, J., Lissin, D., Kash, S. F., & Baekkeskov, S. (1999). The hydrophilic isoform of glutamate decarboxylase, GAD67, is targeted to membranes and nerve terminals independent of dimerization with the hydrophobic membrane-anchored isoform, GAD65. *J.Biol.Chem.* **274**, 37200-37209.

Kananura, C., Haug, K., Sander, T., Runge, U., Gu, W., Hallmann, K., Rebstock, J., Heils, A., & Steinlein, O. K. (2002). A splice-site mutation in GABRG2 associated with childhood absence epilepsy and febrile convulsions. *Arch.Neurol.* **59**, 1137-1141.

Kanematsu, T. & Hirata, M. (2002). [The analysis of protein-protein interaction with special reference to PRIP-1]. *Nippon Yakurigaku Zasshi* **119**, 241-246.

Kanematsu, T., Fujii, M., Mizokami, A., Kittler, J. T., Nabekura, J., Moss, S. J., & Hirata, M. (2007). Phospholipase C-related inactive protein is implicated in the constitutive internalization of GABAA receptors mediated by clathrin and AP2 adaptor complex. *J.Neurochem.* **101**, 898-905.

Kang, J. Q. & Macdonald, R. L. (2004). The $GABA_A$ receptor gamma2 subunit R43Q mutation linked to childhood absence epilepsy and febrile seizures causes retention of alpha1beta2gamma2S receptors in the endoplasmic reticulum. *J.Neurosci.* **24**, 8672-8677.

Kapur, J. & Macdonald, R. L. (1997). Rapid seizure-induced reduction of benzodiazepine and Zn2+ sensitivity of hippocampal dentate granule cell GABAA receptors. *J.Neurosci.* **17**, 7532-7540.

Kash, T. L., Jenkins, A., Kelley, J. C., Trudell, J. R., & Harrison, N. L. (2003). Coupling of agonist binding to channel gating in the GABA(A) receptor. *Nature* **421**, 272-275.

Kaur, K.H., Baur, R., Sigel, E. (2009). Unanticipated structural and functional properties of delta subunit containing GABAA receptors. J. Biol. Chem. **284**, 7889-7896.

Kelley, S. P., Dunlop, J. I., Kirkness, E. F., Lambert, J. J., & Peters, J. A. (2003). A cytoplasmic region determines single-channel conductance in 5-HT3 receptors. *Nature* **424**, 321-324.

Keramidas, A., Moorhouse, A. J., Schofield, P. R., & Barry, P. H. (2004). Ligand-gated ion channels: mechanisms underlying ion selectivity. *Prog.Biophys.Mol.Biol.* **86**, 161-204.

Keramidas, A., Kash, T. L., & Harrison, N. L. (2006). The pre-M1 segment of the alpha1 subunit is a transduction element in the activation of the GABAA receptor. *J.Physiol* **575**, 11-22.

Khan, Z. U., Gutierrez, A., & De Blas, A. L. (1994). Short and long form gamma 2 subunits of the GABAA/benzodiazepine receptors. *J.Neurochem.* **63**, 1466-1476.

Kim, D.Y., Fenoglio, K.A., Kerrigan, J.F., Rho, J.M. (2009). Bicarbonate contributes to GABAA receptor-mediated neuronal excitation in surgically resected human hypothalamic hamartomas. Epilepsy Research **83**, 89-93.

Kirkness, E. F. & Fraser, C. M. (1993). A strong promoter element is located between alternative exons of a gene encoding the human gamma-aminobutyric acid-type A receptor beta 3 subunit (GABRB3). *J.Biol.Chem.* **268**, 4420-4428.

Kittler, J. T. & Moss, S. J. (2003). Modulation of GABAA receptor activity by phosphorylation and receptor trafficking: implications for the efficacy of synaptic inhibition. *Curr.Opin.Neurobiol.* **13**, 341-347.

Kittler, J. T., Chen, G., Honing, S., Bogdanov, Y., McAinsh, K., Arancibia-Carcamo, I. L., Jovanovic, J. N., Pangalos, M. N., Haucke, V., Yan, Z., & Moss, S. J. (2005). Phospho-dependent binding of the clathrin AP2 adaptor complex to GABAA receptors regulates the efficacy of inhibitory synaptic transmission. *Proc.Natl.Acad.Sci.U.S.A* **102** , 14871-14876.

Klausberger, T., Fuchs, K., Mayer, B., Ehya, N., & Sieghart, W. (2000). GABA(A) receptor assembly. Identification and structure of gamma(2) sequences forming the intersubunit contacts with alpha(1) and beta(3) subunits. *J.Biol.Chem.* **275**, 8921-8928.

Klausberger, T., Ehya, N., Fuchs, K., Fuchs, T., Ebert, V., Sarto, I., & Sieghart, W. (2001). Detection and binding properties of GABA(A) receptor assembly intermediates. *J.Biol.Chem.* **276**, 16024-16032.

Kneussel, M. & Betz, H. (2000). Receptors, gephyrin and gephyrin-associated proteins: novel insights into the assembly of inhibitory postsynaptic membrane specializations. *J.Physiol* **525 Pt 1**, 1-9.

Knight, A. R., Hartnett, C., Marks, C., Brown, M., Gallager, D., Tallman, J., & Ramabhadran, T. V. (1998). Molecular size of recombinant alpha1beta1 and alpha1beta1gamma2 GABAA receptors expressed in Sf9 cells. *Receptors.Channels* **6**, 1-18.

Korn, S. J. & Horn, R. (1988). Statistical discrimination of fractal and Markov models of single-channel gating. *Biophys.J.* **54**, 871-877.

Korn, S. J., Giacchino, J. L., Chamberlin, N. L., & Dingledine, R. (1987). Epileptiform burst activity induced by potassium in the hippocampus and its regulation by GABA-mediated inhibition. *J.Neurophysiol.* **57**, 325-340.

Krystal, J. H., Staley, J., Mason, G., Petrakis, I. L., Kaufman, J., Harris, R. A., Gelernter, J., & Lappalainen, J. (2006). Gamma-aminobutyric acid type A receptors and alcoholism: intoxication, dependence, vulnerability, and treatment. *Arch.Gen.Psychiatry* **63**, 957-968.

Kulik, A., Nishimaru, H., Ballanyi, K. (2000). Role of bicarbonate and chloride in GABA- and glycine-induced depolarization and [Ca2+]i rise in fetal rat motoneurons in situ. J. Neurosci. **20**, 7905-7913

Kullmann, D. M., Ruiz, A., Rusakov, D. M., Scott, R., Semyanov, A., & Walker, M. C. (2005). Presynaptic, extrasynaptic and axonal GABAA receptors in the CNS: where and why? *Prog.Biophys.Mol.Biol.* **87**, 33-46.

Lagrange, A. H., Botzolakis, E. J., & Macdonald, R. L. (2007). Enhanced macroscopic desensitization shapes the response of alpha4 subtype-containing GABAA receptors to synaptic and extrasynaptic GABA. *J.Physiol* **578**, 655-676.

Langosch, D., Thomas, L., & Betz, H. (1988). Conserved quaternary structure of ligand-gated ion channels: the postsynaptic glycine receptor is a pentamer. *Proc.Natl.Acad.Sci.U.S.A* **85**, 7394-7398.

Langosch, D., Laube, B., Rundstrom, N., Schmieden, V., Bormann, J., & Betz, H. (1994). Decreased agonist affinity and chloride conductance of mutant glycine receptors associated with human hereditary hyperekplexia. *EMBO J.* **13**, 4223-4228.

Lape, R., Colquhoun, D., & Sivilotti, L. G. (2008). On the nature of partial agonism in the nicotinic receptor superfamily. *Nature* **454**, 722-727.

Laurie, D. J., Seeburg, P. H., & Wisden, W. (1992). The distribution of 13 GABAA receptor subunit mRNAs in the rat brain. II. Olfactory bulb and cerebellum. *J.Neurosci.* **12**, 1063-1076.

Laurie, D. J., Wisden, W., & Seeburg, P. H. (1992). The distribution of thirteen GABAA receptor subunit mRNAs in the rat brain. III. Embryonic and postnatal development. *J.Neurosci.* **12**, 4151-4172.

Lerma, J., Herranz, A. S., Herreras, O., Abraira, V., & Martin, d. R. (1986). In vivo determination of extracellular concentration of amino acids in the rat hippocampus. A method based on brain dialysis and computerized analysis. *Brain Res.* **384**, 145-155.

Levitan, E. S., Schofield, P. R., Burt, D. R., Rhee, L. M., Wisden, W., Kohler, M., Fujita, N., Rodriguez, H. F., Stephenson, A., Darlison, M. G., & . (1988). Structural and functional basis for GABAA receptor heterogeneity. *Nature* **335**, 76-79.

Li, M. & De Blas, A. L. (1997). Coexistence of two beta subunit isoforms in the same gamma-aminobutyric acid type A receptor. *J.Biol.Chem.* **272**, 16564-16569.

Liang, S. L., Carlson, G. C., & Coulter, D. A. (2006). Dynamic regulation of synaptic GABA release by the glutamate-glutamine cycle in hippocampal area CA1. *J.Neurosci.* **26**, 8537-8548.

Liu, C. & Reppert, S. M. (2000). GABA synchronizes clock cells within the suprachiasmatic circadian clock. *Neuron* **25**, 123-128.

Liu, F., Wan, Q., Pristupa, Z. B., Yu, X. M., Wang, Y. T., & Niznik, H. B. (2000). Direct protein-protein coupling enables cross-talk between dopamine D5 and gamma-aminobutyric acid A receptors. *Nature* **403**, 274-280.

Liu, X., Krause, W. C., & Davis, R. L. (2007). GABAA receptor RDL inhibits Drosophila olfactory associative learning. *Neuron* **56**, 1090-1102.

Lo, W. Y., Botzolakis, E. J., Tang, X., & Macdonald, R. L. (2008). A conserved Cys-loop receptor aspartate residue in the M3-M4 cytoplasmic loop is required for GABAA receptor assembly. *J.Biol.Chem.* **283**, 29740-29752.

Lopez-Chavez, A., Miledi, R., & Martinez-Torres, A. (2005). Cloning and functional expression of the bovine GABA(C) rho2 subunit. Molecular evidence of a widespread distribution in the CNS. *Neurosci.Res.* **53**, 421-427.

Luddens, H. & Wisden, W. (1991). Function and pharmacology of multiple GABAA receptor subunits. *Trends Pharmacol.Sci.* **12**, 49-51.

Luddens, H., Killisch, I., & Seeburg, P. H. (1991). More than one alpha variant may exist in a GABAA/benzodiazepine receptor complex. *J.Recept.Res.* **11**, 535-551.

Maattanen, P., Kozlov, G., Gehring, K., & Thomas, D. Y. (2006). ERp57 and PDI: multifunctional protein disulfide isomerases with similar domain architectures but differing substrate-partner associations. *Biochem.Cell Biol.* **84**, 881-889.

Macdonald, R. L., Rogers, C. J., & Twyman, R. E. (1989). Kinetic properties of the GABAA receptor main conductance state of mouse spinal cord neurones in culture. *J.Physiol* **410**, 479-499.

Macdonald, R. L. & Olsen, R. W. (1994). GABAA receptor channels. *Annu.Rev.Neurosci.* **17**, 569-602.

Macdonald, R. L., Kang, J. Q., Gallagher, M. J., & Feng, H. J. (2006). GABA(A) receptor mutations associated with generalized epilepsies. *Adv.Pharmacol.* **54**, 147-169.

Mackenzie, B. & Erickson, J. D. (2004). Sodium-coupled neutral amino acid (System N/A) transporters of the SLC38 gene family. *Pflugers Arch.* **447**, 784-795.

Maconochie, D. J., Zempel, J. M., & Steinbach, J. H. (1994). How quickly can GABAA receptors open? *Neuron* **12**, 61-71.

Maguire, J. & Mody, I. (2008). GABA(A)R plasticity during pregnancy: relevance to postpartum depression. *Neuron* **59**, 207-213.

Maher, B. J. & Westbrook, G. L. (2008). Co-transmission of dopamine and GABA in periglomerular cells. *J.Neurophysiol.* **99**, 1559-1564.

Malan, T. P., Mata, H. P., & Porreca, F. (2002). Spinal GABA(A) and GABA(B) receptor pharmacology in a rat model of neuropathic pain. *Anesthesiology* **96**, 1161-1167.

Maljevic, S., Krampfl, K., Cobilanschi, J., Tilgen, N., Beyer, S., Weber, Y. G., Schlesinger, F., Ursu, D., Melzer, W., Cossette, P., Bufler, J., Lerche, H., & Heils, A. (2006). A mutation in the GABA(A) receptor alpha(1)-subunit is associated with absence epilepsy. *Ann.Neurol.* **59**, 983-987.

Mamalaki, C., Barnard, E. A., & Stephenson, F. A. (1989). Molecular size of the gamma-aminobutyric acidA receptor purified from mammalian cerebral cortex. *J.Neurochem.* **52**, 124-134.

Maricq, A. V., Peterson, A. S., Brake, A. J., Myers, R. M., & Julius, D. (1991). Primary structure and functional expression of the 5HT3 receptor, a serotonin-gated ion channel. *Science* **254**, 432-437.

Martin, D. L. (1993). Short-term control of GABA synthesis in brain. *Prog.Biophys.Mol.Biol.* **60**, 17-28.

Martin, D. L. & Rimvall, K. (1993). Regulation of gamma-aminobutyric acid synthesis in the brain. *J.Neurochem.* **60**, 395-407.

McClellan, K. M., Calver, A. R., & Tobet, S. A. (2008). GABAB receptors role in cell migration and positioning within the ventromedial nucleus of the hypothalamus. *Neuroscience* **151**, 1119-1131.

McKernan, R. M. & Whiting, P. J. (1996). Which GABAA-receptor subtypes really occur in the brain? *Trends Neurosci.* **19**, 139-143.

McLean, P. J., Farb, D. H., & Russek, S. J. (1995). Mapping of the alpha 4 subunit gene (GABRA4) to human chromosome 4 defines an alpha 2-alpha 4-beta 1-gamma 1

gene cluster: further evidence that modern GABAA receptor gene clusters are derived from an ancestral cluster. *Genomics* **26**, 580-586.

McManus, O. B., Weiss, D. S., Spivak, C. E., Blatz, A. L., & Magleby, K. L. (1988). Fractal models are inadequate for the kinetics of four different ion channels. *Biophys.J.* **54**, 859-870.

McNally, G. P., Augustyn, K. A., & Richardson, R. (2008). GABA(A) receptors determine the temporal dynamics of memory retention. *Learn.Mem.* **15**, 106-111.

Mejia, C., Garcia-Alcocer, G., Berumen, L. C., Rosas-Arellano, A., Miledi, R., & Martinez-Torres, A. (2008). Expression of GABArho subunits during rat cerebellum development. *Neurosci.Lett.* **432**, 1-6.

Mercik, K., Pytel, M., Cherubini, E., & Mozrzymas, J. W. (2006). Effect of extracellular pH on recombinant alpha1beta2gamma2 and alpha1beta2 GABAA receptors. *Neuropharmacology* **51** , 305-314.

Middleton, S. J., Racca, C., Cunningham, M. O., Traub, R. D., Monyer, H., Knopfel, T., Schofield, I. S., Jenkins, A., & Whittington, M. A. (2008). High-frequency network oscillations in cerebellar cortex. *Neuron* **58**, 763-774.

Mihic, S. J., Ye, Q., Wick, M. J., Koltchine, V. V., Krasowski, M. D., Finn, S. E., Mascia, M. P., Valenzuela, C. F., Hanson, K. K., Greenblatt, E. P., Harris, R. A., & Harrison, N. L. (1997). Sites of alcohol and volatile anaesthetic action on GABA(A) and glycine receptors. *Nature* **389**, 385-389.

Milligan, C. J., Buckley, N. J., Garret, M., Deuchars, J., & Deuchars, S. A. (2004). Evidence for inhibition mediated by coassembly of GABAA and GABAC receptor subunits in native central neurons. *J.Neurosci.* **24**, 7241-7250.

Minelli, A., Brecha, N. C., Karschin, C., DeBiasi, S., & Conti, F. (1995). GAT-1, a high-affinity GABA plasma membrane transporter, is localized to neurons and astroglia in the cerebral cortex. *J.Neurosci.* **15**, 7734-7746.

Mintz, E. M., Jasnow, A. M., Gillespie, C. F., Huhman, K. L., & Albers, H. E. (2002). GABA interacts with photic signaling in the suprachiasmatic nucleus to regulate circadian phase shifts. *Neuroscience* **109**, 773-778.

Mintz, I. M. & Bean, B. P. (1993). GABAB receptor inhibition of P-type Ca2+ channels in central neurons. *Neuron* **10**, 889-898.

Miyazawa, A., Fujiyoshi, Y., & Unwin, N. (2003). Structure and gating mechanism of the acetylcholine receptor pore. *Nature* **423**, 949-955.

Moragues, N., Ciofi, P., Lafon, P., Odessa, M. F., Tramu, G., & Garret, M. (2000). cDNA cloning and expression of a gamma-aminobutyric acid A receptor epsilon-subunit in rat brain. *Eur.J.Neurosci.* **12**, 4318-4330.

Moragues, N., Ciofi, P., Tramu, G., & Garret, M. (2002). Localisation of GABA(A) receptor epsilon-subunit in cholinergic and aminergic neurones and evidence for co-distribution with the theta-subunit in rat brain. *Neuroscience* **111**, 657-669.

Mortensen, M. & Smart, T. G. (2006). Extrasynaptic alphabeta subunit GABAA receptors on rat hippocampal pyramidal neurons. *J.Physiol* **577**, 841-856.

Mozrzymas, J. W., Barberis, A., Mercik, K., & Zarnowska, E. D. (2003). Binding sites, singly bound states, and conformation coupling shape GABA-evoked currents. *J.Neurophysiol.* **89**, 871-883.

Mozrzymas, J. W. & Barberis, A. (2004). Changes of GABA(A)receptor activation kinetics in hippocampal neurons cultured for different periods of time. *Cell Mol.Biol.Lett.* **9**, 61-67.

Mozrzymas, J. W., Barberis, A., & Vicini, S. (2007). GABAergic currents in RT and VB thalamic nuclei follow kinetic pattern of alpha3- and alpha1-subunit-containing GABAA receptors. *Eur.J.Neurosci.* **26**, 657-665.

Nayeem, N., Green, T. P., Martin, I. L., & Barnard, E. A. (1994). Quaternary structure of the native GABAA receptor determined by electron microscopic image analysis. *J.Neurochem.* **62**, 815-818.

Neelands, T. R. & Macdonald, R. L. (1999). Incorporation of the pi subunit into functional gamma-aminobutyric Acid(A) receptors. *Mol.Pharmacol.* **56**, 598-610.

Neelands, T. R., Fisher, J. L., Bianchi, M., & Macdonald, R. L. (1999). Spontaneous and gamma-aminobutyric acid (GABA)-activated GABA(A) receptor channels formed by epsilon subunit-containing isoforms. *Mol.Pharmacol.* **55**, 168-178.

Newland, C. F., Colquhoun, D., & Cull-Candy, S. G. (1991). Single channels activated by high concentrations of GABA in superior cervical ganglion neurones of the rat. *J.Physiol* **432**, 203-233.

Noda, M., Takahashi, H., Tanabe, T., Toyosato, M., Kikyotani, S., Furutani, Y., Hirose, T., Takashima, H., Inayama, S., Miyata, T., & Numa, S. (1983). Structural homology of Torpedo californica acetylcholine receptor subunits. *Nature* **302**, 528-532.

Nusser, Z., Sieghart, W., & Somogyi, P. (1998). Segregation of different GABAA receptors to synaptic and extrasynaptic membranes of cerebellar granule cells. *J.Neurosci.* **18**, 1693-1703.

Nusser, Z., Hajos, N., Somogyi, P., & Mody, I. (1998). Increased number of synaptic GABA(A) receptors underlies potentiation at hippocampal inhibitory synapses. *Nature* **395**, 172-177.

O'Mara, M., Cromer, B., Parker, M., & Chung, S. H. (2005). Homology model of the GABAA receptor examined using Brownian dynamics. *Biophys.J.* **88**, 3286-3299.

Ohlson, J., Pedersen, J. S., Haussler, D., & Ohman, M. (2007). Editing modifies the GABA(A) receptor subunit alpha3. *RNA.* **13**, 698-703.

Olsen, R. W. & Tobin, A. J. (1990). Molecular biology of GABAA receptors. *FASEB J.* **4**, 1469-1480.

Olsen, R. W., Chang, C. S., Li, G., Hanchar, H. J., & Wallner, M. (2004). Fishing for allosteric sites on GABA(A) receptors. *Biochem.Pharmacol.* **68**, 1675-1684.

Olsen, R. W. & Sieghart, W. (2008). GABA(A) receptors: Subtypes provide diversity of function and pharmacology. *Neuropharmacology*.

Otis, T. S. & Mody, I. (1992). Modulation of decay kinetics and frequency of GABAA receptor-mediated spontaneous inhibitory postsynaptic currents in hippocampal neurons. *Neuroscience* **49**, 13-32.

Otis, T. S. & Mody, I. (1992). Differential activation of GABAA and GABAB receptors by spontaneously released transmitter. *J.Neurophysiol.* **67**, 227-235.

Otis, T. S., De Koninck, Y., & Mody, I. (1994). Lasting potentiation of inhibition is associated with an increased number of gamma-aminobutyric acid type A receptors activated during miniature inhibitory postsynaptic currents. *Proc.Natl.Acad.Sci.U.S.A* **91**, 7698-7702.

Overstreet, L. S., Jones, M. V., & Westbrook, G. L. (2000). Slow desensitization regulates the availability of synaptic GABA(A) receptors. *J.Neurosci.* **20**, 7914-7921.

Owens, D. F. & Kriegstein, A. R. (2002). Is there more to GABA than synaptic inhibition? *Nat.Rev.Neurosci.* **3**, 715-727.

Pan, Y. & Qian, H. (2005). Interactions between rho and gamma2 subunits of the GABA receptor. *J.Neurochem.* **94**, 482-490.

Pan, Y., Ripps, H., & Qian, H. (2006). Random assembly of GABA rho1 and rho2 subunits in the formation of heteromeric GABA(C) receptors. *Cell Mol.Neurobiol.* **26**, 289-305.

Pan, Z. H. (2001). Voltage-activated Ca2+ channels and ionotropic GABA receptors localized at axon terminals of mammalian retinal bipolar cells. *Vis.Neurosci.* **18**, 279-288.

Perkins, K.L., Wong, R.K. (1997). The depolarizing GABA response. Can. J. Physiol. Pharmacol. **75**, 516-519.

Peters, J. A., Kelley, S. P., Dunlop, J. I., Kirkness, E. F., Hales, T. G., & Lambert, J. J. (2004). The 5-hydroxytryptamine type 3 (5-HT3) receptor reveals a novel determinant of single-channel conductance. *Biochem.Soc.Trans.* **32**, 547-552.

Picton, A. J. & Fisher, J. L. (2007). Effect of the alpha subunit subtype on the macroscopic kinetic properties of recombinant GABA(A) receptors. *Brain Res.* **1165**, 40-49.

Pirker, S., Schwarzer, C., Wieselthaler, A., Sieghart, W., & Sperk, G. (2000). GABA(A) receptors: immunocytochemical distribution of 13 subunits in the adult rat brain. *Neuroscience* **101**, 815-850.

Plested, A. J., Groot-Kormelink, P. J., Colquhoun, D., & Sivilotti, L. G. (2007). Single-channel study of the spasmodic mutation alpha1A52S in recombinant rat glycine receptors. *J.Physiol* **581**, 51-73.

Poulter, M. O., Brown, L. A., Tynan, S., Willick, G., William, R., & McIntyre, D. C. (1999). Differential expression of alpha1, alpha2, alpha3, and alpha5 GABAA receptor subunits in seizure-prone and seizure-resistant rat models of temporal lobe epilepsy. *J.Neurosci.* **19**, 4654-4661.

Pritchett, D. B., Sontheimer, H., Shivers, B. D., Ymer, S., Kettenmann, H., Schofield, P. R., & Seeburg, P. H. (1989). Importance of a novel GABAA receptor subunit for benzodiazepine pharmacology. *Nature* **338**, 582-585.

Qian, H. & Ripps, H. (1999). Response kinetics and pharmacological properties of heteromeric receptors formed by coassembly of GABA rho- and gamma 2-subunits. *Proc.Biol.Sci.* **266**, 2419-2425.

Qian, H. & Pan, Y. (2002). Co-assembly of GABA rho subunits with the GABA(A) receptor gamma(2) subunit cloned from white perch retina. *Brain Res.Mol.Brain Res.* **103**, 62-70.

Quirk, K., Gillard, N. P., Ragan, C. I., Whiting, P. J., & McKernan, R. M. (1994). gamma-Aminobutyric acid type A receptors in the rat brain can contain both gamma 2 and gamma 3 subunits, but gamma 1 does not exist in combination with another gamma subunit. *Mol.Pharmacol.* **45**, 1061-1070.

Quirk, K., Whiting, P. J., Ragan, C. I., & McKernan, R. M. (1995). Characterisation of delta-subunit containing GABAA receptors from rat brain. *Eur.J.Pharmacol.* **290**, 175-181.

Richardson, J. E., Garcia, P. S., O'Toole, K. K., Derry, J. M., Bell, S. V., & Jenkins, A. (2007). A conserved tyrosine in the beta2 subunit M4 segment is a determinant of gamma-aminobutyric acid type A receptor sensitivity to propofol. *Anesthesiology* **107**, 412-418.

Rivera, C., Voipio, J., Payne, J. A., Ruusuvuori, E., Lahtinen, H., Lamsa, K., Pirvola, U., Saarma, M., & Kaila, K. (1999). The K+/Cl- co-transporter KCC2 renders GABA hyperpolarizing during neuronal maturation. *Nature* **397**, 251-255.

Roberts, E. & Frankel, S. (1950). gamma-Aminobutyric acid in brain: its formation from glutamic acid. *J.Biol.Chem.* **187**, 55-63.

Rothberg, B. S. & Magleby, K. L. (2000). Voltage and Ca2+ activation of single large-conductance Ca2+-activated K+ channels described by a two-tiered allosteric gating mechanism. *J.Gen.Physiol* **116**, 75-99.

Rudolph, U. & Mohler, H. (2004). Analysis of GABAA receptor function and dissection of the pharmacology of benzodiazepines and general anesthetics through mouse genetics. *Annu.Rev.Pharmacol.Toxicol.* **44**, 475-498.

Rula, E. Y., Lagrange, A. H., Jacobs, M. M., Hu, N., Macdonald, R. L., & Emeson, R. B. (2008). Developmental modulation of GABA(A) receptor function by RNA editing. *J.Neurosci.* **28**, 6196-6201.

Russek, S. J. & Farb, D. H. (1994). Mapping of the beta 2 subunit gene (GABRB2) to microdissected human chromosome 5q34-q35 defines a gene cluster for the most abundant GABAA receptor isoform. *Genomics* **23**, 528-533.

Sancar, F. & Czajkowski, C. (2004). A GABAA receptor mutation linked to human epilepsy (gamma2R43Q) impairs cell surface expression of alphabetagamma receptors. *J.Biol.Chem.* **279**, 47034-47039.

Sarang, S. S., Lukyanova, S. M., Brown, D. D., Cummings, B. S., Gullans, S. R., & Schnellmann, R. G. (2008). Identification, coassembly, and activity of gamma-aminobutyric acid receptor subunits in renal proximal tubular cells. *J.Pharmacol.Exp.Ther.* **324**, 376-382.

Sarto-Jackson, I. & Sieghart, W. (2008). Assembly of GABA(A) receptors (Review). *Mol.Membr.Biol.* **25**, 302-310.

Saxena, N. C. & Macdonald, R. L. (1994). Assembly of GABAA receptor subunits: role of the delta subunit. *J.Neurosci.* **14**, 7077-7086.

Saxena, N. C. & Macdonald, R. L. (1996). Properties of putative cerebellar gamma-aminobutyric acid A receptor isoforms. *Mol.Pharmacol.* **49**, 567-579.

Scheller, M. & Forman, S. A. (2002). Coupled and uncoupled gating and desensitization effects by pore domain mutations in GABA(A) receptors. *J.Neurosci.* **22**, 8411-8421.

Schneiderman, J. H. (1997). The role of long-term potentiation in persistent epileptiform burst-induced hyperexcitability following GABAA receptor blockade. *Neuroscience* **81**, 1111-1122.

Schofield, C. M. & Harrison, N. L. (2005). Transmembrane residues define the action of isoflurane at the GABAA receptor alpha-3 subunit. *Brain Res.* **1032**, 30-35.

Schofield, P. R., Darlison, M. G., Fujita, N., Burt, D. R., Stephenson, F. A., Rodriguez, H., Rhee, L. M., Ramachandran, J., Reale, V., Glencorse, T. A., & . (1987). Sequence and functional expression of the GABA A receptor shows a ligand-gated receptor super-family. *Nature* **328**, 221-227.

Schoppa, N. E. & Sigworth, F. J. (1998). Activation of Shaker potassium channels. III. An activation gating model for wild-type and V2 mutant channels. *J.Gen.Physiol* **111**, 313-342.

Schoppa, N. E. & Sigworth, F. J. (1998). Activation of Shaker potassium channels. II. Kinetics of the V2 mutant channel. *J.Gen.Physiol* **111**, 295-311.

Schwartzkroin, P. A. & Prince, D. A. (1980). Changes in excitatory and inhibitory synaptic potentials leading to epileptogenic activity. *Brain Res.* **183**, 61-76.

Schweitzer, P., Roberto, M., Madamba, S. G., & Siggins, G. R. (2004). gamma-hydroxybutyrate increases a potassium current and decreases the H-current in hippocampal neurons via GABAB receptors. *J.Pharmacol.Exp.Ther.* **311**, 172-179.

Serafini, R., Bracamontes, J., & Steinbach, J. H. (2000). Structural domains of the human GABAA receptor 3 subunit involved in the actions of pentobarbital. *J.Physiol* **524 Pt 3**, 649-676.

Shelley, C. & Magleby, K. L. (2008). Linking exponential components to kinetic states in markov models for single-channel gating. *J.Gen.Physiol* **132**, 295-312.

Shivers, B. D., Killisch, I., Sprengel, R., Sontheimer, H., Kohler, M., Schofield, P. R., & Seeburg, P. H. (1989). Two novel GABAA receptor subunits exist in distinct neuronal subpopulations. *Neuron* **3**, 327-337.

Sieghart, W. & Sperk, G. (2002). Subunit composition, distribution and function of GABA(A) receptor subtypes. *Curr.Top.Med.Chem.* **2**, 795-816.

Sigg, D. & Bezanilla, F. (2003). A physical model of potassium channel activation: from energy landscape to gating kinetics. *Biophys.J.* **84**, 3703-3716.

Simon, J., Wakimoto, H., Fujita, N., Lalande, M., & Barnard, E. A. (2004). Analysis of the set of GABA(A) receptor genes in the human genome. *J.Biol.Chem.* **279**, 41422-41435.

Smith, G. B. & Olsen, R. W. (1995). Functional domains of GABAA receptors. *Trends Pharmacol.Sci.* **16**, 162-168.

Smith, K. R., McAinsh, K., Chen, G., Arancibia-Carcamo, I. L., Haucke, V., Yan, Z., Moss, S. J., & Kittler, J. T. (2008). Regulation of inhibitory synaptic transmission by a conserved atypical interaction of GABA(A) receptor beta- and gamma-subunits with the clathrin AP2 adaptor. *Neuropharmacology*.

Sommer, B., Poustka, A., Spurr, N. K., & Seeburg, P. H. (1990). The murine GABAA receptor delta-subunit gene: structure and assignment to human chromosome 1. *DNA Cell Biol.* **9**, 561-568.

Steffensen, S. C., Svingos, A. L., Pickel, V. M., & Henriksen, S. J. (1998). Electrophysiological characterization of GABAergic neurons in the ventral tegmental area. *J.Neurosci.* **18**, 8003-8015.

Stein, V. & Nicoll, R. A. (2003). GABA generates excitement. *Neuron* **37**, 375-378.

Steriade, M. (2005). Sleep, epilepsy and thalamic reticular inhibitory neurons. *Trends Neurosci.* **28**, 317-324.

Strecker, G. J., Park, W. K., & Dudek, F. E. (1999). Zinc and flunitrazepam modulation of GABA-mediated currents in rat suprachiasmatic neurons. *J.Neurophysiol.* **81**, 184-191.

Sur, C., Farrar, S. J., Kerby, J., Whiting, P. J., Atack, J. R., & McKernan, R. M. (1999). Preferential coassembly of alpha4 and delta subunits of the gamma-aminobutyric acidA receptor in rat thalamus. *Mol.Pharmacol.* **56**, 110-115.

Tanaka, M., Olsen, R. W., Medina, M. T., Schwartz, E., Alonso, M. E., Duron, R. M., Castro-Ortega, R., Martinez-Juarez, I. E., Pascual-Castroviejo, I., Machado-Salas, J., Silva, R., Bailey, J. N., Bai, D., Ochoa, A., Jara-Prado, A., Pineda, G., Macdonald, R. L., & Delgado-Escueta, A. V. (2008). Hyperglycosylation and reduced GABA currents of mutated GABRB3 polypeptide in remitting childhood absence epilepsy. *Am.J.Hum.Genet.* **82**, 1249-1261.

Taylor, P. M., Thomas, P., Gorrie, G. H., Connolly, C. N., Smart, T. G., & Moss, S. J. (1999). Identification of amino acid residues within GABA(A) receptor beta subunits that mediate both homomeric and heteromeric receptor expression. *J.Neurosci.* **19**, 6360-6371.

Taylor, P. M., Connolly, C. N., Kittler, J. T., Gorrie, G. H., Hosie, A., Smart, T. G., & Moss, S. J. (2000). Identification of residues within GABA(A) receptor alpha subunits that mediate specific assembly with receptor beta subunits. *J.Neurosci.* **20**, 1297-1306.

Tobimatsu, T., Fujita, Y., Fukuda, K., Tanaka, K., Mori, Y., Konno, T., Mishina, M., & Numa, S. (1987). Effects of substitution of putative transmembrane segments on nicotinic acetylcholine receptor function. *FEBS Lett.* **222**, 56-62.

Traynels, S. F. & Dingledine, R. (1988). Potassium-induced spontaneous electrographic seizures in the rat hippocampal slice. *J.Neurophysiol.* **59**, 259-276.

Tretter, V., Ehya, N., Fuchs, K., & Sieghart, W. (1997). Stoichiometry and assembly of a recombinant GABAA receptor subtype. *J.Neurosci.* **17**, 2728-2737.

Tretter, V., Jacob, T. C., Mukherjee, J., Fritschy, J. M., Pangalos, M. N., & Moss, S. J. (2008). The clustering of GABA(A) receptor subtypes at inhibitory synapses is facilitated via the direct binding of receptor alpha 2 subunits to gephyrin. *J.Neurosci.* **28**, 1356-1365.

Trudell, J. R. & Bertaccini, E. (2004). Comparative modeling of a GABAA alpha1 receptor using three crystal structures as templates. *J.Mol.Graph.Model.* **23**, 39-49.

Twyman, R. E., Rogers, C. J., & Macdonald, R. L. (1989). Differential regulation of gamma-aminobutyric acid receptor channels by diazepam and phenobarbital. *Ann.Neurol.* **25**, 213-220.

Twyman, R. E., Rogers, C. J., & Macdonald, R. L. (1989). Pentobarbital and picrotoxin have reciprocal actions on single GABAA receptor channels. *Neurosci.Lett.* **96**, 89-95.

Twyman, R. E., Rogers, C. J., & Macdonald, R. L. (1990). Intraburst kinetic properties of the GABAA receptor main conductance state of mouse spinal cord neurones in culture. *J.Physiol* **423**, 193-220.

Twyman, R. E. & Macdonald, R. L. (1992). Neurosteroid regulation of GABAA receptor single-channel kinetic properties of mouse spinal cord neurons in culture. *J.Physiol* **456**, 215-245.

Twyman, R. E., Green, R. M., & Macdonald, R. L. (1992). Kinetics of open channel block by penicillin of single GABAA receptor channels from mouse spinal cord neurones in culture. *J.Physiol* **445**, 97-127.

Unwin, N. (1993). Nicotinic acetylcholine receptor at 9 A resolution. *J.Mol.Biol.* **229**, 1101-1124.

Unwin, N. (2005). Refined structure of the nicotinic acetylcholine receptor at 4A resolution. *J.Mol.Biol.* **346**, 967-989.

Uusi-Oukari, M., Heikkila, J., Sinkkonen, S. T., Makela, R., Hauer, B., Homanics, G. E., Sieghart, W., Wisden, W., & Korpi, E. R. (2000). Long-range interactions in neuronal gene expression: evidence from gene targeting in the GABA(A) receptor beta2-alpha6-alpha1-gamma2 subunit gene cluster. *Mol.Cell Neurosci.* **16**, 34-41.

Ventriglia, F. & Di, M., V (2003). Stochastic fluctuations of the quantal EPSC amplitude in computer simulated excitatory synapses of hippocampus. *Biosystems* **71**, 195-204.

Vicini, S., Ferguson, C., Prybylowski, K., Kralic, J., Morrow, A. L., & Homanics, G. E. (2001). GABA(A) receptor alpha1 subunit deletion prevents developmental changes of inhibitory synaptic currents in cerebellar neurons. *J.Neurosci.* **21**, 3009-3016.

Wagner, D. A., Goldschen-Ohm, M. P., Hales, T. G., & Jones, M. V. (2005). Kinetics and spontaneous open probability conferred by the epsilon subunit of the GABAA receptor. *J.Neurosci.* **25**, 10462-10468.

Wagner, P. G. & Dekin, M. S. (1993). GABAb receptors are coupled to a barium-insensitive outward rectifying potassium conductance in premotor respiratory neurons. *J.Neurophysiol.* **69**, 286-289.

Wanamaker, C. P. & Green, W. N. (2007). Endoplasmic reticulum chaperones stabilize nicotinic receptor subunits and regulate receptor assembly. *J.Biol.Chem.* **282**, 31113-31123.

Wang, H., Bedford, F. K., Brandon, N. J., Moss, S. J., & Olsen, R. W. (1999). GABA(A)-receptor-associated protein links GABA(A) receptors and the cytoskeleton. *Nature* **397**, 69-72.

Wang, W. & Shakes, D. C. (1996). Molecular evolution of the 14-3-3 protein family. *J.Mol.Evol.* **43**, 384-398.

Weiss, D. S. & Magleby, K. L. (1989). Gating scheme for single GABA-activated Cl-channels determined from stability plots, dwell-time distributions, and adjacent-interval durations. *J.Neurosci.* **9**, 1314-1324.

Wendt, A., Birnir, B., Buschard, K., Gromada, J., Salehi, A., Sewing, S., Rorsman, P., & Braun, M. (2004). Glucose inhibition of glucagon secretion from rat alpha-cells is mediated by GABA released from neighboring beta-cells. *Diabetes* **53**, 1038-1045.

Whiting, P., McKernan, R. M., & Iversen, L. L. (1990). Another mechanism for creating diversity in gamma-aminobutyrate type A receptors: RNA splicing directs expression of two forms of gamma 2 phosphorylation site. *Proc.Natl.Acad.Sci.U.S.A* **87**, 9966-9970.

Wilcox, A. S., Warrington, J. A., Gardiner, K., Berger, R., Whiting, P., Altherr, M. R., Wasmuth, J. J., Patterson, D., & Sikela, J. M. (1992). Human chromosomal localization of genes encoding the gamma 1 and gamma 2 subunits of the gamma-aminobutyric acid receptor indicates that members of this gene family are often clustered in the genome. *Proc.Natl.Acad.Sci.U.S.A* **89**, 5857-5861.

Wilke, K., Gaul, R., Klauck, S. M., & Poustka, A. (1997). A gene in human chromosome band Xq28 (GABRE) defines a putative new subunit class of the GABAA neurotransmitter receptor. *Genomics* **45**, 1-10.

Wilkin, G. P., Hudson, A. L., Hill, D. R., & Bowery, N. G. (1981). Autoradiographic localization of GABAB receptors in rat cerebellum. *Nature* **294**, 584-587.

Wilkins, M. E., Hosie, A. M., & Smart, T. G. (2002). Identification of a beta subunit TM2 residue mediating proton modulation of GABA type A receptors. *J.Neurosci.* **22**, 5328-5333.

Wisden, W., Laurie, D. J., Monyer, H., & Seeburg, P. H. (1992). The distribution of 13 GABAA receptor subunit mRNAs in the rat brain. I. Telencephalon, diencephalon, mesencephalon. *J.Neurosci.* **12**, 1040-1062.

Wong, C. G., Bottiglieri, T., & Snead, O. C., III (2003). GABA, gamma-hydroxybutyric acid, and neurological disease. *Ann.Neurol.* **54 Suppl 6**, S3-12.

Wotring, V. E. & Weiss, D. S. (2008). Charge scan reveals an extended region at the intracellular end of the GABA receptor pore that can influence ion selectivity. *J.Gen.Physiol* **131**, 87-97.

Wuenschell, C. W., Fisher, R. S., Kaufman, D. L., & Tobin, A. J. (1986). In situ hybridization to localize mRNA encoding the neurotransmitter synthetic enzyme glutamate decarboxylase in mouse cerebellum. *Proc.Natl.Acad.Sci.U.S.A* **83**, 6193-6197.

Xu, M. & Akabas, M. H. (1996). Identification of channel-lining residues in the M2 membrane-spanning segment of the GABA(A) receptor alpha1 subunit. *J.Gen.Physiol* **107**, 195-205.

Ymer, S., Schofield, P. R., Draguhn, A., Werner, P., Kohler, M., & Seeburg, P. H. (1989). GABAA receptor beta subunit heterogeneity: functional expression of cloned cDNAs. *EMBO J.* **8**, 1665-1670.

Ymer, S., Schofield, P. R., Shivers, B. D., Pritchett, D. B., Luddens, H., Kohler, M., Werner, P., Sontheimer, H., Kettenmann, H., & Seeburg, P. H. (1989). Molecular studies of the GABAA receptor. *J.Protein Chem.* **8**, 352-355.

Zagotta, W. N., Hoshi, T., & Aldrich, R. W. (1994). Shaker potassium channel gating. III: Evaluation of kinetic models for activation. *J.Gen.Physiol* **103**, 321-362.

Zhang, D., Pan, Z. H., Awobuluyi, M., & Lipton, S. A. (2001). Structure and function of GABA(C) receptors: a comparison of native versus recombinant receptors. *Trends Pharmacol.Sci.* **22**, 121-132.

Zhang, J. H., Araki, T., Sato, M., & Tohyama, M. (1991). Distribution of GABAA-receptor alpha 1 subunit gene expression in the rat forebrain. *Brain Res.Mol.Brain Res.* **11**, 239-247.

Zoli, M., Jansson, A., Sykova, E., Agnati, L. F., & Fuxe, K. (1999). Volume transmission in the CNS and its relevance for neuropsychopharmacology. *Trends Pharmacol.Sci.* **20**, 142-150.

CHAPTER II

MICROSCOPIC KINETIC DETERMINANTS OF MACROSCOPIC CURRENTS: INSIGHTS FROM COUPLING AND UNCOUPLING OF $GABA_A$ RECEPTOR DESENSITIZATION AND DEACTIVATION

Emmanuel J. Botzolakis, Matt T. Bianchi, Kevin F. Haas,
Janet L. Fisher, and Robert L. Macdonald

ABSTRACT

The time course of inhibitory postsynaptic currents (IPSCs) reflects $GABA_A$ receptor deactivation, the process of current relaxation following transient activation. Fast desensitization has been demonstrated to prolong deactivation, and these processes have been described as being "coupled". However, the relationship between desensitization and deactivation remains poorly understood. We investigated the "uncoupling" of $GABA_A$ receptor macroscopic desensitization and deactivation using experimental conditions that affected these two processes differently. Changing agonist affinity preferentially altered deactivation, changing agonist concentration preferentially altered macroscopic desensitization, and a pore-domain mutation prolonged deactivation despite blocking fast desensitization. To gain insight into the mechanistic basis for coupling and uncoupling, simulations were used to systematically evaluate the interplay between agonist affinity, gating efficacy, and desensitized state stability in shaping macroscopic desensitization and deactivation. We found that the influence of individual kinetic transitions on macroscopic currents depended not only on model connectivity, but also on the relationship among transitions within a given model. In addition, changing

single rate constants differentially affected macroscopic desensitization and deactivation, thus providing parsimonious kinetic explanations for experimentally observed uncoupling. Finally, these findings permitted development of an algorithmic framework for kinetic interpretation of experimental manipulations that alter macroscopic current properties.

INTRODUCTION

Transient synaptic release of GABA onto clusters of post-synaptic αβγ $GABA_A$ receptors represents a major mechanism of inhibition in the brain. The time course of $GABA_A$ receptor synaptic currents influences the complex behavior of inhibitory circuits, and many clinically useful drugs that potentiate $GABA_A$ receptor function act by prolonging IPSCs. Because IPSC duration depends primarily on post-synaptic $GABA_A$ receptor properties, the kinetic principles governing channel behavior have been the focus of active experimental investigation (Twyman and Macdonald, 1990; Jones and Westbrook, 1995; Galarreta and Hestrin, 1997; Haas and Macdonald, 1999; Bai et al, 1999; Mozrzymas et al., 2003). In particular, $GABA_A$ receptor deactivation, the process by which activated receptors relax toward the resting state, shapes the decay rate (and thus charge transfer) of IPSCs. This process can be studied experimentally by activating $GABA_A$ receptors with brief pulses of high concentration GABA and taking the ensuing deactivation time course as a model of synaptic currents.

Early work by Jones and Westbrook (1995, 1996) demonstrated that the fast phase of macroscopic desensitization played an important physiological role in augmenting IPSC duration, as the underlying desensitized state provided a surrogate high affinity conformation that prolonged the time during which an activated receptor could re-open. The importance of fast desensitization in shaping IPSCs has been validated by subsequent studies (Galarreta and Hestrin, 1997; Mozrzymas et al., 2003), and extended to include possible roles for slower phases of desensitization (Overstreet et al., 2000; Bianchi and Macdonald, 2002). This phenomenon of desensitization-deactivation "coupling", defined as increased macroscopic desensitization in the context of prolonged

deactivation (or decreased macroscopic desensitization in the context of accelerated deactivation), has been observed with changes in subunit composition (Haas and Macdonald, 1999; Bianchi et al., 2001; Lagrange et al., 2007), allosteric modulators (Bianchi et al., 2002; Feng and Macdonald, 2004), post-translational modifications (Hinkle and Macdonald, 2003), and disease-related mutations (Buhr et al., 2002).

While it is clear that desensitized states prolong the time course of deactivation, other receptor conformations (both conducting and non-conducting) are predicted to serve similar roles. Indeed, for Markovian models of ligand-gated ion channels, every agonist bound state delays unbinding in non-cyclic kinetic schemes (for example, Twyman et al., 1990; Celentano and Wong; 1994; Jones and Westbrook, 1995; Haas and Macdonald, 1999). This delay is unrelated to microscopic affinity (which also affects unbinding); occupancy of any kinetic state not associated with a binding/unbinding step is said to "trap" agonist (Bianchi and Macdonald, 2001a). The functional consequence of trapping is that additional transitions among open and closed states occur prior to agonist unbinding, the macroscopic correlate of which is a prolonged time course of deactivation. Although cyclic models have been proposed for cys-loop receptors (for example, Grosman and Auerbach, 2001; Scheller and Forman, 2002; Chang et al., 2002) and are not predicted to exhibit trapping *per se*, open and desensitized states will nonetheless prolong deactivation if they are high affinity states (low unbinding rate constants).

How other receptor conformations influence macroscopic desensitization, however, has received less attention (Mozrzymas et al., 2003). In many experimental circumstances, desensitization and deactivation appeared to be "uncoupled" (Bianchi et al., 2001b; Scheller and Forman, 2002; Fisher 2004; Mercik et al., 2006; Barberis et al.,

2007), such that decreased extents of macroscopic desensitization were associated with prolonged time courses of deactivation (or increased extents of macroscopic desensitization with accelerated deactivation time courses). This suggested that the kinetic determinants of macroscopic desensitization were distinct from those of deactivation, despite the known sensitivity of both processes to all rate constants in the gating scheme (Mozrzymas et al., 2003). To explore the kinetic basis for coupling and uncoupling (purely phenomenological descriptions of macroscopic currents), we focused on experimental manipulations that affected desensitization and deactivation differently: $GABA_A$ receptor agonists of different affinity, a range of concentrations of GABA application, and a pore-domain mutation that blocked fast desensitization. In addition, using kinetic simulations, we investigated the relative roles of agonist affinity, efficacy, desensitized state stability, and model connectivity in shaping macroscopic current properties. Analysis of simulated currents generated from a spectrum of rate constants and gating schemes provided mechanistic insight into experimental observations of coupling and uncoupling, and established a preliminary framework for interpretation of changes in macroscopic current properties due to the effects of mutations or allosteric modulators.

MATERIALS AND METHODS

Cell culture and expression of recombinant $GABA_A$ receptors

The cDNAs encoding rat α1, α6, β1, β3, γ2L, δ, and α1(L245S) $GABA_A$ receptor subunits were subcloned into the pCMVNeo vector. Human embryonic kidney cells (HEK293T; a gift from P. Connely, COR Therapeutics, San Francisco, CA) were maintained in DMEM supplemented with 10% fetal bovine serum and penicillin/streptomycin at 37°C in 5% CO_2 / 95% air. Experiments shown in Figure 2 were conducted using mouse L929 fibroblasts. Cells were transfected with 4 μg of each subunit plasmid and 1-2 μg of pHOOK (Invitrogen, Carlsbad, CA) for immunomagnetic bead selection of transfected cells using a modified calcium phosphate technique (Fisher et al., 1997). The next day, cells were replated and recordings were made at room temperature 18-30 hours later.

Electrophysiology

On recording days, transfected fibroblasts were bathed in an external solution consisting of (in mM): NaCl 142; KCl 8; $MgCl_2$ 6; $CaCl_2$ 1; HEPES 10; glucose 10 (pH adjusted to 7.4 with NaOH, ~330 mOsm). For whole cell studies, thin-walled borosilicate glass electrodes (World Precision Instruments, Pittsburgh, PA, USA) were pulled with a P-2000 laser puller (Sutter Instrument Co., San Rafael, CA, USA) and heat-polished to resistances of 0.5-1.5 MΩ. The internal solution consisted of (in mM): KCl 153; $MgCl_2$ 1; MgATP 2; HEPES 10; EGTA 5 (pH adjusted to 7.3 with KOH prior to ATP addition, ~300 mOsm). ATP was added on the day of recording. This combination

of internal and external solutions produced a chloride equilibrium potential near 0 mV. For excised patch experiments, thick-walled borosilicate glass was used with resistances of 5-15 MΩ after heat-polishing. Electrodes used for single channel recordings were coated with Q-Dope. Cells and patches were voltage-clamped using an Axon 200A or 200B amplifier (Axon Instruments, Foster City, CA). GABA was applied (via gravity) with a rapid perfusion system consisting of pulled multi-barrel square glass connected to a Warner Perfusion Fast-Step (Warner Instrument Corp., Hamden, CT), or "theta" glass mounted on a piezo-electric translator (Burleigh Instruments, Victor, NY). The solution exchange time for excised patch experiments was 400 μs or less, as determined after each recording by blowing off the patch and then stepping a dilute external solution across the open electrode tip. For whole cell experiments, solution flow rates were decreased by lowering the height of the source solutions so that open tip exchange times were ~ 1 ms, although slower exchange probably occurred around intact cells. All chemicals were from Sigma-Aldrich.

Analysis of currents

Currents were low-pass filtered at 2 kHz by the internal 4 pole Bessel filter of the amplifier, digitized at 10-20 kHz, and analyzed using the pCLAMP8 or 9 software suite (Axon Instruments, Foster City, CA). For experiments using outside out patches, multiple applications were made at 30-90 second intervals and averaged prior to kinetic analysis. The desensitization and deactivation time courses were fit using the Levenberg-Marquardt least squares method with multiple component exponential functions of the form $\Sigma\, a_n e^{(-t/\tau_n)}$, where n is the number of exponential components, a is the relative

(fractional) amplitude of the component at time = 0, *t* is time, and τ is the time constant. The number of components was incremented until additional components did not significantly improve the fit as determined by an F-test performed on residuals. Fitting the decay during 400 ms and 6 second applications sometimes revealed 3 or 4 exponential components, respectively. To simplify comparisons, no more than 2 or 3 components, respectively, were considered for analysis. A weighted summation of biphasic deactivation time courses ($a_f * \tau_f + a_s * \tau_s$) was used. Three component fits were not considered. Single channel recordings were obtained after 3-4 minutes of incubation in 1 mM GABA. Currents were idealized using a 50% threshold method with the Fetchan program of the pClamp suite, and binned histograms were fitted with multiple exponential functions using Interval5 software (Dr. B. Pallotta, University of North Carolina, Chapel Hill). Only main conductance state openings (approximately 2 pA at –75 mV) were included in the analysis. However, brief openings that reached threshold were accepted in the idealization. All patches contained more than one channel as indicated by overlapped openings. Although these openings were ignored in the idealization, the presence of multiple openings complicates the analysis of closed times (artificially shortened), opening frequency (artificially increased), and open probability (artificially increased). Numerical data were expressed as mean ± SEM. Statistical significance, using Student's *t* test (paired or unpaired as appropriate) was taken as $p < 0.05$.

Simulations

Kinetic modeling was carried out with Berkeley Madonna 3.1 (www.berkeleymadonna.com), a differential equation solver, using the fourth order Runge-Kutta method with a time interval of 10-100 μs.

RESULTS

Agonists with different affinities for the $GABA_A$ receptor altered deactivation without altering macroscopic desensitization

We tested the hypothesis that deactivation could be altered independent of macroscopic desensitization using ligands with higher (muscimol) or lower (THIP) affinity than GABA for $GABA_A$ receptors. Since muscimol (Twyman and Macdonald, unpublished observation) and THIP (Mortensen et al., 2004) evoked single channel currents similar to those evoked by GABA, we predicted that macroscopic desensitization would be similar for all three agonists when applied at nearly-saturating concentrations, as activated receptors would transition within the same di-liganded portion of the receptor gating scheme. In contrast, we expected that deactivation would be markedly different for each of the three agonists, as the unbinding rate plays an important role in determining how quickly activated receptors return to the resting state (Jones et al, 1998, Li and Pearce, 2000).

Macroscopic desensitization of α1β1γ2L receptor currents was investigated in response to rapid application of EC-equivalent concentrations of each agonist, approximated from whole cell concentration-response curves generated using a Y-tube perfusion system (not shown). Outside-out patches were obtained from transfected L929 fibroblasts, and agonists were applied rapidly with the concentration-jump technique (see methods). GABA- and THIP-evoked currents desensitized to similar extents during 400 ms applications (66.1 $\pm$ 6.1 %; n = 6, for 100 μM GABA; 59.6 $\pm$ 5.0 %; n = 11, for 10 mM THIP) (Figure 1A1, 1B1). Also, 8 of 11 patches exposed to THIP exhibited a

biphasic desensitization time course that included a fast (~20 ms or less) phase. The rate and extent of the fast phase of desensitization was similar between the biphasic currents evoked by GABA (12.1 ± 3.1 ms; 51.1 ± 6.7 %; n = 6) and THIP (11.2 ± 2.2 ms; 49.7 ± 6.0 %; n = 11). Currents evoked by muscimol (30 μM) activated more slowly (5.7 ± 0.9 ms; n = 4) than those evoked by THIP (2.2 ± 0.4 ms; n = 11) or GABA (1.8 ± 0.2 ms; n = 6) currents (not shown). However, the extent of desensitization (53.2 ± 4.9 %; n = 4) and the rate and relative proportion of fast desensitization (17.4 ± 5.6 ms; 44.5 ± 4.5 %; n = 4) of biphasic currents activated by muscimol were not different than those observed for GABA or THIP (Figure 1C1).

In contrast, the deactivation time course depended strongly on agonist affinity (Figure 1A1, 1B1, 1C1). To further explore this difference, brief (5 ms) applications of each agonist were applied (Figure 1A2, 1B2, 1C2). For muscimol, some of these applications were made using a longer duration (30 ms) to ensure that peak current was obtained. Since the resulting deactivation time courses were similar between these two conditions, the results were pooled. The weighted time constants of current deactivation were 10.5 ± 0.9 ms (n = 5) for THIP, 61.3 ± 6.8 ms (n = 5) for GABA, and 198.1 ± 48.0 ms (n = 6) for muscimol (Figure 1D). Whereas brief GABA- and muscimol-evoked currents decayed bi-phasically, in 4 of 5 THIP-evoked currents, the decay was dominated by a fast phase (>95%). These results were similar to those of Jones et al. (1998), who reported that currents evoked by muscimol and the low affinity agonist β-alanine had longer and shorter deactivation time courses, respectively, than those evoked by GABA, despite identical desensitization kinetics.

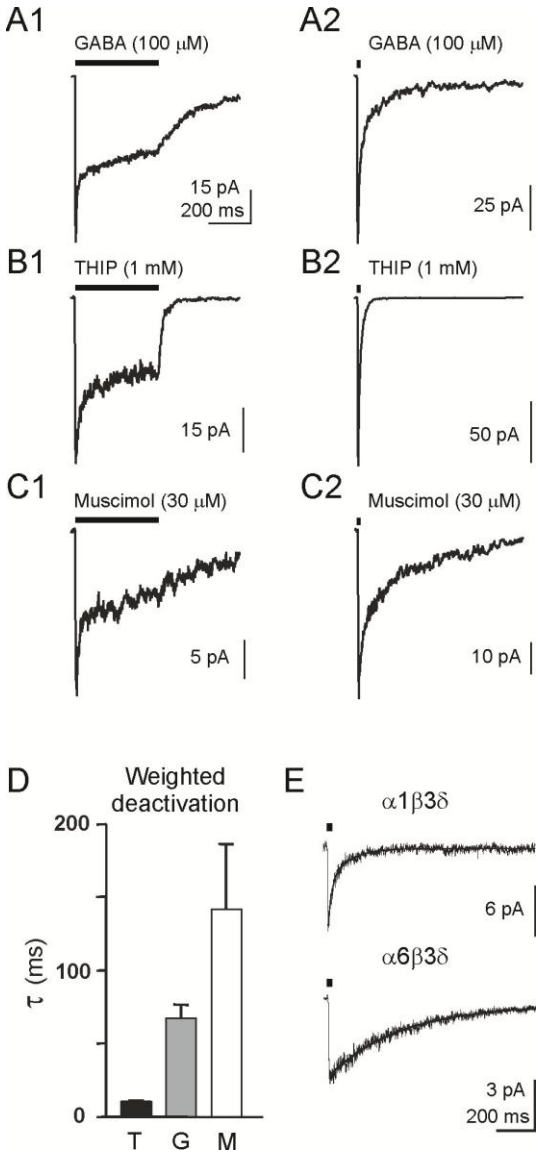

Figure 1. Macroscopic desensitization and deactivation of α1β1γ2L $GABA_A$ receptor currents evoked by different agonists

Currents were obtained from outside-out membrane patches using concentration jumps of 400 or 5 ms duration into equivalent concentrations of GABA (A1, A2), THIP (B1, B2), or Muscimol (C1, C2). The currents displayed were obtained from different patches. The horizontal scale bar in panel A1 applies to panels A-C. The agonist pulse duration is shown by a filled bar above each trace. Quantification of macroscopic desensitization is given in the text. D. Weighted time constants of deactivation following brief pulses of 1 mM THIP (T; gray bar), 100 μM GABA (G; filled bar), and 30 μM Muscimol (M; open bar). E. Deactivation currents from patches containing α1β3δ (top trace) and α6β3δ receptors (bottom trace) following a 5 ms pulse of 1 mM GABA (filled bar). The horizontal scale bar applies to both traces.

This apparent uncoupling of desensitization and deactivation demonstrated that the unbinding rate constant could dominate the deactivation time course, even in the presence of fast desensitization. To explore this observation, deactivation time courses were measured following activation of different receptor isoforms by the same agonist (note that changes in agonist affinity can also be related to subunit composition). While kinetic models of α6 subunit-containing αβδ receptors are unavailable, their low GABA EC_{50} compared to α1 subunit-containing receptors has been attributed to increased affinity (Saxena and Macdonald, 1996; Fisher et al., 1997; Fisher 2004). When excised patches containing α1β3δ or α6β3δ receptors were exposed to brief (5 ms) pulses of GABA (1 mM), those containing the α6 subunit had markedly slower deactivation (Figure 1E). Neither receptor isoform, however, exhibited fast desensitization (Bianchi et al., 2002). Taken together, these data suggested that fast desensitization was neither necessary nor sufficient for prolonged deactivation. In addition, the data also raised the more general questions: under what conditions could other rate constants in the gating scheme dominate the deactivation time course, and in what context would this also be manifested as desensitization-deactivation uncoupling?

Different agonist concentrations altered macroscopic desensitization without affecting deactivation

One interpretation of the apparent increase in macroscopic desensitization observed with increasing agonist concentrations (Figure 2A) is that desensitized states are preferentially accessed during activation with high agonist concentrations. However, the slow activation observed with low agonist concentrations may mask the manifestation of an inherently concentration-independent desensitization process (Celentano and Wong,

1994), similar to slow agonist perfusion (Bianchi and Macdonald, 2002). Indeed, "pre-desensitization" has been shown using pre-incubations of low GABA concentrations prior to test jumps into a saturating GABA concentration (Overstreet et al., 2001; Lagrange et al., 2007). If desensitized states were accessible at low GABA concentrations, similar deactivation time courses would be predicted over a broad range of GABA concentrations despite variable macroscopic desensitization (i.e., uncoupling). In contrast, if desensitized state accessibility decreased with lower GABA concentrations, the observed loss of macroscopic desensitization would be associated with an accelerated deactivation time course (i.e., coupling).

Macroscopic desensitization was measured during 4-6 second applications of different GABA concentrations to cells expressing α1β3γ2L receptors (Figure 2A). Although the extent of desensitization varied from 0% to 80% over this concentration range (Figure 2B), deactivation time courses were indistinguishable at concentrations from 1 mM (near-saturating) to 1 μM (approximately EC_{10}) (Figure 2C, D), providing an additional experimental example of desensitization-deactivation uncoupling. The deactivation time course was significantly faster only following the 300 nM GABA applications (Figure 2D), possibly caused by a significant mono-liganded component at this low concentration. Similar results were obtained in excised patches, eliminating the possibility that our findings were an artifact of the slower solution exchange characteristic of whole-cell recording (not shown). This suggested that the underlying kinetic processes shaping deactivation were unchanged over a wide range of GABA

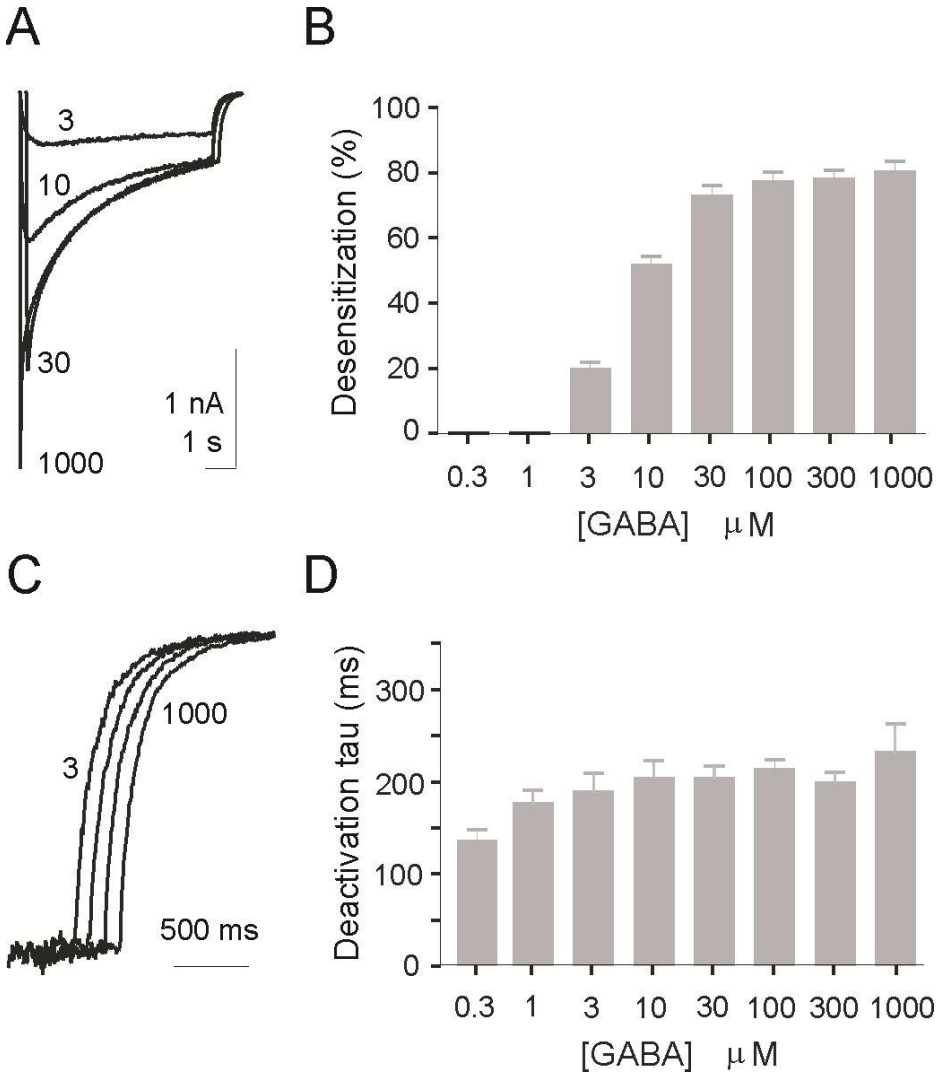

Figure 2. Macroscopic desensitization and deactivation of α1β3γ2L receptor currents evoked by different GABA concentrations

A. Representative traces from a single cell exposed to increasing concentrations of GABA were labeled with concentration in μM. The 30 μM trace was staggered horizontally for clarity. B. The extent of macroscopic desensitization, measured as % current loss during the GABA pulse, was plotted for each concentration. C. Deactivation currents expanded from the traces shown in panel A. The traces were staggered horizontally to illustrate their similar time courses. D. The weighted deactivation time constant was shown for 8 concentrations of GABA (4-6 second applications each). Only the deactivation following the 300 nM concentration was significantly faster than the others.

concentrations, and thus, that accessibility of desensitized states was not compromised. As in the previous section, this demonstrated that prolonged deactivation was possible even in the absence of fast macroscopic desensitization, and provided an additional example of uncoupling.

A channel mutation blocked macroscopic desensitization without accelerating deactivation

Mutations of the conserved pore-lining TM2 9'leucine in the cys-loop family of receptors to the polar residues serine or threonine have been shown to alter macroscopic current properties via an increase in single channel mean open time (Revah et al, 1991; Yakel et al, 1993; Filatov and White, 1995; Thompson et al, 1999). Specifically, during rapid kinetic studies of the α1(L9'T)β2γ2L receptor mutation, the extent of macroscopic desensitization was found to decrease despite a prolonged deactivation time course (Scheller and Forman, 2002). To better understand the mechanistic basis for this desensitization-deactivation uncoupling, we analyzed the kinetic properties of a similar mutation in the $GABA_A$ receptor α1 subunit.

α1(L9'S)β3γ2L receptors exhibited a left-shifted whole cell GABA EC_{50} of ~300 nM (Figure 3A), as well as bicuculline-sensitive spontaneous activity (not shown), consistent with previous studies (Labarca et al, 1995; Chang and Weiss, 1999; Thompson et al, 1999, Bianchi and Macdonald, 2001b; Scheller and Forman, 2002). During a 6 second application of GABA to excised outside-out patches, macroscopic desensitization of α1(L9'S)β3γ2L currents was slower and less extensive than that of α1β3γ2L currents (Figure 3B). In contrast to α1β3γ2L currents, which desensitized with three exponential

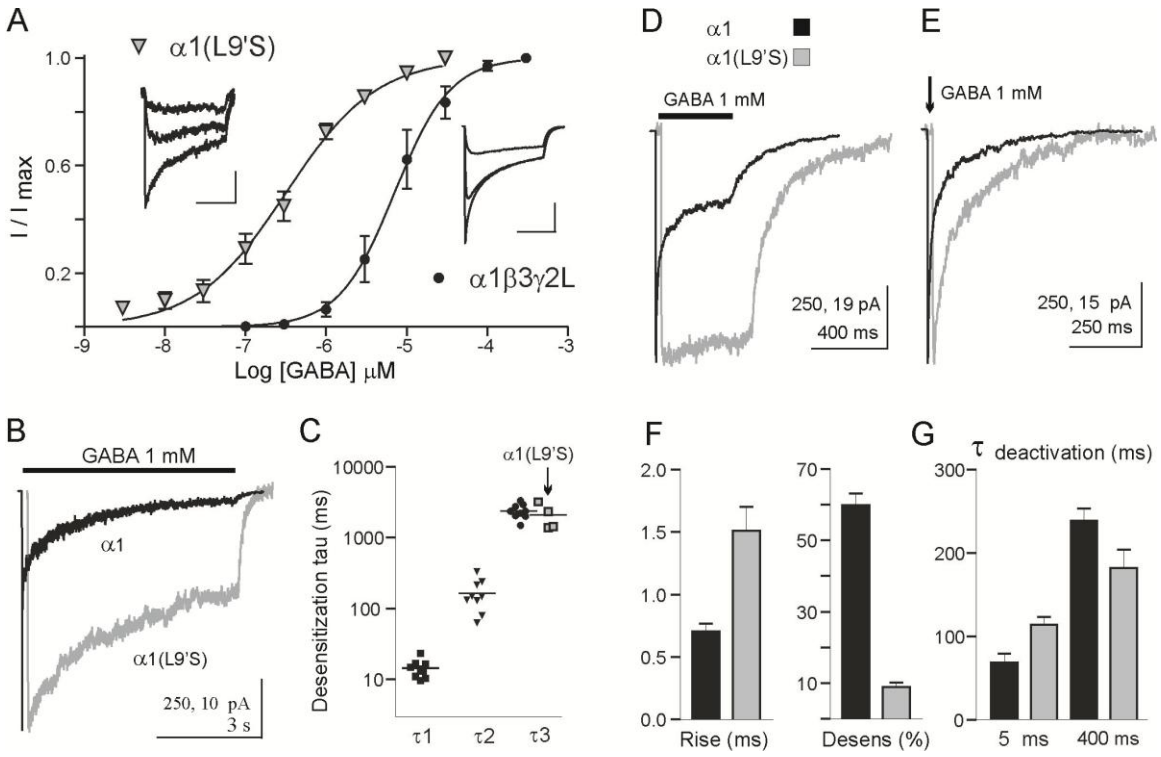

Figure 3. Characterization of α1(L9'S)β3γ2L GABA$_A$ receptor currents

A. Concentration-response curves obtained for α1β3γ2L (filled circles) and α1(L9'S)β3γ2L (gray triangles) receptors. Representative current traces from individual cells are shown at concentrations of 3, 10, and 100 μM for α1β3γ2L receptors, and 0.03, 0.1, and 10 μM for α1(L9'S)β3γ2L receptors. Vertical scale bars are 1.0 nA and 50 pA for α1β3γ2L and α1(L9'S)β3γ2L receptors, respectively. Horizontal scale bars are 3 s for both isoforms. B. Currents evoked by 6 s applications of 1 mM GABA to outside out patches containing α1β3γ2L (black trace) and α1(L9'S)β3γ2L (gray trace) receptors. Traces were normalized to peak and slightly staggered horizontally for comparison. C. Scatter plot of the time constants obtained from exponential fitting of the desensitization time course. Three time constants were required to fit the time course of α1β3γ2L receptor desensitization (filled symbols), while α1(L9'S)β3γ2L receptor desensitization was mono-exponential (gray symbols). Note the logarithmic axis. D, E. α1β3γ2L (black traces) and α1(L9'S)β3γ2L (gray traces) receptor currents were evoked by 400 ms (Panel D) and 5 ms (Panel E) concentration jumps into 1 mM GABA. F. Activation rates (left), as indicated by the 10-90% rise time observed for 400 ms concentration jumps, were shown for both isoforms. The extent of macroscopic desensitization was plotted as the loss of current during the 400 ms application (right). G. The weighted deactivation time constant was shown for α1β3γ2L (solid bars) and α1(L9'S)β3γ2L (gray bars) receptor currents following 5 ms (left) and 400 ms (right) application durations. Filled squares in Panel D indicate isoform color for bar graphs in Panels F and G.

components (Figure 3C, filled symbols), α1(L9'S)β3γ2L currents desensitized with a single exponential component (Figure 3C, open squares), similar to the results of Scheller and Forman (2002). The single α1(L9'S)β3γ2L desensitization time constant (2098 ± 435 ms; n = 4) was not different from the longest wild-type desensitization time constant (τ3; 2395 ± 184 ms; n = 9), but its relative contribution was increased from 37.0 ± 3.0 % to 57.5 ± 6.3 %.

Shorter duration pulses of GABA (1 mM) were used to investigate the effects of the α1(L9'S) subunit mutation on deactivation (Figure 3D, 400 ms; Figure 4E, 5 ms). The 10-90% rise times were significantly increased by the α1(L9'S) subunit mutation from 0.71 ± 0.07 ms to 1.51 ± 0.19 ms (Figure 3F, left). For 400 ms pulses, the extent of desensitization was minimal for α1(L9'S)β3γ2L compared to wild-type receptors (Figure 3F, right), while the deactivation time courses of α1β3γ2L (238.7 ± 14.7 ms, n = 6) and α1(L9'S)β3γ2L (181.8 ± 21.9 ms, n = 9) currents were similar. Consistent with prior reports, this uncoupling manifested as the loss of fast desensitization without accelerated deactivation time course. After 5 ms pulses, deactivation was faster than after 400 ms pulses for both mutant and wild-type receptors, although the time course was significantly longer for the mutant (114.0 ± 9.4 ms) in comparison to wild-type (68.4 ± 10.9 ms) receptors (Figure 3G). Thus, with longer GABA exposure, prolongation of deactivation for the wild-type current (~300% increase) was greater than for the mutant current (~40% increase) (Figure 3G).

The dependence of the deactivation time course on the duration of GABA exposure has been suggested to reflect increasing occupancy of desensitized states (Jones and Westbrook, 1995). Thus, the failure to observe such an increase with the α1(L9'S)

mutation, particularly given the absence of fast macroscopic desensitization, could indicate failure to access desensitized state(s). However, this would be expected to accelerate deactivation, while in this case, deactivation was prolonged following synaptic pulse durations. We hypothesized that increased efficacy could account for the constellation of findings, as this would be consistent with prolonged deactivation after brief pulses, decreased macroscopic desensitization, and a left-shifted GABA EC_{50}. Moreover, since deactivation following prolonged agonist exposure is dominated by the ability of long-lived desensitized states to delay agonist unbinding, this would also be consistent with a similar deactivation time course following long applications.

Changes in gating efficacy accounted for slow deactivation despite reduced desensitization of α1(L9'S)β3γ2L receptor currents

Although it has been proposed that increased spontaneous channel activity reflects increased efficacy of liganded gating (Grosman and Auerbach, 2000; Scheller and Forman, 2002), spontaneous openings may involve a different reaction pathway than the gating of liganded receptors, thus necessitating single channel analysis. To test the hypothesis that prolonged deactivation after brief pulses (despite absent fast desensitization) in α1(L9'S) mutants was due to increased gating efficacy, we obtained single channel recordings from α1β3γ2L and α1(L9'S)β3γ2L receptor channels (Figure 4A and 4B). Both mean open time (2.5 versus 1.8 ms) and burst duration (18.6 versus 3.7 ms) were significantly increased by the mutation. Open duration histograms for α1β3γ2L and α1(L9'S)β3γ2L receptor single channel currents were both fitted best by three exponential functions (Figure 4C and 4D). The increase in mean open and burst

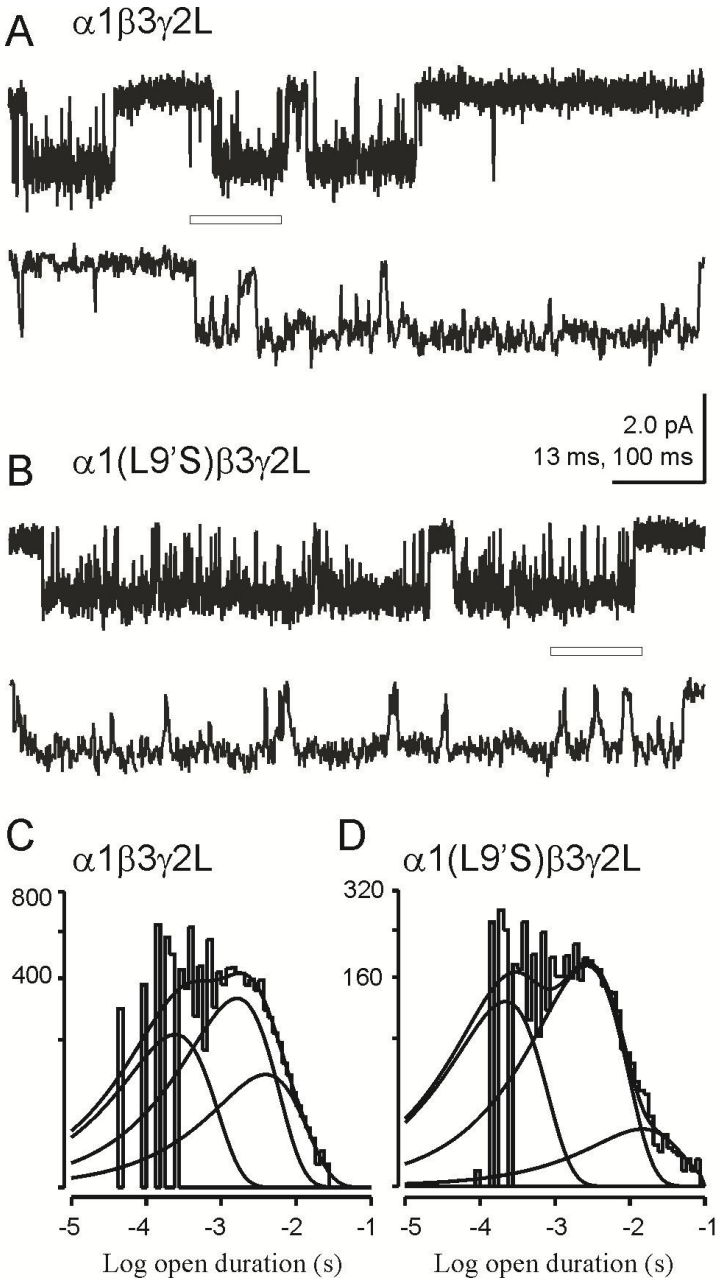

Figure 4. Single channel analysis of α1(L9'S)β3γ2L receptors

A. Representative α1β3γ2L receptor single channel events recorded from an outside-out patch voltage clamped at –75 mV are shown. A portion of the continuous trace (open bar) is expanded below. Channel openings are visible as downward deflections from the baseline current. B. Continuous trace showing α1(L9'S)β3γ2L receptor single channel events for comparison. C, D. Open time histograms for WT (Panel C) and L9'S mutant (Panel D) single channel recordings. Open durations were fitted best with three exponential functions in each case (overlapping curves in each plot). The sum of the three exponentials was shown as the top curve in each plot.

durations were accounted for in part by longer time constants associated with the two longest open components (O2 and O3). Opening frequency, open probability, and closed time distributions were not investigated, since the patches used for analysis contained multiple channels (overlapped openings). While development of an exhaustive kinetic scheme of the mutated receptors was not possible with this limited data set, the results suggested that increased efficacy could explain prolonged deactivation despite reduced macroscopic desensitization, and supported the idea that multiple rate constants in the gating scheme (not just the agonist binding and unbinding rates) could mediate desensitization-deactivation uncoupling.

Kinetic modeling explored the role of microscopic kinetic parameters on macroscopic desensitization and deactivation

Although comprehensive kinetic models have been developed that account for both the microscopic and macroscopic properties of $GABA_A$ receptors (Haas and Macdonald, 1999; Figure 5A), simple models are often sufficient to illustrate the salient features of GABA-evoked currents such as rapid activation, extensive macroscopic desensitization, and prolonged deactivation. In addition, with fewer free parameters, they facilitate systematic exploration of relationships between individual rate constants and macroscopic current properties. Historically, two simple models have been commonly used to describe the behavior of ligand-gated ion channels. Katz and colleagues described cholinergic responses with a linear scheme of binding, isomerisation to the open state, and subsequent entry into the desensitized state (Katz and Thesleff, 1957; Figure 5B). Jones and Westbrook (1995) explained $GABA_A$ receptor desensitization

A

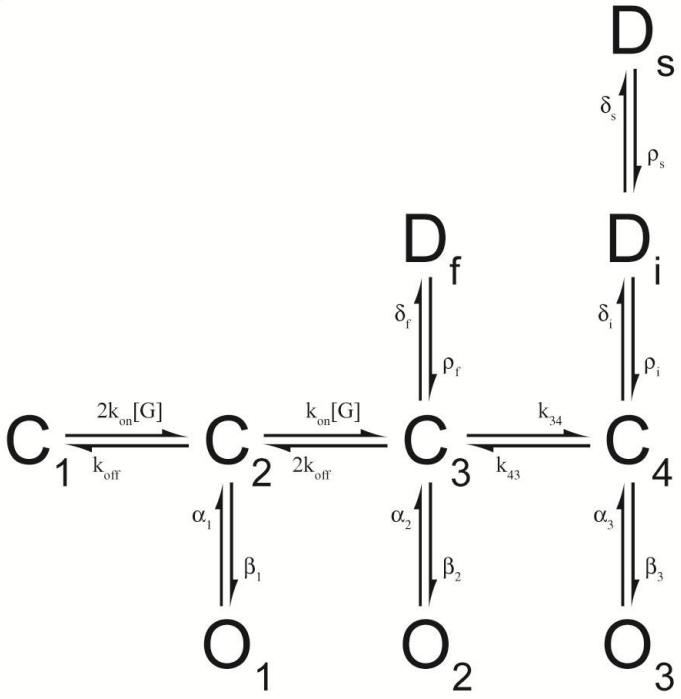
D s
δ s
ρ s
D f
D i
δ f
ρ f
δ i
ρ i
C 1
2k on[G]
k off
C 2
k on[G]
2k off
C 3
k 34
k 43
C 4
α 1
β 1
α 2
β 2
α 3
β 3
O 1
O 2
O 3

B

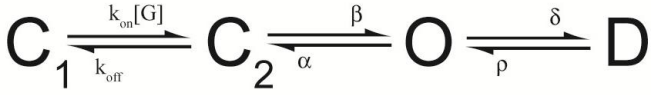
C 1
k on[G]
k off
C 2
β
α
O
δ
ρ
D

C

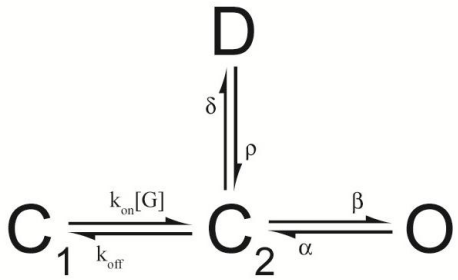
D
δ
ρ
C 1
k on[G]
k off
C 2
β
α
O

Figure 5. Kinetic models of ligand-gated ion channel function

A. Comprehensive kinetic scheme for the α1β3γ2L receptor isoform taken from Haas and Macdonald (1999). For simplicity, the two distal "intraburst" closed states connected to each open state were omitted from the display. Closed (C), open (O), and desensitized (Df, "fast"; Di, "intermediate"; Ds, "slow") states were reversibly interconnected. The microscopic transitions associated with agonist binding were labeled k_{on} and k_{off} for association and dissociation rate constants, respectively. Each agonist binding step was taken to be equivalent and independent in this scheme (the first binding and unbinding rates were therefore multiplied by 2). [G], concentration of GABA. B. 4-state kinetic model, in linear arrangement. A single binding step connects C1 and C2. The O state is accessed from C2, and is arranged in series with the D state D. C. 4-state kinetic model, in branched arrangement. D and O states are arranged in parallel, each being directly accessible following sojourns in the ligand-bound closed state. All rate constants referred to in the text and in subsequent figures have units of s^{-1}, except for the binding rate, k_{on}, which is multiplied by the concentration of ligand, and thus has units of $s^{-1} M^{-1}$.

using a branched arrangement of states, which at high agonist concentration, reduces to the scheme shown in Figure 5C. In both cases, the single non-conducting state not associated with a binding step was designated the desensitized (D) state. This was supported by the fact that no combination of rate constants supported macroscopic desensitization in the absence of this state (Appendix IV).

To gain insight into the mechanistic basis for coupling and uncoupling, simulations were conducted to explore the effects of agonist affinity, agonist concentration, open state efficacy, and desensitized state stability (defined as the ratio of the entry rate, δ, to the exit rate, ρ) on macroscopic desensitization and deactivation. While the comprehensive α1β3γ2L receptor model was used to recapitulate our experimental findings, the simple 4-state models were used to systematically evaluate the impact of each kinetic parameter on macroscopic currents. By co-varying rate constants, the kinetic conditions for which deactivation was either coupled to or uncoupled from macroscopic desensitization were determined. In this manner, we elucidated patterns

relevant to the experimental setting, where neither the kinetic model nor the relevant underlying transitions are typically known.

The relationships among agonist unbinding, macroscopic desensitization, and deactivation

Our experimental observations using agonists of different affinity suggested that unbinding, the terminating step in the relaxation of activated receptors to the resting state, could have a dominant influence on deactivation independent of the rate or extent of macroscopic desensitization. This form of desensitization-deactivation uncoupling was further examined using the comprehensive α1β3γ2L receptor model (Figure 5A) (Haas and Macdonald, 1999). For a 30-fold increase (Figure 6A1) or decrease (Figure 6A2) in k_{off}, the peak current amplitude and shape of macroscopic desensitization were nearly overlapping during activation by a near-saturating GABA concentration, while deactivation differed markedly (current with the "wild-type" k_{off} is marked with an asterisk). Additional increases in k_{off} resulted in decreased peak amplitude, attributable to substantial shifts in GABA EC_{50} that rendered 1 mM GABA sub-saturating and thus slowed macroscopic activation (which also resulted in decreased apparent desensitization; not shown). The same phenomena were also observed for alterations in k_{off} using the 4-state branched and linear models (not shown). These results confirmed that deactivation could be markedly altered by changes in unbinding that produced little effect on macroscopic desensitization, similar to our experimental observations with currents evoked by agonists of different affinity (Figure 1; Jones et al., 1998).

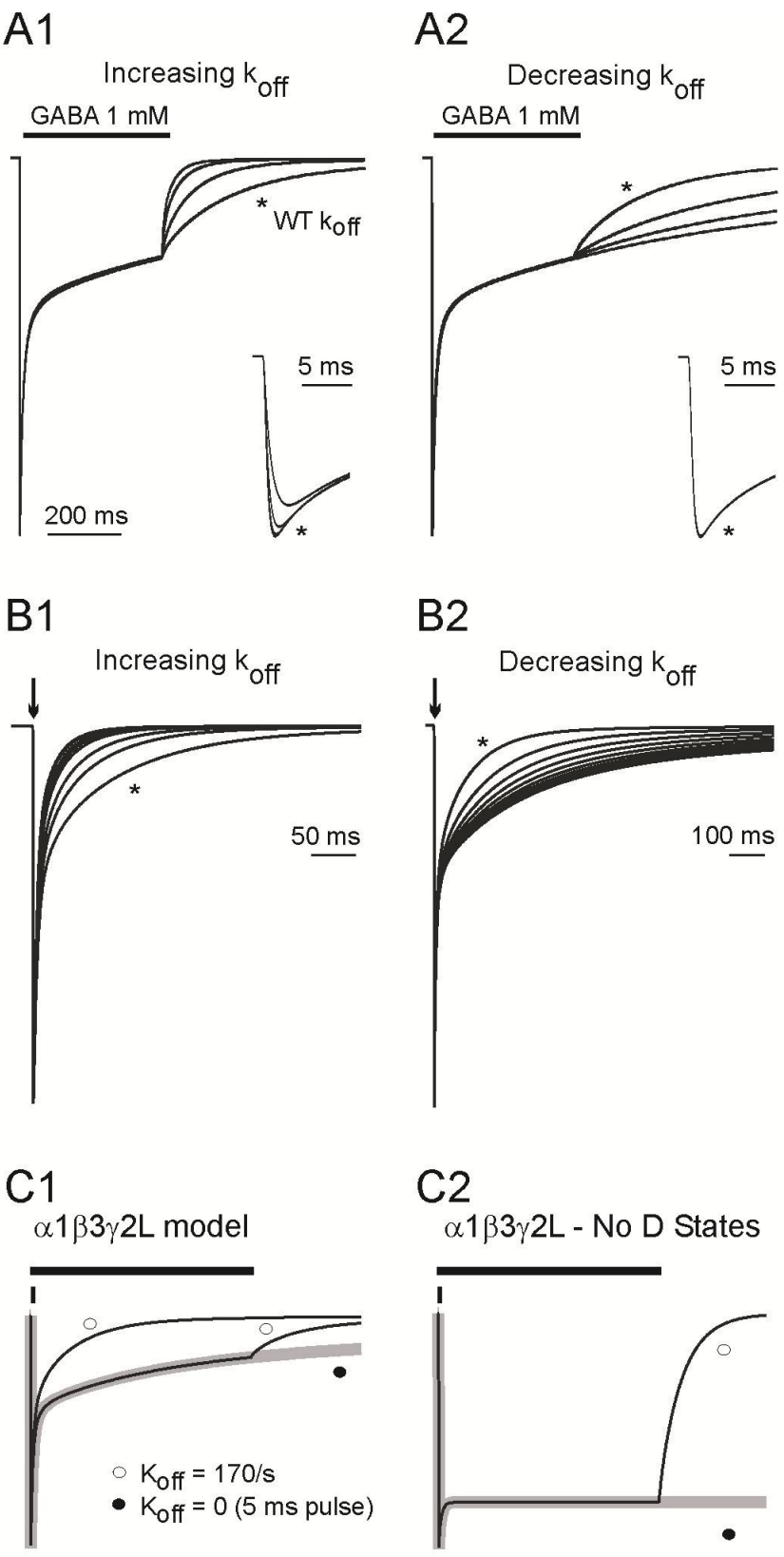
A1
Increasing k_{off}
GABA 1 mM
WT k_{off}
5 ms
200 ms
A2
Decreasing k_{off}
GABA 1 mM
5 ms
B1
Increasing k_{off}
50 ms
B2
Decreasing k_{off}
100 ms
C1
α1β3γ2L model
K_{off} = 170/s
K_{off} = 0 (5 ms pulse)
C2
α1β3γ2L - No D States

Figure 6. Predicted effects of altering microscopic unbinding on macroscopic desensitization and deactivation

A. Simulated responses to 400 ms applications of near-saturating GABA (1 mM) were overlapped for various values of k_{off} using the comprehensive α1β3γ2L receptor model (Figure 5A). In the left panel, k_{off} = 5100, 1700, 510, and 170 s^{-1}. In the right panel, koff = 170, 51, 17, and 5.1 s^{-1}. Currents were not normalized. Insets show the first 10 ms of the overlapped traces to illustrate the effect of altering k_{off} on activation rate and peak current amplitude. * indicates "wild-type" deactivation, where k_{off} = 170 s^{-1}. B. Simulated current responses to 5 ms applications of GABA (1 mM) for wild type (*) and either increasing (B1; k_{off} varied from 170 to 170,000 s^{-1}) or decreasing (B2; k_{off} varied from 170 to 0 s^{-1}) unbinding rates. For the two fastest k_{off} traces, the GABA concentration was raised to 20 mM to overcome the extremely low affinity. C. In the left panel, simulated responses of the α1β3γ2L model to 5 or 1000 ms pulses (black lines, open circles) were overlaid with a simulated response to a 5 ms pulse when k_{off} was set to zero (gray line, filled circle). In the right panel, the response of the same model, but without D states, to a 1 second application of 1 mM GABA (black line, open circle) is overlaid with a 5 ms application for which k_{off} was set to zero (gray line, filled circle). The small amount of macroscopic desensitization that persisted even in the absence of desensitized states was due to C4 serving as a "branched" D state relative to O2.

Macroscopic desensitization sets a boundary condition for deactivation time course

To investigate the relationship between k_{off} and deactivation under synaptic conditions, currents evoked by brief GABA pulses were simulated using the α1β3γ2L model in the context of increasing (Figure 6B1) or decreasing (Figure 6B2) k_{off}. The resulting deactivation currents were multi-phasic, with the fast phase demonstrating less sensitivity to changes in k_{off} than the slower phases (Figure 6B1, 6B2). Overall, both slow and fast phases of deactivation became faster with increasing k_{off} until approaching a limit at higher k_{off} values (Figure 6B1). Similarly, with decreasing k_{off}, both slow and fast phases of deactivation became slower until approaching a limit at lower k_{off} values (Figure 6B2). The observation of a fast limit under conditions of extremely rapid unbinding was not surprising, since open receptors must close before unbinding, in which case, open durations (or in the case of more complex models, burst/cluster durations)

become rate limiting. The basis for the slow limit, however, was less clear. Given that the slowly desensitizing α6β3δ isoform also deactivated slowly (Figure 1E), we hypothesized that *macroscopic* desensitization served to *limit* the deactivation time course. Although this initially seemed counterintuitive, additional simulations revealed a simple kinetic basis for this phenomenon.

The simulated response to a 5 ms pulse of 1 mM GABA using the kinetic scheme of Figure 5A and the default value for k_{off} (Figure 6C1, left open circle) was compared to the response of the same brief pulse in the extreme case when k_{off} was set to zero (Figure 6C1, filled circle). As expected, when unbinding could not occur, the deactivation time course was markedly prolonged. Interestingly, when the response to a 1 second application of 1 mM GABA was overlaid on these responses (Figure 6C1, right open circle), it was found to follow a time course identical to that of deactivation following the 5 ms pulse when k_{off} was set to zero (Figure 6C1, filled circle). The overlap between deactivation following the 5 ms pulse (where unbinding was impossible) and macroscopic desensitization during the 1 second pulse (where unbinding was possible, but functionally irrelevant given the near-saturating agonist concentration) occurred simply because receptors were fully liganded in both conditions, and as a result, behaved in the same manner. Similar constraints on the deactivation time course by macroscopic desensitization were also evident with the 4-state models (not shown).

The idea that the time course of deactivation could not be slower than macroscopic desensitization was illustrated further by repeating the simulations of Figure 6C1 in the absence of all three D states. We compared the currents generated by a 1 second pulse of 1 mM GABA using the default value for k_{off} (Figure 6C2, open circle)

with a 5 ms pulse where k_{off} was set to zero (Figure 6C2, filled circle). Again, deactivation following the brief pulse followed the same time course as that of macroscopic desensitization during the 1 second pulse. However, compared to deactivation in the context of all three D states, the overall time course was markedly prolonged (compare Figure 6C1 to Figure 6C2; filled circles). Thus, when unbinding was impossible, desensitization-deactivation uncoupling always occurred, as decreased macroscopic desensitization allowed for prolonged deactivation, while increased macroscopic desensitization forced deactivation to accelerate.

It should be noted that the constraint imposed by macroscopic desensitization on deactivation actually depended on the duration of agonist application. For example, the constraint imposed on the fast phase of deactivation was limited to brief applications, because macroscopic desensitization manifested a fast phase selectively in this time domain. In other words, only if an agonist pulse terminated prior to the onset of a given phase of macroscopic desensitization could that phase constrain deactivation. Thus, while deactivation following brief pulses was constrained by all phases of macroscopic desensitization, deactivation following prolonged pulses, where macroscopic fast desensitization had already occurred, was only constrained by slower phases of desensitization.

Although the extreme case of irreversible binding was used to illustrate the complex interplay between macroscopic desensitization and deactivation, the interpretations are applicable to the continuum of rate constants likely to occur biologically. The implication of fast macroscopic desensitization in shaping the fast phase of deactivation is of particular physiological relevance since rapid desensitization

has been widely observed in native and recombinant $GABA_A$ receptor currents (Celentano and Wong, 1994; Jones and Westbrook, 1995; Tia et al., 1997, Haas and Macdonald, 1999; Li and Pearce, 2000; Burkat et al., 2001; Mozrzymas et al., 2003; Scheller and Forman, 2002; Yang et al., 2002). In summary, the simulations suggested that the effect of agonist affinity on deactivation was not actually independent of macroscopic desensitization. *Instead, agonist affinity determined the "position" of deactivation between two limits: a fast limit dictated by channel gating, and a slow one imparted by the shape of macroscopic desensitization.*

The relationships among agonist concentration, macroscopic desensitization, and deactivation

Higher concentrations of GABA evoke faster and more extensively desensitizing currents (Figure 2A), but it is important to distinguish between two possible explanations for this phenomenon: increased D state occupancy, or improved resolution of the concentration-independent desensitization process. While the experimental observation of similar deactivation time courses for currents evoked by concentrations above ~EC_{20} (3 μM) suggested that relative occupancy of microscopic states was similar over this range of concentrations, we further explored this hypothesis using kinetic simulations. Using the α1β3γ2L model (Figure 5A), currents evoked by four different agonist concentrations were simulated (Figure 7A). Total D state occupancy (sum of D_f + D_i + D_s) is represented in the upward traces, while total O state occupancy (sum of O1 + O2 + O3) is represented in the downward traces (i.e., the currents). When the current evoked by 10 μM GABA (~EC_{30}) was compared with the current evoked by 1 mM GABA

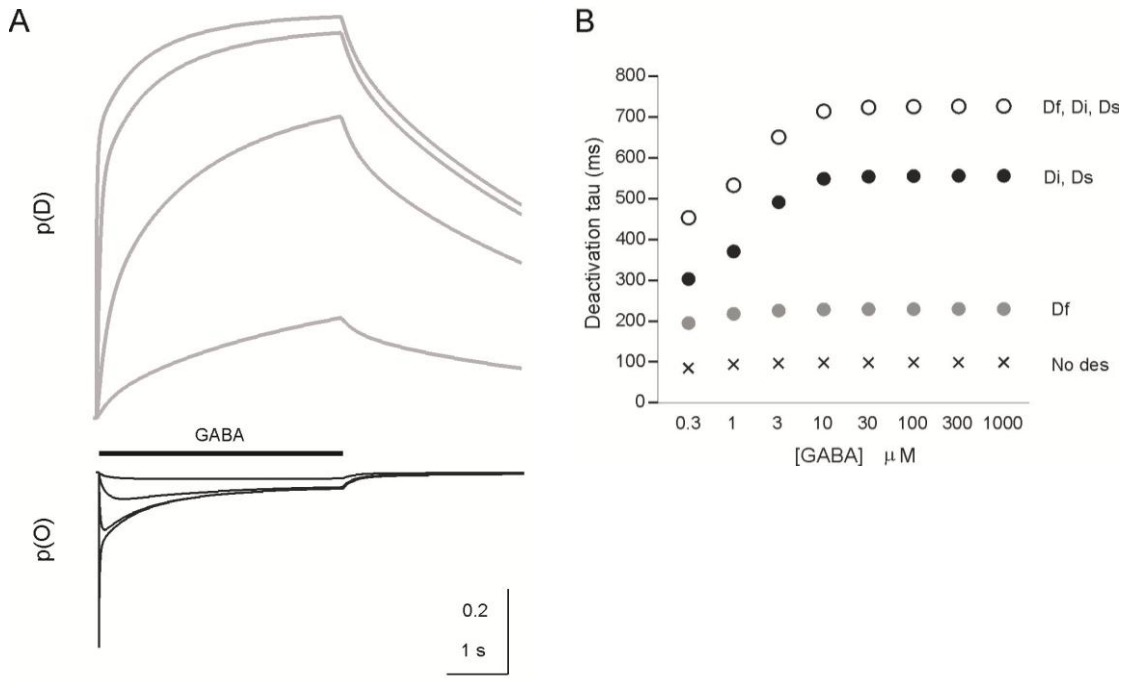

Figure 7. Predicted concentration dependence of macroscopic desensitization and deactivation

A. The sum of desensitized state (upward traces) and open state (downward traces) occupancies are shown for 4 agonist concentrations (1, 3, 10, and 1000 μM) using the comprehensive α1β3γ2L receptor model from Figure 5A. The top of the upward traces and the bottom of the downward traces corresponds to 1000 μM. The calibration bars apply to both sets of traces. The vertical calibration represents a probability of receptor occupancy of 0.2. Note that the currents (downward traces) and the D state probability curves (upward traces) represent the combined occupancy of all 3 O and D states, respectively. B. Weighted deactivation time constant of simulated currents generated with the α1β3γ2L model over a range of GABA concentrations applied for 400 ms. For each concentration, simulations were generated using the "wild-type" rate constants (open circles), setting the entry rate into Df to zero (filled circles), setting the entry rates into both Di and Ds to zero (gray circles), and setting entry rates into all 3 desensitized states to zero (x). The labels to the right of the circles indicated the desensitized states that remained accessible for a set of simulations. The longer deactivation predicted by the model relative to the experimental data may be attributed to a long time constant that is unlikely to be resolved experimentally because its small amplitude would be difficult to distinguish from baseline noise.

(~EC_{100}), marked differences were observed in the extent of macroscopic desensitization, though the fractional occupancy of D states was similar (Figure 7A). This clearly demonstrated that increasing concentrations of GABA did not produce increasing extents of macroscopic desensitization due to increased accessibility of D states. Equilibrium occupancy of O states was also similar in this concentration range, indicating that increasing the GABA concentration did not substantially affect the equilibrium occupancy of fully-liganded receptors. Consistent with this result, simulated deactivation was faster only following applications of very low GABA concentrations (Figure 7B). Interestingly, the simulated current generated by 0.3 μM GABA (Figure 7A, smallest current) was associated with several-fold higher probability of D state occupancy (Figure 7A, smallest of the upward traces) than of O state occupancy, despite the extent of macroscopic desensitization being <1%. Taken together, these findings demonstrated that the extent of macroscopic desensitization was a poor predictor of desensitized state occupancy.

To investigate the kinetic basis for this concentration relationship, we measured deactivation over this concentration range for simulations in which one or more D states were eliminated. Eliminating D_f accelerated deactivation similarly at each concentration (Figure 7B, filled circles) relative to the intact scheme (Figure 7B, open circles), suggesting that this state contributed to deactivation similarly at all tested concentrations. Eliminating the two slower D states, however, accelerated deactivation and blunted the concentration-dependence (Figure 7B, gray circles), suggesting that receptors activated by very low agonist concentrations were unable to achieve sufficient occupancy of these slowly equilibrating states. Because low concentrations forced receptors to spend more

time in mono- and unliganded states, receptors had fewer opportunities to enter slowly equilibrating D states (which were only accessible to di-liganded receptors). In support of this slow equilibration idea, increasing the application duration (>25 seconds) for low concentrations (300 nM and 1 μM GABA) allowed receptors time to equilibrate among slower D states, significantly prolonging the time course of deactivation (not shown). In other words, increasing the fractional occupancy of slowly equilibrating D states (D_i and D_s) could be accomplished either by increasing the concentration of agonist for a given duration application, or by increasing the application duration for low concentrations.

The relationship between macroscopic desensitization and the stability of open and desensitized states

Although macroscopic desensitization is not possible without D states, extracting microscopic information about D states from current traces remains a significant challenge, as other states are known to contribute to macroscopic current shape (Mozrzymas et al., 2003; Celentano and Hawkes, 2004; Appendix III). We therefore examined the extent of macroscopic desensitization (percent of current lost) for branched and linear 4-state models (Figure 5), over a range of entry and exit rate constants from O and D states spanning two orders of magnitude (60 s^{-1} to 6000 s^{-1}). Plotting the extent of macroscopic desensitization (on the ordinate) against each pair of rate constants yielded a "landscape" illustrating the dependence of macroscopic desensitization on the relative stability (defined as the ratio of the entry rate to the exit rate) of O (β/α) and D (δ/ρ) states (Figure 8). For example, in Figures 8A and 8B, the extent of macroscopic desensitization of the branched model was evaluated over a range of β and α values (right

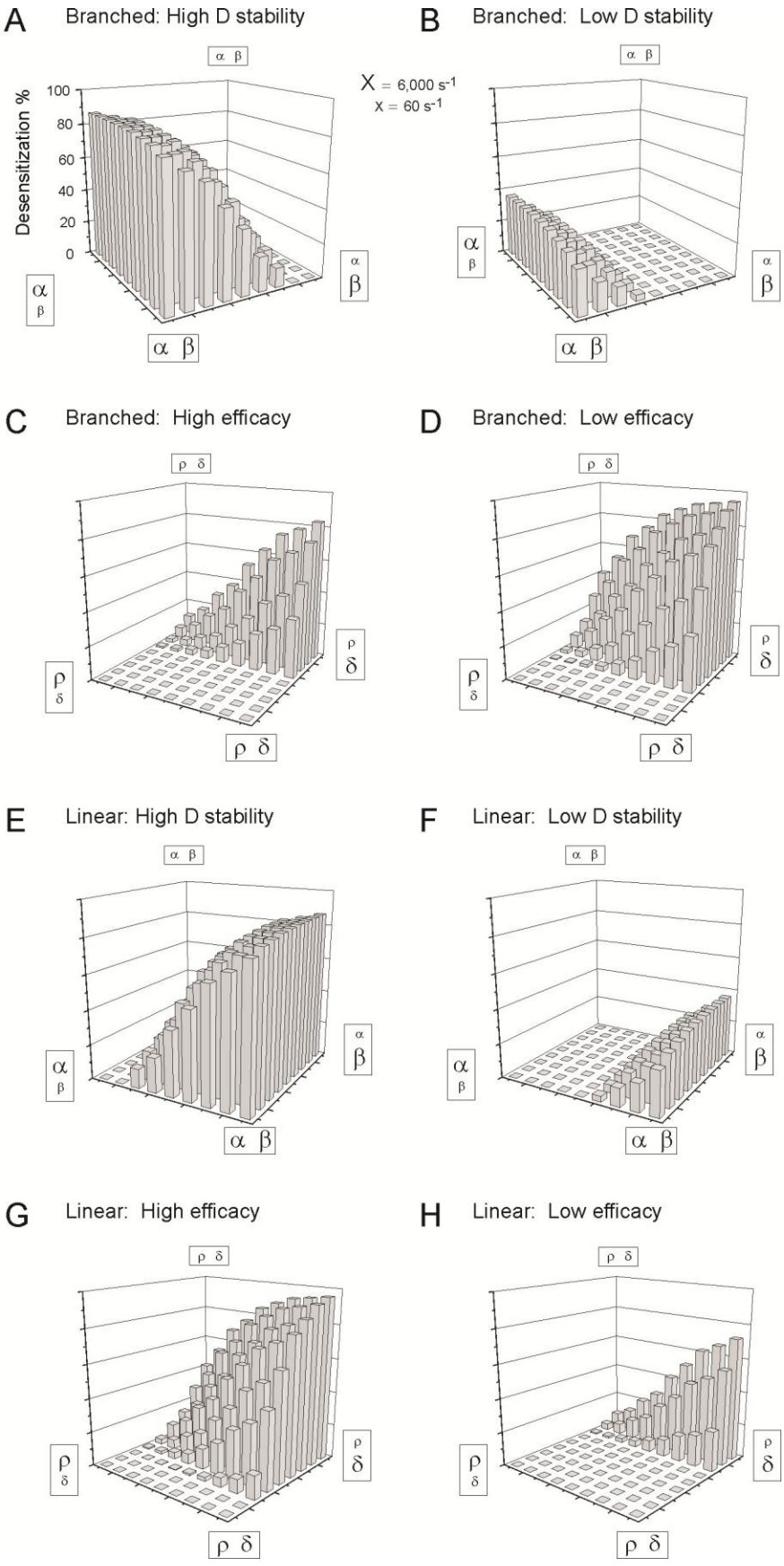
A
Branched: High D stability
B
Branched: Low D stability
X = 6,000 s-1
X = 60 s-1
Desensitization %
100
80
60
40
20
0
α β
C
Branched: High efficacy
D
Branched: Low efficacy
ρ δ
E
Linear: High D stability
F
Linear: Low D stability
G
Linear: High efficacy
H
Linear: Low efficacy

Figure 8. Dependence of the extent of macroscopic desensitization on the stability of open and desensitized states for branched and linear kinetic schemes

Landscape plots illustrate the extent of macroscopic desensitization (Z axis) for branched (A-D) and linear (E-H) kinetic schemes over a range of β/α and δ/ρ combinations. The Z axis labels of panel A apply to all 8 plots. Each grid shows the 81 combinations of rate constants used to generate the simulated currents (not shown), the values of which are indicated in the four corners of each plot by variable letter sizes. Large letters correspond to 6000 s^{-1}, small letters correspond to 60 s^{-1}, and the rate constant values in between were 3000, 2000, 1000, 600, 300, 200 and 100 s^{-1} (not labeled). The top 4 landscapes were generated using the branched 4-state model (Figure 5C), and the bottom 4 were generated using the linear 4-state model (Figure 5B). For all panels, $k_{on} = 10^6\ s^{-1}M^{-1}$, $k_{off} = 300\ s^{-1}$, and the GABA concentration was 1 mM. For panels in which the O state transitions were varied (A, B, E, F), the D state rate constants were $\delta = 1.0$ and $\rho = 0.1$ for "high D stability" panels, and $\delta = 0.6$ and $\rho = 0.6$ for "low D stability" panels. For panels in which the D state transitions were varied, the O state rate constants were $\beta = 3.0$; and $\alpha = 0.6$ for "high efficacy" panels and $\beta = 0.3$; and $\alpha = 2.0$ for "low efficacy" panels. Note that in simulations of the linear kinetic scheme, efficacy was actually changing in the δ x ρ grids because open duration was determined by the reciprocal sum of the two "closing" rate constants: α and δ.

and left corners represented the highest and lowest O state stabilities, respectively), in the context of either more (panel A) or less (panel B) D state stability. Note that for these simplified schemes, the percent of current lost was considered a suitable index of macroscopic desensitization, as faster time constants correlated in most cases with more extensive desensitization (not shown).

When efficacy (O state stability; β/α) was varied in the branched model, the extent of macroscopic desensitization was greatest for high values of α (brief openings), and least when α was low (long openings) (Figure 8A, B). Increasing β (higher opening frequency) reduced the extent of macroscopic desensitization, while decreasing β (lower opening frequency) increased the extent. Although varying β had much less of an effect than varying α, these landscape patterns were consistent with the idea that increasing efficacy caused the branched model to shift towards a C-C-O arrangement, which cannot

macroscopically desensitize (Appendix IV). When D state stability was varied in the branched model, the extent of macroscopic desensitization was greatest for high values of δ and low values of ρ (Figures 8C, 8D). Overall, the high efficacy condition (Figure 8C) displayed less macroscopic desensitization than the low efficacy condition (Figure 8D), again reflecting the inability of C-C-O arrangements to macroscopically desensitize. Note, however, that high values of δ were not always associated with macroscopic desensitization, even for low efficacy receptors (Figure 8D). Indeed, macroscopic desensitization was only possible when α was greater than ρ (Appendix IV). When this condition was violated, neither increasing δ nor decreasing β restored macroscopic desensitization, even when this drove D state fractional occupancy above 90% (not shown).

Varying efficacy in the linear model produced patterns of macroscopic desensitization distinct from those of the branched model (Figures 8E, 8F). The extent of macroscopic desensitization was greatest when efficacy was highest and was more sensitive to changing β than α. In addition, while both models predicted extensive macroscopic desensitization for high values of δ and low values of ρ (Figures 8C, 8D, 8G, 8H), high efficacy receptors in the linear model were more susceptible to changes in D state stability than low efficacy receptors (Figures 8G, 8H). Interestingly, the rate constant relationships that determined whether macroscopic desensitization occurred were also different. Unlike the branched model, macroscopic desensitization was possible in the linear model only when β was greater than ρ (Appendix IV). When this condition was violated, altering other rate constants could not restore macroscopic

desensitization, even when this yielded D state fractional occupancies above 90% (not shown).

These results demonstrated that tremendous variation in macroscopic desensitization could arise despite constant D state stability (note the constant δ/ρ ratio along the diagonal between the nearest and furthest corners of Figure 8D). Conversely, the landscapes demonstrated regions of negligible macroscopic desensitization despite marked changes D state stability. Thus, current shape was a poor predictor of D state fractional occupancy, suggesting that failure to observe macroscopic desensitization should not, by itself, be considered evidence against the presence of D states. Although macroscopic currents are shaped by all rate constants in the gating scheme (Mozrzymas et al., 2003; Appendix III), these results also suggested that only certain rate constants determine whether macroscopic desensitization can occur (Appendix IV).

The relationship between deactivation and the stability of open and desensitized states

Similar to the approach taken in the previous section to determine the relationship between individual rate constants and the extent of macroscopic desensitization, landscape plots were generated from weighted deactivation time courses following simulated 100 ms agonist pulses for branched (Figures 9A-D) and linear (Figures 9E-H) schemes. For the branched model, increasing efficacy prolonged deactivation while decreasing efficacy accelerated deactivation, in the context of both high (Figure 9A) and low (Figure 9B) D state stabilities. These deactivation landscapes, however, trended in the opposite direction compared to their corresponding desensitization landscapes

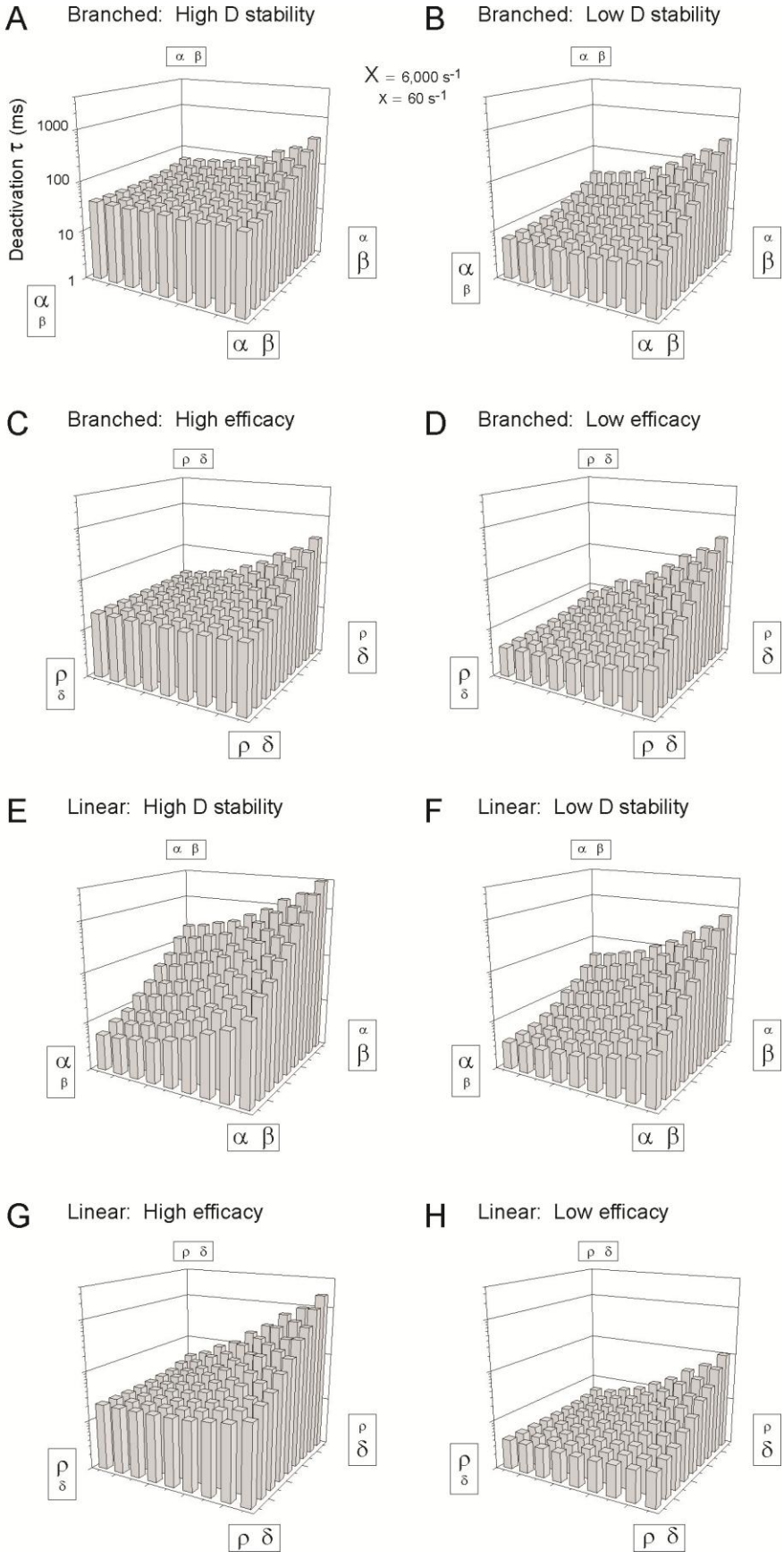
A
Branched: High D stability
B
Branched: Low D stability
X = 6,000 s-1
X = 60 s-1
Deactivation τ (ms)
1000
100
10
1
α β
C
Branched: High efficacy
D
Branched: Low efficacy
ρ δ
E
Linear: High D stability
F
Linear: Low D stability
G
Linear: High efficacy
H
Linear: Low efficacy

Figure 9. Dependence of deactivation time course on the stability of the open and desensitized states for branched and linear schemes

Landscape plots illustrate the weighted deactivation time constant (Z axis) for branched (A-D) and linear (E-H) kinetic schemes over a range of β/α and δ/ρ combinations. The Z axis labels in panel A apply to all 8 panels. See the legend of Figure 8 for plot descriptions and rate constants.

(compare Figures 9A, 9B to Figures 8A, 8B), thus revealing a pattern of uncoupling: regions with the slowest deactivation showed the least macroscopic desensitization, while those with the fastest deactivation showed the most macroscopic desensitization. Figures 9C and 9D illustrated branched model deactivation when D state stability was varied in the context of high and low efficacy. Deactivation was slowest for the most stable D state conditions and fastest for the least stable D state conditions for both high and low efficacy conditions, matching the relationship between deactivation and efficacy (Figures 9A and 9B). These deactivation landscapes trended in the same direction as their corresponding desensitization landscapes (compare Figures 9C, 9D to Figures 8C, 8D), thus illustrating desensitization-deactivation coupling. Note, however, that deactivation varied substantially even for regions that lacked macroscopic desensitization.

Similar to the branched model, increasing and decreasing O or D state stabilities in the linear model corresponded to longer and shorter deactivation time courses, respectively (Figures 9E-9H). This suggested that unlike macroscopic desensitization, the effect of stabilizing O and D states on deactivation was independent of model connectivity, consistent with the idea that weighted deactivation time courses simply reflect the mean time receptors are agonist bound, which increases when O and/or D

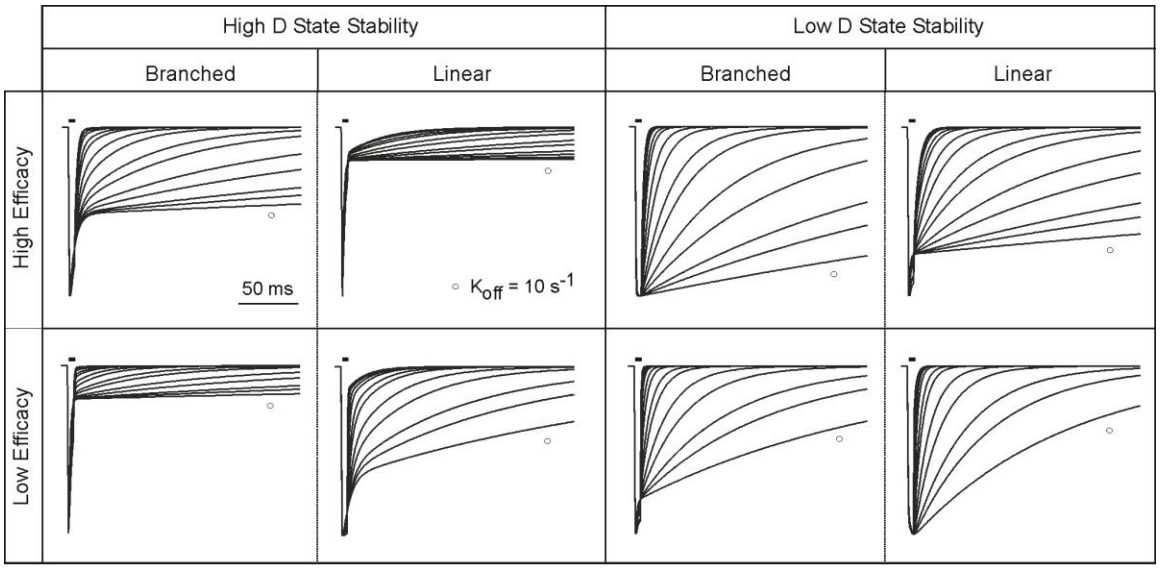

Figure 10. The interplay between agonist affinity, gating efficacy, desensitized state stability, and model connectivity on current deactivation

Simulated responses of linear and branched kinetic models (Figure 5B, C) to 5 ms pulses of nearly-saturating GABA concentrations (1 mM to 20 mM; higher concentrations were required when k_{off} was high) in the context of different O and D state stabilities. Within each panel, k_{off} was varied from 10 s^{-1} to 100,000 s^{-1}. All other rate constants were identical to those used in Figures 8 and 9. Horizontal scale bar applies to all traces. Open circles in each panel indicate traces corresponding to the slowest unbinding rate.

states are stabilized (Appendix II). Exceptions to this relationship between time bound and deactivation include irreversible microscopic desensitization, and small amplitude components not resolvable through baseline noise (neither case is considered here).

There were, however, notable quantitative differences between branched and linear deactivation landscapes. Compared to the branched model (Figures 9A-D to Figures 9E-H), stabilizing O and/or D states in the linear model resulted in slower deactivation (Figures 9E-H, right corners). This was related to O and D states being directly interconnected, which allowed transitions without any chance of unbinding. It should also be noted that while deactivation was typically biphasic for both models, the

magnitude and relative contribution of each phase depended greatly on state connectivity. This was particularly evident for deactivation following brief pulses, whose time course was constrained by macroscopic desensitization (Figure 6). For example, while deactivation in the linear model had the most prominent fast phase when efficacy was high (which corresponded to extensive macroscopic desensitization; Figure 8), the opposite was true for the branched model (Figure 10).

Interestingly, all deactivation landscapes obtained with the linear model trended in the same direction as their corresponding desensitization landscapes, suggesting that linear arrangements primarily supported desensitization-deactivation coupling (compare Figures 9E-H with Figures 8E-H). As with the branched model, however, changes in deactivation were observed even when corresponding grid positions lacked macroscopic desensitization, providing additional landscape regions of apparent uncoupling. These results suggested that neither coupling nor uncoupling was the rule *per se* for $GABA_A$ receptors. Instead, it appeared that both phenomena were theoretically possible for any given kinetic scheme, the result of desensitization and deactivation having markedly different kinetic determinants.

DISCUSSION

Coupling and uncoupling of macroscopic desensitization and deactivation

It is common practice to use the term "coupled" to describe correlated observations, such as that of fast desensitization with slow deactivation. We described several experimental conditions that differed from the typical correlation of fast desensitization with slow deactivation, or of slow desensitization with fast deactivation. Such "uncoupling" resulted from macroscopic desensitization and deactivation being differentially sensitive to changes in certain rate constants, and consequently, able to vary independently. We found the kinetic determinants of macroscopic desensitization to be complex, depending not only on the relationship between subsets of rate constants, but also on the specific connectivity of states (Appendix IV).

While we limited our simulations to non-cyclic gating schemes, coupling and uncoupling are also theoretically possible for schemes containing cyclic features (Scheller and Forman, 2002), as macroscopic desensitization and deactivation have different kinetic determinants under these circumstances as well. We did not, however, systematically evaluate the behavior of cyclic schemes, as they introduced a higher level of kinetic complexity to the simulations (for example, maintaining microscopic reversibility precluded alterations of individual rate constants). In addition, our prior data suggested that unbinding does not occur from fully-liganded open or pre-open states (Bianchi and Macdonald, 2001a), which argues against the presence of cyclic features.

The relationship between macroscopic current shape and microscopic rate constants

Our simulations emphasized that macroscopic phenomena could not be attributed to individual states or rate constants; rather, they were shaped by all transitions within a given scheme, as well as the connectivity of states (Mozrzymas et al., 2003; Appendix III). As a result, the terminology used to describe an experimental observation may inappropriately suggest relevance to a microscopic process. For this reason, Colquhoun (1998) has argued against using "affinity" or even "apparent affinity" interchangeably with EC_{50}. Similarly, the phenomenological description of fading current during continued agonist application as "desensitization" implies relevance to microscopic D states; however, simulations indicated that macroscopic desensitization provides little or no information about the fractional occupancy or stability of D states. Even "flat" currents do not preclude existence of D states; indeed, the fractional occupancy of D states can actually exceed that of O states (Figure 7). Moreover, describing macroscopic desensitization requires observation of an initial peak amplitude, which may imply that microscopic desensitization is a kinetic process mechanistically preceded by channel opening (Colquhoun and Hawkes, 1995). Our simulations, however, demonstrated that D states may achieve substantial occupancy before currents reach peak, and therefore, before any loss of macroscopic current can be measured.

The influence of agonist affinity on desensitization and deactivation

Both the extent and time course of macroscopic desensitization were relatively insensitive to changes in agonist affinity in the setting of a near-saturating GABA concentration. This occurred because the effective binding rate (k_{on} x [GABA]) was

orders of magnitude higher than the unbinding rate (k_{off}), and as a result, changes in affinity could not affect the relative distribution of receptors in the gating scheme (which were essentially fully-liganded). In contrast, deactivation was highly sensitive to agonist affinity, as the unbinding rate was an important determinant of the rate at which receptors returned to the resting state. While this represented one example of apparent uncoupling between desensitization and deactivation, it should be noted that altering affinity in the context of sub-saturating agonist concentrations causes desensitization-deactivation coupling. Under these conditions, increasing agonist affinity not only prolongs deactivation, but also increases the extent of macroscopic desensitization (as if a higher concentration of agonist was applied; see Figure 7).

Although the unbinding rate played a dominant role in shaping deactivation under certain circumstances, it was clear that multiple microscopic parameters contributed to the deactivation time course, including the unbinding rate constant, the entry and exit rates from O and D states, and the gating scheme connectivity. Interestingly, macroscopic desensitization constrained the effect of agonist affinity on deactivation by providing a slow limit to its time course. This constraint had particular relevance to brief (such as synaptic) pulses, where the fast phase of deactivation could not be slower than the fast phase of macroscopic desensitization. An unexpected consequence of this finding was that deactivation of currents lacking fast macroscopic desensitization should theoretically be unconstrained (Figures 2E and 6D), a concept that may be important for understanding the kinetic basis for prolonged deactivation in the slowly desensitizing but high affinity α4βδ and α6βδ isoforms. Thus, not only can prolonged deactivation occur

without macroscopic desensitization, but the presence of fast macroscopic desensitization may actually accelerate early phases of deactivation.

The influence of gating efficacy on macroscopic desensitization and deactivation

Whether unbinding from the O state is assumed to be impossible (non-cyclic schemes) or less probable than unbinding from other states (cyclic schemes), increasing efficacy in branched arrangements is predicted to prolong deactivation (Figure 9A, 9B). Since increased O state occupancy shifts the gating scheme towards the C-C-O arrangement (which cannot macroscopically desensitize; Appendix IV), this reduces the extent of macroscopic desensitization (Figure 8A, 8B), thereby providing an example of uncoupling. In the linear model, however, the concept of efficacy is more complex. Increasing efficacy can technically occur in two ways (since there are two routes for channel closure): increasing β/α or decreasing δ/ρ. Increasing β/α prolongs deactivation because of increased time spent in both O and D states. Increasing efficacy via decreasing δ/ρ, however, increases O state occupancy while decreasing D state occupancy. In our simulations, the changes in D state occupancy dominated, likely due to the more distal positioning of the D state relative to the unbinding step. Thus, unlike in the branched model, increasing efficacy in the linear scheme can either prolong (via β/α) or accelerate (via δ/ρ) deactivation. Either way, altered efficacy in the linear scheme is always associated with coupling. If efficacy is increased via increasing β/α, deactivation is prolonged and the extent of macroscopic desensitization is increased (Figures 8E, 8F, 9E, 9F). If efficacy is increased via decreasing δ/ρ, deactivation is

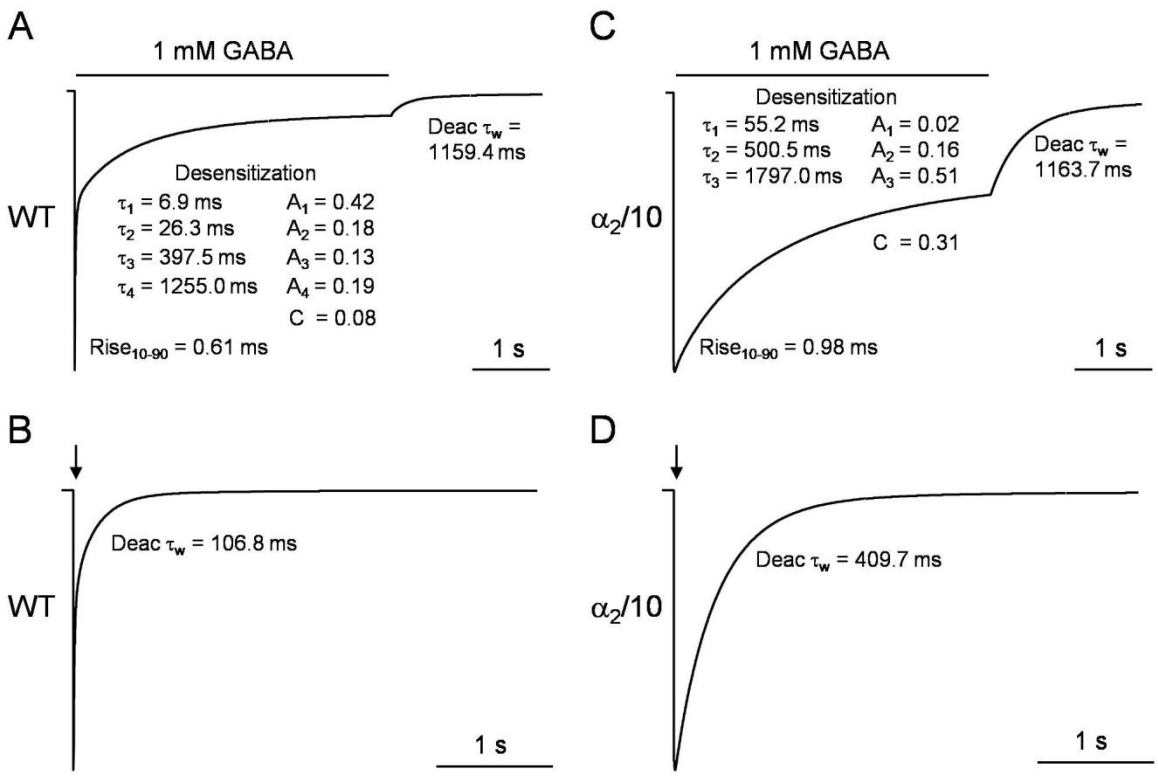

Figure 11. Predicted effects of increased efficacy on macroscopic current properties using a comprehensive model of $GABA_A$ receptor function

Using the α1β3γ2L receptor kinetic model (Figure 5A), the effect of increasing efficacy (via decreasing the exit rate from the O2 state) was evaluated on current rise time ("$Rise_{10-90}$"), extent and time course of macroscopic desensitization ("Desensitization"), and weighted deactivation time course ("Deact τ_w"). "τ_n" and "A_n" indicate the time constant and relative contribution of each exponential component to the time course of macroscopic desensitization, respectively. "C" indicates the fraction of current remaining at the end of the GABA pulse. Values for deactivation reflect exponential fitting of curents for 10 s following pulse termination (not shown). A, B. Simulated responses to prolonged (4 s) and brief (5 ms) applications of 1 mM GABA to wild-type receptors (WT). C, D. Simulated responses to prolonged (4 s) and brief (5 ms) applications of 1 mM GABA to higher efficacy receptors, achieved by decreasing the exit rate from O2 (α2/10). Note that decreasing α2 ten-fold increases the mean dwell time in O2 less than two-fold, the result of multiple routes existing for channel closure.

accelerated and the extent of macroscopic desensitization is decreased (Figures 8G, 8H, 9G, 9H). Therefore, uncoupling in the context of altered efficacy necessitates a branched arrangement.

Several experimental observations argue against a purely linear kinetic arrangement for $GABA_A$ receptors. Barbiturates prolong IPSC duration via increased gating efficacy (Twyman, et al., 1989) while decreasing the extent of macroscopic desensitization (Feng, et al., 2004), consistent with a branched arrangement. Increased efficacy in the context of uncoupling due to mutations in the pore-domain supports this idea (Figures 3 and 4). Although altered efficacy may be only one of several kinetic alterations caused by the α1(L9'S) mutation, preliminary simulations using the comprehensive α1β3γ2L model (Figure 5), whose O and D states are in branched arrangement, confirm that increasing efficacy can recapitulate the decreased macroscopic desensitization, prolonged deactivation following brief but not long applications, and slower rise time (Figure 11).

Predictive microscopic kinetic value of observed changes in macroscopic desensitization and deactivation

Although the complex kinetic basis underlying current shape essentially precludes direct extraction of microscopic parameters, the differential sensitivities of macroscopic desensitization and deactivation to various kinetic parameters can help distinguish between model arrangements and guide mechanistic interpretations (Figure 12). For example, given an experimental observation of decreased macroscopic desensitization (from a mutation or allosteric modulator), changes in deactivation could be used to

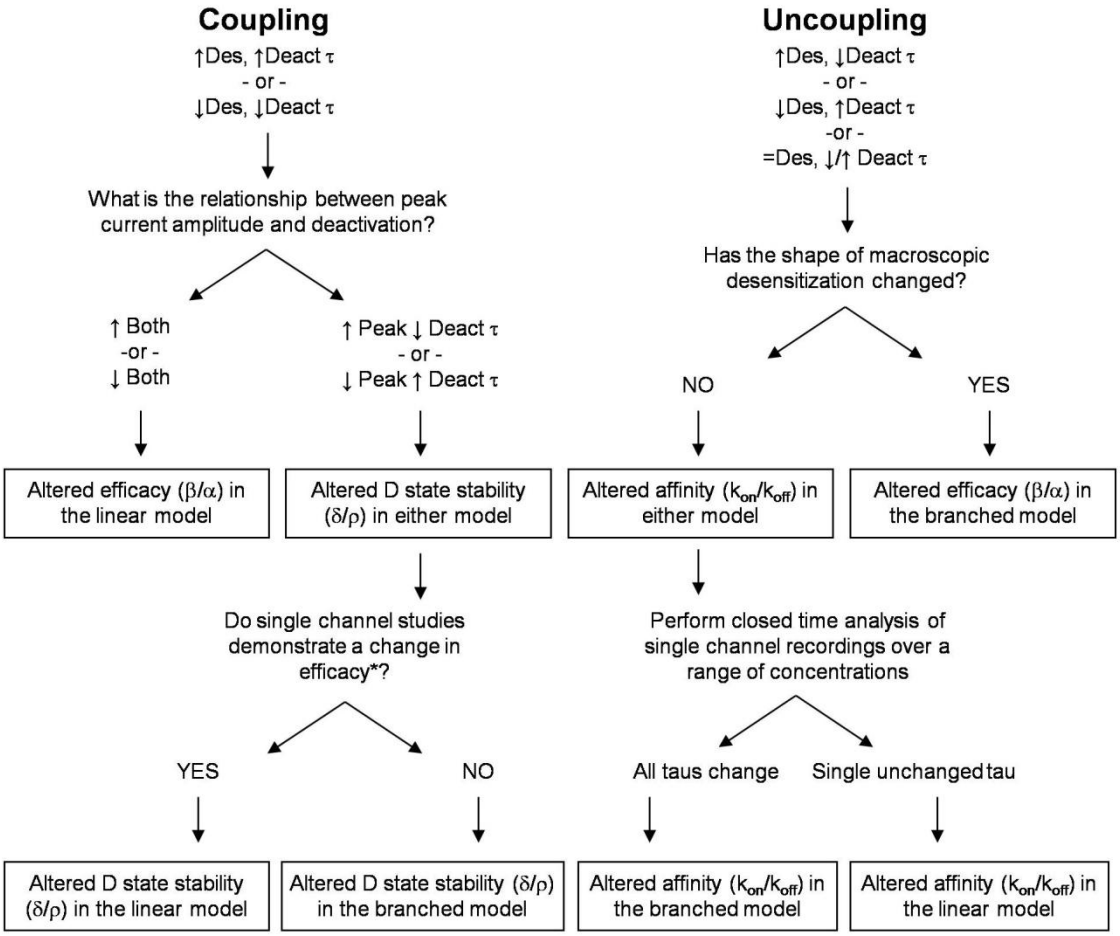

Figure 12. Flowchart for interpreting changes in $GABA_A$ receptor current kinetics

The flowchart depicts an algorithmic approach for interpreting the effect of a kinetic perturbation (due to a mutation or allosteric modulator) on $GABA_A$ receptor macroscopic currents. By analyzing macroscopic current properties ("Des", extent of desensitization; "Deact τ", weighted deactivation time constant) and single channel kinetic properties, both the relevant microscopic transition (β/α, δ/ρ, k_{on}/k_{off}) and the arrangement of O and D states (branched or linear) can be determined assuming a simple 4-state kinetic scheme. The abbreviations "↑ Des", "↓ Des", and "= Des" refer to increased, decreased, and unchanged extents of macroscopic desensitization, respectively, when receptors are activated by a nearly-saturating GABA concentration. "↑ Deact τ" and "↓ Deact τ" refer to prolonged and shortened time courses of deactivation, respectively. * indicates that for linear models, changes in either β/α or δ/ρ will change efficacy, since receptors can open and close via two independent pathways.

constrain the number of potentially responsible microscopic transitions. If deactivation was prolonged (uncoupling), this would be consistent with increased efficacy in a branched model, a prediction testable using single channel recording. However, if deactivation was accelerated (coupling), this could result from destabilization of the D state in either kinetic scheme or from decreased efficacy in the linear scheme. Comparing peak current amplitudes would then be useful, since destabilization of the D state and decreased efficacy should have opposite effects (increased and decreased peak current amplitudes, respectively). If peak current amplitude was increased, single channel studies could then be employed to distinguish between D state destabilization in branched and linear schemes. If the D state was destabilized in the branched model, then efficacy should be unchanged. If, however, the D state was destabilized in the linear model, then efficacy would be expected to increase.

Single channel studies might also be helpful for distinguishing branched and linear arrangements in the special case of unchanged desensitization but altered deactivation, an example of uncoupling presumably reflecting altered microscopic affinity. In this case, evaluation of the concentration sensitivity of the closed time distribution can expose different arrangements of D states. Only linear arrangements can yield a fixed (concentration-independent) time constant, since only then do a subset of all closures correspond with certainty to sojourns in a single closed state (Colquhoun and Hawkes, 1982). In contrast, branched D states are directly connected with the pre-open state, which is directly connected with the unbound state. Thus, individual closures may include transitions among all three closed states, causing the time constants to depend on a complex relationship between all rate constants connecting these states. Since one of

these rates (the effective binding rate) depends on the agonist concentration, all time constants will be concentration sensitive, even though entry and exit rates from the D state are not themselves concentration dependent. It should be noted that while this approach is valid in theory, in practice, even branched arrangements can appear to have fixed time constants when D states are very long-lived. Nonetheless, if all time constants in the closed time distribution vary with concentration, then it can be concluded that all non-conducting states in the gating scheme are connected.

Despite the mentioned limitations, the goal of this algorithmic approach was to collapse the spectrum of potential explanations for a given macroscopic observation into a smaller and potentially testable set of hypotheses. Although the observations outlined here represent characterization of simplified models that likely underestimate the complexity of $GABA_A$ receptor kinetics, it is clear that even in these simplified cases, macroscopic current interpretation can be complex or even counterintuitive. The likelihood that $GABA_A$ receptors obey even more complex kinetic rules emphasizes the necessity for establishing more quantitative frameworks to transition from macroscopic observations to microscopic models.

REFERENCES

Bai D, Pennefather PS, MacDonald JF and Orser BA (1999) The general anesthetic propofol slows deactivation and desensitization of GABA(A) receptors. J Neurosci 19: 10635-10646.

Barberis A, Mozrzymas JW, Ortinski PI and Vicini S (2007) Desensitization and binding properties determine distinct alpha1beta2gamma2 and alpha3beta2gamma2 GABA(A) receptor-channel kinetic behavior. Eur J Neurosci 25: 2726-2740.

Bianchi MT, Haas KF and Macdonald RL (2001) Structural determinants of fast desensitization and desensitization-deactivation coupling in $GABA_A$ receptors. J Neurosci 21: 1127-1136.

Bianchi MT and Macdonald RL (2001a) Agonist trapping by $GABA_A$ receptor channels. J Neurosci 21: 9083-9091.

Bianchi MT and Macdonald RL (2001b) Mutation of the 9' leucine in the GABA(A) receptor gamma2L subunit produces an apparent decrease in desensitization by stabilizing open states without altering desensitized states. Neuropharmacol 41: 737-744.

Bianchi MT and Macdonald RL (2002) Slow phases of GABA(A) receptor desensitization: structural determinants and possible relevance for synaptic function. J Physiol 544: 3-18.

Bianchi MT, Haas KF and Macdonald RL (2002) Alpha1 and alpha6 subunits specify distinct desensitization, deactivation and neurosteroid modulation of GABA(A) receptors containing the delta subunit. Neuropharmacol 43: 492-502.

Buhr A, Bianchi MT, Baur R, Courtet P, Pignay V, Boulenger JP, Gallati S, Hinkle DJ, Macdonald RL and Sigel E (2002) Functional characterization of the new human GABA(A) receptor mutation beta3 (R192H). Hum Genet 111: 154-160.

Burkat PM, Yang J and Gingrich KJ (2001) Dominant gating governing transient $GABA_A$ receptor activity: A first latency and P(o/o) analysis. J Neurosci 21: 7026-7036.

Celentano and Hawkes (2004) Use of the covariance matrix in directly fitting kinetic parameters: application to $GABA_A$ receptors. Biophys J 87: 276-294.

Celentano JJ and Wong RKS (1994) Multiphasic desensitization of the $GABA_A$ receptor in outside-out patches. Biophys J 66: 1039-1050.

Chang Y and Weiss DS (1999) Allosteric activation mechanism of the α1β2γ2 γ-aminobutyric acid type A receptor revealed by mutation of the conserved M2 leucine. Biophys J 77: 2542-2551.

Chang Y, Ghansah E, Chen Y, Ye J and Weiss DS. Desensitization mechanism of GABA receptors revealed by single oocyte binding and receptor function. J Neurosci 22: 7982-7990.

Colquhoun D and Hawkes AG (1982) On the stochastic properties of bursts of single ion channel openings and of clusters of bursts. Philos Trans R Soc Lond B Biol Sci 300: 1-59.

Colquhoun D and Hawkes AG (1995) Desensitization of N-methyl-D-aspartate receptors: a problem of interpretation. Proc Natl Acad Sci USA 92:10327-10329.

Colquhoun D (1998) Binding, gating, affinity and efficacy: the interpretation of structure-activity relationships for agonists and of the effects of mutating receptors. Br J Pharmacol 125: 924-947.

Feng HJ, Bianchi MT and Macdonald RL (2004) Pentobarbital differentially modulates alpha1beta3delta and alpha1beta3gamma2L GABA-A receptor currents. Mol Pharmacol 66: 988-1003.

Feng HJ and Macdonald RL (2004) Multiple actions of propofol on alphabetagamma and alphabetadelta GABAA receptors. Mol Pharmacol 66: 1517-1524.

Filatov GN and White MW (1995) The role of conserved leucines in the M2 domain of the acetylcholine receptor in channel gating. Mol Pharmacol 48: 379-384.

Fisher JL, Zhang J and Macdonald RL (1997) The role of alpha1 and alpha6 subtype amino-terminal domains in allosteric regulation of gamma-aminobutyric acid a receptors. Mol Pharmacol 52: 714-724.

Fisher JL (2004) The alpha 1 and alpha 6 subunit subtypes of the mammalian GABA(A) receptor confer distinct channel gating kinetics. J Physiol 561: 433-448.

Galarreta M and Hestrin S (1997) Properties of $GABA_A$ receptors underlying inhibitory synaptic currents in neocortical pyramidal neurons. J Neurosci 17:7220-7227.

Grosman C and Auerbach A (2000) Kinetic, mechanistic, and structural aspects of unliganded gating of acetylcholine receptor channels. J Gen Physiol 115:621-635.

Grosman C and Auerbach A (2001) The dissociation of acetylcholine from open nicotinic receptor channels. Proc Natl Acad Sci 98:14102-14107.

Haas KF and Macdonald RL (1999) $GABA_A$ receptor subunit γ2 and δ subtypes confer unique kinetic properties on recombinant $GABA_A$ receptor currents in mouse fibroblasts. J Physiol 514: 27-45.

Hinkle DJ and Macdonald RL (2003) Beta subunit phoshorylation selectively increases fast desensitization and prolongs deactivation of alpha1beta1gamma2L and alpha1beta3gamma2L GABA(A) receptor currents. J Neurosci 23: 11698-11710.

Jones MV and Westbrook GL (1995) Desensitized states prolong $GABA_A$ channel responses to brief agonist pulses. Neuron 15: 181-191.

Jones MV and Westbrook GL (1996) The impact of receptor desensitization on fast synaptic transmission. Trends Neurosci 19: 96-101.

Jones MV, Sahara Y, Dzubay JA and Westbrook GL (1998) Defining affinity with the $GABA_A$ receptor. J Neurosci 18: 8590-8604.

Katz B and Thesleff S (1957) A study of the desensitization produced by acetylcholine at the motor end-plate. J Physiol 138: 63-80.

Labarca C, Nowak MW, Zhang H, Tang L, Deshpande P and Lester HA (1995) Channel gating governed symmetrically by conserved leucine residues in the M2 domain of nicotinic receptors. Nature 376: 514-516.

Lagrange AH, Botzolakis EJ and Macdonald RL (2007) Enhanced macroscopic desensitization shapes the response of alpha4 subtype-containing GABAA receptors to synaptic and extrasynaptic GABA. J Physiol 578: 655-676.

Li X and Pearce R (2000) Effects of halothane on GABAA receptor kinetics: evidence for slowed agonist unbinding. J Neurosci 20: 899-907.

Mercik K, Pytel M, Cherubini E and Mozrzymas JW (2006) Effect of extracellular pH on recombinant alpha1beta2gamma2 and alpha1beta2 GABAA receptors. Neuropharmacology 51: 305-314.

Mortensen M, Kristiansen U, Ebert B, Frolund B, Krogsgaard-Larsen P and Smart TG (2004) Activation of single heteromeric $GABA_A$ receptor ion channels by full and partial agonists. J Physiol 557: 389-413.

Mozrzymas JW, Barberis A, Mercik K and Zarnowska ED (2003) Binding sites, singly bound states, and conformational coupling shape GABA-evoked currents. J Neurophysiol 89: 871-883.

Olsen RW and Macdonald RL: $GABA_A$ Receptor Complex: Structure and Function, in Egebjerg, J., Schousboe, A., Krogsgaard-Larsen, P. (eds), Glutamate and GABA Receptors and Transporters: Structure, Function, and Pharmacology, Chapt 9, pp. 203-235, London and Francis, 2002.

Overstreet LS, Jones MV and Westbrook GL (2000) Slow desensitization regulates the availability of synaptic GABA(A) receptors. J Neurosci 20: 7914-7921.

Revah F, Bertrand D, Galzi JL Devillers-Thiery A, Mulle C, Hussy N, Bertrand S, Ballivet M and Changeux JP (1991) Mutations in the channel domain alter desensitization of a neuronal nicotinic receptor. Nature 353: 846-849.

Scheller M and Forman SA (2002) Coupled and uncoupled gating and desensitization effects by pore-domain mutations in GABA(A) receptors. J Neurosci 22: 8411-8421.

Thompson S-A, Smith MZ, Wingrove PB, Whiting PJ and Wafford KA (1999) Mutation at the putative $GABA_A$ ion channel gate reveals changes in allosteric modulation. Br J Pharmacol 127: 1349-1358.

Tia S, Wang JF, Kotchabhakdi N and Vicini S (1997) Distinct deactivation and desensitization kinetics of recombinant $GABA_A$ receptors. Neuropharmacology 35: 1375-1382.

Twyman RE, Rogers CJ and Macdonald RL (1990) Intraburst kinetic properties of the $GABA_A$ receptor main conductance state of mouse spinal cord neurones in culture. J Physiol (Lond) 423: 193-219.

Twyman RE, Rogers CJ and Macdonald RL (1989) Differential regulation of gamma-aminobutyric acid receptor channels by diazepam and phenobarbital. Ann Neurol 25: 213-220.

Yakel JL, Lagrutta A, Adelman JP and North RA (1993) Single amino acid substitution affects desensitization kinetics of the 5-hydroxytryptamine type 3 receptor expressed in *Xenopus* oocytes. Proc Natl Acad Sci USA 90: 5030-5033.

Yang P, Jones BL and Henderson LP (2002) Mechanisms of anabolic androgenic steroid modulation of alpha(1)beta(3)gamma(2L) GABA(A) receptors. Neuropharmacol 43: 619-633.

CHAPTER III

BENZODIAZEPINE MODULATION OF $GABA_A$ RECEPTOR OPENING FREQUENCY DEPENDS ON ACTIVATION CONTEXT: A PATCH CLAMP AND SIMULATION STUDY

Emmanuel J. Botzolakis, Matt T. Bianchi, Andre H. Lagrange, and Robert L. Macdonald

ABSTRACT

Benzodiazepines (BDZs) are $GABA_A$ receptor modulators with anxiolytic, hypnotic, and anti-convulsant properties. BDZs are understood to potentiate $GABA_A$ receptor function by increasing channel opening frequency, in contrast to barbiturates, which increase channel open duration. However, the *in vitro* evidence demonstrating increased opening frequency involved prolonged exposure to sub-saturating GABA concentrations, conditions most similar to those found in extrasynaptic areas. In contrast, synaptic $GABA_A$ receptors are transiently activated by high GABA concentrations. To determine if BDZ modulation of single-channel opening frequency would be different for BDZ-sensitive receptors activated under synaptic versus extrasynaptic conditions, a combination of patch-clamp recording and kinetic modeling was used. Consistent with the original experimental findings, BDZs were found to increase receptor affinity for GABA by decreasing the unbinding rate. While this mechanism was predicted to increase opening frequency under extrasynaptic conditions, simulations predicted that the same mechanism under synaptic conditions would increase the number, but not the frequency, of single-channel openings. Thus, a single mechanism (slower GABA

unbinding) can produce differential changes in opening frequency under synaptic versus extrasynaptic conditions. The functional impact of BDZs on $GABA_A$ receptors therefore depends upon the physiological context of receptor activation.

INTRODUCTION

As the predominant source of fast synaptic inhibition in the brain, $GABA_A$ receptors have been the focus of emerging hypotheses not only of seizure pathophysiology, but also of anticonvulsant drug pharmacology. However, their role as the therapeutic target of benzodiazepines (BDZs) remained controversial for some time. While BDZs were observed to enhance $GABA_A$ receptor currents during intracellular recording from cultured neurons (Choh, et al., 1977; Macdonald and Barker, 1978), others studies suggested that BDZs were antagonists of $GABA_A$ receptors (Gahwiler, 1976; Mathers, 1987), and still others indicated actions at glycine receptors (Young, et al., 1974). Not until the development of single-channel recording (Colquhoun, 1991) was direct evidence presented that BDZs enhanced $GABA_A$ receptor responses (Rogers, et al., 1994; Twyman, et al., 1989). Specifically, BDZs were reported to increase single-channel opening frequency without altering mean open duration, an effect attributed to an increased affinity of GABA for the receptor (Rogers, et al., 1994). Barbiturates, in contrast, were reported to increase the duration of openings without increasing their frequency (Macdonald, et al., 1989; Twyman, et al., 1989).

However, the *in vitro* electrophysiological evidence demonstrating BDZ-mediated increased opening frequency involved conditions most similar to those occurring in extrasynaptic areas, where receptors are persistently activated by sub-saturating concentrations of ambient GABA (~1 μM or less) (Farrant and Nusser, 2005). Under these conditions, binding of GABA to the receptor is infrequent, and because GABA is always present, receptors are free to repeatedly bind and unbind GABA. Synaptic receptors, in contrast, are transiently activated (~1 ms) by saturating concentrations of

GABA (~1 mM) (Jones and Westbrook, 1996), such that receptors are predominantly GABA-bound, and the majority of channel activity (which can last 10s-100s of milliseconds) occurs without the prospect of rebinding. Given that BDZs were reported to increase the affinity of GABA for the receptor, a mechanism that favors GABA-bound receptor conformations, this suggests that the effects of BDZs on opening frequency would be different for receptors activated under synaptic versus extrasynaptic conditions. Although extrasynaptic receptors are enriched for BDZ-insensitive receptor isoforms (i.e., those containing the δ subunit), BDZ-sensitive receptor isoforms (i.e., those containing the γ subunit) occur commonly in extrasynaptic locations as well (Glykys, et al., 2008; Glykys and Mody, 2007), and in some cases, are actually more abundant than BDZ-insensitive receptors (Farrant and Nusser, 2005). Therefore, the potential context-dependence of BDZ modulation of $GABA_A$ receptor function remains an important mechanistic issue.

MATERIALS AND METHODS

Cell culture and electrophysiology

HEK293T cells were maintained in FBS-supplemented DMEM (Invitrogen, Grand Island, NY) and co-transfected with rat α1, β3, and γ2L $GABA_A$ receptor subunit cDNAs using Fugene 6 (Roche Diagnostics, Indianapolis, IN). Co-transfection of cDNA encoding the pHook surface antibody allowed for immunomagnetic selection of positively-transfected cells. Electrophysiological recordings were performed the day after selection, as described previously (Bianchi and Macdonald, 2001). Briefly, patched cells were gently lifted from the culture dish and exposed to drug-containing solution via a rapid solution switching system (Hinkle, et al., 2003). Solution exchange times were consistently < 400 μs when measured at the open patch electrode, but were slightly slower around the lifted cell. Currents were recorded using an Axopatch 200A amplifier (Molecular Devices, Foster City, CA), low-pass filtered at 2 kHz, and digitized with the Digidata 1322A data acquisition system (Molecular Devices). Diazepam was pre-applied for 1.0 sec prior to co-application with GABA. Consecutive applications were separated by at least 45 sec to allow for complete GABA and diazepam unbinding. GABA and diazepam were obtained from Sigma-Aldrich (St. Louis, MO).

Kinetic Simulations

Simulations of macroscopic currents (100s of receptors) were conducted using Berkeley Madonna (www.berkeleymadonna.com) software that solves the probability that a receptor will occupy any state of a kinetic model as a function of time. QUB

(www.qub.buffalo.edu) software was used for single channel simulations such that resting (C_u), bound closed (C_b and D), and bound open (O) states could be distinguished via assigning different (arbitrary) current levels (C_u = 0 units, C_b and D = -2 units, and O = -6 units, respectively) to each state. For equilibrium ("extrasynaptic") simulations, 10 ms after the start of the trial, 1 μM GABA was applied for 1990 ms. 10 such trials constituted a batch. For phasic ("synaptic") simulations, 10 ms after the start of a trial, 1 mM GABA was applied for 1 ms. Channel openings were then observed for 490 ms. 50 such trials were analyzed per batch, and batches were averaged for analysis. GraphPad Prism (www.graphpad.com) was used for statistical analysis. All data were plotted as mean $\pm$ SEM, and statistical significance was taken as $p < 0.05$ using ANOVA followed by Tukey post-hoc analysis.

RESULTS

$GABA_A$ receptor macroscopic current properties were predicted to have different sensitivities to changes in GABA affinity

BDZs have been shown to enhance $GABA_A$ receptor currents by increasing the affinity of GABA for the receptor (defined as the ratio of the binding to the unbinding rate) (Twyman, et al., 1989), causing a "left shift" of the GABA concentration-response curve (Ghansah and Weiss, 1999). This mechanism predicts that BDZs should increase peak current amplitude only when receptors are activated by sub-saturating concentrations of GABA. Once receptors are activated by a saturating GABA concentration, no further increase in peak current should be possible through increasing agonist binding affinity (Ghansah and Weiss, 1999). Furthermore, desensitization (the loss of current in the continued presence of agonist) should not be affected by BDZs during application of a saturating concentration of GABA, again because binding sites are already saturated (Bianchi, et al., 2007). In contrast, the sensitivity of deactivation (the process by which currents return to baseline following GABA washout) to BDZs should depend on whether BDZs increased affinity by increasing the binding rate or decreasing the unbinding rate. Since deactivation occurs in the absence of free GABA, its time course should be insensitive to changes in the binding rate (defined as the product of the "true" binding rate and the GABA concentration, which equals zero during deactivation). In contrast, deactivation should be highly sensitive to slower unbinding, which increases the average time receptors spend GABA-bound, thus allowing for additional openings.

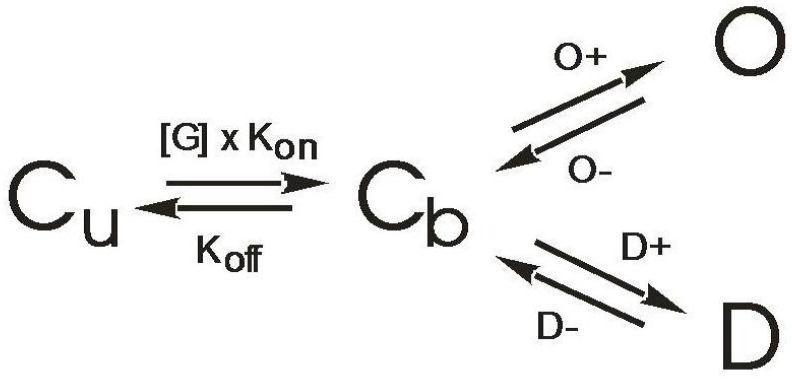

Figure 1. Simplified 4-state kinetic model of $GABA_A$ receptor function.

The model contains a single unbound closed state (C_u). Agonist binding initiates the transition from C_u to the bound closed state (C_b). This state can reversibly transition into either the open (O) or the desensitized (D) state. Note that the binding rate is the product of K_{on} and the GABA concentration, which have units of $M^{-1}s^{-1}$ and M, respectively. The remaining rate constants have units of s^{-1}. Model rate constants are: $K_{on} = 5 \times 10^6$; K_{off} = 1000; O+ = 800; O- = 500; D+ = 800; D- = 100.

These predictions were tested using a simple kinetic model of $GABA_A$ receptor function, previously shown to be useful for investigating the relationship between microscopic and macroscopic current kinetics (Figure 1) (Bianchi, et al., 2007) While this simplified model does not capture the rich kinetic behavior of $GABA_A$ receptors (Haas and Macdonald, 1999), it provides qualitative representation of the salient features of $GABA_A$ receptor currents (fast activation, fast desensitization, and relatively slow deactivation). In this model, receptors can occupy one of 4 states: a resting closed state (closed-unbound, C_u), a GABA-bound closed state (closed-bound, C_b), a GABA-bound open state (open, O), and an additional GABA-bound closed state that permits desensitization to occur (desensitized, D). As predicted, increasing affinity by increasing K_{on} (Figure 2A) or decreasing K_{off} (Figure 2B) increased peak amplitude when

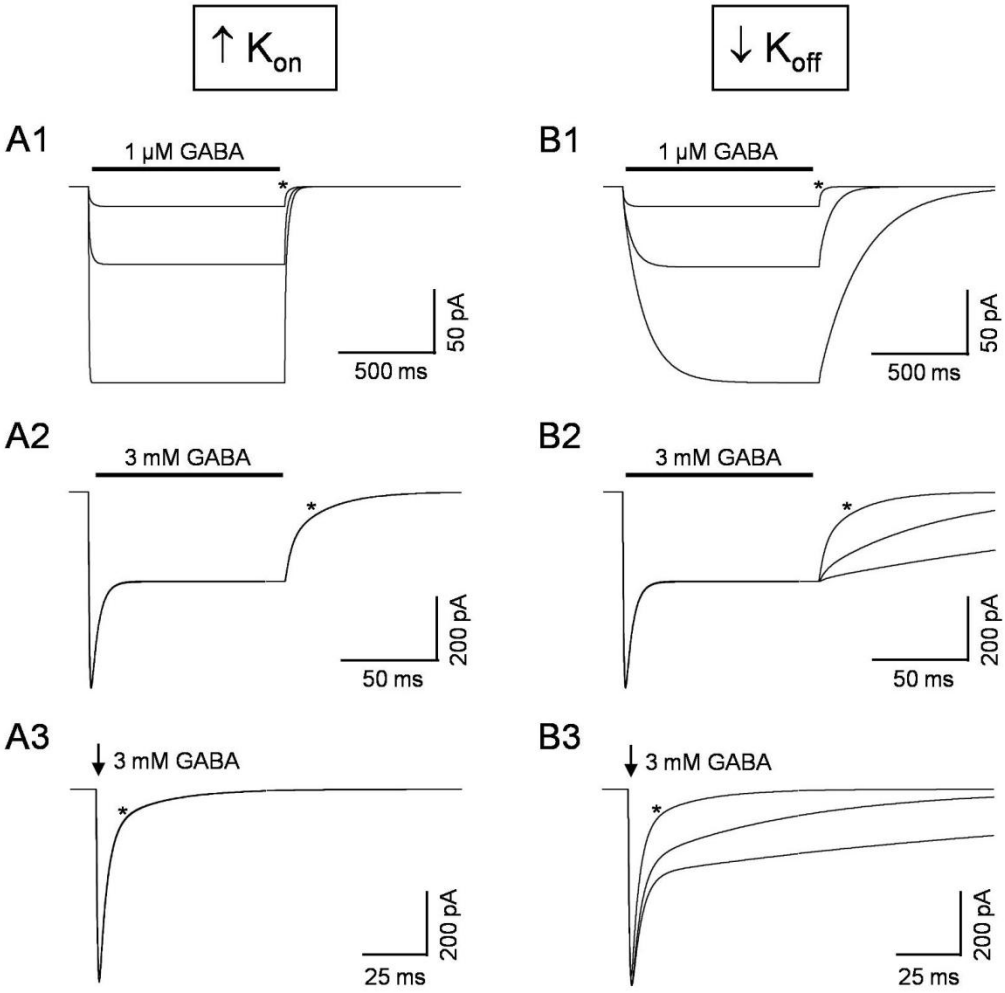

Figure 2. The effect of increasing GABA affinity by increasing K_{on} or decreasing K_{off} on macroscopic current properties.

Increasing receptor affinity for GABA can be accomplished either by increasing K_{on} (left column) or decreasing K_{off} (right column). A. Increasing GABA affinity by increasing K_{on} increased current amplitudes in the context of a sub-saturating (1 μM; ~EC_2) GABA concentration (Panel A1), but had no appreciable effect on currents evoked by a saturating (3 mM; ~EC_{99}) GABA concentration, either after long (Panel A2) or short (Panel A3) duration GABA applications. The asterisk (*) indicates the baseline current (K_{on} = $5x10^6$), and currents evoked in the context of progressively higher values of K_{on} ($2.5x10^7$ and $1x10^8$) were superimposed. B. Increasing GABA affinity by decreasing K_{off} also increased current amplitudes in the context of a sub-saturating GABA concentration (Panel B1) but not in the context of a saturating GABA concentration (Panels B2, B3). However, deactivation was substantially prolonged with decreasing K_{off} at all GABA concentrations, independent of the application duration. The asterisk (*) indicates the baseline current (K_{off} = 1000), and currents evoked in the context of progressively lower values of K_{on} (200 and 50) were superimposed. Currents are downward-going by convention.

currents were evoked by a sub-saturating GABA concentration (Figure 2A1, 2B1), but neither did so when currents were evoked by a saturating GABA concentration (Figure 2A2, 2B2). Desensitization occurring in the presence of a saturating GABA concentration was also not affected by increased affinity, either by increasing K_{on} or decreasing K_{off} (Figure 2A2, 2B2). Deactivation, in contrast, was highly sensitive to increases in affinity, even in the context of saturating GABA, but only by decreasing K_{off}. This was true for deactivation following prolonged exposures to GABA (Figure 2A2, 2B2) and also for deactivation following "synaptic" (1 ms) pulses (Figure 2A3, 2B3). Similar results were obtained using comprehensive models containing multiple open, closed, and desensitized states (Haas and Macdonald, 1999; Lagrange, et al., 2007).

BDZs enhanced $GABA_A$ receptor currents by decreasing the GABA unbinding rate

Although single-channel studies have suggested that BDZs enhance $GABA_A$ receptor currents by increasing GABA affinity, it remains unclear whether this is mediated by an increased rate of GABA binding or a decreased rate of GABA unbinding (Lavoie and Twyman, 1996). Therefore, guided by the kinetic simulations in the previous section, we re-evaluated BDZ-mediated increase in GABA affinity using electrophysiolgy. Whole-cell patch-clamp recordings were obtained from HEK293T cells transiently expressing $\alpha1\beta3\gamma2L$ $GABA_A$ receptors (Figure 3). GABA was applied with or without 1 μM diazepam (DZP) using a rapid solution exchange system. DZP was pre-applied for 1 sec to allow for equilibration (the slight baseline shift with BDZ pre-application may reflect a low-affinity direct activation mechanism) (Bianchi and

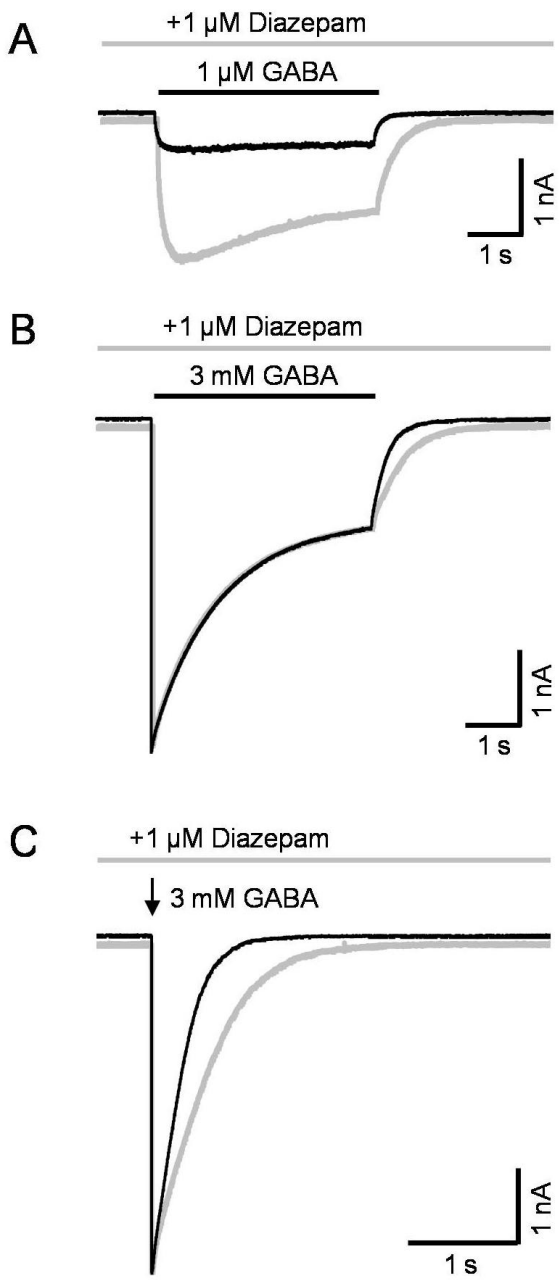

Figure 3. Modulation of $GABA_A$ receptor currents by diazepam.

A, Currents evoked from cells expressing α1β3γ2L $GABA_A$ receptors by a sub-saturating GABA concentration (1 μM; black line) were enhanced by concurrent application of diazepam (1 μM; gray line). B, Similar experimental protocol as in Panel A, using a saturating GABA concentration (3 mM). Note that the current amplitude and shape of desensitization (i.e., during the GABA application; black bar above traces) were unchanged by diazepam. In contrast, current deactivation (i.e., after the GABA application) was prolonged by diazepam. C, Diazepam prolonged deactivation after a brief (5 ms, "synaptic") pulse of saturating GABA.

Macdonald, 2001). Consistent with BDZs increasing the affinity of GABA for the receptor, DZP co-application increased the peak amplitude and desensitization of currents evoked by a sub-saturating concentration of GABA (1 μM, ~EC_{25}) (Figure 3A), but had no effect on the amplitude or desensitization of currents evoked by a saturating concentration of GABA (3 mM, ~EC_{99}) (Figure 3B). Deactivation, however, was always prolonged in the presence of DZP, for both low and high GABA concentrations (Figure 3A, B), and for brief (5 ms) synaptic-like pulses of GABA (Figure 3C). Taken together, these findings suggested that BDZs increased GABA affinity by decreasing the GABA unbinding rate, K_{off}. Although we cannot exclude a mixed mechanism that involves both K_{on} and K_{off}, the data are incompatible with BDZs modulating K_{on} alone.

Decreasing the GABA unbinding rate is predicted to increase opening frequency of $GABA_A$ receptors activated under tonic "extrasynaptic" conditions

Single-channel opening frequency is defined as the number of openings per unit time. Since individual openings must be flanked by closures, opening frequency is determined by the average time channels spend open and by the average time channels spend closed (this determines the average interval between openings). However, when channels are capable of accessing multiple closed states, as in the kinetic model shown in Figure 1, the overall average closed time depends not only on the average lifetime of each individual closed state (which equals the reciprocal sum of the exit rates from each state), but also on the weighted likelihood of reaching each closed state (which is determined by a more complex relationship between rates) (Colquhoun and Hawkes, 1982). For receptors activated under extrasynaptic conditions (i.e., prolonged exposure to a sub-saturating concentration of GABA), the average lifetime of the C_u state is relatively long

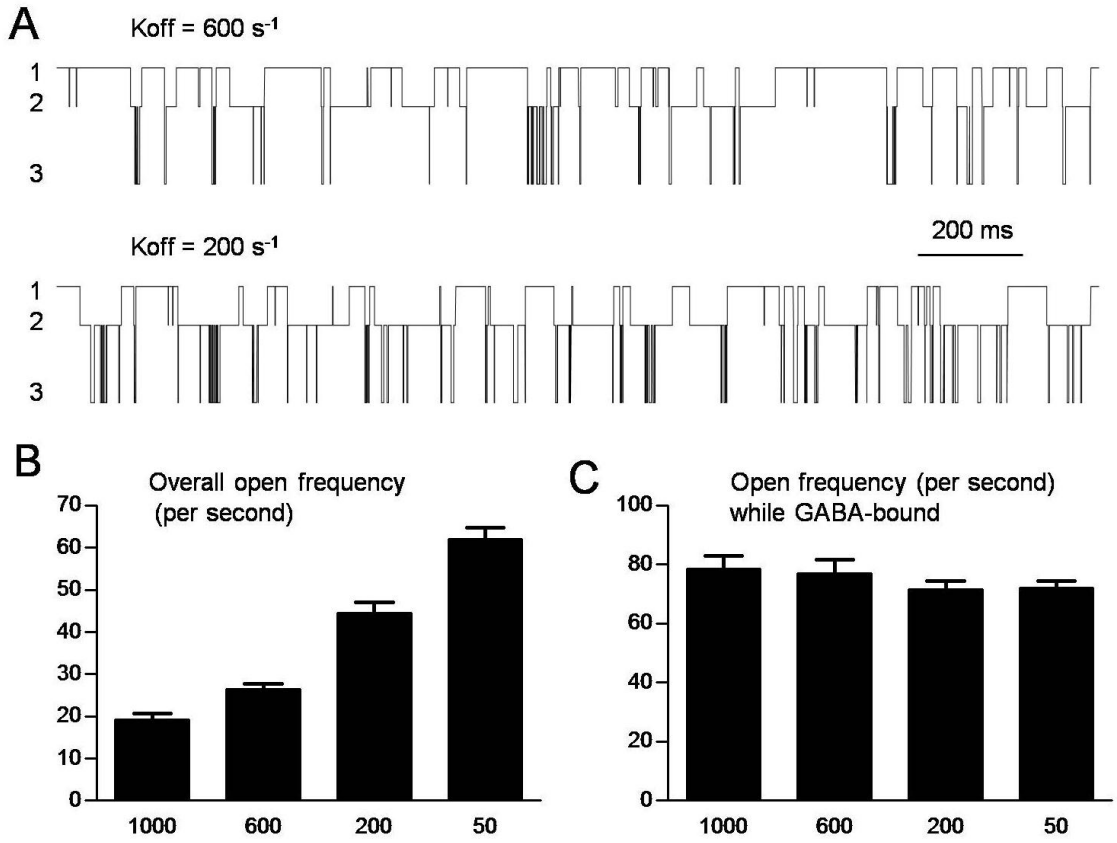

Figure 4. Simulated single-channel activity under "extrasynaptic" conditions

A. Simulated single-channel activity in response to continuous exposure to 1 μM GABA when K_{off} is 600 s^{-1} (top trace) and when K_{off} is 200 s^{-1} (bottom trace). The current levels designate receptor presence in the C_u (level 1), C_b or D (level 2), and O (level 3) states. Decreasing K_{off} (which increases GABA affinity) leads to an increase in the frequency of openings (currents reaching the 3rd current level), and less time spent in the resting unbound state (the baseline current level). The horizontal time bar applies to both traces. B. Overall opening frequency, including time spent in the unbound state, increased as K_{off} decreased, with significant differences in comparison of every pair of columns. C. Opening frequency, restricted to the time during which the channel was GABA-bound, did not increase as K_{off} was decreased. In this and subsequent panels, the column labels indicate the value of K_{off} in units of s^{-1}.

(since the effective binding rate is determined by the product of K_{on} and the GABA concentration), and therefore, contributes substantially to the average closed time. By decreasing K_{off}, BDZs decrease the likelihood that receptors enter this long-lived state, thus decreasing the average closed time. In other words, with slower unbinding, the average length of channel closure becomes dominated by the time spent in two closed states (C_b and D) as opposed to three (C_u, C_b, and D). Thus, BDZs are predicted to decrease the interval between openings and, therefore, increase opening frequency.

To evaluate this phenomenon explicitly, single-channel activity was simulated using the simple kinetic model (Figure 1) under extrasynaptic conditions: a low concentration of GABA (1 μM) applied for an extended period of time (2000 ms) (Figure 4). Increasing BDZ concentration was simulated by varying K_{off} from 1000 s^{-1} (baseline) to progressively lower values (600, 200, and 50 s^{-1}). The "EC_X" notation denotes the GABA concentration producing *X* percent of maximal current amplitude. Based on simulated concentration-response curves (not shown), 1 μM GABA was approximately EC_2 when K_{off} was 1000, EC_{15} when K_{off} was 600, EC_{25} when K_{off} was 200, and EC_{35} when K_{off} was 50 s^{-1}. The use of a simplified model and a single concentration of BDZ precluded direct comparison of the magnitude of BDZ modulation with that seen in the patch clamp experiments, although this would not alter the interpretations of our simulation data.

Unlike "real" single-channel recordings, where one cannot explicitly distinguish different states with the same conductance (such as different closed states), the simulations allowed us to unambiguously determine the receptor occupation of each state by assigning them different current levels (Figure 4A; see Methods). We were

specifically interested in distinguishing the unbound state (C_u, level 1) from the GABA-bound non-conducting states (C_b and D, level 2), and also from the single GABA-bound conducting state (O, level 3). As expected, the transition profile in the presence of BDZ (lower trace) consisted of less time in the unbound closed state (level 1) and more time in the bound closed (level 2) and open (level 3) states than did the transition profile in the absence of BDZ (top trace). Note that in both cases channels spent only a fraction of the total GABA-bound time in the open state; the remainder of bound time was spent in C_b and D. Since decreasing the unbinding rate did not affect channel mean open time (not shown), this shift of receptor occupancy towards the GABA-bound conformations increased overall channel opening frequency (Figure 4B).

However, when analysis was restricted to the time when receptors were GABA-bound (something that can only be accomplished *in silico*), opening frequency was not found to increase (Figure 4C). This critical difference reflects the fact that the increase in overall frequency (which is what was measured in the previously reported experiments using prolonged exposure to low GABA concentrations) was mediated entirely by decreased occupancy of the unbound closed state (C_u). Therefore, when we eliminated this state from our calculations, the effect on opening frequency disappeared. In other words, the observed frequency change simply reflected the ability of receptors to bind and rebind GABA in the experimental conditions, as opposed to a fundamental change in receptor kinetics.

Interestingly, opening frequency actually tended to decrease with lower values of K_{off}. Although seemingly counterintuitive, this reflected the fact that decreasing the unbinding rate actually increased the average lifetime of the C_b state, which partly

determined the GABA-bound closed time. The magnitude of this decrease in frequency was small simply because the average lifetime of the C_b state was short compared to that of the D state, which dominated the GABA-bound closed time.

Decreasing the GABA unbinding rate is predicted to increase the number, but not the frequency, of single-channel openings under phasic "synaptic" conditions

Synaptic receptors are activated under markedly different conditions from those traditionally used to evaluate the effects of BDZs on single-channels, suggesting that BDZs will have a different effect on their opening frequency. Indeed, if receptors are fully-saturated by vesicular release of GABA, then receptor occupancy in C_u approaches zero. This limits the ability of BDZs to affect opening frequency, as decreasing the unbinding rate cannot further increase the fraction of receptors that are GABA-bound (a "ceiling" effect). Importantly, this inability to affect opening frequency is independent of the duration of the GABA transient: as long as the GABA concentration is high, the C_u species is negligible, and thus frequency will not be increased whether the GABA transient is 1 ms (as in our simulations) or 5 ms (as in our experiments). Although our simulations and experiments do not address the potential contributions of altered diffusion and/or transporter function on the time-course of the GABA transient, it should be noted that even if receptors are not saturated, once GABA is cleared from the synaptic cleft, all subsequent openings shaping the synaptic current necessarily reflect transitions among GABA-bound states (i.e., C_b, D, and O). Our results, however, demonstrated that decreasing the unbinding rate cannot increase opening frequency when channel activity does not involve the C_u state (Figure 4), suggesting that BDZs would not increase opening frequency under synaptic conditions.

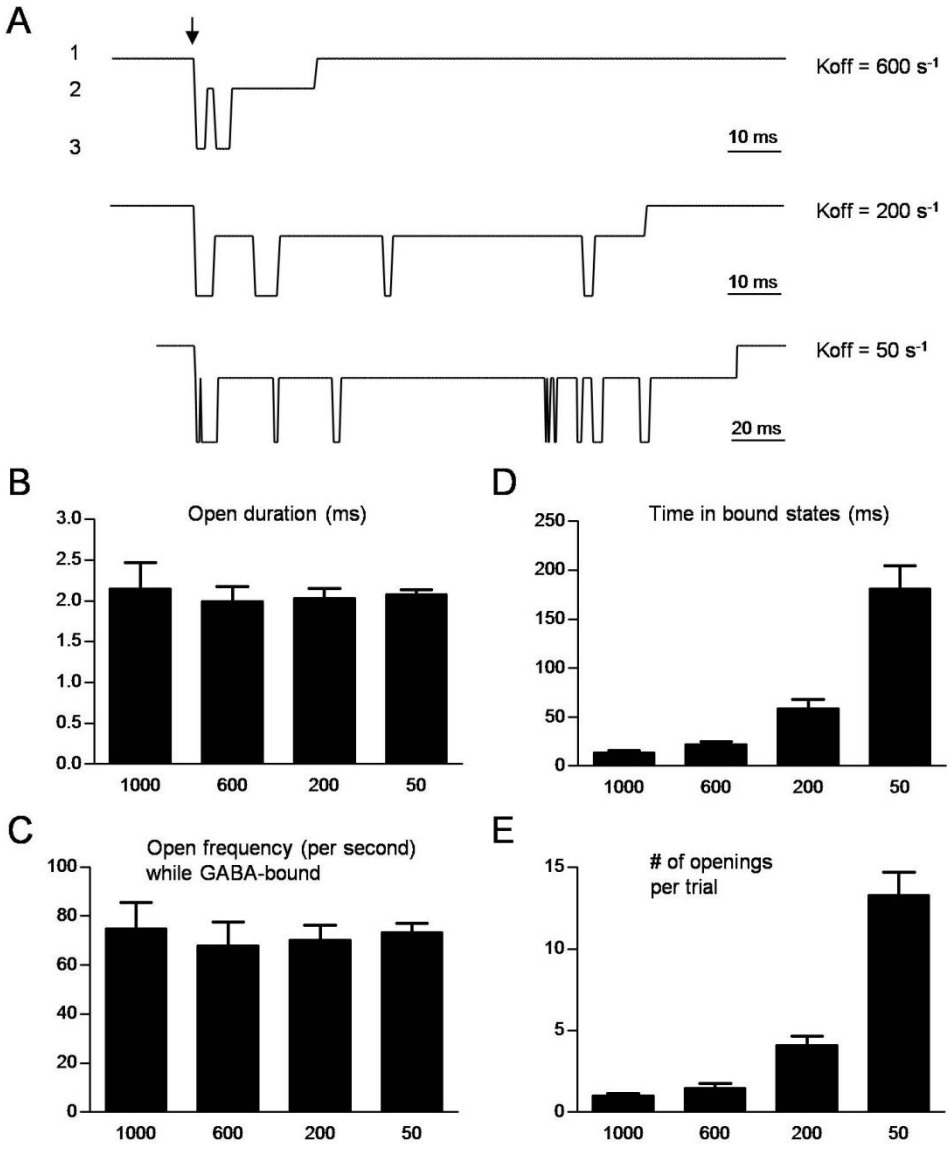

Figure 5. Simulated single-channel activity under "synaptic" conditions

A. Simulated single-channel activity in response to a 1 ms pulse of 1 mM GABA when K_{off} is 600 s^{-1} (top trace), 200 s^{-1} (middle trace), and 50 s^{-1} (bottom trace). The current levels designate receptor presence in the C_u (level 1), C_b or D (level 2), and O (level 3) states. B. Mean open duration (ms) was not significantly altered by changes in K_{off}. In this and subsequent panels, the column labels indicate the value of K_{off} in units of s^{-1}. C. Mean opening frequency, measured while channels were bound by GABA, was not significantly altered by changes in K_{off}. D. The time spent in the bound states increased as K_{off} decreased, with significant differences in every pair-wise column comparison except between K_{off} = 1000 and K_{off} = 600. E. The mean number of openings per trial pulse of GABA increased as K_{off} decreased, with significant differences in comparison of every pair of columns except between K_{off} = 1000 and K_{off} = 600.

To test this hypothesis, single-channel responses to 1 ms pulses of 1 mM GABA were simulated (Figure 5). As in the previous section, K_{off} was set to 1000 s^{-1} in the baseline condition, and increasing BDZ concentrations were simulated using progressively lower K_{off} values (600, 200, and 50 s^{-1}) (Figure 5A). Unbinding (entry into C_u) was considered a terminal event for calculations of opening frequency, since we assumed that rebinding was negligible under synaptic conditions. Opening frequency was therefore defined as the number of openings divided by the time spent GABA-bound. Note that being able to determine precisely the moment of unbinding overcomes a critical limitation for testing this hypothesis experimentally, where unbinding is not associated with a change in channel conductance and thus cannot be measured or inferred. In other words, with "real" experiments, one cannot justify how long to "watch" for openings after a GABA pulse is delivered, yet this duration specifies the denominator for calculations of opening frequency. As expected, neither the open durations (Figure 5B) nor the opening frequency (Figure 5C) were increased by decreasing the unbinding rate. However, slower unbinding increased the average time receptors spent GABA-bound (Figure 5D), which increased the total number of openings (Figure 5E). Thus, under synaptic conditions, BDZs are predicted to increase the number of channel openings without increasing opening frequency.

DISCUSSION

The unique conditions of synaptic transmission prevent BDZs from increasing single-channel opening frequency

Electrophysiological studies have demonstrated that BDZs increase single-channel opening frequency by increasing GABA affinity (Rogers, et al., 1994; Twyman, et al., 1989). However, these experiments were performed using low concentrations of GABA, which allowed channels to spend considerable time in the unbound closed state (C_u), and prolonged exposure to GABA, which allowed channels to repeatedly access this state (i.e., bind and unbind GABA). In this context, which resembles extrasynaptic transmission *in vivo*, BDZs were able to increase opening frequency by decreasing the contribution of the C_u state to the overall average closed time. This state, however, plays a minimal role in opening frequency when receptors are activated under synaptic conditions for two main reasons. First, receptor occupancy in C_u rapidly approaches zero with the high concentrations of GABA reached in synapses. Second, the high rate at which free GABA is cleared from the synaptic cleft renders rebinding (and therefore, the contribution of the C_u state to the average closed interval) minimal under synaptic conditions, even if synaptic $GABA_A$ receptors are not saturated (Perrais and Ropert, 1999; Poncer, et al., 1996). Thus, BDZs are not predicted to increase the single-channel opening frequency of synaptic $GABA_A$ receptors.

BDZs enhance synaptic currents by increasing the number of single-channel openings

If BDZs cannot increase single-channel opening frequency of receptors activated under synaptic conditions, what then explains their ability to enhance synaptic currents

(Nusser and Mody, 2002)? Our simulations demonstrated that by delaying GABA unbinding, BDZs increase the average time receptors are GABA-bound, thus increasing the total number of channel openings following a brief pulse of GABA. Indeed, once a receptor enters the C_b state, the likelihood of unbinding GABA versus continuing to transition among GABA-bound states is determined by the ratio of the unbinding rate (K_{off}) to the sum of the alternatives (entry into O and D). Thus, by decreasing K_{off}, BDZs extend the window of time during which individual receptors can transition among GABA-bound states, prolonging synaptic currents. Unlike stabilizing desensitized states, which also prolongs synaptic currents by increasing the average time receptors are GABA-bound (Bianchi, et al., 2007; Jones and Westbrook, 1995), delaying unbinding by decreasing K_{off} necessarily increases synaptic charge transfer. This is because decreasing K_{off} increases the number of channels available for opening at each moment in time after the GABA pulse (i.e., the "population" opening frequency increases), which increases the total number of openings.

BDZs are predicted to increase single-channel opening frequency of extrasynaptic $GABA_A$ receptors

Increasing evidence suggests that extrasynaptic $GABA_A$ receptors make important contributions to inhibitory signaling (Kullmann, et al., 2005). In contrast to synaptic signaling that is brief, point-to-point, and involves high neurotransmitter concentrations, extrasynaptic communication involves low and slowly changing concentrations of neurotransmitters diffusing over larger distances than the synaptic cleft (Kullmann, et al., 2005). Although the physiological relevance of extrasynaptic transmission remains poorly understood, the effects of BDZs observed on single-channel currents evoked under

equilibrium conditions may prove relevant for understanding how this subset of $GABA_A$ receptors are modulated by BDZs. While the majority of extrasynaptic receptors include the δ subunit, which renders them insensitive to BDZs (McKernan and Whiting, 1996; Mehta and Ticku, 1999), γ subunit-containing receptors sensitive to the effects of BDZs have also been found outside synapses in a number of brain regions including the hippocampus (Glykys and Mody, 2007). Our simulations predicted that BDZs would in fact increase single-channel opening frequency of BDZ-sensitive extrasynaptic receptors. Although the relative importance of synaptic and extrasynaptic $GABA_A$ receptors to neurological diseases such as epilepsy remains uncertain, the dependence of BDZ modulation on activation context may have important relevance for anticonvulsant treatment. For example, BDZs may prolong synaptic currents in situations in which they are pathologically brief such as the γ2 subunit mutation, K289M, associated with generalized epilepsy with febrile seizures plus (Bianchi, et al., 2002). It is conceivable that extrasynaptic receptors (which may depend upon ambient rather than synaptic GABA) can be modulated by BDZs independent of synaptic inhibition or when synaptic inhibition is pathologically compromised.

Single-channel opening frequency is sensitive to multiple kinetic mechanisms

Although single-channel opening frequency is a relatively straightforward experimental measurement, there are in fact a variety of "mechanisms" that influence opening frequency. For example, just as decreasing K_{off} can increase opening frequency by decreasing the average channel closed time (under extrasynaptic conditions), frequency can also be increased by decreasing the entry rate or increasing the exit rate

from the desensitized state. Interestingly, opening frequency can also be increased by decreasing the time spent in the open state (by increasing the exit rate O^-), as this will decrease the length of each open-closed cycle. However, increasing opening frequency in this manner will actually decrease overall channel open probability. Thus, changes in opening frequency alone can neither specify a kinetic mechanism nor provide information regarding channel effectiveness (the open duration must also be known). This distinction between observation (opening frequency) and mechanism (increased affinity via K_{off}) forms the basis for our demonstration of "context-dependent" BDZ modulation of $GABA_A$ receptor opening frequency. Thus, a single mechanism (increased affinity via decreasing K_{off}) yields different functional impacts on opening frequency (and macroscopic current properties) depending on the context in which receptors are activated. Despite this kinetic difference, $GABA_A$ receptor function is enhanced by BDZs in both synaptic and extrasynaptic contexts. Although detailed kinetic models of most $GABA_A$ receptor isoforms have not been established, the mechanistic arguments of this study are likely to apply in general to BDZ-sensitive isoforms, because they hold for any model in which binding precedes transitions to open, pre-open and desensitized states, regardless of their number or connectivity.

REFERENCES

Bianchi, M.T., Botzolakis, E.J., Haas, K.F., Fisher, J.L., Macdonald, R.L., 2007. Microscopic kinetic determinants of macroscopic currents: insights from coupling and uncoupling of $GABA_A$ receptor desensitization and deactivation. J Physiol 584, 769-787.

Bianchi, M.T., Macdonald, R.L., 2001. Agonist Trapping by $GABA_A$ Receptor Channels. J Neurosci 21, 9083-9091.

Bianchi, M.T., Song, L., Zhang, H., Macdonald, R.L., 2002. Two different mechanisms of disinhibition produced by $GABA_A$ receptor mutations linked to epilepsy in humans. J Neurosci 22, 5321-5327.

Choh, D.W., Farb, D.H., Fischbach, G.D., 1977. Chlordiazepoxide selectively augments GABA action in spinal cord cell cultures. Nature 269, 342-344.

Colquhoun, D., 1991. Neher and Sakmann win Nobel Prize for patch-clamp work. Trends Pharmacol Sci 12, 449.

Colquhoun, D., Hawkes, A.G., 1982. On the stochastic properties of bursts of single ion channel openings and of clusters of bursts. Philos Trans R Soc Lond B Biol Sci 300, 1-59.

Farrant, M., Nusser, Z., 2005. Variations on an inhibitory theme: phasic and tonic activation of GABA(A) receptors. Nat Rev Neurosci 6, 215-229.

Gahwiler, B.H., 1976. Diazepam and chlordiazepoxide: powerful GABA antagonsits in explants of rat cerebellum. Brain Res 107, 176-179.

Ghansah, E., Weiss, D.S., 1999. Benzodiazepines do not modulate desensitization of recombinant alpha1beta2gamma2 GABA(A) receptors. Neuroreport 10, 817-821.

Glykys, J., Mann, E.O., Mody, I., 2008. Which GABA(A) receptor subunits are necessary for tonic inhibition in the hippocampus? J Neurosci 28, 1421-1426.

Glykys, J., Mody, I., 2007. Activation of $GABA_A$ receptors: views from outside the synaptic cleft. Neuron 56, 763-770.

Haas, K.F., Macdonald, R.L., 1999. $GABA_A$ receptor subunit gamma2 and delta subtypes confer unique kinetic properties on recombinant $GABA_A$ receptor currents in mouse fibroblasts. J Physiol 514 (Pt 1), 27-45.

Hinkle, D.J., Bianchi, M.T., Macdonald, R.L., 2003. Modifications of a commercial perfusion system for use in ultrafast solution exchange during patch clamp recording. Biotechniques 35, 472-474, 476.

Jones, M.V., Westbrook, G.L., 1995. Desensitized states prolong $GABA_A$ channel responses to brief agonist pulses. Neuron 15, 181-191.

Jones, M.V., Westbrook, G.L., 1996. The impact of receptor desensitization on fast synaptic transmission. Trends Neurosci 19, 96-101.

Kullmann, D.M., Ruiz, A., Rusakov, D.M., Scott, R., Semyanov, A., Walker, M.C., 2005. Presynaptic, extrasynaptic and axonal $GABA_A$ receptors in the CNS: where and why? Prog Biophys Mol Biol 87, 33-46.

Lagrange, A.H., Botzolakis, E.J., Macdonald, R.L., 2007. Enhanced macroscopic desensitization shapes the response of alpha4 subtype-containing $GABA_A$ receptors to synaptic and extrasynaptic GABA. J Physiol 578, 655-676.

Lavoie, A.M., Twyman, R.E., 1996. Direct evidence for diazepam modulation of $GABA_A$ receptor microscopic affinity. Neuropharmacology 35, 1383-1392.

Macdonald, R., Barker, J.L., 1978. Benzodiazepines specifically modulate GABA-mediated postsynaptic inhibition in cultured mammalian neurones. Nature 271, 563-564.

MacDonald, R.L., Rogers, C.J., Twyman, R.E., 1989. Barbiturate regulation of kinetic properties of the GABAA receptor channel of mouse spinal neurones in culture. J Physiol 417, 483-500.

Mathers, D.A., 1987. The $GABA_A$ receptor: new insights from single-channel recording. Synapse 1, 96-101.

McKernan, R.M., Whiting, P.J., 1996. Which $GABA_A$ -receptor subtypes really occur in the brain? Trends Neurosci 19, 139-143.

Mehta, A.K., Ticku, M.K., 1999. An update on $GABA_A$ receptors. Brain Res Brain Res Rev 29, 196-217.

Nusser, Z., Mody, I., 2002. Selective modulation of tonic and phasic inhibitions in dentate gyrus granule cells. J Neurophysiol 87, 2624-2628.

Perrais, D., Ropert, N., 1999. Effect of zolpidem on miniature IPSCs and occupancy of postsynaptic $GABA_A$ receptors in central synapses. J Neurosci 19, 578-588.

Poncer, J.C., Durr, R., Gahwiler, B.H., Thompson, S.M., 1996. Modulation of synaptic $GABA_A$ receptor function by benzodiazepines in area CA3 of rat hippocampal slice cultures. Neuropharmacology 35, 1169-1179.

Rogers, C.J., Twyman, R.E., Macdonald, R.L., 1994. Benzodiazepine and beta-carboline regulation of single $GABA_A$ receptor channels of mouse spinal neurones in culture. J Physiol 475, 69-82.

Twyman, R.E., Rogers, C.J., Macdonald, R.L., 1989. Differential regulation of gamma-aminobutyric acid receptor channels by diazepam and phenobarbital. Ann Neurol 25, 213-220.

Young, A.B., Zukin, S.R., Snyder, S.H., 1974. Interaction of benzodiazepines with central nervous glycine receptors: possible mechanism of action. Proc Natl Acad Sci U S A 71, 2246-2250.

CHAPTER IV

CONTEXT-DEPENDENT MODULATION OF SYNAPTIC AND EXTRASYNAPTIC $GABA_A$ RECEPTORS BY PENICILLIN: IMPLICATIONS FOR PHASIC AND TONIC INHIBITION

Emmanuel J. Botzolakis, Hua-Jun Feng, and Robert L. Macdonald

ABSTRACT

$GABA_A$ receptors mediate two modes of inhibitory neurotransmission, each involving different subsets of receptor isoforms and different contexts of receptor activation. While "phasic" inhibition results from transient activation of synaptic receptors by nearly-saturating concentrations of GABA, "tonic" inhibition results from persistent activation of extrasynaptic receptors by sub-saturating concentrations of ambient GABA. Penicillin, an open-channel blocker of $GABA_A$ receptors, selectively inhibits hippocampal phasic currents. To distinguish between isoform-specific and context-dependent modulation as possible explanations for this selectivity, the effects of penicillin were evaluated on the properties of recombinant $GABA_A$ receptor isoforms expressed in HEK293T cells. When co-applied with saturating GABA, penicillin decreased peak currents, altered desensitization, and prolonged deactivation of both synaptic and extrasynaptic isoforms. However, when activated in their respective physiological contexts, synaptic and extrasynaptic isoforms had markedly different sensitivities to penicillin. Currents evoked from synaptic isoforms under phasic conditions were substantially inhibited, while those evoked from extrasynaptic isoforms

under tonic conditions were minimally affected. Although this behavior was unexpected for an open-channel blocker, kinetic simulations using simple models of channel function provided intuitive explanations for each of the experimental findings and exposed a previously unrecognized similarity between the roles of blocked and desensitized states in shaping macroscopic currents. We therefore concluded that the reported inability of penicillin to modulate tonic currents could not simply be attributed to insensitivity of extrasynaptic receptors, but rather, reflected an inability to modulate these receptors in their specific context of activation.

INTRODUCTION

$GABA_A$ receptors are heteropentameric ligand-gated chloride channels responsible for the majority of fast inhibitory neurotransmission in the mammalian brain (Olsen and Macdonald, 2002; Luscher and Keller, 2004). Seven subunit families (α, β, γ, δ, ε, θ, and π) are known to exist (Olsen and Macdonald, 2002; Luscher and Keller, 2004), with αβγ and αβδ isoforms representing the majority of neuronal $GABA_A$ receptors (McKernan and Whiting, 1996). In general, αβγ receptors are targeted to synapses (though some γ subunit-containing receptors may also be found extrasynaptically), while αβδ receptors are targeted to extra- or perisynaptic areas (Essrich et al., 1998; Nusser et al., 1998; Wei et al., 2003; Semyanov et al., 2004; Sun et al., 2004).

Following vesicular release, a nearly-saturating concentration of GABA activates synaptic receptors before being rapidly cleared by diffusion and reuptake. This transient activation, thought to occur in the sub-millisecond time scale (Mozrzymas, 2004), gives rise to inhibitory post-synaptic currents (IPSCs) and is termed "phasic" inhibition. Increasing evidence, however, suggests that GABA may escape from synapses, allowing for activation of extrasynaptic receptors (Glykys and Mody, 2007). The persistent increase in chloride conductance resulting from prolonged exposure to sub-saturating concentrations of ambient GABA gives rise to "tonic" inhibition and represents an important alternate mode of GABAergic transmission, one thought to be less spatially and temporally constrained (Mody and Pearce, 2004; Farrant and Nusser, 2005). Understanding how pharmacological agents differentially modulate these two modes of neuronal inhibition is of increasing interest, as they may play distinct roles in the

pathogenesis of epilepsy and other neurological disorders (Macdonald et al., 2006; Peng et al., 2004).

Penicillin is a known convulsant that reduces GABA-evoked currents (Macdonald and Barker, 1977; Horne et al., 1992; Katayama et al., 1992; Tsuda et al., 1994; Behrends, 2000; Sugimoto et al., 2002) and blocks spontaneous activity of $GABA_A$ receptors (Krishek et al., 1996; Tierney et al., 1996; Lindquist et al., 2004). This negative modulation is thought to be mediated by open-channel block, as single channel studies have reported reduced open duration with increased channel opening frequency and burst length (Chow and Mathers, 1986; Twyman et al., 1992). Interestingly, evidence from electrophysiological studies in hippocampal neurons indicated that penicillin selectively inhibited phasic currents (Yeung et al., 2003). Given that different receptor isoforms are thought to mediate phasic and tonic inhibition (Farrant and Nusser, 2005), and subunit composition is known to influence receptor pharmacology (Wohlfarth et al., 2002; Feng and Macdonald, 2004; Feng et al., 2004), one parsimonious explanation for this observation is that extrasynaptic isoforms are simply insensitive to penicillin (i.e., isoform-specific modulation).

Alternatively, it is possible that penicillin modulates both synaptic and extrasynaptic isoforms, but that its effects are highly dependent on the "context" of receptor activation (i.e., context-dependent modulation). Unlike tonic currents, which are mediated by receptors activated under conditions of near-equilibrium by low concentrations of GABA, phasic currents are mediated by receptors activated under conditions of extreme non-equilibrium by high concentrations of GABA. As a result, the distribution of receptors among available states in the gating scheme is likely to be

markedly different for conditions of phasic and tonic activation, and depending on the relationship between the kinetics of open-channel block and those of receptor gating, could give the appearance of selectivity for phasic, but not tonic, currents (e.g., if the blocking rate was high but the overall blocker affinity was low). Indeed, sensitivity to the context of receptor activation, both in terms of exposure duration and agonist concentration, has previously been described for positive and negative $GABA_A$ receptor modulators (Barberis et al., 2002; Bianchi and Macdonald, 2003; Feng et al., 2004) and also for open-channel blockers of NMDA-type glutamate receptors (Lipton, 2006).

To distinguish between isoform-specific and context-dependent modulation as potential mechanisms underlying the selective modulation of phasic currents, the effects of penicillin were evaluated on currents evoked from recombinant synaptic and extrasynaptic $GABA_A$ receptor isoforms expressed in HEK293T cells. In addition, simulations using simple models of $GABA_A$ receptor function explored the relationship between the microscopic kinetics of open-channel block and the macroscopic properties of currents evoked under phasic or tonic conditions. Both the simulations and the experimental results demonstrated that open-channel blockers can have seemingly counterintuitive effects on macroscopic current properties, and interestingly, that these effects are highly dependent on the context of receptor activation.

MATERIALS AND METHODS

Cell culture and expression of recombinant $GABA_A$ receptors

Human embryonic kidney (HEK293T) cells were cultured in Dulbecco's Modified Eagle Medium (Invitrogen, Grand Island, NY, USA) supplemented with 10% fetal bovine serum (Invitrogen), 100 i.u./ml penicillin, and 100 μg/ml streptomycin (Life Technologies, Grand Island, NY, USA) and maintained at 37°C in humidified 5% CO_2 / 95% air. Cells were seeded at moderate density in 60-mm culture dishes (Corning Glassworks, Corning, NY, USA) and transfected 24 hr later with 2 μg per cDNA encoding rat α (α1, α4, α5, or α6), β3, and either γ2L or δ $GABA_A$ receptor subunits using a modified calcium phosphate precipitation method (Feng et al., 2004). Two μg of pHOOK (Invitrogen, Carlsbad, CA, USA), which encodes for the surface antibody sFv, were co-transfected for immunomagnetic selection 24 hrs later (Greenfield et al., 1997). Following selection, cells were re-plated in 35-mm culture dishes and currents were recorded 24 hr later using standard patch clamp techniques. Collagen-coated dishes were used for macropatch recordings.

Electrophysiology

Patch clamp recordings were obtained at room temperature with cells bathed in an external solution composed of (in mM) 142 NaCl, 1 $CaCl_2$, 6 $MgCl_2$, 8 KCl, 10 glucose, and 10 HEPES (pH 7.4). Recording electrodes were pulled using a P-87 Flaming Brown Micropipette Puller (Sutter Instruments, San Rafael, CA, USA), fire polished on an MF-9 microforge (Narishige, Tokyo, Japan), and filled with an internal solution consisting of

(in mM) 153 KCl, 1 $MgCl_2$, 10 HEPES, 2 MgATP, and 5 EGTA (pH 7.3). Open tip resistances of the recording electrodes were typically 1.0–1.6 MΩ. Whole-cell or macropatch currents were recorded using an Axopatch 200A amplifier (Molecular Devices, Foster City, CA, USA), low-pass filtered at 2 kHz using the internal 4-Pole Bessel filter of the amplifier, digitized with the Digidata 1322A data acquisition system (Molecular Devices), and stored for offline analysis. Both GABA and penicillin G (benzylpenicillin, sodium salt) were purchased from Sigma-Aldrich (St. Louis, MO, USA) and prepared as stock solutions. Working solutions were made on the day of the experiment by diluting stock solutions with external solution. Drugs were gravity-fed using 4-barrel square glass tubing connected to a Perfusion Fast-Step system (Warner Instruments, Hamden, CT, USA). The 10-90% rise times of open electrode tip liquid junction currents were consistently <2.0 ms. Penicillin was pre-applied for 1.5 sec prior to co-application with GABA. 4 sec pulses of 1 mM GABA were used to evaluate macroscopic current kinetics, 5 ms pulses of 1 mM GABA were used to mimic phasic activation, and 30 sec pulses of 1 μM GABA were used to mimic tonic activation. Consecutive drug applications were separated by at least 45 sec in external solution to allow for complete GABA and penicillin unbinding.

Data analysis and simulations

Data were analyzed offline using Clampfit 8.1 (Molecular Devices). The extent of current inhibition by penicillin (% of GABA current) was determined by dividing the current evoked during co-application of GABA and penicillin by the current evoked by GABA alone. The extent of desensitization was determined by dividing the amount of

current lost (residual current subtracted from peak current) by peak current. The time course of deactivation was fit using the standard Levenberg-Marquardt method to the form $\Sigma\, a_n e^{(-t/\tau_n)}$, where n is the number of the exponential components, a is the relative amplitude, t is time, and τ is the time constant. A weighted τ in the form of $(a_1\tau_1 + a_2\tau_2) / (a_1 + a_2)$ was calculated for comparison of deactivation time courses. The net charge transfer of a pulse was defined as the area between the adjusted baseline and the current. Data were reported as mean ± SEM. A paired Student's *t* test was performed to compare individual current features before and after penicillin co-application. An unpaired Student's *t* test was used to compare current features. Statistical significance was taken as $p<0.05$.

Kinetic simulations were carried out using Berkeley Madonna 3.1 (www.berkeleymadonna.com), a differential equation solving program, using the fourth order Runge-Kutta method with a time interval of 10 μs. Analyses of simulated currents were identical to those of real currents.

RESULTS

Penicillin altered the kinetic properties of synaptic and extrasynaptic $GABA_A$ receptor isoform currents

To explore the effects of penicillin on the macroscopic current properties of synaptic and extrasynaptic $GABA_A$ receptors, a saturating concentration of GABA (1 mM) was co-applied with penicillin (1 mM) for 4 sec using rapid solution exchange to lifted HEK293T cells transiently transfected with α (α1, α4, α5, or α6), β3, and either γ2L or δ subunits. These eight subunit combinations were chosen as a representative sample of receptor isoforms thought to be expressed in synaptic or extrasynaptic areas (Wisden et al., 1992; Saxena and Macdonald, 1994; McKernan and Whiting, 1996; Sur et al., 1999; Brunig et al., 2002; Poltl et al., 2003; Caraiscos et al., 2004; Peng et al., 2004; Glykys et al., 2007). For the purposes of this study, only α1βγ and α6βγ subunit combinations were considered "synaptic"; the remaining subunit combinations were considered "extrasynaptic". Note that although the α4βγ isoform has been detected in synapses under certain conditions (Hsu et al., 2003; Liang et al., 2006; Zhang et al., 2007), its role in normal synaptic physiology remains unclear.

Penicillin altered the kinetic properties of all γ2L subunit-containing receptor isoform currents (Figure 1A-D). Peak currents were substantially decreased for each isoform (α1β3γ2L: 47.1 ± 8.1% of control, n = 6, $p<0.01$; α4β3γ2L: 41.8 ± 3.8% of control, n = 12, $p<0.001$; α5β3γ2L: 37.7 ± 3.6% of control, n = 8, $p<0.01$; α6β3γ2L: 54.3 ± 6.7% of control, n = 10, $p<0.05$) (Figure 1E), as were residual currents (α1β3γ2L: 32.3 ± 4.4% of control, $p<0.01$; α4β3γ2L: 59.0 ± 4.0% of control, $p<0.01$; α5β3γ2L: 44.9 ±

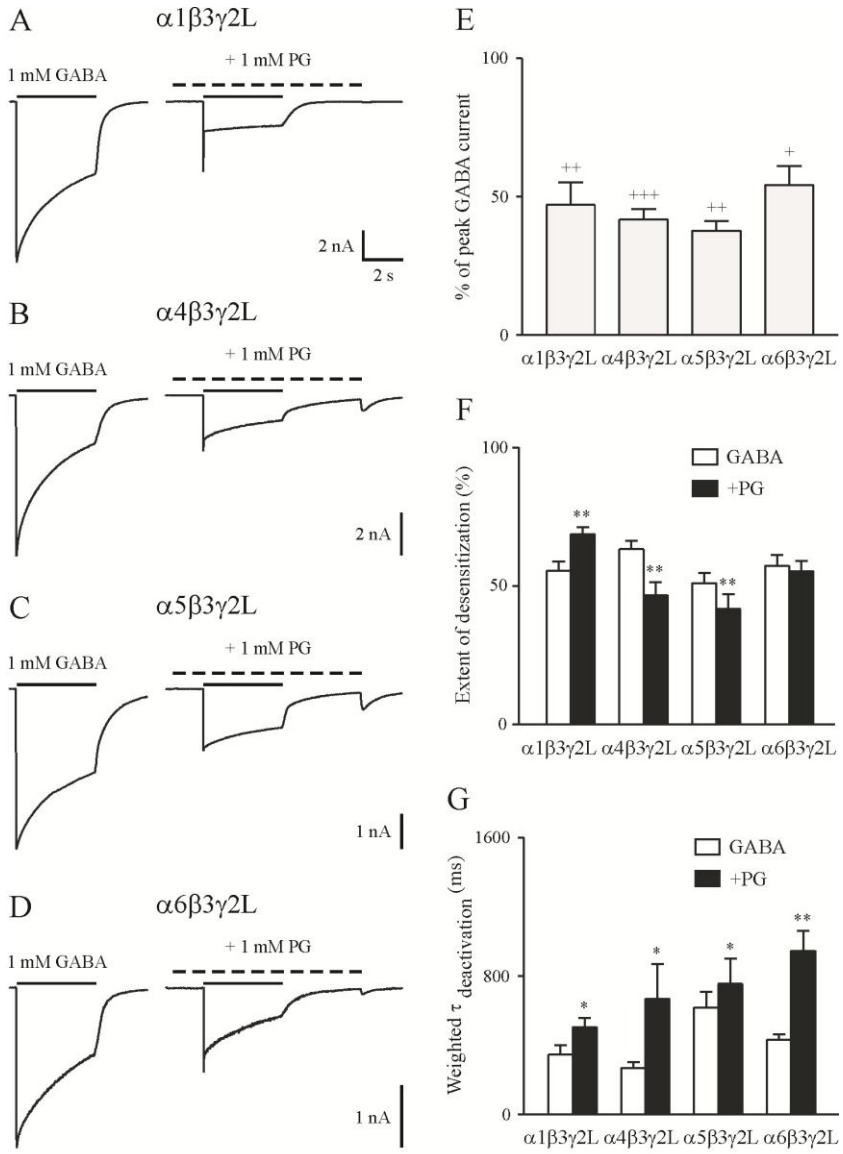

Figure 1. Penicillin altered the macroscopic current properties of γ2L subunit-containing $GABA_A$ receptors.

A-D, Whole-cell currents were evoked by 1 mM GABA either alone (left) or in the presence of 1 mM penicillin G (PG) (right) for α1β3γ2L, α4β3γ2L, α5β3γ2L, and α6β3γ2L receptors, respectively. The solid line above each trace indicates the duration of GABA application. The dashed line denotes the duration of penicillin application. E, Penicillin decreased peak current amplitudes. F, Penicillin had variable effects on the extent of desensitization. G, Penicillin increased the weighted time constant (τ) of deactivation. Error bars denote SEM. + The peak current evoked by co-application of GABA and penicillin was significantly reduced compared to the GABA control current at $p<0.05$; ++ $p<0.01$; +++ $p<0.001$. * Significantly different from GABA control current desensitization or deactivation at $p<0.05$; ** $p<0.01$.

4.3% of control, $p<0.01$; $\alpha6\beta3\gamma2L$: 55.3 ± 5.3% of control, $p<0.05$). While the extent of desensitization increased for $\alpha1\beta3\gamma2L$ receptors compared to control (55.5 ± 3.3% vs 68.7 ± 2.6%, $p<0.01$), it decreased for $\alpha4\beta3\gamma2L$ (63.3 ± 3.1% vs 46.7 ± 4.6%, $p<0.01$) and $\alpha5\beta3\gamma2L$ (51.1 ± 3.7% vs 41.7 ± 5.4%, $p<0.01$) receptors, and was unchanged for $\alpha6\beta3\gamma2L$ receptors (57.3 ± 3.9% vs 55.3 ± 3.7%, $p>0.05$) (Figure 1F). Interestingly, despite the variable effects on desensitization, all γ2L subunit-containing receptors had prolonged deactivation in the presence of penicillin compared to control currents ($\alpha1\beta3\gamma2L$: 345.8 ± 53.2 ms vs 504.6 ± 51.7 ms, $p<0.05$; $\alpha4\beta3\gamma2L$: 268.5 ± 34.2 ms vs 668.2 ± 201.8 ms, $p<0.05$; $\alpha5\beta3\gamma2L$: 617.7 ± 92.6 ms vs 755.3 ± 144.7 ms, $p<0.05$; $\alpha6\beta3\gamma2L$: 432.4 ± 32.4 ms vs 946.4 ± 116.8 ms, $p<0.01$) (Figure 1G) and had rebound currents upon penicillin washout (Figure 1A-D).

Penicillin also altered the kinetic properties of δ subunit-containing receptor isoform currents (Figure 2A-D). As with γ2L subunit-containing receptors, peak currents were reduced ($\alpha1\beta3\delta$: 78.3 ± 7.3% of control, n = 9, $p<0.05$; $\alpha4\beta3\delta$: 54.2 ± 1.2% of control, n = 6, $p<0.01$; $\alpha5\beta3\delta$: 69.6 ± 5.2% of control, n = 5, $p = 0.07$; $\alpha6\beta3\delta$: 69.3 ± 4.3% of control, n = 6, $p<0.05$) (Figure 2E). Residual currents, however, were only decreased for $\alpha4\beta3\delta$ and $\alpha6\beta3\delta$ receptors ($\alpha1\beta3\delta$: 95.6 ± 3.0% of control, $p>0.05$; $\alpha4\beta3\delta$: 65.8 ± 2.6% of control, $p<0.01$; $\alpha5\beta3\delta$: 101.7 ± 3.9% of control, $p>0.05$; $\alpha6\beta3\delta$: 65.0 ± 4.6% of control, $p<0.05$). The higher sensitivity of peak compared to residual currents caused the extent of desensitization to decrease for the majority of δ subunit-containing receptors ($\alpha1\beta3\delta$: 24.8 ± 6.5% vs 7.4 ± 1.7%, $p<0.05$; $\alpha4\beta3\delta$: 53.4 ± 2.1% vs

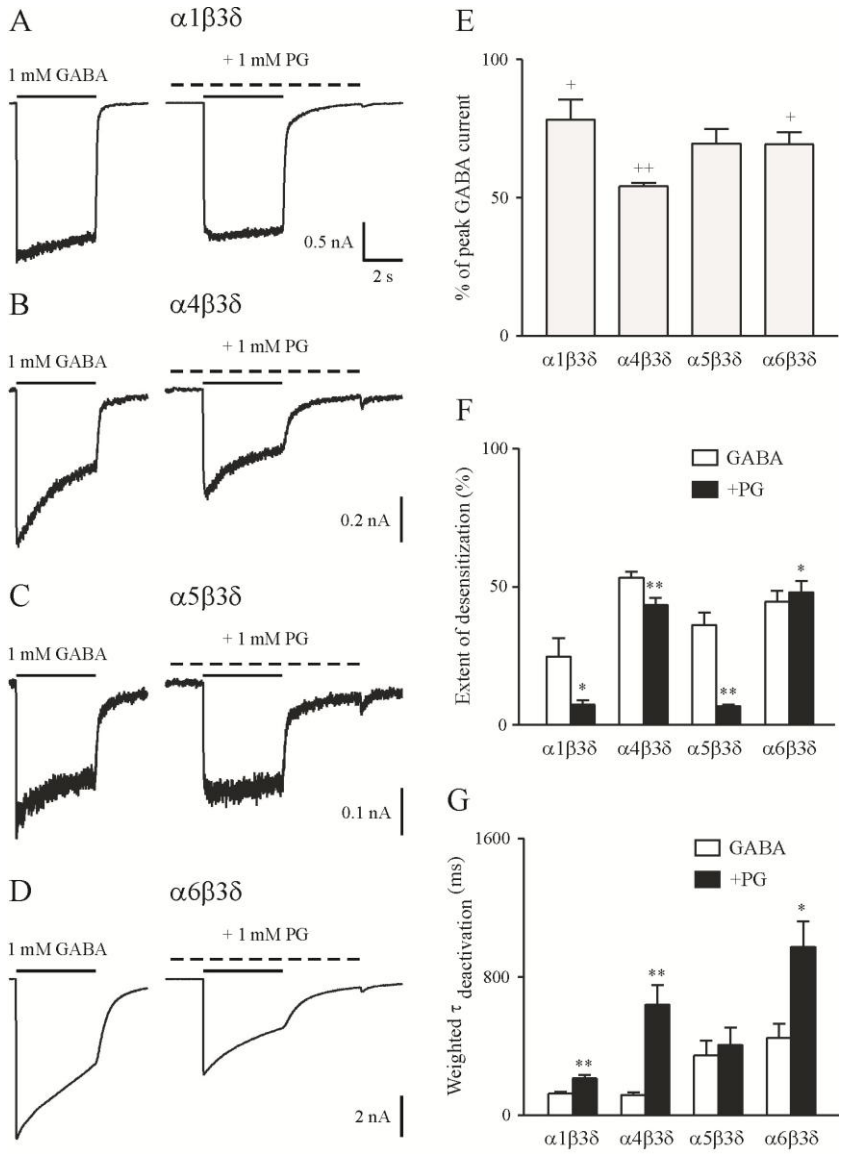

Figure 2. Penicillin altered the macroscopic current properties of δ subunit-containing $GABA_A$ receptors.

A-D, Whole-cell currents were evoked by 1 mM GABA either alone (left) or in the presence of 1 mM penicillin G (PG) (right) for α1β3δ, α4β3δ, α5β3δ, and α6β3δ receptors, respectively. The solid line above each current trace indicates the duration of GABA application. The dashed line denotes the duration of penicillin application. E, Penicillin decreased peak current amplitudes. F, Penicillin had variable effects on the extent of desensitization. G, Penicillin increased the weighted time constant (τ) of deactivation. Error bars denote SEM. + Significantly reduced compared to the GABA control current at $p<0.05$; ++ $p<0.01$. * Significantly different from GABA control current desensitization or deactivation at $p<0.05$; ** $p<0.01$.

43.5 ± 2.5%, $p<0.01$; α5β3δ: 36.2 ± 4.4% vs 6.8 ± 0.5%, $p<0.01$), with only α6 subunit-containing receptors having a slightly increased extent of desensitization (44.7 ± 3.9% vs 48.0 ± 4.1%, $p<0.05$) (Figure 2F). With the exception of α5 subunit-containing receptors, deactivation was prolonged for all δ subunit-containing receptors (α1β3δ: 125.3 ± 10.5 ms vs 214.5 ± 19.5 ms, $p<0.01$; α4β3δ: 117.8 ± 13.5 ms vs 641.0 ± 112.4 ms, $p<0.01$; α5β3δ: 345.7 ± 87.4 ms vs 407.9 ± 100.4 ms, $p>0.05$; α6β3δ: 449.1 ± 80.9 ms vs 975.7 ± 147.7 ms, $p<0.05$) (Figure 2G). In addition, all δ subunit-containing receptors had rebound currents upon penicillin washout (Figure 2A-D). Note that α5β3δ receptors were expressed poorly in HEK293T cells, and we thus obtained currents from only 5 cells.

In summary, penicillin reduced peak current amplitudes, prolonged deactivation, and induced rebound currents for both synaptic and extrasynaptic $GABA_A$ receptor isoforms (Table 1), suggesting that the reported inability of penicillin to modulate tonic inhibition in previous studies (Yeung et al., 2003) could not simply be attributed to insensitivity of extrasynaptic receptors. However, the finding that the extent of desensitization was decreased for most extrasynaptic receptor isoforms (the result of peak currents having higher sensitivity than residual currents) suggested that these isoforms might simply appear insensitive to penicillin when activated under near-equilibrium conditions. We thus explored the possibility that the "context" of receptor activation was responsible for the apparent selectivity of penicillin for phasic currents.

Table 1. Summary of the effects of penicillin on the macroscopic current properties of synaptic and extrasynaptic $GABA_A$ receptor isoforms (4 sec application of 1 mM GABA vs co-application of 1 mM GABA and 1 mM penicillin)

	I_{peak} amplitude	Desensitization	Deactivation
α1β3γ2L	↓	↑	↑
α1β3δ	↓	↓	↑
α4β3γ2L	↓	↓	↑
α4β3δ	↓	↓	↑
α5β3γ2L	↓	↓	↑
α5β3δ	NS	↓	NS
α6β3γ2L	↓	NS	↑
α6β3δ	↓	↑	↑

↑/↓, denotes increased or decreased peak current amplitude, extent of desensitization, or weighted deactivation time constant; NS, not significantly different from the GABA control current.

Currents evoked from synaptic $GABA_A$ receptor isoforms in the context of phasic activation were significantly inhibited by penicillin

To investigate its potential effects on phasic inhibition, penicillin (1 mM) was co-applied with a brief pulse (5 ms) of saturating GABA (1 mM) to the synaptic α1β3γ2L and α6β3γ2L $GABA_A$ receptor isoforms. These experimental conditions are thought to

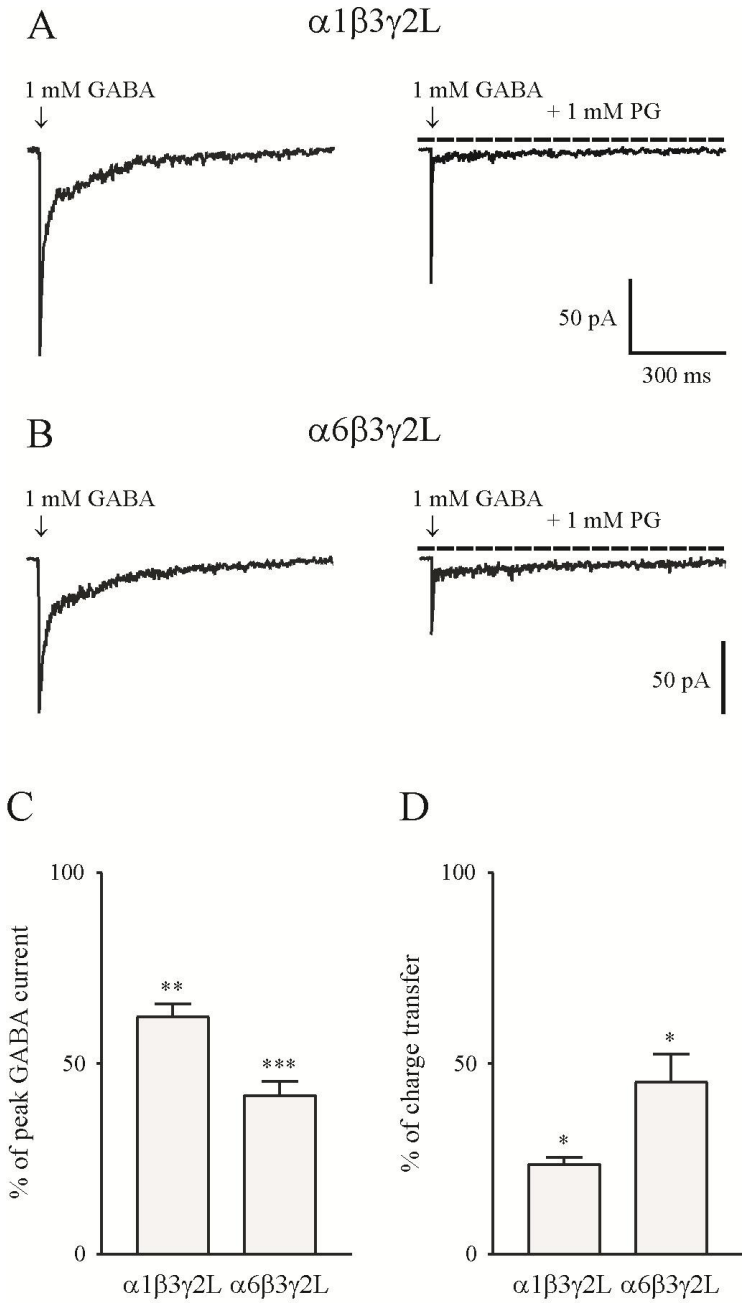

Figure 3. Penicillin substantially inhibited currents evoked from synaptic $GABA_A$ receptor isoforms under phasic conditions.

A, B, Macropatch currents were evoked by a brief (5 ms) application of 1 mM GABA either alone (left) or in the presence of 1 mM penicillin G (PG) (right) for α1β3γ2L and α6β3γ2L receptors, respectively. The solid arrow above each current trace indicates the brief duration of GABA application. The dashed line denotes the duration of penicillin application. C, Penicillin decreased peak current amplitudes. D, Penicillin decreased total charge transfer. Error bars denote SEM. * Significantly different from GABA control current at $p<0.05$; ** $p<0.01$; *** $p<0.001$.

mimic those of phasic activation, as the resulting currents have kinetic properties similar to those of IPSCs (Jones and Westbrook, 1995). To further increase the temporal resolution of the recordings, they were performed on excised outside-out patches from transiently transfected HEK293T cells.

Compared to currents evoked by brief pulses of GABA alone, co-application of GABA with penicillin reduced the peak current amplitude of $\alpha1\beta3\gamma2L$ receptors (62.3 ± 3.3% of control, n = 5, $p<0.01$) (Figure 3A, C). In addition, penicillin accelerated the deactivation time course from 64.7 ± 4.6 ms to 25.9 ± 5.4 ms ($p<0.001$), an unexpected finding given that deactivation was significantly prolonged following longer applications (Figure 1G). Combined, these effects caused a substantial decrease in the net charge transfer following an individual GABA pulse (23.7 ± 1.8% of control, $p<0.05$) (Figure 3D). Penicillin also reduced the peak current amplitude (41.6 ± 3.9% of control, n = 11, $p<0.001$) (Figure 3B, C) and accelerated deactivation (109.8 ± 13.5 ms vs 72.5 ± 9.5 ms, $p<0.05$) of $\alpha6\beta3\gamma2L$ receptors. As with $\alpha1\beta3\gamma2L$ receptors, these effects combined to substantially decrease the net charge transfer following an individual brief GABA pulse (45.1 ± 7.3% of control, $p<0.05$) (Figure 3D).

Currents evoked from extrasynaptic $GABA_A$ receptor isoforms in the context of tonic activation were minimally inhibited by penicillin

To investigate its potential effects on tonic inhibition, penicillin (1 mM) was co-applied with a long pulse (30 sec) of sub-saturating GABA (1 μM) to the extrasynaptic $\alpha4\beta3\delta$, $\alpha4\beta3\gamma2L$, and $\alpha5\beta3\gamma2L$ receptor isoforms. This subset of receptor isoforms is thought to mediate the majority of the tonic current in hippocampal neurons (Wisden et

al., 1992; Caraiscos et al., 2004; Chandra et al., 2006), which was found to be penicillin insensitive (Yeung et al., 2003). Prolonged drug application allowed for currents to reach a pseudo-equilibrium, as would be expected for those that mediate tonic inhibition.

For $\alpha4\beta3\delta$ receptors, the effects of penicillin were surprisingly limited to the peak current (Figure 4A). Indeed, while peak currents were reduced in the presence of penicillin ($74.8 \pm 2.9\%$ of control, $n = 10$, $p<0.01$), equilibrium currents were essentially unchanged ($93.7 \pm 4.1\%$ of control, $p>0.05$). The higher sensitivity of peak currents (peak vs equilibrium, $p<0.01$) caused the extent of desensitization to decrease from $40.0 \pm 1.2\%$ to $24.7 \pm 2.8\%$ ($p<0.01$). Penicillin also preferentially modulated peak currents of $\alpha4\beta3\gamma2L$ (Figure 4B; peak: $72.3 \pm 3.9\%$ of control, $n = 10$, $p<0.01$; equilibrium: $85.0 \pm 3.0\%$ of control, $p<0.01$; peak vs equilibrium, $p<0.05$) and $\alpha5\beta3\gamma2L$ (Figure 4C; peak: $58.1 \pm 4.2\%$ of control, $n = 12$, $p<0.01$; equilibrium: $77.8 \pm 4.7\%$ of control, $p<0.01$; peak vs equilibrium, $p<0.01$) receptors. As a result, the extent of desensitization was decreased from $34.9 \pm 3.3\%$ to $23.6 \pm 2.4\%$ ($p<0.001$) and from $35.4 \pm 3.9\%$ to $14.2 \pm 3.2\%$ ($p<0.001$) for $\alpha4\beta3\gamma2L$ and $\alpha5\beta3\gamma2L$ receptor currents, respectively.

Thus, while peak currents were significantly reduced for each of these extrasynaptic receptor isoforms, equilibrium currents were less affected (Figure 4D, E). Although preferential modulation of peak currents (i.e., decreased extent of desensitization) was also observed for these same isoforms in the context of saturating GABA (Figure 1F, 2F), the combination of lowering the GABA concentration and extending the duration of GABA exposure rendered equilibrium currents even less

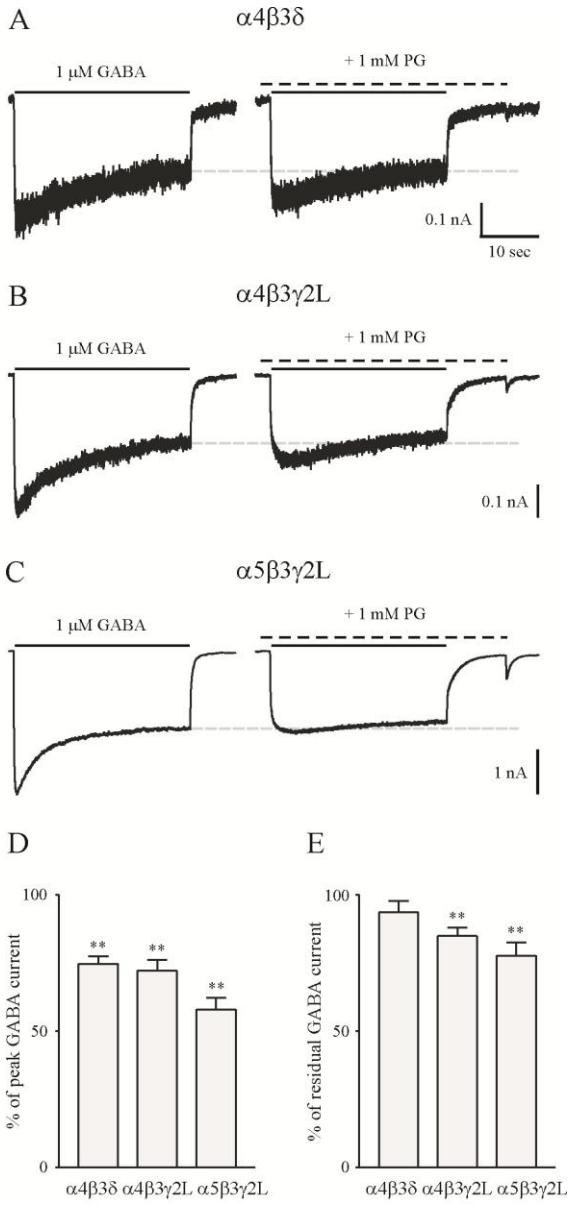

Figure 4. Penicillin had minimal effect on currents evoked from extrasynaptic $GABA_A$ receptor isoforms under tonic conditions.

A-C, Whole-cell currents were evoked by a long pulse (30 sec) of 1 μM GABA either alone (left) or in the presence of 1 mM penicillin G (PG) for α4β3δ, α4β3γ2L, and α5β3γ2L receptors, respectively. The solid line above each current trace indicates the duration of GABA application. The dashed black line denotes the duration of penicillin application. The dashed gray line indicates the amount of control steady-state current. D, Penicillin reduced peak current amplitudes. E, Penicillin had limited effect on residual current amplitudes. Error bars represent SEM. ** Significantly different from GABA control peak or steady state current amplitude at $p<0.01$.

sensitive to penicillin. This suggested that the reported selectivity of penicillin for phasic currents resulted not from an inability to modulate extrasynaptic receptors, but rather, from an inability to modulate these receptors in their native "context" of activation.

Simple kinetic models qualitatively reproduced the effects of open-channel block on $GABA_A$ receptor macroscopic current properties

The experimental findings in the previous sections suggested that open-channel block could have complex effects on macroscopic current properties. Although penicillin decreased peak currents and prolonged deactivation, its effects on the extent of desensitization were isoform specific. Moreover, while currents evoked under synaptic conditions were particularly vulnerable to penicillin, currents evoked under extrasynaptic conditions were relatively insensitive. To determine the kinetic basis for these findings, the effects of open-channel block were evaluated on macroscopic current properties using Markov models of $GABA_A$ receptor function.

Although comprehensive kinetic models have been proposed that account for both the microscopic and macroscopic properties of $GABA_A$ receptors (Haas and Macdonald, 1999; Lema and Auerbach, 2006; Lagrange et al., 2007), simple models are often sufficient to illustrate the salient features of GABA-evoked currents. Two such models, proven useful for investigating the relationship between macroscopic currents and microscopic kinetics, are shown in Figure 5 (panels A1 and B1; Bianchi et al., 2007). In the "linear" model (Figure 5A1), receptors transition into the desensitized (D) state directly from the open (O) state, while in the "branched" model (Figure 5B1) transitions into the D state proceed from the pre-open state (C_2). Since penicillin is thought to act

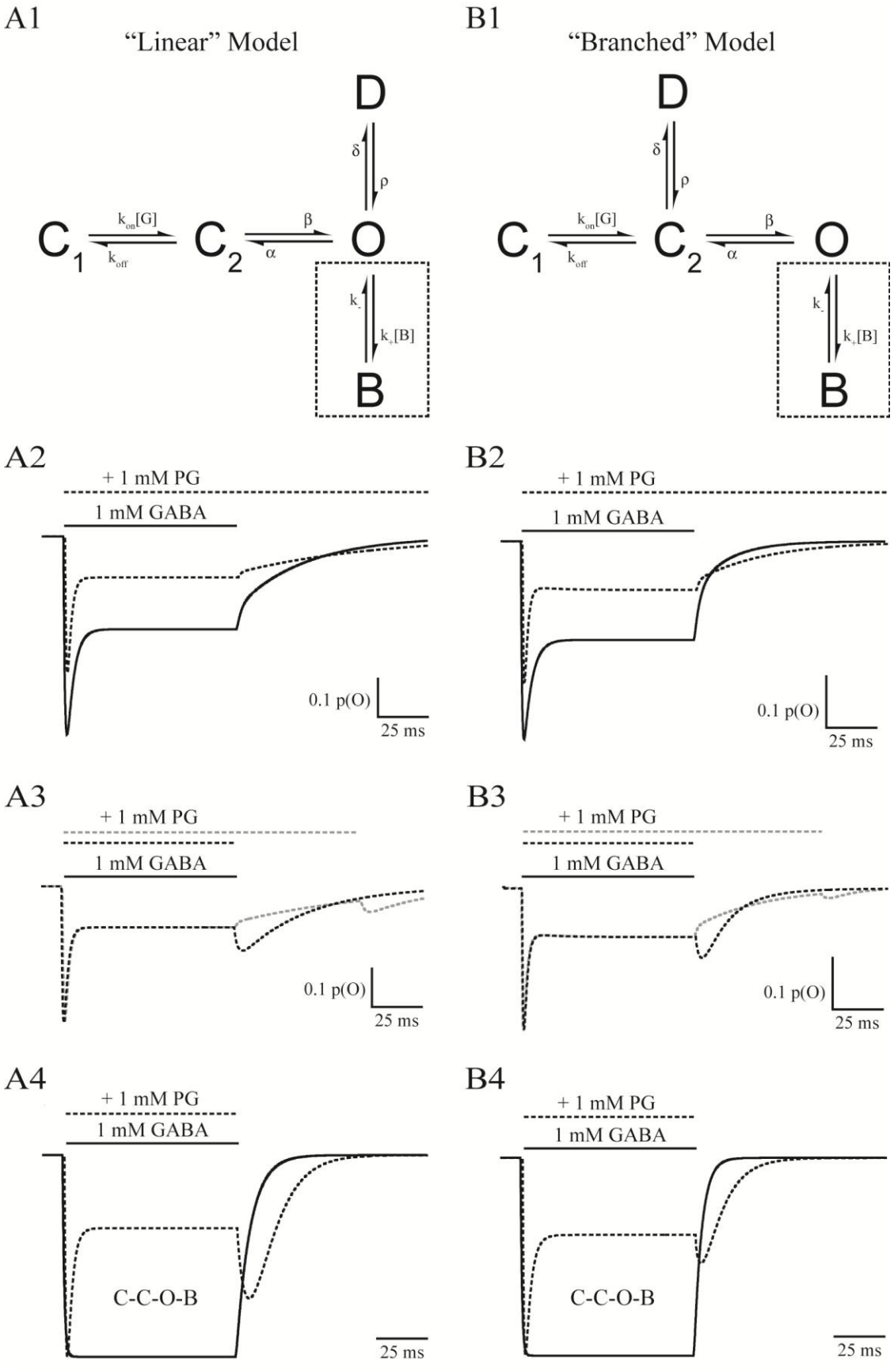
A1
"Linear" Model
D
δ
ρ
k_{on}[G]
k_{off}
C1
C2
β
α
O
k_-
k_+[B]
B
B1
"Branched" Model
A2
+ 1 mM PG
1 mM GABA
0.1 p(O)
25 ms
B2
A3
B3
A4
C-C-O-B
B4

Figure 5. The effects of penicillin-mediated open-channel block on macroscopic currents were simulated using simple kinetic models of $GABA_A$ receptor function.

A1, 4-state kinetic model, with closed (C), open (O), and desensitized (D) states in "linear" arrangement, was used to generate simulated GABA currents. Agonist binding occurs between C_1 and C_2. Open-channel block was simulated by adding a blocked state (B) to the O state (dashed box). Rate constants were: k_{on} = 7000, k_{off} = 1.0, β = 1.0, α = 0.3, δ = 0.3, ρ = 0.1, k+ = 550, k- = 0.1. All rates had units of ms^{-1}, except for the agonist binding (k_{on}) and blocker binding (k+) rates, which were multiplied by the concentration of GABA [G] and blocker [B], respectively, and thus had units of $ms^{-1}M^{-1}$. B1, 4-state kinetic model, with O and D states in "branched" arrangement, was used to generate simulated GABA currents. Rate constants were: k_{on} = 7000, k_{off} = 1.0, β = 1.0, α = 0.6, δ = 0.6, ρ = 0.1, k+ = 550, k- = 0.1. Note that while the original single channel studies assigned different blocking and unblocking rates for each O state (Twyman et al., 1992), the averaged values of k+ and k- were used here since linear and branched models contained a single O state. The remaining rate constants were chosen to qualitatively reproduce the macroscopic current properties of $\alpha\beta\gamma$ receptors (Haas and Macdonald, 1999; Lagrange et al., 2007). A2, B2, Currents were simulated from linear (Panel A2) and branched (Panel B2) models to 100 ms pulses of 1 mM GABA either in the presence (dashed traces) or absence (solid traces) of 1 mM penicillin G (PG). A3, B3, Currents were simulated from linear (Panel A3) and branched (Panel B3) models to 100 ms pulses of 1 mM GABA and 1 mM penicillin, with washout of penicillin occurring either simultaneously or 50 ms after GABA washout. Note the rebound currents upon penicillin washout, which became smaller in amplitude if deactivation was permitted before washout. A4, B4, Currents (scaled to peak) were simulated from linear (Panel A4) and branched (Panel B4) models to 100 ms pulses of 1 mM GABA either with (solid traces) or without (dashed traces) 1 mM penicillin when the D state entry rate was set to zero.

via open-channel block (Twyman et al., 1992), its effects were modeled by reversibly connecting a non-conducting state to the O state (Figure 5A1, B1; dashed boxes). Receptors entered this "blocked" state (B) via a concentration-dependent blocking rate (k+) and returned via a concentration-independent unblocking rate (k-), with k- being taken as the inverse of the brief closed time associated with penicillin block and k+ being chosen to account for the concentration-dependent increase in burst length (Twyman et al., 1992).

For both kinetic arrangements, simulated co-application of 1 mM GABA with 1 mM penicillin generated currents with reduced peak amplitudes, increased extents of desensitization, prolonged time courses of deactivation, and rebound upon penicillin washout, compared to currents evoked by GABA alone (Figure 5A2, B2, A3, B3). With the exception of the extent of desensitization, these results were qualitatively similar to our experimental observations, and were consistent with the expected effects of open-channel block on macroscopic currents. For example, since penicillin was modeled by adding a non-conducting state to the gating scheme, receptor occupancy in all other states should have decreased, the result being currents with smaller amplitudes (Figure 5A2, B2). In addition, since GABA unbinding could only occur from C2, addition of the blocked state effectively increased receptor mean bound time (Appendix II). Much like desensitized states, this allowed for additional openings prior to GABA unbinding, the macroscopic correlate of which is prolonged deactivation (Figure 5A2, B2) (Jones and Westbrook, 1995; Bianchi et al., 2007). The observation of a rebound current upon blocker washout was also to be expected, the result of surging open state occupancy following blocker unbinding (Figure 5A3, B3).

Blocking and unblocking rates played distinct roles in modulating the extent of desensitization

Although the kinetic simulations in the previous section qualitatively reproduced many of our experimental observations, it remained unclear how open-channel block could support decreased or unchanged extents of desensitization (Figures 1F, 2F). Indeed, since the B state was arranged in series with the O state, just as the D state was arranged in the linear model, we expected desensitization to increase, as receptors could

now close via an additional route. Support for the idea that the B state was serving as an additional D state came from the observation that desensitization was still possible in the absence of the D state (Figure 5A4, B4; dashed traces), while no desensitization was observed in the absence of both D and B states (Figure 5A4, B4; solid traces).

To reconcile our experimental findings with the simulations, we systematically explored the relationship between the rates of open-channel block and the extent of desensitization (Figure 6A1-A4). Using the default blocking rate ($k+ = 550\ ms^{-1}$) and the linear model (Figure 5A1), decreasing the unblocking rate (k-) over two orders of magnitude progressively increased desensitization (Figure 6A1). This corresponded to increased desensitization for the lowest unblocking rate ($k- = 0.01\ ms^{-1}$) compared to the GABA control current (dashed line), but slightly decreased desensitization for the highest unblocking rate ($k- = 1.0\ ms^{-1}$). This same trend was observed in the context of a higher blocking rate ($k+ = 5500\ ms^{-1}$), though the effect was substantially more pronounced (Figure 6A2). Interestingly, the unblocking rate supporting decreased desensitization was the same for both blocking rates ($k- = 1.0\ ms^{-1}$), as were the unblocking rates supporting essentially unchanged ($k- = 0.3\ ms^{-1}$) or increased ($k- = 0.1, 0.03, 0.01\ ms^{-1}$) desensitization. This suggested that blocking and unblocking rates played different roles in determining the sensitivity of desensitization to open-channel block: *the unblocking rate determined the direction of change (increased, decreased, or unchanged) while the blocking rate served mainly to modulate the magnitude of the change.*

This idea was supported by the observation that increasing the blocking rate in the context of the default unblocking rate ($k- = 0.1\ ms^{-1}$) caused only increased

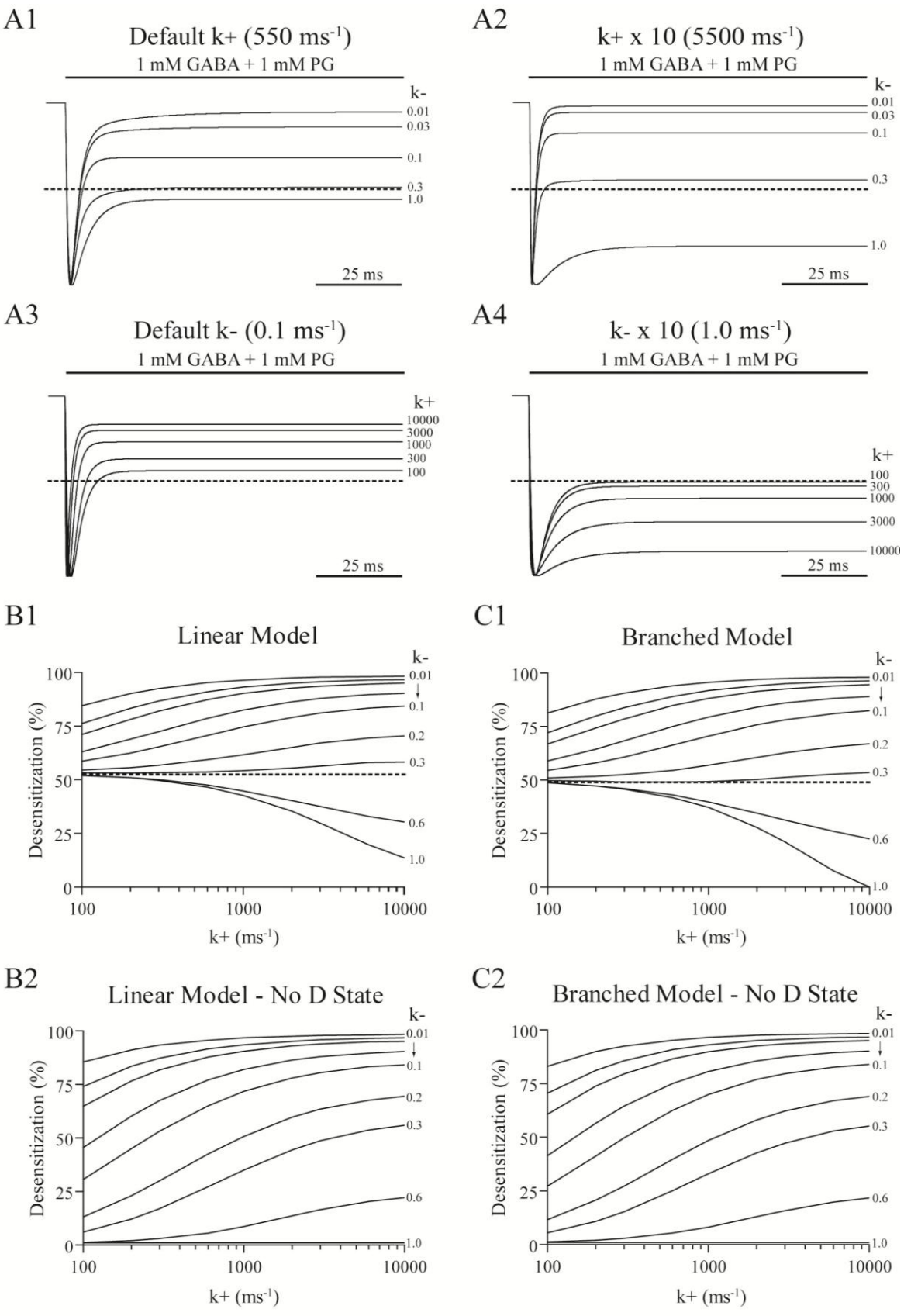
A1
Default k+ (550 ms-1)
1 mM GABA + 1 mM PG
k-
0.01
0.03
0.1
0.3
1.0
25 ms
A2
k+ x 10 (5500 ms-1)
1 mM GABA + 1 mM PG
k-
0.01
0.03
0.1
0.3
1.0
25 ms
A3
Default k- (0.1 ms-1)
1 mM GABA + 1 mM PG
k+
10000
3000
1000
300
100
25 ms
A4
k- x 10 (1.0 ms-1)
1 mM GABA + 1 mM PG
k+
100
300
1000
3000
10000
25 ms
B1
Linear Model
Desensitization (%)
k+ (ms-1)
C1
Branched Model
Desensitization (%)
k+ (ms-1)
B2
Linear Model - No D State
Desensitization (%)
k+ (ms-1)
C2
Branched Model - No D State
Desensitization (%)
k+ (ms-1)

Figure 6. The extent of macroscopic desensitization was differentially sensitive to blocking and unblocking rate constants.

A, Currents (normalized to peak) were simulated for the linear model to 100 ms co-applications of 1 mM GABA and 1 mM penicillin G (PG). In panels A1 and A2, the unblocking rate was varied in the context of either the default blocking rate (Panel A1; k+ = 550) or a higher blocking rate (Panel A2; k+ = 5500). In panels A3 and A4, the blocking rate was varied in the context of either the default unblocking rate (Panel A3; k- = 0.1) or a higher unblocking rate (Panel A4; k- = 1.0). Horizontal dashed lines indicate the residual current remaining in the absence of penicillin. B1-2, C1-2, The extent of desensitization was evaluated for simulated currents evoked by 100 ms pulses of 1 mM GABA to linear (Panels B1 and B2) and branched (Panel C1 and C2) models over a range of blocking (k+ = 100, 200, 300, 600, 1000, 2000, 3000, 6000, and 10000) and unblocking (k- = 0.01, 0.02, 0.03, 0.06, 0.1, 0.2, 0.3, 0.6, 1.0) rates in the presence of 1 mM penicillin. In Panels B2 and C2, the D state entry rate was set to zero. Dashed horizontal lines indicate the extent of desensitization in the absence of penicillin for each condition.

desensitization (Figure 6A3), while increasing the blocking rate in the context of a larger unblocking rate (k- = 1.0 ms^{-1}) caused only decreased desensitization (Figure 6A4). Interestingly, differences in blocker affinity were insufficient to explain this behavior, as blockers of similar affinity could have different effects on desensitization (compare k+ = 1000 ms^{-1} in Figure 6A3 to k+ = 10000 ms^{-1} in Figure 6A4, where k- was also 10 fold higher), and conversely, those with different affinities could have similar effects (compare k- = 0.3 ms^{-1} in Figure 6A1 to k- = 0.3 ms^{-1} in Figure 6A2, where k+ was 10 fold higher). Similar patterns were observed with the branched model (not shown), suggesting that this effect did not depend on D state connectivity.

Blocked states decreased the extent of macroscopic desensitization by competing with existing desensitized states for occupancy

While the simulations demonstrated that both increased and decreased (or even unchanged) extents of desensitization were possible with open-channel block, the kinetic

basis for this observation remained unclear. One possibility was that certain combinations of blocking and unblocking rates rendered the B state "non-desensitizing" (i.e., unable to support macroscopic desensitization despite being arranged like a linear D state). Indeed, previous kinetic studies have demonstrated that O and D states in linear arrangement cause macroscopic desensitization only when specific microscopic conditions are met (Bianchi et al., 2007; Appendix IV). Addition of non-desensitizing states might therefore decrease desensitization by decreasing the contribution of the existing D state to the macroscopic current. To test this hypothesis, blocking and unblocking rates were co-varied, and the extent of desensitization supported by the B state alone was compared to that in the presence of both B and D states (Figure 6B1, C1, B2, C2).

Using the default rate constants for linear and branched models, the distinct roles played by blocking and unblocking rates in shaping desensitization were again evident (Figure 6B1, C1). However, when blocking and unblocking rates were co-varied in the absence of the D state, the curves were markedly different (compare Figure 6B2, C2 to Figure 6B1, C1). Only increases in desensitization were observed, reflecting the fact that models lacking a D state (i.e., C-C-O arrangements) could not macroscopically desensitize at baseline (Figure 5A4, B4; Appendix IV). However, not all combinations of blocking and unblocking rates supported desensitization. Desensitization was not observed for the highest unblocking rate tested ($k_- = 1.0\ ms^{-1}$), or for higher unblocking rates (not shown), independent of the magnitude of the blocking rate (Figure 6B2, C2; bottom curves). This was true even for blocking rates two orders of magnitude higher than those shown, which reduced current amplitudes to less than 1% of control and

increased occupancy of the B state above 99% (not shown). Interestingly, the maximum unblocking rate supporting desensitization was determined by the channel opening rate (β). This relationship was also reported by Bianchi et al (2007) for β and the exit rate from the D state (ρ) in the linear model, supporting the idea that open-channel block was analogous to adding a linear D state to the gating scheme.

By comparing the results in Panels B1 and C1 with those in Panels B2 and C2 (Figure 6), the kinetic basis for the ability of open-channel block to both increase and decrease desensitization became apparent. This was best illustrated by the curves corresponding to the highest unblocking rate (Figures B1, C1; k- = 1.0 ms^{-1}). When the blocking rate was low (k+ = 100 ms^{-1}), desensitization was nearly identical to that of the control current (dashed line). This reflected low B state occupancy, as transitions into this state were infrequent (due to the low blocking rate), and when they occurred, were short-lived (due to the high unblocking rate). Thus, the models behaved as if the B state did not exist. At the other extreme, however, when the blocking rate was high (k+ = 10000 ms^{-1}), receptors in the O state were more likely to transition into the B than into the D state. In this case, the model behaved as if the D state did not exist, and the extent of desensitization was primarily determined by the relationship between entry and exit rates from O and B states. Use of the high unblocking rate (k- = 1.0 ms^{-1}), however, yielded non-desensitizing currents for all blocking rates (Figure 6B2, C2; bottom curves). Thus, increasing the blocking rate shifted the behavior of the kinetic model from that of the macroscopically *desensitizing* C-O-D arrangement towards that of the macroscopically *non-desensitizing* C-O-B arrangement, resulting in less desensitization. Conversely, in cases where the C-O-B sub-scheme supported more desensitization than

the C-O-D sub-scheme (for example, compare Figure 6B2, C2 when k- = 0.01 ms^{-1} to the control extent of desensitization in Figure 6B1, C1), increasing the blocking rate increased desensitization (Figure 6B1, C1; top curve). Indeed, this same effect could be appreciated for each unblocking rate, as desensitization was nearly the same with high blocking rates regardless of whether the D state was present (compare values at the far right of Figures 6B1 and 6B2 to those of Figures 6C1 and 6C2, respectively). *Therefore, whether desensitization appeared to increase, decrease, or remain unchanged following addition of the blocker depended simply on the relative contributions of the desensitized and blocked states to the macroscopic current.*

The observation that different combinations of blocking and unblocking rates could support dramatically different extents of desensitization provided a parsimonious explanation for the experimentally observed variability in desensitization. However, it should be emphasized that in principle, blocking and unblocking rates could have been similar for all isoforms, with variable effects being observed on desensitization due to inherent differences in the gating schemes of synaptic and extrasynaptic receptor isoforms (Haas and Macdonald, 1999; Lagrange et al., 2007). Although systematic analysis of the interplay between the stability of O, D, and B states was beyond the scope of the present study, preliminary simulations demonstrated that the effects of open-channel block depended on the kinetics of channel gating, as both increased and decreased desensitization was possible for any given combination of blocking and unblocking rates depending on the relative stabilities of O and D states (Figure 7).

Open-channel block can selectively modulate either peak or residual currents.

The simulations in the previous sections confirmed that open-channel block could decrease the extent of desensitization, as observed experimentally for the majority of receptor isoforms. Interestingly, for certain receptor isoforms (e.g., α1β3δ and α5β3δ), this decrease was mediated almost entirely by inhibition of peak currents; residual currents were essentially unaffected (Figure 2). To determine the kinetic basis for this observation, the sensitivity of peak and residual currents to open-channel block was evaluated. Each set of simulations was performed with the linear model in the context of either increased (Figure 8A1, A2) or decreased (Figure 8B1, B2) D state stability (defined as δ/ρ), allowing for an expanded view of the kinetic parameter space.

Interestingly, a striking difference was noted between the relative contribution of blocking and unblocking rates to peak and residual currents. While residual currents were sensitive to both rates (Figures 8A2, B2), peak currents were primarily sensitive to changes in the blocking rate (Figure 8A1, B1). Although somewhat counterintuitive, it was noted that current rise times (10-90%) were rapid (~1 ms) for both high and low D state stability conditions (Figure 8C1, D1; solid traces). As a result, unblocking rates below 1.0 ms^{-1} did not cause further reductions in the peak current, as they supported dwell times in the B state of >1 ms, and therefore, permitted channel reopening (on average) only after currents reached peak. Thus, for any given blocking rate, there was a limit to the ability of open-channel block to inhibit peak currents, which was determined by the relationship between the current rise time in the absence of blocker and the unblocking rate. Support for this idea came from increasing the highest unblocking rate

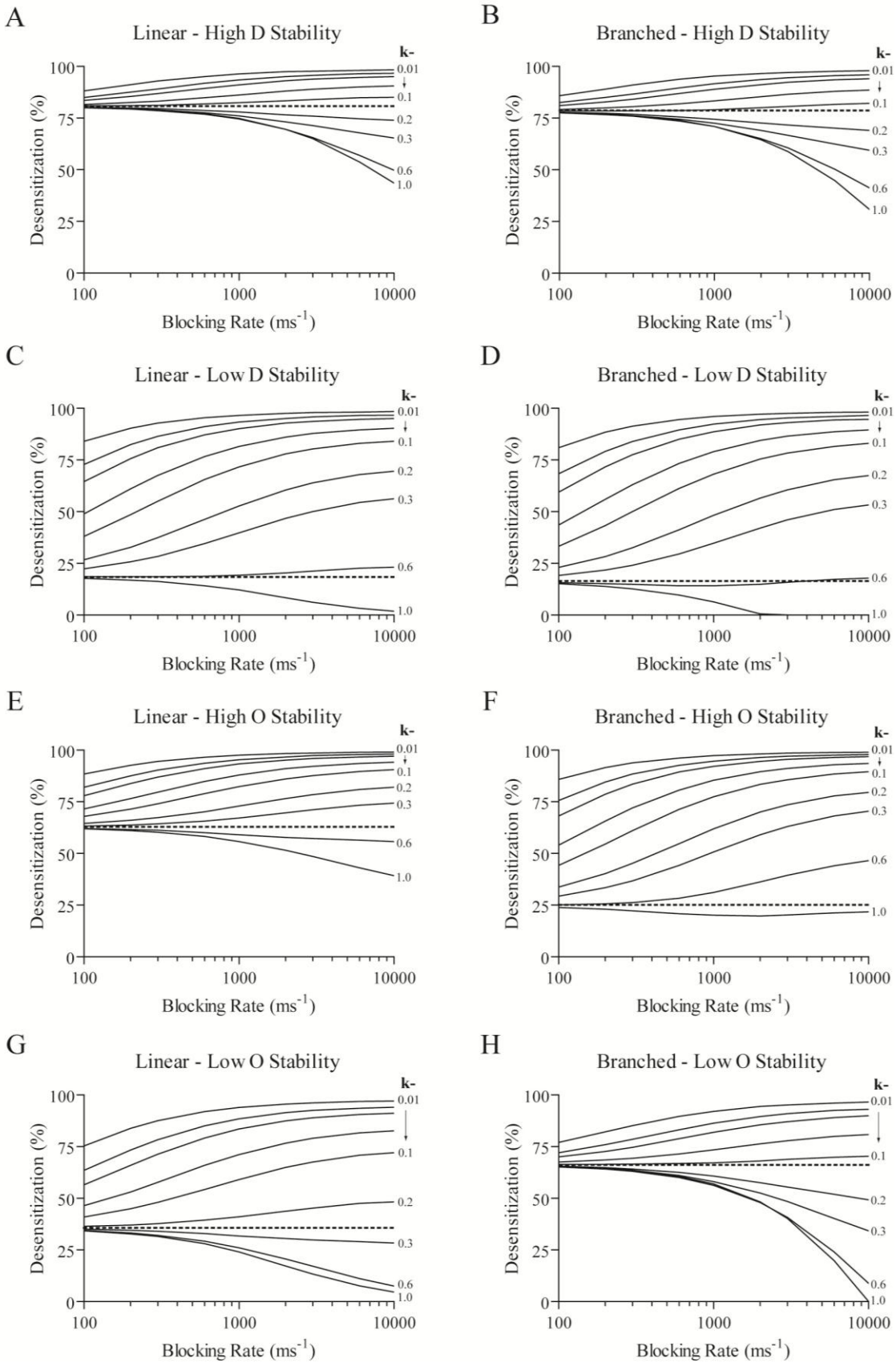
A
Linear - High D Stability
B
Branched - High D Stability
C
Linear - Low D Stability
D
Branched - Low D Stability
E
Linear - High O Stability
F
Branched - High O Stability
G
Linear - Low O Stability
H
Branched - Low O Stability
k-
0.01
0.1
0.2
0.3
0.6
1.0
Desensitization (%)
Blocking Rate (ms-1)
100
1000
10000
0
25
50
75

Figure 7. Gating kinetics influenced the sensitivity of macroscopic desensitization to open-channel block.

A-D, The extent of desensitization was evaluated for linear (Panels A and C) and branched (Panels B and D) models over a range of blocking and unblocking rates in the context of either four-fold increased (Panels A and B) or decreased (Panels C and D) D state stability (δ/ρ). Increased stability was achieved by increasing δ and decreasing ρ two-fold each, while decreased stability was achieved by decreasing δ and increasing ρ two-fold each. See the legends of Figures 6 and 7 for rate constants and simulation conditions. Dashed horizontal lines indicate the extent of desensitization in the absence of penicillin. E-H, The extent of desensitization was evaluated for linear (Panels E and G) and branched (Panels F and H) models over a range of blocking and unblocking rates in the context of four-fold increased (Panels E and F) or decreased (Panels G and H) O state stability (β/α). Increased stability was achieved by increasing β and decreasing α two-fold each, while decreased stability was achieved by decreasing β and increasing α two-fold each. Note that when the unblocking rate was set to 0.3 ms^{-1}, both increased (Panels C, D, E, F) and decreased (Panels A, B, G, H) extents of macroscopic desensitization were possible, and that the direction of change was not always related to the amount of macroscopic desensitization observed at baseline (i.e., both decreased and increased extents of desensitization were possible independent of whether control desensitization was high (Panels A and E) or low (Panels C and G)).

by an order of magnitude (so that channel reopening was more likely during current activation), which substantially right-shifted the inhibition curve (not shown). A similar right-shift could also be obtained by altering the kinetics of channel gating, such that current rise time was substantially increased (by decreasing the channel opening rate; not shown).

In contrast, there was no limit to the ability of open-channel block to inhibit residual currents, as an infinitely low unblocking rate would simply cause the blocked state to become absorbing, driving open state occupancy to zero (Appendix II). Under certain conditions, this allowed for selective modulation of peak or residual currents. For example, when the blocking rate was low (k+ = 100), peak currents were always $\geq$ 90%

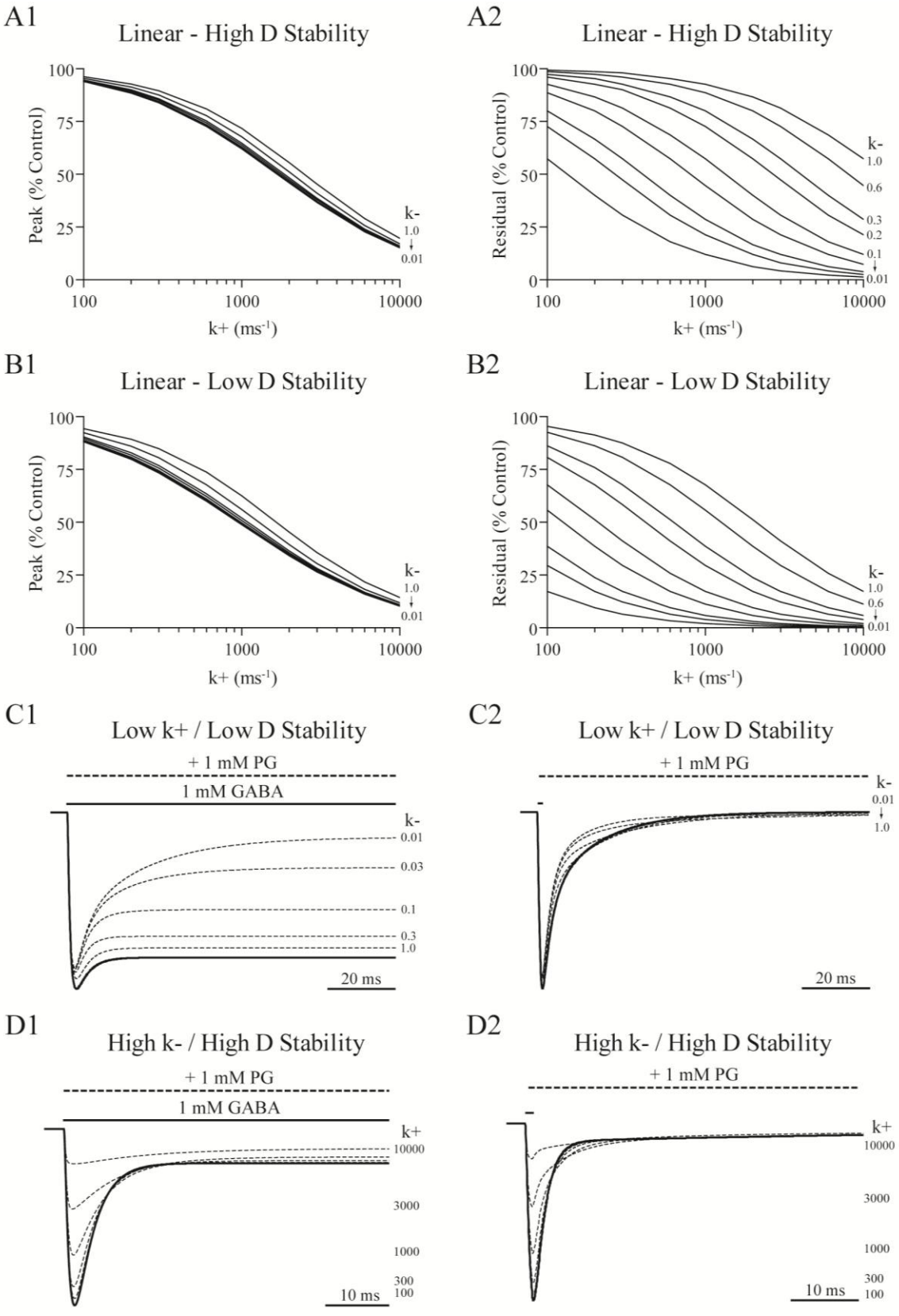
A1
Linear - High D Stability
Peak (% Control)
k+ (ms-1)
k-
1.0
0.01
A2
Linear - High D Stability
Residual (% Control)
k+ (ms-1)
k-
1.0
0.6
0.3
0.2
0.1
0.01
B1
Linear - Low D Stability
Peak (% Control)
k+ (ms-1)
k-
1.0
0.01
B2
Linear - Low D Stability
Residual (% Control)
k+ (ms-1)
k-
1.0
0.6
0.01
C1
Low k+ / Low D Stability
+ 1 mM PG
1 mM GABA
k-
0.01
0.03
0.1
0.3
1.0
20 ms
C2
Low k+ / Low D Stability
+ 1 mM PG
k-
0.01
1.0
20 ms
D1
High k- / High D Stability
+ 1 mM PG
1 mM GABA
k+
10000
3000
1000
300
100
10 ms
D2
High k- / High D Stability
+ 1 mM PG
k+
10000
3000
1000
300
100
10 ms

Figure 8. Peak and residual currents had different sensitivities to blocking and unblocking rate constants.

A, B, Peak (Panels A1 and B1) and residual (Panels A2 and B2) currents had different sensitivities to open-channel block in the context of increased (Panels A1 and A2) or decreased (Panels A2 and B2) D state stability. Increased stability was achieved by increasing δ and decreasing ρ two-fold each, while decreased stability was achieved by decreasing δ and increasing ρ two-fold each. C, Currents were simulated with either 100 ms (Panel C1) or 1 ms (Panel C2) pulses of 1 mM GABA in the presence of 1 mM penicillin G (PG) in the context of low blocking (k+ = 100) and low D state stability (δ/ρ = 0.75). D, Currents were simulated with either 50 ms (Panel D1) or 1 ms (Panel D2) pulses of 1 mM GABA in the presence of 1 mM penicillin in the context of high blocking (k+ = 10000) and high D state stability (δ/ρ = 12). Responses simulated with 1 mM GABA alone are shown in black. Peak currents were not normalized. All simulations were performed with the linear model (Figure 5A1; see figure legend for rate constants).

of control, the result of transitions into the B state being infrequent during current activation (Figure 8A1, B1). However, when combined with the lowest unblocking rate (k- = 0.01), substantial reductions were observed in the residual current (Figure 8A2, B2). This effect was more apparent with low D state stability (Figure 8B2), as this allowed for higher B state fractional occupancy with any given combination of blocking and unblocking rates (compare Figure 8A2 to Figure 8B2). Thus, blockers with relatively low blocking and unblocking rates would have limited capacity to modulate early phases of current activation, giving the appearance of selectivity for currents evoked under tonic conditions (Figure 8C1, 8C2).

Conversely, certain combinations of rate constants preferentially modulated peak currents. For example, when the blocking rate was increased by two orders of magnitude (k+ = 10,000), peak currents were reduced to ~20% of control (Figure 8A1, B1). However, when combined with the largest unblocking rate (k- = 1.0), residual currents were inhibited less than peak currents (Figure 8A2, B2). This effect was more

pronounced under conditions of increased D state stability (Figure 8A2), where ~60% of the residual current remained. In fact, when D state stability was increased by an additional order of magnitude, this same combination of blocking and unblocking rates had only minimal effect on residual current, despite causing a similar reduction in peak current (not shown). Thus, it appeared that highly stable D states "buffered" O state equilibrium occupancy from the effects of open-channel block (Appendix II). In this context, blockers with relatively high blocking and unblocking rates would appear to selectively modulate early phases of current activation (Figure 8D1), which would substantially reduce phasic currents (Figure 8D2).

Decreasing the GABA concentration further decreased the sensitivity of residual currents to open-channel block

The observation that increasing D state stability limited the ability of open-channel block to modulate residual currents suggested that stabilizing other non-conducting states might have a similar (and possibly compounding) effect. Consistent with this idea, residual currents evoked by prolonged exposure to sub-saturating GABA (to mimic tonic inhibition) were only minimally affected by penicillin (Figure 4), despite having clear sensitivity when evoked by nearly-saturating GABA (Figures 1, 2). This was best illustrated by $\alpha4\beta3\delta$ receptors, whose residual currents were inhibited ~40% by penicillin when evoked by 1 mM GABA, but <10% when evoked by 1 μM GABA. Since decreasing the GABA concentration should increase fractional occupancy of the unliganded non-conducting state, we hypothesized that much like stabilizing D state, this might also "buffer" O state occupancy from the effects of open-channel block.

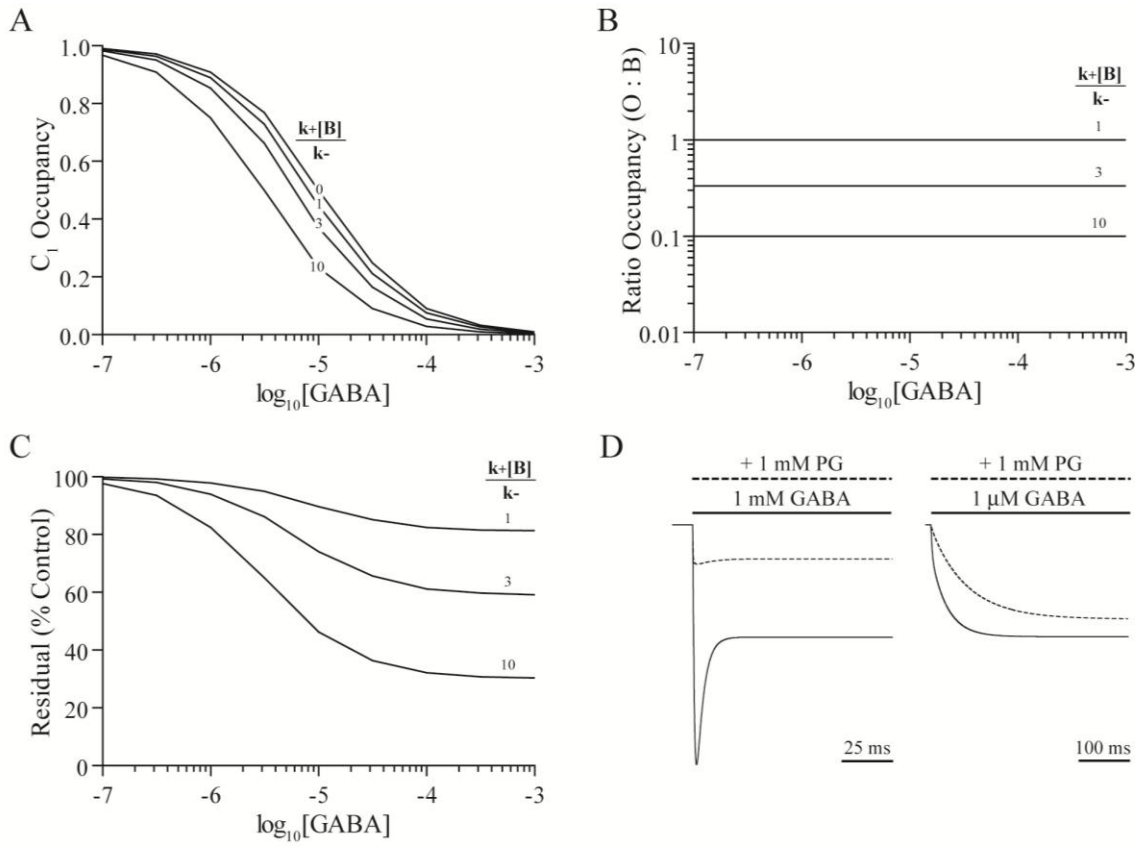

Figure 9. Decreasing the GABA concentration decreased the sensitivity of residual currents to open-channel block.

A, The equilibrium fractional occupancy of the unbound state (C_1) increased as the GABA concentration and B state stability (defined as the ratio of the effective blocking rate, k+[Blocker], to the unblocking rate, k-) decreased. B, The ratio of O state occupancy to B state occupancy was unchanged across GABA concentrations for any given B state stability. C, The sensitivity of residual currents to open-channel block decreased with decreasing GABA concentration and B state stability. D, Currents were simulated with 1 mM GABA (left) and 1 µM GABA (right) either alone (solid traces) or in the presence of 1 mM penicillin G (PG; dashed traces) when B state stability was high (k+[PG]/k- = 10). Currents evoked by GABA alone (black traces) were scaled to the amplitude of residual currents. All simulations were performed with the linear model (Figure 5A; see legend for rate constants).

To test this hypothesis, simulated residual currents evoked by prolonged co-applications (30 s) of GABA and 1 mM penicillin were evaluated over a range of GABA concentrations (Figure 9). As expected, decreasing the GABA concentration increased equilibrium occupancy of C_1 (Figure 9A) and decreased occupancy of all other states (not shown). In addition, increasing B state stability left-shifted the concentration-occupancy curve. This likely reflected the decreased GABA EC_{50} (not shown), as increasing B state stability should have the same effect on EC_{50} as stabilizing any other fully-liganded state in the gating scheme (Colquhoun, 1998). Interestingly, while decreasing the GABA concentration did not alter the ratio of O to B state occupancies (Figure 9B), it substantially decreased the sensitivity of residual currents to open-channel block (Figure 9C). This phenomenon was observed even when B state occupancy was substantially higher than O state occupancy (e.g., when k+[B]/k- = 10; Figure 8C, D). Similar behavior was observed using the branched model (Figure 5B1) and previously published kinetic models of $\alpha1\beta3\gamma2L$ and $\alpha4\beta3\gamma2L$ receptors (Lagrange et al., 2007) (Figure 10), indicating that this effect was independent of the number and connectivity of states in the gating scheme.

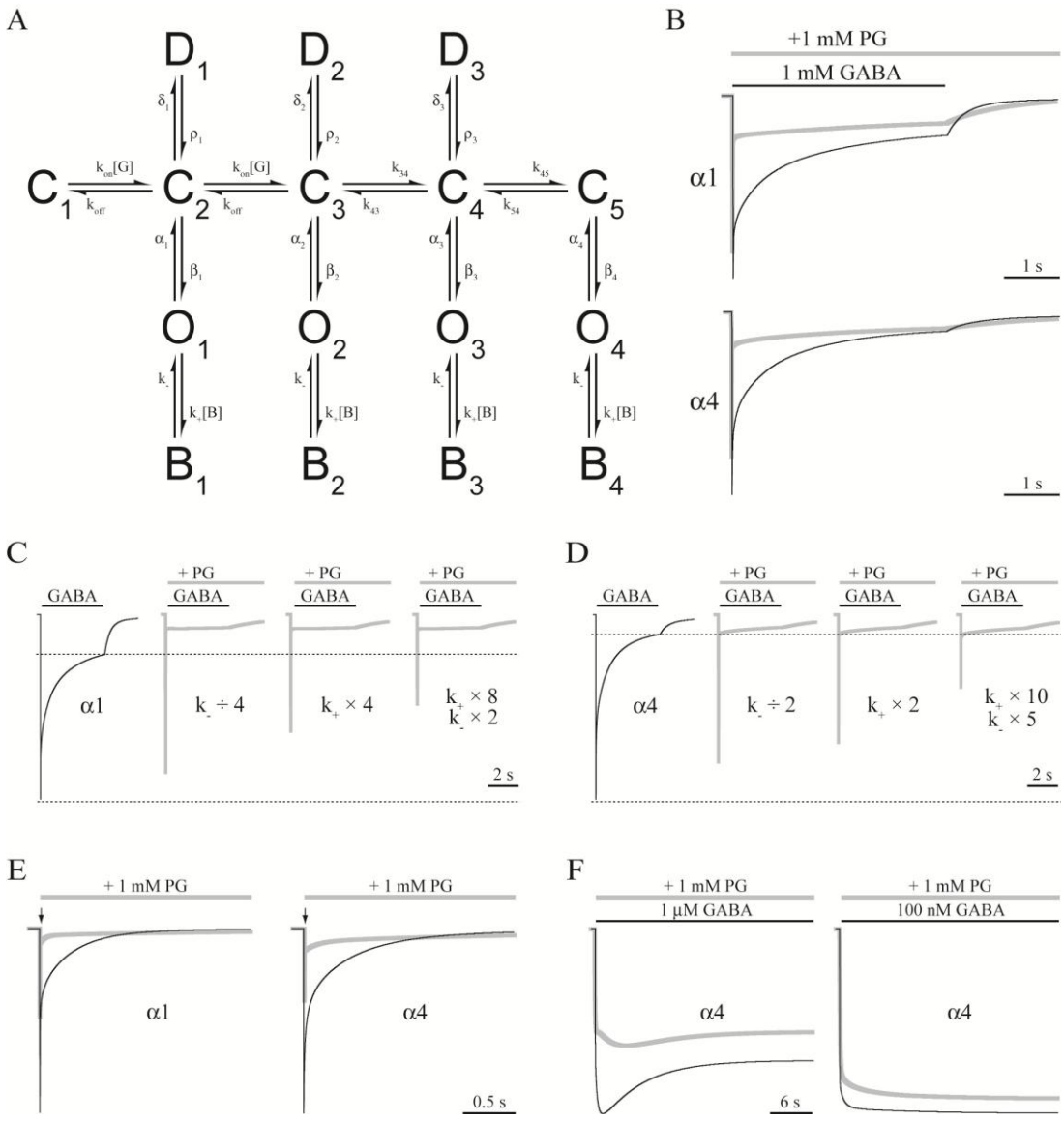
A
B
+1 mM PG
1 mM GABA
α1
α4
1 s
C
D
GABA
+ PG
α1
α4
2 s
E
F
+ 1 mM PG
1 µM GABA
100 nM GABA
0.5 s
6 s

Figure 10. Context-dependent modulation was also observed with a comprehensive model of $GABA_A$ receptor function.

A, Comprehensive kinetic model of $GABA_A$ receptor function for the α1β3γ2L and α4β3γ2L receptor isoforms (for rate constants, see Lagrange et al., 2007). Blocked states (B) were connected to each open state using the default blocking (k+) and unblocking (k-) rates (see Figure 5 legend). B, Simulated responses to 1 mM GABA either alone (black) or in the presence of 1 mM penicillin (PG; grey) for the α1β3γ2L (top) and α4β3γ2L (bottom) receptor isoforms. Note that the reduction of peak and residual currents was less than that observed experimentally (see Figure 1), suggesting that penicillin had a higher affinity for these isoforms (note that the original single-channel studies were performed in spinal cord neurons, which express different receptor isoforms; Twyman, et al., 1992). C, D, Blocking and unblocking rates were optimized for the α1β3γ2L (Panel C) and α4β3γ2L (Panel D) receptor isoforms such that peak and residual currents were inhibited to the extent observed experimentally. The control current is shown on the far left, followed by currents obtained in the presence of penicillin at each step of the optimization process. Final values are shown at the far right. Dashed lines indicate the amplitude of peak and residual currents for the GABA control. Note that the final values should be taken only as approximations, as they are based entirely on macroscopic data and assume the rates of blockade are identical for all O states. E, Simulated responses to brief (1 ms) pulses of 1 mM GABA either alone (black) or in the presence of 1 mM penicillin (grey) predict that both α1β3γ2L (left) and α4β3γ2L (right) isoforms would be highly sensitive to penicillin when activated under phasic conditions. F, Simulated responses of the α4β3γ2L receptor isoform to prolonged application (30 s) of either 1 μM (left) or 100 nM (right) GABA either alone (black) or in the presence of 1 mM penicillin (grey) predicts that this isoform would be minimally sensitive to penicillin when activated under tonic conditions. Similar results were obtained for the α1β3γ2L receptor (not shown). Control currents were scaled to their peaks.

DISCUSSION

Penicillin produced context-dependent modulation of $GABA_A$ receptor currents

Preferential modulation of phasic or tonic inhibition is generally attributed to synaptic and extrasynaptic receptor isoforms having different sensitivities to a given pharmacological agent (Nusser and Mody, 2002; Stell and Mody, 2002; Farrant and Nusser, 2005). The observation that penicillin selectively inhibited phasic currents has thus been suggested to reflect specificity for synaptic isoforms (Yeung et al., 2003). However, we found that penicillin modulated GABA currents evoked from both synaptic and extrasynaptic isoforms, indicating that isoform-specificity was insufficient to account for the apparent insensitivity of tonic currents. We therefore explored the possibility that the markedly different contexts of receptor activation associated with phasic and tonic inhibition were responsible for their different sensitivities to penicillin. Consistent with this hypothesis, we found that currents evoked by prolonged exposure to sub-saturating GABA (i.e., tonic activation) were relatively insensitive to penicillin, while those evoked by brief pulses of nearly-saturating GABA (i.e., phasic activation) were highly sensitive. Although we did not evaluate the effects of penicillin on every known $GABA_A$ receptor isoform, the results were nonetheless consistent with the idea that the context of receptor activation, and not the subset of receptor isoforms present in synaptic and extrasynaptic compartments, was responsible for the reported selectivity of penicillin for phasic currents.

Penicillin had variable effects on $GABA_A$ receptor macroscopic current properties

Penicillin has previously been demonstrated to negatively modulate $GABA_A$ receptor currents (Macdonald and Barker, 1977; Horne et al., 1992; Katayama et al., 1992; Tsuda et al., 1994; Behrends, 2000; Sugimoto et al., 2002) by an open-channel block mechanism (Twyman et al., 1992). Consistent with these studies, we found that penicillin decreased peak current amplitudes for both synaptic and extrasynaptic receptor isoforms when evoked by saturating GABA. This suggested that phasic currents would always be inhibited by penicillin, regardless of which subset of receptor isoforms is localized to synapses. Penicillin is therefore likely to have widespread effects on phasic inhibition, which may underlie its potent pro-convulsant properties and ability to produce epileptiform activity *in vitro* (Schneiderman et al., 1994; Uysal et al., 1996; Schneiderman 1997; Jimenez et al., 2000; Shen and Lai, 2002). It should be emphasized, however, that the widespread sensitivity of $GABA_A$ receptor peak currents to penicillin is not a fundamental property of open-channel blockade. Indeed, our simulations demonstrated that addition of blocked states can theoretically have minimal effect on peak current if, for example, the current rise time is much faster than the blocking rate (Figure 8). In this case, open-channel block would appear selective for tonic, as opposed to phasic, inhibition.

Interestingly, penicillin had variable effects on the extent of desensitization, with increased, decreased, and even unchanged extents being observed with different receptor isoforms. Although unexpected for an open-channel block mechanism, particularly since the blocked state provided an additional route for channel closure, our simulations demonstrated that macroscopic current shape does not specify uniquely the precise

arrangement of states in the microscopic gating scheme (Mozrzymas et al., 2003; Bianchi et al., 2007). In other words, the fact that individual receptors must open before becoming blocked does not necessarily mean that the resulting macroscopic currents will be affected only after they have reached peak. Much like desensitized states (Bianchi et al., 2007), substantial occupancy of blocked states can be achieved even during current activation. As a result, blocked states can influence both peak and residual currents, and depending on the relationship between the kinetics of block and those of channel gating, can have markedly different effects on each of these current properties, causing the extent of desensitization to change. While the physiological significance of altered desensitization remains unclear (since prolonged exposure to high concentrations of GABA is not thought to occur *in vivo*), increasing evidence suggests that the shape of desensitization influences the pattern of current responses during repetitive stimulation (Bianchi and Macdonald, 2002; Pugh and Raman, 2005; Lagrange et al., 2007).

Although the effects on desensitization were highly variable, all receptor isoforms displayed prolonged deactivation in the presence of penicillin (in the case of decreased desensitization, this provided a novel experimental example of desensitization-deactivation "uncoupling"; Bianchi et al., 2007). Somewhat paradoxically, however, penicillin accelerated deactivation following brief pulses, a finding consistent with the reported ability of penicillin to accelerate IPSC decay in hippocampal neurons (Mtchedlishvili and Kapur, 2005). While this behavior was also observed during our kinetic simulations (Figure 8C2), it should be emphasized that only the fast phase of deactivation was accelerated by open-channel block. Similar to the effect of stabilizing desensitized states (Bianchi et al., 2007), the accelerated fast phase was accompanied by

a markedly prolonged slow phase (Figure 8C2; note that traces corresponding to deactivation in the presence of blocker did not return to baseline), causing the weighted deactivation time course to actually be prolonged (not shown). Slow phases, however, may be difficult to resolve experimentally above background noise if they are relatively low amplitude, giving the appearance of accelerated deactivation.

Thus, while the effects of penicillin on macroscopic current properties were complex and often counterintuitive, our simulations using simple models of $GABA_A$ receptor function demonstrated that these effects were entirely consistent with simple open-channel block. In addition, the simulations exposed a striking similarity between the roles played by blocked and desensitized states in shaping the macroscopic current, suggesting that open-channel blockers could be useful experimental tools for exploring the relationship between microscopic and macroscopic desensitization. Unlike native desensitized states, the entry rate into the blocked state can be precisely controlled simply by varying the blocker concentration, the orientation of the blocked state with respect to the open state is always known, and the exit rate from the blocked state can be unambiguously determined with single channel analysis.

Receptor activation by low concentrations of GABA contributed to the apparent insensitivity of tonic currents to penicillin

For an open-channel blocker to alter the extent of desensitization, it must have different effects on peak and residual currents. Implicit in this definition, however, is the capacity to differentially modulate phasic and tonic inhibition. For example, preferential inhibition of peak currents predicts that non-equilibrium phases of receptor activation will be more sensitive than near-equilibrium phases, meaning that phasic currents should

be affected more than tonic currents. Conversely, preferential inhibition of residual currents predicts that near-equilibrium phases of receptor activation will be more sensitive than non-equilibrium phases, meaning that tonic currents should be affected more than phasic currents. The observation that the extent of desensitization was decreased for most extrasynaptic isoforms (the result of preferential inhibition of peak currents) was therefore consistent with the observation that tonic currents were less sensitive to penicillin than phasic currents (Yeung et al., 2003). This, however, could not fully explain the apparent insensitivity of tonic currents. Despite the decreased extent of desensitization observed for most extrasynaptic receptor isoforms, residual currents activated by a nearly-saturating GABA concentration were still substantially inhibited by penicillin (Figures 1, 2), suggesting that tonic currents should have been reduced to some degree. However, only a small reduction was reported in the root-mean-square noise of tonic currents; the magnitude of the tonic current itself was unchanged (Yeung et al., 2003; Mtchedlishvili and Kapur, 2005).

Interestingly, residual currents were considerably less sensitive to penicillin when evoked by sub-saturating GABA (compare residual currents in Figures 1 and 2 to those in Figure 4). While this could potentially have been explained by lower affinity of the blocker for mono-liganded compared to di-liganded open states, single channel studies have reported that penicillin actually had the highest affinity for the mono-liganded open state (Twyman et al., 1992). An alternative explanation was provided by the simulations, where it was observed that decreasing the GABA concentration buffered open state occupancy from the effects of open-channel block by stabilizing the unliganded state. This phenomenon was independent of the specific connectivity or number of states in the

gating scheme, suggesting that tonic currents would be minimally sensitive to penicillin regardless of which receptor isoforms comprised the extrasynaptic pool.

Thus, our results demonstrated that the "context" of receptor activation, both in terms of agonist concentration and time course of exposure, was an important determinant of the sensitivity of $GABA_A$ receptor currents to penicillin. While it remains unclear whether such context-dependent modulation is possible with other known $GABA_A$ receptor modulators, preliminary simulations suggested that this behavior was not unique to open-channel block. For example, phasic and tonic currents could also have markedly different sensitivities to modulators that "block" non-conducting states, and even to modulators that stabilize open states (not shown). The latter are of particular interest, as the ability to selectively enhance equilibrium or non-equilibrium currents would have important therapeutic implications for disease states caused by impairments in tonic or phasic inhibition, respectively.

REFERENCES

Barberis, A., Petrini, E.M., Cherubini, E., Mozrzymas, J.W., 2002. Allosteric interaction of zinc with recombinant $\alpha1\beta2\gamma2$ and $\alpha1\beta2$ $GABA_A$ receptors. Neuropharmacology 43, 607-618.

Behrends, J.C., 2000. Modulation by bicuculline and penicillin of the block by t-butyl-bicyclo-phosphorothionate (TBPS) of $GABA_A$-receptor mediated Cl^--current responses in rat striatal neurones. Br J Pharmacol 129, 402-408.

Bianchi, M.T., Macdonald, R.L., 2002. Slow phases of $GABA_A$ receptor desensitization: structural determinants and possible relevance for synaptic function. J Physiol 544, 3-18.

Bianchi, M.T., Botzolakis, E.J., Haas, K.F., Fisher, J., Macdonald, R.L., 2007. Microscopic kinetic determinants of macroscopic currents: insights from coupling and uncoupling of $GABA_A$ receptor desensitization and deactivation. J Physiol 584, 769-787.

Bianchi, M.T., Macdonald, R.L., 2003. Neurosteroids shift partial agonist activation of $GABA_A$ receptor channels from low- to high-efficacy gating patterns. J Neurosci 23, 10934-10943.

Brunig, I., Scotti, E., Sidler, C., Fritschy, J.M., 2002. Intact sorting, targeting, and clustering of γ-aminobutyric acid A receptor subtypes in hippocampal neurons in vitro. J Comp Neurol 443, 43-55.

Caraiscos, V.B., Newell, J.G., You-Ten, K.E., Elliott, E.M., Rosahl, T.W., Wafford, K.A., MacDonald, J.F., Orser, B.A., 2004. Selective enhancement of tonic GABAergic inhibition in murine hippocampal neurons by low concentrations of the volatile anesthetic isoflurane. J Neurosci 24, 8454-8458.

Chandra, D., Jia, F., Liang, J., Suryznarayanan, A., Werner, D.F., Spigelman, I., Houser, C.R., Olsen, R.W., Harrison, N.L., Homanics, G.E., 2006. $GABA_A$ receptor $\alpha4$ subunits mediate extrasynaptic inhibition in thalamus and dentate gyrus and the action of gaboxadol. Proc Natl Acad Sci USA 103, 15230-15235.

Chow, P., Mathers, D., 1986. Convulsant doses of penicillin shorten the lifetime of GABA-induced channels in cultured central neurones. Br J Pharmacol 88, 541-547.

Colquhoun, D., 1998. Binding, gating, affinity and efficacy: The interpretation of structure-activity relationships for agonists and of the effects of mutating receptors. Br J Pharmacol 125, 923-947.

Essrich, C., Lorez, M., Benson, J.A., Fritschy, J.M., Luscher, B., 1998. Postsynaptic clustering of major $GABA_A$ receptor subtypes requires the $\gamma 2$ subunit and gephyrin. Nat Neurosci 1, 563-571.

Farrant, M., Nusser, Z., 2005. Variations on an inhibitory theme: phasic and tonic activation of $GABA_A$ receptors. Nat Rev Neurosci 6, 215-229.

Feng, H.J., Macdonald, R.L., 2004. Multiple actions of propofol on $\alpha\beta\gamma$ and $\alpha\beta\delta$ $GABA_A$ receptors. Mol Pharmacol 66, 1517-1524.

Feng, H.J., Bianchi, M.T., Macdonald, R.L., 2004. Pentobarbital differentially modulates $\alpha 1\beta 3\delta$ and $\alpha 1\beta 3\gamma 2L$ $GABA_A$ receptor currents. Mol Pharmacol 66, 988-1003.

Glykys, J., Mody, I., 2007. The main source of ambient GABA responsible for tonic inhibition in the mouse hippocampus. J Physiol 582, 1163-1178.

Glykys, J., Peng, Z., Chandra, D., Homanics, G.E., Houser, C.R., Mody, I., 2007. A new naturally occurring $GABA_A$ receptor subunit partnership with high sensitivity to ethanol. Nat Neurosci 10, 40-48.

Greenfield, L.J. Jr., Sun, F., Neelands, T.R., Burgard, E.C., Donnelly, J.L., Macdonald, R.L., 1997. Expression of functional $GABA_A$ receptors in transfected L929 cells isolated by immunomagnetic bead separation. Neuropharmacology 36, 63-73.

Haas, K.F., Macdonald, R.L., 1999. $GABA_A$ receptor subunit $\gamma 2$ and δ subtypes confer unique kinetic properties on recombinant $GABA_A$ receptor currents in mouse fibroblasts. J Physiol 514, 27-45.

Horne, A.L., Hadingham, K.L., Macaulay, A.J., Whiting, P., Kemp, J.A., 1992. The pharmacology of recombinant $GABA_A$ receptors containing bovine $\alpha 1$, $\beta 1$, $\gamma 2L$ subunits stably transfected into mouse fibroblast L-cells. Br J Pharmacol 107, 732-737.

Hsu, F., Waldeck, R., Faber, D., Smith, S.S., 2003. Neurosteroid effects of GABAergic synaptic plasticity in hippocampus. J Neurophysiol 89, 1929-1940.

Jimenez, F., Velasco, F., Carrillo-Ruiz, J., Villanueva, F.E., Velasco, M., Ponce, H., 2000. Seizures induced by penicillin microinjections in the mesencephalic tegmentum. Epilepsy Res 38, 33-44.

Jones, M.V., Westbrook, G.L., 1995. Desensitized states prolong $GABA_A$ channel responses to brief agonist pulses. Neuron 15, 181-191.

Katayama, N., Tokutomi, N., Nabekura, J., Akaike, N., 1992. Penicillin-induced triphasic modulation of $GABA_A$ receptor-operated chloride current in frog sensory neuron. Brain Res 595, 249-255.

Krishek, B.J., Moss, S.J., Smart, T.G., 1996. Homomeric β1 γ-aminobutyric acid A receptor-ion channels: evaluation of pharmacological and physiological properties. Mol Pharmacol 49, 494-504.

Lagrange, A.H., Botzolakis, E.J., Macdonald, R.L., 2007. Enhanced macroscopic desensitization shapes the response of α4 subunit-containing $GABA_A$ receptors to synaptic and extrasynaptic GABA. J Physiol 578, 655-676.

Lema, G.M., Auerbach, A., 2006. Modes and models of $GABA_A$ receptor gating. J Physiol 572, 183-200.

Liang, J., Zhang, N., Cagetti, E., Houser, C., Olsen, R.W., Spigelman, I., 2006. Chronic intermittent ethanol-induced switch of ethanol actions from extrasynaptic to synaptic hippocampal $GABA_A$ receptors. J Neurosci 26, 1749-1758.

Lindquist, C.E., Dalziel, J.E., Cromer, B.A., Birnir, B., 2004. Penicillin blocks human α1β1 and α1β1γ2S $GABA_A$ channels that open spontaneously. Eur J Pharmacol 496, 23-32.

Lipton, S.A., 2006. Paradigm shift in neuroprotection by NMDA receptor blockade: Memantine and beyond. Nat Rev Drug Discov 5, 160-170.

Luscher, B., Keller, C.A., 2004. Regulation of $GABA_A$ receptor trafficking, channel activity, and functional plasticity of inhibitory synapses. Pharmacol Ther 102, 195-221.

Macdonald, R.L., Barker, J.L., 1977. Pentylenetetrazol and penicillin are selective antagonists of GABA-mediated post-synaptic inhibition in cultured mammalian neurons. Nature 267, 720-721.

Macdonald, R.L., Kang, J.Q., Gallagher, M.J., Feng, H.J., 2006. $GABA_A$ receptor mutations associated with generalized epilepsies. Adv Pharmacol 54, 147-169.

McKernan, R.M., Whiting, P.J., 1996. Which $GABA_A$-receptor subtypes really occur in the brain? Trends Neurosci 19, 139-143.

Mody, I., Pearce, R.A., 2004. Diversity of inhibitory neurotransmission through $GABA_A$ receptors. Trends Neurosci 27, 569-575.

Mozrzymas, J.W., Barberis, A., Mercik, K., Zarnowska, E.D., 2003. Binding sites, singly bound states, and conformation coupling shape GABA-evoked currents. J Neurophysiol 89, 871-883.

Mozrzymas, J.W., 2004. Dynamism of $GABA_A$ receptor activation shapes the "personality" of inhibitory synapses. Neuropharmacology 47, 945-960.

Mtchedlishvili, Z., Kapur, J., 2005. High-Affinity, Slowly Desensitizing $GABA_A$ Receptors Mediate Tonic Inhibition in Hippocampal Dentate Granule Cells. Mol Pharmacol 69, 564-575.

Nusser, Z., Sieghart, W., Somogyi, P., 1998. Segregation of different $GABA_A$ receptors to synaptic and extrasynaptic membranes of cerebellar granule cells. J Neurosci 18, 1693-1703.

Nusser, Z., Mody, I., 2002. Selective modulation of tonic and phasic inhibitions in dentate gyrus granule cells. J Neurophysiol 87, 2624-2628.

Olsen, R.W., Macdonald, R.L., 2002. $GABA_A$ receptor complex: structure and function. In: Egebjerg, J., Schousboe, A., Krogsgaard-Larsen, P., (Eds), Glutamate and GABA Receptors and Transporters: Structure, Function and Pharmacology. Taylor and Francis, London, pp. 202-235.

Peng, Z., Huang, C.S., Stell, B.M., Mody, I., Houser, C.R., 2004. Altered expression of the δ subunit of the $GABA_A$ receptor in a mouse model of temporal lobe epilepsy. J Neurosci 24, 8629-8639.

Poltl, A., Hauer, B., Fuchs, K., Tretter, V., Sieghart, W., 2003. Subunit composition and quantitative importance of $GABA_A$ receptor subtypes in the cerebellum of mouse and rat. J Neurochem 87, 1444-1455.

Pugh, J.R., Raman, I.M., 2005. $GABA_A$ receptor kinetics in the cerebellar nuclei: evidence for detection of transmitter from distant release sites. Biophys J 88, 1740-1754.

Saxena, N.C., Macdonald, R.L., 1994. Assembly of $GABA_A$ receptor subunits: role of the δ subunit. J Neurosci 14, 7077-7086.

Schneiderman, J.H., Sterling, C.A., Luo, R., 1994. Hippocampal plasticity following epileptiform bursting produced by $GABA_A$ antagonists. Neuroscience 59, 259-273.

Schneiderman, J.H., 1997. The role of long-term potentiation in persistent epileptiform burst-induced hyperexcitability following $GABA_A$ receptor blockade. Neuroscience 81, 1111-1122.

Semyanov, A., Walker, M.C., Kullmann, D.M., Silver, R.A., 2004. Tonically active $GABA_A$ receptors: modulating gain and maintaining the tone. Trends Neurosci 27, 262-269.

Shen, E.Y., Lai, Y.J., 2002. In vivo microdialysis study of excitatory and inhibitory amino acid levels in the hippocampus following penicillin-induced seizures in mature rats. Acta Paediatr Taiwan 43, 313-318.

Stell, B.M., Mody, I., 2002. Receptors with different affinities mediate phasic and tonic $GABA_A$ conductances in hippocampal neurons. J Neurosci 22, 1-5.

Sugimoto, M., Fukami, S., Kayakiri, H., Yamazaki, S., Matsuoka, N., Uchida, I., Mashimo, T., 2002. The β-lactam antibiotics, penicillin-G and cefoselis have different mechanisms and sites of action at $GABA_A$ receptors. Br J Pharmacol 135, 427-432.

Sun, C., Sieghart, W., Kapur, J., 2004. Distribution of α1, α4, γ2, and δ subunits of $GABA_A$ receptors in hippocampal granule cells. Brain Res 1029, 207-216.

Sur, C., Farrar, S.J., Kerby, J., Whiting, P.J., Atack, J.R., McKernan, R.M., 1999. Preferential coassembly of α4 and δ subunits of the γ-aminobutyric $acid_A$ receptor in rat thalamus. Mol Pharmacol 56, 110-115.

Tierney, M.L., Birnir, B., Pillai, N.P., Clements, J.D., Howitt, S.M., Cox, G.B., Gage, P.W., 1996. Effects of mutating leucine to threonine in the M2 segment of α1 and β1 subunits of $GABA_A$ α1β1 receptors. J Membr Biol 154, 11-21.

Tsuda, A., Ito, M., Kishi, K., Shiraishi, H., Tsuda, H., Mori, C., 1994. Effect of penicillin on GABA-gated chloride ion influx. Neurochem Res 19, 1-4.

Twyman, R.E., Green, R.M., Macdonald, R.L., 1992. Kinetics of open channel block by penicillin of single $GABA_A$ receptor channels from mouse spinal cord neurones in culture. J Physiol 445, 97-127.

Uysal, H., Kuli, P., Caglar, S., Inan, L.E., Akarsu, E.S., Palaoglu, O., Ayhan, I.H., 1996. Antiseizure activity of insulin: insulin inhibits pentylenetetrazole, penicillin and kainic acid-induced seizures in rats. Epilepsy Res 25, 185-190.

Wei, W., Zhang, N., Peng, Z., Houser, C.R., Mody, I., 2003. Perisynaptic localization of δ subunit-containing $GABA_A$ receptors and their activation by GABA spillover in the mouse dentate gyrus. J Neurosci 23, 10650-10661.

Wisden, W., Laurie, D.J., Monyer, H., Seeburg, P.H., 1992. The distribution of 13 $GABA_A$ receptor subunit mRNAs in the rat brain. I. Telencephalon, diencephalon, mesencephalon. J Neurosci 12, 1040-1062.

Wohlfarth, K.M., Bianchi, M.T., Macdonald, R.L., 2002. Enhanced neurosteroid potentiation of ternary $GABA_A$ receptors containing the δ subunit. J Neurosci 22, 1541-1549.

Yeung, J.Y., Canning, K.J., Zhu, G., Pennefather, P., MacDonald, J.F., Orser, B.A., 2003. Tonically activated $GABA_A$ receptors in hippocampal neurons are high-affinity, low-conductance sensors for extracellular GABA. Mol Pharmacol 63, 2-8.

Zhang, N., Wel, W., Mody, I., Houser, C.R., 2007. Altered localization of $GABA_A$ receptor subunits on dentate granule cell dendrites influences tonic and phasic inhibition in a mouse model of epilepsy. J Neurosci 27, 7520-7531.

CHAPTER V

IDENTITY OF THE $GABA_A$ RECEPTOR α SUBUNIT INFLUENCES MACROSCOPIC CURRENT KINETICS: IMPLICATIONS FOR SYNAPTIC AND EXTRASYNAPTIC TRANSMISSION

Emmanuel J. Botzolakis, Andre H. Lagrange, and Robert L. Macdonald

ABSTRACT

Up-regulation of the $GABA_A$ receptor α4β3γ2L receptor isoform has been shown in multiple animal models of chronic epilepsy. However, little is known about its functional properties, limiting our understanding of its role in normal and abnormal neuronal physiology. We therefore compared the properties of the α4β3γ2L receptor isoform to those of the more widely distributed α1β3γ2L receptor isoform using a combination of whole cell recording and kinetic modeling. While peak current amplitudes and GABA EC_{50} values were similar for both isoforms, currents evoked from α4β3γ2L receptors had more fast desensitization and deactivated more slowly than those evoked from α1β3γ2L receptors. To determine how these kinetic differences would affect $GABA_A$ receptor responses under physiologically relevant conditions, a comprehensive kinetic model was generated for each isoform and evaluated under synaptic and extrasynaptic contexts of activation. The simulations predicted that currents evoked by repetitive, brief GABA applications would be more strongly attenuated for the α4β3γ2L receptor. In addition, they predicted that exposure to prolonged low levels of GABA, similar to those that might be present in the extrasynaptic space, would greatly

suppress the response of α4β3γ2L currents to higher concentrations of GABA. Thus, while similar to α1β3γ2L receptors in their ability to respond to brief and low frequency synaptic inputs, α4β3γ2L receptors are less efficacious when exposed to prolonged tonic GABA or during repetitive stimulation. Taken together, these data suggest that enhanced desensitization limits the range of GABA applications to which receptors can respond maximally.

INTRODUCTION

$GABA_A$ receptors are pentameric cys-loop receptors composed primarily of two α subunits, two β subunits, and either a γ or a δ subunit selected from six α, three β, three γ, and one δ subunit subtype. The distribution of specific subtypes is highly brain region and cell type specific, and varies during development and in certain disease states. Interestingly, the pharmacological properties of $GABA_A$ receptors are highly dependent upon the specific α subunit subtype included. For example, when assembled with β and γ subunits, $GABA_A$ receptors containing α1, 2, 3, or 5 subtypes are highly diazepam sensitive. However, α1 subtype-containing receptors are more sensitive to zolpidem than receptors containing α2 or α3 subtypes, and those containing α5 subtypes are completely insensitive to this drug. In contrast, $GABA_A$ receptors containing α4 or α6 subtypes are insensitive to both diazepam and zolpidem. Furthermore, the imidazobenzodiazepine Ro 15-4513, which is an inverse benzodiazepine receptor agonist at $GABA_A$ receptors containing α1, α2, α3 or α5 subtypes, actually enhances currents from $GABA_A$ receptors containing α4 or α6 subtypes.

Unlike the pharmacological properties of $GABA_A$ receptors composed of different α subtypes, relatively little is known about their kinetic properties. This limits our understanding of the role played by $GABA_A$ receptors in either normal or abnormal inhibitory neurotransmission, as receptor kinetics determine the efficiency of both synaptic and extrasynaptic signaling. Indeed, GABAergic inhibitory post-synaptic current (IPSC) time courses are determined primarily by the rates of $GABA_A$ receptor activation and deactivation. Moreover, while the role of desensitization in synaptic transmission not yet clear, there is evidence that the underlying desensitized states delay

GABA unbinding, thereby prolonging current deactivation (Jones & Westbrook, 1995). In addition, slow desensitization may be important for shaping receptor responses under conditions of high frequency stimulation (Bianchi & Macdonald, 2002). Receptor kinetic properties also determine the effectiveness of extrasynaptic GABAergic transmission. Although this mode of inhibitory signaling involves near-equilibrium conditions, meaning that extrasynaptic $GABA_A$ receptors need not be rapidly activating, highly desensitizing, or slowly deactivating, these processes may nonetheless be important for determining receptor responses to fluctuations in the ambient GABA concentration.

As a result, altered expression and distribution of different α subunit-containing $GABA_A$ receptor isoforms could potentially have profound effects on inhibitory neurotransmission. Interestingly, several animal models of epilepsy have demonstrated an up-regulation of α4 subtype protein expression (Schwarzer *et al.* 1997; Sperk *et al.* 1998; Brooks-Kayal *et al.* 1998). In addition, one model of CNS hyperexcitability, chronic intermittent ethanol, shifts the subcellular localization of α4 subtype-containing receptors from a perisynaptic to a central synaptic location (Liang *et al.* 2006). In both cases, however, it remains unclear whether α4 subtype up-regulation contributes to the generation of seizures or, alternatively, is a response to the hyperexcitable state. Indeed, without knowing the kinetic properties of α4 subunit-containing receptors, it is impossible to even speculate as to whether this change in receptor expression is causative or compensatory. As a first attempt to address this issue, we compared the functional properties of recombinant α4β3γ2 and α1β3γ2 receptor isoforms using a combination of whole-cell patch-clamp recording and kinetic modeling.

MATERIALS AND METHODS

Cell culture and expression of recombinant $GABA_A$ receptors

$GABA_A$ receptor α1, α4, β3 and γ2L subunit cDNAs were individually subcloned into the mammalian expression vector pCMV-neo. Deletion of an extraneous genomic sequence in the 5' untranslated region of the α4 subtype cDNA resulted in improved expression, as previously described (Wallner *et al.* 2003). All cDNAs were sequenced by the Vanderbilt University Medical Centre sequencing core to confirm that they matched the published sequences for mature rat peptides (accession numbers NP_899155, NP_542154, P63079 and NP_899156 for the α1, α4, β3, and γ2 proteins, respectively).

Human embryonic kidney (HEK293T) cells were plated at a density of 200,000 – 400,000 cells per 60-mm culture dish and maintained in Dulbecco's modified Eagle's medium (Invitrogen, Carlsbad, CA, USA) supplemented with 10% fetal bovine serum and 100 IU ml^{-1} each of penicillin and streptomycin (Invitrogen) at 37°C in 5% CO_2–95% O_2. On day one, cells were transfected using a previously established calcium phosphate precipitation technique (Angelotti *et al.* 1993). A total of 12 μg of $GABA_A$ receptor subunit-containing DNA, with 4 μg of each subunit plasmid (ratio 1 : 1 : 1) for αβ3γ2L receptors. Two micrograms of pHook-1 (Invitrogen) were also added so that immunomagnetic bead selection could be performed on day two (Greenfield *et al.* 1997). Following selection, the cells were plated on 35-mm dishes, and recordings were made on day three, approximately 18–36 h after selection.

Electrophysiological recording and drug application

Whole cell voltage-clamp recordings were performed on transfected HEK293T cells. All experiments were performed using at least two separate transfected batches of cells on at least two separate days of recording. Cells were bathed in an external solution consisting of (in mM): NaCl 142, $CaCl_2$ 1, KCl 8, $MgCl_2$ 6, glucose 10, HEPES 10 (pH 7.4, ~320–340 mosmol l^{-1}). All recordings were performed at room temperature. Glass micropipettes were formed from thin-walled borosilicate glass with a filament (World Precision Instruments, Sarasota, FL, USA) with a P2000 laser electrode puller (Sutter Instruments, San Rafael, CA, USA) and fire polished with a microforge (Narishige, East Meadow, NY, USA). Microelectrodes used for lifted cell recording had resistances of 1–2 MΩ when filled with an internal solution consisting of (in mM): KCl 153, $MgCl_2$ 1, HEPES 10, EGTA 5, Mg^{2+}-ATP 2 (pH 7.3, ~300–310 mosmol l^{-1}). This combination of external and internal solutions produced a chloride equilibrium potential (E_{Cl}) of approximately 0 mV.

Membrane voltages were clamped at –20 mV using an Axopatch 200A amplifier (Axon Instruments, Union City, CA, USA) amplifier. GABA was applied to the lifted cells via a three-, four-, or six-barrelled square glass (Friedrich and Dimmock, Millville, NJ, USA). These multi-barrelled pipettes were pulled on a P-87 Flaming-Brown (Sutter Instruments, San Rafael, CA, USA) electrode puller with custom made platinum–iridium filament and sanded to a final diameter of 200–400 µm for each barrel. The multi-barrelled pipettes were attached to a Warner SF-77B Perfusion Fast-Step (Warner Instrument Corporation, Hamden, CT, USA), allowing for rapid solution changes. All GABA application protocols began with a cell positioned in the flow of external bath

solution from which the multi-barrelled array was repositioned such that the unmoved cell and electrode were now exposed to GABA. The drug application was initiated by an analog pulse triggered by the pCLAMP 9 software (Axon Instruments) that caused the motor of the Warner Fast-Step to reposition the multi-barrelled array from one barrel to another (e.g., external solution to GABA). Exchange times were routinely measured and always found to be 0.3–0.7 ms at an open electrode tip by stepping from control to dilute external solution. The exchange around an intact cell was measured in a subset of cells by stepping into 10 μM GABA and then another step into 10 μM GABA in external solution in which NaCl was replaced by NaSCN. The resulting current had a 10–90% rise time of 0.9 ± 0.1 ms (n = 9; data not shown) using a drug application pipette with 0.35 ms open-tip exchange time.

For generation of concentration–response relationships, peak $GABA_A$ receptor currents evoked by randomly sequenced concentrations of GABA were recorded with at least 45 s of wash between each application. This time was empirically determined to be sufficient for complete recovery from desensitization. To assess possible changes in the transmembrane chloride ion concentration gradient, pCLAMP 9 generated a 500 ms ramp voltage step from –50 mV to +50 mV. The current–voltage relationship was determined at the beginning and end of each prolonged exposure to 1 μM GABA, as well as at the end of the wash in external solution. The responses during concentration–response determinations and pre-application studies were normalized to the current elicited by 1 mM GABA after a prolonged wash in external solution during each sweep. Data were excluded if there was a greater than 10% rundown of the maximal response between sweeps.

Data analysis

Currents were low-pass filtered at 2 kHz, digitized at 5–10 kHz, and analyzed using the pCLAMP 9 software suite. For cells with very small (< 50 pA) currents, rise time, desensitization and deactivation were not determined. Current amplitudes and 10–90% rise times were measured using the Axon Instruments Clampfit 9 software package. The desensitization and deactivation time courses of $GABA_A$ receptor currents were fitted using the Levenberg-Marquardt least squares method with up to six component exponential functions of the form $\sum a_n e^{(-t/\tau^n)} + C$, where t is time, n is the best number of exponential components, a_n is the relative amplitude of the nth component, τ_n is the time constant of the nth component, and C is the residual current at the end of the GABA application. Additional components were accepted only if they significantly improved the fit, as determined by an F-test automatically performed by the analysis software on the sum of squared residuals. The time course of deactivation was summarized as a weighted time constant, defined by the following expression: $\frac{\sum a_n \tau_n}{\sum a_n}$. GraphPad Prism 4 (GraphPad Software Inc, San Diego, CA, USA) was used to fit the concentration–response results to a sigmoidal function using the equation:

$$I = \frac{I_{\max}}{1 + 10^{(\log_{EC50} - \log_{drug}) \times \text{Hill slope}}},$$

where I is the peak current at a given GABA concentration, and I_{max} is the maximal peak current. Numerical data were expressed as means ± SEM. Statistical analysis was performed using GraphPad Prism 4. Data were compared using a Mann-Whitney test for pairs of data, or a Kruskal-Wallis test for comparing three or more groups. Statistical significance was taken as $P < 0.05$.

Kinetic modeling

Using QuB version 1.4 (http://www.qub.buffalo.edu), a modified version of the α1β3γ2L GABA receptor model proposed by Haas & Macdonald (1999) was fitted to representative α1β3γ2L and α4β3γ2L whole cell currents. For each GABA concentration used in the fitting process, a representative current was generated by averaging the responses of three to eight cells whose peak currents were normalized to the 1 mM GABA peak current. Before using this averaged current for fitting, it was verified against the average kinetic properties of individual cells at the same GABA concentration.

Since mono-liganded states should have negligible occupancy in the presence of saturating concentrations of GABA, we first fitted an averaged current elicited by 10 mM GABA to a version of the model including only the di-liganded states. This reduced the number of free parameters, thus decreasing the time required for each fitting iteration. To further reduce the number of free parameters, the exit rates from di-liganded open states were fixed so that mean open times would be consistent with previously published single channel data for these receptor isoforms (Haas & Macdonald, 1999; Akk *et al.* 2004). Once an adequate fit was obtained (i.e., when the log likelihood ratio changed by less than 0.5 between iterations), the currents were refitted to a model with scaled rate constants to obtain open time distributions consistent with the published single channel data. Closed time distributions were not considered during the fitting process, as the longest components tend to be artificially shortened due to the presences of multiple channels in most patches. Nonetheless, it should be noted that the di-liganded portion of our model contains five closed states. This gives rise to a closed time distribution with five components, a number consistent with published reports for both receptor isoforms.

After fitting the model to currents elicited by 10 mM GABA, all di-liganded rate constants were fixed, and mono- and unliganded non-conducting states were added to generate two GABA binding steps. The two GABA binding sites were assumed have equal affinity. To obtain an estimate of the unbinding rates, this model was first fitted to the time course of current deactivation following a brief GABA application (5 ms, 1 mM). Mono-liganded open and desensitized states were then added, and the model was refitted to currents elicited by the lowest GABA concentration that permitted significant activation and macroscopic desensitization (3 and 10 μM for α4β3γ2 and α1β3γ2 receptor isoforms, respectively). The final kinetic model for each receptor isoform was verified by generating theoretical currents with the differential equation solving program Berkeley-Madonna 8.0 (http://www.berkeleymadonna.com) using the fourth-order Runge-Kutta method and time intervals of 10–100 μs.

RESULTS

To investigate the influence of the α4 subunit subtype on the physiological properties of αβγ $GABA_A$ receptor currents, we used whole-cell voltage-clamp recording and a rapid drug delivery system to apply GABA to lifted HEK293T cells that had been co-transfected with β3, γ2L, and either α1 or α4 subtypes. We chose the combination of α4, β3, and γ2L subunits because rodent brain α4 subtypes co-precipitate with β2/3 subunits (Bencsits *et al.* 1999) and are among the subtypes co-expressed in thalamus and hippocampus (Pirker *et al.* 2000). Moreover, multiple models of epilepsy have found a consistent up-regulation of α4 subtype expression in the hippocampal dentate gyrus, where β3 is the predominant β subunit subtype. Furthermore, low levels of endogenous β3 subtypes have been detected by RT-PCR in HEK293 cells (Kirkness & Fraser, 1993; Davies *et al.* 2000). We therefore used the β3 subtype to prevent possible contamination with multiple β subtypes. Although α1β2γ2 receptors are the most abundant native receptors in mammalian brain, we used α1β3γ2L receptors to permit comparison of the effects of different α subtypes on receptor current kinetic properties, without the possible confound of different β subtypes.

α4β3γ2L receptor currents desensitized more rapidly and extensively than α1β3γ2L receptor currents

To characterize the effect of α subtypes on current desensitization, α4β3γ2L and α1β3γ2L currents were recorded during prolonged (4 second) applications of a high concentration of GABA (1 mM). While α4β3γ2L and α1β3γ2L receptor currents had similar peak amplitudes (data not shown), α4β3γ2L currents desensitized more rapidly

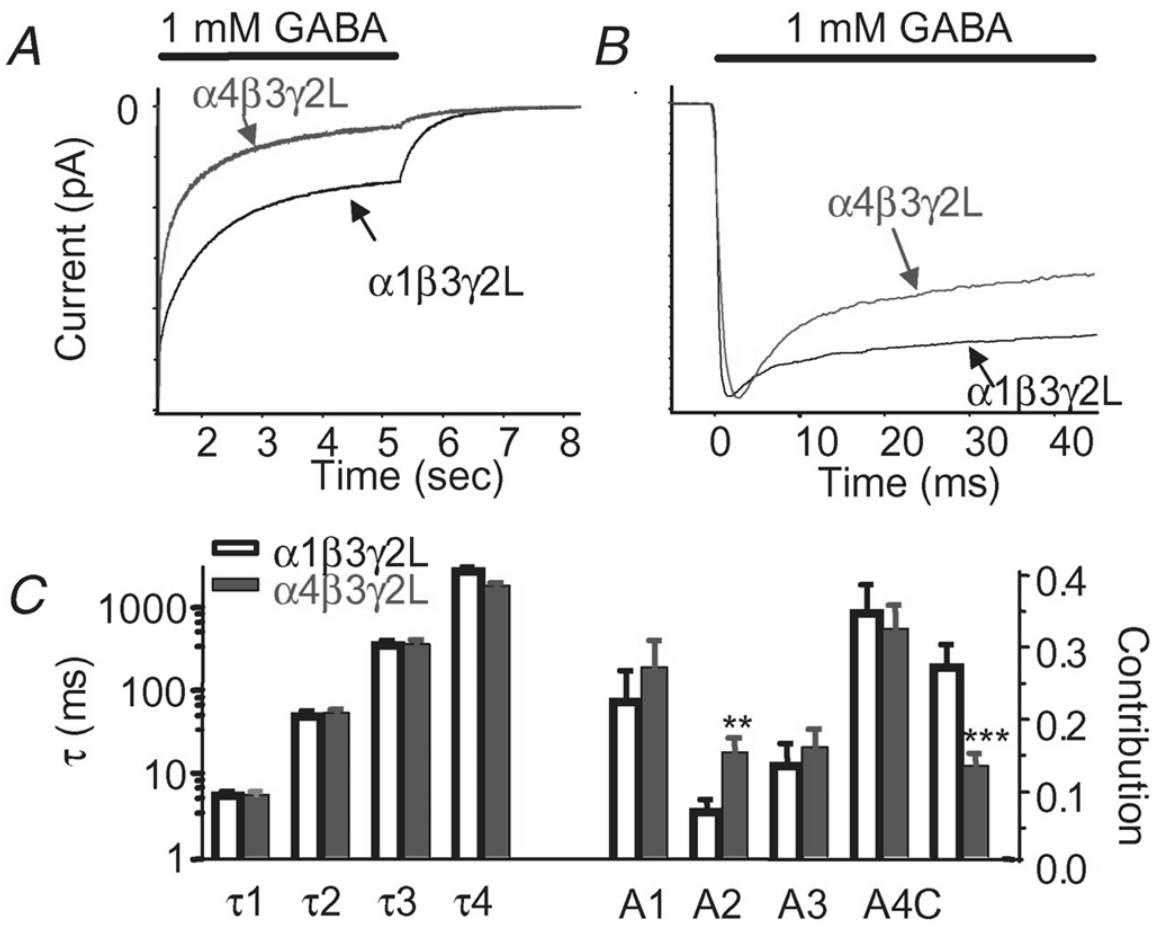

Figure 1. Desensitization of α4β3γ2L currents was faster and more extensive than that of α1β3γ2L currents.

A) Representative currents illustrated the rapid and extensive desensitization that occurred during a 4 sec application of 1 mM GABA. Peak currents were normalized to allow for comparison of their kinetic properties. B.) The same currents were presented on an expanded time scale. C.) Although the desensitization time constants were similar for α1β3γ2L and α4β3γ2L currents, there was a greater contribution of fast (τ <100 ms) desensitization in α4β3γ2L currents. Moreover, α4β3γ2L currents had less residual current at the end of 4 sec of GABA. ** p<.01, *** p<.001 α1β3γ2L versus α4β3γ2L currents.

and extensively than α1β3γ2L currents (Figure 1A and 1B). All currents were fitted best with a three or four component exponential function with time constants that fell into four discrete groups, τ_1 (< 15 ms), τ_2 (20–100 ms), τ_3 (110–800), and τ_4 (800–4800 ms)

(Figure 1C). The α4β3γ2L currents had a greater contribution of fast (< 100 ms) desensitization than α1β3γ2L receptors (Figure 1C), although the actual time constants of desensitization were similar for both receptors. Moreover, α4β3γ2L receptors had more overall desensitization, as assessed by the residual current at the end of the 4 s GABA application.

The rapidly changing membrane conductance during GABA application introduces a transient series resistance error that cannot be compensated with our recording system. In theory, this could lead to underestimation of the true peak amplitude and degree of rapid desensitization. However, if this were the case, we would expect those cells with larger currents to have a smaller fraction of fast desensitization. Similar to previous work from our laboratory (Bianchi & Macdonald, 2002), we found no such correlation between current amplitude and desensitization (data not shown). Moreover, since the peak amplitudes of α4β3γ2L and α1β3γ2L receptors were the same, any transient series resistance errors should have been the same in both groups.

α4β3γ2L receptor currents deactivated more slowly than α1β3γ2L receptor currents

Synaptic inhibitory neurotransmission involves very brief exposure to high concentrations of GABA. To characterize the response of these receptors to a more synaptically relevant application of GABA, cells were exposed to 1 mM GABA for 5 ms, the briefest application that we were able to achieve reproducibly with our drug delivery system. Both α4β3γ2L and α1β3γ2L receptor currents decayed slowly after a brief exposure to GABA (Figure 2A). However, α4β3γ2L currents deactivated more slowly,

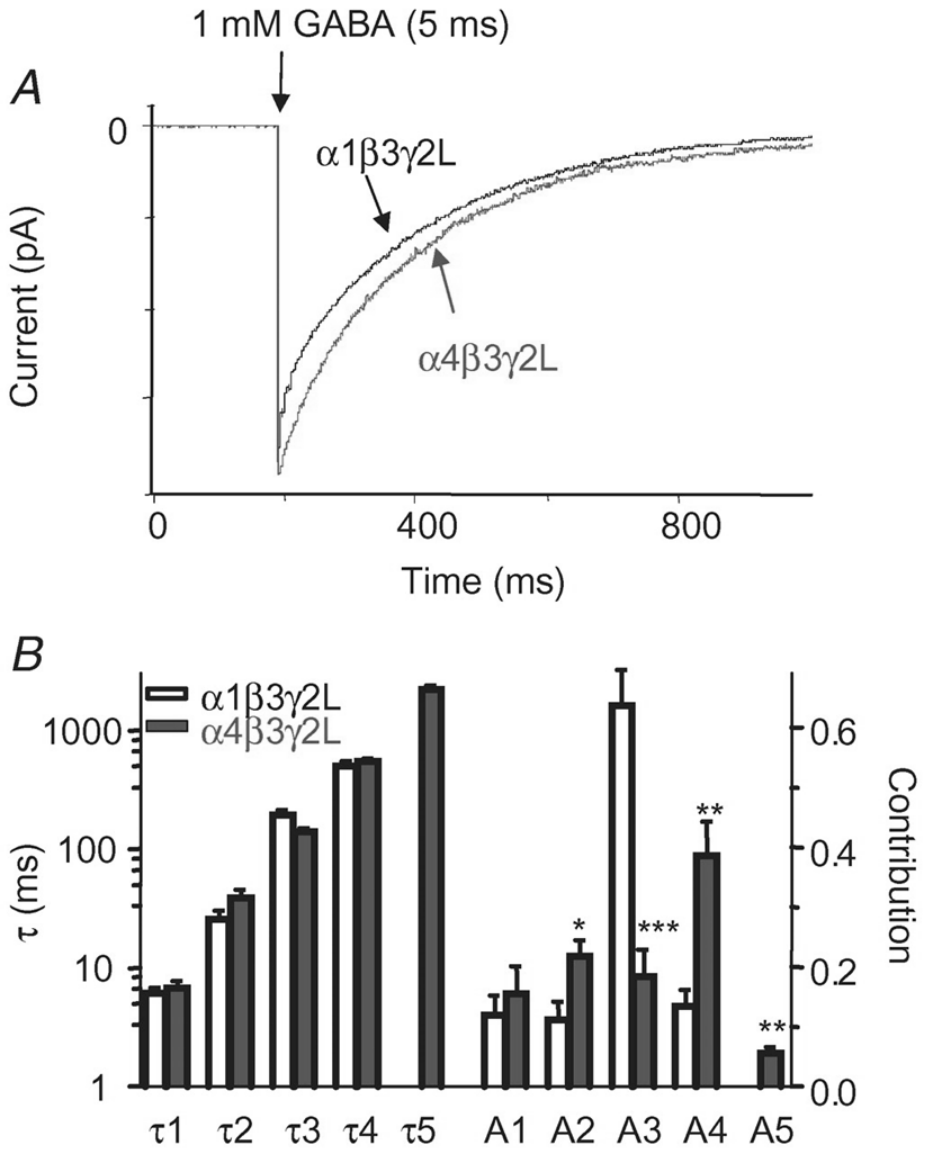

Figure 2. α4β3γ2L receptor currents deactivated more slowly than those of α1β3γ2L receptors.

A) α4β3γ2L currents deactivated more slowly after a brief application of saturating GABA (1 mM, 5 ms). B) Summary of the deactivation kinetics. The α1β3γ2L current weighted deactivation time constant was 200 ± 24 ms (n = 13) and was largely determined by a single time constant (τ3). In contrast, α4β3γ2L current deactivation was more complicated and prolonged, with an overall weighted deactivation time constant of 371 ± 55 ms (n = 18), which was significantly longer than α1β3γ2L currents ($p<.05$). * $p<.05$, ** $p<.01$, *** $p<.0001$ α1β3γ2L versus α4β3γ2L currents

with a weighted time constant of 371 ± 54 ms (n = 18) *versus* 200 ± 24 ms (n = 13, P < 0.05) for α1β3γ2L currents. Deactivation of α1β3γ2L current was relatively simple, with two (1 of 13 cells), three (6 of 13 cells), or four (6 of 13 cells) time constants, but the major part of the deactivation was due to a single component (τ_3, 100–300 ms). In contrast, α4β3γ2L current deactivation tended to be more complex, requiring three (7 of 18 cells), four (8 of 18 cells) or five (3 of 18 cells) components to accurately fit the deactivation time course. Furthermore, unlike α1β3γ2L current deactivation, no single component dominated the deactivation time course (Figure 2B).

Interestingly, in most published reports, only one or two component exponential functions are generally used to fit IPSC decay. The basis for this difference is uncertain, but may be due to the fact that our recombinant currents were significantly larger than most IPSCs, which may have allowed us to detect greater kinetic complexity than would be possible from the smaller IPSC currents. Different fitting techniques are another potential source of confusion when comparing studies among laboratories. To address this issue, all of the currents in these studies were also fitted with a two-component exponential function. Although this approach provided less precise fits of the data, there was no change in the overall weighted time constant compared to the more complicated fits described above (data not shown).

α4β3γ2L and α1β3γ2L receptors had similar sensitivities to GABA

In addition to the synaptic receptors mediating IPSCs, another population of $GABA_A$ receptors found outside the synaptic cleft respond to tonic, low levels of GABA

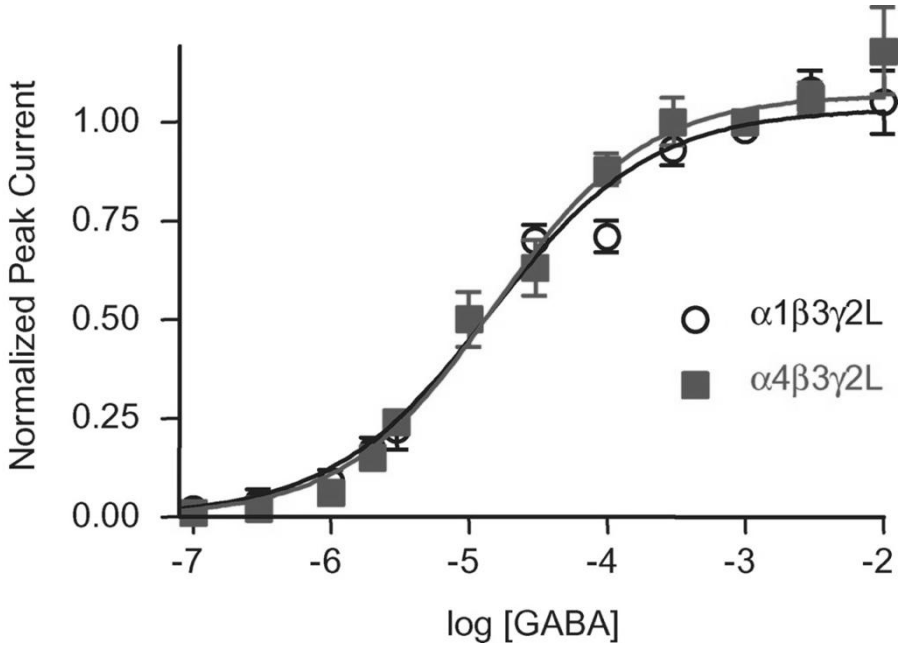

Figure 3. α1β3γ2L and α4β3γ2L receptor peak currents had similar sensitivities to GABA.

The GABA potency, as determined by complete concentration response studies in individual neurons showed that the peak current EC_{50}s (12 ± 2 μM (n = 9) and 17 ± 4 μM (n = 12)) were not different for α1β3γ2L and α4β3γ2l currents, respectively. Similar results were obtained when the data from all cells were pooled and then fitted as a group (EC_{50} = 14 μM (95% CI = 12 – 17 μM) and 15 μM (95% CI = 14-17 μM), for α1β3γ2L and α4β3γ2l currents, respectively).

(≤ 1 μM). Despite the small size of these tonic currents, their longevity allows a large overall charge transfer that can significantly alter neuronal excitability. Effective inhibition by extrasynaptic receptors would be best served by highly sensitive $GABA_A$ receptors that are able to respond during prolonged exposure to low GABA concentrations. Concentration–response curves were generated by applying varying GABA concentrations in random order with at least a 45 s wash between applications of each concentration (Figure 3). Since there was substantial cell-to-cell variability in

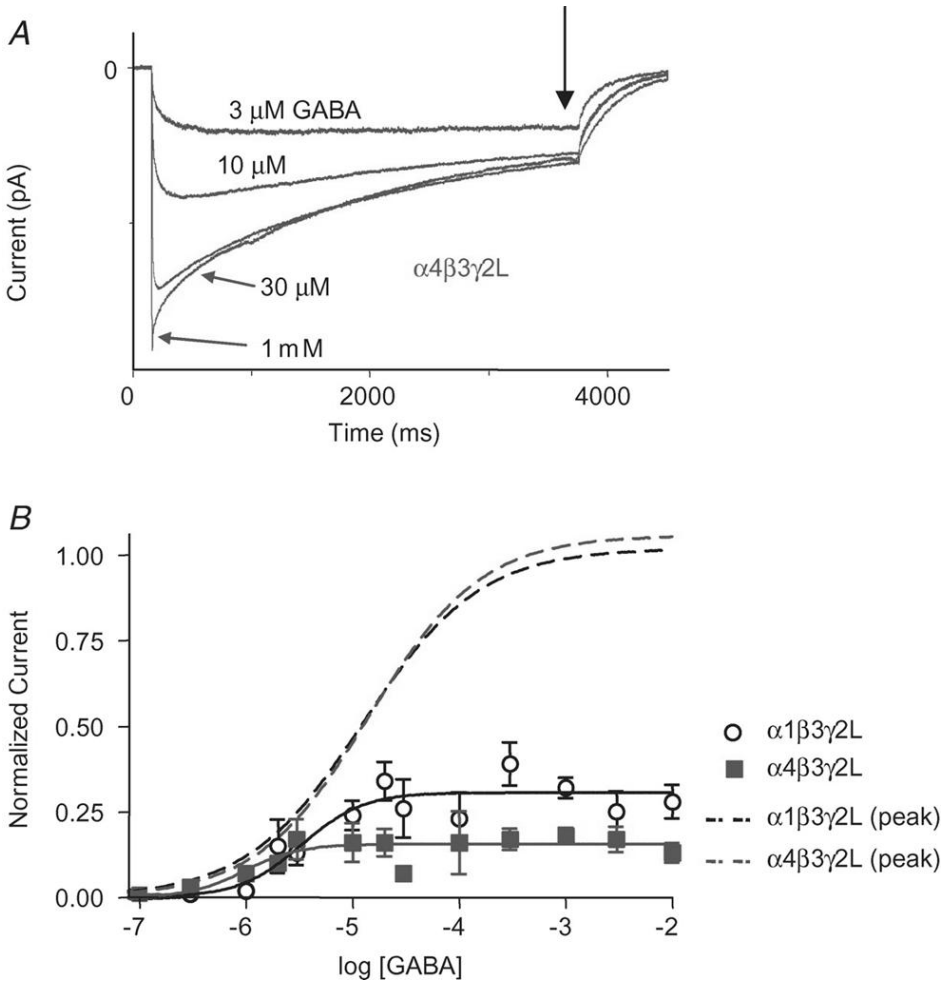

Figure 4. Desensitization attenuated receptor responses to prolonged GABA applications.

A) Representative α4β3γ2L currents illustrating the effect of desensitization to differentially influence peak and pseudo-steady state currents in a concentration dependent manner. Unlike the peak current, the pseudo-steady state current measured after 4 sec of GABA (arrow) was responsive to a very limited range of GABA concentrations, with maximal stimulation occurring at approximately 10 μM. B) Prolonged GABA application to α1β3γ2L receptors strongly suppressed the maximal GABA response (I_{max} = 31% of 1mM peak current; 95% CI = 29 – 32%) and also caused an apparent leftward shift of the concentration-response curves (EC_{50} = 3.3 μM; 95% CI = 2.4 – 4.5 μM GABA). The highly desensitizing α4β3γ2L receptors had an even more limited response to prolonged GABA application (I_{max} = 15%; 95% CI = 15-16%) (EC_{50} = 1.0 μM; 95% CI = 0.7 – 1.3 μM GABA) Comparing the response of α1β3γ2L versus α4β3γ2L receptors to 4 sec of 1 mM GABA confirmed that the highly desensitizing α4β3γ2L currents were more suppressed during prolonged GABA application ($p < 0.001$). For comparison, peak current concentration response data from Figure 7 were replotted here as dashed lines.

current size, a near-maximal (1 mM) GABA concentration was applied intermittently to allow normalization of peak currents and to assess current run-down during the experiments. The GABA EC_{50} values were similar for both α1β3γ2L and α4β3γ2L receptors (Figure 3; GABA EC_{50} values were 14 μM (95% CI = 12–17 μM) and 15 μM (95% CI = 14–17 μM) for pooled data from α1β3γ2L and α4β3γ2L peak currents, respectively).

Tonic GABA receptor currents measured in neurons are thought to be caused by low levels of extrasynaptic GABA that change much more slowly than GABA levels in the synaptic cleft. Therefore, we determined the pseudo-steady-state concentration-dependent response of α1β3γ2L and α4β3γ2L receptors to prolonged GABA application. Various concentrations of GABA were applied for 4 seconds, and the current at the end of the GABA application was measured (Figure 4A, arrow). At GABA concentrations above 10 μM, the response to prolonged GABA was lower for α4β3γ2L than for α1β3γ2L receptors (Figure 4B). It is worth noting that the concentration dependence of these pseudo-steady-state currents had remarkably limited dynamic ranges. A maximal pseudo-steady-state response was seen with 10 μM GABA, although higher concentrations were able to accelerate the rates of activation and desensitization (Figure 4B). In the range of GABA concentrations likely to be present in the extrasynaptic spaces (1–2 μM), the responses of α4β3γ2L and α1β3γ2L receptors were similar.

Development of a comprehensive kinetic model of α4β3γ2L and α1β3γ2L $GABA_A$ receptor function

To make more quantitative predictions about the potential physiological roles of

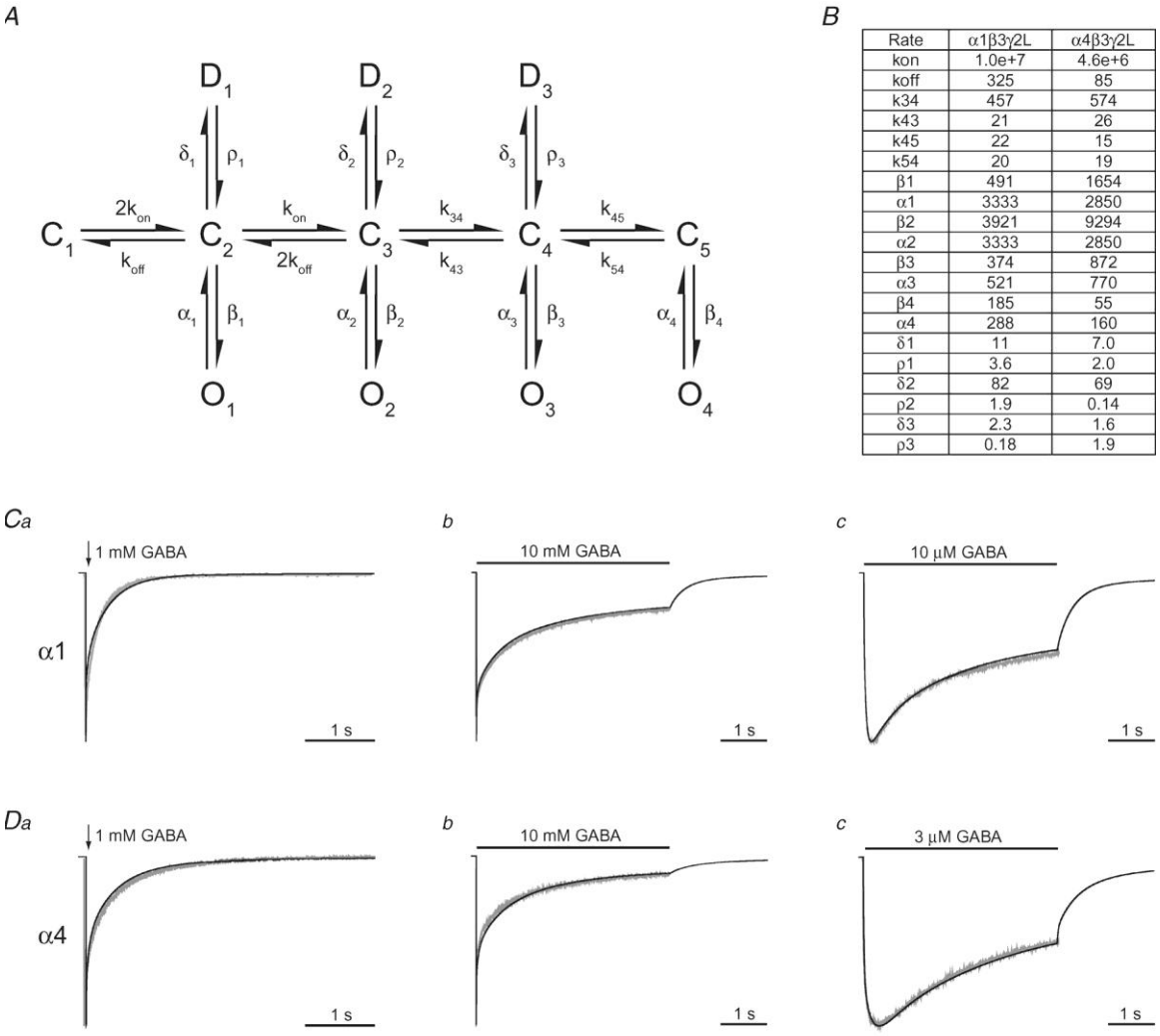

Rate	α1β3γ2L	α4β3γ2L
kon	1.0e+7	4.6e+6
koff	325	85
k34	457	574
k43	21	26
k45	22	15
k54	20	19
β1	491	1654
α1	3333	2850
β2	3921	9294
α2	3333	2850
β3	374	872
α3	521	770
β4	185	55
α4	288	160
δ1	11	7.0
ρ1	3.6	2.0
δ2	82	69
ρ2	1.9	0.14
δ3	2.3	1.6
ρ3	0.18	1.9

Figure 5. Kinetic model for the α1β3γ2L and α4β3γ2L receptor isoforms.

A) Modified version of the kinetic model proposed for the α1β3γ2L receptor isoform by Haas & Macdonald (1999) is shown (O, open; C, closed; D, desensitized). B) rate constants for the α1β3γ2L and α4β3γ2L receptor isoforms were determined by fitting the time course of macroscopic currents evoked by saturating and sub-saturating GABA concentrations to the kinetic model in A after constraints were imposed based on published single-channel data (see Methods). Units for all rate constants are s^{-1} except for k_{on} (M^{-1} s^{-1}). C1, D1) the optimized responses of α1β3γ2L and α4β3γ2L receptors to a 5 ms square pulse of GABA (1 mM; arrow) are superimposed on averaged currents evoked under similar conditions. C2, D2) the optimized responses of the α1β3γ2L and α4β3γ2L receptors to a 4 sec square pulse of a saturating GABA concentration (10 mM; filled bars) are superimposed on the averaged data traces used for fitting the di-liganded rate constants (see Methods). C3, D3) the optimized responses of the α1β3γ2L and α4β3γ2L receptors to a 4 sec square pulse of sub-saturating GABA concentrations (10 and 3 μM, respectively; filled bars) are superimposed on the averaged data traces used for fitting of the mono-liganded rate constants (see Methods).

α1 and α4 subtype-containing $GABA_A$ receptors, a kinetic model was generated for these receptor isoforms that accounted for not only the observed macroscopic properties described above, but also for the previously published single channel properties (Haas & Macdonald, 1999; Akk *et al.* 2004) (Figure 5). This model was based largely on the previous work of Haas & Macdonald (1999), but has been expanded to account for several additional microscopic and macroscopic kinetic observations. Specifically, single channel recordings from α1βγ $GABA_A$ receptors have consistently demonstrated three open states, with the relative contribution of the shortest open state (O_1) being concentration dependent at GABA concentrations below 10 μM (Fisher & Macdonald, 1997). Although this suggests the presence of an additional GABA binding step distal to O_1, a feature found in most of the existing models, it remains unclear why a residual component of O_1 persists at higher concentrations. One possible explanation is that two open states with similar mean open times exist, one of which is mono-liganded and the other di-liganded. We have therefore added two additional states to the Haas & Macdonald (1999) kinetic model: a di-liganded closed (C_3) and a di-liganded open state (O_2). The addition of the closed state is intended to preserve the known burst characteristics of these receptors such that only one type of opening is observed per burst (Twyman *et al.* 1990). As with α1βγ receptors, single channel recordings from α4βγ receptors also demonstrated the presence of three open states that are concentration independent at GABA concentrations above 10 μM (Akk *et al.* 2004). We therefore applied the same kinetic model to those receptors.

Table 1. Kinetic models accurately predict the single channel and macroscopic current responses of α1β3γ2L and α4β3γ2L receptor isoforms to a variety of GABA application protocols.

Parameter	α1β3γ2L		α4β3γ2L	
	Measured	**Simulated**	**Measured**	**Simulated**
Open Intervals (1 mM GABA)				
τ_1 (ms)	0.30*	0.30	0.35^{+}	0.35
Fraction O_1	0.24*	0.24	0.34^{+}	0.32
τ_2 (ms)	1.92*	1.92	1.30^{+}	1.30
Fraction O_2	0.48*	0.49	0.63^{+}	0.65
τ_3 (ms)	3.47*	3.47	6.30^{+}	6.25
Fraction O_3	0.28*	0.27	0.03^{+}	0.03
Mean Open Time (ms)	2.14*	1.97	1.13^{+}	1.16
P_o	0.11*	0.08	0.35$^{+◊}$	0.06
Desensitization (4 sec, 1 mM GABA)				
τ_1 (ms)	6 ± 1	3	7 ± 1	7
Contribution A_1	0.18 ± 0.03	0.18	0.25 ± 0.03	0.25
τ_2 (ms)	56 ± 5	36	58 ± 4	49
Contribution A_2	0.07 ± 0.01	0.10	0.13 ± 0.02	0.16
τ_3 (ms)	431 ± 45	373	373 ± 41	392
Contribution A_3	0.17 ± 0.03	0.22	0.17 ± 0.02	0.19
τ_4 (ms)	2652 ± 250	1848	1934 ± 161	1406
Contribution A_4	0.33 ± 0.03	0.32	0.33 ± 0.03	0.30
Residual Current	0.25 ± 0.02	0.18	0.12 ± 0.02	0.09
Deactivation (5 ms, 1 mM GABA)				
Weighted τ (ms)	200 ± 24	214	371 ± 55	359
EC_{50}				
Peak (μM)	14	14	15	15
4 sec (μM)	3.0	1.8	1.0	0.6
Repetitive Stimulation (5 ms, 1 mM GABA)				
2 pulses – 12.5 Hz (final/initial peak)	0.84 ± 0.02	0.77	0.60 ± 0.05	0.63
2 pulses – 1 Hz (final/initial peak)	0.89 ± 0.01	0.85	0.68 ± 0.04	0.65
2 pulses – 0.05 Hz (final/initial peak)	0.99 ± 0.01	0.99	0.92 ± 0.02	0.96
4 pulses – 10 Hz (final/initial peak)	0.75 ± 0.03	0.62	0.52 ± 0.06	0.46

* Haas & Macdonald, 1999.
$^{+}$ Akk, Bracamontes, & Steinbach, 2004.
$^{◊}$ Note that this value overestimates the true P_o as it only reflects intra-cluster P_o.

For both receptor isoforms, we also modified the arrangement of the desensitized states. We found that an accurate fit of the currents evoked by low concentrations of GABA was only possible when a mono-liganded closed state (D_1) was added, as has been previously suggested (Jones & Westbrook, 1995; Mozrzymas *et al.* 2003). Furthermore, we did not find that a D state connected to the terminal pre-open state (C_5) significantly improved our fits. Without very long GABA applications (> 10 seconds), however, we cannot rule out the possibility that there may be even slower phases of desensitization than those described here, which may necessitate additional states. It should be noted that while at least four phases of desensitization were observed in the presence of saturating GABA concentrations (see above), the model proposed here includes only two di-liganded desensitized states. The cause of this discrepancy is two-fold. First, it reflects the fact that macroscopic current kinetic properties do not directly correspond to specific microscopic rate constants or any precise connectivity between states. Instead, macroscopic current properties represent a complex mixture of all rate constants in the underlying kinetic scheme, such that the number of desensitized states need not directly correspond to the number of time constants required for fitting of macroscopic desensitization. Indeed, our model with two desensitized states gives rise to currents that require four exponential components to adequately fit the time course of macroscopic desensitization (Table 1). Second, it raises the important question: what is a desensitized state? From the standpoint of charge transfer, desensitized states are simply non-conducting states. While it is tempting to propose that the dwell time in a given state

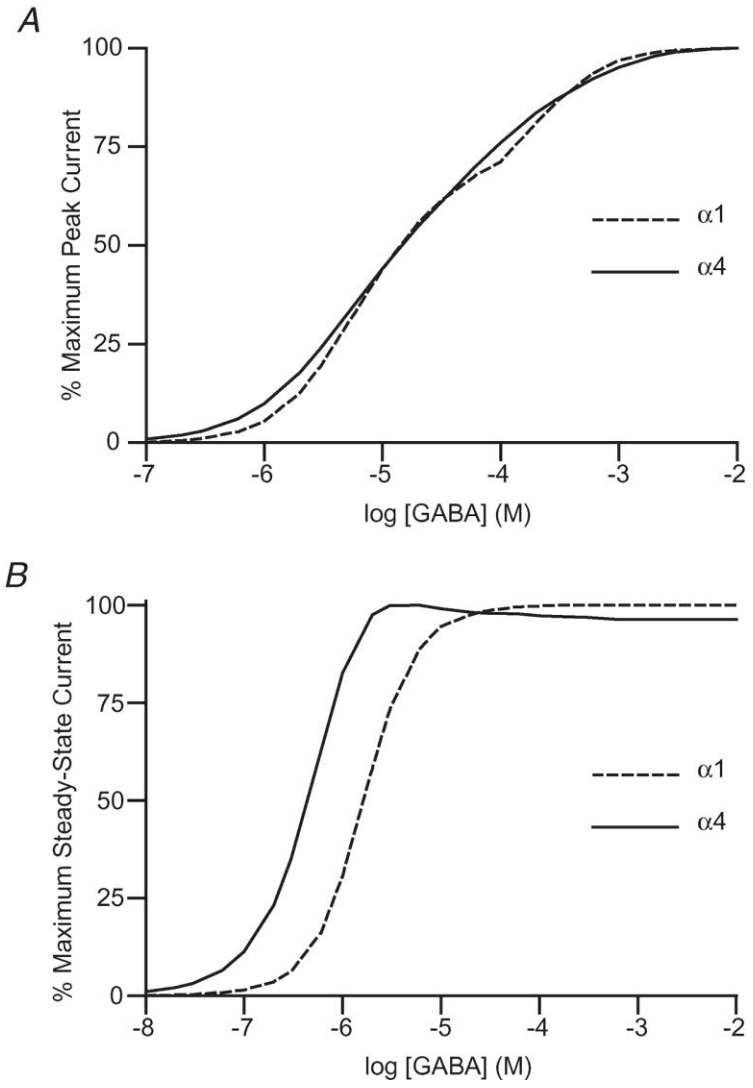

Figure 6. Kinetic model accurately predicts the concentration dependence of α1β3γ2L and α4β3γ2L receptor peak and steady-state responses to GABA.

Using the α1β3γ2L and α4β3γ2L kinetic models, simulations of receptor activation were performed using square 4 sec GABA pulses. A) peak currents at various GABA concentrations are compared to the peak current evoked by a square pulse of 10 mM GABA, above which the peak current amplitude did not change. Although slight differences in the shape of the concentration response profiles are evident, the EC_{50}s are virtually identical for these two receptor isoforms (α1, 14 μM; α4, 15 μM). B) as above, except that 45 sec square pulses of GABA were used to allow for the occupancies of all states in the kinetic model to reach equilibrium. As with peak currents, the models predict that α1 and α4 receptors have similar steady-state current EC_{50}s (α1, 1.8 μM; α4, 0.6 μM). Note that peak steady-state current for α4 receptors occurs at ~ 3 μM, reflecting the lower O state occupancy of di-liganded receptors than of mono-liganded receptors for this isoform at very low GABA concentrations.

determines if it should be designated as 'desensitized' (as we have chosen to do here in the interest of clarity), it should be noted that both the α1 and α4 models continue to undergo fast macroscopic desensitization in the absence of these desensitized states (data not shown). This suggests that other non-conducting states such as C_4 and C_5, while much shorter lived, may also play the role of desensitized states.

Our studies and those of Akk *et al.* (2004) used slightly different transfection techniques and GABA subunit combinations. Furthermore, without repeating the single channel recording of others, we were not able to directly fit our model to actual single channel data and cannot exclude the possibility that other gating schemes might describe our results equally well. We have therefore chosen not to make further mechanistic arguments about the microscopic kinetic properties of these receptors based on these kinetic models. Rather, we sought to use these models to help predict the responses of these receptor isoforms to GABA application protocols that were not experimentally testable with our current techniques. As shown in Figures 5 and 6, and in Table 1, the kinetic models accurately fit the experimentally determined single channel, whole cell, and pharmacological data quite accurately. Thus, we used this model to explore the responses of α1 and α4 subtype containing receptors to GABA under a variety of physiological conditions.

α4β3γ2L and α1β3γ2L $GABA_A$ receptors were predicted to respond differently to changes in the duration of the synaptic transient

We first used the kinetic models to predict the responses of α1 *versus* α4 subtype-containing $GABA_A$ receptors to brief pulses of saturating GABA, as might be expected in

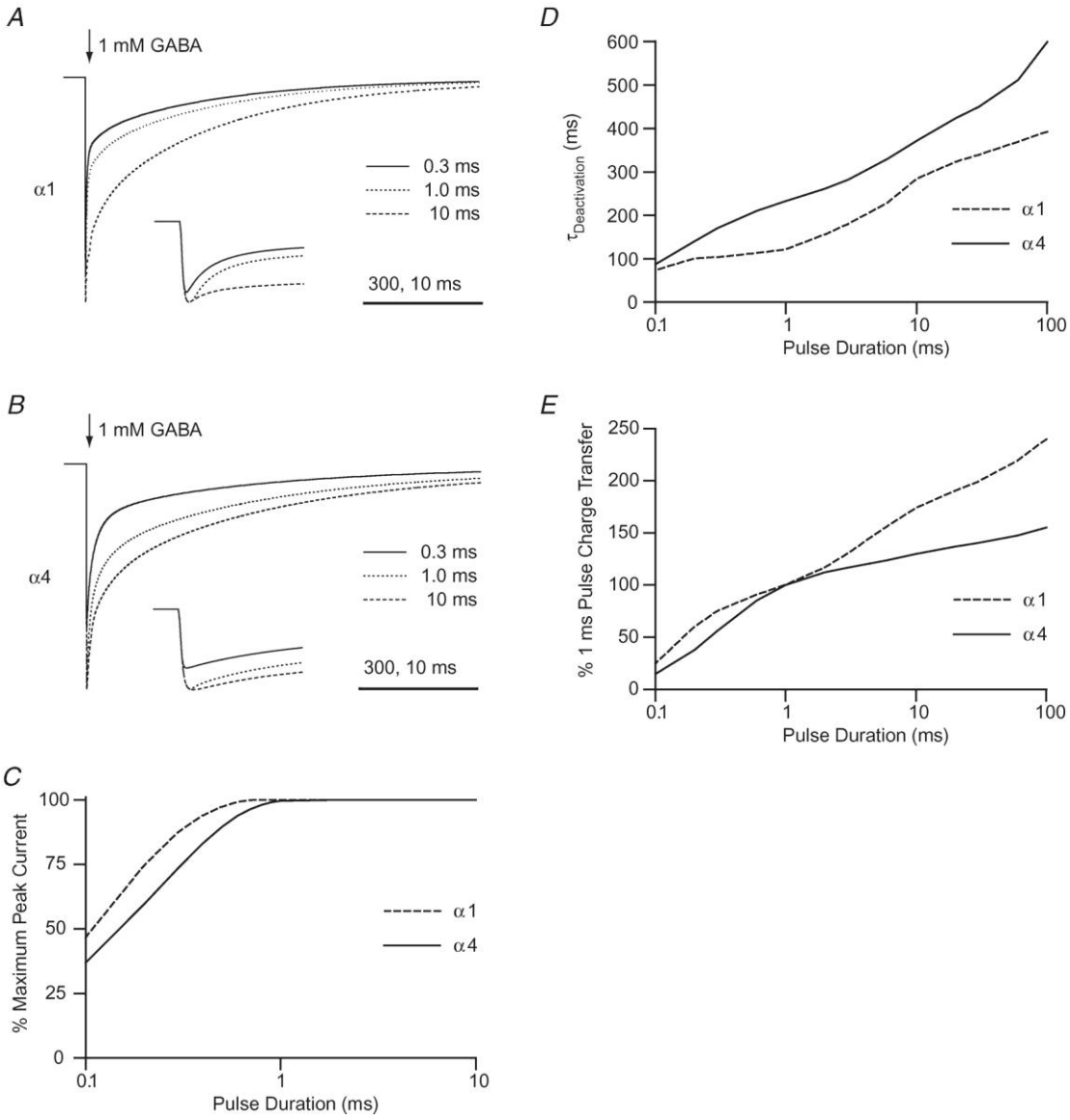

Figure 7. The kinetic properties of α1β3γ2L and α4β3γ2L receptor isoforms have a unique dependence on the duration of GABA application.

A) Incrementally increasing the GABA pulse (1 mM; arrow) duration to α1β3γ2L receptors from 0.3 ms (solid line) to 1.0 ms (short dashed line) slightly increased the peak current amplitude, with little effect on the subsequent deactivation rate. Further increasing the GABA application duration to 10 ms (long dashed line) did not further increase the peak amplitude, but did prolong the deactivation (see inset). B) Unlike the α1β3γ2L receptor isoform, increasing the GABA pulse (1 mM; arrow) duration from 0.3 ms (solid line) to 1.0 ms (short dashed line) elicited α4β3γ2L currents with both increased peak amplitude and prolonged deactivation. Like α1 containing receptors, a further increase in GABA duration to 10 ms (long dashed line) had no further effect on peak current but does continues to prolong deactivation. C) Brief GABA pulse durations

Figure 7 (continued)

(< 1 ms) elicit a smaller normalized peak response from α4β3γ2L currents than from α1β3γ2L receptor isoforms, likely a consequence of the slower activation observed with α4β3γ2L receptors. D) deactivation is slower for α4β3γ2L receptors than for α1β3γ2L receptors at all GABA pulse durations. For pulse durations < 1 ms, however, deactivation for α1β3γ2L receptors remains relatively stable, while deactivation for α4β3γ2L receptors continues to accelerate. E) Due to the combination of accelerated deactivation and heightened sensitivity of peak current amplitudes to pulses < 1 ms, the charge transfer of α4β3γ2L receptors are more sensitive than α1β3γ2L receptor to changes in synaptically relevant durations of GABA exposure. Furthermore, for pulses longer than 1 ms, conditions analogous to bursts of high frequency neurotransmitter release, charge transfer is relatively stable for α4β3γ2L receptors while charge transfer continues to increase for α1β3γ2L receptors.

synapses. During extremely brief (100 μs) GABA applications, the peak currents of both α1β3γ2L and α4β3γ2L currents were truncated, but this effect was more pronounced for α4β3γ2L currents (Figure 7A and 7B), reflecting the slower rise time of this isoform (data not shown). As GABA durations were prolonged within the synaptically relevant range (0.1–1.0 ms), there was a gradual increase in peak currents for both isoforms, although the α4β3γ2L receptor required longer GABA applications to reach its maximal peak current (Figure 7C). The rate of deactivation after an extremely brief (100 μs) GABA application was similar for α1β3γ2L and α4β3γ2L currents (Figure 7D). However, the deactivation rate of α4β3γ2L currents became progressively prolonged with longer GABA exposures while deactivation of α1β3γ2L currents was relatively constant following synaptically relevant applications of GABA and only became progressively prolonged after GABA exposures longer than 1 ms. Because charge transfer after a single synaptic event depends on both peak current and the time course of deactivation, inhibition mediated by α1β3γ2L currents depended linearly on the duration of GABA

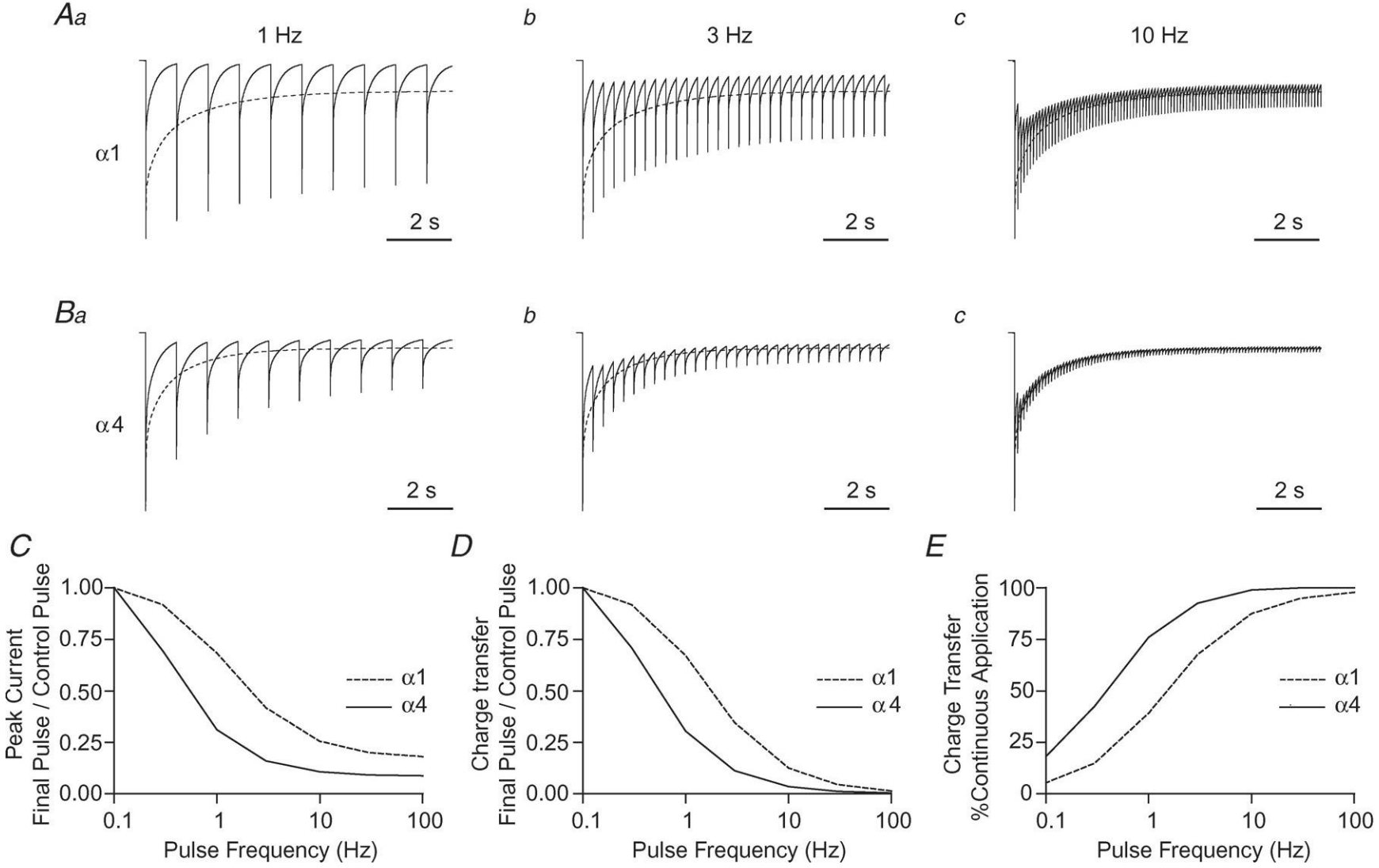
Aa
1 Hz
α1
2 s
b
3 Hz
2 s
c
10 Hz
2 s
Ba
α4
2 s
b
2 s
c
2 s
C
Peak Current
Final Pulse / Control Pulse
1.00
0.75
0.50
0.25
0.00
0.1
1
10
100
Pulse Frequency (Hz)
α1
α4
D
Charge transfer
Final Pulse / Control Pulse
1.00
0.75
0.50
0.25
0.00
0.1
1
10
100
Pulse Frequency (Hz)
α1
α4
E
Charge Transfer
%Continuous Application
100
75
50
25
0
0.1
1
10
100
Pulse Frequency (Hz)
α1
α4

Figure 8. α4β3γ2L and α1β3γ2L receptors respond to different frequencies of stimulation during repetitive GABA exposure.

A, B) using the kinetic models for the α1β3γ2L and α4β3γ2L receptors, simulations of pulse trains were performed to evaluate the response of these isoforms to repetitive stimulation. 1 ms square pulses of 1 mM GABA were applied at the indicated frequencies for 10 sec. For comparison, the responses are superimposed on the response to a continuous application of 1 mM GABA (dashed line). Note that the shape of the response to repeated stimulation for both receptor isoforms begins to approach that of the continuous application at higher frequencies. C) the peak current of the final pulse in the pulse train is compared to a control 1 mM pulse. Although the peak response of both isoforms is attenuated with high frequency stimulation, α4β3γ2L peak currents are more sensitive than α1β3γ2L peak currents. D) charge transfer of the final pulse in the pulse train is compared to a control 1 mM pulse. As with peak currents, the charge transfer following a GABA pulse applied to α4β3γ2L receptors is more sensitive to high frequency stimulation than the charge transfer of α1β3γ2L receptors. E) the total charge transfer of the 10 sec pulse train is compared at each frequency to the total charge transfer of a continuous GABA application. Compared to α1β3γ2L receptors, α4β3γ2L receptors approach maximal charge transfer at much lower frequencies. Indeed, the entire frequency-response curve is shifted to the left for α4 containing receptors, suggesting that these receptors may act as low-pass filters compared to α1 containing receptors.

application. In contrast, since both peak current and deactivation time course of α4β3γ2L currents were very sensitive to the duration of GABA, the overall charge transfer was strongly shaped by small changes in the duration of synaptically relevant (< 1 ms) GABA (Figure 7E).

α4β3γ2L and α1β3γ2L $GABA_A$ receptors were predicted to respond differently to changes in the frequency of neuronal firing

As a next step toward understanding the potential role of α1 *versus* α4 subtype containing receptors in synaptic physiology, we used the models to predict the responses of these receptors to repetitive, brief applications of GABA (1 ms, 1 mM) (Figure 8A and 8B). The responses of α1β3γ2L and α4β3γ2L receptors to repetitive exposure of brief pulses of GABA were associated with a progressively diminished peak current (Figure

8C) and charge transfer per pulse (Figure 8D), thereby limiting the overall charge transfer that occurred during a long barrage of inhibitory synaptic input, as might occur during a seizure. The overall charge transfer of both α1β3γ2L and α4β3γ2L currents exhibited a steep dependence on stimulus frequency, but α4β3γ2L currents were attenuated by repetitive stimulation at lower frequencies than α1β3γ2L currents (Figure 8E). Similar results were obtained by modeling repetitive 100 μs pulses of GABA (data not shown). Thus, assuming equal receptor densities and similar peak current open probabilities, synapses with α4 subtype-containing receptors would have a stronger inhibitory drive at low stimulus frequencies than those with α1 subtype-containing receptors given their longer deactivation time course. However, α4 subtype containing synapses would also be expected to respond to a narrower range of IPSC frequencies compared to α1 subtype-containing synapses.

α4β3γ2L and α1β3γ2L $GABA_A$ receptors were predicted to respond differently to changes in the levels of ambient GABA

In normal animals, α4 subtype-containing receptors occupy a primarily perisynaptic position on hippocampal dentate granule cells. These receptors would be expected to respond to synaptic overflow of GABA, which may be largely influenced by changes in GABA reuptake. There is also evidence for synaptic crosstalk among synapses that appears to involve overflow from one synapse to another (Overstreet & Westbrook, 2003). Furthermore, there are complex changes in the expression of GABA transporters associated with epilepsy (Dalby, 2003) with the potential to modify the basal GABA levels in both the synaptic and extrasynaptic spaces. We therefore sought to

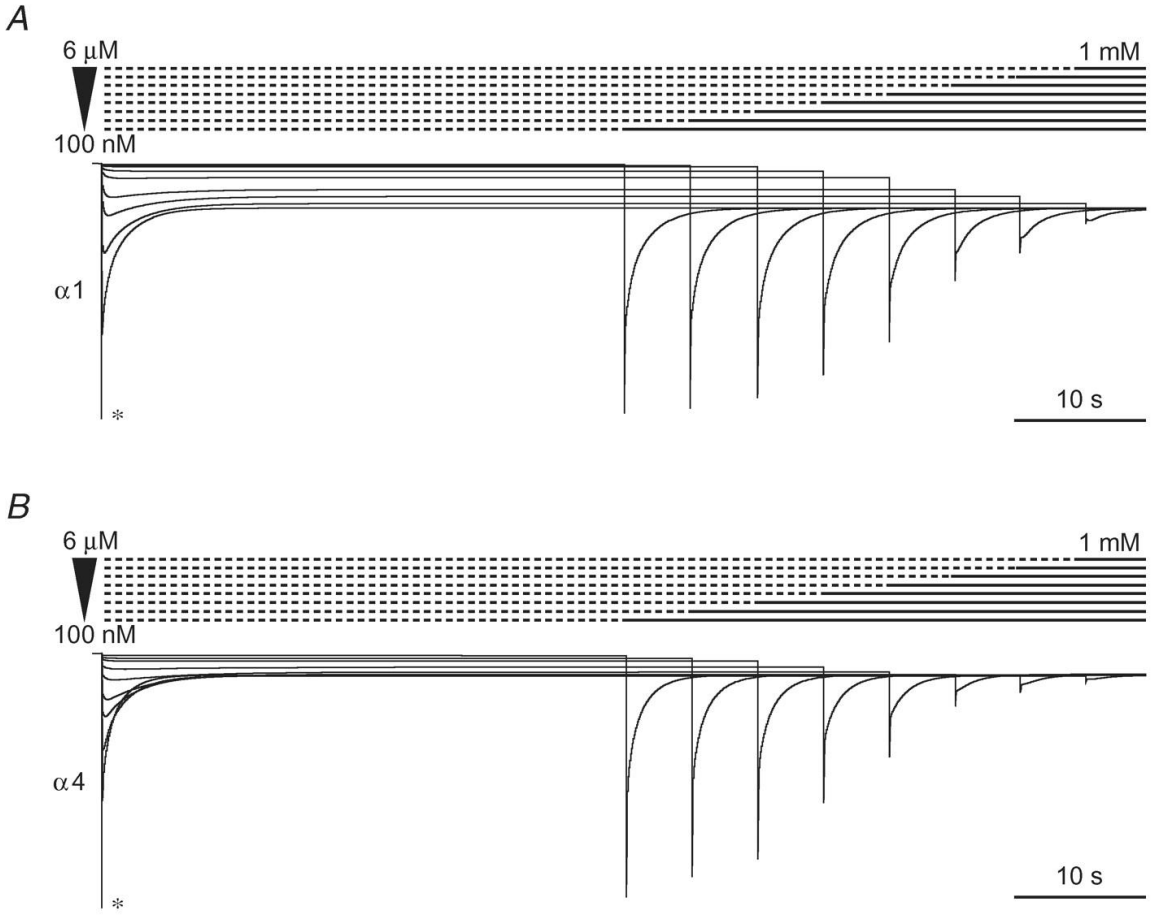
A
6 µM
1 mM
100 nM
α1
10 s
B
6 µM
1 mM
100 nM
α4
10 s

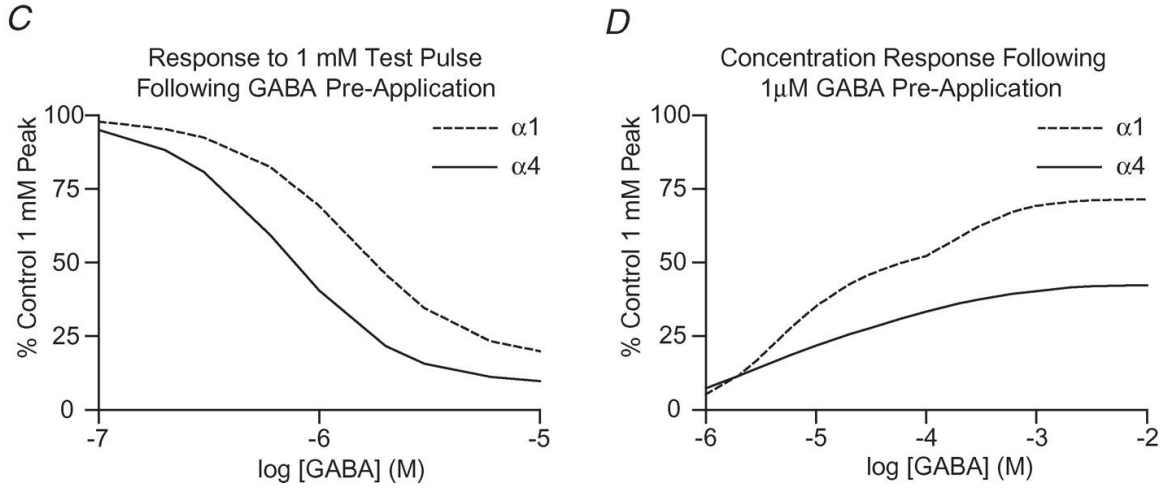
C
Response to 1 mM Test Pulse
Following GABA Pre-Application
α1
α4
% Control 1 mM Peak
100
75
50
25
0
-7
-6
-5
log [GABA] (M)
D
Concentration Response Following
1µM GABA Pre-Application
α1
α4
% Control 1 mM Peak
100
75
50
25
0
-6
-5
-4
-3
-2
log [GABA] (M)

Figure 9. α4β3γ2L receptors are more inhibited than α1β3γ2L receptors during prolonged exposure to low levels of GABA.

A) low concentrations of GABA (dashed lines) ranging from 100 nM to 6 μM (100 nM, 200 nM, 300 nM, 600 nM, 1 μM, 2 μM, 3 μM, and 6 μM) were applied to the α1β3γ2L kinetic model for a minimum of 40 sec prior to being exchanged for 1 mM GABA for the remainder of the 80 sec trace (solid lines). The length of the pre-applications was varied for illustrative purposes only, and does not affect the results (equilibrium occupancy is reached by all states in the kinetic model before the earliest time point). The control 1 mM pulse is indicated with an asterisk. B) simulations were performed as in A, except using the α4β3γ2L kinetic model. C) peak currents evoked by 1 mM GABA following pre-application with various GABA concentrations are compared to the control 1 mM GABA application. Following all pre-applied concentrations of GABA, α4β3γ2L receptor peak current responses to 1 mM GABA were more attenuated compared to those from α1β3γ2L receptors. D) after pre-application with 1 μM GABA, receptors were switched into various concentrations of GABA. The resulting peak currents were compared to peak currents evoked by a control 1 mM application. At all but the lowest GABA concentrations, α4β3γ2L receptors responded more weakly compared to α1β3γ2L receptors.

explore how these receptors responded following exposure to low levels of GABA. We first used the model to predict the response to a synaptically relevant GABA concentration (1 mM) following prior exposure to low GABA concentrations. Exposure to low levels of tonic GABA greatly attenuated the response to 1 mM GABA (Figure 9). For illustrative purposes, the duration of low GABA concentrations was varied to offset the subsequent responses to 1 mM GABA; identical results were obtained with a single fixed duration of low GABA. The responses of α4β3γ2L receptors were particularly sensitive to attenuation during application of very low concentrations of GABA (Figure 9C). Alternatively, perisynaptic and extrasynaptic GABA receptors may be constantly bathed in low levels of GABA but still need to react to small changes in ambient GABA in response to changes in nearby neuronal activity. Consistent with our whole cell current data (not shown), prior exposure to a physiologically relevant low GABA concentration

(1 μM) strongly suppressed the response to higher concentrations of GABA, with this suppression being especially apparent for α4β3γ2L receptors.

DISCUSSION

The role of α4 subunit-containing receptor isoforms in normal and abnormal neuronal physiology

To date, the α4 subtype has been most extensively studied in the thalamus and hippocampus, where it assembles with δ subunits. The high GABA sensitivity of α4βδ receptors allows them to respond to the persistent low levels of GABA present in the extrasynaptic space, thereby conveying a long-lasting tonic current with the ability to powerfully modify neuronal excitability (Nusser & Mody, 2002; Jia *et al.* 2005; Cope *et al.* 2005). In contrast, the physiological significance of α4βγ $GABA_A$ receptors remains unclear. Based on immunoprecipitation studies and analysis of benzodiazepine-insensitive Ro 15-4513 binding of native brain receptors, α4βγ receptors appear to be at least as abundant as α4βδ receptors (Benke *et al.* 1997; Bencsits *et al.* 1999), suggesting they also contribute substantially to inhibitory tone.

Although the predominant γ subunit-containing isoform in the central nervous system is the α1β2γ2 isoform, the α4 subtype is relatively abundant in brain regions involved in both partial and generalized epilepsies, including cortex, hippocampus, and thalamus (Pirker *et al.* 2000). Furthermore, this subtype may be involved in both synaptic and extrasynaptic neurotransmission, depending on the brain region and physiological state of the animal (Hsu *et al.* 2003; Belelli *et al.* 2005; Cope *et al.* 2005). In addition, α4 subtype up-regulation has been consistently found in multiple models of temporal lobe epilepsy, and is correlated with up-regulation of γ2 subunit expression and down-regulation of δ subunit expression (Peng *et al.* 2004; Nishimura *et al.* 2005). However, it

is unclear whether α4 subtype up-regulation contributes to the generation of seizures or, alternatively, is a compensatory response to the hyperexcitable state.

As a first step towards elucidating the role of α4βγ $GABA_A$ receptors in both normal and abnormal physiology, we used a variety of GABA application protocols to perform a direct comparison of the kinetic properties of recombinant α4β3γ2L and α1β3γ2L receptors. We found that α4β3γ2L currents deactivated more slowly than α1β3γ2L currents, a kinetic change predicted to increase synaptic charge transfer, and consequently, enhance GABAergic inhibition in the normal physiological state. However, α4β3γ2L receptors desensitized more rapidly and extensively, had slower recovery from desensitization, had greater loss of peak current amplitude in response to repetitive stimulation, and had more suppressed responses following exposure to low GABA concentrations. These findings argue against a compensatory role for the α4β3γ2L receptor isoform during seizures, as this constellation of kinetic changes would be predicted to substantially reduce the magnitude of GABAergic inhibition, which would promote neuronal hyperexcitability. Instead, the results raise the intriguing possibility that increasing α4β3γ2L receptor isoform expression may actually be involved in the pathogenesis of epilepsy.

The kinetic basis for the different macroscopic current properties of α4β3γ2L and α1β3γ2L $GABA_A$ receptors

While the structural basis for the altered kinetic properties is currently unknown, it is of interest that the single channel properties of α4βγ receptors (Akk *et al.* 2004) are similar to those of α1βγ receptors (Fisher & Macdonald, 1997; Steinbach & Akk, 2001), suggesting that the microscopic kinetic processes underlying activation of these two

isoforms are analogous. This suggests that, following agonist binding, α4βγ receptors also gain access to multiple open and closed states, many of which are long-lived. Progressive accumulation of receptors into long-lived non-conducting states, referred to as desensitized states, gives rise to the phenomenon of macroscopic desensitization (Jones & Westbrook, 1995; Haas & Macdonald, 1999). Since these states cannot release bound GABA (Bianchi & Macdonald, 2001*a*), receptors must transition though multiple intermediate closed and open GABA-bound states in order to unbind GABA, the macroscopic correlate of which is prolonged deactivation (Jones & Westbrook, 1995; Haas & Macdonald, 1999). Thus, one parsimonious interpretation of our results is that α4β3γ2L receptors have an increased steady-state occupancy of desensitized states, which would explain both the increase in the extent of macroscopic desensitization and the prolongation of deactivation observed with α4β3γ2L currents (i.e., desensitization-deactivation coupling; Bianchi *et al.* 2007). Consistent with this hypothesis, our modeling studies suggested that α4β3γ2L receptors accessed desensitized states with higher stability (defined as the ratio of the entry rate (δ) to the exit rate (ρ)) compared to those of α1β3γ2L receptors. Indeed, the combined stabilities of the D_2 and D_3 states (note that D_1 is only relevant at sub-saturating GABA concentrations) were much higher in the α4β3γ2L receptor kinetic model, and consequently, were associated with lower equilibrium occupancies of open states (i.e., less residual current; data not shown).

It should be emphasized, however, that occupancy of desensitized states does not necessarily correlate with either the rate or extent of macroscopic desensitization (Bianchi *et al*. 2007). Desensitization is highly sensitive to the entry and exit rates from all states in the gating scheme, including open states. In fact, high occupancy

desensitized states can, depending on the rate constants and state connectivity, support non-desensitizing macroscopic currents. For example, kinetic schemes whose desensitized states are in "branched" arrangement with the open states (as is the case for the kinetic models proposed here) can only desensitize when the exit rate from the open state is larger than the exit rate from the desensitized state, with more desensitization being observed as the ratio of these two rates increases (Bianchi *et al*. 2007; Appendix IV). Thus, from a kinetic standpoint, the enhanced macroscopic desensitization observed for α4β3γ2L receptors cannot simply be attributed to enhanced D state stability. Instead, it is more likely that one of the branched arrangements embedded within the comprehensive model contains O and D states with highly disparate exit rates (or, at least, more disparate than those found in the α1β3γ2L receptor model). Consistent with this prediction, while the highest occupancy open state (O_2) had a similar exit rate in both α1β3γ2L and α4β3γ2L receptor models, its partnering desensitized state (D_2) had an order of magnitude lower exit rate in the α4β3γ2L receptor model.

α4β3γ2L receptors as synaptic $GABA_A$ receptors

Since high concentrations of GABA are thought to exist in the synaptic cleft for only very brief periods of time (< 1 ms), effective synaptic $GABA_A$ receptors should activate very quickly and deactivate slowly. Within individual synapses, however, there is significant variability in the peak amplitude and duration of IPSCs that appears to be due to fluctuations in both peak GABA concentration and duration (Nusser *et al.* 2001; Mozrzymas, 2004). Similar to native receptors, the activation rates reported here were quite dependent on GABA concentrations (Maconochie *et al.* 1994) and were consistently

slower for α4β3γ2L receptors during all but the highest GABA concentrations. Therefore, while the concentration time course of synaptic GABA may contribute to the shape of postsynaptic responses, our results suggest it may do so differently in α1β3γ2L and α4β3γ2L receptor-containing synapses. While multiple studies have found increased α4 subtype expression in epileptic animals (Schwarzer *et al.* 1997; Brooks-Kayal *et al.* 1998; Sperk *et al.* 1998), it is currently unclear whether this is associated with an increased number of α4 subtype-containing receptors that are actually within the synapses. One model of CNS hyperexcitability, chronic intermittent ethanol, produces animals with a lowered seizure threshold and an increased expression of α4 subunits in the hippocampus. In these animals, the subcellular localization of α4 subtype-containing receptors shifts from a primarily perisynaptic to a central synaptic location on dentate granule cells (Liang *et al.* 2006). If the same phenomenon proves true in epileptic animals, our results would predict that α4β3γ2L receptor-containing synapses would have attenuated peak currents during brief synaptic GABA. Our results also predict, however, that these responses would have prolonged decay times compared to α1β3γ2L currents, thus suggesting a possible compensatory role for up-regulation of α4 subtype-containing $GABA_A$ receptors. In the hippocampal dentate region of epileptic animals, there is a loss of interneurons and an associated reduction in IPSC frequency (Kobayashi & Buckmaster, 2003; Cohen *et al.* 2003; Naylor *et al.* 2005). The prolonged responses conveyed by α4 subtype-containing synapses may help to normalize the charge transfer over time. However, because of the observed coupling between desensitization and deactivation, α4βγ receptors are rendered relatively insensitive to prolonged repetitive stimulation, especially at frequencies above 2–5 Hz. Therefore, α4βγ receptors may serve

as low pass frequency filters, which respond best to brief low frequency barrages of synaptic activity, but poorly to high frequency bursts of synaptic input. Similar to our findings, studies using brain slices have shown prolonged IPSCs in dentate granule cells during status epilepticus or chronic epilepsy (Cohen *et al.* 2003; Shao & Dudek, 2005; Naylor *et al.* 2005). However it is unknown what role, if any, enhanced α4 subtype expression plays in altered inhibitory neurotransmission in epileptic rats. One of the few reports describing the physiological significance of increased α4 subtype expression used recordings from CA1 pyramidal neurons following neurosteroid withdrawal. Pharmacological characterization of the IPSCs and comparison with recombinant $GABA_A$ receptors suggest that synaptic α1βγ $GABA_A$ receptors may be replaced by α4βγ and/or α4βδ receptors (Hsu *et al.* 2003; Smith & Gong, 2005). Interestingly, in contrast to our studies, the IPSCs in neurosteroid withdrawn neurons are significantly shortened. This discrepancy may be related to several technical differences, but one likely explanation is that the different findings are due to differences in the β subtype. Work in other models of epilepsy have also found accelerated IPSC decay in CA1 pyramidal neurons (Mangan & Bertram, 1997; Morin *et al.* 1998), where the predominant β subtype is β2. However, the enhanced α4 subtype expression in epileptic animals is found in the dentate gyrus where the β3 subtype is highly expressed. Consistent with this, preliminary work has found that the deactivation of α4β2γ2L currents is very brief compared to α4β3γ2L currents (Lagrange & Macdonald, 2005). Thus, the physiological consequences of α4 subtype expression on synaptic transmission may be very different from region to region, depending on the other $GABA_A$ receptor subtypes that are available for assembly.

α4β3γ2L receptors as extrasynaptic $GABA_A$ receptors

In addition to brief IPSCs, many neurons also have a long-lasting 'tonic' current that is largely conveyed by extrasynaptic $GABA_A$ receptors in response to ambient low levels of GABA. Although this tonic current is small in amplitude, its long duration allows the transfer of substantial charge and may play an important role in regulating neuronal excitability (Mody, 2001). The GABAergic tonic current is most commonly mediated by αβδ and occasionally by α5βγ receptors (Nusser *et al.* 1998; Spigelman *et al.* 2003; Caraiscos *et al.* 2004; Cope *et al.* 2005; Belelli *et al.* 2005). Pharmacological experiments have suggested that α4βγ receptors may also convey part of the tonic current in some brain regions, and that the subcellular distribution of synaptic and extrasynaptic α1 and α4 subtypes may be altered in pathological conditions (Liang *et al.* 2004; Liang *et al.* 2006). We found that during prolonged GABA application both α1β3γ2L and α4β3γ2L receptors responded to a remarkably limited range of GABA concentrations, with a maximal response evoked by < 10 μM GABA. Therefore, small changes in GABA concentration (on the order of 1–2 μM) would have a relatively large effect on the current produced by extrasynaptic α1βγ or α4βγ receptors. However, persistent low levels of GABA renders $GABA_A$ receptors largely insensitive to higher GABA concentrations (Overstreet *et al.* 2000), an effect that is much more pronounced with the highly desensitizing α4βγ receptors. As such, it is conceivable that drug treatments that increase the levels of extrasynaptic GABA may differentially suppress the ability of extrasynaptic α4βγ receptors to respond to variations in ambient GABA that may occur during status epilepticus (Naylor *et al.* 2005).

Future directions in understanding the response of $GABA_A$ receptors to physiological contexts of activation

These studies used recombinant $GABA_A$ receptor proteins in an immortalized cell line to elucidate the kinetic properties of specific $GABA_A$ receptor subunit combinations. It is possible that modulatory factors, such as protein phosphorylation, neurosteroids, or anchoring proteins differentially alter the kinetics of one $GABA_A$ receptor isoform, but not another. Moreover, in some brain regions, a given $GABA_A$ receptor population may be composed of receptors containing multiple α or β subtypes within the same receptor (Fritschy *et al.* 1992; Mertens *et al.* 1993). For example, using immunoprecipitation it has been shown that α4 subtypes may exist in combination with α1, α2, or α3 subunits (Benke *et al.* 1997). The kinetic properties of $GABA_A$ receptors with a mixture of α subunits are currently unpredictable and will need to be specifically tested.

In summary, α4βγ $GABA_A$ receptors produce rapidly desensitizing and slowly deactivating currents. Based on these findings, disease states in which α1βγ receptors are replaced by α4βγ receptors would be expected to be associated with impaired inhibitory neurotransmission. These changes would alter both synaptic and extrasynaptic inhibition in a frequency and GABA concentration-dependent fashion. Since epilepsy is a network phenomenon, further experiments in brain slices will be needed to specifically test whether altered α4 subtype expression in epilepsy is actually associated with the changes in CNS neurotransmission predicted by these studies. Nonetheless, our results provide a basis for testable hypotheses about the role of altered synaptic and extrasynaptic inhibitory neurotransmission in epilepsy.

REFERENCES

Akk G, Bracamontes J & Steinbach JH (2004). Activation of $GABA_A$ receptors containing the α4 subunit by GABA and pentobarbital. *J Physiol* 556, 387–399.

Angelotti TP & Macdonald RL (1993). Assembly of $GABA_A$ receptor subunits: α1β1 and α1β1γ2S subunits produce unique ion channels with dissimilar single-channel properties. *J Neurosci* 13, 1429–1440.

Angelotti TP, Uhler MD & Macdonald RL (1993). Assembly of $GABA_A$ receptor subunits: analysis of transient single-cell expression utilizing a fluorescent substrate/marker gene technique. *J Neurosci* 13, 1418–1428.

Belelli D, Peden DR, Rosahl TW, Wafford KA & Lambert JJ (2005). Extrasynaptic $GABA_A$ receptors of thalamocortical neurons: a molecular target for hypnotics. *J Neurosci* 25, 11513–11520.

Bencsits E, Ebert V, Tretter V & Sieghart W (1999). A significant part of native γ-aminobutyric $acid_A$ receptors containing α4 subunits do not contain γor δ subunits. *J Biol Chem* 274, 19613–19616.

Benke D, Michel C & Mohler H (1997). $GABA_A$ receptors containing the α4-subunit. Prevalence, distribution, pharmacology, and subunit architecture in situ. *J Neurochem* 69, 806–814.

Bianchi MT & Macdonald RL (2001*a*). Agonist trapping by $GABA_A$ receptor channels. *J Neurosci* 21, 9083–9091.

Bianchi MT & Macdonald RL (2001*b*). Mutation of the 9' leucine in the $GABA_A$ receptor γ2L subunit produces an apparent decrease in desensitization by stabilizing open states without altering desensitized states. *Neuropharmacology* 41, 737–744.

Bianchi MT & Macdonald RL (2002). Slow phases of $GABA_A$ receptor desensitization: structural determinants and possible relevance for synaptic function. *J Physiol* 544, 3–18.

Bianchi MT, Botzolakis EJ, Haas KF, Fisher J & Macdonald RL (2007). Microscopic kinetic determinants of macroscopic currents: insights from coupling and uncoupling of $GABA_A$ receptor desensitization and deactivation. *J Physiol* 584, 769-787.

Brooks-Kayal AR, Shumate MD, Jin H, Rikhter TY & Coulter DA (1998). Selective changes in single cell $GABA_A$ receptor subunit expression and function in temporal lobe epilepsy. *Nat Med* 4, 1166–1172.

Caraiscos VB, Elliott EM, You T, Cheng VY, Belelli D, Newell JG, Jackson MF, Lambert JJ, Rosahl TW, Wafford KA, MacDonald JF & Orser BA (2004). Tonic inhibition in mouse hippocampal CA1 pyramidal neurons is mediated by α5 subunit-containing γ-aminobutyric acid type A receptors. *Proc Natl Acad Sci U S A* 101, 3662–3667.

Chang Y, Wang R, Barot S & Weiss DS (1996). Stoichiometry of a recombinant $GABA_A$ receptor. *J Neurosci* 16, 5415–5424.

Cohen AS, Lin DD, Quirk GL & Coulter DA (2003). Dentate granule cell $GABA_A$ receptors in epileptic hippocampus: enhanced synaptic efficacy and altered pharmacology. *Eur J Neurosci* 17, 1607–1616.

Cope DW, Hughes SW & Crunelli V (2005). $GABA_A$ receptor-mediated tonic inhibition in thalamic neurons. *J Neurosci* 25, 11553–11563.

Dalby NO (2003). Inhibition of γ-aminobutyric acid uptake: anatomy, physiology and effects against epileptic seizures. *Eur J Pharmacol* 479, 127–137.

Davies PA, Hoffmann EB, Carlisle HJ, Tyndale RF & Hales TG (2000). The influence of an endogenous β3 subunit on recombinant $GABA_A$ receptor assembly and pharmacology in WSS-1 cells and transiently transfected HEK293 cells. *Neuropharmacology* 39, 611–620.

Draguhn A, Verdorn TA, Ewert M, Seeburg PH & Sakmann B (1990). Functional and molecular distinction between recombinant rat $GABA_A$ receptor subtypes by Zn^{2+}. *Neuron* 5, 781–788.

Farrar SJ, Whiting PJ, Bonnert TP & McKernan RM (1999). Stoichiometry of a ligand-gated ion channel determined by fluorescence energy transfer. *J Biol Chem* 274, 10100–10104.

Fisher JL & Macdonald RL (1997). Single channel properties of recombinant $GABA_A$ receptors containing γ2 or δsubtypes expressed with α1 and β3 subtypes in mouse L929 cells. *J Physiol* 505, 283–297.

Fritschy JM, Benke D, Mertens S, Oertel WH, Bachi T & Mohler H (1992). Five subtypes of type A γ-aminobutyric acid receptors identified in neurons by double and triple immunofluorescence staining with subunit-specific antibodies. *Proc Natl Acad Sci U S A* 89, 6726–6730.

Greenfield LJ Jr, Sun F, Neelands TR, Burgard EC, Donnelly JL & Macdonald RL (1997). Expression of functional $GABA_A$ receptors in transfected L929 cells isolated by immunomagnetic bead separation. *Neuropharmacology* 36, 63–73.

Haas KF & Macdonald RL (1999). $GABA_A$ receptor subunit γ2 and δsubtypes confer unique kinetic properties on recombinant $GABA_A$ receptor currents in mouse fibroblasts. *J Physiol* 514, 27–45.

Hsu FC, Waldeck R, Faber DS & Smith SS (2003). Neurosteroid effects on GABAergic synaptic plasticity in hippocampus. *J Neurophysiol* 89, 1929–1940.

Jia F, Pignataro L, Schofield CM, Yue M, Harrison NL & Goldstein PA (2005). An extrasynaptic $GABA_A$ receptor mediates tonic inhibition in thalamic VB neurons. *J Neurophysiol* 94, 4491–4501.

Jones MV & Westbrook GL (1995). Desensitized states prolong $GABA_A$ channel responses to brief agonist pulses. *Neuron* 15, 181–191.

Kirkness EF & Fraser CM (1993). A strong promoter element is located between alternative exons of a gene encoding the human γ-aminobutyric acid-type A receptor β3 subunit (GABRB3). *J Biol Chem* 268, 4420–4428.

Kobayashi M & Buckmaster PS (2003). Reduced inhibition of dentate granule cells in a model of temporal lobe epilepsy. *J Neurosci* 23, 2440–2452.

Lagrange AH & Macdonald RL (2005). Enhanced desensitization in α-4 containing $GABA_A$ receptors. *Epilepsia* 46 (Suppl 8), 113.

Liang J, Cagetti E, Olsen RW & Spigelman I (2004). Altered pharmacology of synaptic and extrasynaptic $GABA_A$ receptors on CA1 hippocampal neurons is consistent with subunit changes in a model of alcohol withdrawal and dependence. *J Pharmacol Exp Ther* 310, 1234–1245.

Liang J, Zhang N, Cagetti E, Houser CR, Olsen RW & Spigelman I (2006). Chronic intermittent ethanol-induced switch of ethanol actions from extrasynaptic to synaptic hippocampal $GABA_A$ receptors. *J Neurosci* 26, 1749–1758.

Macdonald RL, Rogers CJ & Twyman RE (1989). Kinetic properties of the $GABA_A$ receptor main conductance state of mouse spinal cord neurones in culture. *J Physiol* 410, 479–499.

Maconochie DJ, Zempel JM & Steinbach JH (1994). How quickly can $GABA_A$ receptors open? *Neuron* 12, 61–71.

Mangan PS & Bertram EH III (1997). Shortened-duration $GABA_A$ receptor-mediated synaptic potentials underlie enhanced CA1 excitability in a chronic model of temporal lobe epilepsy. *Neuroscience* 80, 1101–1111.

Mangan PS, Sun C, Carpenter M, Goodkin HP, Sieghart W & Kapur J (2005). Cultured hippocampal pyramidal neurons express two kinds of $GABA_A$ receptors. *Mol Pharmacol* 67, 775–788.

Mertens S, Benke D & Mohler H (1993). $GABA_A$ receptor populations with novel subunit combinations and drug binding profiles identified in brain by α5- and δ-subunit-specific immunopurification. *J Biol Chem* 268, 5965–5973.

Mody I (2001). Distinguishing between $GABA_A$ receptors responsible for tonic and phasic conductances. *Neurochem Res* 26, 907–913.

Morin F, Beaulieu C & Lacaille JC (1998). Cell-specific alterations in synaptic properties of hippocampal CA1 interneurons after kainate treatment. *J Neurophysiol* 80, 2836–2847.

Mozrzymas JW (2004). Dynamism of $GABA_A$ receptor activation shapes the 'personality' of inhibitory synapses. *Neuropharmacology* 47, 945–960.

Mozrzymas JW, Barberis A, Mercik K & Zarnowska ED (2003). Binding sites, singly bound states, and conformation coupling shape GABA-evoked currents. *J Neurophysiol* 89, 871–883.

Naylor DE, Liu H & Wasterlain CG (2005). Trafficking of $GABA_A$ receptors, loss of inhibition, and a mechanism for pharmacoresistance in status epilepticus. *J Neurosci* 25, 7724–7733.

Nishimura T, Schwarzer C, Gasser E, Kato N, Vezzani A & Sperk G (2005). Altered expression of $GABA_A$ and $GABA_B$ receptor subunit mRNAs in the hippocampus after kindling and electrically induced status epilepticus. *Neuroscience* 134, 691–704.

Nusser Z & Mody I (2002). Selective modulation of tonic and phasic inhibitions in dentate gyrus granule cells. *J Neurophysiol* 87, 2624–2628.

Nusser Z, Naylor D & Mody I (2001). Synapse-specific contribution of the variation of transmitter concentration to the decay of inhibitory postsynaptic currents. *Biophys J* 80, 1251–1261.

Nusser Z, Sieghart W & Somogyi P (1998). Segregation of different $GABA_A$ receptors to synaptic and extrasynaptic membranes of cerebellar granule cells. *J Neurosci* 18, 1693–1703.

Overstreet LS, Jones MV & Westbrook GL (2000). Slow desensitization regulates the availability of synaptic $GABA_A$ receptors. *J Neurosci* 20, 7914–7921.

Overstreet LS & Westbrook GL (2003). Synapse density regulates independence at unitary inhibitory synapses. *J Neurosci* 23, 2618–2626.

Peng Z, Huang CS, Stell BM, Mody I & Houser CR (2004). Altered expression of the δ subunit of the $GABA_A$ receptor in a mouse model of temporal lobe epilepsy. *J Neurosci* 24, 8629–8639.

Pirker S, Schwarzer C, Wieselthaler A, Sieghart W & Sperk G (2000). $GABA_A$ receptors: immunocytochemical distribution of 13 subunits in the adult rat brain. *Neuroscience* 101, 815–850.

Schwarzer C, Tsunashima K, Wanzenbock C, Fuchs K, Sieghart W & Sperk G (1997). $GABA_A$ receptor subunits in the rat hippocampus II: altered distribution in kainic acid-induced temporal lobe epilepsy. *Neuroscience* 80, 1001–1017.

Shao LR & Dudek FE (2005). Changes in mIPSCs and sIPSCs after kainate treatment: evidence for loss of inhibitory input to dentate granule cells and possible compensatory responses. *J Neurophysiol* 94, 952–960.

Smith SS & Gong QH (2005). Neurosteroid administration and withdrawal alter $GABA_A$ receptor kinetics in CA1 hippocampus of female rats. *J Physiol* 564, 421–436.

Sperk G, Schwarzer C, Tsunashima K & Kandlhofer S (1998). Expression of $GABA_A$ receptor subunits in the hippocampus of the rat after kainic acid-induced seizures. *Epilepsy Res* 32, 129–139.

Spigelman I, Li Z, Liang J, Cagetti E, Samzadeh S, Mihalek RM, Homanics GE & Olsen RW (2003). Reduced inhibition and sensitivity to neurosteroids in hippocampus of mice lacking the $GABA_A$ receptor δsubunit. *J Neurophysiol* 90, 903–910.

Steinbach JH & Akk G (2001). Modulation of $GABA_A$ receptor channel gating by pentobarbital. *J Physiol* 537, 715–733.

Tretter V, Ehya N, Fuchs K & Sieghart W (1997). Stoichiometry and assembly of a recombinant $GABA_A$ receptor subtype. *J Neurosci* 17, 2728–2737.

Twyman RE, Rogers CJ & Macdonald RL (1990). Intraburst kinetic properties of the $GABA_A$ receptor main conductance state of mouse spinal cord neurones in culture. *J Physiol* 423, 193–220.

Verdoorn TA, Draguhn A, Ymer S, Seeburg PH & Sakmann B (1990). Functional properties of recombinant rat $GABA_A$ receptors depend upon subunit composition. *Neuron* 4, 919–928.

Wagner DA, Czajkowski C & Jones MV (2004). An arginine involved in GABA binding and unbinding but not gating of the $GABA_A$ receptor. *J Neurosci* 24, 2733–2741.

Wallner M, Hanchar HJ & Olsen RW (2003). Ethanol enhances $\alpha 4\beta 3\delta$ and $\alpha 6\beta 3\delta$ γ-aminobutyric acid type A receptors at low concentrations known to affect humans. *Proc Natl Acad Sci U S A* 100, 15218–15223.

Zezula J, Slany A & Sieghart W (1996). Interaction of allosteric ligands with $GABA_A$ receptors containing one, two, or three different subunits. *Eur J Pharmacol* 301, 207–214.

CHAPTER VI

ACHIEVING SYNAPTICALLY RELEVANT PULSES OF NEUROTRANSMITTER USING PDMS MICROFLUIDICS

Emmanuel J. Botzolakis, Ankit Maheshwari, Hua-Jun Feng, Andre H. Lagrange, Jesse H. Shaver, Nicholas J. Kassebaum, Raghav Venkataraman, Franz J. Baudenbacher, and Robert L. Macdonald

ABSTRACT

Fast synaptic transmission is mediated by post-synaptic ligand-gated ion channels (LGICs) transiently activated by neurotransmitter released from pre-synaptic vesicles. Although disruption of synaptic transmission has long been implicated in numerous Neurological and Psychiatric disorders, effective and practical methods for studying LGICs *in vitro* under synaptically relevant conditions remain unavailable. Here, we describe a novel microfluidic approach to solution-switching that allows for precise temporal control over the neurotransmitter transient while substantially increasing experimental throughput, flexibility, reproducibility, and cost-effectiveness. When this system was used to apply ultra-brief (~400 μs) GABA pulses to recombinant $GABA_A$ receptors, members of the Cys-loop family of LGICs, the resulting currents resembled hippocampal inhibitory post-synaptic currents and differed from currents evoked by longer, conventional pulses, illustrating the importance of evaluating LGICs on a synaptic timescale. This methodology should therefore allow the effects of disease-causing mutations and allosteric modulators to be evaluated *in vitro* under physiologically relevant conditions.

INTRODUCTION

Ligand-gated ion channels (LGICs) mediate fast synaptic transmission in the central and peripheral nervous systems. They are targeted by numerous clinically important drugs and have been implicated in a variety of Neurological and Psychiatric disorders (Kullmann and Hanna, 2002; Macdonald et al., 2004; Vincent et al., 2006). However, despite decades of research, effective and practical methods for studying LGICs *in vitro* under physiologically relevant conditions remain unavailable (Mozrzymas, 2008), largely reflecting the short timescale on which synaptic transmission occurs. Increasing evidence suggests that neurotransmitter levels in the synaptic cleft rise extremely rapidly following release from pre-synaptic vesicles, only to be cleared after hundreds of microseconds by a combination of diffusion, reuptake, and for some neurotransmitters, enzymatic hydrolysis (Holmes, 1995; Clements, 1996; Glavinovic, 1999; Ventriglia and Di, V, 2003). Mimicking the synaptic transient in the experimental setting thus requires not only that neurotransmitter be applied rapidly, but also that it be applied briefly.

Failure to activate LGICs under synaptically relevant conditions, however, can cause the effects of disease-causing mutations and potential therapeutic compounds to be obscured or even missed entirely (Mozrzymas et al., 2007). Indeed, LGIC currents are known to be exquisitely sensitive to both the rate and duration of neurotransmitter exposure. For example, because most LGICs activate in the millisecond time domain before undergoing rapid and extensive desensitization, slowly changing the concentration of neurotransmitter can lead to underestimation of current amplitudes (Jones and Westbrook, 1996; Bianchi and Macdonald, 2002). Conversely, prolonged

neurotransmitter applications can lead to overestimation of current amplitudes, particularly when intrinsic current rise times are much longer than the synaptic transient (Mozrzymas, 2004; Lagrange et al., 2007; Rula et al., 2008). Prolonged applications can also artificially prolong deactivation (the process by which currents return to baseline), the result of receptor accumulation in long-lived "desensitized" states from which neurotransmitter cannot directly unbind (Jones and Westbrook, 1995; Lagrange et al., 2007; Rula et al., 2008).

Currently, solution switching has proven the most effective technique for generating brief neurotransmitter pulses (Franke et al., 1987; Jonas, 1995; Clements, 1997; Hinkle et al., 2003). In contrast to photoactivation of "caged" neurotransmitter (Niu et al., 1996), this method does not require use of expensive reagents or radiation sources, is not constrained by the existing library of photoactivatable compounds, and most importantly, provides better control over the rate of neurotransmitter application and washout. Solution switching is typically accomplished by reversibly translating parallel control and neurotransmitter-containing solution streams generated from an array of glass capillary tubing across stationary cells or excised membrane patches. This approach allows neurotransmitter to be applied extremely rapidly to experimental preparations, with solution exchange times less than 100 μs having been reported (Mozrzymas et al., 2007). Terminating the neurotransmitter pulse after synaptically relevant durations (i.e., 300-600 μs), however, has yet to be performed reliably (Jonas, 1995; Clements, 1997; Hinkle et al., 2003; Mozrzymas et al., 2007; Mozrzymas, 2008).

To study LGICs under physiologically relevant conditions, we took a microfluidic approach to solution switching. In contrast to existing systems, we fabricated drug

application devices from polydimethylsiloxane (PDMS), an inexpensive, durable, and biocompatible polymer, using photolithography and replica molding. This allowed for the miniaturization and customization of device features, which dramatically reduced the width of individual channels and their septa while increasing experimental flexibility and throughput. By translating ultra-thin fluid streams generated by these devices across stationary excised membrane patches with a stepper motor, solution exchange times as brief as ~100 μs and application durations as brief as ~400 μs were achieved reproducibly. When applied to recombinant $GABA_A$ receptors, members of the Cys-loop family of LGICs, these ultra-brief GABA pulses yielded currents with kinetic properties similar to those of hippocampal inhibitory post-synaptic currents (IPSCs) and different from currents evoked by conventional, longer pulses. We thus anticipate that this novel approach to solution switching will provide new insights into the role of different receptor isoforms, allosteric modulators, and disease-causing mutations in synaptic physiology.

MATERIALS AND METHODS

Fabrication of microfluidic device molds from SU-8 using photolithography

Device molds were fabricated in a class-100 clean room at the Vanderbilt Institute for Integrative Biosystems Research and Education at Vanderbilt University. SU-8 2050 (MicroChem, Newton, MA), a negative-tone photoepoxy, was dispensed onto a polished silicon wafer (mechanical grade) on a spinner. To uniformly coat the wafer, the rotational speed was ramped at 100 rpm/s to 500 rpm and held for 5 seconds. To achieve a final film thickness of 100 μm, the speed was then increased to 1750 rpm at 300 rpm/s and held for 30 seconds. Next, the coated wafer was soft baked for 5 minutes at 65°C and then for an additional 15 minutes at 95°C. The coated wafer was subsequently patterned with a customized chromium mask by contact photolithography using 230 mJ/cm^2 of UV radiation (Figure 1a). The patterned wafer was subjected to a post-exposure bake of 5 minutes at 65°C followed by 10 minutes at 95°C. The unexposed SU-8 was removed from the wafer by incubation in SU-8 Developer (MicroChem, Newton, MA) for 30 minutes, leaving behind an SU-8 complementary replica of the microfluidic device (Figure 1b). For prolonged stability, the resulting SU-8 mold was hard baked by temperature-ramping from 25°C to 200°C over 30 minutes and allowed to cool at room temperature overnight.

Fabrication of microfluidic devices from PDMS using replica molding

Microfluidic devices were fabricated from the SU-8 masters. Each device consisted of two layers of Sylgard 184 PDMS (Dow Corning Corp., Midland, MI), a

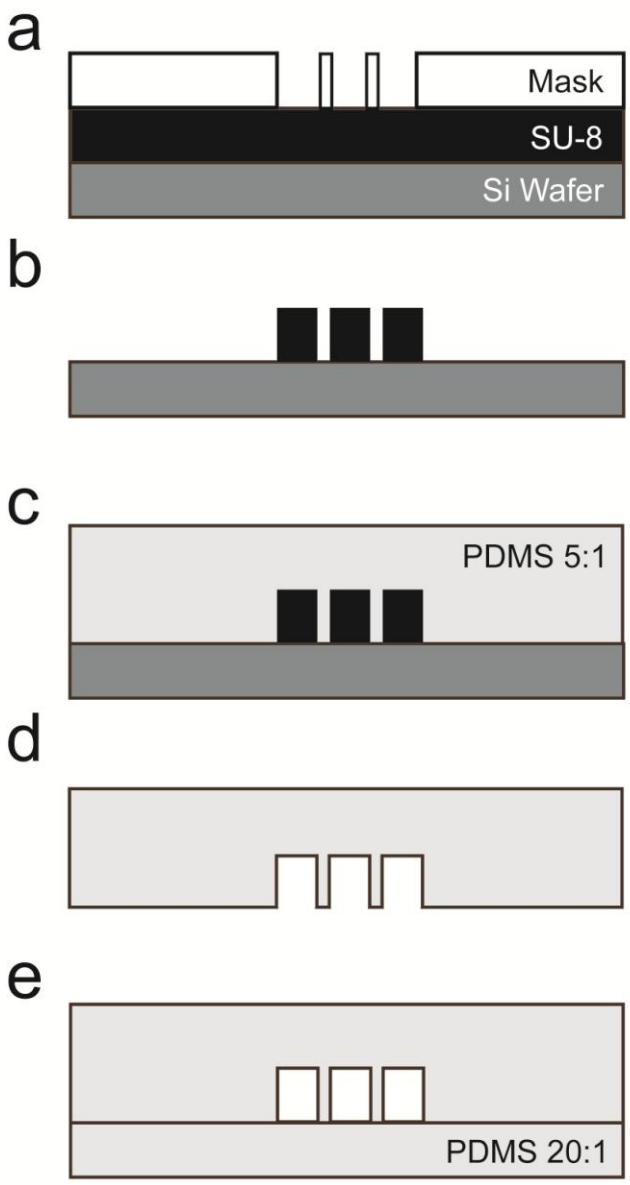

Figure 1. Overview of PDMS microfluidic device fabrication using photolithography and replica molding

a) The SU-8 photoepoxy is patterned with using the chrome mask by contact photolithography. b) Unexposed SU-8 photoepoxy is removed, leaving behind the device mold. c) PDMS is poured over the SU-8 mold to generate the "imprinted" layer. d) After baking, the imprinted layer is peeled away from the SU-8 mold. e) The imprinted layer of PDMS is bonded with an "unimprinted" layer to seal off the channels. Chrome mask, SU-8 photoepoxy, silicon wafer, and PDMS are indicated by the white, black, dark grey, and light grey layers, respectively. The pre-polymer to catalyst ratio is indicated within the PDMS layers.

silicone-based organic polymer widely used for microfluidic applications. Although PDMS is hydrophobic, unreactive to most reagents, non-toxic, and stable over a wide temperature range (McDonald and Whitesides, 2002; Mata et al., 2005), it should be noted that the hydrophobic nature of PDMS renders it incompatible with most organic solvents, which cause the material to swell. One PDMS layer was "imprinted" with a replica of the device design (i.e., the fluidic channels), and the other was left "unimprinted", serving as a cover for the fluidic channels. To generate the imprinted layer, PDMS was prepared with a 5:1 ratio of pre-polymer to catalyst and poured over the SU-8 molds to a thickness of 5 mm (Figure 1c). The PDMS was degassed in a vacuum chamber for 15-30 minutes and allowed to fully cure by incubation at 65°C for 4 hours. Once cured, the imprinted PDMS layer was peeled from the SU-8 molds (Figure 1d), and the circular solution input ports were cored using a blunt 18-gauge syringe needle. To generate the unimprinted layer, PDMS was prepared with a 20:1 ratio of pre-polymer to catalyst and poured to a final thickness of 2 mm in a 10 cm culture dish (Corning Glassworks). The unimprinted PDMS layer was also degassed in a vacuum chamber for 15-30 minutes, but allowed to only partially cure for 30-45 minutes at 65°. The imprinted layer was then placed on the unimprinted layer (Figure 1e), and the two were incubated at 65°C for 3 hours to fully cure and form a monolithic sealed device. Completed microfluidic devices were cut out using a surgical scalpel, and polyethylene tubing (Becton Dickinson, Sparks, MD) was connected to the solution input ports.

Cell culture and expression of recombinant $GABA_A$ receptors

Human $GABA_A$ receptor α1, β3, and γ2S subunits were individually sub-cloned into the pcDNA3.1+ mammalian expression vector (Invitrogen, Grand Island, NY). The coding region of each vector was sequenced by the Vanderbilt University Medical Center DNA Sequencing Facility and verified against published sequences (accession numbers NM_000806, NM_000814, and NM_000816 for the α1, β3, and γ2S subunits, respectively). HEK293T cells (American Type Culture Collection, Manassas, VA) were maintained at 37°C in humidified 5% CO_2 / 95% air using Dulbecco's Modified Eagle Medium (Invitrogen) supplemented with 10% fetal bovine serum (Invitrogen), 100 i.u./ml penicillin (Invitrogen), and 100 μg/ml streptomycin (Invitrogen). Cells were plated at a density of ~10^6 cells per 10 cm culture dish (Corning Glassworks, Corning, NY) and passaged every 2-4 days using trypsin-EDTA (Invitrogen). For electrophysiological recordings, cells were plated at a density of $4x10^5$ cells per 6 cm culture dish (Corning Glassworks) and transfected ~24 hours later with equal amounts (1 μg/subunit) of α1, β3, and γ2S subunit cDNA. One μg of pHook-1 cDNA (encoding the cell surface antibody sFv) was included so positively transfected cells could be selected 24 hours later by immunomagnetic bead separation. All transfections were performed using FuGene6 (Roche Diagnostics, Indianapolis, IN) per manufacturer recommendations. The day after transfection, cells were selected and re-plated at low density on collagen-coated 35 mm dishes for electrophysiological recording the next day.

Electrophysiology

Patch clamp recordings were performed at room temperature from excised outside-out membrane patches. Cells were maintained during recordings in a bath solution consisting of (in mM): 142 NaCl, 8 KCl, 6 $MgCl_2$, 1 $CaCl_2$, 10 glucose, and 10 HEPES (pH adjusted to 7.4; 325-330 mOsm). All chemicals used for solution preparation were purchased from Sigma-Aldrich (St. Louis, MO). Recording pipettes were pulled from thin-walled borosilicate capillary glass (Fisher, Pittsburgh, PA) on a Sutter P-2000 micropipette electrode puller (Sutter Instruments, San Rafael, CA) and fire polished with a microforge (Narishige, East Meadow, NY). When filled with a pipette solution consisting of (in mM) 153 KCl, 1 $MgCl_2$, 5 EGTA, 10 HEPES, and 2 MgATP (pH adjusted to 7.3; 300-310 mOsm) and submerged in the bath solution, this yielded open tip resistances of ~2 MΩ and a chloride equilibrium potential (E_{Cl}) of ~0 mV. Currents were recorded at a holding potential of -20 mV using an Axopatch 200A amplifier (Molecular Devices, Foster City, CA), low-pass filtered at 2 kHz (5 kHz for open-tip experiments) using a 4-Pole Bessel filter, digitized at 10 kHz (20 kHz for open-tip experiments) using the Digidata 1322A (Molecular Devices), and stored offline for analysis. All results shown are from a minimum of two days of experiments, each from a different batch of transfected cells. GABA was prepared as a stock solution. Working solutions were made on the day of the experiment by diluting stock solutions with the bath solution. All solutions were brought to room temperature prior to the experiments to minimize formation of bubbles in the microfluidic devices.

Data analysis

Current kinetic properties were analyzed using Clampfit 9 (Molecular Devices). Rise time was defined as the time required for currents to increase from 10% to 90% of their peak. The time course of deactivation was fit using the Levenberg-Marquardt least squares method to the form $\sum a_n e^{(-t/\tau_n)} + C$, where t is time, *n* is the number of components, *a* is the relative amplitude, τ is the time constant, and C is the fraction of current remaining, with $\sum a_n = 1$. Additional components were accepted only if they significantly improved the fit, as determined by an F-test automatically performed by the analysis software on the sum of squared residuals. Deactivation was typically biphasic, though as many as four components could be resolved with larger amplitude currents. To facilitate comparison, the time course of deactivation was summarized as a weighted time constant in the form $\sum a_n \tau_n$ with $\sum a_n = 1$. The time course of peak current decay during repetitive stimulation was also fit to a sum of exponential functions, though typically, only a single component was required. Solution exchange time was defined as the time for an open-tip liquid-junction current to increase from 10% to 90% of its maximum value. Pulse duration was defined as the time an open-tip liquid-junction current spent at ≥ 90% of its maximum value. Data were reported as mean ± SEM. A paired Student's *t* test (one-tailed) was performed to compare the responses of an individual excised patch to different experimental protocols. Statistical significance was taken as $p < 0.05$.

RESULTS

Custom microfluidic devices capable of generating synaptically relevant neurotransmitter pulses were fabricated from PDMS

Generating synaptic neurotransmitter pulses with conventional approaches to solution switching remains technically challenging, as most commercially available translators cannot reverse their motion to terminate the application (i.e., switch back to the control solution stream) after only hundreds of microseconds. High-velocity piezoelectric translators are currently used to overcome this limitation; however, they often suffer from resonant "ringing" after very brief excursions, which produces unwanted fluidic oscillations (Jonas, 1995; Clements, 1997; Mozrzymas et al., 2007); they require the use of high voltages, which requires electrical shielding to prevent additional noise contributions (Jonas, 1995; Clements, 1997; Heckmann and Pawlu, 2002); and they have a limited range of motion (typically 20-80 μm), which substantially limits the potential complexity of experimental protocols. Thus, if LGICs are to be studied *in vitro* under physiologically relevant conditions, an alternate approach is needed. One proposed method involves simultaneously delivering three, as opposed to two, parallel solution streams to the experimental preparation (Tang, 2001). Indeed, if only the central stream is loaded with neurotransmitter, then switching directly from the first to the third stream allows both application and washout of neurotransmitter to occur in a single motion. Ultra-brief pulses could therefore be generated simply by decreasing the width of the central solution stream. However, achieving solution channels less than ~100 μm wide is not practical with glass capillary tubing, as heating and pulling the glass

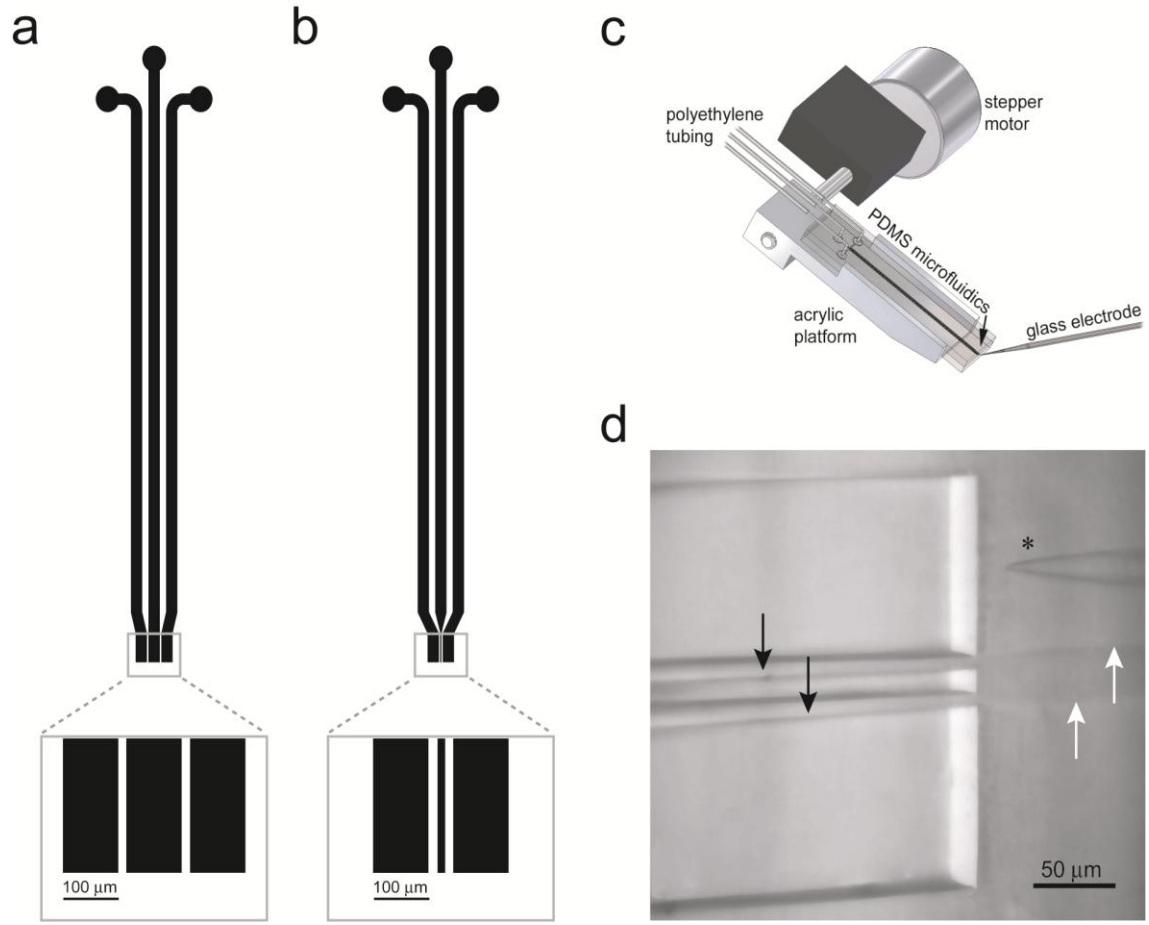

Figure 2. Microfluidic device design and integration for electrophysiological recording

a) Standard 3-channel design (length not to scale). Individual channels (black) are 100 µm wide and separated by 50 µm septa (white) that taper to a final thickness of 10 µm. The circular enlargements at the origin of each channel (top) permit solution access via polyethylene tubing. b) Modified 3-channel design for application of synaptically relevant agonist pulses. Dimensions are identical to those of the standard 3-channel device except for the width of the central channel, which tapers to a final width of 10 µm. c) Schematic of the experimental setup. PDMS devices were connected to a stepper motor via an acrylic platform, allowing for translation of parallel solution streams across a stationary recording electrode. d) Top-down view of a modified 3-channel microfluidic device (black arrows indicate device septa) and recording electrode (indicated by asterisk, *) submerged in bath solution, as typically arranged for electrophysiological recordings. Outer and central channels are shown delivering high and low osmolarity solution streams, respectively, allowing for visualization of solution interfaces (white arrows). Note that channels were ~80 µm high, though they appear smaller due to the image perspective.

to achieve the necessary dimensions is not only labor intensive, but also causes application devices to be inherently fragile and rarely reproducible.

To overcome this obstacle, custom microfluidic devices were fabricated from PDMS using photolithography and replica molding (see Methods). This approach allowed for micro-miniaturization of device features, while substantially improving device durability and reproducibility. The standard design, intended to mimic existing glass devices (Hinkle et al., 2003), employed three identical channels, each being 3 cm long and 100 μm wide (Figure 2a). To generate ultra-brief pulses, the standard design was modified such that the central channel tapered to a final width of 50, 25, or 10 μm (Figure 2b). All channels originated from circular solution access ports 300 μm in diameter (for connecting reagent reservoirs via polyethylene tubing) and were separated at their exits by 10 μm septa (to minimize the width of solution interfaces, allowing for rapid solution exchange; Figures 3, 4). Due to current aspect ratio limitations, decreasing the widths of channels or their septa below 10 μm was not possible without decreasing channel heights, which needed to be at least 50-100 μm to facilitate channel visualization and electrode positioning. To rapidly translate the microfluidic devices during electrophysiological recordings, they were secured on an acrylic platform and connected to a Warner Instruments SF-77B stepper motor (Figure 2c). Since this system has a reported translational velocity of ~35 μm/ms (http://www.warneronline.com), we predicted the microfluidic devices with the narrowest central channels (i.e., 10 and 25 μm) would be capable of generating synaptically relevant neurotransmitter pulses.

Device performance was characterized by loading outer and central channels with high and low (1:10 dilution) osmolarity solutions, respectively. This allowed electrode

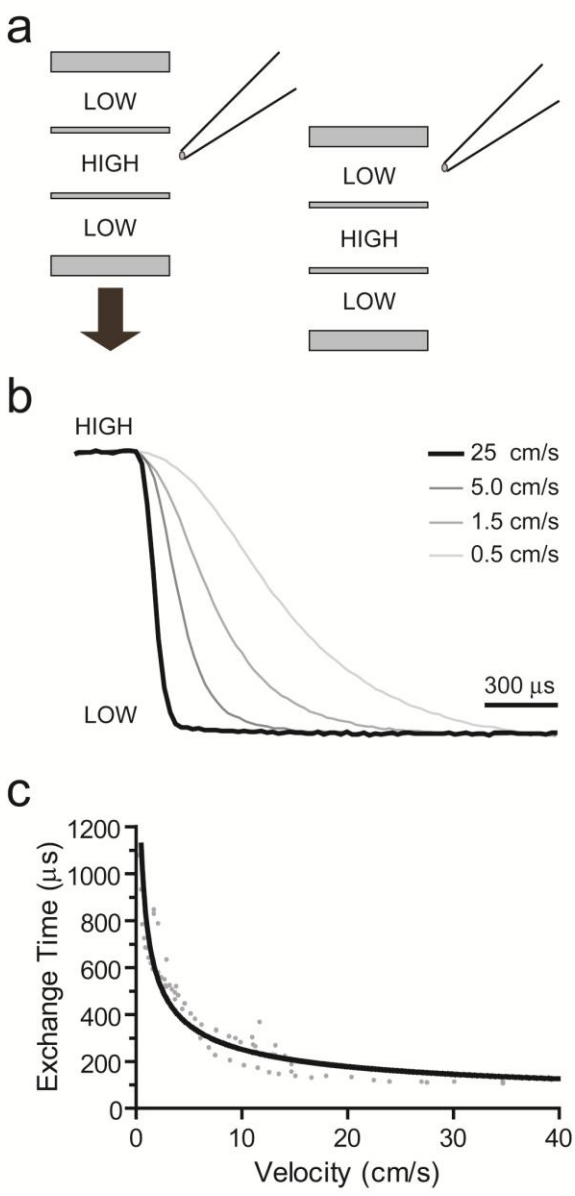

Figure 3. Relationship between solution velocity and solution exchange time

a) Schematic depicting protocol for achieving rapid solution exchange. The standard 3-channel device (PDMS septa represented by grey bars; not to scale) is depicted in the starting position (left) with the recording pipette positioned in the high solute (HIGH) fluid stream. Repositioning the device orthogonal to its long axis (black arrow) rapidly exposes the recording pipette to the adjacent low solute (LOW) fluid stream (right). b) Representative liquid junction currents obtained using the protocol in Panel A at different solution velocities. Solution exchange times for these currents were 108, 294, 614, and 1074 µs (for velocities of 25, 5, 1.5, and 0.5 cm/s, respectively). c) Relationship between solution velocity and solution exchange time. The data were fit using a non-linear regression ($t = 794.6/\sqrt{v}$; $r^2 = 0.87$).

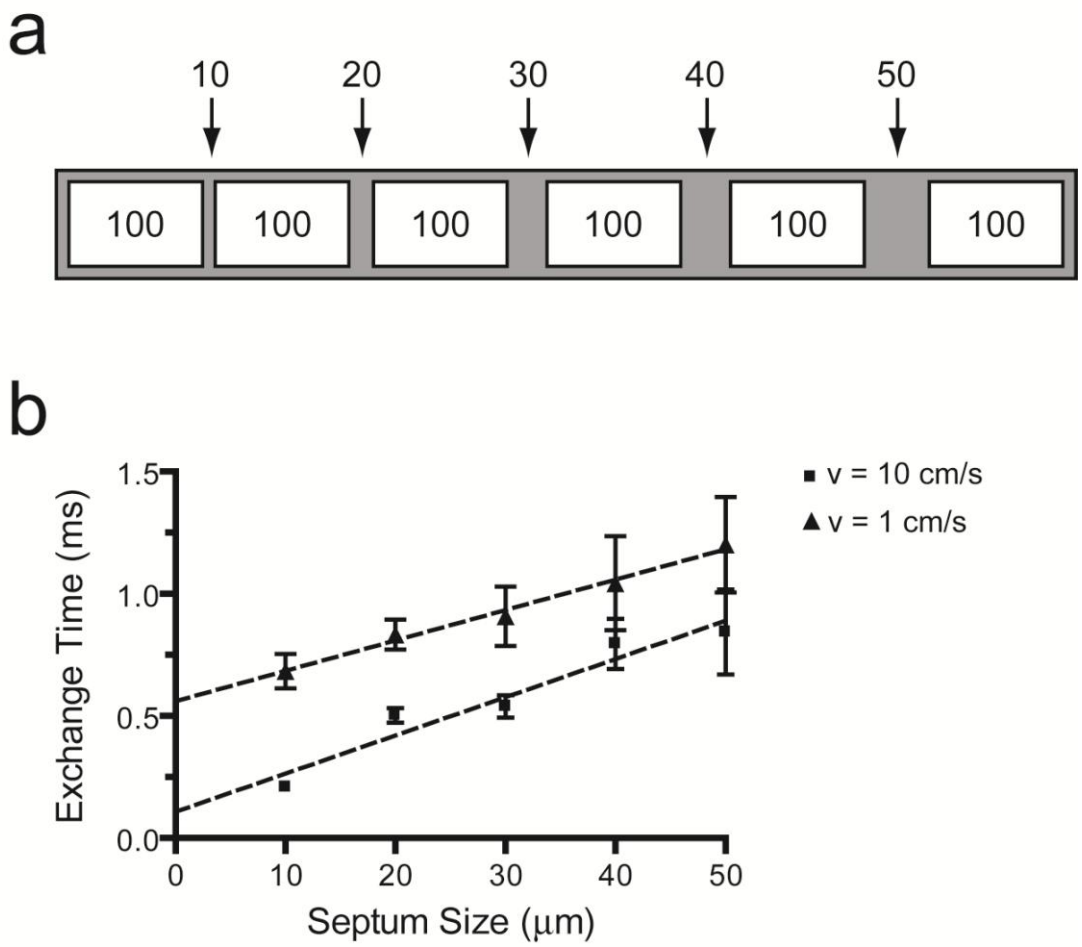

Figure 4. Solution exchange time depended on septal thickness and fluid velocity

a) Schematic of channel exits in a custom microfluidic device containing six channels (white) separated by septa (grey) of increasing thickness. The numbers in and above the device correspond to the width of the channels and septa, respectively, in μm. b) Exchange time as a function of fluid velocity and septal thickness. The data were fit using a linear regression (r^2 = 0.99 and 0.94 for 1 cm/s and 10 cm/s fluid velocities, respectively). Although not always visible, error bars representing the SEM were included for all points.

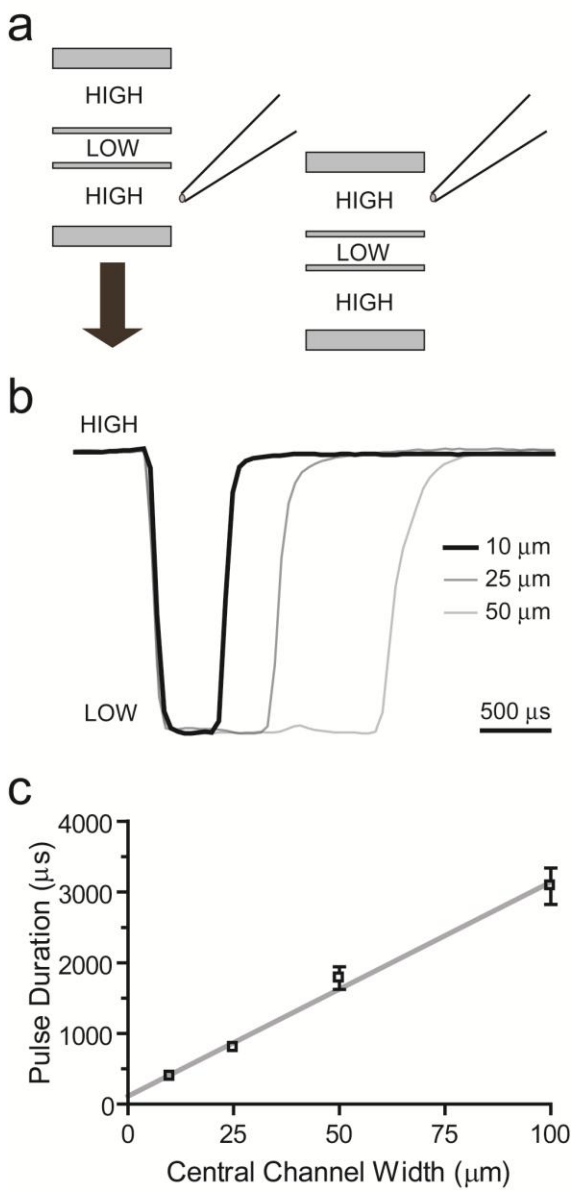

Figure 5. Microfluidic device characterization

a) Schematic depicting protocol for generating brief neurotransmitter pulses. A modified 3-channel device (not to scale) is shown in the starting position (left) with the recording pipette positioned in the high osmolarity (HIGH) fluid stream. With a single lateral movement of the device (black arrow), the recording pipette is exposed briefly to the low osmolarity (LOW) stream and then to the second high osmolarity stream (right). b) Representative open-tip liquid junction currents obtained using the protocol in Panel A using devices with different central channel widths. Pulse durations for these currents were 410, 810, and 1620 μs (for the 10, 25, and 50 μm central channels, respectively). c) Relationship between central channel width and pulse duration. The data were fit using a linear regression (see Results; r^2=0.99). Although not always visible, error bars representing the SEM were included for all points.

positioning relative to the channels to be monitored as a function of time, as solutions with different osmolarities yield different liquid-junction currents. Recordings began with an "open-tip" electrode positioned in one of the outer high osmolarity solution streams 25-50 μm from the channel exits (Figure 2d). Maintaining a minimum of this distance from the channel exits prevented the electrode from passing through the solution "dead space" immediately distal to the septa, and instead, allowed it to pass through a narrower and more laminar solution interface (Sachs, 1999). To generate the brief pulse, the microfluidic device was translated orthogonally to its long axis with a single motion such that after being exposed to the first high osmolarity stream, the electrode was then exposed to the low osmolarity stream, and then to the second high osmolarity stream (Figure 5a). With a fluid velocity of ~25 cm/s (the maximum sustainable by excised membrane patches; data not shown), solution exchange times were consistently ~100 μs (Figure 3) and exposure durations to the low osmolarity solution stream were 391 ± 47, 799 ± 49, 1783 ± 159, and 3082 ± 259 ms when central channel widths were 10, 25, 50, and 100 μm, respectively (n = 5 devices) (Figure 5b, 5c). These values were unaffected by using different osmolarity solutions or by repeatedly translating the devices at rates up to 80 Hz (data not shown). Pulse duration was linearly related to the width of the central channel (r^2 = 0.99), with a slope of 30.2 ± 1.9 μs/μm (Figure 5c). This corresponded to an average translational velocity of ~33 μm/ms, a value only slightly lower than that reported by the manufacturer (likely reflecting the larger mass of the acrylic platform and PDMS device compared to glass capillary tubing).

Currents evoked from $GABA_A$ receptors were exquisitely sensitive to the duration of GABA application

Although synaptic LGICs are thought to be exposed to neurotransmitter for only 300-600 μs, pulse lengths of 1 – 10 ms have historically been used to mimic synaptic transmission (Colquhoun et al., 1992; Jones and Westbrook, 1995; Lagrange et al., 2007; Bianchi et al., 2007; Rula et al., 2008). To determine if this difference in pulse length could alter the kinetic properties of LGICs, we compared the peak amplitude, deactivation time course, and sensitivity to high-frequency stimulation of $GABA_A$ receptor currents evoked by either a "synaptic" 400 μs or a more "conventional" 10 ms pulse of 1 mM GABA (a synaptically relevant concentration). The 400 μs pulse was generated by translating the modified 3-channel device (Figure 2b) containing the 10 μm central channel using the protocol described in the previous section (Figure 5a), except that high and low osmolarity solutions were replaced by control and GABA-containing bath solutions, respectively. The 10 ms pulse was generated by translating the standard 3-channel device (Figure 2a), again with control and GABA-containing bath solutions in place of high and low osmolarity solutions, respectively, using the traditional approach to solution switching (i.e., after exposing the recording electrode to the GABA-containing stream, it was then re-exposed to the original control stream by translating the microfluidic device in the opposite direction). Experiments were performed on outside-out membrane patches excised from HEK293T cells expressing the α1β3γ2S receptor, an isoform expressed in adult hippocampal synapses (Pirker et al., 2000; Herd et al., 2008). To facilitate application of both pulse lengths to the same excised patch, a combination device containing both the standard and modified channel designs was used (Figure 6). Note that solution exchange times and application durations are known to be similar for

"open-tip" and "patched" recording electrodes (Colquhoun et al., 1992; Mozrzymas et al., 2003).

Compared to currents evoked by conventional 10 ms pulses, those evoked by the more synaptically relevant 400 μs pulses had smaller peak amplitudes (169.9 ± 55.3 pA vs. 225.4 ± 56.4 pA; n = 10; $p < 0.01$) (Figure 7a, 7b). This difference could not be attributed to differences in the rates of GABA application, as solution exchange times were consistently ~100 μs for all application protocols at a fluid velocity of 25 cm/s (Figure 3, 5) and were routinely checked before and after recording sessions. In addition, this difference could not be attributed to current "rundown" between applications, as 10 ms pulses were applied before and after the 400 μs pulse, and the average of those

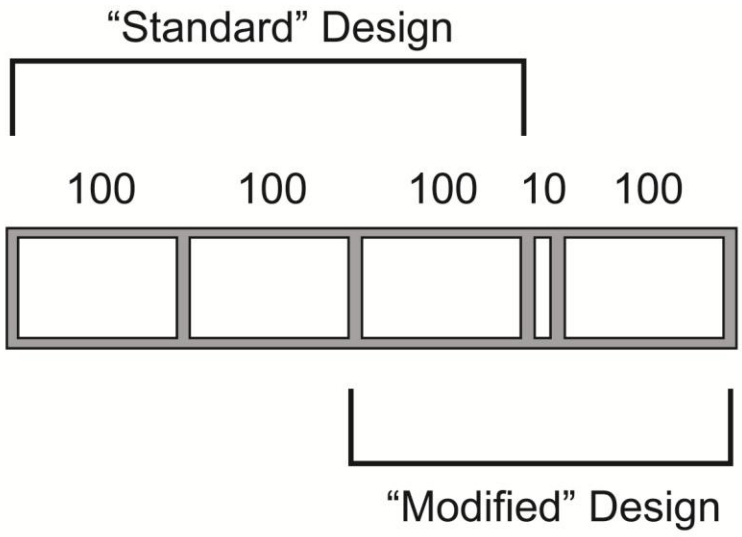

Figure 6. Schematic of a custom microfluidic device that allows for application of synaptic (400 μs) and conventional (10 ms) pulse lengths to the same lifted cell or excised membrane patch

Channel exits in a custom microfluidic device that incorporates both the standard (Figure 2a) and modified (Figure 2b) designs are shown. Channels (white) are separated by 10 μm septa (grey). The numbers above the device indicate the width of the channels in μm.

responses was used for comparison. Instead, the smaller peak amplitude of currents evoked by synaptic pulses reflected the fact that α1β3γ2S receptors were relatively slow to activate (Figure 7c, 7d). In other words, while 10 ms pulses provided ample time for currents to reach their peak amplitude, 400 μs pulses terminated receptor activation, causing currents to be truncated. Indeed, while maximal rise slopes were similar for 400 μs and 10 ms pulses (Figure 7c), indicating that the kinetics of receptor activation were similar following both application protocols, current rise time was substantially shorter following the 400 μs pulse (0.61 ± 0.05 vs. 1.33 ± 0.14 ms; n = 10; $p < 0.001$) (Figure 7c, 7d). In fact, the rise time of currents evoked by 400 μs GABA pulses was approximately equal to the sum of the pulse duration (~0.4 ms) and the solution exchange time (~0.2 ms; i.e., ~0.1 ms × 2, since the electrode must enter and exit the GABA stream), consistent with the idea that activation of this particular receptor isoform was limited by the duration of GABA exposure.

In addition, activating $GABA_A$ receptors with ultra-brief as opposed to conventional pulses decreased the weighted time constant of deactivation (10.67 ± 2.44 ms vs. 17.99 ± 4.58 ms; n = 10; $p < 0.01$) (Figure 7e, 7f), suggesting that limiting the duration of GABA exposure decreased receptor accumulation in long-lived conformations, which serve to delay GABA unbinding (Jones and Westbrook, 1995; Bianchi et al., 2007). Deactivation was typically bi-phasic (although as many as four components could be resolved with larger currents), and interestingly, while the relative amplitudes of fast and slow phases were similar for synaptic and conventional pulses (A1: 0.71 ± 0.05 vs. 0.83 ± 0.04; A2: 0.29 ± 0.05 vs. 0.17 ± 0.04; $p > 0.05$ in both cases), synaptic pulses were associated with faster time constants of deactivation (τ1: 1.83 ± 0.38

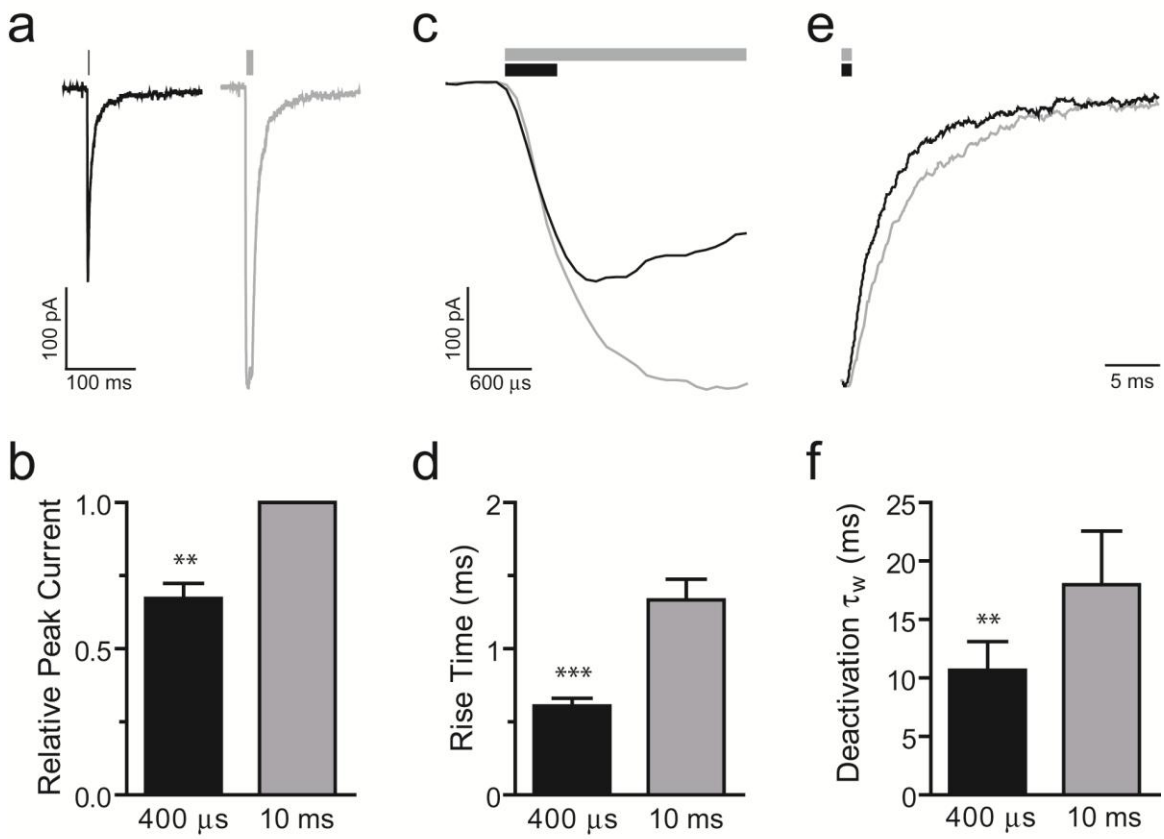

Figure 7. Effect of pulse duration on α1β3γ2S $GABA_A$ receptor current kinetics

a) Representative currents evoked by 400 µs (left) or 10 ms (right) pulses of 1 mM GABA applied to the same outside-out patch. b) The effect of pulse duration on peak current amplitude. c) Comparison of current activation during 400 µs (black) or 10 ms (grey) pulses of 1 mM GABA. d) The effect of pulse duration on current rise time. e) Comparison of current deactivation following 400 µs (black) or 10 ms (grey) pulses of 1 mM GABA. Currents were normalized to their amplitudes at the start of GABA washout. f) The effect of pulse duration on the weighted time constant of deactivation. Filled bars above currents indicate duration of GABA exposure. ** $p < 0.01$; *** $p < 0.001$

ms vs. 3.32 ± 0.47 ms; τ2: 20.88 ± 5.04 ms vs. 55.24 ± 8.66 ms; $p < 0.01$ in both cases). Synaptic pulses also decreased the sensitivity of $GABA_A$ receptors to repetitive stimulation (Figure 8), which has been demonstrated to progressively decrease peak current amplitudes (Jones and Westbrook, 1995; Lagrange et al., 2007; Rula et al., 2008). While this was not apparent at low stimulation frequencies (1 Hz; Figure 8a, 8b), where the inter-pulse interval was sufficiently long to allow currents evoked by both synaptic and conventional pulses to fully deactivate, a substantial reduction was noted in the rate at which peak current amplitudes decayed when evoked by high frequency synaptic, as opposed to conventional, pulses (20 Hz; Figure 8c, 8d). Indeed, when the peak amplitude of the last current was compared to that of the first current in a 20 Hz pulse train, 62 ± 11 % of the current amplitude remained when synaptic pulses were used, while only 27 ± 8 % remained when conventional pulses were used ($n = 3$; $p < 0.05$) (Figure 8e, 8f). As with the effect on peak current, these effects of pulse length on deactivation and repetitive stimulation could not be attributed to differences in the rate of GABA washout, as solution exchange times were similar for all experimental protocols (data not shown).

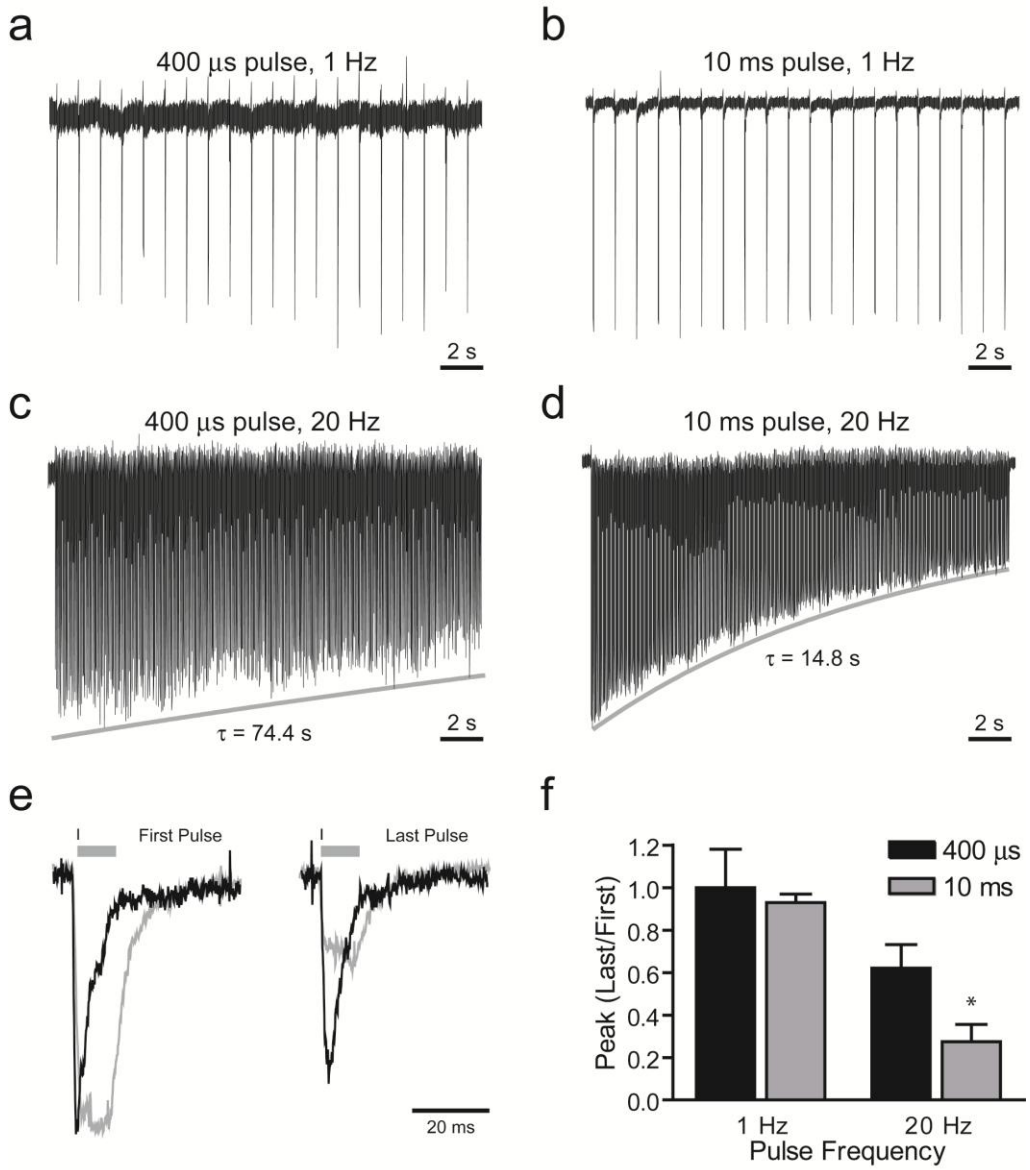

Figure 8. Effect of pulse duration on α1β3γ2S $GABA_A$ receptor current responses during repetitive stimulation

a-d) Representative current responses from 400 µs (Panels a and c) and 10 ms (Panels b and d) pulses of 1 mM GABA applied at frequencies of 1 Hz (Panels a and b) or 20 Hz (Panels c and d). Note that there was no appreciable reduction of peak currents at 1 Hz for either pulse length, while there was a gradual reduction of peak current amplitudes at 20 Hz. To facilitate comparison of the rates of peak current reduction during repetitive stimulation, the maximal responses in Panels a and c were normalized to those of Panels b and d. E) Representative currents evoked by the first (left) and last (right) pulses in the 20 Hz condition for either 400 µs (black) or 10 ms (grey) pulses. Currents were normalized to the first pulse in the train. F) Longer GABA pulses are associated with more pronounced loss of peak current amplitude during high frequency repetitive stimulation. * $p < 0.05$

DISCUSSION

The fact that synaptic transmission occurs on a sub-millisecond timescale has made studying LGICs *in vitro* under physiologically relevant conditions technically challenging. Indeed, mimicking the synaptic transient requires that neurotransmitter be applied not only extremely rapidly, but also extremely briefly. Here, we describe the design, fabrication, optimization, and implementation of a novel microfluidic solution-switching system that allows for solution exchange times as brief as ~100 μs and pulse durations as brief as ~400 μs, thus fulfilling both of these requirements. When applied to recombinant α1β3γ2S $GABA_A$ receptors, an isoform expressed highly in adult hippocampal synapses (Pirker et al., 2000; Herd et al., 2008), currents evoked by ultra-brief pulses of GABA had kinetic properties similar to those of inhibitory post-synaptic currents (IPSCs) recorded from adult hippocampal CA1 pyramidal neurons, including sub-millisecond rise times and biphasic deactivation time courses with weighted time constants of ~10 ms (Cohen et al., 2000). These kinetic properties, however, were substantially altered for currents evoked by longer, conventional pulses of GABA, consistent with the predictions of several theoretical modeling studies (Glavinovic, 1999; Mozrzymas, 2004; Lagrange et al., 2007). This raises the possibility that approximating synaptic conditions with longer neurotransmitter pulses could obscure the effects of disease-causing mutations or potential therapeutic compounds on LGIC currents, particularly when there are large differences between the length of application durations and intrinsic current rise times (i.e., the time required for currents to reach peak during continuous neurotransmitter exposure) (Mozrzymas, 2004; Mozrzymas et al., 2007).

The advantages of using PDMS microfluidic devices for studying LGIC currents, however, extend beyond their ability to effectively mimic the timescale of synaptic transmission. In contrast to existing rapid application systems, which typically allow for the delivery of only a few solution streams (Jonas, 1995; Clements, 1997; Hinkle et al., 2003), PDMS-based systems can, in principle, deliver tens to hundreds of solutions to experimental preparations. This tremendously increases the throughput of electrophysiological studies (see Figure 9 for an example of a 12-channel microfluidic device used to determine the concentration response and pharmacological profiles of the $\alpha4\beta3\gamma2L$ $GABA_A$ receptor isoform), and importantly, permits more complex experimental protocols to be performed. For example, different device designs can be included on the same microfluidic chip, thereby allowing neurotransmitter to be applied for different lengths of time (by varying central channel width; Figure 6) and/or at different rates (by varying septum width; Figure 4). Fabricating microfluidic devices from PDMS also makes them more durable and reproducible. Indeed, there is little risk of breaking PDMS devices even when they include micron-scale features, and should this occur, the replica molding process ensures that all replacement devices will be nearly identical to the original. Furthermore, taking a microfluidic approach to solution switching substantially reduces the cost of electrophysiological experiments, as PDMS-based devices are cheaper to fabricate, consume less reagent, and with short setup times, are less labor intensive.

The future for this microfluidic approach to solution switching thus appears highly promising, and new techniques are poised to further enhance its capabilities. Optimized methods for PDMS microfabrication allow for devices with higher aspect

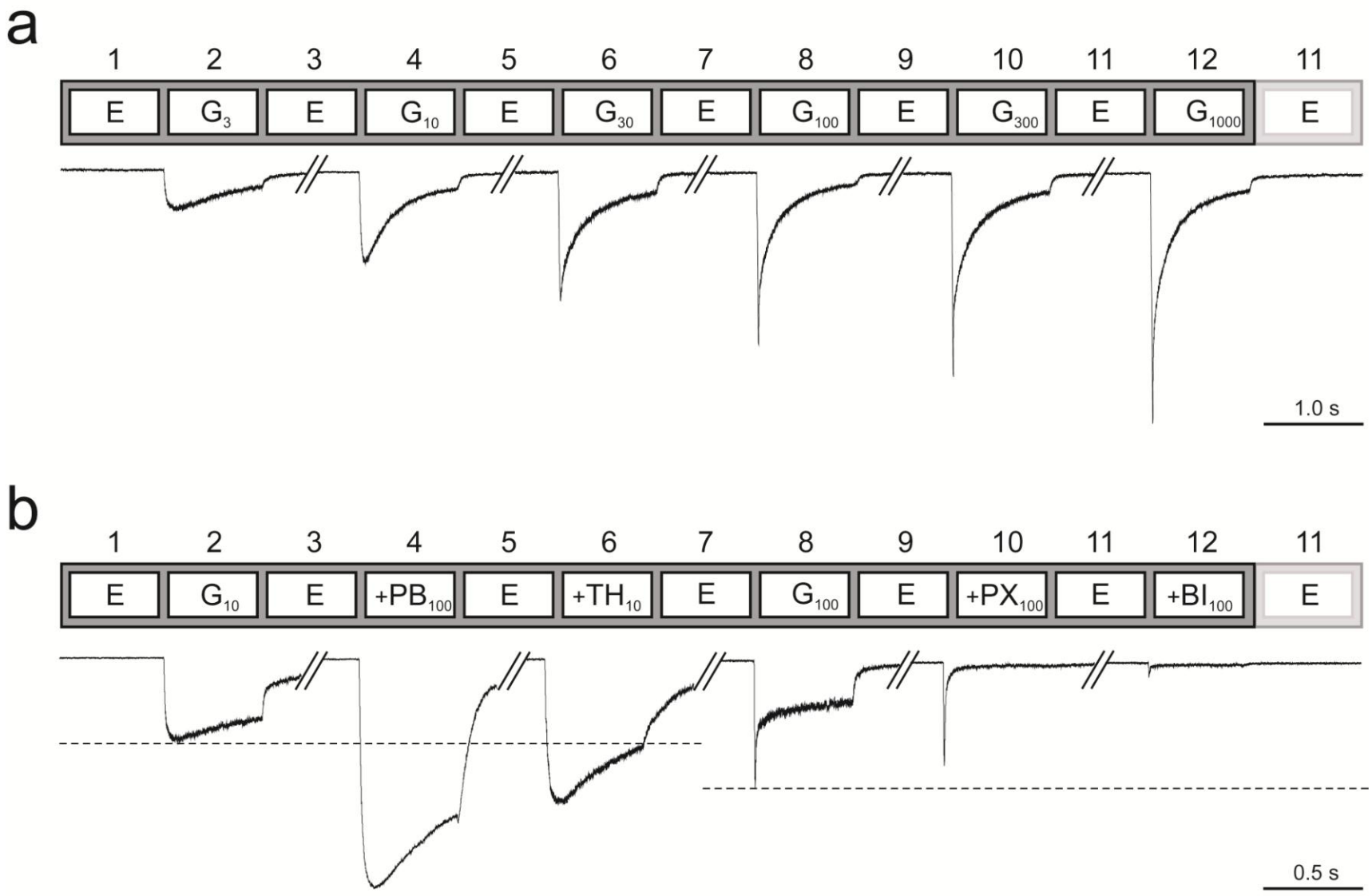
a
1 2 3 4 5 6 7 8 9 10 11 12 11
E G3 E G10 E G30 E G100 E G300 E G1000 E
1.0 s
b
1 2 3 4 5 6 7 8 9 10 11 12 11
E G10 E +PB100 E +TH10 E G100 E +PX100 E +BI100 E
0.5 s

Figure 9. Schematic of a microfluidic device that allows for efficient screening of LGIC concentration response and pharmacological profiles

a) Channel exits in a custom 12-channel device are shown (numbered above device for clarity; not to scale). Even-numbered channels were loaded with GABA solutions (G) of increasing concentration (subscript denotes concentration in μM). Odd-numbered channels were loaded with external bath solution (E). Shown below the device are the corresponding currents (normalized to the 1000 μM trace) evoked from lifted whole cells expressing rat α4β3γ2L $GABA_A$ receptors. One-second GABA applications were separated by 45-second washes in external solution to allow for complete agonist unbinding (omitted traces indicated by //). Following exposure to the final GABA solution (channel 12), neurotransmitter washout was accomplished by stepping the device in reverse to channel 11 (indicated by light gray box; far right). b) As above, except that even-numbered channels contained either low (10 μM; lanes 2, 4, and 6) or high (100 μM; lanes 8, 10, and 12) concentrations of GABA along with either a putative agonist or antagonist (PB = pentobarbital; TH = THDOC; PX = picrotoxin; BI = bicuculline; subscript denotes concentration in μM). Agonists (PB and TH) and antagonists (PX and BI) were co-applied with 10 μM and 100 μM GABA, respectively. Dashed lines indicate control peak current amplitudes for reference.

ratios (Liu et al., 2005), meaning that the widths of individual channels and their septa could be further decreased. This, combined with the availability of higher velocity stepper translators (Haydon Switch and Instrument Corp., Waterbury, CT), should allow for faster solution exchange times and briefer pulse durations. Moreover, given the recent development of microfluidic design elements that allow concentration gradients to be generated within individual channels (Chung et al., 2005), modulating the shape of the neurotransmitter transient should now be feasible. In other words, if the central neurotransmitter-containing solution stream is replaced with one that contains a neurotransmitter gradient, then passing this stream across the recording pipette will generate a non-square neurotransmitter waveform. This will allow the experimental neurotransmitter transient not only to be brief, but also to mimic the shape of the synaptic neurotransmitter transient, whose decay is better described by an exponential function

(Clements, 1996). We thus anticipate that our novel approach to solution switching will allow for LGIC currents to be evaluated in vitro under a wide range of physiologically relevant conditions.

REFERENCES

Bianchi MT, Botzolakis EJ, Haas KF, Fisher JL, Macdonald RL. Microscopic kinetic determinants of macroscopic currents: insights from coupling and uncoupling of $GABA_A$ receptor desensitization and deactivation. J Physiol 2007;584:769-787.

Bianchi MT, Macdonald RL. Slow phases of GABA(A) receptor desensitization: structural determinants and possible relevance for synaptic function. J Physiol 2002;544:3-18.

Chung BG, Flanagan LA, Rhee SW, Schwartz PH, Lee AP, Monuki ES, Jeon NL. Human neural stem cell growth and differentiation in a gradient-generating microfluidic device. Lab Chip 2005;5:401-406.

Clements J. Very Fast Drug Application to Dissociated Cells and Membrane Patches. In Martin R, editor. Neuroscience Methods: A Guide for Advanced Students. Overseas Publishers Association: Amsterdam, 1997; 73-79.

Clements JD. Transmitter timecourse in the synaptic cleft: its role in central synaptic function. Trends Neurosci 1996;19:163-171.

Cohen AS, Lin DD, Coulter DA. Protracted postnatal development of inhibitory synaptic transmission in rat hippocampal area CA1 neurons. J Neurophysiol 2000;84:2465-2476.

Colquhoun D, Jonas P, Sakmann B. Action of brief pulses of glutamate on AMPA/kainate receptors in patches from different neurones of rat hippocampal slices. J Physiol 1992;458:261-287.

Franke C, Hatt H, Dudel J. Liquid filament switch for ultra-fast exchanges of solutions at excised patches of synaptic membrane of crayfish muscle. Neurosci Lett 1987;77:199-204.

Glavinovic MI. Monte carlo simulation of vesicular release, spatiotemporal distribution of glutamate in synaptic cleft and generation of postsynaptic currents. Pflugers Arch 1999;437:462-470.

Heckmann M, Pawlu C. Fast-Drug Application. In Walz W, Boulton AA, Baker GB, editors. Patch-clamp Analysis: Advanced Techniques. Humana Press: Totowa, 2002; 217-229.

Herd MB, Haythornthwaite AR, Rosahl TW, Wafford KA, Homanics GE, Lambert JJ, Belelli D. The expression of GABAA beta subunit isoforms in synaptic and extrasynaptic receptor populations of mouse dentate gyrus granule cells. J Physiol 2008;586:989-1004.

Hinkle DJ, Bianchi MT, Macdonald RL. Modifications of a commercial perfusion system for use in ultrafast solution exchange during patch clamp recording. Biotechniques 2003;35:472-4, 476.

Holmes WR. Modeling the effect of glutamate diffusion and uptake on NMDA and non-NMDA receptor saturation. Biophys J 1995;69:1734-1747.

Jonas P. Fast application of agonists to isolated membrane patches. In Sakmann B, Neher E, editors. Single Channel Recording. Plenum Press: New York, 1995; 231-243.

Jones MV, Westbrook GL. Desensitized states prolong GABAA channel responses to brief agonist pulses. Neuron 1995;15:181-191.

Jones MV, Westbrook GL. The impact of receptor desensitization on fast synaptic transmission. Trends Neurosci 1996;19:96-101.

Kullmann DM, Hanna MG. Neurological disorders caused by inherited ion-channel mutations. Lancet Neurol 2002;1:157-166.

Lagrange AH, Botzolakis EJ, Macdonald RL. Enhanced macroscopic desensitization shapes the response of {alpha}4 subtype-containing GABAA receptors to synaptic and extrasynaptic GABA. J Physiol 2007;578:655-676.

Liu G, Tian Y, Kan Y. Fabrication of high-aspect-ratio microstructures using SU8 photoresist. Microsystem Technologies-Micro-and Nanosystems-Information Storage and Processing Systems 2005;11:343-346.

Macdonald RL, Gallagher MJ, Feng HJ, Kang J. GABA(A) receptor epilepsy mutations. Biochem Pharmacol 2004;68:1497-1506.

Mata A, Fleischman AJ, Roy S. Characterization of polydimethylsiloxane (PDMS) properties for biomedical micro/nanosystems. Biomed Microdevices 2005; 7:281-293.

McDonald JC, Whitesides GM. Poly(dimethylsiloxane) as a material for fabricating microfluidic devices. Acc Chem Res 2002;35:491-499.

Mozrzymas JW, Barberis A, Mercik K, Zarnowska ED. Binding sites, singly bound states, and conformation coupling shape GABA-evoked currents. J Neurophysiol 2003;89:871-883.

Mozrzymas JW. Dynamism of GABA(A) receptor activation shapes the "personality" of inhibitory synapses. Neuropharmacology 2004;47:945-960.

Mozrzymas JW. Electrophysiological description of mechanisms determining synaptic transmission and its modulation. Acta Neurobiol Exp (Wars) 2008;68:256-263.

Mozrzymas JW, Wojtowicz T, Piast M, Lebida K, Wyrembek P, Mercik K. GABA transient sets the susceptibility of mIPSCs to modulation by benzodiazepine receptor agonists in rat hippocampal neurons. J Physiol 2007;585:29-46.

Niu L, Wieboldt R, Ramesh D, Carpenter BK, Hess GP. Synthesis and characterization of a caged receptor ligand suitable for chemical kinetic investigations of the glycine receptor in the 3-microseconds time domain. Biochemistry 1996;35:8136-8142.

Pirker S, Schwarzer C, Wieselthaler A, Sieghart W, Sperk G. GABA(A) receptors: immunocytochemical distribution of 13 subunits in the adult rat brain. Neuroscience 2000;101:815-850.

Rula EY, Lagrange AH, Jacobs MM, Hu N, Macdonald RL, Emeson RB. Developmental modulation of GABA(A) receptor function by RNA editing. J Neurosci 2008;28:6196-6201.

Sachs F. Practical limits on the maximal speed of solution exchange for patch clamp experiments. Biophys J 1999;77:682-690.

Tang CM. Rapid solution application methods. Curr Protoc Neurosci 2001;Chapter 6:Unit.

Ventriglia F, Di M, V. Stochastic fluctuations of the quantal EPSC amplitude in computer simulated excitatory synapses of hippocampus. Biosystems 2003;71:195-204.

Vincent A, Lang B, Kleopa KA. Autoimmune channelopathies and related neurological disorders. Neuron 2006;52:123-138.

CHAPTER VII

THE ROLE OF MACROSCOPIC DESENSITIZATION AND DEACTIVATION IN SHAPING $GABA_A$ RECEPTOR CURRENTS EVOKED BY REPETITIVE STIMULATION

Emmanuel J. Botzolakis, Matt T. Bianchi, and Robert L. Macdonald

ABSTRACT

Repetitive activation of $GABA_A$ receptors gives rise to currents with progressively smaller peak amplitudes (repetitive pulse inhibition, RPI), a phenomenon important for normal signal processing and recently implicated in the pathogenesis of temporal lobe epilepsy. Although RPI is assumed to reflect accumulation and trapping of $GABA_A$ receptors in long-lived desensitized states, certain receptor isoforms (e.g., αβδ receptors) exhibit minimal RPI despite having access to such states. To better understand the kinetic basis for RPI, we evaluated the relationship between desensitization and the sensitivity of currents to repetitive activation using a combination of electrophysiological studies of recombinant α1β3γ2L receptors expressed in HEK293T cells and Markov modeling of $GABA_A$ receptor function. The results demonstrated that while desensitized states were necessary for $GABA_A$ receptor currents to exhibit RPI, they were not sufficient and did not necessarily need to be long-lived. In contrast, the phenomenon of macroscopic desensitization (the loss of current in the continued presence of agonist) was both necessary and sufficient for RPI. Interestingly, this macroscopic current property defined a boundary condition for the time course of RPI: increasing the frequency of

receptor activation drove the rate and extent of RPI towards the limit set by macroscopic desensitization. Weighted deactivation time course accounted for differences between the kinetics of RPI and those of macroscopic desensitization, with faster deactivation decreasing and slower deactivation increasing the rate and extent of RPI. Taken together, the results demonstrate that RPI is shaped primarily by macroscopic phenomena, and therefore, cannot be attributed to individual microscopic parameters (such as desensitized state occupancy). Moreover, the results suggest that macroscopic desensitization has important physiological relevance, as alterations in its kinetic properties are predicted to have profound effects on the inhibitory signaling mediated by $GABA_A$ receptors under conditions of high frequency synaptic transmission.

INTRODUCTION

Sustained neuronal firing leads to a progressive reduction in the amplitude of inhibitory post-synaptic currents (IPSCs) (Ben-Ari, et al., 1979, 1981; Connors, et al., 1982; Wong and Watkins, 1982; Numann and Wong, 1984; McCarren and Alger, 1985; Huguenard and Alger, 1986; Deisz and Prince, 1989; Thompson and Gähwiler, 1989; Fukuda, et al., 1993; Galarreta and Hestrin, 1998; Varela, et al., 1999), a form of short-term plasticity that provides synapses with a rapid and powerful mechanism for negative feedback. This phenomenon, commonly referred to as "repetitive pulse inhibition (RPI)" (or alternatively, "frequency-dependent" or "use-dependent" depression), is thought to be important for normal signal processing (Metherate and Ashe, 1994; Reyes et al., 1998; Galaretta and Hestrin, 1998; Varela, et al., 1999; Fortune and Rose, 2001; Grande and Spain, 2005) and has been implicated in the pathogenesis of some forms of epilepsy (Palma et al., 2002; Roseti et al., 2008; Mazzuferi et al., 2010). While there is considerable evidence that pre-synaptic factors such as depletion of GABA from synaptic vesicles, enhanced GABA reuptake, and autoinhibitory feedback via $GABA_B$ receptors contribute to this phenomenon (Krnjevic, 1984; Varela et al., 1999; McCarren and Alger, 1985; Deisz and Prince, 1989; Thompson and Gähwiler, 1989; Davies and Collingridge, 1993; Fukuda, et al., 1993), post-synaptic factors such as dissipation of the chloride gradient, internalization of $GABA_A$ receptors, and accumulation of $GABA_A$ receptors in desensitized states are also thought to play an important role (Ben-Ari, et al., 1979, 1981; Desarmenien et al., 1980; Wong and Watkins, 1982; Numann and Wong, 1984; McCarren and Alger, 1985; Huguenard and Alger, 1986; Thompson and Gähwiler, 1989; Galarreta and Hestrin, 1997, 1998).

Of the post-synaptic factors, the least understood in terms of its role in shaping RPI is $GABA_A$ receptor desensitization. Indeed, while the relationship between desensitization and the shape of individual IPSCs has been examined in detail (Jones and Westbrook, 1995, 1996; Galarreta and Hestrin, 1997; Haas and Macdonald, 1999; Bianchi et al., 2007), how desensitization shapes IPSCs in the setting of repetitive stimulation has only started to be explored (Bianchi and Macdonald, 2002; Lagrange et al., 2007). Loss of current in the setting of repetitive activation is traditionally attributed to receptor accumulation in desensitized states (Jones and Wesbtrook, 1996), defined as long-lived non-conducting states from which agonist cannot directly unbind (Bianchi and Macdonald, 2001). Support for this hypothesis comes from *in vitro* studies of the predominant $GABA_A$ receptor isoform in synapses ($\alpha1\beta2/3\gamma2$), which exhibits extensive RPI that correlates with receptor accumulation in desensitized states (Jones and Westbrook, 1995; Galarreta and Hestrin, 1997; Bianchi and Macdonald, 2002; Lagrange et al., 2007). However, other $GABA_A$ receptor isoforms (e.g., $\alpha1\beta2/3\delta$) access similar long-lived non-conducting states and yet exhibit only minimal RPI (Haas and Macdonald, 1999; Bianchi and Macdonald, 2002). Moreover, in some cases (e.g., $\alpha1\beta2/3\delta$ and $\alpha3\beta2/3\gamma2$), RPI is paradoxically preceded by the phenomenon of repeated pulse enhancement (RPE), where current amplitudes become progressively larger with repetitive activation. Thus, accumulation of receptors in desensitized states can actually be associated with increased current amplitudes (Bianchi and Macdonald, 2002; Rula et al., 2008).

One possible explanation for the apparent discrepancy between experimentally observed RPI (or RPE) and the ability of receptors to access desensitized states is that

RPI, like other macroscopic phenomena, cannot simply be attributed to individual microscopic parameters. Despite the common attribution of macroscopic behavior to individual rate constants, it is well known that macroscopic current kinetics actually reflect a complex interplay between all rate constants in the underlying gating scheme (Colquhoun, 1981; Bianchi et al., 2007). For example, the time course of macroscopic desensitization (the loss of current in the continued presence of agonist; also referred to as current "sag") is known to depend on the entry and exit rates not only of desensitized states, but also of open states (Bianchi et al., 2007). Similarly, the time course of deactivation (the return of currents to baseline following agonist washout) depends primarily on the mean time receptors remain agonist-bound, which is determined not only by the agonist unbinding rate(s), but also by every other rate constant connecting agonist-bound states (Bianchi et al., 2007; Appendix II). Put another way, while any particular change in a microscopic parameter "maps" clearly to a macroscopic current, the reverse is not true – changes in macroscopic current properties could have been generated by any of a number of microscopic parameters (sometimes referred to as the "inverse problem" in engineering).

To better understand the kinetic basis for RPI, a combination of patch-clamp electrophysiology and mathematical modeling was used to evaluate the relationship between the shape of currents evoked by trains of saturating GABA pulses and intrinsic receptor kinetics. The results demonstrated that desensitized states were in fact necessary for the phenomenon of RPI to be observed, consistent with prior hypotheses linking RPI to discreet kinetic states. However, desensitized states were not sufficient and did not necessarily need to be long-lived. In contrast, the presence of macroscopic

desensitization was both necessary and sufficient for RPI to occur (i.e., any Markov model that gave rise to a macroscopically desensitizing current also supported RPI). Interestingly, macroscopic desensitization was found to represent a boundary condition for the time course of RPI. This suggests that macroscopic desensitization has important physiological relevance, despite its experimental "visualization" requiring agonist exposure for periods of time orders of magnitude longer than are thought to occur at synapses.

MATERIALS AND METHODS

Cell culture and expression of recombinant $GABA_A$ receptors

Rat $GABA_A$ receptor α1, β3, and γ2L subunits were individually sub-cloned into the pcDNA3.1+ mammalian expression vector (Invitrogen, Grand Island, NY). The coding region of each vector was sequenced by the Vanderbilt University Medical Center DNA Sequencing Facility and verified against published sequences. HEK293T cells (American Type Culture Collection, Manassas, VA) were maintained at 37°C in humidified 5% CO_2 / 95% air using Dulbecco's Modified Eagle Medium (Invitrogen) supplemented with 10% fetal bovine serum (Invitrogen), 100 i.u./ml penicillin (Invitrogen), and 100 μg/ml streptomycin (Invitrogen). Cells were plated at a density of ~10^6 cells per 10 cm culture dish (Corning Glassworks, Corning, NY) and passaged every 2-4 days using trypsin-EDTA (Invitrogen). For electrophysiological recordings, cells were plated at a density of $4x10^5$ cells per 6 cm culture dish (Corning Glassworks) and transfected ~24 hours later with equal amounts (1 μg/subunit) of α1, β3, and γ2S subunit cDNA. One μg of pHook-1 cDNA (encoding the cell surface antibody sFv) was included so positively transfected cells could be selected 24 hours later by immunomagnetic bead separation. All transfections were performed using FuGene6 (Roche Diagnostics, Indianapolis, IN) per manufacturer recommendations. The day after transfection, cells were selected and re-plated at low density on collagen-coated 35 mm dishes for electrophysiological recording the next day.

Electrophysiology

Patch clamp recordings were performed at room temperature from excised outside-out membrane patches. Cells were maintained during recordings in a bath solution consisting of (in mM): 142 NaCl, 8 KCl, 6 $MgCl_2$, 1 $CaCl_2$, 10 glucose, and 10 HEPES (pH adjusted to 7.4; 325-330 mOsm). All chemicals used for solution preparation were purchased from Sigma-Aldrich (St. Louis, MO). Recording pipettes were pulled from thin-walled borosilicate capillary glass (Fisher, Pittsburgh, PA) on a Sutter P-2000 micropipette electrode puller (Sutter Instruments, San Rafael, CA) and fire polished with a microforge (Narishige, East Meadow, NY). When filled with a pipette solution consisting of (in mM) 153 KCl, 1 $MgCl_2$, 5 EGTA, 10 HEPES, and 2 MgATP (pH adjusted to 7.3; 300-310 mOsm) and submerged in the bath solution, this yielded open tip resistances of ~2 MΩ and a chloride equilibrium potential (E_{Cl}) of ~0 mV. Currents were recorded at a holding potential of -20 mV using an Axopatch 200B amplifier (Molecular Devices, Foster City, CA), low-pass filtered at 2 kHz using a 4-Pole Bessel filter, digitized at 10 kHz using the Digidata 1322A (Molecular Devices), and stored offline for analysis. GABA was prepared as a stock solution. Working solutions were made on the day of the experiment by diluting stock solutions with the bath solution.

Kinetic Simulations

Kinetic simulations were carried out with Berkeley Madonna 3.1 (www.berkeleymadonna.com), a differential equation solver, using the fourth order Runge-Kutta method with a time interval of 10 μs. For the branched model, default rates

were (s^{-1}) K_{on} = 7 x 10^6, K_{off} = 300, β = 1000, α = 300, δ = 100, and ρ = 3. For the linear model, default rates were (s^{-1}) K_{on} = 7 x 10^6, K_{off} = 300, β = 1000, α = 300, δ = 100, and ρ = 10. 1 ms pulses of 10 mM GABA were used during the pulse-trains unless otherwise stated. Occupancies of open and desensitized states were normalized in Clampfit 9.2 for display, and virtual currents were generated by assuming activation of 100 receptors with a 26 pS conductance voltage-clamped at -75 mV. Proof of the kinetic conditions supporting macroscopic desensitization for simple Markov models of $GABA_A$ receptor function are shown Appendix IV and V.

RESULTS

Repetitive activation of $GABA_A$ receptors leads to progressive reduction of peak current amplitudes

To illustrate the phenomenon of repeated pulse inhibition (RPI), brief (5 ms) pulses of a saturating GABA concentration (1 mM) were applied at increasing frequencies (1 – 20 Hz) for 20 seconds to membrane patches excised from HEK293T cells expressing recombinant α1β3γ2L $GABA_A$ receptors, an isoform commonly found in inhibitory synapses (Farrant and Nusser, 2005). Brief pulses of GABA were generated using a rapid solution switching system, as previously described (Hinkle et al., 2003). Of note, while this pulse duration was approximately an order of magnitude longer than the synaptic GABA transient *in vivo* (Clements, 1996; Glavinovic, 1999), experimental data (Jones and Westbrook, 1995) and simulations using comprehensive Markov models for the α1β3γ2L isoform (Haas and Macdonald, 1999; Lagrange et al., 2007) predicted that this would not significantly affect macroscopic current kinetics following single or multiple GABA pulses (data not shown).

The results demonstrated that both the extent (defined as the ratio of peak current amplitude evoked by the last GABA pulse to that evoked by the first GABA pulse) and the time course (defined as the rate of current amplitude loss) of RPI increased sharply with increasing stimulation frequency (Figure 1). This loss of current amplitude was completely reversible with prolonged exposure to control solution (~60 second wash; data not shown), suggesting that it did not reflect receptor internalization or loss of the chloride gradient, a finding consistent with previous studies (Celentano and Wong, 1994; Bianchi and Macdonald, 2002). Of note, a wash period of 20 seconds was

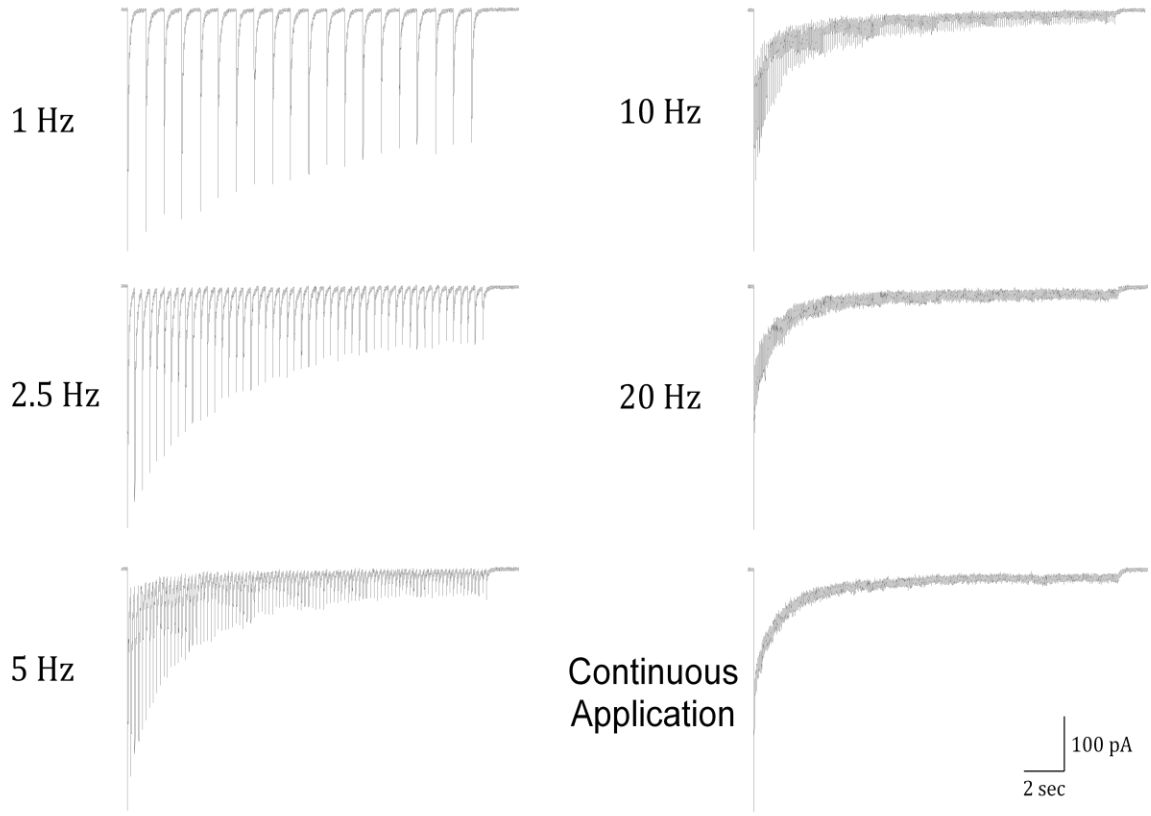

Figure 1. Repeated stimulation of α1β3γ2L $GABA_A$ receptors decreases the amplitude of currents evoked by brief pulses of GABA.

the minimum necessary to prevent RPI from occurring in the first place (i.e., RPI was observed at frequencies above 0.05 Hz; data not shown). Interestingly, both the extent and the time course of RPI reached a maximum when the stimulation frequency was 20 Hz. Indeed, the currents generated with pulse trains at 20 Hz were nearly identical to those generated by a single continuous pulse (which is essentially the equivalent of an infinitely high stimulation frequency). The similarity of the currents evoked by high frequency stimulation to those evoked by continuous application could not be attributed

to malfunction of the drug application system, as open tip recordings of liquid junction currents (generated by replacing the GABA-containing solution with diluted control solution) demonstrated complete washout between pulses and similar solution exchange times at all stimulation frequencies (data not shown).

The relationship between desensitization and repeated pulse inhibition was explored using kinetic models of $GABA_A$ receptor function

The data shown in the previous section demonstrated that increasing the frequency of $GABA_A$ receptor activation increased the rate and extent of RPI, and ultimately, with progressively higher stimulation frequencies, gave rise to currents that closely approximated those generated by a continuous application of GABA. In other words, the shape of currents evoked by continuous application appeared to represent a boundary condition for currents generated by repetitive activation, such that current lost due to repetitive activation could never exceed current lost in the setting of continuous application (i.e., the rate and extent of RPI could never exceed the rate and extent of macroscopic desensitization). We therefore hypothesized that, under conditions where currents failed to exhibit *macroscopic* desensitization, RPI would not be observed, independent of the presence or fractional occupancy of *microscopic* desensitized states (note that while desensitized states are necessary, they are not sufficient to cause macroscopic desensitization; Bianchi et al., 2007). If true, this could explain the failure of the αβδ isoform to exhibit significant RPI (Bianchi and Macdonald, 2002), despite its known ability to access long-lived desensitized states (Haas and Macdonald, 1999).

To test this hypothesis, we generated simple 4-state Markov models of $GABA_A$ receptor function. In the “linear" model (Figure 2, top), receptors transitioned into the

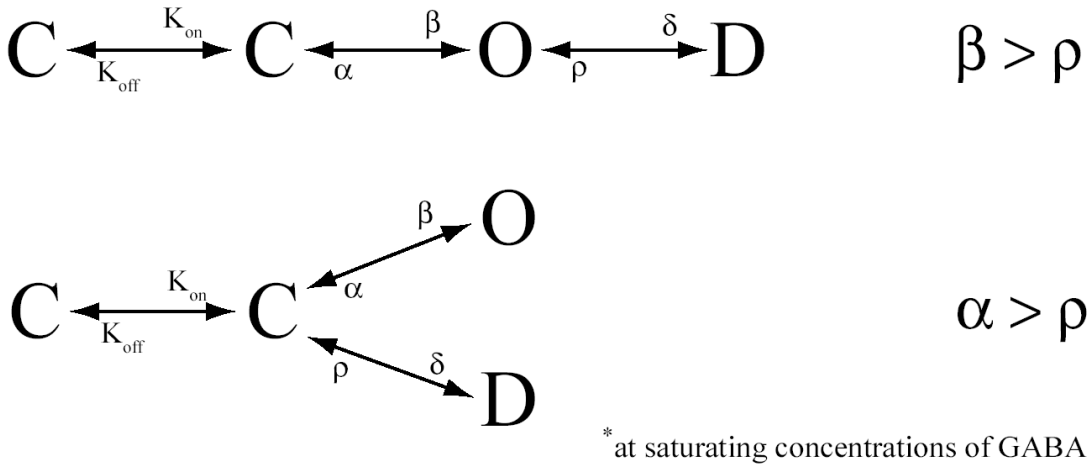

Figure 2. Requirements for macroscopic desensitization in simple models of $GABA_A$ receptor function.

desensitized (D) state directly from the open (O) state, while in the "branched" model (Figure 2, bottom) transitions into the D state occurred via the pre-open state (C_2). Although comprehensive models that account for both the microscopic and macroscopic kinetic properties of $GABA_A$ receptors have been proposed (Haas and Macdonald, 1999; Lema and Auerbach, 2006; Lagrange et al., 2007), simple models are often sufficient to illustrate the salient features of GABA-evoked currents (Jones and Westbrook, 1996; Bianchi et al., 2007; Feng et al., 2009). More importantly, simple models permit the microscopic conditions supporting macroscopic desensitization to be solved analytically (Figure 2; for proofs see Appendix IV and V). For example, in the branched model, macroscopic desensitization was possible only when the exit rate from the O state (α) was larger than the exit rate from the D state (ρ). In contrast, the linear model only exhibited macroscopic desensitization when the entry rate into the O state (β) was larger than the exit rate from the D state (ρ).

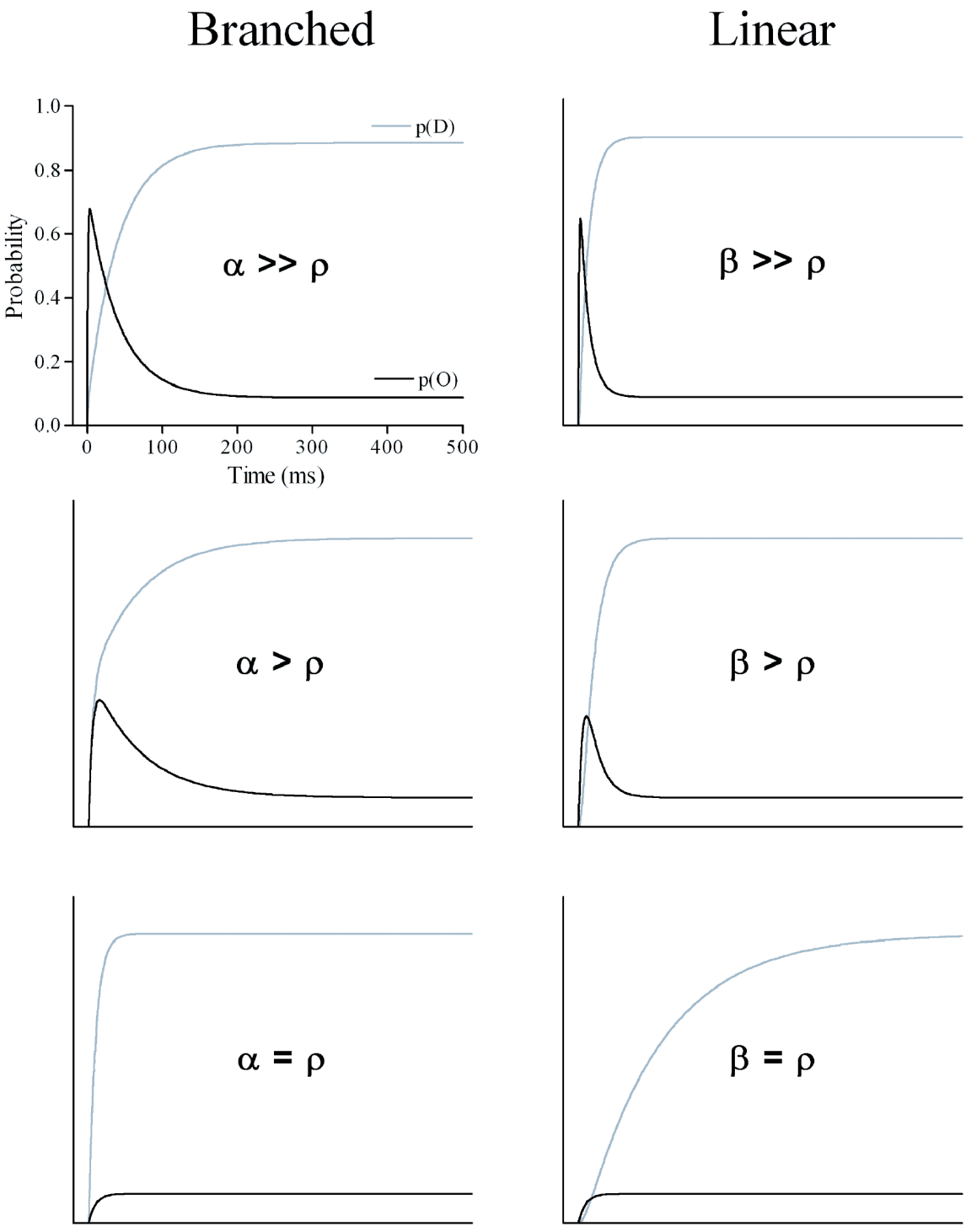

Figure 3. High occupancy microscopic desensitized states were not sufficient for macroscopic currents to undergo desensitization.

Knowledge of these kinetic relationships allowed for models to be generated with high occupancy D states but without the ability to macroscopically desensitize, a situation analogous to the previously described αβδ isoform and to the αβγ isoform activated by low GABA concentrations (Haas and Macdonald, 1999; Bianchi and Macdonald, 2002). This is illustrated in Figure 3 for branched and linear models. For example, when α was set equal to ρ in the branched model (or when β was set equal to ρ in the linear model), the fractional occupancy of the O state, p(O), did not overshoot its equilibrium value (the equivalent of a macroscopic current without desensitization), despite the fractional occupancy of the D state, p(D), approaching an equilibrium value of 0.9. However, when α was much larger than ρ in the branched model (or when β was much larger than ρ in the linear model), peak p(O) was much larger than equilibrium p(O) (the equivalent of a current with macroscopic desensitization), and yet p(D) again approached an equilibrium value of 0.9. Note that an identical p(D) was possible in each condition despite increasing values of α or β (which should have increased and decreased p(D), respectively) because changes in α and β were always accompanied by an identical change in the partnering rate constant (i.e., if α was increased by an order of magnitude, so was β).

Using these models, we evaluated the relationship between RPI and desensitization, both in terms of macroscopic time course and microscopic D state kinetics (Figure 4). In the left column ($\alpha >> \rho$), the branched model supporting extensive macroscopic desensitization was subjected to either brief pulses (1 ms) of saturating GABA at frequencies of 10, 30, and 100 Hz or to a continuous application of saturating GABA. In the middle and right columns, the same protocols were applied to the

branched models supporting moderate ($\alpha > \rho$) or absent ($\alpha = \rho$) macroscopic desensitization, respectively. For each condition, p(D) was shown as an upward trace, while the resulting current (which is directly proportional to p(O)) was shown as a downward trace. Although the results are shown only for the branched model, it should be emphasized that nearly identical results were obtained for the linear model, indicating the results were independent of model connectivity (thought we did not explore cyclic models).

Consistent with our hypothesis, the results demonstrated that RPI was not possible for receptors that failed to exhibit macroscopic desensitization, even in the setting of high occupancy D states. Indeed, despite all three variations of the branched model exhibiting progressive receptor accumulation in the D state with repetitive activation, the resulting macroscopic currents had markedly different kinetic profiles. For example, while the highly desensitizing model ($\alpha >> \rho$) exhibited rapid and extensive RPI at even the lowest tested frequency (10 Hz), the non-desensitizing model ($\alpha = \rho$) failed to exhibit RPI at even the highest tested frequency (100 Hz). Like the highly desensitizing model ($\alpha >> \rho$), the moderately desensitizing model ($\alpha > \rho$) exhibited RPI at all stimulation frequencies. However, the rate and extent of RPI were always less in that case, supporting the idea that macroscopic desensitization dictated the maximum possible rate and extent of RPI. Interestingly, the non-desensitizing model actually exhibited enhancement of current amplitudes (repeated pulse enhancement, RPE) with repetitive activation, despite the occupancy of the D state increasing with each successive pulse. RPE was also observed with the moderately desensitizing model ($\alpha > \rho$) at 30 and 100 Hz, though this was followed by RPI.

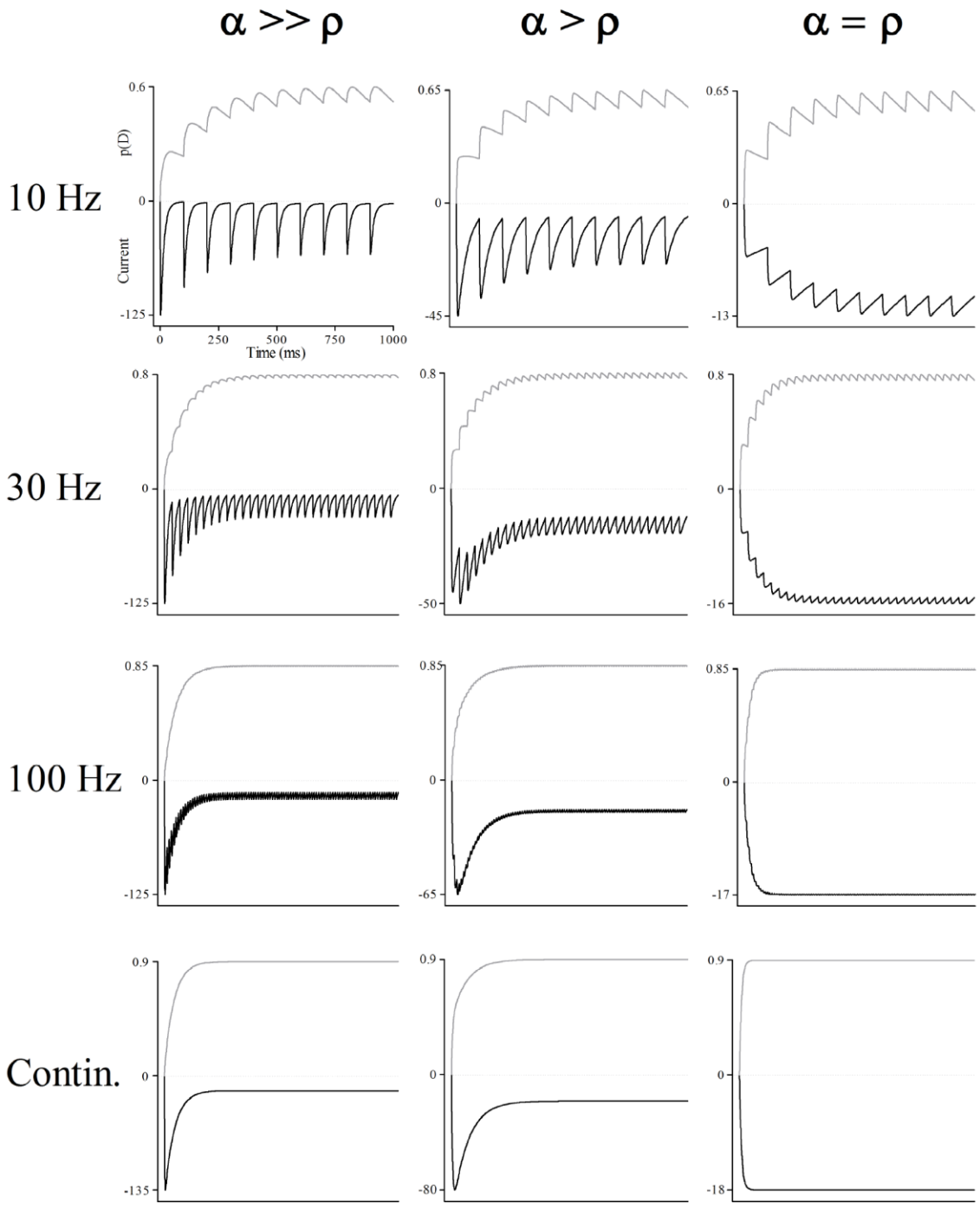

Figure 4. Lack of macroscopic desensitization precludes repeated pulse inhibition, even in the presence of high occupancy desensitized states.

The simulations performed to demonstrate this fundamental relationship between macroscopic desensitization and RPI, however, required the use of kinetic models that differed by more than one parameter (i.e., to keep relative equilibrium occupancies of O and D states constant, multiple rate constants had to be altered). To illustrate this relationship in an even more direct manner, simulations were performed using a single model activated using different GABA concentrations. Indeed, decreasing the GABA concentration is known to decrease the rate and extent of macroscopic desensitization, as this prevents the synchronous activation of receptors needed to resolve the true peak current (Jones and Westbrook, 1996; Bianchi and Macdonald, 2002; Bianchi et al., 2007). However, decreasing the GABA concentration does not prevent receptors from occupying microscopic D states, and in fact, preserves the relative occupancies of O and D states (so long as all O and D states are located distal to the GABA binding step; Appendix I). In other words, GABA concentrations that fail to induce macroscopic desensitization can still drive the vast majority of GABA-bound receptors into the D state. To illustrate this phenomenon, currents were evoked by repetitive stimulation using the highly desensitizing ($\alpha >> \rho$) branched model over a wide range of GABA concentrations (Figure 5). In the left column, the model was activated by brief (1 ms) pulses of saturating (10 mM) GABA at frequencies of 10, 30, and 100 Hz, and also by continuous application. In the middle and right columns, the same protocols were applied but with sub-saturating GABA concentrations (10 μM and 10 nM, respectively).

Consistent with the results from Figure 4, the activation patterns clearly supported the hypothesis that macroscopic desensitization, and not microscopic D state kinetics per se, was the driving force behind the phenomenon of RPI. For example, application of a

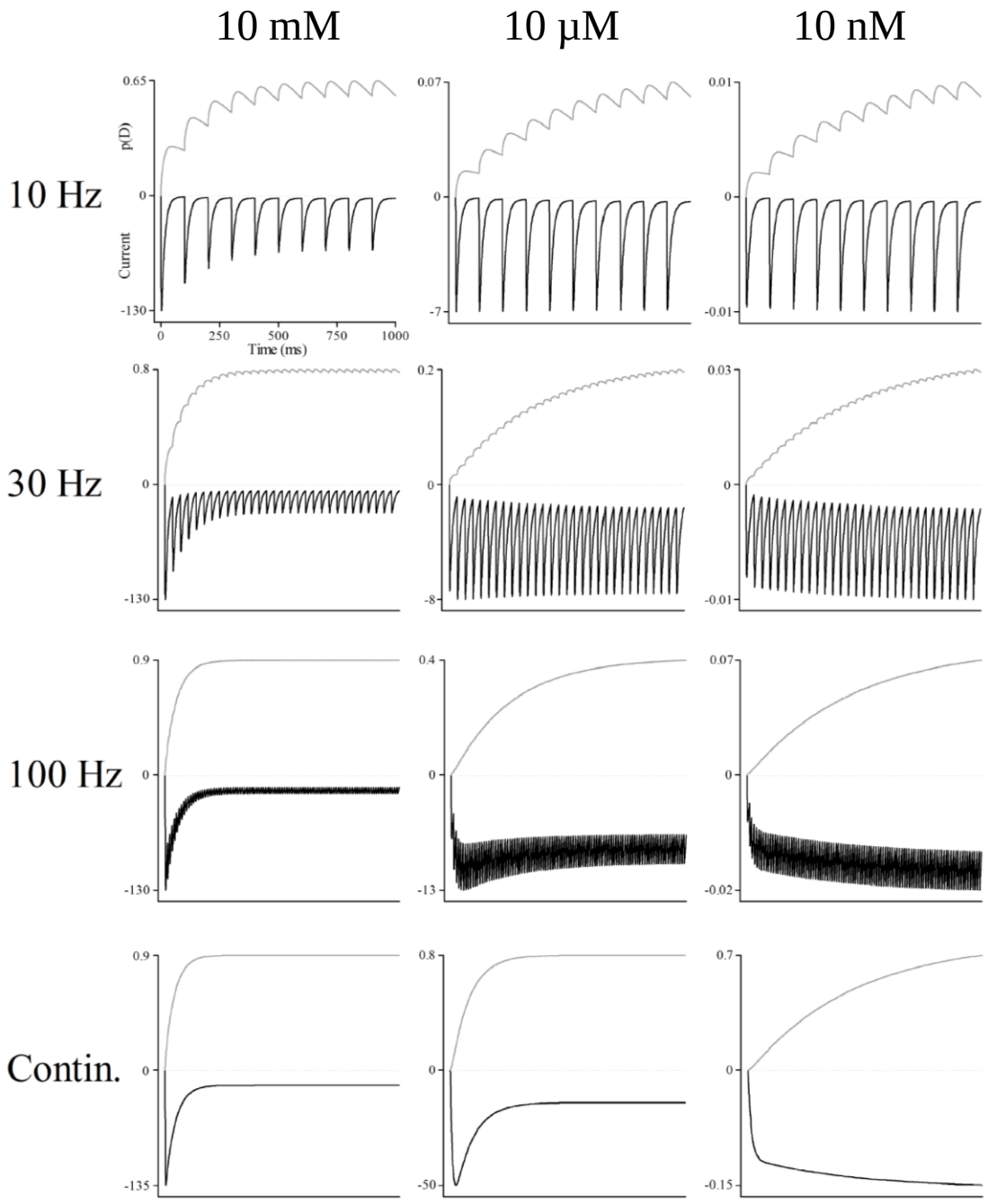

Figure 5. Decreasing the GABA concentration decreased the amount of repeated pulse inhibition by decreasing the extent of macroscopic desensitization, and not by preventing receptor entry into desensitized states.

continuous pulse of 10 nM GABA yielded a non-desensitizing macroscopic current (despite causing accumulation of receptors in the D state), and pulse trains applying this same concentration failed to elicit RPI, even at the highest stimulation frequencies. In contrast, the GABA concentrations supporting macroscopic desensitization (10 mM and 10 μM) always yielded currents that exhibited RPI, though lower concentrations required use of higher stimulation frequencies. This effect was not dependent on the size or complexity of the kinetic model used for the simulations, as both the 4-state linear model and comprehensive models of the α1β3γ2L and α4β3γ2L isoforms (Haas and Macdonald, 1999; Lagrange et al., 2007) behaved similarly when activated by concentrations of GABA sufficiently low to avoid macroscopic desensitization (data not shown). Of note, the phenomenon of RPE was again present in several conditions despite the concurrent accumulation of receptors in the D state, including the 10 μM condition, which ultimately underwent RPI.

Faster deactivation shifts the time course of repeated pulse inhibition away from the limit imposed by macroscopic desensitization

The results in the previous section demonstrated that macroscopic desensitization was both necessary and sufficient to cause RPI, and importantly, that the time course of macroscopic desensitization represented a boundary condition for maximal rate and extent of RPI. But what determined the difference between the time course of RPI at any given frequency and the limit set by macroscopic desensitization? We hypothesized that this difference was related to the time course of deactivation (the return of macroscopic current to baseline upon termination of an agonist pulse), which determines the rate at which receptors become available for subsequent activation. For example, if deactivation

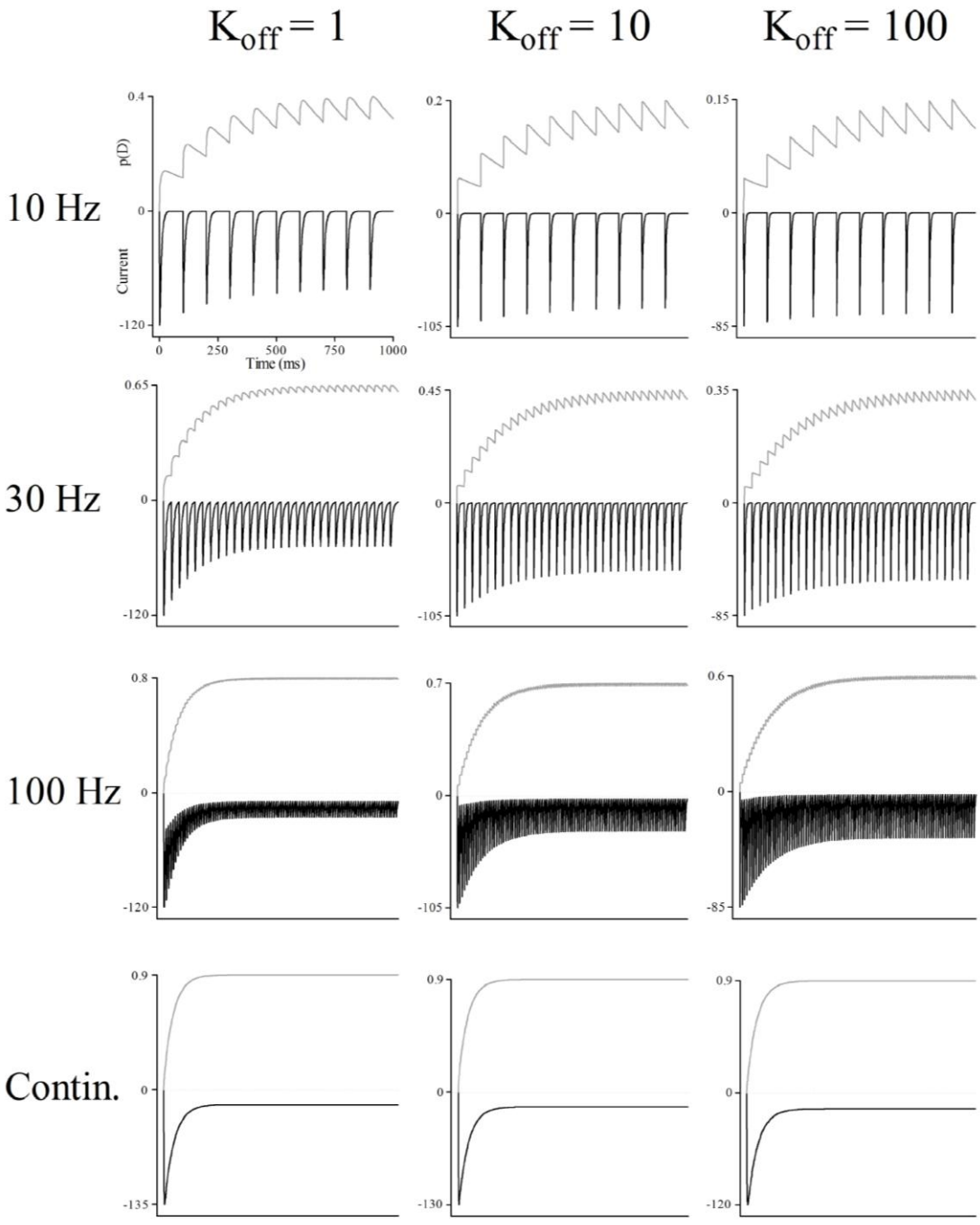

Figure 6. Faster deactivation shifts the time course of repeated pulse inhibition away from the time course of macroscopic desensitization.

is significantly faster than the inter-pulse interval, then the vast majority of receptors should be available for reactivation by subsequent pulses, thus reducing the rate and extent of RPI. In contrast, if deactivation is extremely slow, meaning that nearly all receptors remain GABA-bound at the time of reactivation, then near-maximal RPI would be expected (that is, within the limit imposed by macroscopic desensitization).

To test this hypothesis, currents were evoked by repetitive stimulation using the highly desensitizing ($\alpha >> \rho$) branched model over a wide range of unbinding rates (K_{off}) (Figure 6). For each value of K_{off}, the model was again activated by brief (1 ms) pulses of saturating (10 mM) GABA at frequencies of 10, 30, and 100 Hz, and also by continuous application. Note that varying the unbinding rate in the setting of a saturating GABA concentration has minimal effect on macroscopic current kinetics during GABA exposure, as the fractional occupancy of the unbound state is effectively zero under these conditions (Bianchi et al., 2007). However, because the unbinding rate is an important determinant of the mean time receptors are GABA-bound (though not the only determinant; see Appendix II), it significantly influences the deactivation time course, when the GABA concentration is zero (Bianchi et al., 2007). Thus, varying K_{off} in the setting of saturating GABA allows for the effect of deactivation to be evaluated independent of macroscopic desensitization.

Consistent with our hypothesis, the results demonstrated that deactivation was an important determinant of RPI kinetics, with faster deactivation decreasing and slower deactivation increasing the rate and extent of RPI. For example, compared to the slowest unbinding rate (K_{off} = 1 s^{-1}), increasing the unbinding rate by two orders of magnitude (K_{off} = 100 s^{-1}) nearly eliminated RPI at 10 Hz and significantly decreased the amount of

RPI observed at 30 and 100 Hz. In fact, the rate and extent of RPI observed at 30 and 100 Hz for the slowest unbinding rate (K_{off} = 1 s^{-1}) was comparable to that observed at 10 and 30 Hz, respectively, for the fastest unbinding rate (K_{off} = 100 s^{-1}). Thus, changes in the deactivation time course changed the frequency response properties of model, such that slower deactivation shifted the shape of RPI towards the limit imposed by macroscopic desensitization, while faster deactivation shifted it away (i.e., towards a non-desensitizing macroscopic current). Of note, however, the change in frequency response was not due to D state accessibility or occupancy, as equilibrium p(D) remained at ~0.9 for all values of K_{off} in the setting of a continuous application of saturating GABA.

Changes in the kinetics of repeated pulse inhibition could not be used to infer either the magnitude or the direction of change in D state occupancy

The results in the previous sections demonstrated that, in contrast to leading hypotheses in the literature, RPI was in fact a poor predictor of receptor occupancy in D states. This is consistent with previous studies of other macroscopic phenomena, whose kinetic properties are determined by a complex interplay between multiple rate constants in the underlying gating scheme (Bianchi et al., 2007). However, it has been argued that despite this complex relationship between microscopic and macroscopic receptor properties, experimental increases in the rate and/or extent of RPI (due to disease-causing mutations or allosteric modulators) are nevertheless indicative of overall increases in the fractional occupancy of D states. To test this hypothesis, rate constants in the branched and linear models were systematically varied either alone or in combination over several orders of magnitude, and the response of each model to pulse trains of increasing frequency was evaluated (the results of this extremely large data set are not shown).

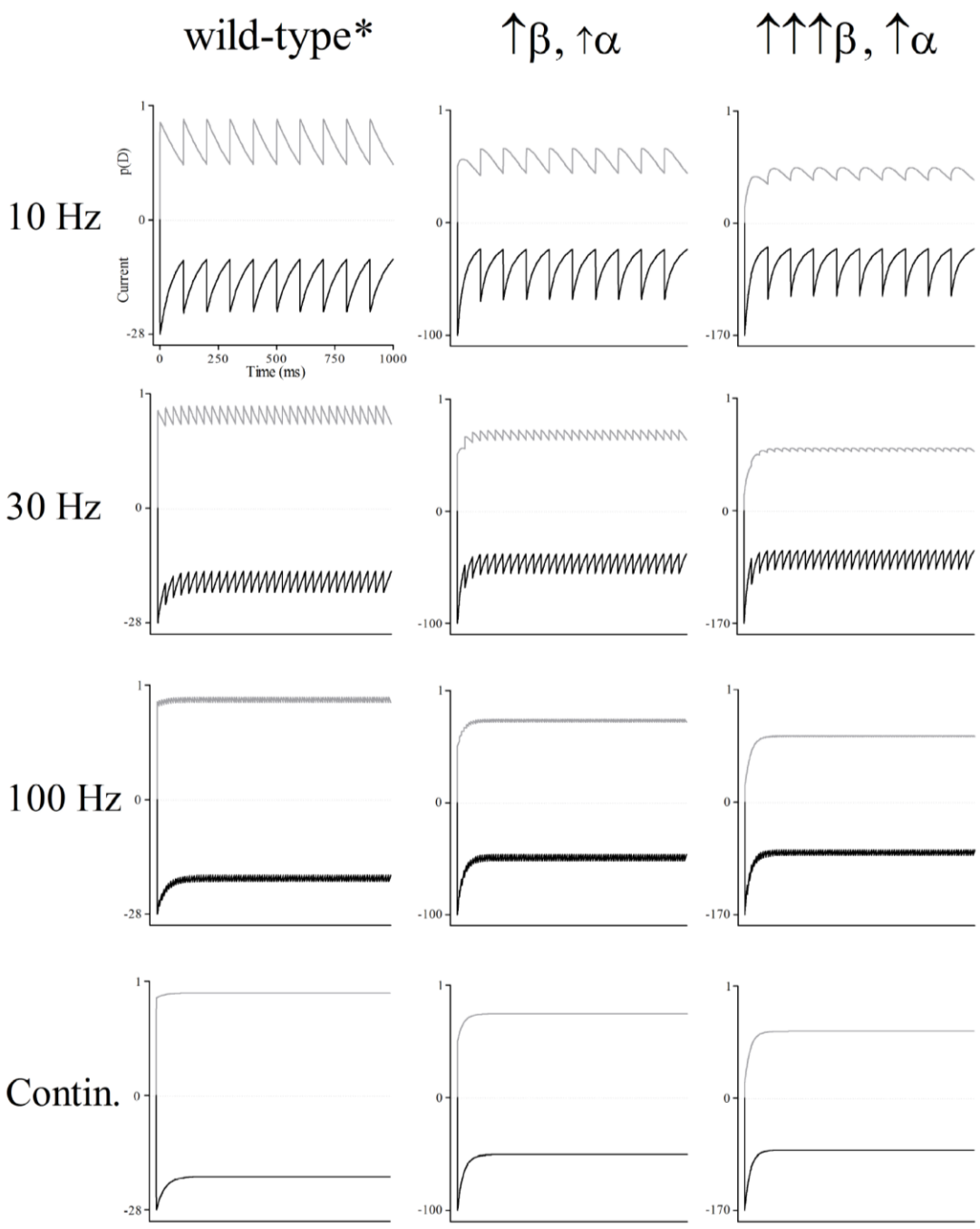

*Figure 7. Increased repeated pulse inhibition can occur despite decreased desensitized state occupancy. * indicates modified rate constants, see text.*

Consistent with our hypothesis, the simulations showed that no single rate constant in either model could cause the extent of RPI to change in a direction opposite that of D state occupancy (i.e., increased or decreased RPI was always associated with increased or decreased D state occupancy, respectively). For example, in the branched model, either increasing β or decreasing α led to dereased RPI (because these changes decreased the extent of macroscopic desensitization; Bianchi et al., 2007) and D state occupancy (increasing efficacy (β/α) in the branched model increased O state occupancy at the expense of occupancy in all other states; Appendix I). In the linear model, either increasing β or decreasing α led to increased RPI (because these changes increased the extent of macroscopic desensitization; Bianchi et al., 2007) and D state occupancy (increasing efficacy in the linear model increases occupancy of both O and D states; Appendix I). In both models, increasing δ or decreasing ρ always increased RPI (because these changes increased the extent of macroscopic desensitization; Bianchi et al., 2007) and increased D state occupancy (Appendix I).

However, changes in RPI extent did not necessarily parallel those of D state occupancy when multiple rate constants were changed, a scenario often encountered with disease-causing mutations and allosteric modulators. An example is shown in Figure 7, where the response of the branched model to pulse trains of 10, 30, and 100 Hz or to continuous application in the setting of increased channel efficacy (β/α) mediated by a simultaneous increase in *both* the channel opening (β) and closing (α) rate. The "wild type" condition (K_{on} = 7x10^6, K_{off} = 3000, β = 1000, α = 30, δ = 6000, and ρ = 20 s^{-1}) is shown in the left column, while conditions of increased efficacy are shown in the middle (β = 6000 and α = 60 s^{-1}) and right (β = 3x10^4 and α = 120 s^{-1}) columns. As in previous

figures, p(D) was shown as an upward trace, while the resulting currents were shown as downward traces (note that currents were scaled to peak p(O) to facilitate comparison of RPI extent). The results demonstrate that so long as the channel opening rate (β) increases more than the channel closing rate (α), the extent of RPI increases despite p(D) decreasing. This reflects the fact that increased efficacy in branched models necessarily decreases p(D) (Appendix I). However, when increases in efficacy are accompanied by an increase in the channel closing rate (α), the extent of macroscopic desensitization increases, reflecting the increased disparity between the channel closing rate (α) and the resensitization rate (ρ) (Appendix V). This same effect was observed in the branched model with decreases in D state stability (δ/ρ) that were mediated by greater reductions in the desensitization rate (δ) than the resensitization rate (ρ) – the reduction in D state stability (δ/ρ) necessarily reduced D state occupancy, but because of the increased disparity between the channel closing rate (α) and the resensitization rate (ρ), the extent of desensitization actually increased (data not shown).

DISCUSSION

The phenomenon of repeated pulse inhibition depends on the relationships among macroscopic, and not microscopic, $GABA_A$ receptor properties

Simulations using simple Markov models of $GABA_A$ receptor function demonstrated that the extent and rate of RPI, like all other macroscopic current properties (e.g., activation, desensitization, deactivation), could not be attributed to individual microscopic kinetic parameters such as the lifetime or fractional occupancy of desensitized states. Indeed, for any given desensitized state occupancy, a wide range of RPI profiles were possible, including the absence of RPI or even the phenomenon of RPE (Figure 4). Even relative changes in D state occupancy could not be inferred from changes in RPI kinetics, as illustrated by the example of increasing channel efficacy, which increased RPI extent while decreasing D state occupancy (Figure 7). Despite these complexities, our simulations definitively demonstrated that RPI could not occur in the absence of desensitized states (i.e., C-C-O models do not exhibit RPI at any stimulation frequency; data not shown). In other words, D states were necessary (though they did not necessarily need to be long-lived) but not sufficient for RPI to be observed.

Interestingly, despite the emphasis on microscopic "mechanisms" throughout the literature of ion channel biophysics, we have demonstrated that in fact macroscopic desensitization was critical, being both necessary and sufficient for RPI to be observed. This fundamental relationship was demonstrated using a variety of modeling approaches, and appeared to be independent of model size or connectivity (though we limited our simulations to non-cyclic gating schemes). Thus, the relationship between macroscopic desensitization and RPI may generalize not only to other ligand-gated channels, but also

to voltage-gated channels (where the analogous phenomenon to macroscopic desensitization is termed "inactivation"). Interestingly, the time course of macroscopic desensitization was found to impose a limit on RPI kinetics, such that the rate and extent of RPI could approach but never exceed that of macroscopic desensitization, regardless of the underlying D state kinetics. Given that firing frequencies considerably higher than those tested in this study have been documented throughout the brain in both normal and abnormal conditions, the results suggest that macroscopic desensitization may have broad physiological significance, despite the fact that experimental visualization of this phenomenon requires application of agonist for physiologically irrelevant durations (a prominent criticism of early desensitization studies).

However, the results demonstrated that RPI kinetics were influenced not only by the time course macroscopic desensitization, but also by the time course of deactivation. This extends the physiological significance of deactivation, which is already thought to be the primary determinant of IPSC decay rate (Jones and Westbrook, 1995; Galarreta and Hestrin, 1997). Indeed, while macroscopic desensitization facilitated RPI, deactivation attenuated RPI by promoting receptor availability for reactivation. In other words, deactivation determined the position of RPI between two boundaries – that of macroscopic desensitization and that of full recovery (i.e., no RPI). The functional consequence of changes in deactivation time course was a shift in the frequency response profile of the receptor. Compared to slowly deactivating currents, those with rapid deactivation required higher stimulation frequencies to exhibit RPI, and higher frequencies to reach the limit imposed by macroscopic desensitization. Thus, the low-

pass frequency filter imposed by RPI on $GABA_A$ receptor responses is determined, at least in part, by deactivation.

Of note, the sensitivity of RPI to both macroscopic desensitization and deactivation implied that the phenomenon would be exquisitely sensitive to changes in certain rate constants and relatively insensitive to changes in others, reflecting the fact that these current properties can be differentially sensitive to changes in certain rate constants, a phenomenon termed desensitization-deactivation uncoupling (Bianchi et al., 2007). For example, in the linear model, increasing the channel opening rate (β) not only increased the rate and extent of macroscopic desensitization (Bianchi et al., 2007), but also prolonged deactivation (by increasing the mean bound time; Appendix II), the combination of which markedly increased the rate and extent of RPI (data not shown). Conversely, in the branched model, increasing the channel opening rate (β) decreased the rate and extent of macroscopic desensitization (Bianchi et al., 2007) but prolonged deactivation (by increasing the mean bound time; Appendix II), the result being offsetting effects on RPI kinetics (data not shown).

Unexpectedly, understanding how desensitization and deactivation shaped RPI provided an intuitive kinetic explanation for the phenomenon of repeated pulse enhancement (RPE), which in addition to being observed in many of our simulations, has also been observed in a variety of experimental settings (Nathan and Lambert, 1991; Lambert and Wilson, 1994; Wilcox and Dichter, 1994; Fleidervish and Gutnick, 1995). Simply, both phenomena reflect a system attempting to reach equilibrium. What differs is the manner in which the underlying system accomplishes this task. In the case of currents that exhibit macroscopic desensitization, equilibrium occupancy of the O state is

less than the transient peak occupancy (i.e., currents overshoot their equilibrium value). Thus, if the first pulse is of sufficient duration to achieve peak O state occupancy, then subsequent activation can only cause O state occupancy to decrease, as this drives the system closer to its equilibrium value. The only way that subsequent activation can achieve the same O state occupancy is if all receptors have returned to the unbound state, meaning that deactivation is shorter than the inter-pulse interval. But in the case of currents that fail to exhibit macroscopic desensitization, peak and equilibrium O state occupancy are one and the same (i.e., currents do not overshoot their equilibrium values). Thus, only if the first pulse is of infinite duration will peak O state occupancy ever be achieved. For any shorter pulse length, O state occupancy will be less than maximal, and subsequent activation will drive the system closer to equilibrium, giving the appearance of current enhancement.

The physiological significance of macroscopic desensitization

Macroscopic desensitization has been observed for nearly all ligand-gated ion channels (Jones and Westbrook, 1996; Bianchi and Macdonald, 2002; Mohammadi et al., 2003; Robert and Howe, 2003; Schorge and Colquhoun, 2003; Tsuneki et al., 2007). In the case of $GABA_A$ receptors, desensitization can be extensive and multi-phasic, with as many as four components having been identified (time constants ranging from ~10 ms to ~10 s) (Celentano and Wong, 1994; Haas and Macdonald, 1999; Bianchi and Macdonald, 2002; Lagrange et al., 2007). Desensitization kinetics are highly dependent on subunit composition (Bianchi et al., 2002; Fisher, 2007; Lagrange et al., 2007). For example, while γ subunit-containing isoforms give rise to macroscopic currents that desensitize

rapidly and extensively, those containing δ subunits desensitize slowly and to a much lesser extent (Haas and Macdonald, 1999; Bianchi and Macdonald, 2002). The subunit-dependence of desensitization is of particular interest given the subunit-dependence of receptor subcellular localization. Receptor isoforms containing γ subunits are found primarily in synapses, where they are transiently activated by nearly-saturating concentrations of GABA ("phasic" inhibition). In contrast, those containing δ subunits are targeted extrasynaptically, where they are persistently activated by sub-saturating concentrations of ambient GABA ("tonic" inhibition) (Farrant and Nusser, 2005). Desensitization has therefore been suggested to represent an important mechanism for tuning receptor responses to specific contexts of activation (Jones and Westbrook, 1995, 1996; Bianchi and Macdonald, 2002; Overstreet et al., 2002; Lagrange et al., 2007).

However, the physiological relevance of desensitization has remained a matter of some debate. Even the fastest phase of desensitization occurs with a time constant over an order of magnitude longer than the presumed duration of the synaptic transient (~10 ms vs. <1 ms, respectively; Clements, 1996; Bianchi and Macdonald, 2002; Mozrzymas, 2004), prompting some investigators to call desensitization "more of an experimental nuisance than a physiologically interesting phenomenon" (Colquhoun and Sakmann, 1998). Others have disagreed, arguing that the underlying D state provides an additional agonist-bound conformation from which channels can re-open, extending the duration of synaptic currents (Jones and Westbrook, 1995, 1996). While true, it should be emphasized that addition of D states to kinetic models necessarily decreases open probability, meaning that regardless of deactivation time course, net charge transfer must decrease. Moreover, it was recently demonstrated fast desensitization actually

accelerates early phases of IPSC decay, suggesting that desensitization serves to reshape rather than to enhance IPSCs (Bianchi et al., 2007). Unfortunately, such a role appears to be reserved for fast desensitization, as elimination of intermediate and slow desensitized states from comprehensive kinetic models had minimal predicted effects on either the amplitude or decay of individual IPSCs (Haas and Macdonald, 1999).

The results of this and one other study (Bianchi and Macdonald, 2002), however, suggest that the unique property conferred by macroscopic desensitization is the ability to modulate signal intensity in the setting of repetitive activation. In the case of receptor isoforms that exhibit multi-phasic macroscopic desensitization, this finding implies that all phases will have relevance in the setting of high frequency stimulation, not just the slow phases. The difference is that slow phases can only influence RPI kinetics after prolonged repetitive activation, whereas fast phases can manifest themselves after even short bursts.

REFERENCES

Ben-Ari, Y., Krnjevic, K., & Reinhardt, W. (1979). Hippocampal seizures and failure of inhibition. *Can. J. Physiol. Pharmacol.* 57, 1462-1466.

Ben-Ari, Y., Krnjevic, K., Reiffenstein, R. J., & Reinhardt, W. (1981). Inhibitory conductance changes and action of γ-aminobutyrate in rat hippocampus. *Neuroscience* 6, 2445-2463.

Bianchi, M. T., Haas, K. F., & Macdonald, R. L. (2001). Structural determinants of fast desensitization and desensitization-deactivation coupling in GABAa receptors. *J.Neurosci.* 21, 1127-1136.

Bianchi, M. T. & Macdonald, R. L. (2001). Mutation of the 9' leucine in the GABA(A) receptor gamma2L subunit produces an apparent decrease in desensitization by stabilizing open states without altering desensitized states. *Neuropharmacology* 41, 737-744.

Bianchi, M. T. & Macdonald, R. L. (2001). Agonist Trapping by GABAA Receptor Channels. *J.Neurosci.* 21, 9083-9091.

Bianchi, M. T. & Macdonald, R. L. (2002). Slow phases of GABA(A) receptor desensitization: structural determinants and possible relevance for synaptic function. *J.Physiol* 544, 3-18.

Bianchi, M. T., Botzolakis, E. J., Haas, K. F., Fisher, J. L., & Macdonald, R. L. (2007). Microscopic kinetic determinants of macroscopic currents: insights from coupling and uncoupling of GABAA receptor desensitization and deactivation. *J.Physiol* 584, 769-787.

Burkat, P. M., Yang, J., & Gingrich, K. J. (2001). Dominant gating governing transient GABA(A) receptor activity: a first latency and Po/o analysis. *J.Neurosci.* 21, 7026-7036.

Celentano, J. J. & Wong, R. K. (1994). Multiphasic desensitization of the $GABA_A$ receptor in outside-out patches. *Biophys.J.* 66, 1039-1050.

Colquhoun, D. & Hawkes, A. G. (1981). On the stochastic properties of single ion channels. *Proc.R.Soc.Lond.B.Biol.Sci.* 211, 205-235.

Colquhoun, D. & Sakmann, B. (1998). From muscle endplate to brain synapses: a short history of synapses and agonist-activated ion channels. *Neuron*, 20, 381-387.

Clements, J. D. (1996). Transmitter timecourse in the synaptic cleft: its role in central synaptic function. *Trends Neurosci.* 19, 163-171.

Connors, B. W., Gutnick, M. J., & Prince, D. A. (1982). Electrophysiological properties of neocortical neurons in vitro. *J.Neurophysiol* 48, 1302-1320.

Davies, C. H. & Collingridge, G. L. (1993). The physiological regulation of synaptic inhibition by GABAB autoreceptors in rat hippocampus. *J.Physiol* 472, 245-265.

Deisz, R. A. & Prince, D. A. Frequency-dependent depression of inhibition in guinea-pig neocortex in vitro by $GABA_B$ receptor feed-back on GABA release. *J.Physiol* 412, 513-541.

Desarmenien, M., Feltz, P., & Headley, P. M. (1980). Does glial uptake affect GABA responses? An intracellular study on rat dorsal root ganglion neurons in vitro. *J.Physiol.* 307, 163-182.

Farrant, M. & Nusser, Z. (2005). Variations on an inhibitory theme: phasic and tonic activation of GABA(A) receptors. *Nat.Rev.Neurosci*. 6, 215-229.

Feng, H. J., Botzolakis, E. J., & Macdonald, R. L. (2009). Context-dependent modulation of alphabetagamma and alphabetadelta GABAA receptors by penicillin: implications for phasic and tonic inhibition. *Neuropharmacology* 56, 161-173.

Fisher, J. L. & Macdonald, R. L. (1997). Single channel properties of recombinant GABAA receptors containing gamma 2 or delta subtypes expressed with alpha 1 and beta 3 subtypes in mouse L929 cells. *J.Physiol* 505 (Pt 2), 283-297.

Fleidervish, I. A. & Gutnick, M. J. (1995). Paired-pulse facilitation of IPSCs in slices of immature and mature mouse somatosensory neocortex. *J.Neurophysiol*. 73, 2591-2595.

Fortune, E. S. & Rose, G. J. (2001). Short-term synaptic plasticity as a temporal filter. *Trends Neurosci.* 24, 381-385.

Fukuda, A., Mody, I., & Prince, D. A. (1993). Differential ontogenesis of presynaptic and postsynaptic $GABA_B$ inhibition in rat somatosensory cortex. *J.Neurophysiol.* 70, 448-452.

Galarreta, M. & Hestrin, S. (1997). Properties of $GABA_A$ receptors underlying inhibitory synaptic currents in neocortical pyramidal neurons. *J.Neurosci.* 17, 7220-7227.

Galarreta, M. & Hestrin, S. (1998). Frequency-dependent synaptic depression and the balance of excitation and inhibition in the neocortex. *Nat. Neurosci.* 1, 587-594.

Glavinovic, M. I. (1999). Monte carlo simulation of vesicular release, spatiotemporal distribution of glutamate in synaptic cleft and generation of postsynaptic currents. *Pflugers Arch.* 437, 462-470.

Grande, L.A. & Spain, W. J. (2005). Synaptic depression as a timing device. *Physiology (Bethesda)* 20, 201-210.

Haas, K. F. & Macdonald, R. L. (1999). GABAA receptor subunit gamma2 and delta subtypes confer unique kinetic properties on recombinant GABAA receptor currents in mouse fibroblasts. *J.Physiol* 514 (Pt 1), 27-45.

Hinkle, D. J., Bianchi, M. T., & Macdonald, R. L. (2003). Modifications of a commercial perfusion system for use in ultrafast solution exchange during patch clamp recording. *Biotechniques* 35, 472-474.

Huguenard, J. R. & Alger, B. E. (1986). Whole-cell voltage-clamp study of the fading of GABA-activated currents in acutely dissociated hippocampal neurons. *J.Neurophysiol.* 56, 1-18.

Jones, M. V. & Westbrook, G. L. (1995). Desensitized states prolong GABAA channel responses to brief agonist pulses. *Neuron* 15, 181-191.

Jones, M. V. & Westbrook, G. L. (1996). The impact of receptor desensitization on fast synaptic transmission. *Trends Neurosci.* 19, 96-101.

Krnjevic, K. (1984). Some functional consequences of GABA uptake by brain cells. *Neurosci.Lett.* 47, 283-287.

Lagrange, A. H., Botzolakis, E. J., & Macdonald, R. L. (2007). Enhanced macroscopic desensitization shapes the response of alpha4 subtype-containing GABAA receptors to synaptic and extrasynaptic GABA. *J.Physiol.* 578, 655-676.

Lambert, N. A. & Wilson, W. A. (1994). Temporally distinct mechanisms of use-dependent depression at inhibitory synapses in the rat hippocampus in vitro. *J.Neurophysiol.* 72, 121-130.

Lema, G. M. & Auerbach, A. (2006). Modes and models of GABA(A) receptor gating. *J.Physiol.* 572, 183-200.

Macdonald, R. L. & Olsen, R. W. (1994). GABAA receptor channels. *Annu.Rev.Neurosci.* 17, 569-602.

Maconochie, D. J., Zempel, J. M., & Steinbach, J. H. (1994). How quickly can GABAA receptors open? *Neuron* 12, 61-71.

Mazzuferi, M., Palma, E., Martinello, K., Maiolino, F., Roseti, C., Fucile, S., Fabene, P. F., Schio, F., Pellitteri, M., Sperk, G., Miledi, R., Eusebi, F., & Simonato, M. (2010). Enhancement of GABA(A)-current run-down in the hippocampus occurs at the first spontaneous seizure in a model of temporal lobe epilepsy. *Proc.Natl.Acad.Sci.U.S.A.* 107, 3180-3185.

McCarren, M. & Alger, B. E. (1985). Use-dependent depression of IPSPs in rat hippocampal pyramidal cells in vitro. *J.Neurophysiol.* 53, 557-571.

McManus, O. B., Weiss, D. S., Spivak, C. E., Blatz, A. L., & Magleby, K. L. (1988). Fractal models are inadequate for the kinetics of four different ion channels. *Biophys.J.* 54, 859-870.

Metherate, R. & Ashe, J. H. (1994). Facilitation of an NMDA receptor-mediated EPSP by paired-pulse stimulation in rat neocortex via depression of GABAergic IPSPs. *J.Physiol.* 481, 331-348.

Mohammadi, B., Krampfl, K., Cetinkaya, C., Moschref, H., Grosskreutz, J., Dengler, R., and Bufler, J. (2003). Kinetic analysis of recombinant alpha(1) and alpha(1)beta glycine receptor channels. *Eur.Biophys.J.* 32, 529-536.

Mozrzymas, J. W., Barberis, A., Mercik, K., & Zarnowska, E. D. (2003). Binding sites, singly bound states, and conformation coupling shape GABA-evoked currents. *J.Neurophysiol.* 89, 871-883.

Mozrzymas, J. W. (2004). Dynamism of GABA(A) receptor activation shapes the "personality" of inhibitory synapses. *Neuropharmacology* 47, 945-960.

Nathan, T. and Lambert, J. D. (1991). Depression of the fast IPSP underlies paired-pulse facilitation in area CA1 of the rat hippocampus. *J.Neurophysiol*. 66, 1704-1715.

Numann, R. E. & Wong, R. K. S. (1984). Voltage-clamp study on GABA response desensitization in single pyramidal cells dissociated from the hippocampus of adult guinea pig. *Neurosci. Lett.* 47, 289-294.

Overstreet, L. S., Jones, M. V., & Westbrook, G. L. (2000). Slow desensitization regulates the availability of synaptic GABA(A) receptors. *J.Neurosci.* 20, 7914-7921.

Palma, E, Esposito, V., Mileo, A. M., DiGennaro, G., Quarato, P., Giangaspero, F., Scoppetta, C., Onorati, P., Trettei, F., Miledi, R., & Eusebi, F. (2002). Expression of human epileptic temporal lobe neurotransmitter receptors in Xenopus oocytes: An innovative approach to study epilepsy. *Proc.Natl.Acad.Sci.U.S.A.* 99, 15078-15083.

Reyes, A., Lujan, R., Rozov, A., Burnashev, N., Somogyi, P., & Sakmann, B. (1998). Target-cell-specific facilitation and depression in neocortical circuits. *Nat.Neurosci*. 1, 279-285.

Robert, A. & Howe, J. R. (2003). How AMPA receptor desensitization depends on receptor occupancy. *J.Neurosci*. 23, 847-858.

Roseti, C., Martinelo, K., Fucile, S., Piccari, V., Mascia, A., DiGennaro, G., Quarato, P. P., Manfredi, M., Esposito, V., Cantore, G., Arcella, A., Simonato, M., Fredholm, B. B., Limatola, C., Miledi, R., & Eusebi, F. (2008). Adenosine receptor antagonists alter the stability of human epileptic GABAA receptors. *Proc.Natl.Acad.Sci.U.S.A.* 105, 15118-15123.

Rula, E. Y., Lagrange, A. H., Jacobs, M. M., Hu, N., Macdonald, R. L., & Emeson, R. B. (2008). Developmental modulation of GABA(A) receptor function by RNA editing. *J.Neurosci.* 28, 6196-6201.

Scheller, M. & Forman, S. A. (2002). Coupled and uncoupled gating and desensitization effects by pore domain mutations in GABA(A) receptors. *J.Neurosci.* 22, 8411-8421.

Schorge, S. & Colquhoun, D. (2003). Studies of NMDA receptor function and stoichiometry with truncated and tandem subunits. *J.Neurosci*. 23, 1151-1158.

Shelley, C. & Magleby, K. L. (2008). Linking exponential components to kinetic states in markov models for single-channel gating. *J.Gen.Physiol* 132, 295-312.

Thompson, S. M. & Gahwiler, B. H. (1989). Activity-dependent disinhibition. I. Repetitive stimulation reduces IPSP driving force and conductance in the hippocampus in vitro. *J.Neurophysiol* 61, 501-511.

Thompson, S. M. & Gahwiler, B. H. (1989). Activity-dependent disinhibition. III. Desensitization and $GABA_B$ receptor-mediated presynaptic inhibition in the hippocampus in vitro. *J.Neurophysiol* 61, 524-533.

Tsuneki, H., Kobayashi, S., Takagi, K., Kagawa, S., Tsunoda, M., Murata, M., Matsuoka, T., Wada, T., Kurachi, M., Kimura, I., & Sasaoka, T. (2007). Novel G423S mutation of human alpha7 nicotinic receptor promotes agonist-induces desensitization by a protein kinase C-dependent mechanism. *Mol.Pharmacol*. 71, 777-786.

Varela, J. A., Song, S., Turrigiano, G. G., & Nelson, S. B. (1999). Differential depression at excitatory and inhibitory synapses in visual cortex. *J.Neurosci.* 19, 4293-4304.

Wilcox, K.S. & Dichter, M. A. (1994). Paired pulse depression in cultured hippocampal neurons is due to a presynaptic mechanism independent of GABAB autoreceptor activation. *J.Neurosci*. 14, 1775-1788.

Wong, R. K. & Watkins, D. J. (1982). Cellular factors influencing GABA response in hippocampal pyramidal cells. *J.Neurophysiol* 48, 938-951.

CHAPTER VIII

CONCLUSION

Emmanuel J. Botzolakis and Robert L. Macdonald

The relationship microscopic and macroscopic kinetic phenomena

The primary goals of this dissertation were to determine the microscopic kinetic factors that shape $GABA_A$ receptor macroscopic currents, to use this information to develop an algorithm for interpreting the effects of mutations and modulators, and to apply this algorithm to answer long-standing questions in the field of $GABA_A$ receptor research. These goals were accomplished through a combination of theoretical studies using Markov models of $GABA_A$ receptor function, which systematically evaluated the relationship between microscopic rate constants and macroscopic current properties, and electrophysiological studies of recombinant $GABA_A$ receptors expressed in HEK293T cells, which tested the hypotheses generated by the theoretical studies and illustrated the utility of the algorithmic approach.

Both the theoretical and electrophysiological studies demonstrated that macroscopic current properties depended on a complex interplay among all rate constants in the gating scheme, and consequently, that changes in individual macroscopic current properties could not be attributed with any degree of certainty to changes in individual rate constants. For example, while delaying agonist unbinding could prolong the time course of deactivation, so could increasing the stability of open and/or desensitized states

(Chapter II). This reflected the fact that stabilizing fully liganded states increased the mean time receptors were GABA-bound (since unbinding can only occur from a subset of all states), which allowed channel activity to persist for an extended period of time (Appendix II). The relationship between macroscopic desensitization and the stability of open and desensitized states was more complex, depending not only on every rate constant in the gating scheme, but also on the arrangement of states in the model (i.e., "branched" vs. "linear" desensitized states; Chapter II). In the linear model, macroscopic desensitization was increased when either open or desensitized states were stabilized. However, in the branched model, macroscopic desensitization was increased only when desensitized states were stabilized; stabilizing open states actually decreased macroscopic desensitization (Chapter II). This reflected the fact that stabilizing the open state in the branched model shifted its behavior towards that of the C-C-O arrangement, which could not undergo macroscopic desensitization (Appendix IV). Interestingly, while all rate constants influenced the extent and time course of macroscopic desensitization, only a subset of rate constants determined whether macroscopic desensitization could actually occur. For example, the linear model could only desensitize when the channel opening rate (β) was larger than the resensitization rate (ρ). In contrast, the branched model could only desensitize when the channel closing rate (α) was larger than the resensitization rate (ρ) (Appendix IV). Like desensitization and deactivation, every other macroscopic current property (rise time, amplitude, EC_{50}, paired pulse recovery, etc.) was also found to have a complex dependence on microscopic rate constants (Botzolakis, Bianchi, Smith, and Macdonald, unpublished observations).

Admittedly, these findings were somewhat discouraging, as they suggested that the relationships between macroscopic currents and microscopic rate constants were possibly too complex to allow mechanistic insight to be obtained from macroscopic observations alone. However, it was soon realized that combining macroscopic observations could impose tremendous constraints on the possible explanations for the macroscopic effects of a given mutation or modulator. Indeed, while the time course of desensitization and deactivation were both influenced by all rate constants in the gating scheme, their differential sensitivities to changes in certain rate constants could be exploited to include or exclude rate constants from consideration. For example, deactivation was prolonged whenever changing a rate constant increased receptor mean bound time; however, only a subset of rate constants increased mean bound time and yet decreased the extent of macroscopic desensitization (Chapter II; Appendix II). In fact, such an observation could only be explained with increases in single channel efficacy (i.e., increased channel opening rate or decreased channel closing rate) and only with kinetic models that contained a branched desensitized state. Thus, by asking just two macroscopic "questions" (Is the extent of macroscopic desensitization increased or decreased? Is deactivation accelerated or prolonged?) the microscopic transition targeted by certain mutations and modulators could be exposed (Chapter II). Moreover, with only one additional "question" (Is peak current increased or decreased?), every state transition in simple 4-state models of $GABA_A$ receptor function could be identified as the target of a mutation or modulator. These questions, combined with a few basic single channel experiments, were used to generate the first experimental algorithm for interpreting changes in macroscopic currents in terms of microscopic mechanisms. Preliminary

studies indicate that adding a fourth "question" (Is current rise time faster or slower?) will allow the algorithm to be extended further, such that the actual rate constant, and not just the reversible state transition, could be identified (Botzolakis, Smith, and Macdonald, unpublished observations). This suggested that microscopic transitions in even larger kinetic schemes could eventually be identified, the caveat simply being that more "questions" will be required as the number of states is increased.

Our preliminary "four-question" algorithm, however, was sufficient to identify the rate constant targeted by the most widely prescribed class of $GABA_A$ receptor modulator, the benzodiazepines. Up to this point, there has been considerable disagreement regarding the mechanism of action of these drugs. While single channel studies have made compelling arguments that benzodiazepines increase receptor affinity for GABA (Twyman et al., 1989; Rogers et al., 1994), other studies have suggested that benzodiazepines act by increasing efficacy (Rusch and Forman, 1005; Campo-Soria et al., 2006). By applying the algorithm to whole cell currents evoked from recombinant $\alpha1\beta3\gamma2$ $GABA_A$ receptors, however, we demonstrated not only that benzodiazepines act by increasing GABA affinity, but also that this increase was specifically mediated by a slower unbinding rate, as this was the only mechanism by which macroscopic desensitization could appear unchanged (when evoked by saturating concentrations of GABA) in the context of prolonged deactivation (Chapter III). In fact, this pattern of desensitization and deactivation appeared to be the macroscopic "fingerprint" of changes in the microscopic unbinding rate, as it was independent of the connectivity or number of states in the gating scheme (Chapter II). Interestingly, this pattern was also observed when currents were evoked by different agonists (GABA, muscimol, and THIP),

suggesting they differed not in terms of their mode of channel gating, but rather, in terms of their microscopic affinity for the receptor (Chapter II).

In addition to allowing the experimental algorithm to be generated, understanding the kinetic determinants of desensitization and deactivation provided simple explanations for several unresolved issues in the field of $GABA_A$ receptor biophysics. First, while fast desensitization has been shown to prolong deactivation, a phenomenon referred to as desensitization-deactivation "coupling", numerous examples of desensitization-deactivation "uncoupling" have been reported (Bianchi et al., 2001; Scheller and Forman, 2002; Fisher, 2004; Mercik et al., 2006; Barberis et al., 2007; Chapter II). The kinetic basis for uncoupling, however, was not entirely clear. If macroscopic desensitization required the presence of microscopic desensitized states, and the presence of those states delayed agonist unbinding, then how could increased macroscopic desensitization ever be associated with faster deactivation (or vice versa)? The answer was provided by our simulations, which as discussed above, demonstrated that the macroscopic phenomenon of desensitization was as intimately linked to the process of channel opening and closing as it was to the process of entering and exiting desensitized states. Even the rates of binding and unbinding could influence the time course of macroscopic desensitization. Changing many of these rate constants, however, had opposite effects on desensitization and deactivation, thus giving the appearance of uncoupling (Chapter II). In fact, our simulations indicated that coupling was as likely to be observed as uncoupling: of the 12 microscopic transitions systematically evaluated for their ability to modulate macroscopic desensitization and deactivation, 6 could were found to promote coupling (linear model:

α, β, δ, and ρ; branched model: δ and ρ) and 6 were found to promote uncoupling (linear model: K_{on} and K_{off}; branched model: K_{on}, K_{off}, α, β).

Second, the arrangement of desensitized states in kinetic models of $GABA_A$ receptor function has thus far been somewhat arbitrary. Granted, branched arrangements have typically provided the best fits of macroscopic and microscopic data (Chapter VI), but optimized mathematical fitting is by no means adequate proof for such an arrangement, as it assumes the core gating scheme to which desensitized states are being added is already correct. However, the fact that desensitization-deactivation uncoupling has been observed with several mutations and pharmacological agents that altered channel efficacy (e.g., the TM2 9' leucine mutation and the anticonvulsant barbiturates, respectively; Chapter II; Twyman et al., 1989; Feng et al., 2004) strongly suggested the existence of a branch point in the underlying channel gating scheme. Indeed, purely linear state arrangements could not cause desensitization and deactivation to appear uncoupled, except in the special case of altered agonist binding or unbinding rates, as discussed above (Chapter II, III). That being said, the possibility that receptors have access to both types of desensitized states cannot be excluded. In fact, it is worth mentioning that existing comprehensive models technically already include both types of states, as the distal closed states responsible for channel bursting have an arrangement with respect to the open states identical to that of linear desensitized states. While some might argue that these states do not have sufficiently long lifetimes to warrant classification as "desensitized" states, it should be emphasized that in linear arrangements, the requirements for macroscopic desensitization are such that the open state can actually have a longer lifetime than that of the desensitized state, and yet, still

support substantial macroscopic desensitization (i.e., desensitization requires that $\beta > \rho$, but dwell time in the open state is equal to $1/(\alpha + \delta)$).

Third, the minimal macroscopic desensitization observed with currents from δ-subunit containing receptors has long seemed at odds with the known ability of these isoforms to enter closed states with lifetimes and proportions similar to (if not greater than) those of γ-subunit containing isoforms, which undergo rapid and extensive macroscopic desensitization (Fisher and Macdonald, 1997; Haas and Macdonald, 1999). While somewhat counterintuitive, the fact that macroscopic desensitization has specific microscopic requirements provides a simple explanation for this phenomenon. Consider, for example, the branched arrangement where exit rates from open and desensitized states are equal (i.e., $\alpha = \rho$). So long as this kinetic relationship is maintained, macroscopic desensitization will never be observed (Appendix IV), even if the entry rate into the desensitized state (δ) is increased by several orders of magnitude such that the vast majority of receptors are found in the desensitized state at equilibrium (Appendix I). Thus, the absence of macroscopic desensitization should never be taken to indicate the absence of microscopic desensitized states. The converse, however, is not true – macroscopic desensitization necessitates the existence of microscopic desensitized states, as C-C-O arrangements were proven to always generate "flat" currents (Appendix IV). Even then, however, neither the rate nor the extent of macroscopic desensitization was found to correspond to the entry/exit rates or fractional occupancy of the desensitized state (Chapter II).

Fourth, while it has been known for some time that simple open channel block can have unusual effects on macroscopic currents (Ascher, et al., 1978; Marty, 1978;

Lipton, 2005, 2006), the kinetic bases for these effects remain unclear. The ability of an open channel blocker to decrease the extent of macroscopic desensitization is perhaps most counterintuitive (Chapter IV), as blocked states were expected to provide channels with an additional route for closure (besides that already provided by existing desensitized states), and therefore, to increase current desensitization. The simulations, however, demonstrated that open channel block was no different than adding a linear desensitized state to the gating scheme, which as discussed above, can only cause macroscopic desensitization under certain conditions ($\beta > \rho$). By analogy, when the exit rate from the blocked state (k+) was equal to or greater than the channel opening rate (β), a macroscopically non-desensitizing (i.e., flat) current was favored. Consequently, stabilizing non-desensitizing blocked states (by increasing the concentration of blocker) necessarily gave the appearance of attenuated macroscopic desensitization, as this decreased the contribution of the existing desensitized states (which supported macroscopic desensitization) to the macroscopic current.

The physiological significance of macroscopic desensitization and deactivation

Having exposed the microscopic determinants of desensitization and deactivation, the next goal of this dissertation was to determine the possible physiological relevance of these macroscopic phenomena. While it is generally agreed that the time course of deactivation determines the rate of IPSC decay, this only pertains to deactivation following brief GABA pulses (~1 ms), which are intended to mimic the synaptic GABA transient. But what of deactivation following longer pulses of GABA, which typically has a much longer time course? Is this process only of interest to kineticists, who apply it

as a constraint during fitting of microscopic rate constants to putative gating schemes? And what about macroscopic desensitization, which by definition, is the loss of current in the continued presence of agonist? Does the fact that receptors are exposed to GABA *in vivo* for 1 millisecond or less (Clements, 1996; Mozrzymas, 2004), and not for 100s to 1000s of milliseconds, automatically make this phenomenon physiologically irrelevant? To gain insight into the possible biological significance of desensitization and deactivation, we explored how changes in these macroscopic properties affected receptor currents evoked under three distinct physiological contexts. This included the classic synaptic context, where receptors are transiently activated by nearly saturating concentrations of GABA; the perisynaptic context, where receptors are also transiently activated, but by lower concentrations of GABA and likely in the context of baseline GABA exposure; and the extrasynaptic context, where receptors are persistently activated by extremely low concentrations of ambient GABA.

From the synaptic standpoint, investigators have argued that desensitization is an important determinant of IPSC decay, as the underlying desensitized state provides receptors with additional opportunities to re-open, thus enhancing GABAergic synaptic transmission by prolonging receptor deactivation (Jones and Westbrook, 1995, 1996). This explanation, however, has long left something to be desired. Although our simulations clearly supported the idea that stabilizing desensitized states prolongs current deactivation, to conclude that desensitized states enhance charge transfer ignores their known ability to decrease peak current amplitudes (Haas and Macdonald, 1999). Indeed, our simulations indicate that it is impossible to increase IPSC charge transfer by adding a non-conducting state to the gating scheme (Botzolakis and Macdonald, unpublished

observations). Moreover, both the simulations (Chapters II and IV) and the experimental results (Chapter IV) demonstrated that stabilizing desensitized states had mixed effects on deactivation time course; while fast phases were accelerated, slow phases were markedly prolonged. This suggested that the role of desensitized states was not to enhance charge transfer, but rather, to redistribute it. In other words, compared to receptors that lack desensitized states, those with access to desensitized states gave rise to IPSCs that delivered less charge initially but more charge later on. Interestingly, the limit of this effect was an IPSC that actually resembled a "tonic" current, as receptors with extremely high desensitized state stability had low open probability and high mean GABA bound times (Appendix I, II), the combination of which was predicted to yield small but sustained currents.

Despite the clear ability of desensitized states to influence IPSC shape, the physiological relevance of their macroscopic manifestation was less clear. In fact, some investigators have gone so far as to call macroscopic desensitization more of an experimental nuisance than a biologically interesting phenomenon. Our simulations, however, revealed that the time course of macroscopic desensitization represents an important boundary condition for IPSC decay, as the time course of current deactivation can never be slower than that of macroscopic desensitization (Chapter II). This was demonstrated by decreasing the GABA unbinding rate in the context of receptor activation by a saturating concentration of GABA, which caused the deactivation time course to approach that of macroscopic desensitization. Indeed, the magnitude of the unbinding rate appeared to determine the position of deactivation between two limits, the slow limit being determined by desensitization and the fast limit being determined by

channel mean open time (or burst/cluster length, depending on the gating scheme). While the existence of a slow limit imparted by macroscopic desensitization was somewhat counterintuitive, this occurred simply because receptors that cannot unbind GABA are functionally no different from those that unbind but are immediately re-bound with GABA (i.e., receptors are fully liganded in both cases). Thus, receptors that give rise to rapidly desensitizing currents will necessarily evoke IPSCs with fast decay components, while those that give rise to slowly desensitizing currents will evoke IPSCs whose time course depends highly on agonist affinity. Interestingly, this suggests that allosteric modulators that act primarily by increasing GABA affinity (such as benzodiazepines) will have the greatest effects on the shape of IPSCs mediated by non-desensitizing receptors.

The simulations also demonstrated that the time course of macroscopic desensitization represented an important boundary condition for the pattern of current responses evoked by high frequency stimulation, a phenomenon termed "repeated pulse inhibition" (Chapter V, VII). Specifically, we found that the rate and extent of repeated pulse inhibition could never be faster or greater, respectively, than the rate and extent of macroscopic desensitization. The existence of this kinetic boundary reflected the simple fact that for any pulse duration, there was a stimulation frequency that effectively exposed receptors to agonist continuously, which represented the maximal amount of current that could be lost. Consequently, receptors that yielded macroscopically non-desensitizing currents did not exhibit repeated pulse inhibition, no matter how high the stimulation frequency (Chapter VII). Conversely, receptors that yielded macroscopically desensitizing currents necessarily exhibited repeated pulse inhibition, provided of course

that the stimulation frequency was high enough to prevent complete receptor unbinding between successive pulses. Given the lack of any clear relationship between macroscopic desensitization and the occupancy of open, closed, or desensitized states (except that observing the macroscopic phenomenon necessitates the existence of a desensitized state; see above), it should be emphasized that kinetic data obtained from experimental protocols involving pulse trains should not under any circumstances be used to extract microscopic kinetic information. This includes the commonly employed experimental paradigm of paired-pulse recovery, often used as an index of receptor recovery from desensitized states.

However, the dependence of repeated pulse inhibition on the phenomenon of macroscopic desensitization did provide valuable information regarding the frequency domain within which different receptor isoforms could respond (Chapter V, VII). Desensitization served as a low-pass filter for receptor responses, decreasing the amplitude of successive IPSCs, and the multi-phasic nature of desensitization allowed the amount of filtering to be modulated with time, such that longer exposures to high frequency stimulation yielded progressively more filtering. Indeed, while fast desensitization was most relevant during short bursts of repetitive stimulation, slow desensitization was most relevant during sustained repetitive stimulation. This finding was consistent with the results of previous studies that showed that receptors lacking fast desensitization could still exhibit repeated pulse inhibition, but only in the context of long pulse trains or short pulse trains involving longer pulse durations (Bianchi and Macdonald, 2002). The idea that slow desensitization was primarily relevant under conditions of sustained exposure to agonist was further supported by the observation that

the kinetic properties of a single IPSC (evoked by brief exposure to GABA) were virtually identical when slow desensitized states were removed from comprehensive models of $GABA_A$ receptor function, but not when fast desensitized states were removed (Haas and Macdonald, 1999). Notably, the time course of deactivation also played an important role in filtering receptor responses to high frequency stimulation, as it determined the rate of receptor recovery between successive pulses. Specifically, slower deactivation caused the amount of repeated pulse inhibition to increase for any given amount of macroscopic desensitization and any given stimulation frequency, thus left-shifting the frequency response profile. Interestingly, considering the context of high frequency stimulation exposed a role for the longer deactivation time course observed with longer GABA exposures *in vitro*. This reflected the increasing occupancy of slow desensitized states with sustained receptor activation, which caused IPSCs later in the pulse train to have slower decay than those occurring earlier in the train (Chapter VII).

Our simulations suggested that desensitization and deactivation may also have physiological significance for receptors activated under nonsynaptic conditions. In the perisynaptic context, our simulations demonstrated that isoforms with more desensitization and slower deactivation were substantially less responsive to test pulses of saturating GABA following pre-application of sub-saturating GABA (Chapter V). It should be noted, however, that we did not independently evaluate the role of desensitization and deactivation in this context of receptor activation, and so it was difficult to know which macroscopic property was more relevant, or if differences in these particular macroscopic properties were even responsible for the phenomenon. Indeed, among other kinetic differences, the less responsive isoform also had a lower

steady-state GABA EC_{50}, meaning that pre-exposure to any given GABA concentration would have driven more receptors into fully liganded states. However, it should be noted that even if this were the case, a non-desensitizing receptor would have responded in exactly the same manner with or without pre-application, as the lack of macroscopic desensitization precludes any loss of current amplitude due to repeated exposure (see above). This suggested that enhanced macroscopic desensitization was at least partly responsible for this phenomenon, and consequently, that desensitization might be of physiological relevance to receptors that mediate nonsynaptic forms of GABAergic transmission (Overstreet et al., 2000). Interestingly, our studies of open channel block suggested that desensitized states may also buffer open state occupancy from fluctuations in the GABA concentration or exposure to negative modulators, thus ensuring stability of the tonic current. For example, open channel block was found to have decreasing effects on channel opening probability with increasing desensitized state occupancy (Chapter IV, Appendix II). While we can only speculate as to the evolutionary significance of this finding, it should be noted that tonic currents are thought to be responsible for three times as much charge transfer as phasic currents, and consequently, protecting this current from environmental toxins may have been a high priority in the development of GABAergic systems.

Future Directions

The kinetic studies presented in this dissertation have raised more questions than they have answered. In hopes that some brave soul will continue this work where we left off, the following is a long list of possible future directions.

Chapter II: While the studies in this chapter demonstrated the complex relationship between microscopic rate constants and macroscopic current properties, our focus was on understanding the kinetic determinants of macroscopic desensitization and deactivation. Consequently, the relationship between affinity, efficacy, desensitized state stability, and other macroscopic current properties such as current rise time, peak current EC_{50} (note that the solutions presented in Appendix II refer to equilibrium EC_{50}), paired-pulse recovery, and current rebound (which, incidentally, can occur with blockade of any fully liganded state) remains unclear. In addition, our studies involved gross measurements of macroscopic current properties (i.e., extent of desensitization; weighted deactivation time course); the relationships between microscopic rate constants and different phases of desensitization and deactivation were not systematically evaluated. Once available, however this information should allow for generation of a substantially more comprehensive algorithm for interpreting the effects of mutations and modulators, and may even expose conditions where microscopic information can actually be extracted from macroscopic observations. The data shown in Appendix V, for example, illustrate how simply varying the concentration of agonist can expose the microscopic exit rate from the desensitized state, at least for models containing only a single open state.

Chapter III: Applying our preliminary algorithm to benzodiazepines illustrated the potential power of combining macroscopic observations to constrain mechanistic hypotheses. It would therefore be of interest to apply the algorithm (or, better still, an expanded version of the algorithm; see above) to other modulators and mutations. Indeed, the mechanism of action of many clinically relevant compounds and disease-causing mutations remains controversial, reflecting the general lack of appreciation for

the complex relationship between microscopic and macroscopic currents. Macro-micro issues aside, this chapter also touches on the issue of context-dependent modulation, a topic only starting to be explored in the literature. Specifically, we found that benzodiazepines had distinct effects on macroscopic current shape and microscopic channel opening frequency depending on the mode of receptor activation. This suggests that disorders characterized by deficits in phasic or tonic inhibition could be treated not by compounds that selectively modulate synaptic or extrasynaptic receptor isoforms, but rather, by drugs that modulate receptors selectively under certain contexts of activation.

Chapter IV: This chapter addressed issues similar to those addressed in Chapter III, namely the macro-micro relationship and the idea of context-dependent modulation. As for the former, the idea that open channel block is analogous to addition of a linear desensitized state offers a unique method for systematically evaluating the relationship between microscopic and macroscopic desensitization in an actual experimental context. Indeed, using single channel analysis, the entry and exit rates from the blocked state can be determined, and by simply varying the concentration of blocker, precise control can be gained over the entry rate into the blocked (i.e., linear desensitized) state. It is worth noting that there are few experimental approaches that allow for the magnitude of a single rate constant in the gating scheme to be controlled. The most well known is changing the concentration of agonist, which changes the effective binding rate, the other being receptor activation in the presence of benzodiazepines, which as demonstrated in Chapter III, lowers the unbinding rate. As for the demonstration that open channel blockers also modulate receptors in a context-dependent manner (reflecting the dependence of open channel block on channel open probability), it would be of interest to explore whether

other negative modulators are similarly dependent upon GABA concentration. Based on the mathematical analysis shown in Appendix II, it seems likely that this would be the case not only for negative modulators, but also for positive modulators. If so, then the validity of using pharmacological agents to determine which receptor isoforms mediate phasic and tonic currents would need to be re-examined.

Chapter V: Increasing evidence suggests that most $GABA_A$ receptor isoforms access similar numbers of open and closed states and have similar bursting structure (i.e., one type of opening per burst), but have very different open, closed, burst, and cluster durations. This suggests that $GABA_A$ receptor isoforms operate according to the same core gating scheme, but that subunit composition determines the magnitude of the rate constants governing the state transitions. Although the feasibility of using a common core gating structure to describe the behavior of different receptor isoforms was presented in this chapter, this needs to be tested with other isoforms. One of the greatest challenges would be to explain the behavior of αβδ receptors in terms of a limited αβγ receptor gating scheme and to apply such an "embedded" model to explain the effects of neurosteroids, which convert αβδ currents into αβγ-like currents, possibly by granting αβδ receptors access to a previously restricted portion of the gating scheme (Bianchi and Macdonald, 2003). In addition, it is worth noting that different receptor isoforms tend to undergo macroscopic desensitization according to a time course with similar time constants but very different relative contributions (at saturating concentrations of GABA). This raises the intriguing possibility that differences in current shape reflect differences in the manner that receptors access the fully liganded gating scheme, and not the actual gating scheme itself. Indeed, for the time constants of a macroscopic time

course to be similar, the underlying model connectivity and rate constants must be similar. But by accessing the gating scheme from different starting positions (i.e., after binding GABA, receptors might enter a fast desensitized state as opposed to the traditional pre-open state), the relative contributions of each component would be very different, despite the time constants themselves being unchanged (Appendix III, IV).

Chapter VI: The microfluidic system presented in this chapter represents a major advance in solution exchange, as we can now activate $GABA_A$ receptors *in vitro* under physiologically relevant conditions. The full potential of this approach, however, has yet to be achieved. For example, while our system can exchange solutions in <100 μs, there is no reason that faster times cannot be achieved. The simplest way to do this would be to translate the devices with a faster motor, many of which are commercially available. In addition, the septal thickness could conceivably be reduced further, perhaps to as little as 1-5 μm. Since solution exchange time is linearly related to both septal thickness and translational velocity, even a two-fold improvement in both aspects would decrease exchange times to only ~25 μs, more than enough to synchronously activate even the most rapidly activating $GABA_A$ receptors. Similarly, there is no reason that pulse durations even shorter than 400 μs could not be achieved. This would only require increasing translational velocity and/or decreasing the width of the central channel. Moreover, there is no reason that the shape of the pulse must be square. PDMS microfabrication is already being used to generate concentration gradients, which if used to replace the existing central stream (which delivers a single concentration of GABA), would allow for even more physiologically relevant GABA pulses to be generated. For example, while a GABA transient with a rapid rise but multi-exponential decay could be

used to mimic the synaptic transient, one with a relatively slow rise and slow decay could be used to mimic the perisynaptic environment. The shape of the waveform could even be modified to replicate disease states, where GABA reuptake is either enhanced or impaired.

Chapter VII: The results from this chapter and those before it argue strongly against the idea that macroscopic desensitization and deactivation are physiologically irrelevant phenomena. However, all of the included studies involved either theoretical modeling or electrophysiological studies using recombinant receptors expressed in heterologous cells. Convincing the scientific community will undoubtedly require work in primary culture, where both pre- and postsynaptic factors are in play. Indeed, it is possible that changes in presynaptic factors, such as the concentration of GABA in the cleft or the rate of clearance due to reuptake, are more important in the physiological setting than postsynaptic receptor properties. One of the simplest experiments for testing this hypothesis is to study the phenomenon of repeated pulse inhibition in neuronal slice preparations under conditions that selectively modulate postsynaptic receptor desensitization or deactivation. For example, as shown in Chapter II, desensitization can be targeted selectively by reducing the GABA concentration, and as shown in Chapter III, deactivation can be targeted selectively by adding benzodiazepines. If the importance of postsynaptic receptor properties is confirmed, it will be of enormous interest to determine how clinically relevant drugs such as benzodiazepines and barbiturates influence the time course of repeated pulse inhibition.

REFERENCES

Ascher, P., Marty, A., & Neild, T. O. (1978). The mode of action of antagonists of the excitatory response to acetylcholine in Aplysia neurones. *J.Physiol* **278**, 207-235.

Barberis, A., Mozrzymas, J. W., Ortinski, P. I., & Vicini, S. (2007). Desensitization and binding properties determine distinct alpha1beta2gamma2 and alpha3beta2gamma2 GABA(A) receptor-channel kinetic behavior. *Eur.J.Neurosci.* **25**, 2726-2740.

Bianchi, M. T. & Macdonald, R. L. (2001). Mutation of the 9' leucine in the GABA(A) receptor gamma2L subunit produces an apparent decrease in desensitization by stabilizing open states without altering desensitized states. *Neuropharmacology* **41**, 737-744.

Bianchi, M. T. & Macdonald, R. L. (2002). Slow phases of GABA(A) receptor desensitization: structural determinants and possible relevance for synaptic function. *J.Physiol* **544**, 3-18.

Campo-Soria, C., Chang, Y., & Weiss, D. S. (2006). Mechanism of action of benzodiazepines on GABAA receptors. *Br.J.Pharmacol.* **148**, 984-990.

Clements, J. D. (1996). Transmitter timecourse in the synaptic cleft: its role in central synaptic function. *Trends Neurosci.* **19**, 163-171.

Feng, H. J., Bianchi, M. T., & Macdonald, R. L. (2004). Pentobarbital differentially modulates alpha1beta3delta and alpha1beta3gamma2L GABAA receptor currents. *Mol.Pharmacol.* **66**, 988-1003.

Fisher, J. L. & Macdonald, R. L. (1997). Single channel properties of recombinant GABAA receptors containing gamma 2 or delta subtypes expressed with alpha 1 and beta 3 subtypes in mouse L929 cells. *J.Physiol* **505 (Pt 2)**, 283-297.

Fisher, J. L. (2004). The alpha 1 and alpha 6 subunit subtypes of the mammalian GABA(A) receptor confer distinct channel gating kinetics. *J.Physiol* **561**, 433-448.

Haas, K. F. & Macdonald, R. L. (1999). GABAA receptor subunit gamma2 and delta subtypes confer unique kinetic properties on recombinant GABAA receptor currents in mouse fibroblasts. *J.Physiol* **514 (Pt 1)**, 27-45.

Jones, M. V. & Westbrook, G. L. (1995). Desensitized states prolong GABAA channel responses to brief agonist pulses. *Neuron* **15**, 181-191.

Jones, M. V. & Westbrook, G. L. (1996). The impact of receptor desensitization on fast synaptic transmission. *Trends Neurosci.* **19**, 96-101.

Lipton, S. A. (2005). The molecular basis of memantine action in Alzheimer's disease and other neurologic disorders: low-affinity, uncompetitive antagonism. *Curr.Alzheimer Res.* **2** , 155-165.

Lipton, S. A. (2006). Paradigm shift in neuroprotection by NMDA receptor blockade: memantine and beyond. *Nat.Rev.Drug Discov.* **5**, 160-170.

Marty, A. & Ascher, P. (1978). Slow relaxations of acetylcholine-induced potassium currents in Aplysia neurones. *Nature* **274**, 494-497.

Mercik, K., Pytel, M., Cherubini, E., & Mozrzymas, J. W. (2006). Effect of extracellular pH on recombinant alpha1beta2gamma2 and alpha1beta2 GABAA receptors. *Neuropharmacology* **51** , 305-314.

Mozrzymas, J. W. (2004). Dynamism of GABA(A) receptor activation shapes the "personality" of inhibitory synapses. *Neuropharmacology* **47**, 945-960.

Overstreet, L. S., Jones, M. V., & Westbrook, G. L. (2000). Slow desensitization regulates the availability of synaptic GABA(A) receptors. *J.Neurosci.* **20**, 7914-7921.

Rogers, C. J., Twyman, R. E., & Macdonald, R. L. (1994). Benzodiazepine and beta-carboline regulation of single GABAA receptor channels of mouse spinal neurones in culture. *J.Physiol* **475**, 69-82.

Rusch, D. & Forman, S. A. (2005). Classic benzodiazepines modulate the open-close equilibrium in alpha1beta2gamma2L gamma-aminobutyric acid type A receptors. *Anesthesiology* **102**, 783-792.

Scheller, M. & Forman, S. A. (2002). Coupled and uncoupled gating and desensitization effects by pore domain mutations in GABA(A) receptors. *J.Neurosci.* **22**, 8411-8421.

Twyman, R. E., Rogers, C. J., & Macdonald, R. L. (1989). Differential regulation of gamma-aminobutyric acid receptor channels by diazepam and phenobarbital. *Ann.Neurol.* **25**, 213-220.

Twyman, R. E., Rogers, C. J., & Macdonald, R. L. (1989). Pentobarbital and picrotoxin have reciprocal actions on single GABAA receptor channels. *Neurosci.Lett.* **96**, 89-95.

APPENDIX I

ANALYTIC SOLUTIONS OF EQUILIBRIUM FRACTIONAL OCCUPANCY FOR MARKOV MODELS OF $GABA_A$ RECEPTOR FUNCTION

Emmanuel J. Botzolakis, Matt T. Bianchi, Farid Hekmat, and Robert L. Macdonald

I. Solution of equilibrium fractional occupancy for states in the $\mathcal{C} \underset{\alpha}{\overset{\beta}{\rightleftharpoons}} \mathcal{O}$ reaction scheme, which is represented by the following system of first-order differential equations:

$$\mathcal{C}' = -\mathcal{C}\beta + \mathcal{O}\alpha \tag{1}$$

$$\mathcal{O}' = \mathcal{C}\beta - \mathcal{O}\alpha \tag{2}$$

A. *Macroscopic Solution*

i. $$\underset{t \to \infty}{\mathcal{O}(t)} = \frac{\#\ receptors\ \ in\ \mathcal{O}}{\#\ receptors} = \frac{(\#\ receptors\ \ in\ \mathcal{O})}{(\#\ receptors\ \ in\ \mathcal{O}) + (\#\ receptors\ \ in\ \mathcal{C})}$$

$$= \frac{\mathcal{O}}{\mathcal{O} + \mathcal{C}} = \frac{1}{1 + \frac{\mathcal{C}}{\mathcal{O}}} \tag{3}$$

as t → ∞, $\mathcal{C}' = \mathcal{O}' = 0$

from (1) and (2), $\mathcal{C}\beta = \mathcal{O}\alpha$, or alternatively,

$$\frac{\mathcal{C}}{\mathcal{O}} = \frac{\alpha}{\beta} \tag{4}$$

substituting (4) into (3)

$$\boxed{\underset{t \to \infty}{\mathcal{O}(t)} = \frac{1}{1 + \frac{\alpha}{\beta}}} \tag{5}$$

ii. $\underset{t \to \infty}{\mathcal{C}(t)} = \frac{\#\ receptors\ \ in\ \mathcal{C}}{\#\ receptors} = \frac{(\#\ receptors\ \ in\ \mathcal{C})}{(\#\ receptors\ \ in\ \mathcal{C}) + (\#\ receptors\ \ in\ \mathcal{O})}$

$$= \frac{\mathcal{C}}{\mathcal{C} + \mathcal{O}} = \frac{1}{1 + \frac{\mathcal{O}}{\mathcal{C}}} \tag{6}$$

substituting (4) into (6)

$$\boxed{\underset{t \to \infty}{\mathcal{C}(t)} = \frac{1}{1 + \frac{\beta}{\alpha}}} \tag{7}$$

B. *Microscopic Solution*

i. $p(\mathcal{O}) = \frac{mean\ \ open\ \ time}{mean\ \ lengt\ h\ of\ \ open - closed\ \ cycle}$

$$= \frac{(mean\ \ dwell\ \ time\ \ in\ \mathcal{O})}{(mean\ \ dwell\ \ time\ \ in\ \mathcal{O}) + (mean\ \ dwell\ \ time\ \ in\ \mathcal{C})} \tag{8}$$

if the mean dwell time in state $\mathcal{N}$ equals the reciprocal sum of the exit rates from state $\mathcal{N}$, then

mean dwell time in $\mathcal{O} = \frac{1}{\alpha}$ (9)

mean dwell time in $\mathcal{C} = \frac{1}{\beta}$ (10)

substituting (9) and (10) into (8)

$p(\mathcal{O}) = \frac{\frac{1}{\alpha}}{\frac{1}{\alpha} + \frac{1}{\beta}}$, or alternatively,

$\boxed{p(\mathcal{O}) = \frac{1}{1 + \frac{\alpha}{\beta}}}$ (note that this is identical to (5))

ii. $p(\mathcal{C}) = \frac{mean\ \ closed\ \ time}{mean\ \ lengt\ h\ of\ \ open - closed\ \ cycle}$

$$= \frac{(mean\ \ dwell\ \ time\ \ in\ \mathcal{C})}{(mean\ \ dwell\ \ time\ \ in\ \mathcal{O}) + (mean\ \ dwell\ \ time\ \ in\ \mathcal{C})} \tag{11}$$

substituting (9) and (10) into (11)

$p(\mathcal{C}) = \frac{\frac{1}{\beta}}{\frac{1}{\alpha}+\frac{1}{\beta}}$, or alternatively,

$$\boxed{p(\mathcal{C}) = \frac{1}{1+\frac{\beta}{\alpha}}}$$ (note that this is identical to (8))

II. Solution of equilibrium fractional occupancy for states in the $\mathcal{C}_1 \underset{K_{off}}{\overset{K_{on}[GABA]}{\rightleftarrows}} \mathcal{C}_2 \underset{\alpha}{\overset{\beta}{\rightleftarrows}} \mathcal{O}$ reaction scheme, which is represented by the following system of first-order differential equations:

$$\mathcal{C}_1{}' = -\mathcal{C}_1 K_{on}[GABA] + \mathcal{C}_2 K_{off} \tag{12}$$

$$\mathcal{C}_2{}' = \mathcal{C}_1 K_{on}[GABA] - \mathcal{C}_2\left(K_{off} + \beta\right) + \mathcal{O}\alpha \tag{13}$$

$$\mathcal{O}' = \mathcal{C}_2\beta - \mathcal{O}\alpha \tag{14}$$

A. *Macroscopic Solution*

i. $\underset{t \to \infty}{\mathcal{O}(t)} = \frac{\#\ receptors\ \ in\ \mathcal{O}}{\#\ receptors}$

$$= \frac{(\#\ receptors\ \ in\ \mathcal{O})}{(\#\ receptors\ \ in\ \mathcal{O}) + (\#\ receptors\ \ in\ \mathcal{C}_1) + (\#\ receptors\ \ in\ \mathcal{C}_2)}$$

$$= \frac{\mathcal{O}}{\mathcal{O} + \mathcal{C}_1 + \mathcal{C}_2} = \frac{1}{1 + \frac{\mathcal{C}_1}{\mathcal{O}} + \frac{\mathcal{C}_2}{\mathcal{O}}} \tag{15}$$

as t → ∞, $\mathcal{C}_1{}' = \mathcal{C}_2{}' = \mathcal{O}' = 0$

from (14), $\mathcal{C}_2\beta = \mathcal{O}\alpha$, or alternatively,

$$\frac{\mathcal{C}_2}{\mathcal{O}} = \frac{\alpha}{\beta} \tag{16}$$

from (12), $\mathcal{C}_1 K_{on}[GABA] = \mathcal{C}_2 K_{off}$, or alternatively,

$$\frac{\mathcal{C}_2}{\mathcal{C}_1} = \frac{K_{on}[GABA]}{K_{off}} \tag{17}$$

solving (16) for $\mathcal{C}_2$ and substituting into (17)

$$\frac{\mathcal{C}_1}{\mathcal{O}} = \frac{\alpha K_{off}}{\beta K_{on}[GABA]} \tag{18}$$

substituting (16) and (18) into (15)

$$\boxed{\underset{t \to \infty}{\mathcal{O}(t)} = \frac{1}{1 + \frac{\alpha}{\beta} + \frac{\alpha K_{off}}{\beta K_{on}[GABA\ ]}}} \tag{19}$$

ii. $$\underset{t \to \infty}{\mathcal{C}1(t)} = \frac{\#\ receptors\ \ in\ \mathcal{C}_1}{\#\ receptors}$$

$$= \frac{(\#\ receptors\ \ in\ \mathcal{C}_1)}{(\#\ receptors\ \ in\ \mathcal{O}) + (\#\ receptors\ \ in\ \mathcal{C}_1) + (\#\ receptors\ \ in\ \mathcal{C}_2)}$$

$$= \frac{\mathcal{C}_1}{\mathcal{O} + \mathcal{C}_1 + \mathcal{C}_2} = \frac{1}{1 + \frac{\mathcal{O}}{\mathcal{C}_1} + \frac{\mathcal{C}_2}{\mathcal{C}_1}} \tag{20}$$

substituting (17) and (18) into (20)

$$\boxed{\underset{t \to \infty}{\mathcal{C}_1(t)} = \frac{1}{1 + \frac{K_{on}[GABA\ ]}{K_{off}} + \frac{\beta K_{on}[GABA\ ]}{\alpha K_{off}}}} \tag{21}$$

iii. $$\underset{t \to \infty}{\mathcal{C}_2(t)} = \frac{\#\ receptors\ \ in\ \mathcal{C}_2}{\#\ receptors}$$

$$= \frac{(\#\ receptors\ \ in\ \mathcal{C}_2)}{(\#\ receptors\ \ in\ \mathcal{O}) + (\#\ receptors\ \ in\ \mathcal{C}_1) + (\#\ receptors\ \ in\ \mathcal{C}_2)}$$

$$= \frac{\mathcal{C}_2}{\mathcal{O} + \mathcal{C}_1 + \mathcal{C}_2} = \frac{1}{1 + \frac{\mathcal{O}}{\mathcal{C}_2} + \frac{\mathcal{C}_1}{\mathcal{C}_2}} \tag{22}$$

substituting (16) and (17) into (22)

$$\boxed{\underset{t \to \infty}{\mathcal{C}_2(t)} = \frac{1}{1 + \frac{K_{off}}{K_{on}[GABA\ ]} + \frac{\beta}{\alpha}}} \tag{23}$$

B. *Microscopic Solution*

i. $$p(\mathcal{O}) = \frac{(mean\ \ dwell\ \ time\ \ in\ \mathcal{O})(probability\ \ \ of\ \mathcal{O}\ transition\ \ \ from\ \mathcal{C}_2)}{\sum\ (mean\ \ dwell\ \ time\ \ in\ \mathcal{N})(probability\ \ \ of\ \mathcal{N} transition\ \ \ from\ neighbors)} \tag{24}$$

if the mean dwell time in state $\mathcal{N}$ equals the reciprocal sum of the exit rates from state $\mathcal{N}$, then

mean dwell time in $\mathcal{O} = \frac{1}{\alpha}$ (25)

mean dwell time in $\mathcal{C}_1 = \frac{1}{K_{on\,[GABA\ ]}}$ (26)

mean dwell time in $\mathcal{C}_2 = \frac{1}{\beta + K_{off}}$ (27)

probability of $\mathcal{C}_1 \rightarrow \mathcal{C}_2$ transition = 1 (no other option once in $\mathcal{C}_1$) (28)

probability of $\mathcal{C}_2 \rightarrow \mathcal{C}_1$transition = $\frac{K_{off}}{\beta + K_{off}}$ (29)

probability of $\mathcal{C}_2 \rightarrow \mathcal{O}$ transition = $\frac{\beta}{\beta + K_{off}}$ (30)

probability of $\mathcal{O} \rightarrow \mathcal{C}_2$ transition = 1 (no other option once in $\mathcal{O}$) (31)

substituting (25 – 31) into (24)

$$p(\mathcal{O}) = \frac{\left(\frac{1}{\alpha}\right)\left(\frac{\beta}{\beta + K_{off}}\right)}{\left(\frac{1}{\alpha}\right)\left(\frac{\beta}{\beta + K_{off}}\right) + \left(\frac{1}{\beta + K_{off}}\right) + \left(\frac{1}{K_{on\,[GABA\ ]}}\right)\left(\frac{K_{off}}{\beta + K_{off}}\right)}$$

or alternatively,

$$\boxed{p(\mathcal{O}) = \frac{1}{1 + \frac{\alpha}{\beta} + \frac{\alpha K_{off}}{\beta K_{on\,[GABA\ ]}}}}$$ (note that this is identical to (19))

ii. $p(\mathcal{C}_1) = \frac{(mean\ \ dwell\ \ time\ \ in\ \mathcal{C}_1)(probability\ \ \ of\ \mathcal{C}_1\ transition\ from\ \mathcal{C}_2)}{\sum(mean\ \ dwell\ \ time\ \ in\ \mathcal{N})(probability\ \ \ of\ \mathcal{N}transition\ \ \ from\ neighbors)}$ (32)

substituting (25 – 31) into (32)

$$p(\mathcal{C}_1) = \frac{\left(\frac{1}{K_{on[GABA]}}\right)\left(\frac{K_{off}}{\beta + K_{off}}\right)}{\left(\frac{1}{\alpha}\right)\left(\frac{\beta}{\beta + K_{off}}\right) + \left(\frac{1}{\beta + K_{off}}\right) + \left(\frac{1}{K_{on[GABA]}}\right)\left(\frac{K_{off}}{\beta + K_{off}}\right)}$$

or alternatively,

$$\boxed{p(\mathcal{C}_1) = \frac{1}{1 + \frac{K_{on\,[GABA\ ]}}{K_{off}} + \frac{\beta K_{on\,[GABA\ ]}}{\alpha K_{off}}}}$$

(note that this is identical to (22))

iii. $$p(\mathcal{C}_2) = \frac{(mean\ \ dwell\ \ time\ \ in\ \mathcal{C}_2)(probability\ \ \ of\ \mathcal{C}_2\ transition\ from\ \mathcal{C}_1\ and\ \mathcal{O})}{\sum(mean\ \ dwell\ \ time\ \ in\ \mathcal{N})(probability\ \ \ of\ \mathcal{N} transition\ \ \ from\ neighbors)} \quad (33)$$

substituting (25 – 31) into (33)

$$p(\mathcal{C}_2) = \frac{\left(\frac{1}{\beta + K_{off}}\right)}{\left(\frac{1}{\alpha}\right)\left(\frac{\beta}{\beta + K_{off}}\right) + \left(\frac{1}{\beta + K_{off}}\right) + \left(\frac{1}{K_{on}[GABA]}\right)\left(\frac{K_{off}}{\beta + K_{off}}\right)}$$

$$\boxed{p(\mathcal{C}_2) = \frac{1}{1 + \frac{K_{off}}{K_{on}\,[GABA\ ]} + \frac{\beta}{\alpha}}}$$ (note that this is identical to (24))

III. Solution of equilibrium fractional occupancy for states in the $\mathcal{C}_1 \underset{K_{off}}{\overset{K_{on}\,[GABA\ ]}{\rightleftarrows}} \mathcal{C}_2 \underset{\alpha}{\overset{\beta}{\rightleftarrows}} \mathcal{O} \underset{\rho}{\overset{\delta}{\rightleftarrows}} \mathcal{D}$ reaction scheme, which is represented by the following system of first-order differential equations:

$$\mathcal{C}_1{}' = -\mathcal{C}_1 K_{on}[GABA] + \mathcal{C}_2 K_{off} \quad (34)$$

$$\mathcal{C}_2{}' = \mathcal{C}_1 K_{on}[GABA] - \mathcal{C}_2\left(K_{off} + \beta\right) + \mathcal{O}\alpha \quad (35)$$

$$\mathcal{O}' = \mathcal{C}_2\beta - \mathcal{O}(\alpha + \delta) + \mathcal{D}\rho \quad (36)$$

$$\mathcal{D}' = \mathcal{O}\delta - \mathcal{D}\rho \quad (37)$$

A. *Macroscopic Solution*

i. $$\underset{t \to \infty}{\mathcal{O}(t)} = \frac{\#\ receptors\ \ open}{\#\ receptors}$$

$$= \frac{(\#\ receptors\ \ in\ \mathcal{O})}{(\#\ receptors\ \ in\ \mathcal{O}) + (\#\ receptors\ \ in\ \mathcal{C}_1) + (\#\ receptors\ \ in\ \mathcal{C}_2) + (\#\ receptors\ \ in\ \mathcal{D})}$$

$$= \frac{\mathcal{O}}{\mathcal{O} + \mathcal{C}_1 + \mathcal{C}_2 + \mathcal{D}} = \frac{1}{1 + \frac{\mathcal{C}_1}{\mathcal{O}} + \frac{\mathcal{C}_2}{\mathcal{O}} + \frac{\mathcal{D}}{\mathcal{O}}} \quad (38)$$

as t → ∞, $\mathcal{C}_1{}' = \mathcal{C}_2{}' = \mathcal{O}' = \mathcal{D}' = 0$

from (37), $\mathcal{O}\delta = \mathcal{D}\rho$, or alternatively,

$$\frac{\mathcal{D}}{\mathcal{O}} = \frac{\delta}{\rho} \tag{39}$$

from (36), $\mathcal{O}(\alpha + \delta) = \mathcal{C}_2\beta + \mathcal{D}\rho$ (40)

solving (39) for $\mathcal{D}$ and substituting into (40)

$$\frac{\mathcal{C}_2}{\mathcal{O}} = \frac{\alpha}{\beta} \tag{41}$$

from (34), $\mathcal{C}_1 K_{on}[GABA] = \mathcal{C}_2 K_{off}$, or alternatively

$$\frac{\mathcal{C}_2}{\mathcal{C}_1} = \frac{K_{on}}{K_{off}} \tag{42}$$

solving (41) for $\mathcal{C}_2$ and substituting into (42)

$$\frac{\mathcal{C}_1}{\mathcal{O}} = \frac{\alpha K_{off}}{\beta K_{on}[GABA]} \tag{43}$$

substituting (39), (41), and (43) into (38)

$$\boxed{\underset{t \to \infty}{\mathcal{O}(t)} = \frac{1}{1 + \frac{\alpha}{\beta} + \frac{\alpha K_{off}}{\beta K_{on}[GABA]} + \frac{\delta}{\rho}}} \tag{44}$$

ii. $\underset{t \to \infty}{\mathcal{C}_1(t)} = \frac{\#\ receptors\ \ in\ \mathcal{C}_1}{\#\ receptors}$

$$= \frac{(\#\ receptors\ \ in\ \mathcal{C}_1)}{(\#\ receptors\ \ in\ \mathcal{O}) + (\#\ receptors\ \ in\ \mathcal{C}_1) + (\#\ receptors\ \ in\ \mathcal{C}_2) + (\#\ receptors\ \ in\ \mathcal{D})}$$

$$= \frac{\mathcal{C}_1}{\mathcal{O} + \mathcal{C}_1 + \mathcal{C}_2 + \mathcal{D}} = \frac{1}{1 + \frac{\mathcal{O}}{\mathcal{C}_1} + \frac{\mathcal{C}_2}{\mathcal{C}_1} + \frac{\mathcal{D}}{\mathcal{C}_1}} \tag{45}$$

solving (39) for $\mathcal{O}$ and substituting into (43)

$$\frac{\mathcal{D}}{\mathcal{C}_1} = \frac{\beta\delta K_{on}[GABA]}{\alpha\rho K_{off}} \tag{46}$$

substituting (42), (43), and (46) into (45)

$$\boxed{\underset{t \to \infty}{\mathcal{C}_1(t)} = \frac{1}{1 + \frac{K_{on}[GABA]}{K_{off}} + \frac{\beta K_{on}[GABA]}{\alpha K_{off}} + \frac{\beta\delta K_{on}[GABA]}{\alpha\rho K_{off}}}} \tag{47}$$

iii. $\underset{t \to \infty}{\mathcal{C}_2(t)} = \frac{\#\ receptors\ \ in\ \mathcal{C}_2}{\#\ receptors}$

$$= \frac{(\#\ receptors\ \ in\ \mathcal{C}_2)}{(\#\ receptors\ \ in\ \mathcal{O}) + (\#\ receptors\ \ in\ \mathcal{C}_1) + (\#\ receptors\ \ in\ \mathcal{C}_2) + (\#\ receptors\ \ in\ \mathcal{D})}$$

$$= \frac{\mathcal{C}_2}{\mathcal{O} + \mathcal{C}_1 + \mathcal{C}_2 + \mathcal{D}} = \frac{1}{1 + \frac{\mathcal{C}_1}{\mathcal{C}_2} + \frac{\mathcal{O}}{\mathcal{C}_2} + \frac{\mathcal{D}}{\mathcal{C}_2}} \tag{48}$$

solving (39) for $\mathcal{O}$ and substituting into (41)

$$\frac{\mathcal{D}}{\mathcal{C}_2} = \frac{\beta\delta}{\alpha\rho} \tag{49}$$

substituting (41), (42), and (49) into (48)

$$\boxed{\underset{t \to \infty}{\mathcal{C}_2(t)} = \frac{1}{1 + \frac{K_{off}}{K_{on}[GABA\ ]} + \frac{\beta}{\alpha} + \frac{\beta\delta}{\alpha\rho}}} \tag{50}$$

iv. $\underset{t \to \infty}{\mathcal{D}(t)} = \frac{\#\ receptors\ \ in\ \mathcal{D}}{\#\ receptors}$

$$= \frac{(\#\ receptors\ \ in\ \mathcal{D})}{(\#\ receptors\ \ in\ \mathcal{O}) + (\#\ receptors\ \ in\ \mathcal{C}_1) + (\#\ receptors\ \ in\ \mathcal{C}_2) + (\#\ receptors\ \ in\ \mathcal{D})}$$

$$= \frac{\mathcal{D}}{\mathcal{O} + \mathcal{C}_1 + \mathcal{C}_2 + \mathcal{D}} = \frac{1}{1 + \frac{\mathcal{C}_1}{\mathcal{D}} + \frac{\mathcal{C}_2}{\mathcal{D}} + \frac{\mathcal{O}}{\mathcal{D}}} \tag{51}$$

substituting (39), (46), and (49) into (51)

$$\boxed{\underset{t \to \infty}{\mathcal{D}(t)} = \frac{1}{1 + \frac{\alpha\rho\, K_{off}}{\beta\delta\, K_{on}[GABA\ ]} + \frac{\alpha\rho}{\beta\delta} + \frac{\rho}{\delta}}} \tag{52}$$

B. *Microscopic Solution*

i. $p(\mathcal{O}) = \frac{(mean\ \ dwell\ \ time\ \ in\ \mathcal{O})(probability\ \ \ of\ \mathcal{O}\ transition\ \ \ from\ \mathcal{C}_2\ and\ \mathcal{D})}{\sum\ (mean\ \ dwell\ \ time\ \ in\ \mathcal{N})(probability\ \ \ of\ \mathcal{N} transition\ \ \ from\ \ neig\,hbors)}$ (53)

if the mean dwell time in state $\mathcal{N}$ equals the reciprocal sum of the exit rates from state $\mathcal{N}$, then

mean dwell time in $\mathcal{O} = \frac{1}{\alpha + \delta}$ (54)

mean dwell time in $\mathcal{C}_1 = \frac{1}{K_{on\,[GABA\ ]}}$ (55)

mean dwell time in $\mathcal{C}_2 = \frac{1}{\beta + K_{off}}$ (56)

mean dwell time in $\mathcal{D} = \frac{1}{\rho}$ (57)

probability of $\mathcal{C}_1 \rightarrow \mathcal{C}_2$ transition = 1 (no other option once in $\mathcal{C}_1$) (58)

probability of $\mathcal{C}_2 \rightarrow \mathcal{C}_1$transition = $\frac{K_{off}}{\beta + K_{off}}$ (59)

probability of $\mathcal{C}_2 \rightarrow \mathcal{O}$ transition = $\frac{\beta}{\beta + K_{off}}$ (60)

probability of $\mathcal{O} \rightarrow \mathcal{C}_2$ transition = $\frac{\alpha}{\alpha + \delta}$ (61)

probability of $\mathcal{O} \rightarrow \mathcal{D}$ transition = $\frac{\delta}{\alpha + \delta}$ (62)

probability of $\mathcal{D} \rightarrow \mathcal{O}$ transition = 1 (no other option once in $\mathcal{D}$) (63)

substituting (54 – 63) into (53)

$$p(\mathcal{O}) = \frac{\left(\frac{1}{\alpha+\delta}\right)\left(\frac{\beta}{\beta+K_{off}}\right)}{\left(\frac{1}{\alpha+\delta}\right)\left(\frac{\beta}{\beta+K_{off}}\right)+\left(\frac{1}{\beta+K_{off}}\right)\left(\frac{\alpha}{\alpha+\delta}\right)+\left(\frac{1}{K_{on\,[GABA\ ]}}\right)\left(\frac{K_{off}}{\beta+K_{off}}\right)\left(\frac{\alpha}{\alpha+\delta}\right)+\left(\frac{1}{\rho}\right)\left(\frac{\delta}{\alpha+\delta}\right)\left(\frac{\beta}{\beta+K_{off}}\right)}$$

or alternatively,

$$\boxed{p(\mathcal{O}) = \frac{1}{1+\frac{\alpha}{\beta}+\frac{\alpha K_{off}}{\beta K_{on\,[GABA\ ]}}+\frac{\delta}{\rho}}}$$ (note that this is identical to (44))

ii. $p(\mathcal{C}_1) = \frac{(mean\ \ dwell\ \ time\ \ in\ \mathcal{C}_1)(probability\ \ \ of\ \mathcal{C}_1\ transition\ \ \ from\ \mathcal{C}_2)}{\sum(mean\ \ dwell\ \ time\ \ in\ \mathcal{N})(probability\ \ \ of\ \mathcal{N}transition\ \ \ from\ neig\,hbors)}$ (64)

substituting (54 – 63) into (64)

$$p(\mathcal{C}_1) = \frac{\left(\frac{1}{K_{on\,[GABA\ ]}}\right)\left(\frac{K_{off}}{\beta+K_{off}}\right)\left(\frac{\alpha}{\alpha+\delta}\right)}{\left(\frac{1}{\alpha+\delta}\right)\left(\frac{\beta}{\beta+K_{off}}\right)+\left(\frac{1}{\beta+K_{off}}\right)\left(\frac{\alpha}{\alpha+\delta}\right)+\left(\frac{1}{K_{on\,[GABA\ ]}}\right)\left(\frac{K_{off}}{\beta+K_{off}}\right)\left(\frac{\alpha}{\alpha+\delta}\right)+\left(\frac{1}{\rho}\right)\left(\frac{\delta}{\alpha+\delta}\right)\left(\frac{\beta}{\beta+K_{off}}\right)}$$

or alternatively,

$$\boxed{p(\mathcal{C}_1) = \frac{1}{1+\frac{K_{on\,[GABA\ ]}}{K_{off}}+\frac{\beta K_{on\,[GABA\ ]}}{\alpha K_{off}}+\frac{\beta\delta K_{on\,[GABA\ ]}}{\alpha\rho K_{off}}}}$$

(note that this is identical to (47))

iii. $$p(\mathcal{C}_2) = \frac{(mean\ \ dwell\ \ time\ \ in\ \mathcal{C}_2)(probability\ \ \ of\ \mathcal{C}_2\ transition\ \ \ from\ \mathcal{C}_1\ and\ \mathcal{O})}{\sum(mean\ \ dwell\ \ time\ \ in\ \mathcal{N})(probability\ \ \ of\ \mathcal{N}transition\ \ \ from\ \ neig\ hbors)} \quad (65)$$

substituting (54 – 63) into (65)

$$p(\mathcal{C}_2) = \frac{\left(\frac{1}{\beta + K_{off}}\right)\left(\frac{\alpha}{\alpha+\delta}\right)}{\left(\frac{1}{\alpha+\delta}\right)\left(\frac{\beta}{\beta+K_{off}}\right) + \left(\frac{1}{\beta+K_{off}}\right)\left(\frac{\alpha}{\alpha+\delta}\right) + \left(\frac{1}{K_{on}[GABA\ ]}\right)\left(\frac{K_{off}}{\beta+K_{off}}\right)\left(\frac{\alpha}{\alpha+\delta}\right) + \left(\frac{1}{\rho}\right)\left(\frac{\delta}{\alpha+\delta}\right)\left(\frac{\beta}{\beta+K_{off}}\right)}$$

or alternatively,

$$\boxed{p(\mathcal{C}_2) = \frac{1}{1 + \frac{K_{off}}{K_{on}[GABA\ ]} + \frac{\beta}{\alpha} + \frac{\beta\delta}{\alpha\rho}}}$$ (note that this is identical to (50))

iv. $$p(\mathcal{D}) = \frac{(mean\ \ dwell\ \ time\ \ in\ \mathcal{D})(probability\ \ \ of\ \mathcal{D}\ transition\ \ \ from\ \mathcal{O})}{\sum(mean\ \ dwell\ \ time\ \ in\ \mathcal{N})(probability\ \ \ of\ \mathcal{N}transition\ \ \ from\ \ neig\ hbors)} \quad (66)$$

substituting (54 – 63) into (66)

$$p(\mathcal{D}) = \frac{\left(\frac{1}{\rho}\right)\left(\frac{\delta}{\alpha+\delta}\right)\left(\frac{\beta}{\beta+K_{off}}\right)}{\left(\frac{1}{\alpha+\delta}\right)\left(\frac{\beta}{\beta+K_{off}}\right) + \left(\frac{1}{\beta+K_{off}}\right)\left(\frac{\alpha}{\alpha+\delta}\right) + \left(\frac{1}{K_{on}[GABA\ ]}\right)\left(\frac{K_{off}}{\beta+K_{off}}\right)\left(\frac{\alpha}{\alpha+\delta}\right) + \left(\frac{1}{\rho}\right)\left(\frac{\delta}{\alpha+\delta}\right)\left(\frac{\beta}{\beta+K_{off}}\right)}$$

or alternatively,

$$\boxed{p(\mathcal{D}) = \frac{1}{1 + \frac{\alpha\rho\, K_{off}}{\beta\delta\, K_{on}[GABA\ ]} + \frac{\alpha\rho}{\beta\delta} + \frac{\rho}{\delta}}}$$ (note that this is identical to (52))

IV. Solution of equilibrium fractional occupancy for the

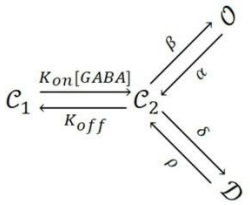

reaction scheme, which is represented by the following system of first-order differential equations:

$$\mathcal{C}_1{}' = -\mathcal{C}_1 K_{on}[GABA] + \mathcal{C}_2 K_{off} \quad (67)$$

$$\mathcal{C}_2{}' = \mathcal{C}_1 K_{on}[GABA] - \mathcal{C}_2\left(K_{off} + \beta + \delta\right) + \mathcal{O}\alpha + \mathcal{D}\rho \tag{68}$$

$$\mathcal{O}' = \mathcal{C}_2\beta - \mathcal{O}\alpha \tag{69}$$

$$\mathcal{D}' = \mathcal{C}_2\delta - \mathcal{D}\rho \tag{70}$$

A. *Macroscopic Solution*

i. $\underset{t \to \infty}{\mathcal{O}(t)} = \frac{\#\ receptors\ \ open}{\#\ receptors}$

$$= \frac{(\#\ receptors\ \ in\ \mathcal{O})}{(\#\ receptors\ \ in\ \mathcal{O}) + (\#\ receptors\ \ in\ \mathcal{C}_1) + (\#\ receptors\ \ in\ \mathcal{C}_2) + (\#\ receptors\ \ in\ \mathcal{D})}$$

$$= \frac{\mathcal{O}}{\mathcal{O} + \mathcal{C}_1 + \mathcal{C}_2 + \mathcal{D}} = \frac{1}{1 + \frac{\mathcal{C}_1}{\mathcal{O}} + \frac{\mathcal{C}_2}{\mathcal{O}} + \frac{\mathcal{D}}{\mathcal{O}}} \tag{71}$$

as t → ∞, $\mathcal{C}_1{}' = \mathcal{C}_2{}' = \mathcal{O}' = \mathcal{D}' = 0$

from (69), $\mathcal{O}\alpha = \mathcal{C}_2\beta$, or alternatively,

$$\frac{\mathcal{C}_2}{\mathcal{O}} = \frac{\alpha}{\beta} \tag{72}$$

from (67), $\mathcal{C}_1 K_{on}[GABA] = \mathcal{C}_2 K_{off}$, or alternatively,

$$\frac{\mathcal{C}_2}{\mathcal{C}_1} = \frac{K_{on}[GABA]}{K_{off}} \tag{73}$$

solving (73) for $\mathcal{C}_2$ and substituting into (72)

$$\frac{\mathcal{C}_1}{\mathcal{O}} = \frac{\alpha K_{off}}{\beta K_{on}[GABA]} \tag{74}$$

from (53), $\mathcal{D}\rho = \mathcal{C}_2\delta$, or alternatively,

$$\frac{\mathcal{C}_2}{\mathcal{D}} = \frac{\rho}{\delta} \tag{75}$$

solving (75) for $\mathcal{C}_2$ and substituting into (72)

$$\frac{\mathcal{D}}{\mathcal{O}} = \frac{\alpha\delta}{\beta\rho} \tag{76}$$

substituting (72), (74), and (76) into (71)

$$\boxed{\underset{t \to \infty}{\mathcal{O}(t)} = \frac{1}{1 + \frac{\alpha}{\beta} + \frac{\alpha K_{off}}{\beta K_{on}[GABA]} + \frac{\alpha\delta}{\beta\rho}}} \tag{77}$$

ii. $$\underset{t \to \infty}{\mathcal{C}_1(t)} = \frac{\#\, receptors \;\; in\; \mathcal{C}_1}{\#\, receptors}$$

$$= \frac{(\#\, receptors \;\; in\; \mathcal{C}_1)}{(\#\, receptors \;\; in\; \mathcal{O}) + (\#\, receptors \;\; in\; \mathcal{C}_1) + (\#\, receptors \;\; in\; \mathcal{C}_2) + (\#\, receptors \;\; in\; \mathcal{D})}$$

$$= \frac{\mathcal{C}_1}{\mathcal{O} + \mathcal{C}_1 + \mathcal{C}_2 + \mathcal{D}} = \frac{1}{1 + \frac{\mathcal{O}}{\mathcal{C}_1} + \frac{\mathcal{C}_2}{\mathcal{C}_1} + \frac{\mathcal{D}}{\mathcal{C}_1}} \tag{78}$$

solving (74) for $\mathcal{O}$ and substituting into (76)

$$\frac{\mathcal{D}}{\mathcal{C}_1} = \frac{\delta K_{on}[GABA]}{\rho K_{off}} \tag{79}$$

substituting (73), (74), and (79) into (78)

$$\boxed{\underset{t \to \infty}{\mathcal{C}_1(t)} = \frac{1}{1 + \frac{K_{on}[GABA]}{K_{off}} + \frac{\beta K_{on}[GABA]}{\alpha K_{off}} + \frac{\delta K_{on}[GABA]}{\rho K_{off}}}} \tag{80}$$

iii. $$\underset{t \to \infty}{\mathcal{C}_2(t)} = \frac{\#\, receptors \;\; in\; \mathcal{C}_2}{\#\, receptors}$$

$$= \frac{(\#\, receptors \;\; in\; \mathcal{C}_2)}{(\#\, receptors \;\; in\; \mathcal{O}) + (\#\, receptors \;\; in\; \mathcal{C}_1) + (\#\, receptors \;\; in\; \mathcal{C}_2) + (\#\, receptors \;\; in\; \mathcal{D})}$$

$$= \frac{\mathcal{C}_2}{\mathcal{O} + \mathcal{C}_1 + \mathcal{C}_2 + \mathcal{D}} = \frac{1}{1 + \frac{\mathcal{C}_1}{\mathcal{C}_2} + \frac{\mathcal{O}}{\mathcal{C}_2} + \frac{\mathcal{D}}{\mathcal{C}_2}} \tag{81}$$

substituting (72), (73), and (75) into (81)

$$\boxed{\underset{t \to \infty}{\mathcal{C}_2(t)} = \frac{1}{1 + \frac{K_{off}}{K_{on}[GABA]} + \frac{\beta}{\alpha} + \frac{\delta}{\rho}}} \tag{82}$$

iv. $$\underset{t \to \infty}{\mathcal{D}(t)} = \frac{\#\, receptors \;\; in\; \mathcal{D}}{\#\, receptors}$$

$$= \frac{(\#\, receptors \;\; in\; \mathcal{D})}{(\#\, receptors \;\; in\; \mathcal{O}) + (\#\, receptors \;\; in\; \mathcal{C}_1) + (\#\, receptors \;\; in\; \mathcal{C}_2) + (\#\, receptors \;\; in\; \mathcal{D})}$$

$$= \frac{\mathcal{D}}{\mathcal{O} + \mathcal{C}_1 + \mathcal{C}_2 + \mathcal{D}} = \frac{1}{1 + \frac{\mathcal{C}_1}{\mathcal{D}} + \frac{\mathcal{C}_2}{\mathcal{D}} + \frac{\mathcal{O}}{\mathcal{D}}} \tag{83}$$

substituting (75), (76), and (79) into (83)

$$\boxed{\underset{t \to \infty}{\mathcal{D}(t)} = \frac{1}{1 + \frac{\rho K_{off}}{\delta K_{on}[GABA\ ]} + \frac{\beta\rho}{\alpha\delta} + \frac{\rho}{\delta}}} \quad (84)$$

B. *Microscopic Solution*

i. $$p(\mathcal{O}) = \frac{(mean\ \ dwell\ \ time\ \ in\ \mathcal{O})(probability\ \ \ of\ \mathcal{O}\ transition\ \ \ from\ \ \mathcal{C}_2)}{\sum (mean\ \ dwell\ \ time\ \ in\ \mathcal{N})(probability\ \ \ of\ \mathcal{N} transition\ \ \ from\ \ neig\,hbors)} \quad (85)$$

if the mean dwell time in state $\mathcal{N}$ equals the reciprocal sum of the exit rates from state $\mathcal{N}$, then

mean dwell time in $\mathcal{O} = \frac{1}{\alpha}$ (86)

mean dwell time in $\mathcal{C}_1 = \frac{1}{K_{on}[GABA\ ]}$ (87)

mean dwell time in $\mathcal{C}_2 = \frac{1}{\beta + \delta + K_{off}}$ (88)

mean dwell time in $\mathcal{D} = \frac{1}{\rho}$ (89)

probability of $\mathcal{C}_1 \rightarrow \mathcal{C}_2$ transition = 1 (no other option once in $\mathcal{C}_1$) (90)

probability of $\mathcal{C}_2 \rightarrow \mathcal{C}_1$transition = $\frac{K_{off}}{\beta + \delta + K_{off}}$ (91)

probability of $\mathcal{C}_2 \rightarrow \mathcal{O}$ transition = $\frac{\beta}{\beta + \delta + K_{off}}$ (92)

probability of $\mathcal{O} \rightarrow \mathcal{C}_2$ transition = 1 (no other option once in $\mathcal{O}$) (93)

probability of $\mathcal{C}_2 \rightarrow \mathcal{D}$ transition = $\frac{\delta}{\beta + \delta + K_{off}}$ (94)

probability of $\mathcal{D} \rightarrow \mathcal{C}_2$ transition = 1 (no other option once in $\mathcal{D}$) (95)

substituting (86 – 95) into (85)

$$p(\mathcal{O}) = \frac{\left(\frac{1}{\alpha}\right)\left(\frac{\beta}{\beta + \delta + K_{off}}\right)}{\left(\frac{1}{\alpha}\right)\left(\frac{\beta}{\beta + \delta + K_{off}}\right) + \left(\frac{1}{\beta + \delta + K_{off}}\right) + \left(\frac{1}{K_{on}[GABA\ ]}\right)\left(\frac{K_{off}}{\beta + \delta + K_{off}}\right) + \left(\frac{1}{\rho}\right)\left(\frac{\delta}{\beta + \delta + K_{off}}\right)}$$

or alternatively,

$$\boxed{p(\mathcal{O}) = \frac{1}{1 + \frac{\alpha}{\beta} + \frac{\alpha K_{off}}{\beta K_{on}[GABA]} + \frac{\alpha\delta}{\beta\rho}}}$$

(note that this is identical to (77))

ii. $$p(\mathcal{C}_1) = \frac{(mean\ dwell\ time\ in\ \mathcal{C}_1)(probability\ \ of\ \mathcal{C}_1\ transition\ \ from\ \mathcal{C}_2)}{\sum(mean\ dwell\ time\ in\ \mathcal{N})(probability\ \ of\ \mathcal{N}transition\ \ from\ neighbors)} \quad (96)$$

substituting (86 – 95) into (96)

$$p(\mathcal{C}_1) = \frac{\left(\frac{1}{K_{on}[GABA]}\right)\left(\frac{K_{off}}{\beta + \delta + K_{off}}\right)}{\left(\frac{1}{\alpha}\right)\left(\frac{\beta}{\beta + \delta + K_{off}}\right) + \left(\frac{1}{\beta + \delta + K_{off}}\right) + \left(\frac{1}{K_{on}[GABA]}\right)\left(\frac{K_{off}}{\beta + \delta + K_{off}}\right) + \left(\frac{1}{\rho}\right)\left(\frac{\delta}{\beta + \delta + K_{off}}\right)}$$

or alternatively,

$$\boxed{p(\mathcal{C}_1) = \frac{1}{1 + \frac{K_{on}[GABA]}{K_{off}} + \frac{\beta K_{on}[GABA]}{\alpha K_{off}} + \frac{\delta K_{on}[GABA]}{\rho K_{off}}}}$$

(note that this is identical to (80))

iii. $$p(\mathcal{C}_2) = \frac{(mean\ dwell\ time\ in\ \mathcal{C}_2)(probability\ \ of\ \mathcal{C}_2\ transition\ \ from\ \mathcal{C}_1,\ \mathcal{O},\ \mathcal{D})}{\sum(mean\ dwell\ time\ in\ \mathcal{N})(probability\ \ of\ \mathcal{N}transition\ \ from\ neighbors)} \quad (97)$$

substituting (86 – 95) into (97)

$$p(\mathcal{C}_2) = \frac{\left(\frac{1}{\beta + \delta + K_{off}}\right)}{\left(\frac{1}{\alpha}\right)\left(\frac{\beta}{\beta + \delta + K_{off}}\right) + \left(\frac{1}{\beta + \delta + K_{off}}\right) + \left(\frac{1}{K_{on}[GABA]}\right)\left(\frac{K_{off}}{\beta + \delta + K_{off}}\right) + \left(\frac{1}{\rho}\right)\left(\frac{\delta}{\beta + \delta + K_{off}}\right)}$$

or alternatively,

$$\boxed{p(\mathcal{C}_2) = \frac{1}{1 + \frac{K_{off}}{K_{on}[GABA]} + \frac{\beta}{\alpha} + \frac{\delta}{\rho}}}$$

(note that this is identical to (82))

iv. $$p(\mathcal{D}) = \frac{(mean\ dwell\ time\ in\ \mathcal{D})(probability\ \ of\ \mathcal{D}\ transition\ \ from\ \mathcal{C}_2)}{\sum(mean\ dwell\ time\ in\ \mathcal{N})(probability\ \ of\ \mathcal{N}transition\ \ from\ neighbors)} \quad (98)$$

substituting (86 – 95) into (98)

$$p(\mathcal{D}) = \frac{\left(\frac{1}{\rho}\right)\left(\frac{\delta}{\beta + \delta + K_{off}}\right)}{\left(\frac{1}{\alpha}\right)\left(\frac{\beta}{\beta + \delta + K_{off}}\right) + \left(\frac{1}{\beta + \delta + K_{off}}\right) + \left(\frac{1}{K_{on}[GABA]}\right)\left(\frac{K_{off}}{\beta + \delta + K_{off}}\right) + \left(\frac{1}{\rho}\right)\left(\frac{\delta}{\beta + \delta + K_{off}}\right)}$$

or alternatively,

$$\boxed{p(\mathcal{D}) = \frac{1}{1 + \frac{\rho K_{off}}{\delta K_{on}[GABA\ ]} + \frac{\beta\rho}{\alpha\delta} + \frac{\rho}{\delta}}}$$

(note that this is identical to (84))

V. Shortcut for solving the equilibrium fractional occupancy of state $\mathcal{N}$ in any non-cyclic Markov model, independent of the number of states (the "round trip" formula)

A. Setup an equation in the following form

$$\underset{t \to \infty}{\mathcal{N}(t)} = \frac{1}{1 + \frac{rates}{rates} + \ \ldots\ + \frac{rates}{rates}}$$

B. Increase the number of rate-constant-ratio-terms in the denominator until it equals the number of states in the gating scheme minus 1.

C. Assign each term in the denominator (other than the term that equals 1) to a different state in the gating scheme (other than state $\mathcal{N}$).

D. For each term, the numerator is equal to the product of rate constants that permit the shortest possible transition from the assigned state to $\mathcal{N}$, and the denominator is the product of rate constants that permit the shortest possible transition from $\mathcal{N}$ to the assigned state.

APPENDIX II

ANALYTIC SOLUTIONS OF MEAN CLOSED TIME, MEAN BOUND TIME, OPENING FREQUENCY, AND GABA EC_{50} FOR MARKOV MODELS OF $GABA_A$ RECEPTOR FUNCTION

Emmanuel J. Botzolakis, Matt T. Bianchi, Farid Hekmat, and Robert L. Macdonald

I. Mean closed time (MCT)

A. $\mathcal{C}_1 \underset{K_{off}}{\overset{K_{on}[GABA]}{\rightleftarrows}} \mathcal{C}_2 \underset{\alpha}{\overset{\beta}{\rightleftarrows}} \mathcal{O}$

$$p(\mathcal{O}) = \frac{1}{1+\frac{\alpha}{\beta}+\frac{\alpha K_{off}}{\beta K_{on}[GABA]}} \text{ (Appendix I, eq. 19)} \quad (1)$$

however, it is also true that

$$p(\mathcal{O}) = \frac{mean\ \ open\ \ time}{mean\ \ lengt\,h\ of\ \ open-closed\ \ cycle}$$

$$= \frac{(mean\ \ open\ \ time)}{(mean\ \ open\ \ time)+(mean\ \ closed\ \ time)} \quad (2)$$

since there is a single $\mathcal{O}$ state,

mean open time = mean dwell time in $\mathcal{O} = \frac{1}{\alpha}$ (3)

substituting (3) into (2)

$$p(\mathcal{O}) = \frac{\frac{1}{\alpha}}{\frac{1}{\alpha}+(MCT)} = \frac{1}{1+\alpha(MCT)} \quad (4)$$

setting (1) equal to (4)

$$\frac{1}{1+\alpha(MCT)} = \frac{1}{1+\frac{\alpha}{\beta}+\frac{\alpha K_{off}}{\beta K_{on}[GABA]}}$$

$$\boxed{\text{MCT} = \frac{1}{\beta}\left(1+\frac{K_{off}}{K_{on}[GABA]}\right)} \quad (5)$$

B. $\mathcal{C}_1 \underset{K_{off}}{\overset{K_{on}[GABA]}{\rightleftharpoons}} \mathcal{C}_2 \underset{\alpha}{\overset{\beta}{\rightleftharpoons}} \mathcal{O} \underset{\rho}{\overset{\delta}{\rightleftharpoons}} \mathcal{D}$

$$p(\mathcal{O}) = \frac{1}{1+\frac{\alpha}{\beta}+\frac{\delta}{\rho}+\frac{\alpha K_{off}}{\beta K_{on}[GABA]}} \text{ (Appendix I, eq. 44)} \quad (6)$$

however, it is also true that

$$p(\mathcal{O}) = \frac{mean\ \ open\ \ time}{mean\ \ lengt\ h\ of\ \ open-closed\ \ cycle}$$

$$= \frac{(mean\ \ open\ \ time)}{(mean\ \ open\ \ time) + (mean\ \ closed\ \ time)} \quad (7)$$

since there is a single $\mathcal{O}$ state,

mean open time = mean dwell time in $\mathcal{O} = \frac{1}{\alpha+\delta}$ (8)

substituting (8) into (7)

$$p(\mathcal{O}) = \frac{\left(\frac{1}{\alpha+\delta}\right)}{\left(\frac{1}{\alpha+\delta}\right)+(MCT)} = \frac{1}{1+(\alpha+\delta)(MCT)} \quad (9)$$

setting (6) equal to (9)

$$\frac{1}{1+(\alpha+\delta)(MCT)} = \frac{1}{1+\frac{\alpha}{\beta}+\frac{\delta}{\rho}+\frac{\alpha K_{off}}{\beta K_{on}[GABA]}}$$

$$\boxed{MCT = \frac{\frac{\alpha}{\beta}+\frac{\delta}{\rho}+\frac{\alpha K_{off}}{\beta K_{on}[GABA]}}{\alpha+\delta}} \quad (10)$$

C.

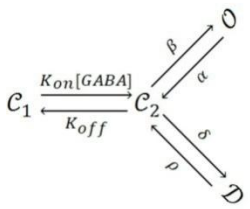

$$p(\mathcal{O}) = \frac{1}{1+\frac{\alpha}{\beta}+\frac{\alpha K_{off}}{\beta K_{on}[GABA]}+\frac{\alpha\delta}{\beta\rho}} \text{ (Appendix I, eq. 77)} \quad (11)$$

however, it is also true that

$$p(\mathcal{O}) = \frac{mean\ \ open\ \ time}{mean\ \ lengt\ h\ of\ \ open-closed\ \ cycle}$$

$$= \frac{(mean\ \ open\ \ time\ )}{(mean\ \ open\ \ time\ ) + (mean\ \ closed\ \ time\ )} \quad (12)$$

since there is a single $\mathcal{O}$ state,

mean open time = mean dwell time in $\mathcal{O} = \frac{1}{\alpha}$ (13)

substituting (13) into (12)

$$p(\mathcal{O}) = \frac{\left(\frac{1}{a}\right)}{\left(\frac{1}{a}\right) + (MCT)} = \frac{1}{1 + a(MCT)} \quad (14)$$

setting (12) equal to (14)

$$\frac{1}{1 + a(MCT)} = \frac{1}{1 + \frac{\alpha}{\beta} + \frac{\alpha K_{off}}{\beta K_{on}[GABA\ ]} + \frac{\alpha\delta}{\beta\rho}}$$

$$\boxed{MCT = \frac{1}{\beta}\left(1 + \frac{K_{off}}{K_{on}[GABA]} + \frac{\delta}{\rho}\right)} \quad (15)$$

D. Shortcut to solving MCT for any non-cyclic Markov model, independent of the number of $\mathcal{C}$ states (assuming the presence of a single $\mathcal{O}$ state)

i. Using the "round trip" formula outlined in Appendix I, Section V, solve for $p(\mathcal{O})$.

ii. Take the inverse of $p(\mathcal{O})$ and subtract 1.

iii. Solve for the mean open time (inverse sum of the exit rates from the $\mathcal{O}$ state).

iv. MCT = the product of (ii) and (iii)

II. Mean bound time (MBT)

A. $\mathcal{C}_1 \underset{K_{off}}{\overset{K_{on}[GABA]}{\rightleftarrows}} \mathcal{C}_2 \underset{\alpha}{\overset{\beta}{\rightleftarrows}} \mathcal{O}$

$$p(\mathcal{C}_1) = \frac{1}{1 + \frac{K_{on}[GABA]}{K_{off}} + \frac{\beta K_{on}[GABA]}{\alpha K_{off}}} \text{ (Appendix I, eq. 21)} \quad (16)$$

however, it is also true that

$$p(\mathcal{C}_1) = \frac{mean\ \ unbound\ \ time}{mean\ \ lengt\,h\ of\ \ unbound\ -bound\ \ cycle}$$

$$= \frac{(mean\ \ unbound\ \ time)}{(mean\ \ unbound\ \ time) + (mean\ \ bound\ \ time)} \quad (17)$$

since there is a single unbound state,

$$\text{mean unbound time = mean dwell time in } \mathcal{C}_1 = \frac{1}{K_{on}[GABA]} \quad (18)$$

substituting (18) into (17)

$$p(\mathcal{C}_1) = \frac{\left(\frac{1}{K_{on}[GABA]}\right)}{\left(\frac{1}{K_{on}[GABA]}\right) + (MBT)} = \frac{1}{1 + (K_{on}[GABA])(MBT)} \quad (19)$$

setting (16) equal to (19)

$$\frac{1}{1 + (K_{on}[GABA])(MBT)} = \frac{1}{1 + \frac{K_{on}[GABA]}{K_{off}} + \frac{\beta K_{on}[GABA]}{\alpha K_{off}}}$$

$$\boxed{MBT = \frac{1}{K_{off}}\left(1 + \frac{\beta}{\alpha}\right)} \quad (20)$$

B. $\mathcal{C}_1 \underset{K_{off}}{\overset{K_{on}[GABA]}{\rightleftarrows}} \mathcal{C}_2 \underset{\alpha}{\overset{\beta}{\rightleftarrows}} \mathcal{O} \underset{\rho}{\overset{\delta}{\rightleftarrows}} \mathcal{D}$

$$p(\mathcal{C}_1) = \frac{1}{1 + \frac{K_{on}[GABA]}{K_{off}} + \frac{\beta K_{on}[GABA]}{\alpha K_{off}} + \frac{\beta\delta K_{on}[GABA]}{\alpha\rho K_{off}}} \text{ (Appendix I, eq. 47)} \quad (21)$$

however, it is also true that

$$p(\mathcal{C}_1) = \frac{mean\ \ unbound\ \ time}{mean\ \ lengt\,h\ of\ \ unbound\ -bound\ \ cycle}$$

$$= \frac{(mean\ \ unbound\ \ time\ )}{(mean\ \ unbound\ \ time\ ) + (mean\ \ bound\ \ time\ )} \tag{22}$$

since there is a single unbound state,

mean unbound time = mean dwell time in $\mathcal{C}_1 = \frac{1}{K_{on}\,[GABA]}$ (23)

substituting (23) into (22)

$$p(\mathcal{C}_1) = \frac{\left(\frac{1}{K_{on}\,[GABA\ ]}\right)}{\left(\frac{1}{K_{on}\,[GABA\ ]}\right) + (MBT)} = \frac{1}{1 + (K_{on}\,[GABA])(MBT)} \tag{24}$$

setting (21) equal to (24)

$$\frac{1}{1 + (K_{on}\,[GABA])(MBT)} = \frac{1}{1 + \frac{K_{on}\,[GABA\ ]}{K_{off}} + \frac{\beta\, K_{on}\,[GABA\ ]}{\alpha K_{off}} + \frac{\beta\delta\, K_{on}\,[GABA\ ]}{\alpha\rho K_{off}}}$$

$$\boxed{MBT = \frac{1}{K_{off}}\left(1 + \frac{\beta}{\alpha} + \frac{\beta\delta}{\alpha\rho}\right)} \tag{25}$$

C.

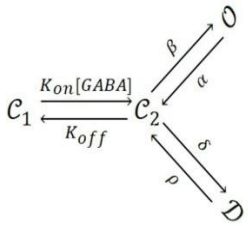

$$p(\mathcal{C}_1) = \frac{1}{1 + \frac{K_{on}\,[GABA\ ]}{K_{off}} + \frac{\beta\, K_{on}\,[GABA\ ]}{\alpha K_{off}} + \frac{\delta\, K_{on}\,[GABA\ ]}{\rho K_{off}}} \text{ (Appendix I, eq. 80)} \tag{26}$$

however, it is also true that

$$p(\mathcal{C}_1) = \frac{mean\ \ unbound\ \ time}{mean\ \ lengt\,h\ of\ \ unbound\ -bound\ \ cycle}$$

$$= \frac{(mean\ \ unbound\ \ time\ )}{(mean\ \ unbound\ \ time\ ) + (mean\ \ bound\ \ time\ )} \tag{27}$$

since there is a single unbound state,

mean unbound time = mean dwell time in $\mathcal{C}_1 = \frac{1}{K_{on}\,[GABA]}$ (28)

substituting (28) into (27)

$$p(\mathcal{C}_1) = \frac{\left(\frac{1}{K_{on}[GABA]}\right)}{\left(\frac{1}{K_{on}[GABA]}\right)+(MBT)} = \frac{1}{1+(K_{on}[GABA])(MBT)} \quad (29)$$

setting (26) equal to (29)

$$\frac{1}{1+(K_{on}[GABA])(MBT)} = \frac{1}{1+\frac{K_{on}[GABA]}{K_{off}}+\frac{\beta K_{on}[GABA]}{\alpha K_{off}}+\frac{\delta K_{on}[GABA]}{\rho K_{off}}}$$

$$\boxed{MBT = \frac{1}{K_{off}}\left(1+\frac{\beta}{\alpha}+\frac{\delta}{\rho}\right)} \quad (30)$$

D. Shortcut to solving MBT for any non-cyclic Markov model, independent of the number of bound states (assuming the presence of a single unbound $\mathcal{C}$ state)

i. Using the "round trip" formula outlined in Appendix I, Section V, solve for $p(\mathcal{C}_1)$.

ii. Take the inverse of $p(\mathcal{C}_1)$ and subtract 1.

iii. Divide this by $K_{on}[GABA]$.

III. Opening frequency ($\mathcal{F}$)

A. $\mathcal{C} \underset{\alpha}{\overset{\beta}{\rightleftharpoons}} \mathcal{O}$

$$\mathcal{F} = \frac{number\ \ of\ openings}{time} = \frac{1\ opening}{mean\ \ lengt\ h\ of\ \ open-closed\ \ cycle}$$

$$= \frac{1\ opening}{(mean\ \ open\ \ time\ ) + (mean\ \ closed\ \ time\ )} \quad (31)$$

mean open time = mean dwell time in $\mathcal{O} = \frac{1}{\alpha}$ (32)

mean closed time = mean dwell time in $\mathcal{C} = \frac{1}{\beta}$ (33)

substituting (33) and (32) into (31)

$$\mathcal{F} = \frac{1}{\frac{1}{\alpha}+\frac{1}{\beta}} = \frac{\alpha}{1+\frac{\alpha}{\beta}} = \frac{\beta}{1+\frac{\beta}{\alpha}} \tag{34}$$

since $p(\mathcal{O}) = \frac{1}{1+\frac{\alpha}{\beta}}$ (Appendix I, eq. 5)

$$\boxed{\mathcal{F} = p(\mathcal{O}) * \alpha} \tag{35}$$

since $p(\mathcal{C}) = \frac{1}{1+\frac{\beta}{\alpha}}$ (Appendix I, eq. 7)

$$\boxed{\mathcal{F} = p(\mathcal{C}) * \beta} \tag{36}$$

B. $\mathcal{C}_1 \underset{K_{off}}{\overset{K_{on}\,[GABA\,]}{\rightleftarrows}} \mathcal{C}_2 \underset{\alpha}{\overset{\beta}{\rightleftarrows}} \mathcal{O}$

$$\mathcal{F} = \frac{number\ \ of\ openings}{time} = \frac{1\ opening}{mean\ \ lengt\,h\ of\ \ open-closed\ \ cycle}$$

$$= \frac{1\ opening}{(mean\ \ open\ \ time\,) + (mean\ \ closed\ \ time\,)} \tag{37}$$

mean open time = mean dwell time in $\mathcal{O} = \frac{1}{\alpha}$ (38)

mean closed time $= \frac{1}{\beta}\left(1 + \frac{K_{off}}{K_{on}\,[GABA]}\right)$ (Appendix II, eq. 5)

substituting (38) and (5) into (37)

$$\mathcal{F} = \frac{1}{\frac{1}{\alpha}+\frac{1}{\beta}\left(1+\frac{K_{off}}{K_{on}\,[GABA\,]}\right)} = \frac{\alpha}{1+\frac{\alpha}{\beta}+\frac{\alpha K_{off}}{\beta K_{on}\,[GABA\,]}} = \frac{\beta}{1+\frac{\beta}{\alpha}+\frac{K_{off}}{K_{on}\,[GABA\,]}} \tag{39}$$

since $p(\mathcal{O}) = \frac{1}{1+\frac{\alpha}{\beta}+\frac{\alpha K_{off}}{\beta K_{on}\,[GABA\,]}}$ (Appendix I, eq. 19)

$$\boxed{\mathcal{F} = p(\mathcal{O}) * \alpha} \tag{40}$$

since $p(\mathcal{C}_2) = \frac{1}{1+\frac{\beta}{\alpha}+\frac{K_{off}}{K_{on}\,[GABA\,]}}$ (Appendix I, eq. 23)

$$\boxed{\mathcal{F} = p(\mathcal{C}_2) * \beta} \tag{41}$$

C. $\mathcal{C}_1 \underset{K_{off}}{\overset{K_{on}\,[GABA\,]}{\rightleftarrows}} \mathcal{C}_2 \underset{\alpha}{\overset{\beta}{\rightleftarrows}} \mathcal{O} \underset{\rho}{\overset{\delta}{\rightleftarrows}} \mathcal{D}$

$$\mathcal{F} = \frac{number\ \ of\ \ openings}{time} = \frac{1\ opening}{mean\ \ lengt\ h\ of\ \ open - closed\ \ cycle}$$

$$= \frac{1\ opening}{(mean\ \ open\ \ time\ ) + (mean\ \ closed\ \ time\ )} \tag{42}$$

mean open time = mean dwell time in $\mathcal{O} = \frac{1}{\alpha + \delta}$ (43)

mean closed time $= \frac{\frac{\alpha}{\beta} + \frac{\delta}{\rho} + \frac{\alpha K_{off}}{\beta K_{on}\,[GABA\,]}}{\alpha + \delta}$ (Appendix II, eq. 10)

substituting (43) and (10) into (42)

$$\mathcal{F} = \frac{1}{\left(\frac{1}{\alpha + \delta}\right) + \left(\frac{\frac{\alpha}{\beta} + \frac{\delta}{\rho} + \frac{\alpha K_{off}}{\beta K_{on}\,[GABA\,]}}{\alpha + \delta}\right)} = \frac{\alpha + \delta}{1 + \frac{\alpha}{\beta} + \frac{\delta}{\rho} + \frac{\alpha K_{off}}{\beta K_{on}\,[GABA\,]}} \tag{44}$$

since $p(\mathcal{O}) = \frac{1}{1 + \frac{\alpha}{\beta} + \frac{\delta}{\rho} + \frac{\alpha K_{off}}{\beta K_{on}\,[GABA\,]}}$ (Appendix I, eq. 44)

$$\boxed{\mathcal{F} = p(\mathcal{O}) * (\alpha + \delta)} \tag{45}$$

rearranging (44)

$$\mathcal{F} = \frac{\alpha}{1 + \frac{\alpha}{\beta} + \frac{\delta}{\rho} + \frac{\alpha K_{off}}{\beta K_{on}\,[GABA\,]}} + \frac{\delta}{1 + \frac{\alpha}{\beta} + \frac{\delta}{\rho} + \frac{\alpha K_{off}}{\beta K_{on}\,[GABA\,]}} \tag{46}$$

$$= \frac{\beta}{1 + \frac{\beta}{\alpha} + \frac{\beta\delta}{\alpha\rho} + \frac{K_{off}}{K_{on}\,[GABA\,]}} + \frac{\rho}{1 + \frac{\alpha\rho}{\beta\delta} + \frac{\rho}{\delta} + \frac{\alpha\rho K_{off}}{\beta\delta K_{on}\,[GABA\,]}}$$

since $p(\mathcal{C}_2) = \frac{1}{1 + \frac{\beta}{\alpha} + \frac{\beta\delta}{\alpha\rho} + \frac{K_{off}}{K_{on}\,[GABA\,]}}$ (Appendix I, eq. 50)

and $p(\mathcal{D}) = \frac{1}{1 + \frac{\alpha\rho}{\beta\delta} + \frac{\rho}{\delta} + \frac{\alpha\rho\, K_{off}}{\beta\delta\, K_{on}\,[GABA\,]}}$ (Appendix I, eq. 52)

$$\boxed{\mathcal{F} = p(\mathcal{C}_2) * \beta + p(\mathcal{D}) * \rho} \tag{47}$$

D.

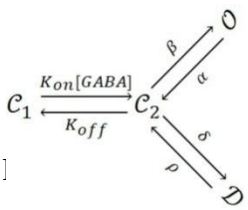

$$\underline{s} = \frac{1}{(mean\ \ open\ \ time\ ) + (mean\ \ closed\ \ time\ )}$$

$$\mathcal{F} = \frac{number\ \ of\ \ openings}{time} = \frac{1\ opening}{mean\ \ lengt\ h\ of\ \ open - closed\ \ cycle}$$

$$= \frac{1\ opening}{(mean\ \ open\ \ time\ ) + (mean\ \ closed\ \ time\ )} \tag{48}$$

mean open time = mean dwell time in $\mathcal{O} = \frac{1}{\alpha}$ (49)

mean closed time $= \frac{1}{\beta}\left(1 + \frac{K_{off}}{K_{on}\,[GABA]} + \frac{\delta}{\rho}\right)$ (Appendix II, eq. 15)

substituting (49) and (15) into (48)

$$\mathcal{F} = \frac{1}{\frac{1}{\alpha} + \frac{1}{\beta}\left(1 + \frac{K_{off}}{K_{on}\,[GABA\ ]} + \frac{\delta}{\rho}\right)} = \frac{\alpha}{1 + \frac{\alpha}{\beta} + \frac{\alpha\delta}{\beta\rho} + \frac{\alpha K_{off}}{\beta K_{on}\,[GABA\ ]}} = \frac{\beta}{1 + \frac{\beta}{\alpha} + \frac{\delta}{\rho} + \frac{K_{off}}{K_{on}\,[GABA\ ]}} \tag{50}$$

since $p(\mathcal{O}) = \frac{1}{1 + \frac{\alpha}{\beta} + \frac{\alpha\delta}{\beta\rho} + \frac{\alpha K_{off}}{\beta K_{on}\,[GABA\ ]}}$ (Appendix I, eq. 77)

$$\boxed{\mathcal{F} = p(\mathcal{O}) * \alpha} \tag{51}$$

since $p(\mathcal{C}_2) = \frac{1}{1 + \frac{\beta}{\alpha} + \frac{\delta}{\rho} + \frac{K_{off}}{K_{on}\,[GABA\ ]}}$ (Appendix I, eq. 82)

$$\boxed{\mathcal{F} = p(\mathcal{C}_2) * \beta} \tag{52}$$

E. $\mathcal{C}_1 \underset{K_{off}}{\overset{K_{on}\,[GABA\ ]}{\rightleftarrows}} \mathcal{C}_2 \underset{\alpha_1}{\overset{\beta_1}{\rightleftarrows}} \mathcal{O}_1 \underset{\alpha_2}{\overset{\beta_2}{\rightleftarrows}} \mathcal{O}_2$

$$\mathcal{F} = \frac{number\ \ of\ \ openings}{time} = \frac{1\ opening}{mean\ \ lengt\ h\ of\ \ open - clos\ ed\ \ cycle}$$

$$= \frac{1\ opening}{(mean\ \ open\ \ time\ ) + (mean\ \ closed\ \ time\ )} \tag{53}$$

mean open time $= \frac{1}{\alpha_1}\left(1 + \frac{\beta_2}{\alpha_2}\right)$ (by analogy to Appendix II, eq. 5) (54)

mean closed time $= \frac{1}{\beta_1}\left(1 + \frac{K_{off}}{K_{on}\,[GABA]}\right)$ (Appendix II, eq. 5) (55)

substituting (54) and (55) into (53)

$$\mathcal{F} = \frac{1}{\frac{1}{\alpha_1}\left(1+\frac{\beta_2}{\alpha_2}\right)+\frac{1}{\beta_1}\left(1+\frac{K_{off}}{K_{on}\,[GABA\,]}\right)} = \frac{\alpha_1}{1+\frac{\beta_2}{\alpha_2}+\frac{\alpha_1}{\beta_1}+\frac{\alpha_1 K_{off}}{\beta_1 K_{on}\,[GABA\,]}} \quad (56)$$

since $p(\mathcal{O}_1) = \frac{1}{1+\frac{\beta_2}{\alpha_2}+\frac{\alpha_1}{\beta_1}+\frac{\alpha_1 K_{off}}{\beta_1 K_{on}\,[GABA\,]}}$ (Appendix I, Section V) (57)

$$\boxed{\mathcal{F} = p(\mathcal{O}_1) * \alpha_1} \quad (58)$$

since $p(\mathcal{C}_2) = \frac{1}{1+\frac{\beta}{\alpha}+\frac{\delta}{\rho}+\frac{K_{off}}{K_{on}\,[GABA\,]}}$ (Appendix I, Section V) (59)

$$\boxed{\mathcal{F} = p(\mathcal{C}_2) * \beta_1} \quad (60)$$

F. Shortcut for solving opening frequency for any non-cyclic Markov model, independent of the number of $\mathcal{C}$ and $\mathcal{O}$ states

i. Identify every transition between $\mathcal{C}$ and $\mathcal{O}$ states.

ii. Determine the equilibrium fractional occupancies (using the "round trip" approach described in Appendix I, Section V) of EITHER the $\mathcal{C}$ or $\mathcal{O}$ states involved in those transitions.

iii. Multiply each of the equilibrium fractional occupancies by the sum of the rate constants that permit transition to the other conductance level.

iv. Opening frequency = the sum of those terms.

IV. GABA EC_{50}

A. $\mathcal{C}_1 \underset{K_{off}}{\overset{K_{on}\,[GABA\,]}{\rightleftarrows}} \mathcal{C}_2 \underset{\alpha}{\overset{\beta}{\rightleftarrows}} \mathcal{O}$

$$p(\mathcal{O}) = \frac{1}{1 + \frac{\alpha}{\beta} + \frac{\alpha K_{off}}{\beta K_{on}[GABA]}}$$ (Appendix I, eq. 19)

or alternatively,

$$p(\mathcal{O}) = \frac{\frac{\beta}{\alpha}}{1 + \frac{\beta}{\alpha} + \frac{K_{off}}{K_{on}[GABA]}} \quad (61)$$

let $\mathcal{E} = \frac{\beta}{\alpha}$ (classical definition of "efficacy") (62)

let $\mathcal{K}_a = \frac{K_{off}}{K_{on}}$ (classical definition of "affinity") (63)

substituting (62) and (63) into (61)

$$p(\mathcal{O}) = \frac{\mathcal{E}}{1 + \mathcal{E} + \frac{\mathcal{K}_a}{[GABA]}} \quad (64)$$

$$p(\mathcal{O})_{max} = \lim_{[\text{GABA}]\to\infty} p(\mathcal{O}) = \lim_{[\text{GABA}]\to\infty} \left(\frac{\mathcal{E}}{1 + \mathcal{E} + \frac{\mathcal{K}_a}{[GABA]}} \right) = \frac{\mathcal{E}}{1 + \mathcal{E}} \quad (65)$$

EC_{50} is, by definition, the [GABA] yielding ½ $p(\mathcal{O})_{max}$

$$\text{½ } p(\mathcal{O})_{max} = \left(\frac{1}{2}\right)\left(\frac{\mathcal{E}}{1 + \mathcal{E}}\right) = \frac{\mathcal{E}}{2 + 2\mathcal{E}} \quad (66)$$

setting (66) equal to (64)

$$\frac{\mathcal{E}}{2 + 2\mathcal{E}} = \frac{\mathcal{E}}{1 + \mathcal{E} + \frac{\mathcal{K}_a}{[GABA]}}$$

solving for $[GABA]$

$$\boxed{[GABA]_{EC_{50}} = \frac{\mathcal{K}_a}{1 + \mathcal{E}}} \quad (67)$$

(note that the above matches the solution shown in Colquhoun, 1998)

B. $\mathcal{C}_1 \underset{K_{off}}{\overset{K_{on}[GABA]}{\rightleftharpoons}} \mathcal{C}_2 \underset{\alpha}{\overset{\beta}{\rightleftharpoons}} \mathcal{O} \underset{\rho}{\overset{\delta}{\rightleftharpoons}} \mathcal{D}$

$$p(\mathcal{O}) = \frac{1}{1 + \frac{\alpha}{\beta} + \frac{\alpha K_{off}}{\beta K_{on}[GABA]} + \frac{\delta}{\rho}}$$ (Appendix I, eq. 44)

or alternatively,

$$p(\mathcal{O}) = \frac{\frac{\beta}{\alpha}}{1 + \frac{\beta}{\alpha} + \frac{K_{off}}{K_{on}[GABA]} + \frac{\beta\delta}{\alpha\rho}} \tag{68}$$

let $\mathcal{E} = \frac{\beta}{\alpha}$ (classical definition of "efficacy") (69)

let $\mathcal{K}_a = \frac{K_{off}}{K_{on}}$ (classical definition of "affinity") (70)

let $\Delta = \frac{\delta}{\rho}$ (Bianchi et al., 2007, definition of $\mathcal{D}$ state "stability") (71)

substituting (69), (70), and (71) into (68)

$$p(\mathcal{O}) = \frac{\mathcal{E}}{1 + \mathcal{E} + \frac{\mathcal{K}_a}{[GABA]} + \mathcal{E}\Delta} \tag{72}$$

$$p(\mathcal{O})_{max} = \lim_{[\text{GABA}]\to\infty} p(\mathcal{O}) = \lim_{[\text{GABA}]\to\infty} \left(\frac{\mathcal{E}}{1 + \mathcal{E} + \frac{\mathcal{K}_a}{[GABA]} + \mathcal{E}\Delta} \right)$$

$$p(\mathcal{O})_{max} = \frac{\mathcal{E}}{1 + \mathcal{E} + \mathcal{E}\Delta} \tag{73}$$

EC_{50} is, by definition, the [GABA] yielding ½ $p(\mathcal{O})_{max}$

$$\text{½ } p(\mathcal{O})_{max} = \left(\frac{1}{2}\right)\left(\frac{\mathcal{E}}{1 + \mathcal{E} + \mathcal{E}\Delta}\right) = \frac{\mathcal{E}}{2 + 2\mathcal{E} + 2\mathcal{E}\Delta} \tag{74}$$

setting (74) equal to (72)

$$\frac{\mathcal{E}}{2 + 2\mathcal{E} + 2\mathcal{E}\Delta} = \frac{\mathcal{E}}{1 + \mathcal{E} + \frac{\mathcal{K}_a}{[GABA]} + \mathcal{E}\Delta}$$

solving for $[GABA]$

$$\boxed{[GABA]_{EC_{50}} = \frac{\mathcal{K}_a}{1 + \mathcal{E} + \mathcal{E}\Delta}} \tag{75}$$

C.

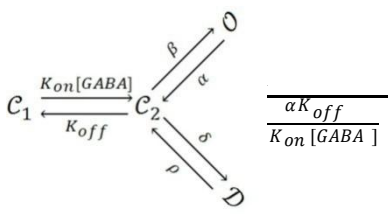

$$\frac{\alpha K_{off}}{K_{on}[GABA]}$$

$$p(\mathcal{O}) = \frac{1}{1 + \frac{\alpha}{\beta} + \frac{\alpha K_{off}}{\beta K_{on}[GABA]} + \frac{\alpha\delta}{\beta\rho}}$$ (Appendix I, eq. 77)

or alternatively,

$$p(\mathcal{O}) = \frac{\frac{\beta}{\alpha}}{1 + \frac{\beta}{\alpha} + \frac{K_{off}}{K_{on}[GABA]} + \frac{\delta}{\rho}} \tag{76}$$

let $\mathcal{E} = \frac{\beta}{\alpha}$ (classical definition of "efficacy") (77)

let $\mathcal{K}_a = \frac{K_{off}}{K_{on}}$ (classical definition of "affinity") (78)

let $\Delta = \frac{\delta}{\rho}$ (Bianchi et al., 2007, definition of $\mathcal{D}$ state "stability") (79)

substituting (77), (78), and (79) into (76)

$$p(\mathcal{O}) = \frac{\mathcal{E}}{1 + \mathcal{E} + \frac{\mathcal{K}_a}{[GABA]} + \Delta} \tag{80}$$

$$p(\mathcal{O})_{max} = \lim_{[\text{GABA}]\to\infty} p(\mathcal{O}) = \lim_{[\text{GABA}]\to\infty} \left(\frac{\mathcal{E}}{1 + \mathcal{E} + \frac{\mathcal{K}_a}{[GABA]} + \Delta} \right)$$

$$p(\mathcal{O})_{max} = \frac{\mathcal{E}}{1 + \mathcal{E} + \Delta} \tag{81}$$

EC_{50} is, by definition, the [GABA] yielding ½ $p(\mathcal{O})_{max}$

$$\text{½ } p(\mathcal{O})_{max} = \left(\frac{1}{2}\right)\left(\frac{\mathcal{E}}{1 + \mathcal{E} + \Delta}\right) = \frac{\mathcal{E}}{2 + 2\mathcal{E} + 2\Delta} \tag{82}$$

setting (74) equal to (72)

$$\frac{\mathcal{E}}{2 + 2\mathcal{E} + 2\Delta} = \frac{\mathcal{E}}{1 + \mathcal{E} + \frac{\mathcal{K}_a}{[GABA]} + \Delta}$$

solving for $[GABA]$

$$\boxed{[GABA]_{EC_{50}} = \frac{\mathcal{K}_a}{1 + \mathcal{E} + \Delta}} \tag{83}$$

APPENDIX III

THE EFFECT OF OPEN CHANNEL BLOCK ON OPEN PROBABILITY, MEAN CLOSED TIME, MEAN BOUND TIME, OPENING FREQUENCY, AND GABA EC_{50} FOR MARKOV MODELS OF $GABA_A$ RECEPTOR FUNCTION

Emmanuel J. Botzolakis, Matt T. Bianchi, Farid Hekmat, and Robert L. Macdonald

I. Open probability

A. $\mathcal{C} \underset{\alpha}{\overset{\beta}{\rightleftharpoons}} \mathcal{O}$

$$p(\mathcal{O})_{C\mathcal{O}} = \frac{1}{1+\frac{\alpha}{\beta}} \text{ (Appendix I, eq. 5)} \quad (1)$$

$$\mathcal{C} \underset{\alpha}{\overset{\beta}{\rightleftharpoons}} \mathcal{O} \underset{K_-}{\overset{K_+[B]}{\rightleftharpoons}} \mathcal{B}$$

$$\boxed{p(\mathcal{O})_{C\mathcal{O}\mathcal{B}} = \frac{1}{1+\frac{\alpha}{\beta}+\frac{K_+[B]}{K_-}}} \text{ (Appendix I, Section V)} \quad (2)$$

$$\frac{p(\mathcal{O})_{C\mathcal{O}}}{p(\mathcal{O})_{C\mathcal{O}\mathcal{B}}} = \frac{1+\frac{\alpha}{\beta}+\frac{K_+[B]}{K_-}}{1+\frac{\alpha}{\beta}} = 1+\frac{\frac{K_+[B]}{K_-}}{1+\frac{\alpha}{\beta}}$$

$$\frac{p(\mathcal{O})_{C\mathcal{O}}}{p(\mathcal{O})_{C\mathcal{O}\mathcal{B}}} = 1+\left(\frac{1}{1+\frac{\alpha}{\beta}}\right)\left(\frac{K_+[B]}{K_-}\right)$$

$$\boxed{\frac{p(\mathcal{O})_{C\mathcal{O}}}{p(\mathcal{O})_{C\mathcal{O}\mathcal{B}}} = 1+(\mathrm{p}(\mathcal{O})_{C\mathcal{O}})\left(\frac{K_+[B]}{K_-}\right)} \quad (3)$$

B. $\mathcal{C}_1 \underset{K_{off}}{\overset{K_{on}[GABA]}{\rightleftharpoons}} \mathcal{C}_2 \underset{\alpha}{\overset{\beta}{\rightleftharpoons}} \mathcal{O}$

$$p(\mathcal{O})_{CC\mathcal{O}} = \frac{1}{1+\frac{\alpha}{\beta}+\frac{\alpha K_{off}}{\beta K_{on}[GABA]}} \text{ (Appendix I, eq. 19)} \quad (4)$$

$$\mathcal{C}_1 \underset{K_{off}}{\overset{K_{on}\,[GABA\,]}{\rightleftarrows}} \mathcal{C}_2 \underset{\alpha}{\overset{\beta}{\rightleftarrows}} \mathcal{O} \underset{K_-}{\overset{K_+[B]}{\rightleftarrows}} \mathcal{B}$$

$$\boxed{p(\mathcal{O})_{CC\mathcal{O}\mathcal{B}} = \frac{1}{1+\frac{\alpha}{\beta}+\frac{\alpha K_{off}}{\beta K_{on}\,[GABA\,]}+\frac{K_+[B]}{K_-}}} \text{ (Appendix I, Section V)} \quad (5)$$

$$\frac{p(\mathcal{O})_{CC\mathcal{O}}}{p(\mathcal{O})_{CC\mathcal{O}\mathcal{B}}} = \frac{1+\frac{\alpha}{\beta}+\frac{\alpha K_{off}}{\beta K_{on}\,[GABA\,]}+\frac{K_+[B]}{K_-}}{1+\frac{\alpha}{\beta}+\frac{\alpha K_{off}}{\beta K_{on}\,[GABA\,]}} = 1+\frac{\frac{K_+[B]}{K_-}}{1+\frac{\alpha}{\beta}+\frac{\alpha K_{off}}{\beta K_{on}\,[GABA\,]}}$$

$$\frac{p(\mathcal{O})_{CC\mathcal{O}}}{p(\mathcal{O})_{CC\mathcal{O}\mathcal{B}}} = 1+\left(\frac{1}{1+\frac{\alpha}{\beta}+\frac{\alpha K_{off}}{\beta K_{on}\,[GABA\,]}}\right)\left(\frac{K_+[B]}{K_-}\right)$$

$$\boxed{\frac{p(\mathcal{O})_{CC\mathcal{O}}}{p(\mathcal{O})_{CC\mathcal{O}\mathcal{B}}} = 1+(\mathrm{p}(\mathcal{O})_{CC\mathcal{O}})\left(\frac{K_+[B]}{K_-}\right)} \quad (6)$$

C. $$\mathcal{C}_1 \underset{K_{off}}{\overset{K_{on}\,[GABA\,]}{\rightleftarrows}} \mathcal{C}_2 \underset{\alpha}{\overset{\beta}{\rightleftarrows}} \mathcal{O} \underset{\rho}{\overset{\delta}{\rightleftarrows}} \mathcal{D}$$

$$p(\mathcal{O})_{CC\mathcal{O}\mathcal{D}} = \frac{1}{1+\frac{\alpha}{\beta}+\frac{\delta}{\rho}+\frac{\alpha K_{off}}{\beta K_{on}\,[GABA\,]}} \text{ (Appendix I, eq. 44)} \quad (7)$$

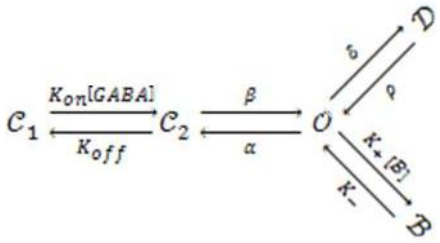

$$\boxed{p(\mathcal{O})_{CC\mathcal{O}\mathcal{D}\mathcal{B}} = \frac{1}{1+\frac{\alpha}{\beta}+\frac{\delta}{\rho}+\frac{\alpha K_{off}}{\beta K_{on}\,[GABA\,]}+\frac{K_+[B]}{K_-}}} \text{ (Appendix I, Section V)} \quad (8)$$

$$\frac{p(\mathcal{O})_{CC\mathcal{O}\mathcal{D}}}{p(\mathcal{O})_{CC\mathcal{O}\mathcal{D}\mathcal{B}}} = \frac{1+\frac{\alpha}{\beta}+\frac{\delta}{\rho}+\frac{\alpha K_{off}}{\beta K_{on}\,[GABA\,]}+\frac{K_+[B]}{K_-}}{1+\frac{\alpha}{\beta}+\frac{\delta}{\rho}+\frac{\alpha K_{off}}{\beta K_{on}\,[GABA\,]}} = 1+\frac{\frac{K_+[B]}{K_-}}{1+\frac{\alpha}{\beta}+\frac{\delta}{\rho}+\frac{\alpha K_{off}}{\beta K_{on}\,[GABA\,]}}$$

$$\frac{p(\mathcal{O})_{CC\mathcal{O}\mathcal{D}}}{p(\mathcal{O})_{CC\mathcal{O}\mathcal{D}\mathcal{B}}} = 1+\left(\frac{1}{1+\frac{\alpha}{\beta}+\frac{\delta}{\rho}+\frac{\alpha K_{off}}{\beta K_{on}\,[GABA\,]}}\right)\left(\frac{K_+[B]}{K_-}\right)$$

$$\boxed{\frac{p(\mathcal{O})_{CC\mathcal{O}\mathcal{D}}}{p(\mathcal{O})_{CC\mathcal{O}\mathcal{D}\mathcal{B}}} = 1+(\mathrm{p}(\mathcal{O})_{CC\mathcal{O}\mathcal{D}})\left(\frac{K_+[B]}{K_-}\right)} \quad (9)$$

D.

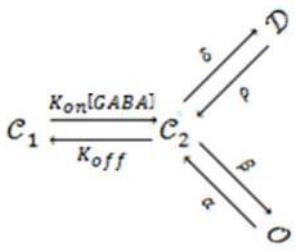

$$p(\mathcal{O})_{CCDO} = \frac{1}{1+\frac{\alpha}{\beta}+\frac{\alpha K_{off}}{\beta K_{on}[GABA\ ]}+\frac{\alpha\delta}{\beta\rho}} \text{ (Appendix I, eq. 77)} \quad (10)$$

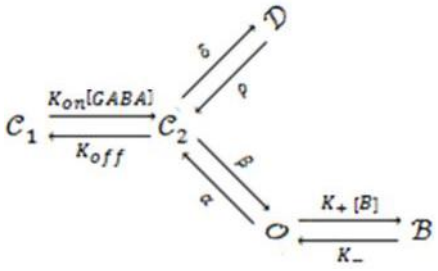

$$\boxed{p(\mathcal{O})_{CCDOB} = \frac{1}{1+\frac{\alpha}{\beta}+\frac{\alpha K_{off}}{\beta K_{on}[GABA\ ]}+\frac{\alpha\delta}{\beta\rho}+\frac{K_+[B]}{K_-}}} \text{ (Appendix I, Section V)} \quad (11)$$

$$\frac{p(\mathcal{O})_{CCDO}}{p(\mathcal{O})_{CCDOB}} = \frac{1+\frac{\alpha}{\beta}+\frac{\alpha K_{off}}{\beta K_{on}[GABA\ ]}+\frac{\alpha\delta}{\beta\rho}+\frac{K_+[B]}{K_-}}{1+\frac{\alpha}{\beta}+\frac{\alpha K_{off}}{\beta K_{on}[GABA\ ]}+\frac{\alpha\delta}{\beta\rho}} = 1+\frac{\frac{K_+[B]}{K_-}}{1+\frac{\alpha}{\beta}+\frac{\alpha K_{off}}{\beta K_{on}[GABA\ ]}+\frac{\alpha\delta}{\beta\rho}}$$

$$\frac{p(\mathcal{O})_{CCDO}}{p(\mathcal{O})_{CCDOB}} = 1+\left(\frac{1}{1+\frac{\alpha}{\beta}+\frac{\alpha K_{off}}{\beta K_{on}[GABA\ ]}+\frac{\alpha\delta}{\beta\rho}}\right)\left(\frac{K_+[B]}{K_-}\right)$$

$$\boxed{\frac{p(\mathcal{O})_{CCDO}}{p(\mathcal{O})_{CCDOB}} = 1+(\mathrm{p}(\mathcal{O})_{CCDO})\left(\frac{K_+[B]}{K_-}\right)} \quad (12)$$

II. Mean closed time (MCT)

A. $\mathcal{C} \underset{\alpha}{\overset{\beta}{\rightleftharpoons}} \mathcal{O}$

since there is only 1 closed state,

$MCT_{\mathcal{CO}}$ = mean dwell time in $\mathcal{C} = \frac{1}{\beta}$ (13)

$$\mathcal{C} \underset{\alpha}{\overset{\beta}{\rightleftarrows}} \mathcal{O} \underset{K_-}{\overset{K_+[B]}{\rightleftarrows}} \mathcal{B}$$

$$\boxed{MCT_{\mathcal{COB}} = \frac{\frac{\alpha}{\beta} + \frac{K_+[B]}{K_-}}{\alpha + (K_+[B])}} \text{ (Appendix II, Section I.D)} \quad (14)$$

$$\frac{MCT_{\mathcal{COB}}}{MCT_{\mathcal{CO}}} = \frac{\alpha + \frac{\beta K_+[B]}{K_-}}{\alpha + (K_+[B])} \quad (15)$$

thus,

$$\frac{MCT_{\mathcal{COB}}}{MCT_{\mathcal{CO}}} > 1 \text{ if } \frac{\beta}{K_-} > 1$$

or alternatively,

$$\boxed{\frac{MCT_{\mathcal{COB}}}{MCT_{\mathcal{CO}}} > 1 \text{ if } \frac{1}{K_-} > \frac{1}{\beta}} \quad (16)$$

(i.e., if mean dwell time in $\mathcal{B}$ > mean dwell time in $\mathcal{C}$)

B. $$\mathcal{C}_1 \underset{K_{off}}{\overset{K_{on}[GABA]}{\rightleftarrows}} \mathcal{C}_2 \underset{\alpha}{\overset{\beta}{\rightleftarrows}} \mathcal{O}$$

$$MCT_{\mathcal{CCO}} = \frac{1}{\beta}\left(1 + \frac{K_{off}}{K_{on}[GABA]}\right) \text{ (Appendix II, eq. 5)} \quad (17)$$

$$\mathcal{C}_1 \underset{K_{off}}{\overset{K_{on}[GABA]}{\rightleftarrows}} \mathcal{C}_2 \underset{\alpha}{\overset{\beta}{\rightleftarrows}} \mathcal{O} \underset{K_-}{\overset{K_+[B]}{\rightleftarrows}} \mathcal{B}$$

$$\boxed{MCT_{\mathcal{CCOB}} = \frac{\frac{\alpha}{\beta} + \frac{\alpha K_{off}}{\beta K_{on}[GABA]} + \frac{K_+[B]}{K_-}}{\alpha + (K_+[B])}} \text{ (Appendix II, Section I.D)} \quad (18)$$

$$\frac{MCT_{\mathcal{CCOB}}}{MCT_{\mathcal{CCO}}} = \frac{\frac{\frac{\alpha}{\beta} + \frac{\alpha K_{off}}{\beta K_{on}[GABA]} + \frac{K_+[B]}{K_-}}{\alpha + (K_+[B])}}{\frac{1}{\beta}\left(1 + \frac{K_{off}}{K_{on}[GABA]}\right)} = \frac{\frac{\alpha}{\beta} + \frac{\alpha K_{off}}{\beta K_{on}[GABA]} + \frac{K_+[B]}{K_-}}{\left(\frac{\alpha}{\beta} + \frac{K_+[B]}{\beta}\right)\left(1 + \frac{K_{off}}{K_{on}[GABA]}\right)}$$

$$\frac{MCT_{\mathcal{CCOB}}}{MCT_{\mathcal{CCO}}} = \frac{\frac{\alpha}{\beta} + \frac{\alpha K_{off}}{\beta K_{on}[GABA]} + \frac{K_+[B]}{K_-}}{\frac{\alpha}{\beta} + \frac{\alpha K_{off}}{\beta K_{on}[GABA]} + \frac{K_+[B]}{\beta} + \frac{K_{off}\ K_+[B]}{\beta K_{on}[GABA]}}$$

$$\frac{MCT_{\mathcal{CCOB}}}{MCT_{\mathcal{CCO}}} = \frac{\frac{\alpha}{K_+[B]} + \frac{\alpha K_{off}}{K_{on}[GABA\ ]K_+[B]} + \frac{\beta}{K_-}}{\frac{\alpha}{K_+[B]} + \frac{\alpha K_{off}}{K_{on}[GABA\ ]K_+[B]} + 1 + \frac{K_{off}}{K_{on}[GABA\ ]}} \tag{19}$$

thus,

$$\frac{MCT_{\mathcal{CCOB}}}{MCT_{\mathcal{CCO}}} > 1 \text{ if } \frac{\beta}{K_-} > \left(1 + \frac{K_{off}}{K_{on}[GABA]}\right)$$

or alternatively,

$$\boxed{\frac{MCT_{\mathcal{CCOB}}}{MCT_{\mathcal{CCO}}} > 1 \text{ if } \frac{1}{K_-} > \frac{1}{\beta}\left(1 + \frac{K_{off}}{K_{on}[GABA]}\right)} \tag{20}$$

(i.e., if mean dwell time in $\mathcal{B} > MCT_{\mathcal{CCO}}$)

C. $\mathcal{C}_1 \underset{K_{off}}{\overset{K_{on}[GABA\ ]}{\rightleftarrows}} \mathcal{C}_2 \underset{\alpha}{\overset{\beta}{\rightleftarrows}} \mathcal{O} \underset{\rho}{\overset{\delta}{\rightleftarrows}} \mathcal{D}$

$$MCT_{\mathcal{CCOD}} = \frac{\frac{\alpha}{\beta} + \frac{\alpha K_{off}}{\beta K_{on}[GABA\ ]} + \frac{\delta}{\rho}}{\alpha + \delta} \text{ (Appendix II, eq. 10)} \tag{21}$$

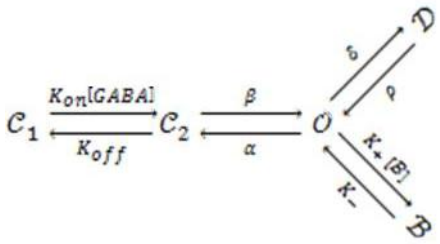

$$\boxed{MCT_{\mathcal{CCODB}} = \frac{\frac{\alpha}{\beta} + \frac{\alpha K_{off}}{\beta K_{on}[GABA\ ]} + \frac{\delta}{\rho} + \frac{K_+[B]}{K_-}}{\alpha + \delta + (K_+[B])}} \text{ (Appendix II, Section I.D)} \tag{22}$$

$$\frac{MCT_{\mathcal{CCODB}}}{MCT_{\mathcal{CCOD}}} = \frac{\frac{\frac{\alpha}{\beta} + \frac{\alpha K_{off}}{\beta K_{on}[GABA\ ]} + \frac{\delta}{\rho} + \frac{K_+[B]}{K_-}}{\alpha + \delta + (K_+[B])}}{\frac{\frac{\alpha}{\beta} + \frac{\alpha K_{off}}{\beta K_{on}[GABA\ ]} + \frac{\delta}{\rho}}{\alpha + \delta}} = \frac{\left(\frac{\alpha}{\beta} + \frac{\alpha K_{off}}{\beta K_{on}[GABA\ ]} + \frac{\delta}{\rho} + \frac{K_+[B]}{K_-}\right)(\alpha + \delta)}{(\alpha + \delta + (K_+[B]))\left(\frac{\alpha}{\beta} + \frac{\alpha K_{off}}{\beta K_{on}[GABA\ ]} + \frac{\delta}{\rho}\right)}$$

$$\frac{MCT_{\mathcal{CCODB}}}{MCT_{\mathcal{CCOD}}} = \frac{\frac{\alpha^2}{\beta} + \frac{\alpha^2 K_{off}}{\beta K_{on}[GABA\ ]} + \frac{\alpha\delta}{\rho} + \frac{\alpha\delta}{\beta} + \frac{\alpha\delta K_{off}}{\beta K_{on}[GABA\ ]} + \frac{\delta^2}{\rho} + \frac{\alpha K_+[B]}{K_-} + \frac{\delta K_+[B]}{K_-}}{\frac{\alpha^2}{\beta} + \frac{\alpha^2 K_{off}}{\beta K_{on}[GABA\ ]} + \frac{\alpha\delta}{\rho} + \frac{\alpha\delta}{\beta} + \frac{\alpha\delta K_{off}}{\beta K_{on}[GABA\ ]} + \frac{\delta^2}{\rho} + \frac{\alpha K_+[B]}{\beta} + \frac{\alpha K_{off} K_+[B]}{\beta K_{on}[GABA\ ]} + \frac{\delta K_+[B]}{\rho}}$$

let X = $\frac{\alpha^2}{\beta} + \frac{\alpha^2 K_{off}}{\beta K_{on}[GABA]} + \frac{\alpha\delta}{\rho} + \frac{\alpha\delta}{\beta} + \frac{\alpha\delta K_{off}}{\beta K_{on}[GABA]} + \frac{\delta^2}{\rho}$

$$\frac{MCT_{\mathcal{CCODB}}}{MCT_{\mathcal{CCOD}}} = \frac{X + \frac{\alpha K_+[B]}{K_-} + \frac{\delta K_+[B]}{K_-}}{X + \frac{\alpha K_+[B]}{\beta} + \frac{\alpha K_{off} K_+[B]}{\beta K_{on}[GABA]} + \frac{\delta K_+[B]}{\rho}} = \frac{\frac{X}{K_+[B]} + \frac{\alpha}{K_-} + \frac{\delta}{K_-}}{\frac{X}{K_+[B]} + \frac{\alpha}{\beta} + \frac{\alpha K_{off}}{\beta K_{on}[GABA]} + \frac{\delta}{\rho}}$$

$$\frac{MCT_{\mathcal{CCODB}}}{MCT_{\mathcal{CCOD}}} = \frac{\frac{X}{K_+[B]} + \frac{\alpha}{K_-} + \frac{\delta}{K_-}}{\frac{X}{K_+[B]} + \frac{\alpha}{\beta} + \frac{\alpha K_{off}}{\beta K_{on}[GABA]} + \frac{\delta}{\rho}} \quad (23)$$

thus,

$$\frac{MCT_{\mathcal{CCODB}}}{MCT_{\mathcal{CCOD}}} > 1 \text{ if } \left(\frac{\alpha + \delta}{K_-}\right) > \left(\frac{\alpha}{\beta} + \frac{\alpha K_{off}}{\beta K_{on}[GABA]} + \frac{\delta}{\rho}\right)$$

or alternatively,

$$\boxed{\frac{MCT_{\mathcal{CCODB}}}{MCT_{\mathcal{CCOD}}} > 1 \text{ if } \frac{1}{K_-} > \frac{\frac{\alpha}{\beta} + \frac{\alpha K_{off}}{\beta K_{on}[GABA]} + \frac{\delta}{\rho}}{\alpha + \delta}} \quad (24)$$

(i.e., if mean dwell time in $\mathcal{B} > MCT_{\mathcal{CCOD}}$)

D.

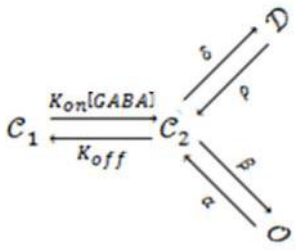

$MCT_{\mathcal{CCDO}} = \frac{1}{\beta}\left(1 + \frac{K_{off}}{K_{on}[GABA]} + \frac{\delta}{\rho}\right)$ (Appendix II, eq. 15) (25)

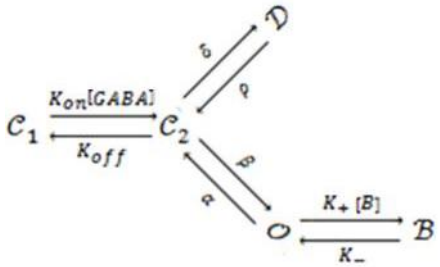

$$\boxed{MCT_{\mathcal{CCDOB}} = \frac{\frac{\alpha}{\beta} + \frac{\alpha K_{off}}{\beta K_{on}[GABA]} + \frac{\alpha\delta}{\beta\rho} + \frac{K_+[B]}{K_-}}{\alpha + (K_+[B])}} \text{ (Appendix II, Section I.D)} \quad (26)$$

$$\frac{MCT_{\mathcal{CCDOB}}}{MCT_{\mathcal{CCDO}}} = \frac{\frac{\frac{\alpha}{\beta} + \frac{\alpha K_{off}}{\beta K_{on}[GABA]} + \frac{\alpha\delta}{\beta\rho} + \frac{K_+[B]}{K_-}}{\alpha + (K_+[B])}}{\frac{1}{\beta}\left(1 + \frac{K_{off}}{K_{on}[GABA]} + \frac{\delta}{\rho}\right)} = \frac{\alpha + \frac{\alpha K_{off}}{K_{on}[GABA]} + \frac{\alpha\delta}{\rho} + \frac{\beta K_+[B]}{K_-}}{(\alpha + (K_+[B]))\left(1 + \frac{K_{off}}{K_{on}[GABA]} + \frac{\delta}{\rho}\right)}$$

$$\frac{MCT_{\mathcal{CCDOB}}}{MCT_{\mathcal{CCDO}}} = \frac{\alpha + \frac{\alpha K_{off}}{K_{on}[GABA]} + \frac{\alpha\delta}{\rho} + \frac{\beta K_+[B]}{K_-}}{\alpha + \frac{\alpha K_{off}}{K_{on}[GABA]} + \frac{\alpha\delta}{\rho} + K_+[B] + \frac{K_{off} K_+[B]}{K_{on}[GABA]} + \frac{\delta K_+[B]}{\rho}}$$

let X = $\alpha + \frac{\alpha K_{off}}{K_{on}[GABA]} + \frac{\alpha\delta}{\rho}$

$$\frac{MCT_{\mathcal{CCDOB}}}{MCT_{\mathcal{CCDO}}} = \frac{X + \frac{\beta K_+[B]}{K_-}}{X + K_+[B] + \frac{K_{off} K_+[B]}{K_{on}[GABA]} + \frac{\delta K_+[B]}{\rho}}$$

$$\frac{MCT_{\mathcal{CCDOB}}}{MCT_{\mathcal{CCDO}}} = \frac{\frac{X}{K_+[B]} + \frac{\beta}{K_-}}{\frac{X}{K_+[B]} + 1 + \frac{K_{off}}{K_{on}[GABA]} + \frac{\delta}{\rho}} \quad (27)$$

thus,

$$\frac{MCT_{\mathcal{CCDOB}}}{MCT_{\mathcal{CCDO}}} > 1 \text{ if } \frac{\beta}{K_-} > \left(1 + \frac{K_{off}}{K_{on}[GABA]} + \frac{\delta}{\rho}\right)$$

or alternatively,

$$\boxed{\frac{MCT_{\mathcal{CCDOB}}}{MCT_{\mathcal{CCDO}}} > 1 \text{ if } \frac{1}{K_-} > \frac{1}{\beta}\left(1 + \frac{K_{off}}{K_{on}[GABA]} + \frac{\delta}{\rho}\right)} \quad (28)$$

(i.e., if mean dwell time in $\mathcal{B} > MCT_{\mathcal{CCDO}}$)

III. Mean bound time (MBT)

A. $\mathcal{C}_1 \underset{K_{off}}{\overset{K_{on}[GABA]}{\rightleftarrows}} \mathcal{C}_2 \underset{\alpha}{\overset{\beta}{\rightleftarrows}} \mathcal{O}$

$$MBT_{CC\mathcal{O}} = \frac{1}{K_{off}}\left(1 + \frac{\beta}{\alpha}\right) \text{ (Appendix II, eq. 20)} \quad (29)$$

$$\mathcal{C}_1 \underset{K_{off}}{\overset{K_{on}[GABA]}{\rightleftarrows}} \mathcal{C}_2 \underset{\alpha}{\overset{\beta}{\rightleftarrows}} \mathcal{O} \underset{K_-}{\overset{K_+[B]}{\rightleftarrows}} \mathcal{B}$$

$$\boxed{MBT_{CCOB} = \frac{1}{K_{off}}\left(1 + \frac{\beta}{\alpha} + \frac{\beta K_+[B]}{\alpha K_-}\right)} \text{ (Appendix II, Section II.D)} \quad (30)$$

$$\frac{MBT_{CCOB}}{MBT_{CCO}} = \frac{\frac{1}{K_{off}}\left(1 + \frac{\beta}{\alpha} + \frac{\beta K_+[B]}{\alpha K_-}\right)}{\frac{1}{K_{off}}\left(1 + \frac{\beta}{\alpha}\right)} = \frac{1 + \frac{\beta}{\alpha} + \frac{\beta K_+[B]}{\alpha K_-}}{1 + \frac{\beta}{\alpha}} = 1 + \frac{\frac{K_+[B]}{K_-}}{1 + \frac{\alpha}{\beta}} \quad (31)$$

since $p(\mathcal{O})_{CCO} = \frac{1}{1 + \frac{\alpha}{\beta} + \frac{\alpha K_{off}}{\beta K_{on}[GABA]}}$ (Appendix I, eq. 19)

and $p(\mathcal{O})_{CCO_{max}} = \lim_{[\text{GABA}]\to\infty} p(\mathcal{O})_{CCO} = \frac{1}{1 + \frac{\alpha}{\beta}}$

$$\boxed{\frac{MBT_{CCOB}}{MBT_{CCO}} = 1 + \left(p(\mathcal{O})_{CCO_{max}}\right)\left(\frac{K_+[B]}{K_-}\right)} \quad (32)$$

B. $\mathcal{C}_1 \underset{K_{off}}{\overset{K_{on}[GABA]}{\rightleftarrows}} \mathcal{C}_2 \underset{\alpha}{\overset{\beta}{\rightleftarrows}} \mathcal{O} \underset{\rho}{\overset{\delta}{\rightleftarrows}} \mathcal{D}$

$$MBT_{CCOD} = \frac{1}{K_{off}}\left(1 + \frac{\beta}{\alpha} + \frac{\beta\delta}{\alpha\rho}\right) \text{ (Appendix II, eq. 25)} \quad (33)$$

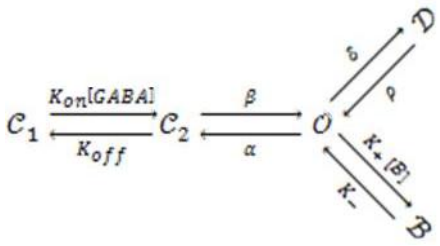

$$\boxed{MBT_{CCODB} = \frac{1}{K_{off}}\left(1 + \frac{\beta}{\alpha} + \frac{\beta\delta}{\alpha\rho} + \frac{\beta K_+[B]}{\alpha K_-}\right)} \text{ (Appendix II, Section II.D)} \quad (34)$$

$$\frac{MBT_{CCODB}}{MBT_{CCOD}} = \frac{\frac{1}{K_{off}}\left(1 + \frac{\beta}{\alpha} + \frac{\beta\delta}{\alpha\rho} + \frac{\beta K_+[B]}{\alpha K_-}\right)}{\frac{1}{K_{off}}\left(1 + \frac{\beta}{\alpha} + \frac{\beta\delta}{\alpha\rho}\right)} = \frac{1 + \frac{\beta}{\alpha} + \frac{\beta\delta}{\alpha\rho} + \frac{\beta K_+[B]}{\alpha K_-}}{1 + \frac{\beta}{\alpha} + \frac{\beta\delta}{\alpha\rho}} = 1 + \frac{\frac{K_+[B]}{K_-}}{1 + \frac{\alpha}{\beta} + \frac{\delta}{\rho}} \quad (35)$$

since $p(\mathcal{O})_{CCOD} = \frac{1}{1 + \frac{\alpha}{\beta} + \frac{\alpha K_{off}}{\beta K_{on}[GABA]} + \frac{\delta}{\rho}}$ (Appendix I, eq. 44)

and $p(\mathcal{O})_{CCOD_{max}} = \lim_{[\text{GABA}]\to\infty} p(\mathcal{O})_{CCOD} = \frac{1}{1 + \frac{\alpha}{\beta} + \frac{\delta}{\rho}}$

$$\boxed{\frac{MBT_{CC\mathcal{O}\mathcal{D}B}}{MBT_{CC\mathcal{O}\mathcal{D}}} = 1 + \left(p(\mathcal{O})_{CC\mathcal{O}\mathcal{D}_{max}}\right)\left(\frac{K_+[B]}{K_-}\right)} \quad (36)$$

C.

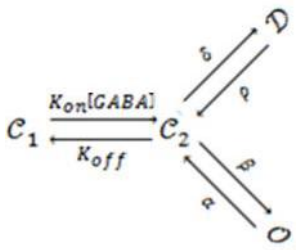

$$MBT_{CC\mathcal{D}\mathcal{O}} = \frac{1}{K_{off}}\left(1 + \frac{\beta}{\alpha} + \frac{\delta}{\rho}\right) \text{ (Appendix II, eq. 30)} \quad (37)$$

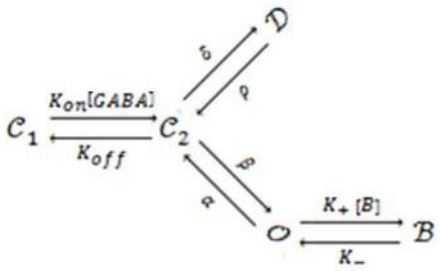

$$\boxed{MBT_{CC\mathcal{D}\mathcal{O}B} = \frac{1}{K_{off}}\left(1 + \frac{\beta}{\alpha} + \frac{\delta}{\rho} + \frac{\beta K_+[B]}{\alpha K_-}\right)} \text{ (Appendix II, Section II.D)} \quad (38)$$

$$\frac{MBT_{CC\mathcal{D}\mathcal{O}B}}{MBT_{CC\mathcal{D}\mathcal{O}}} = \frac{\frac{1}{K_{off}}\left(1 + \frac{\beta}{\alpha} + \frac{\delta}{\rho} + \frac{\beta K_+[B]}{\alpha K_-}\right)}{\frac{1}{K_{off}}\left(1 + \frac{\beta}{\alpha} + \frac{\delta}{\rho}\right)} = \frac{1 + \frac{\beta}{\alpha} + \frac{\delta}{\rho} + \frac{\beta K_+[B]}{\alpha K_-}}{1 + \frac{\beta}{\alpha} + \frac{\delta}{\rho}} = 1 + \frac{\frac{K_+[B]}{K_-}}{1 + \frac{\alpha}{\beta} + \frac{\alpha\delta}{\beta\rho}} \quad (39)$$

since $p(\mathcal{O})_{CC\mathcal{D}\mathcal{O}} = \frac{1}{1 + \frac{\alpha}{\beta} + \frac{\alpha K_{off}}{\beta K_{on}[GABA]} + \frac{\alpha\delta}{\beta\rho}}$ (Appendix I, eq. 77)

and $p(\mathcal{O})_{CC\mathcal{D}\mathcal{O}_{max}} = \lim_{[\text{GABA}]\to\infty} p(\mathcal{O})_{CC\mathcal{D}\mathcal{O}} = \frac{1}{1 + \frac{\alpha}{\beta} + \frac{\alpha\delta}{\beta\rho}}$

$$\boxed{\frac{MBT_{CC\mathcal{D}\mathcal{O}B}}{MBT_{CC\mathcal{D}\mathcal{O}}} = 1 + \left(p(\mathcal{O})_{CC\mathcal{D}\mathcal{O}_{max}}\right)\left(\frac{K_+[B]}{K_-}\right)} \quad (40)$$

IV. Opening frequency ($\mathcal{F}$)

A. $\mathcal{C} \underset{\alpha}{\overset{\beta}{\rightleftarrows}} \mathcal{O}$

$\mathcal{F}_{\mathcal{CO}} = p(\mathcal{O})_{\mathcal{CO}} * \alpha$ (Appendix II, eq. 35) (41)

$p(\mathcal{O})_{\mathcal{CO}} = \frac{1}{1+\frac{\alpha}{\beta}}$ (Appendix I, eq. 5) (42)

substituting (42) into (41)

$\mathcal{F}_{\mathcal{CO}} = \frac{\alpha}{1+\frac{\alpha}{\beta}}$ (43)

$\mathcal{C} \underset{\alpha}{\overset{\beta}{\rightleftarrows}} \mathcal{O} \underset{K_-}{\overset{K_+[B]}{\rightleftarrows}} \mathcal{B}$

$\mathcal{F}_{\mathcal{COB}} = p(\mathcal{O})_{\mathcal{COB}} * (\alpha + K_+[B])$ (Appendix II, Section III.F) (44)

$p(\mathcal{O})_{\mathcal{COB}} = \frac{1}{1+\frac{\alpha}{\beta}+\frac{K_+[B]}{K_-}}$ (Appendix I, Section V) (45)

substituting (45) into (44)

$$\boxed{\mathcal{F}_{\mathcal{COB}} = \frac{\alpha + K_+[B]}{1+\frac{\alpha}{\beta}+\frac{K_+[B]}{K_-}}} \quad (46)$$

$$\frac{\mathcal{F}_{\mathcal{COB}}}{\mathcal{F}_{\mathcal{CO}}} = \frac{\frac{\alpha + K_+[B]}{1+\frac{\alpha}{\beta}+\frac{K_+[B]}{K_-}}}{\frac{\alpha}{1+\frac{\alpha}{\beta}}} = \frac{(\alpha + K_+[B])\left(1+\frac{\alpha}{\beta}\right)}{\alpha\left(1+\frac{\alpha}{\beta}+\frac{K_+[B]}{K_-}\right)} = \frac{\alpha + K_+[B] + \frac{\alpha^2}{\beta} + \frac{\alpha K_+[B]}{\beta}}{\alpha + \frac{\alpha^2}{\beta} + \frac{\alpha K_+[B]}{K_-}}$$

$$\frac{\mathcal{F}_{\mathcal{COB}}}{\mathcal{F}_{\mathcal{CO}}} = \frac{1+\frac{K_+[B]}{\alpha}+\frac{\alpha}{\beta}+\frac{K_+[B]}{\beta}}{1+\frac{\alpha}{\beta}+\frac{K_+[B]}{K_-}} = \frac{1+\frac{\alpha}{\beta}+K_+[B]\left(\frac{1}{\alpha}+\frac{1}{\beta}\right)}{1+\frac{\alpha}{\beta}+\frac{K_+[B]}{K_-}}$$

thus,

$\frac{\mathcal{F}_{\mathcal{COB}}}{\mathcal{F}_{\mathcal{CO}}} > 1$ if $\frac{1}{K_-} < \left(\frac{1}{\alpha}+\frac{1}{\beta}\right)$

or alternatively,

$$\boxed{\frac{\mathcal{F}_{\mathcal{COB}}}{\mathcal{F}_{\mathcal{CO}}} > 1 \text{ if } K_- > \frac{\alpha}{1+\frac{\alpha}{\beta}}} \quad (47)$$

(i.e., if the unblocking rate is greater than $\mathcal{F}_{\mathcal{CO}}$)

B. $\mathcal{C}_1 \underset{K_{off}}{\overset{K_{on}[GABA]}{\rightleftarrows}} \mathcal{C}_2 \underset{\alpha}{\overset{\beta}{\rightleftarrows}} \mathcal{O}$

$$\mathcal{F}_{\mathcal{CCO}} = p(\mathcal{O})_{\mathcal{CCO}} * \alpha \quad \text{(Appendix II, eq. 40)} \tag{48}$$

$$p(\mathcal{O})_{\mathcal{CCO}} = \frac{1}{1 + \frac{\alpha}{\beta} + \frac{\alpha K_{off}}{\beta K_{on}[GABA]}} \quad \text{(Appendix I, eq. 19)} \tag{49}$$

substituting (49) into (48)

$$\mathcal{F}_{\mathcal{CCO}} = \frac{\alpha}{1 + \frac{\alpha}{\beta} + \frac{\alpha K_{off}}{\beta K_{on}[GABA]}} \tag{50}$$

$$\mathcal{C}_1 \underset{K_{off}}{\overset{K_{on}[GABA]}{\rightleftarrows}} \mathcal{C}_2 \underset{\alpha}{\overset{\beta}{\rightleftarrows}} \mathcal{O} \underset{K_-}{\overset{K_+[B]}{\rightleftarrows}} \mathcal{B}$$

$$\mathcal{F}_{\mathcal{CCOB}} = p(\mathcal{O})_{\mathcal{CCOB}} * (\alpha + K_+[B]) \quad \text{(Appendix II, Section III.F)} \tag{51}$$

$$p(\mathcal{O})_{\mathcal{CCOB}} = \frac{1}{1 + \frac{\alpha}{\beta} + \frac{\alpha K_{off}}{\beta K_{on}[GABA]} + \frac{K_+[B]}{K_-}} \quad \text{(Appendix I, Section V)} \tag{52}$$

substituting (52) into (51)

$$\boxed{\mathcal{F}_{\mathcal{CCOB}} = \frac{\alpha + K_+[B]}{1 + \frac{\alpha}{\beta} + \frac{\alpha K_{off}}{\beta K_{on}[GABA]} + \frac{K_+[B]}{K_-}}} \tag{53}$$

$$\frac{\mathcal{F}_{\mathcal{CCOB}}}{\mathcal{F}_{\mathcal{CCO}}} = \frac{\frac{\alpha + K_+[B]}{1 + \frac{\alpha}{\beta} + \frac{\alpha K_{off}}{\beta K_{on}[GABA]} + \frac{K_+[B]}{K_-}}}{\frac{\alpha}{1 + \frac{\alpha}{\beta} + \frac{\alpha K_{off}}{\beta K_{on}[GABA]}}} = \frac{(\alpha + K_+[B])\left(1 + \frac{\alpha}{\beta} + \frac{\alpha K_{off}}{\beta K_{on}[GABA]}\right)}{\alpha\left(1 + \frac{\alpha}{\beta} + \frac{\alpha K_{off}}{\beta K_{on}[GABA]} + \frac{K_+[B]}{K_-}\right)}$$

$$\frac{\mathcal{F}_{\mathcal{CCOB}}}{\mathcal{F}_{\mathcal{CCO}}} = \frac{\alpha + K_+[B] + \frac{\alpha^2}{\beta} + \frac{\alpha K_+[B]}{\beta} + \frac{\alpha^2 K_{off}}{\beta K_{on}[GABA]} + \frac{\alpha K_{off} K_+[B]}{\beta K_{on}[GABA]}}{\alpha + \frac{\alpha^2}{\beta} + \frac{\alpha^2 K_{off}}{\beta K_{on}[GABA]} + \frac{\alpha K_+[B]}{K_-}}$$

$$\frac{\mathcal{F}_{\mathcal{CCOB}}}{\mathcal{F}_{\mathcal{CCO}}} = \frac{1 + \frac{K_+[B]}{\alpha} + \frac{\alpha}{\beta} + \frac{K_+[B]}{\beta} + \frac{\alpha K_{off}}{\beta K_{on}[GABA]} + \frac{K_{off} K_+[B]}{\beta K_{on}[GABA]}}{1 + \frac{\alpha}{\beta} + \frac{\alpha K_{off}}{\beta K_{on}[GABA]} + \frac{K_+[B]}{K_-}}$$

$$\frac{\mathcal{F}_{\mathcal{CCOB}}}{\mathcal{F}_{\mathcal{CCO}}} = \frac{1+\frac{\alpha}{\beta}+\frac{\alpha K_{off}}{\beta K_{on}[GABA\ ]}+K_{+}[B]\left(\frac{1}{\alpha}+\frac{1}{\beta}+\frac{K_{off}}{\beta K_{on}[GABA\ ]}\right)}{1+\frac{\alpha}{\beta}+\frac{\alpha K_{off}}{\beta K_{on}[GABA\ ]}+\frac{K_{+}[B]}{K_{-}}}$$

thus,

$$\frac{\mathcal{F}_{\mathcal{CCOB}}}{\mathcal{F}_{\mathcal{CCO}}} > 1 \text{ if } \frac{1}{K_{-}} < \left(\frac{1}{\alpha}+\frac{1}{\beta}+\frac{K_{off}}{\beta K_{on}[GABA]}\right)$$

or alternatively,

$$\boxed{\frac{\mathcal{F}_{\mathcal{CCOB}}}{\mathcal{F}_{\mathcal{CCO}}} > 1 \text{ if } K_{-} > \frac{\alpha}{1+\frac{\alpha}{\beta}+\frac{\alpha K_{off}}{\beta K_{on}[GABA\ ]}}} \quad (54)$$

(i.e., if the unblocking rate is greater than $\mathcal{F}_{\mathcal{CCO}}$)

C. $\mathcal{C}_1 \underset{K_{off}}{\overset{K_{on}[GABA\ ]}{\rightleftarrows}} \mathcal{C}_2 \underset{\alpha}{\overset{\beta}{\rightleftarrows}} \mathcal{O} \underset{\rho}{\overset{\delta}{\rightleftarrows}} \mathcal{D}$

$$\mathcal{F}_{\mathcal{CCOD}} = p(\mathcal{O})_{\mathcal{CCOD}} * (\alpha+\delta) \text{ (Appendix II, eq. 45)} \quad (55)$$

$$p(\mathcal{O})_{\mathcal{CCOD}} = \frac{1}{1+\frac{\alpha}{\beta}+\frac{\alpha K_{off}}{\beta K_{on}[GABA\ ]}+\frac{\delta}{\rho}} \text{ (Appendix I, eq. 44)} \quad (56)$$

substituting (56) into (55)

$$\mathcal{F}_{\mathcal{CCOD}} = \frac{\alpha+\delta}{1+\frac{\alpha}{\beta}+\frac{\alpha K_{off}}{\beta K_{on}[GABA\ ]}+\frac{\delta}{\rho}} \quad (57)$$

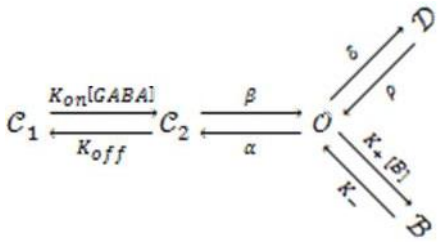

$$\mathcal{F}_{\mathcal{CCODB}} = p(\mathcal{O})_{\mathcal{CCODB}} * (\alpha+\delta+K_{+}[B]) \text{ (Appendix II, Section III.F)} \quad (58)$$

$$p(\mathcal{O})_{\mathcal{CCODB}} = \frac{1}{1+\frac{\alpha}{\beta}+\frac{\alpha K_{off}}{\beta K_{on}[GABA\ ]}+\frac{\delta}{\rho}+\frac{K_{+}[B]}{K_{-}}} \text{ (Appendix I, Section V)} \quad (59)$$

substituting (59) into (58)

$$\boxed{\mathcal{F}_{\mathcal{CCODB}} = \frac{\alpha + \delta + K_+[B]}{1 + \frac{\alpha}{\beta} + \frac{\alpha K_{off}}{\beta K_{on}[GABA]} + \frac{\delta}{\rho} + \frac{K_+[B]}{K_-}}} \tag{60}$$

$$\frac{\mathcal{F}_{\mathcal{CCODB}}}{\mathcal{F}_{\mathcal{CCOD}}} = \frac{\frac{\alpha + \delta + K_+[B]}{1 + \frac{\alpha}{\beta} + \frac{\alpha K_{off}}{\beta K_{on}[GABA]} + \frac{\delta}{\rho} + \frac{K_+[B]}{K_-}}}{\frac{\alpha + \delta}{1 + \frac{\alpha}{\beta} + \frac{\alpha K_{off}}{\beta K_{on}[GABA]} + \frac{\delta}{\rho}}}$$

$$\frac{\mathcal{F}_{\mathcal{CCODB}}}{\mathcal{F}_{\mathcal{CCOD}}} = \frac{(\alpha + \delta + K_+[B])\left(1 + \frac{\alpha}{\beta} + \frac{\alpha K_{off}}{\beta K_{on}[GABA]} + \frac{\delta}{\rho}\right)}{(\alpha + \delta)\left(1 + \frac{\alpha}{\beta} + \frac{\alpha K_{off}}{\beta K_{on}[GABA]} + \frac{\delta}{\rho} + \frac{K_+[B]}{K_-}\right)}$$

$$\frac{\mathcal{F}_{\mathcal{CCODB}}}{\mathcal{F}_{\mathcal{CCOD}}} = \frac{\alpha + \delta + K_+[B] + \frac{\alpha^2}{\beta} + \frac{\alpha\delta}{\beta} + \frac{\alpha K_+[B]}{\beta} + \frac{\alpha^2 K_{off}}{\beta K_{on}[GABA]} + \frac{\alpha\delta K_{off}}{\beta K_{on}[GABA]} + \frac{\alpha K_{off} K_+[B]}{\beta K_{on}[GABA]} + \frac{\alpha\delta}{\rho} + \frac{\delta^2}{\rho} + \frac{\delta K_+[B]}{\rho}}{\alpha + \frac{\alpha^2}{\beta} + \frac{\alpha^2 K_{off}}{\beta K_{on}[GABA]} + \frac{\alpha\delta}{\rho} + \frac{\alpha K_+[B]}{K_-} + \delta + \frac{\alpha\delta}{\beta} + \frac{\alpha\delta K_{off}}{\beta K_{on}[GABA]} + \frac{\delta^2}{\rho} + \frac{\delta K_+[B]}{K_-}}$$

$$\frac{\mathcal{F}_{\mathcal{CCODB}}}{\mathcal{F}_{\mathcal{CCOD}}} = \frac{1 + \frac{\delta}{\alpha} + \frac{K_+[B]}{\alpha} + \frac{\alpha}{\beta} + \frac{\delta}{\beta} + \frac{K_+[B]}{\beta} + \frac{\alpha K_{off}}{\beta K_{on}[GABA]} + \frac{\delta K_{off}}{\beta K_{on}[GABA]} + \frac{K_{off} K_+[B]}{\beta K_{on}[GABA]} + \frac{\delta}{\rho} + \frac{\delta^2}{\alpha\rho} + \frac{\delta K_+[B]}{\alpha\rho}}{1 + \frac{\alpha}{\beta} + \frac{\alpha K_{off}}{\beta K_{on}[GABA]} + \frac{\delta}{\rho} + \frac{K_+[B]}{K_-} + \frac{\delta}{\alpha} + \frac{\delta}{\beta} + \frac{\delta K_{off}}{\beta K_{on}[GABA]} + \frac{\delta^2}{\alpha\rho} + \frac{\delta K_+[B]}{\alpha K_-}}$$

$$\frac{\mathcal{F}_{\mathcal{CCODB}}}{\mathcal{F}_{\mathcal{CCOD}}} = \frac{1 + \frac{\delta}{\alpha} + \frac{\alpha}{\beta} + \frac{\delta}{\beta} + \frac{\delta}{\rho} + \frac{\delta^2}{\alpha\rho} + \frac{\alpha K_{off}}{\beta K_{on}[GABA]} + \frac{\delta K_{off}}{\beta K_{on}[GABA]} + K_+[B]\left(\frac{1}{\alpha} + \frac{1}{\beta} + \frac{K_{off}}{\beta K_{on}[GABA]} + \frac{\delta}{\alpha\rho}\right)}{1 + \frac{\delta}{\alpha} + \frac{\alpha}{\beta} + \frac{\delta}{\beta} + \frac{\delta}{\rho} + \frac{\delta^2}{\alpha\rho} + \frac{\alpha K_{off}}{\beta K_{on}[GABA]} + \frac{\delta K_{off}}{\beta K_{on}[GABA]} + K_+[B]\left(\frac{1}{K_-} + \frac{\delta}{\alpha K_-}\right)}$$

thus,

$$\frac{\mathcal{F}_{\mathcal{CCODB}}}{\mathcal{F}_{\mathcal{CCOD}}} > 1 \text{ if } \frac{1}{K_-}\left(1 + \frac{\delta}{\alpha}\right) < \left(\frac{1}{\alpha} + \frac{1}{\beta} + \frac{K_{off}}{\beta K_{on}[GABA]} + \frac{\delta}{\alpha\rho}\right)$$

or alternatively,

$$\frac{\mathcal{F}_{\mathcal{CCODB}}}{\mathcal{F}_{\mathcal{CCOD}}} > 1 \text{ if } K_- > \frac{1 + \frac{\delta}{\alpha}}{\frac{1}{\alpha} + \frac{1}{\beta} + \frac{K_{off}}{\beta K_{on}[GABA]} + \frac{\delta}{\alpha\rho}}$$

$$\boxed{\frac{\mathcal{F}_{\mathcal{CCODB}}}{\mathcal{F}_{\mathcal{CCOD}}} > 1 \text{ if } K_- > \frac{\alpha + \delta}{1 + \frac{\alpha}{\beta} + \frac{\alpha K_{off}}{\beta K_{on}[GABA]} + \frac{\delta}{\rho}}} \tag{61}$$

(i.e., if the unblocking rate is greater than $\mathcal{F}_{\mathcal{CCOD}}$)

D.

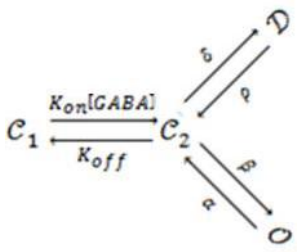

$$\mathcal{F}_{\mathcal{CCDO}} = p(\mathcal{O})_{\mathcal{CCDO}} * (\alpha) \text{ (Appendix II, eq. 51)} \quad (62)$$

$$p(\mathcal{O})_{\mathcal{CCDO}} = \frac{1}{1 + \frac{\alpha}{\beta} + \frac{\alpha K_{off}}{\beta K_{on}[GABA]} + \frac{\alpha\delta}{\beta\rho}} \text{ (Appendix I, eq. 77)} \quad (63)$$

substituting (63) into (62)

$$\mathcal{F}_{\mathcal{CCDO}} = \frac{\alpha}{1 + \frac{\alpha}{\beta} + \frac{\alpha K_{off}}{\beta K_{on}[GABA]} + \frac{\alpha\delta}{\beta\rho}} \quad (64)$$

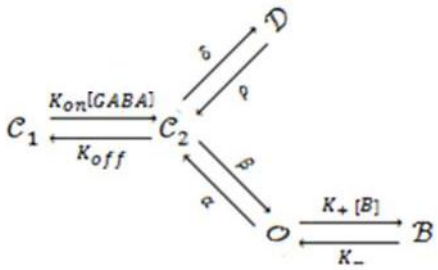

$$\mathcal{F}_{\mathcal{CCDOB}} = p(\mathcal{O})_{\mathcal{CCDOB}} * (\alpha + K_+[B]) \text{ (Appendix II, Section III.F)} \quad (65)$$

$$p(\mathcal{O})_{\mathcal{CCDOB}} = \frac{1}{1 + \frac{\alpha}{\beta} + \frac{\alpha K_{off}}{\beta K_{on}[GABA]} + \frac{\alpha\delta}{\beta\rho} + \frac{K_+[B]}{K_-}} \text{ (Appendix I, Section V)} \quad (66)$$

substituting (66) into (65)

$$\boxed{\mathcal{F}_{\mathcal{CCDOB}} = \frac{\alpha + K_+[B]}{1 + \frac{\alpha}{\beta} + \frac{\alpha K_{off}}{\beta K_{on}[GABA]} + \frac{\alpha\delta}{\beta\rho} + \frac{K_+[B]}{K_-}}} \quad (67)$$

$$\frac{\mathcal{F}_{\mathcal{CCDOB}}}{\mathcal{F}_{\mathcal{CCDO}}} = \frac{\frac{\alpha + K_+[B]}{1 + \frac{\alpha}{\beta} + \frac{\alpha K_{off}}{\beta K_{on}[GABA]} + \frac{\alpha\delta}{\beta\rho} + \frac{K_+[B]}{K_-}}}{\frac{\alpha}{1 + \frac{\alpha}{\beta} + \frac{\alpha K_{off}}{\beta K_{on}[GABA]} + \frac{\alpha\delta}{\beta\rho}}}$$

$$\frac{\mathcal{F}_{\mathcal{CCDOB}}}{\mathcal{F}_{\mathcal{CCDO}}} = \frac{(\alpha + K_+[B])\left(1 + \frac{\alpha}{\beta} + \frac{\alpha K_{off}}{\beta K_{on}[GABA]} + \frac{\alpha\delta}{\beta\rho}\right)}{(\alpha)\left(1 + \frac{\alpha}{\beta} + \frac{\alpha K_{off}}{\beta K_{on}[GABA]} + \frac{\alpha\delta}{\beta\rho} + \frac{K_+[B]}{K_-}\right)}$$

$$\frac{\mathcal{F}_{\mathcal{CCDOB}}}{\mathcal{F}_{\mathcal{CCDO}}} = \frac{\alpha + K_+[B] + \frac{\alpha^2}{\beta} + \frac{\alpha K_+[B]}{\beta} + \frac{\alpha^2 K_{off}}{\beta K_{on}[GABA]} + \frac{\alpha K_{off} K_+[B]}{\beta K_{on}[GABA]} + \frac{\alpha^2\delta}{\beta\rho} + \frac{\alpha\delta K_+[B]}{\beta\rho}}{(\alpha)\left(1 + \frac{\alpha}{\beta} + \frac{\alpha K_{off}}{\beta K_{on}[GABA]} + \frac{\alpha\delta}{\beta\rho} + \frac{K_+[B]}{K_-}\right)}$$

$$\frac{\mathcal{F}_{\mathcal{CCDOB}}}{\mathcal{F}_{\mathcal{CCDO}}} = \frac{1 + \frac{K_+[B]}{\alpha} + \frac{\alpha}{\beta} + \frac{K_+[B]}{\beta} + \frac{\alpha K_{off}}{\beta K_{on}[GABA]} + \frac{K_{off} K_+[B]}{\beta K_{on}[GABA]} + \frac{\alpha\delta}{\beta\rho} + \frac{\delta K_+[B]}{\beta\rho}}{1 + \frac{\alpha}{\beta} + \frac{\alpha K_{off}}{\beta K_{on}[GABA]} + \frac{\alpha\delta}{\beta\rho} + \frac{K_+[B]}{K_-}}$$

$$\frac{\mathcal{F}_{\mathcal{CCDOB}}}{\mathcal{F}_{\mathcal{CCDO}}} = \frac{1 + \frac{\alpha}{\beta} + \frac{\alpha K_{off}}{\beta K_{on}[GABA]} + \frac{\alpha\delta}{\beta\rho} + K_+[B]\left(\frac{1}{\alpha} + \frac{1}{\beta} + \frac{K_{off}}{\beta K_{on}[GABA]} + \frac{\delta}{\beta\rho}\right)}{1 + \frac{\alpha}{\beta} + \frac{\alpha K_{off}}{\beta K_{on}[GABA]} + \frac{\alpha\delta}{\beta\rho} + \frac{K_+[B]}{K_-}}$$

thus,

$$\frac{\mathcal{F}_{\mathcal{CCDOB}}}{\mathcal{F}_{\mathcal{CCDO}}} > 1 \text{ if } \frac{1}{K_-} < \left(\frac{1}{\alpha} + \frac{1}{\beta} + \frac{K_{off}}{\beta K_{on}[GABA]} + \frac{\delta}{\beta\rho}\right)$$

or alternatively,

$$\boxed{\frac{\mathcal{F}_{\mathcal{CCDOB}}}{\mathcal{F}_{\mathcal{CCDO}}} > 1 \text{ if } K_- > \frac{\alpha}{1 + \frac{\alpha}{\beta} + \frac{\alpha K_{off}}{\beta K_{on}[GABA]} + \frac{\alpha\delta}{\beta\rho}}} \tag{68}$$

(i.e., if the unblocking rate is greater than $\mathcal{F}_{\mathcal{CCDO}}$)

V. GABA EC_{50}

A. $\mathcal{C}_1 \underset{K_{off}}{\overset{K_{on}[GABA]}{\rightleftarrows}} \mathcal{C}_2 \underset{\alpha}{\overset{\beta}{\rightleftarrows}} \mathcal{O}$

let $\mathcal{E} = \frac{\beta}{\alpha}$ (classical definition of "efficacy") (69)

let $\mathcal{K}_a = \frac{K_{off}}{K_{on}}$ (classical definition of GABA "affinity") (70)

$\boxed{[GABA]_{EC_{50}} = \frac{\mathcal{K}_a}{1 + \mathcal{E}}}$ (Appendix II, eq. 67)

$\mathcal{C}_1 \underset{K_{off}}{\overset{K_{on}[GABA]}{\rightleftarrows}} \mathcal{C}_2 \underset{\alpha}{\overset{\beta}{\rightleftarrows}} \mathcal{O} \underset{K_-}{\overset{K_+[B]}{\rightleftarrows}} \mathcal{B}$

let $\mathcal{K}_b = \frac{K_-}{K_+}$ (classical definition of blocker "affinity") (71)

$p(\mathcal{O})_{\mathcal{CCOB}} = \frac{1}{1 + \frac{\alpha}{\beta} + \frac{\alpha K_{off}}{\beta K_{on}[GABA]} + \frac{K_+[B]}{K_-}}$ (Appendix III, eq. 5)

or alternatively,

$$p(\mathcal{O})_{\mathcal{CCOB}} = \frac{\frac{\beta}{\alpha}}{1 + \frac{\beta}{\alpha} + \frac{K_{off}}{K_{on}[GABA\ ]} + \frac{\beta K_{+}[B]}{\alpha K_{-}}} \tag{72}$$

substituting (69), (70), and (71) into (72)

$$p(\mathcal{O})_{\mathcal{CCOB}} = \frac{\mathcal{E}}{1 + \mathcal{E} + \frac{\mathcal{K}_a}{[GABA\ ]} + \frac{\mathcal{E}[B]}{\mathcal{K}_b}} \tag{73}$$

$$p(\mathcal{O})_{\mathcal{CCOB}_{max}} = \lim_{[\mathrm{GABA}\ ]\to\infty} p(\mathcal{O})_{\mathcal{CCOB}}$$

$$p(\mathcal{O})_{\mathcal{CCOB}_{max}} = \frac{\mathcal{E}}{1 + \mathcal{E} + \frac{\mathcal{E}[B]}{\mathcal{K}_b}} \tag{74}$$

EC_{50} is, by definition, the [GABA] yielding ½ $p(\mathcal{O})_{\mathcal{CCOB}_{max}}$

$$\left(\frac{1}{2}\right)\left(p(\mathcal{O})_{\mathcal{CCOB}_{max}}\right) = \left(\frac{1}{2}\right)\left(\frac{\mathcal{E}}{1 + \mathcal{E} + \frac{\mathcal{E}[B]}{\mathcal{K}_b}}\right) = \frac{\mathcal{E}}{2 + 2\mathcal{E} + \frac{2\mathcal{E}[B]}{\mathcal{K}_b}} \tag{75}$$

setting (75) equal to (74)

$$\frac{\mathcal{E}}{2 + 2\mathcal{E} + \frac{2\mathcal{E}[B]}{\mathcal{K}_b}} = \frac{\mathcal{E}}{1 + \mathcal{E} + \frac{\mathcal{K}_a}{[GABA\ ]_{EC\ 50}} + \frac{\mathcal{E}[B]}{\mathcal{K}_b}}$$

$$\boxed{[GABA]_{EC_{50}} = \frac{\mathcal{K}_a}{1 + \mathcal{E} + \frac{\mathcal{E}[B]}{\mathcal{K}_b}}} \tag{76}$$

$$\frac{EC_{50\,\mathcal{CCO}}}{EC_{50\,\mathcal{CCOB}}} = \frac{\frac{\mathcal{K}_a}{1 + \mathcal{E}}}{\frac{\mathcal{K}_a}{1 + \mathcal{E} + \frac{\mathcal{E}[B]}{\mathcal{K}_b}}} = \frac{1 + \mathcal{E} + \frac{\mathcal{E}[B]}{\mathcal{K}_b}}{1 + \mathcal{E}} = 1 + \frac{\frac{\mathcal{E}[B]}{\mathcal{K}_b}}{1 + \mathcal{E}}$$

since $p(\mathcal{O})_{\mathcal{CCO}_{max}} = \frac{\mathcal{E}}{1 + \mathcal{E}}$ (Appendix II, eq. 65)

$$\boxed{\frac{EC_{50\,\mathcal{CCO}}}{EC_{50\,\mathcal{CCOB}}} = 1 + \left(p(\mathcal{O})_{\mathcal{CCO}_{max}}\right)\frac{[B]}{\mathcal{K}_b}} \tag{77}$$

B. $\mathcal{C}_1 \underset{K_{off}}{\overset{K_{on}[GABA\ ]}{\rightleftarrows}} \mathcal{C}_2 \underset{\alpha}{\overset{\beta}{\rightleftarrows}} \mathcal{O} \underset{\rho}{\overset{\delta}{\rightleftarrows}} \mathcal{D}$

let $\mathcal{E} = \frac{\beta}{\alpha}$ (classical definition of "efficacy") (78)

let $\mathcal{K}_a = \frac{K_{off}}{K_{on}}$ (classical definition of GABA "affinity") (79)

let $\Delta = \frac{\delta}{\rho}$ (Bianchi et al., 2007, definition of $\mathcal{D}$ state "stability") (80)

$\boxed{[GABA]_{EC_{50}} = \frac{\mathcal{K}_a}{1 + \mathcal{E} + \mathcal{E}\Delta}}$ (Appendix II, eq. 75)

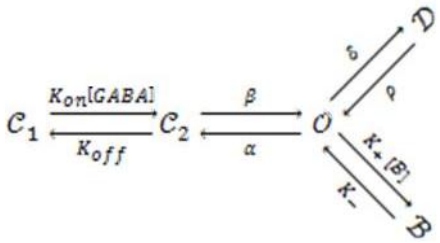

let $\mathcal{K}_b = \frac{K_-}{K_+}$ (classical definition of blocker "affinity") (81)

$p(\mathcal{O})_{\mathcal{CCODB}} = \frac{1}{1 + \frac{\alpha}{\beta} + \frac{\delta}{\rho} + \frac{\alpha K_{off}}{\beta K_{on}[GABA]} + \frac{K_+[B]}{K_-}}$ (Appendix III, eq. 8)

or alternatively,

$$p(\mathcal{O})_{\mathcal{CCODB}} = \frac{\frac{\beta}{\alpha}}{1 + \frac{\beta}{\alpha} + \frac{\beta\delta}{\alpha\rho} + \frac{K_{off}}{K_{on}[GABA]} + \frac{\beta K_+[B]}{\alpha K_-}} \quad (82)$$

substituting (78), (79), (80), and (81) into (82)

$$p(\mathcal{O})_{\mathcal{CCODB}} = \frac{\mathcal{E}}{1 + \mathcal{E} + \mathcal{E}\Delta + \frac{\mathcal{K}_a}{[GABA]} + \frac{\mathcal{E}[B]}{\mathcal{K}_b}} \quad (83)$$

$p(\mathcal{O})_{\mathcal{CCODB}_{max}} = \lim_{[\text{GABA}]\to\infty} p(\mathcal{O})_{\mathcal{CCODB}}$

$$p(\mathcal{O})_{\mathcal{CCODB}_{max}} = \frac{\mathcal{E}}{1 + \mathcal{E} + \mathcal{E}\Delta + \frac{\mathcal{E}[B]}{\mathcal{K}_b}} \quad (84)$$

EC_{50} is, by definition, the [GABA] yielding ½ $p(\mathcal{O})_{\mathcal{CCODB}_{max}}$

$$\left(\frac{1}{2}\right)\left(p(\mathcal{O})_{\mathcal{CCODB}_{max}}\right) = \left(\frac{1}{2}\right)\left(\frac{\mathcal{E}}{1 + \mathcal{E} + \mathcal{E}\Delta + \frac{\mathcal{E}[B]}{\mathcal{K}_b}}\right) = \frac{\mathcal{E}}{2 + 2\mathcal{E} + 2\mathcal{E}\Delta + \frac{2\mathcal{E}[B]}{\mathcal{K}_b}} \quad (85)$$

setting (85) equal to (84)

$$\frac{\mathcal{E}}{2+2\mathcal{E}+2\mathcal{E}\Delta+\frac{2\mathcal{E}[B]}{\mathcal{K}_b}} = \frac{\mathcal{E}}{1+\mathcal{E}+\mathcal{E}\Delta+\frac{\mathcal{K}_a}{[GABA\ ]}+\frac{\mathcal{E}[B]}{\mathcal{K}_b}}$$

$$\boxed{[GABA]_{EC_{50}} = \frac{\mathcal{K}_a}{1+\mathcal{E}+\mathcal{E}\Delta+\frac{\mathcal{E}[B]}{\mathcal{K}_b}}} \tag{86}$$

$$\frac{EC_{50\,\mathcal{CCOD}}}{EC_{50\,\mathcal{CCODB}}} = \frac{\frac{\mathcal{K}_a}{1+\mathcal{E}+\mathcal{E}\Delta}}{\frac{\mathcal{K}_a}{1+\mathcal{E}+\mathcal{E}\Delta+\frac{\mathcal{E}[B]}{\mathcal{K}_b}}} = \frac{1+\mathcal{E}+\mathcal{E}\Delta+\frac{\mathcal{E}[B]}{\mathcal{K}_b}}{1+\mathcal{E}+\mathcal{E}\Delta} = 1+\frac{\frac{\mathcal{E}[B]}{\mathcal{K}_b}}{1+\mathcal{E}+\mathcal{E}\Delta}$$

since $p(\mathcal{O})_{\mathcal{CCOD}_{max}} = \frac{\mathcal{E}}{1+\mathcal{E}+\mathcal{E}\Delta}$ (Appendix II, eq. 73)

$$\boxed{\frac{EC_{50\,\mathcal{CCOD}}}{EC_{50\,\mathcal{CCODB}}} = 1+\left(p(\mathcal{O})_{\mathcal{CCOD}_{max}}\right)\frac{[B]}{\mathcal{K}_b}} \tag{87}$$

C.

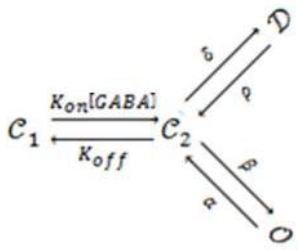

let $\mathcal{E} = \frac{\beta}{\alpha}$ (classical definition of "efficacy") (88)

let $\mathcal{K}_a = \frac{K_{off}}{K_{on}}$ (classical definition of GABA "affinity") (89)

let $\Delta = \frac{\delta}{\rho}$ (Bianchi et al., 2007, definition of $\mathcal{D}$ state "stability") (90)

$\boxed{[GABA]_{EC_{50}} = \frac{\mathcal{K}_a}{1+\mathcal{E}+\Delta}}$ (Appendix II, eq. 83)

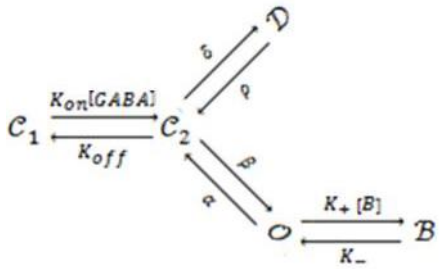

let $\mathcal{K}_b = \frac{K_-}{K_+}$ (classical definition of blocker "affinity") (91)

$p(\mathcal{O})_{\mathcal{CCDOB}} = \frac{1}{1+\frac{\alpha}{\beta}+\frac{\alpha\delta}{\beta\rho}+\frac{\alpha K_{off}}{\beta K_{on}[GABA\ ]}+\frac{K_+[B]}{K_-}}$ (Appendix III, eq. 11)

or alternatively,

$$p(\mathcal{O})_{\mathcal{CCDOB}} = \frac{\frac{\beta}{\alpha}}{1+\frac{\beta}{\alpha}+\frac{\delta}{\rho}+\frac{K_{off}}{K_{on}[GABA\ ]}+\frac{\beta K_+[B]}{\alpha K_-}} \quad (92)$$

substituting (88), (89), (90), and (91) into (92)

$$p(\mathcal{O})_{\mathcal{CCDOB}} = \frac{\mathcal{E}}{1+\mathcal{E}+\Delta+\frac{\mathcal{K}_a}{[GABA\ ]}+\frac{\mathcal{E}[B]}{\mathcal{K}_b}} \quad (93)$$

$p(\mathcal{O})_{\mathcal{CCDOB}_{max}} = \lim_{[\text{GABA }]\to\infty} p(\mathcal{O})_{\mathcal{CCDOB}}$

$$p(\mathcal{O})_{\mathcal{CCDOB}_{max}} = \frac{\mathcal{E}}{1+\mathcal{E}+\Delta+\frac{\mathcal{E}[B]}{\mathcal{K}_b}} \quad (94)$$

EC_{50} is, by definition, the [GABA] yielding ½ $p(\mathcal{O})_{\mathcal{CCDOB}_{max}}$

$$\left(\frac{1}{2}\right)\left(p(\mathcal{O})_{\mathcal{CCDOB}_{max}}\right) = \left(\frac{1}{2}\right)\left(\frac{\mathcal{E}}{1+\mathcal{E}+\Delta+\frac{\mathcal{E}[B]}{\mathcal{K}_b}}\right) = \frac{\mathcal{E}}{2+2\mathcal{E}+2\Delta+\frac{2\mathcal{E}[B]}{\mathcal{K}_b}} \quad (95)$$

setting (95) equal to (94)

$$\frac{\mathcal{E}}{2+2\mathcal{E}+2\Delta+\frac{2\mathcal{E}[B]}{\mathcal{K}_b}} = \frac{\mathcal{E}}{1+\mathcal{E}+\Delta+\frac{\mathcal{K}_a}{[GABA\ ]}+\frac{\mathcal{E}[B]}{\mathcal{K}_b}}$$

$$\boxed{[GABA]_{EC_{50}} = \frac{\mathcal{K}_a}{1+\mathcal{E}+\Delta+\frac{\mathcal{E}[B]}{\mathcal{K}_b}}} \quad (96)$$

$$\frac{EC_{50\,\mathcal{CCDO}}}{EC_{50\,\mathcal{CCDOB}}} = \frac{\frac{\mathcal{K}_a}{1+\mathcal{E}+\Delta}}{\frac{\mathcal{K}_a}{1+\mathcal{E}+\Delta+\frac{\mathcal{E}[B]}{\mathcal{K}_b}}} = \frac{1+\mathcal{E}+\Delta+\frac{\mathcal{E}[B]}{\mathcal{K}_b}}{1+\mathcal{E}+\Delta} = 1+\frac{\frac{\mathcal{E}[B]}{\mathcal{K}_b}}{1+\mathcal{E}+\Delta}$$

since $p(\mathcal{O})_{\mathcal{CCDO}_{max}} = \frac{\mathcal{E}}{1+\mathcal{E}+\Delta}$ (Appendix II, eq. 81)

$$\boxed{\frac{EC_{50\,\mathcal{CCDO}}}{EC_{50\,\mathcal{CCDOB}}} = 1+\left(p(\mathcal{O})_{\mathcal{CCDO}_{max}}\right)\frac{[B]}{\mathcal{K}_b}} \quad (97)$$

APPENDIX IV

ANALYTIC SOLUTIONS OF NON-EQUILIBRIUM FRACTIONAL OCCUPANCY FOR TWO- AND THREE-STATE MARKOV MODELS OF $GABA_A$ RECEPTOR FUNCTION

Emmanuel J. Botzolakis, Matt T. Bianchi, Farid Hekmat, and Robert L. Macdonald

I. Analytic solution of fractional occupancy as a function of time for states in the $\mathcal{C} \underset{\alpha}{\overset{\beta}{\rightleftarrows}} \mathcal{O}$ reaction scheme, which is represented by the following system of first-order differential equations:

$$\mathcal{C}' = -\mathcal{C}\beta + \mathcal{O}\alpha \tag{1}$$

$$\mathcal{O}' = \mathcal{C}\beta - \mathcal{O}\alpha \tag{2}$$

At t = 0, all receptors occupy either $\mathcal{C}$ or $\mathcal{O}$. Thus,

$$\mathcal{C}_\circ + \mathcal{O}_\circ = 1 \tag{3}$$

This system can be represented as the matrix equation

$$\mathcal{N}' = \mathcal{Q}\mathcal{N}, \text{ where} \tag{4}$$

$$\mathcal{N}' = \begin{bmatrix} \mathcal{C}' \\ \mathcal{O}' \end{bmatrix} \tag{5}$$

$$\mathcal{Q} = \begin{bmatrix} -\beta & \alpha \\ \beta & -\alpha \end{bmatrix} \tag{6}$$

$$\mathcal{N} = \begin{bmatrix} \mathcal{C} \\ \mathcal{O} \end{bmatrix} \tag{7}$$

which has the general solution

$$\mathcal{N}(t) = cve^{\lambda t} \tag{8}$$

where v and λ are eigenvectors and eigenvalues of $\mathcal{Q}$, respectively, and c is an integration constant

To obtain the eigenvalues, we set

$$\mathcal{Q}v = \lambda v$$

$$\mathcal{Q}v - \lambda I v = 0$$

$$(\mathcal{Q} - \lambda I)v = 0$$

$$\begin{bmatrix} -\beta - \lambda & \alpha \\ \beta & -\alpha - \lambda \end{bmatrix} v = 0 \tag{9}$$

This system has a non-trivial solution only when

$$\det(\mathcal{Q} - \lambda I) = 0$$

$$(-\beta - \lambda)(-\alpha - \lambda) - (\alpha)(\beta) = 0$$

$$\lambda^2 + \lambda(\alpha + \beta) = 0$$

$$\lambda(\lambda + \alpha + \beta) = 0$$

Solving for the eigenvalues

$$\lambda_1 = 0 \tag{10}$$

$$\lambda_2 = -(\alpha + \beta) \tag{11}$$

Substituting (10) and (11) into (9) and solving the homogenous equation

$$v_1 = \begin{bmatrix} 1 \\ \beta/\alpha \end{bmatrix} \tag{12}$$

$$v_2 = \begin{bmatrix} 1 \\ -1 \end{bmatrix} \tag{13}$$

Substituting (7) and (10 – 13) into (8)

$$\begin{bmatrix} \mathcal{C}(t) \\ \mathcal{O}(t) \end{bmatrix} = c_1 \begin{bmatrix} 1 \\ \beta/\alpha \end{bmatrix} + c_2 \begin{bmatrix} 1 \\ -1 \end{bmatrix} e^{-(\alpha+\beta)t} \tag{14}$$

Solving for the integration constants when $\mathcal{C}_\circ = 1$ and $\mathcal{O}_\circ = 0$

$$c_1 = \frac{\alpha}{\beta + \alpha} \tag{15}$$

$$c_2 = \frac{\beta}{\beta + \alpha} \tag{16}$$

Substituting (15) and (16) into (14)

$$\boxed{\mathcal{C}(t) = \frac{\alpha}{\beta + \alpha} + \left(\frac{\beta}{\beta + \alpha}\right) e^{-(\beta + \alpha)t}} \tag{17}$$

$$\boxed{\mathcal{O}(t) = \frac{\beta}{\beta + \alpha} - \left(\frac{\beta}{\beta + \alpha}\right) e^{-(\beta + \alpha)t}} \tag{18}$$

II. Analytic solution of fractional occupancy as a function of time for states in the $\mathcal{C}_1 \underset{K_{off}}{\overset{K_{on}[GABA]}{\rightleftarrows}} \mathcal{C}_2 \underset{\alpha}{\overset{\beta}{\rightleftarrows}} \mathcal{O}$ reaction scheme, which is represented by the following system of first-order differential equations:

$$\mathcal{C}_1{}' = -\mathcal{C}_1 K_{on}[GABA] + \mathcal{C}_2 K_{off} \tag{19}$$

$$\mathcal{C}_2{}' = \mathcal{C}_1 K_{on}[GABA] - \mathcal{C}_2\left(K_{off} + \beta\right) + \mathcal{O}\alpha \tag{20}$$

$$\mathcal{O}' = \mathcal{C}_2 \beta - \mathcal{O}\alpha \tag{21}$$

At t = 0, all receptors occupy either $\mathcal{C}_1$ or $\mathcal{C}_2$ or $\mathcal{O}$. Thus,

$$\mathcal{C}_{1_o} + \mathcal{C}_{2_o} + \mathcal{O}_o = 1 \tag{22}$$

This system can be represented as the matrix equation

$\mathcal{N}' = \mathcal{Q}\mathcal{N}$, where (4)

$$\mathcal{N}' = \begin{bmatrix} \mathcal{C}_1{}' \\ \mathcal{C}_2{}' \\ \mathcal{O}' \end{bmatrix} \tag{23}$$

$$\mathcal{Q} = \begin{bmatrix} -K_{on}[GABA] & K_{off} & 0 \\ K_{on}[GABA] & -\left(K_{off} + \beta\right) & \alpha \\ 0 & \beta & -\alpha \end{bmatrix} \tag{24}$$

$$\mathcal{N} = \begin{bmatrix} \mathcal{C}_1 \\ \mathcal{C}_2 \\ \mathcal{O} \end{bmatrix} \tag{25}$$

This system has the general solution

$$\mathcal{N}(t) = cve^{\lambda t} \tag{8}$$

where v and λ are eigenvectors and eigenvalues of $\mathcal{Q}$, respectively, and c is an integration constant

To obtain the eigenvalues, we set

$$\mathcal{Q}v = \lambda v$$

$$\mathcal{Q}v - \lambda I v = 0$$

$$(\mathcal{Q} - \lambda I)v = 0$$

$$\begin{bmatrix} -K_{on}[GABA] - \lambda & K_{off} & 0 \\ K_{on}[GABA] & -\left(K_{off} + \beta\right) - \lambda & \alpha \\ 0 & \beta & -\alpha - \lambda \end{bmatrix} v = 0 \tag{26}$$

This system has a non-trivial solution only when

$$\det(\mathcal{Q} - \lambda I) = 0$$

$$\lambda^3 + \lambda^2\left(K_{on}[GABA] + K_{off} + \beta + \alpha\right) + \lambda\left(K_{on}[GABA]\beta + K_{on}[GABA]\alpha + K_{off}\alpha\right) = 0$$

$$\lambda\left(\lambda^2 + \lambda\left(K_{on}[GABA] + K_{off} + \beta + \alpha\right) + \left(K_{on}[GABA]\beta + K_{on}[GABA]\alpha + K_{off}\alpha\right)\right) = 0$$

To simplify, let

$$p = K_{on}[GABA] + K_{off} + \beta + \alpha \tag{27}$$

$$q = \left[p^2 - 4\left(K_{on}[GABA]\beta + K_{on}[GABA]\alpha + K_{off}\alpha\right)\right]^{½} \tag{28}$$

Solving the eigenvalues

$$\lambda_1 = 0 \tag{29}$$

$$\lambda_2 = \frac{-p - q}{2} \tag{30}$$

$$\lambda_3 = \frac{-p + q}{2} \tag{31}$$

Substituting (29 – 31) into (26) and solving the homogenous equation

$$v_1 = \begin{bmatrix} \left(\frac{K_{off}}{K_{on}[GABA]}\right) \\ 1 \\ \left(\frac{\beta}{\alpha}\right) \end{bmatrix} \tag{32}$$

$$v_2 = \begin{bmatrix} \left(\frac{-(\lambda_2+\beta+\alpha)}{\beta}\right) \\ \left(\frac{(\lambda_2+\alpha)}{\beta}\right) \\ 1 \end{bmatrix} \tag{33}$$

$$v_3 = \begin{bmatrix} \left(\frac{-(\lambda_3+\beta+\alpha)}{\beta}\right) \\ \left(\frac{(\lambda_3+\alpha)}{\beta}\right) \\ 1 \end{bmatrix} \tag{34}$$

Substituting (25) and (29 – 34) into (8)

$$\begin{bmatrix} \mathcal{C}_1(t) \\ \mathcal{C}_2(t) \\ \mathcal{O}(t) \end{bmatrix} = c_1 \begin{bmatrix} \left(\frac{K_{off}}{K_{on}[GABA]}\right) \\ 1 \\ \left(\frac{\beta}{\alpha}\right) \end{bmatrix} + c_2 \begin{bmatrix} \left(\frac{-(\lambda_2+\beta+\alpha)}{\beta}\right) \\ \left(\frac{(\lambda_2+\alpha)}{\beta}\right) \\ 1 \end{bmatrix} e^{\lambda_2 t} + c_3 \begin{bmatrix} \left(\frac{-(\lambda_3+\beta+\alpha)}{\beta}\right) \\ \left(\frac{(\lambda_3+\alpha)}{\beta}\right) \\ 1 \end{bmatrix} e^{\lambda_3 t} \tag{35}$$

Solving for the integration constants when $\mathcal{C}_{1_o} = 1$, $\mathcal{C}_{2_o} = 0$, and $\mathcal{O}_o = 0$

$$c_1 = \frac{K_{on}[GABA]\alpha}{\lambda_2\lambda_3} \tag{36}$$

$$c_2 = -\frac{K_{on}[GABA]\beta}{\lambda_2 q} \tag{37}$$

$$c_3 = \frac{K_{on}[GABA]\beta}{\lambda_3 q} \tag{38}$$

Substituting (36 – 38) into (35)

$$\boxed{\mathcal{C}_1(t) = \frac{K_{off}\,\alpha}{\lambda_2\lambda_3} + \frac{K_{on}[GABA](\lambda_2+\beta+\alpha)}{\lambda_2 q} e^{\lambda_2 t} - \frac{K_{on}[GABA](\lambda_3+\beta+\alpha)}{\lambda_3 q} e^{\lambda_3 t}} \tag{39}$$

$$\boxed{\mathcal{C}_2(t) = \frac{K_{on}[GABA]\alpha}{\lambda_2\lambda_3} - \frac{K_{on}[GABA](\lambda_2+\alpha)}{\lambda_2 q} e^{\lambda_2 t} + \frac{K_{on}[GABA](\lambda_3+\alpha)}{\lambda_3 q} e^{\lambda_3 t}} \tag{40}$$

$$\boxed{\mathcal{O}(t) = \frac{K_{on}\,[GABA]\beta}{\lambda_2\lambda_3} - \frac{K_{on}\,[GABA]\beta}{\lambda_2 q}e^{\lambda_2 t} + \frac{K_{on}\,[GABA]\beta}{\lambda_3 q}e^{\lambda_3 t}} \tag{41}$$

III. Analytic solution of fractional occupancy as a function of time for states in the $\mathcal{C}_1 \underset{K_{off}}{\overset{K_{on}\,[GABA\,]}{\rightleftarrows}} \mathcal{C}_2 \underset{\alpha}{\overset{\beta}{\rightleftarrows}} \mathcal{O} \underset{\rho}{\overset{\delta}{\rightleftarrows}} \mathcal{D}$ reaction scheme, which collapses to the $\mathcal{C}_2 \underset{\alpha}{\overset{\beta}{\rightleftarrows}} \mathcal{O} \underset{\rho}{\overset{\delta}{\rightleftarrows}} \mathcal{D}$ reaction scheme as [GABA] $\rightarrow \infty$. This is represented by the following system of first-order differential equations:

$$\mathcal{C}_2{}' = -\mathcal{C}_2\beta + \mathcal{O}\alpha \tag{42}$$

$$\mathcal{O}' = \mathcal{C}_2\beta - \mathcal{O}(\alpha + \delta) + \mathcal{D}\rho \tag{43}$$

$$\mathcal{D}' = \mathcal{O}\delta - \mathcal{D}\rho \tag{44}$$

At t = 0, all receptors occupy either $\mathcal{C}_2$ or $\mathcal{O}$ or $\mathcal{D}$. Thus,

$$\mathcal{C}_{2_o} + \mathcal{O}_o + \mathcal{D}_o = 1 \tag{45}$$

This system can be represented as the matrix equation

$$\mathcal{N}' = \mathcal{Q}\mathcal{N}, \text{ where} \tag{4}$$

$$\mathcal{N}' = \begin{bmatrix} \mathcal{C}_2{}' \\ \mathcal{O}' \\ \mathcal{D}' \end{bmatrix} \tag{46}$$

$$\mathcal{Q} = \begin{bmatrix} -\beta & \alpha & 0 \\ \beta & -(\alpha + \delta) & \rho \\ 0 & \delta & -\rho \end{bmatrix} \tag{47}$$

$$\mathcal{N} = \begin{bmatrix} \mathcal{C}_2 \\ \mathcal{O} \\ \mathcal{D} \end{bmatrix} \tag{48}$$

This system has the general solution

$$\mathcal{N}(t) = cve^{\lambda t} \tag{8}$$

where v and λ are eigenvectors and eigenvalues of $\mathcal{Q}$, respectively, and c is an integration constant

To obtain the eigenvalues, we set

$$\mathcal{Q}v = \lambda v$$

$$\mathcal{Q}v - \lambda I v = 0$$

$$(\mathcal{Q} - \lambda I)v = 0$$

$$\begin{bmatrix} -\beta - \lambda & \alpha & 0 \\ \beta & -(\alpha + \delta) - \lambda & \rho \\ 0 & \delta & -\rho - \lambda \end{bmatrix} v = 0 \tag{49}$$

This system has a non-trivial solution only when

$$\det(\mathcal{Q} - \lambda I) = 0$$

$$\lambda^3 + \lambda^2(\beta + \alpha + \delta + \rho) + \lambda(\beta\delta + \beta\rho + \alpha\rho) = 0$$

$$\lambda\left(\lambda^2 + \lambda(\beta + \alpha + \delta + \rho) + (\beta\delta + \beta\rho + \alpha\rho)\right) = 0$$

To simplify, let

$$p = \beta + \alpha + \delta + \rho \tag{50}$$

$$q = [p^2 - 4(\beta\delta + \beta\rho + \alpha\rho)]^{½} \tag{51}$$

Solving the eigenvalues

$$\lambda_1 = 0 \tag{52}$$

$$\lambda_2 = \frac{-p - q}{2} \tag{53}$$

$$\lambda_3 = \frac{-p + q}{2} \tag{54}$$

Substituting (52 – 54) into (49) and solving the homogenous equation

$$v_1 = \begin{bmatrix} \left(\frac{\alpha}{\beta}\right) \\ 1 \\ \left(\frac{\delta}{\rho}\right) \end{bmatrix} \tag{55}$$

$$v_2 = \begin{bmatrix} \left(\frac{-(\lambda_2+\delta+\rho)}{\delta}\right) \\ \left(\frac{(\lambda_2+\rho)}{\delta}\right) \\ 1 \end{bmatrix} \tag{56}$$

$$v_3 = \begin{bmatrix} \left(\frac{-(\lambda_3+\delta+\rho)}{\delta}\right) \\ \left(\frac{(\lambda_3+\rho)}{\delta}\right) \\ 1 \end{bmatrix} \tag{57}$$

Substituting (48) and (52 – 57) into (8)

$$\begin{bmatrix} \mathcal{C}_2(t) \\ \mathcal{O}(t) \\ \mathcal{D}(t) \end{bmatrix} = c_1 \begin{bmatrix} \left(\frac{\alpha}{\beta}\right) \\ 1 \\ \left(\frac{\delta}{\rho}\right) \end{bmatrix} + c_2 \begin{bmatrix} \left(\frac{-(\lambda_2+\delta+\rho)}{\delta}\right) \\ \left(\frac{(\lambda_2+\rho)}{\delta}\right) \\ 1 \end{bmatrix} e^{\lambda_2 t} + c_3 \begin{bmatrix} \left(\frac{-(\lambda_3+\delta+\rho)}{\delta}\right) \\ \left(\frac{(\lambda_3+\rho)}{\delta}\right) \\ 1 \end{bmatrix} e^{\lambda_3 t} \tag{58}$$

Solving for the integration constants when $\mathcal{C}_{2_o} = 1$, $\mathcal{O}_o = 0$, and $\mathcal{D}_o = 0$

$$c_1 = \frac{\beta\rho}{\lambda_2\lambda_3} \tag{59}$$

$$c_2 = -\frac{\beta\delta}{\lambda_2 q} \tag{60}$$

$$c_3 = \frac{\beta\delta}{\lambda_3 q} \tag{61}$$

Substituting (59 – 61) into (58)

$$\boxed{\mathcal{C}_2(t) = \frac{\alpha\rho}{\lambda_2\lambda_3} + \frac{\beta(\lambda_2+\delta+\rho)}{\lambda_2 q} e^{\lambda_2 t} - \frac{\beta(\lambda_3+\delta+\rho)}{\lambda_3 q} e^{\lambda_3 t}} \tag{62}$$

$$\boxed{\mathcal{O}(t) = \frac{\beta\rho}{\lambda_2\lambda_3} - \frac{\beta(\lambda_2+\rho)}{\lambda_2 q} e^{\lambda_2 t} + \frac{\beta(\lambda_3+\rho)}{\lambda_3 q} e^{\lambda_3 t}} \tag{63}$$

$$\boxed{\mathcal{D}(t) = \frac{\beta\delta}{\lambda_2\lambda_3} - \frac{\beta\delta}{\lambda_2 q} e^{\lambda_2 t} + \frac{\beta\delta}{\lambda_3 q} e^{\lambda_3 t}} \tag{64}$$

IV. Analytic solution of fractional occupancy as a function of time for states in the

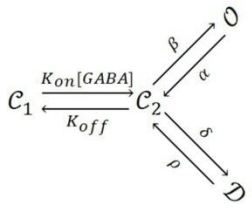

reaction scheme, which collapses to the

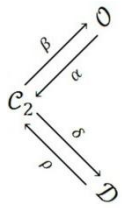

reaction scheme as $[\mathrm{GABA}] \to \infty$. This is represented by the following system of first-order differential equations:

$$\mathcal{O}' = -\mathcal{O}\alpha + \mathcal{C}_2\beta \tag{65}$$

$$\mathcal{C}_2{}' = \mathcal{O}\alpha - \mathcal{C}_2(\beta + \delta) + \mathcal{D}\rho \tag{66}$$

$$\mathcal{D}' = \mathcal{C}_2\delta - \mathcal{D}\rho \tag{67}$$

At t = 0, all receptors occupy either $\mathcal{O}$ or $\mathcal{C}_2$ or $\mathcal{D}$. Thus,

$$\mathcal{O}_o + \mathcal{C}_{2_o} + \mathcal{D}_o = 1 \tag{68}$$

This system can be represented as the matrix equation

$$\mathcal{N}' = \mathcal{Q}\mathcal{N}, \text{ where} \tag{4}$$

$$\mathcal{N}' = \begin{bmatrix} \mathcal{O}' \\ \mathcal{C}_2{}' \\ \mathcal{D}' \end{bmatrix} \tag{69}$$

$$\mathcal{Q} = \begin{bmatrix} -\alpha & \beta & 0 \\ \alpha & -(\beta + \delta) & \rho \\ 0 & \delta & -\rho \end{bmatrix} \tag{70}$$

$$\mathcal{N} = \begin{bmatrix} \mathcal{O} \\ \mathcal{C}_2 \\ \mathcal{D} \end{bmatrix} \tag{71}$$

This system has the general solution

$$\mathcal{N}(t) = cve^{\lambda t} \tag{8}$$

where v and λ are eigenvectors and eigenvalues of $\mathcal{Q}$, respectively, and c is an integration constant

To obtain the eigenvalues, we set

$$\mathcal{Q}v = \lambda v$$

$$\mathcal{Q}v - \lambda I v = 0$$

$$(\mathcal{Q} - \lambda I)v = 0$$

$$\begin{bmatrix} -\alpha - \lambda & \beta & 0 \\ \alpha & -(\beta + \delta) - \lambda & \rho \\ 0 & \delta & -\rho - \lambda \end{bmatrix} v = 0 \tag{72}$$

This system has a non-trivial solution only when

$$\det(\mathcal{Q} - \lambda I) = 0$$

$$\lambda^3 + \lambda^2(\beta + \alpha + \delta + \rho) + \lambda(\alpha\delta + \alpha\rho + \beta\rho) = 0$$

$$\lambda\left(\lambda^2 + \lambda(\beta + \alpha + \delta + \rho) + (\alpha\delta + \alpha\rho + \beta\rho)\right) = 0$$

To simplify, let

$$p = \beta + \alpha + \delta + \rho \tag{73}$$

$$q = [p^2 - 4(\alpha\delta + \alpha\rho + \beta\rho)]^{½} \tag{74}$$

Solving the eigenvalues

$$\lambda_1 = 0 \tag{75}$$

$$\lambda_2 = \frac{-p - q}{2} \tag{76}$$

$$\lambda_3 = \frac{-p + q}{2} \tag{77}$$

Substituting (75 – 77) into (72) and solving the homogenous equation

$$v_1 = \begin{bmatrix} \left(\frac{\beta}{\alpha}\right) \\ 1 \\ \left(\frac{\delta}{\rho}\right) \end{bmatrix} \tag{78}$$

$$v_2 = \begin{bmatrix} \left(\frac{-(\lambda_2+\delta+\rho)}{\delta}\right) \\ \left(\frac{(\lambda_2+\rho)}{\delta}\right) \\ 1 \end{bmatrix} \tag{79}$$

$$v_3 = \begin{bmatrix} \left(\frac{-(\lambda_3+\delta+\rho)}{\delta}\right) \\ \left(\frac{(\lambda_3+\rho)}{\delta}\right) \\ 1 \end{bmatrix} \tag{80}$$

Substituting (71) and (75 – 80) into (8)

$$\begin{bmatrix} \mathcal{O}(t) \\ \mathcal{C}_2(t) \\ \mathcal{D}(t) \end{bmatrix} = c_1 \begin{bmatrix} \left(\frac{\beta}{\alpha}\right) \\ 1 \\ \left(\frac{\delta}{\rho}\right) \end{bmatrix} + c_2 \begin{bmatrix} \left(\frac{-(\lambda_2+\delta+\rho)}{\delta}\right) \\ \left(\frac{(\lambda_2+\rho)}{\delta}\right) \\ 1 \end{bmatrix} e^{\lambda_2 t} + c_3 \begin{bmatrix} \left(\frac{-(\lambda_3+\delta+\rho)}{\delta}\right) \\ \left(\frac{(\lambda_3+\rho)}{\delta}\right) \\ 1 \end{bmatrix} e^{\lambda_3 t} \tag{81}$$

Solving for the integration constants when $\mathcal{O}_o = 0$, $\mathcal{C}_{2_o} = 1$, and $\mathcal{D}_o = 0$

$$c_1 = \frac{\alpha\rho}{\lambda_2\lambda_3} \tag{82}$$

$$c_2 = -\frac{\delta(\lambda_2+\alpha)}{\lambda_2 q} \tag{83}$$

$$c_3 = \frac{\delta(\lambda_3+\alpha)}{\lambda_3 q} \tag{84}$$

Substituting (82 – 84) into (81)

$$\boxed{\mathcal{O}(t) = \frac{\beta\rho}{\lambda_2\lambda_3} + \frac{(\lambda_2+\alpha)(\lambda_2+\delta+\rho)}{\lambda_2 q} e^{\lambda_2 t} - \frac{(\lambda_3+\alpha)(\lambda_3+\delta+\rho)}{\lambda_3 q} e^{\lambda_3 t}} \tag{85}$$

$$\boxed{\mathcal{C}_2(t) = \frac{\alpha\rho}{\lambda_2\lambda_3} - \frac{(\lambda_2+\alpha)(\lambda_2+\rho)}{\lambda_2 q} e^{\lambda_2 t} + \frac{(\lambda_3+\alpha)(\lambda_3+\rho)}{\lambda_3 q} e^{\lambda_3 t}} \tag{86}$$

$$\boxed{\mathcal{D}(t) = \frac{\alpha\delta}{\lambda_2\lambda_3} - \frac{\delta(\lambda_2+\alpha)}{\lambda_2 q} e^{\lambda_2 t} + \frac{\delta(\lambda_3+\alpha)}{\lambda_3 q} e^{\lambda_3 t}} \tag{87}$$

APPENDIX V

THE MICROSCOPIC KINETIC DETERMINANTS OF MACROSCOPIC DESENSITIZATION FOR TWO- AND THREE-STATE MARKOV MODELS OF $GABA_A$ RECEPTOR FUNCTION

Emmanuel J. Botzolakis, Matt T. Bianchi, Farid Hekmat, and Robert L. Macdonald

I. $\mathcal{C} \underset{\alpha}{\overset{\beta}{\rightleftharpoons}} \mathcal{O}$

$$\mathcal{O}(t) = \frac{\beta}{\beta+\alpha} - \left(\frac{\beta}{\beta+\alpha}\right) e^{-(\beta+\alpha)t} \quad \text{(Appendix IV, eq. 18)} \tag{1}$$

For macroscopic desensitization to occur, $\mathcal{O}(\mathrm{t})$ must have a local maximum where

$$\mathcal{O}'(t) = 0 \tag{2}$$

$$\mathcal{O}'(t) = \beta e^{-(\beta+\alpha)t} \tag{3}$$

Setting (2) equal to (3)

$$0 = \beta e^{-(\beta+\alpha)t} \tag{4}$$

Since no solution exists for (4), $\mathcal{O}(t)$ has no local maxima, and consequently, cannot undergo macroscopic desensitization.

II. $\mathcal{C}_1 \underset{K_{off}}{\overset{K_{on}\,[GABA\,]}{\rightleftharpoons}} \mathcal{C}_2 \underset{\alpha}{\overset{\beta}{\rightleftharpoons}} \mathcal{O}$

$$\mathcal{O}(t) = \frac{K_{on}\,[GABA]\beta}{\lambda_2\lambda_3} - \frac{K_{on}\,[GABA]\beta}{\lambda_2(\lambda_3-\lambda_2)} e^{\lambda_2 t} + \frac{K_{on}\,[GABA]\beta}{\lambda_3(\lambda_3-\lambda_2)} e^{\lambda_3 t} \quad \text{(Appendix IV, eq. 41)} \tag{5}$$

For macroscopic desensitization to occur, $\mathcal{O}(\mathrm{t})$ must have a local maximum where

$$\mathcal{O}'(t) = 0 \tag{2}$$

$$\mathcal{O}'(t) = -\frac{K_{on}[GABA]\beta}{(\lambda_3-\lambda_2)}e^{\lambda_2 t} + \frac{K_{on}[GABA]\beta}{(\lambda_3-\lambda_2)}e^{\lambda_3 t} \quad (6)$$

Setting (2) equal to (6)

$$0 = -\frac{K_{on}[GABA]\beta}{(\lambda_3-\lambda_2)}e^{\lambda_2 t} + \frac{K_{on}[GABA]\beta}{(\lambda_3-\lambda_2)}e^{\lambda_3 t}$$

$$e^{\lambda_2 t} = e^{\lambda_3 t}$$

$$\lambda_2 = \lambda_3 \quad (7)$$

However, when $\lambda_2 = \lambda_3$, the denominator in (1) is zero.

Thus, $\mathcal{O}(t)$ has no local maxima, and consequently, cannot undergo macroscopic desensitization.

III. $\mathcal{C}_1 \underset{K_{off}}{\overset{K_{on}[GABA]}{\rightleftarrows}} \mathcal{C}_2 \underset{\alpha}{\overset{\beta}{\rightleftarrows}} \mathcal{O} \underset{\rho}{\overset{\delta}{\rightleftarrows}} \mathcal{D}$, which reduces to the $\mathcal{C}_2 \underset{\alpha}{\overset{\beta}{\rightleftarrows}} \mathcal{O} \underset{\rho}{\overset{\delta}{\rightleftarrows}} \mathcal{D}$ reaction scheme as $[\mathrm{GABA}] \to \infty$.

$$\mathcal{O}(t) = \frac{\beta\rho}{\lambda_2\lambda_3} - \frac{\beta(\lambda_2+\rho)}{\lambda_2(\lambda_3-\lambda_2)}e^{\lambda_2 t} + \frac{\beta(\lambda_3+\rho)}{\lambda_3(\lambda_3-\lambda_2)}e^{\lambda_3 t} \text{ (Appendix IV, eq. 63)} \quad (8)$$

For macroscopic desensitization to occur, $\mathcal{O}(t)$ must have a local maximum where $\mathcal{O}'(t) = 0$ (2)

$$\mathcal{O}'(t) = -\frac{\beta(\lambda_2+\rho)}{(\lambda_3-\lambda_2)}e^{\lambda_2 t} + \frac{\beta(\lambda_3+\rho)}{(\lambda_3-\lambda_2)}e^{\lambda_3 t} \quad (9)$$

Setting (2) equal to (9)

$$0 = -\frac{\beta(\lambda_2+\rho)}{(\lambda_3-\lambda_2)}e^{\lambda_2 t} + \frac{\beta(\lambda_3+\rho)}{(\lambda_3-\lambda_2)}e^{\lambda_3 t}$$

$$(\lambda_2+\rho)e^{\lambda_2 t} = (\lambda_3+\rho)e^{\lambda_3 t}$$

$$e^{(\lambda_3-\lambda_2)t} = \frac{(\lambda_2+\rho)}{(\lambda_3+\rho)}$$

$$t = \frac{\ln\frac{(\lambda_2+\rho)}{(\lambda_3+\rho)}}{(\lambda_3-\lambda_2)} \quad (10)$$

$\lambda_2 = \frac{-p-q}{2}$ (Appendix IV, eq. 53) (11)

$\lambda_3 = \frac{-p+q}{2}$ (Appendix IV, eq. 54) (12)

$p = \beta + \alpha + \delta + \rho$ (Appendix IV, eq. 50) (13)

$q = [p^2 - 4(\beta\delta + \beta\rho + \alpha\rho)]^{½}$ (Appendix IV, eq. 51) (14)

Substituting (11 – 14) into (10)

$$t = \frac{\ln\left(\frac{\left(\frac{-p-q}{2}+\rho\right)}{\left(\frac{-p+q}{2}+\rho\right)}\right)}{\left(\frac{-p+q}{2}\right)-\left(\frac{-p-q}{2}\right)} = \frac{\ln\left(\frac{(-p-q+2\rho)}{(-p+q+2\rho)}\right)}{q} = \frac{\ln\left(\frac{\beta+\alpha+\delta-\rho+q}{\beta+\alpha+\delta-\rho-q}\right)}{q} \quad (15)$$

Let $X = \beta + \alpha + \delta - \rho$ (16)

Substituting (16) into (15)

$$t = \frac{\ln\left(\frac{X+q}{X-q}\right)}{q} \quad (17)$$

Substituting (13) into (14) and rearranging

$q = [(\beta + \alpha + \delta + \rho)^2 - 4(\beta\delta + \beta\rho + \alpha\rho)]^{½} = [(\beta + \alpha - \delta - \rho)^2 + 4\alpha\delta]^{½}$

Since all rate constants are positive, q must also be positive.

Thus, there is a positive solution for t only when $\left(\frac{X+q}{X-q}\right) > 0$

Multiplying the numerator and denominator by $(X - q)$

$\frac{(X+q)(X-q)}{(X-q)(X-q)} > 0$

$$\frac{X^2-q^2}{(X-q)^2} > 0 \quad (18)$$

Since the denominator in (18) must be positive, there is a positive solution for t only when the numerator in (18) is also positive

$$X^2 - q^2 > 0 \quad (19)$$

Substituting (14) and (16) into (19)

$$(\beta + \alpha + \delta - \rho)^2 - (\beta + \alpha + \delta + \rho)^2 - (\beta\delta + \alpha\rho + \beta\rho) > 0$$

$$-4\delta\rho + \beta\delta > 0$$

$$\boxed{\beta > \rho} \quad (20)$$

Thus, $\mathcal{O}(t)$ has a local maximum, meaning that it can undergo macroscopic desensitization, but only when $\beta > \rho$.

III. 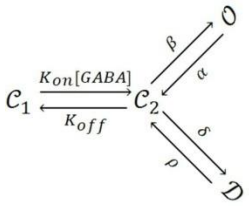 reaction scheme, which reduces to the

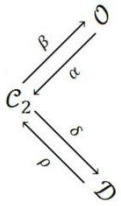 reaction scheme as [GABA] → ∞.

$$\mathcal{O}(t) = \frac{\beta\rho}{\lambda_2\lambda_3} + \frac{(\lambda_2+\alpha)(\lambda_2+\delta+\rho)}{\lambda_2(\lambda_3-\lambda_2)} e^{\lambda_2 t} - \frac{(\lambda_3+\alpha)(\lambda_3+\delta+\rho)}{\lambda_3(\lambda_3-\lambda_2)} e^{\lambda_3 t} \text{ (Appendix IV, eq. 85)} \quad (21)$$

For macroscopic desensitization to occur, $\mathcal{O}(t)$ must have a local maximum where $\mathcal{O}'(t) = 0$ (2)

$$\mathcal{O}'(t) = \frac{(\lambda_2+\alpha)(\lambda_2+\delta+\rho)}{(\lambda_3-\lambda_2)} e^{\lambda_2 t} - \frac{(\lambda_3+\alpha)(\lambda_3+\delta+\rho)}{(\lambda_3-\lambda_2)} e^{\lambda_3 t} \quad (22)$$

Setting (2) equal to (22)

$$0 = \frac{(\lambda_2+\alpha)(\lambda_2+\delta+\rho)}{(\lambda_3-\lambda_2)} e^{\lambda_2 t} - \frac{(\lambda_3+\alpha)(\lambda_3+\delta+\rho)}{(\lambda_3-\lambda_2)} e^{\lambda_3 t}$$

$$(\lambda_2 + \alpha)(\lambda_2 + \delta + \rho)e^{\lambda_2 t} = (\lambda_3 + \alpha)(\lambda_3 + \delta + \rho)e^{\lambda_3 t}$$

$$e^{(\lambda_3-\lambda_2)t} = \frac{(\lambda_2+\alpha)(\lambda_2+\delta+\rho)}{(\lambda_3+\alpha)(\lambda_3+\delta+\rho)}$$

$$t = \frac{\ln\left(\frac{(\lambda_2+\alpha)(\lambda_2+\delta+\rho)}{(\lambda_3+\alpha)(\lambda_3+\delta+\rho)}\right)}{(\lambda_3-\lambda_2)} \quad (23)$$

$\lambda_2 = \frac{-p-q}{2}$ (Appendix IV, eq. 76) (24)

$\lambda_3 = \frac{-p+q}{2}$ (Appendix IV, eq. 77) (25)

$p = \beta + \alpha + \delta + \rho$ (Appendix IV, eq. 73) (26)

$q = [p^2 - 4(\alpha\delta + \alpha\rho + \beta\rho)]^{½}$ (Appendix IV, eq. 74) (27)

Substituting (24 – 27) into (23)

$$t = \frac{\ln\left(\frac{\left(\left(\frac{-p-q}{2}\right)+\alpha\right)\left(\left(\frac{-p-q}{2}\right)+\delta+\rho\right)}{\left(\left(\frac{-p+q}{2}\right)+\alpha\right)\left(\left(\frac{-p+q}{2}\right)+\delta+\rho\right)}\right)}{\left(\frac{-p+q}{2}\right)-\left(\frac{-p-q}{2}\right)} = \frac{\ln\left(\frac{(-p-q+2\alpha)(-p-q+2\delta+2\rho)}{(-p+q+2\alpha)(-p+q+2\delta+2\rho)}\right)}{q}$$

$$t = \frac{\ln\left(\frac{(-q+\alpha-\beta-\delta-\rho)(-q-\alpha-\beta+\delta+\rho)}{(q+\alpha-\beta-\delta-\rho)(q-\alpha-\beta+\delta+\rho)}\right)}{q}$$

$$t = \frac{\ln\left(\frac{q^2-\alpha^2+2\alpha\delta+2\alpha\rho+\beta^2-\delta^2-2\delta\rho-\rho^2+2\beta q}{q^2-\alpha^2+2\alpha\delta+2\alpha\rho+\beta^2-\delta^2-2\delta\rho-\rho^2-2\beta q}\right)}{q} \quad (28)$$

Let $X = q^2 - \alpha^2 + 2\alpha\delta + 2\alpha\rho + \beta^2 - \delta^2 - 2\delta\rho - \rho^2$ (29)

Substituting (29) into (28)

$$t = \frac{\ln\left(\frac{X+2\beta q}{X-2\beta q}\right)}{q} \quad (30)$$

Substituting (26) into (27) and rearranging

$q = [(\beta + \alpha + \delta + \rho)^2 - 4(\alpha\delta + \alpha\rho + \beta\rho)]^{½} = [(\beta + \alpha - \delta - \rho)^2 + 4\beta\delta]^{½}$

Since all rate constants are positive, q must also be positive.

Thus, there is a positive solution for t only when $\left(\frac{X+2\beta q}{X-2\beta q}\right) > 0$

Multiplying the numerator and denominator by $(X - 2\beta q)$

$\frac{(X+2\beta q)(X-2\beta q)}{(X-2\beta q)(X-2\beta q)} > 0$

$$\frac{X^2-4\beta^2q^2}{(X-2\beta q)^2} > 0 \tag{31}$$

Since the denominator in (31) must be positive, there is a positive solution for t only when the numerator in (31) is also positive

$$X^2 - 4\beta^2q^2 > 0 \tag{32}$$

Substituting (27) and (29) into (32) and simplifying

$$16\beta^2\delta(\alpha - \rho) > 0$$

$$(\alpha - \rho) > 0$$

$$\boxed{\alpha > \rho} \tag{33}$$

Thus, $\mathcal{O}(t)$ has a local maximum, meaning that it can undergo macroscopic desensitization, but only when $\alpha > \rho$.